Jane W. Chan
Editor

Optic Nerve Disorders

Diagnosis and Management

Second Edition

Springer

Optic Nerve Disorders

Jane W. Chan
Editor

Optic Nerve Disorders

Diagnosis and Management

Second Edition

Springer

Editor
Jane W. Chan, M.D.
Department of Neurology/Neuro-Ophthalmology
University of Nevada School of Medicine
Reno, NV, USA

ISBN 978-1-4614-0690-7 ISBN 978-1-4614-0691-4 (eBook)
DOI 10.1007/978-1-4614-0691-4
Springer New York Heidelberg Dordrecht London

Library of Congress Control Number: 2014936015

Printed on acid-free paper

Springer is part of Springer Science+Business Media (www.springer.com)

This book is dedicated to my parents, Tom and Rosalie Chan—especially to my mother for her unconditional love and support.

Preface

Since the first edition of this book on optic nerve disorders garnered recognition as one of the best-selling books in neuro-ophthalmology in the world, my close friends encouraged me to embark on another journey of writing to create an improved and updated version. In this second edition, new information on pertinent diagnostic techniques, such as the role of optical coherence tomography (OCT), multifocal visual evoked potential (mfVEP), multifocal electroretinogram (mfERG), neuroimaging, and genetic testing; and therapeutic advancements, such as novel neuroprotective agents, gene therapy, and more effective drugs for optic neuritis/multiple sclerosis based on recent clinical trials, have been incorporated into the various types of optic neuropathies. The chapters have been organized in a similar manner to the first edition with more photos and illustrations, encompassing optic neuritis, papilledema, ischemic optic neuropathies, compressive and infiltrative optic neuropathies, traumatic optic neuropathies, nutritional and toxic optic neuropathies, hereditary optic neuropathies, optic disc tumors, and the applications of OCT and mfVEP and mfERG. A new chapter on the approach to the diagnosis and differentiation of glaucomatous and nonglaucomatous optic neuropathies has been added to highlight the importance of considering glaucoma as another optic neuropathy in the differential diagnosis of optic nerve disorders.

This unique reference is intended to complement other excellent textbooks in neuro-ophthalmology, in which ophthalmologists, neurologists, neuro-ophthalmologists, and neurosurgeons can review practical clinical information for guidance to better help their patients with visual loss. Physicians in training at all levels can also acquire an introduction to the diagnosis and treatment of optic nerve disorders.

Reno, NV, USA — Jane W. Chan, M.D.

Contents

1 Optic Neuritis 1
Jane W. Chan

2 Ischemic Optic Neuropathies 41
Jane W. Chan

3 Papilledema 77
Jane W. Chan

4 Compressive and Infiltrative Optic Neuropathies 109
Jane W. Chan

5 Traumatic Optic Neuropathies 155
Jane W. Chan

6 Nutritional and Toxic Optic Neuropathies 177
Michelle Y. Wang, Alfredo A. Sadun, and Jane W. Chan

7 Hereditary Optic Neuropathies 209
Michelle Y. Wang, Alfredo A. Sadun, and Jane W. Chan

8 Congenital Disc Anomalies 249
Jane W. Chan

9 Optic Disc Tumors 267
Jane W. Chan

10 Approach to the Diagnosis and Differentiation of Glaucomatous and Nonglaucomatous Optic Neuropathies 281
Christopher Kai-shun Leung and Carmen K.M. Chan

11 Application of Optical Coherence Tomography in Neuro-Ophthalmic Disorders 309
Joseph Ho, Geetha Athappilly, Timothy B. Tivnan, and Thomas R. Hedges III

12 The Use of Multifocal Electroretinograms and Multifocal Visual Evoked Potentials in Optic Nerve Disorders 325
Donald C. Hood and Karen Holopigian

Index 353

Contributors

Geetha Athappilly, M.D. Tufts Medical Center, Boston, MA, USA

Lahey Clinic Ophthalmology Department, Burlington, MA, USA

Carmen K.M. Chan, M.B.BChir., M.R.C.P., F.R.C.S.Ed(Ophth). Department of Ophthalmology, Hong Kong Eye Hospital, The Chinese University of Hong Kong, Kowloon, Hong Kong

Jane W. Chan, M.D. Department of Neurology, Neuro-Ophthalmology, University of Nevada School of Medicine, Reno, NV, USA

Thomas R. Hedges III, M.D. Department of Ophthalmology, Tufts Medical Center, Boston, MA, USA

Joseph Ho, M.D. Department of Ophthalmology, New England Eye Center-Tufts Medical Center, Boston, MA, USA

Karen Holopigian, Ph.D. Clinical Sciences and Innovation, Novartis Pharmaceuticals, East Hanover, NJ, USA

Donald C. Hood, B.A., M.Sc., Ph.D., Departments of Psychology and Ophthalmology, Columbia University, New York, NY, USA

Christopher Kai-shun Leung, M.D., M.B.Ch.B., B.MedSc., M.Sc., F.H.K.A.M., F.H.K.C.Ophth. Department of Ophthalmology & Visual Sciences, University Eye Center, Hong Kong Eye Hospital, The Chinese University of Hong Kong, Kowloon, Hong Kong

Alfredo A. Sadun, M.D., Ph.D. Department of Ophthalmology, Doheny Eye Institute, Los Angeles, CA, USA

Timothy B. Tivnan, B.S., C.R.A. Department of Ophthalmology, Lahey Clinic Medical Center, Mashpee, MA, USA

Michelle Y. Wang, M.D. Department of Ophthalmology, Doheny Eye Institute, Los Angeles, CA, USA

Optic Neuritis

1

Jane W. Chan

Introduction

Although neurologists usually diagnose and treat multiple sclerosis (MS), the visual loss that often accompanies this disease often presents to an ophthalmologist or neuro-ophthalmologist for evaluation. It is an inflammation of one or both optic nerves that often results in temporary visual loss. It affects young to middle-aged adults between 16 and 55 years of age. The female-to-male ratio is 2:1. Children often are affected bilaterally, whereas adults are affected unilaterally. The annual incidence of acute optic neuritis (ON) has been estimated in population-based studies to be between 1 and 5 per 100,000 [1, 2]. Clinically definite multiple sclerosis (CDMS) is apparent at the onset of ON in 15–20 % of patients with ON; another 40 % will later experience an MS attack [3]. The clinical diagnosis and advances of understanding of the pathogenesis and current recommended treatment of this disorder are outlined here.

J.W. Chan, M.D. (✉)
Department of Neurology, Neuro-Ophthalmology,
University of Nevada School of Medicine,
975 Kirman Avenue (111), Reno,
Nevada 89502, USA
e-mail: worjun@aol.com

Clinical Presentation of ON

Symptoms

The loss of central vision is the major symptom reported in more than 90 % of patients who have acute ON. Others who have normal visual acuity may complain of loss of peripheral vision to one side in the superior or inferior fields. The patient usually experiences mild orbital pain above or behind the eye, but the pain is mild even with severe visual loss. This dull retrobulbar pain may precede or occur concurrently with the visual loss. It also may be aggravated by upward eye movement and may occasionally last for as long as several weeks. The optic nerve inflammation may stimulate the trigeminal innervation of the optic nerve sheath to cause this orbital pain. As visual acuity decreases over the next several days, the pain usually subsides when visual loss is maximal. Loss of color vision or dullness in the vision is also more commonly noticed by patients than photophobia. Other less common symptoms are perception of phosphenes (flashing lights with noise or eye movement) and decreased depth perception [4].

Signs

Visual Acuity

Visual acuity worsens over several hours, days, or even minutes and ranges in severity from

J.W. Chan (ed.), *Optic Nerve Disorders: Diagnosis and Management*,
DOI 10.1007/978-1-4614-0691-4_1, © Springer Science+Business Media New York 2014

20/20 to no light perception. The degree of visual loss does not correlate with the final visual outcome. Visual loss usually peaks at several days to a week. Maximal improvement in visual function typically occurs within 2–3 weeks and at most within 6 months or more [4].

Visual Field

Patients who have acute ON can present with a wide variety of visual field defects, most commonly a central scotoma. Less frequent defects may include an arcuate scotoma, a superior or inferior altitudinal scotoma, peripheral constriction, a cecocentral scotoma, and a bitemporal or hemianopic defect. In the Optic Neuritis Treatment Trial (ONTT) [5], this wide variety of baseline patterns of visual field loss had limited usefulness in differentiating ON from other optic nerve disorders. During the recovery phase, the central scotoma reduces to a small, dim, central or paracentral defect. Occasionally, an arcuate scotoma may persist. Less severe ON may cause only "blurry vision" and a relative scotoma that eventually resolves. Because of the Uhthoff phenomenon, as will be discussed later, patients whose ON have resolved can have large variations in visual field results on different days and at different times on the same day [5, 6]. Despite the return of visual acuity to 20/20 or better, 32 % of cases have residual visual field defects after 6 months using a Humphrey Field Analyzer [7]. Patients often continue to complain of visual difficulties months after their attack of acute ON. In the ONTT, 215 patients perceived their vision to be worse than it was before their ON, even though 66 % had normal visual acuity, 30 % had normal contrast sensitivity, 55 % had normal color vision, and 58 % had no significant visual field defects [8]. These patients may have subtle visual field defects not detected by conventional perimetry. They complain of disappearing "holes" in their field of vision and the reappearance of the "fill-ins" for these holes while more new holes form. This "Swiss cheese" visual field phenomenon also occurs in other causes of optic nerve disease [8].

In the Optic Neuritis Study Group [9], 48 % of patients who had unilateral ON and no prior ON in the fellow eye had an abnormal visual field in the asymptomatic eye. Approximately 68 % of the asymptomatic fellow eyes had baseline visual field defects that mostly affected the peripheral rim or were diffuse; 62 % of these visual field defects were classified as minimal. Most patients recovered a normal visual field with a varying pattern and location of sensitivity loss. Between 10 and 20 % of these patients believed that their vision was normal, despite having abnormal visual acuity, color vision, or contrast sensitivity. These clinical abnormalities are consistent with the pathologic evidence of demyelination and atrophy found in the optic nerves of patients who have subclinical ON.

The 15-year data from the ONTT [10] revealed that ON does not typically present unilaterally. All of the visual fields from the affected eyes were abnormal. Seventy-five percent from the fellow eyes at baseline were abnormal, and nearly 40 % were abnormal at year 15. At baseline and early in the study, the affected eyes had central diffuse visual field defects which changed to more localized nerve fiber bundle loss, including paracentral, partial arcuate, and arcuate defects, during the first year of the study. Most of the fellow eyes at baseline also had nerve fiber bundle defects that remained during the next 15 years. Therefore, over time, affected and fellow eyes showed similar patterns of visual field defects, with the affected eye being more severely involved. The foveal thresholds (the ability to detect the dimmest light stimulus at the fovea, as measured in decibels (db) between 0 and 50, 50 db being the dimmest stimulus target) also correlated with visual acuity and contrast sensitivity. Optic nerve redundancy was suggested as an explanation for why some patients had normal visual fields, despite severe visual acuity loss and other evidence of nerve fiber bundle damage.

Contrast Sensitivity and Color Vision

Contrast sensitivity and color vision are both reduced in acute ON. The loss of contrast sensitivity is often proportionate to or sometimes worse than the loss of visual acuity [4]. No matter how good the Snellen visual acuity recovery, contrast sensitivity usually remains

abnormal in resolved cases of ON and in subclinical cases [11]. Brightness sensitivity is also reduced in most patients whose unilateral ON has resolved [12].

The color dysfunction is also usually more severe than the visual acuity level [8]. Although Ishihara color plates are most commonly used in the clinic, the Farnsworth–Munsell 100-hue test has been shown to be more sensitive and specific [13]. The shortened version with caps 22–42 has a similar sensitivity for serial monitoring of dyschromatopsia after ON. The dyschromatopsia is related to the time course of the disease. More blue–yellow defects occur in the acute stage of ON, whereas more red–green defects occur after 6 months [13].

Pupillary Abnormality

The relative afferent pupillary defect is almost always present in anterior (swollen disc) or retrobulbar neuritis. If it is not present, then one should seriously consider other ophthalmic problems, such as a coexisting optic neuropathy in the fellow eye or other causes of visual loss unrelated to an optic neuropathy. Subclinical ON in the fellow eye is not uncommon [4].

Fundus Findings

Fundus findings also help to localize the site of the optic nerve lesion. Lesions that are adjacent to the optic nerve head cause papillitis (anterior ON) with minimal blood vessel enlargement and rarely peripapillary hemorrhages. Vitritis is present in anterior ON caused by infections or inflammations (sarcoidosis, syphilis, tuberculosis, Lyme disease) and may be associated with MS as part of an intermediate uveitis. More posterior lesions (retrobulbar ON) do not produce papillitis [4]. Unilateral retrobulbar ON and papillitis both are part of the MS spectrum of presentation [4]. In retrobulbar ON the optic disc is normal. Irrespective of the location of the lesion, 75 % of patients who have MS, including the ones who have had a previous subclinical attack, eventually will develop diffuse or temporal optic disc pallor and nerve fiber layer atrophy [14]. The optic disc swelling and the disc pallor both are nonspecific findings in ON. Peripheral retinal venous sheathing may also be seen in MS, but this finding is not specific for MS as it may also be found in sarcoidosis, pars planitis, intermediate uveitis, lymphoma, and other localized ocular conditions. This sheathing represents the visible clinical sign of perivascular lymphocytic infiltration and edema of MS lesions. The vascular inflammation occurs in a region that lacks myelin and oligodendrocytes, suggesting that the vascular endothelium may be the initial site for the formation of new lesions. The presence of peripheral retinal venous sheathing has been shown to be correlated with the development of MS [15].

Differential Diagnosis of ON

The acute monocular visual loss suggestive of ON should alert the ophthalmologist and neurologist to consider vascular optic nerve disorders [16]. Acute ischemic optic neuropathy (AION) is an infarction of the prelaminar anterior optic nerve as a result of an occlusion of the two main posterior ciliary arteries that supply the optic nerve and choroid. The orbital pain of MS-related ON, when it is severe and when it occurs or worsens during eye movement, is often a useful feature in differentiating acute ON from anterior ischemic optic neuropathy [17]. A course that is painless and does not progress to significantly improved visual function (at least two lines of visual acuity improvement) after several weeks does not suggest ON [3]. Furthermore, altitudinal rather than generalized disc swelling, disc pallor, arterial attenuation, and peripapillary hemorrhages are features much more commonly seen in AION than in ON [18]. AION is much more common in patients who are older than 50 years and who have symptoms of giant cell arteritis and an elevated sedimentation rate. It may also occur independently of giant cell arteritis [4].

Another neuro-ophthalmic disorder to consider in the differential diagnosis of ON is Leber's hereditary optic neuropathy (LHON). Males between 15 and 35 years are more commonly affected than females. Impairment of ganglion cell function results in visual loss that typically begins painlessly and centrally in one eye

followed by the second eye over days or months. Circumpapillary telangiectatic microangiopathy, swelling of the nerve fiber layer around the disc (pseudoedema), and absence of leakage from the disc or papillary region on fluorescein angiography are the key features distinguishing LHON from other causes of optic disc edema [19]. Genetic testing for the mitochondrial DNA mutations, 11778, 3460, 14484, can also help confirm the diagnosis of LHON [20].

Other systemic infections, granulomatous inflammations, and autoimmune diseases besides MS may present with optic disc edema as part of a neuroretinitis, posterior uveitis, or posterior scleritis.

Parainfectious ON usually develops 1–3 weeks after the onset of a viral or bacterial infection [21]. It is more common in children than in adults and may be unilateral, but more often bilateral. It is usually due to demyelination associated with swollen optic discs. It may occur with no evidence of neurologic dysfunction or with a meningitis, meningoencephalitis, or encephalomyelitis. Cerebrospinal fluid (CSF) is usually abnormal when neurologic manifestations are present. Visual recovery after parainfectious ON is often excellent. Postviral ON may be caused by underlying adenovirus [22], coxsackievirus [23], hepatitis A [24] and B [25], cytomegalovirus [26], Epstein–Barr virus (EBV) [27], human immunodeficiency virus type 1 (HIV-1) [28], measles [29], mumps [30], rubella [31], varicella zoster [32], and herpes zoster [33]. ON may also be seen in bacterial infections including anthrax [34], beta-hemolytic streptococcal infections [35], brucellosis [36], cat scratch disease [37], meningococcal infection [38], pertussis [39], tuberculosis [40], typhoid fever [41], and Whipple's disease [42]. Postvaccination ON is more often anterior and bilateral. It may develop after vaccination with Bacillus Calmette Guerin [43], hepatitis B [44], rabies virus [45], tetanus toxoid [46], variola virus [47], and influenza virus [48].

In sarcoidosis the ON may be anterior or retrobulbar. It can be the presenting feature or may occur during the course of the disease. Unlike demyelinating ON, the optic disc may have a lumpy, white appearance suggestive of a granulomatous reaction and may be associated with vitritis. Unlike the course of recovery in primary demyelinating ON, which is not steroid dependent, vision may decrease again in sarcoid once steroids are tapered or stopped. This steroid-dependent course of recovery is atypical for demyelinating ON and suggests an infiltrative or nondemyelinating inflammatory process, such as sarcoidosis [49].

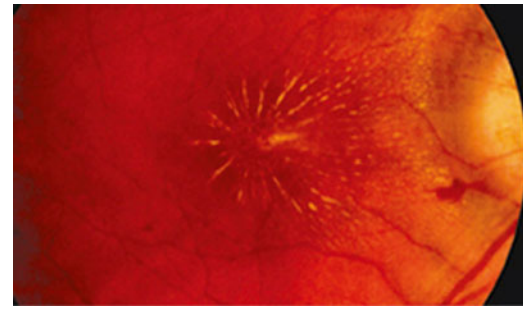

Fig. 1.1 Disc edema, hemorrhages, and a macular star in neuroretinitis are atypical for demyelinating optic neuritis

Both anterior and retrobulbar ON may occur in HIV-infected patients with cryptococcal meningitis [50], cytomegalovirus infection [51, 52], herpesvirus infection [53], syphilis [54], tuberculous meningitis [55], and various fungal infections [56]. Rarely, patients with toxoplasmosis may also develop ON [57, 58]. ON in patients with AIDS may also represent infection of the optic nerve by HIV itself [58, 59].

Regarding spirochetal infections, both anterior and retrobulbar ON may be seen in patients with Lyme disease [60].

In severe acute sphenoid sinusitis, the infection may spread posteriorly to the optic nerve in the orbital apex or within the optic canal causing retrobulbar ON and acute visual loss [61].

In neuroretinitis intraocular inflammation itself may cause optic disc edema (Fig. 1.1). Unlike the visual loss from damage to the optic nerve in demyelinating ON, the visual acuity is limited by the degree of vitreous inflammation or by secondary changes in the macula, such as cystoid macular edema (CME), associated with optic disc edema after cataract extraction. Swelling of the peripapillary retina may be observed in patients with anterior ON [62]. Lipid exudates

in a star configuration may also develop in the macula of the affected eye. Neuroretinitis may be seen in infections involving *Borrelia burgdorferi* (cat scratch disease) [62], toxoplasmosis [63], hepatitis B [64], and influenza [65]. Syphilis can cause both neuroretinitis and optic perineuritis, which are seen more frequently as part of syphilitic meningitis [66]. Coxsackievirus infection may also cause an ON or neuroretinitis [67].

In posterior uveitis, optic disc edema and profound visual loss may occur with inflammation of the retina and choroid. Posterior uveitis may be associated with some form of systemic disease. The bacterial infections include *Treponema pallidum* [68], *B. burgdorferi* [69], *Leptospira interrogans* [70], *Brucella* [71], *Nocardia asteroides* [72], *Mycobacterium tuberculosis* [73], and *Neisseria meningitides* [74]. Viruses causing posterior uveitis include cytomegalovirus [75], herpes simplex [76], herpes zoster [77], rubella [78], rubeola [79], and HIV [80]. Parasites, such as toxoplasmosis [81], *Toxocara canis* [82], and *Onchocerca volvulus* [83] and fungi, such as Candida [84], histoplasma capsulatum [85], *Cryptococcus neoformans* [86], aspergillus [87], *Coccidioides immitis* [88], and *Blastomyces dermatitidis* [89] may also cause optic disc edema in the clinical setting of posterior uveitis.

In the setting of autoimmune-related posterior uveitis, vasculitis of the optic nerve in Wegener's granulomatosis may cause optic disc edema [90, 91]. Papillitis occurs in the acute phase of the posterior uveitis in at least 25 % of cases of Behcet's disease and is related to microvasculitis of the arterioles feeding the optic nerve [92]. Retinopathy more often than choroidopathy is seen in systemic lupus erythematosus; the ON may occur with or without posterior uveitis [93]. Hyperemia of the optic disc and ON, in addition to uveitis, choroiditis, and exudative retinal detachments, can be seen in Vogt–Koyanagi–Harada disease [94].

Various malignancies may also invade the uvea and optic nerve. Up to 18 % of acute leukemias and 16 % of chronic leukemias have some leukemic infiltration of the optic nerve causing optic disc edema and hemorrhage [95]. Intraocular lymphoma, malignant melanoma, and metastatic lesions may also spread to the optic nerve [96–98].

Regarding posterior uveitis in primary ocular disorders, severe disc edema and CME can be commonly seen in birdshot retinochoroiditis [99]. Papillitis occasionally may be present in acute posterior multifocal placoid pigment epitheliopathy [100] and multiple evanescent white dot syndrome [101]. The optic nerve is usually not affected in serpiginous choroiditis, but ON has been reported so far in one patient with recurrent disease [102].

Optic disc edema may be seen in about 20 % of patients with posterior scleritis, which usually presents with unilateral periocular pain and decreased vision with little or no redness. Patients greater than 50 years of age usually have an associated systemic disease and are more likely to experience visual loss, mostly from macular changes or optic atrophy related to the posterior scleritis. The more common associated systemic diseases are rheumatoid arthritis, Wegener's granulomatosis, systemic vasculitis, relapsing polychondritis, and other autoimmune diseases similar to those seen in anterior scleritis, and rarely systemic lymphoma and multiple myeloma [103].

Less commonly, ON may be the only initial manifestation of an underlying autoimmune disease unassociated with MS. Young females present with unilateral or bilateral decreased vision and usually do not have overt signs or symptoms of a preexisting collagen-vascular disease, such as systemic lupus erythematosus. Laboratory tests for antinuclear antibody (ANA) and double-stranded DNA are most useful in confirming the diagnosis of lupus [104]. Patients who have occult symptoms of rheumatic disease or who have positive family histories for collagen vascular diseases may initially present with ON and/or transverse myelitis. The diagnosis of antiphospholipid antibody syndrome in these patients is confirmed by the presence of elevated serum immunoglobulin M (IgM) anticardiolipin antibody [105]. Another form of optic-spinal MS more commonly seen in Asians is associated with significantly high levels of antithyroid autoantibodies. It is thought that this MS variant could represent a pathogenetic link between antithyroid autoimmunity and a subgroup of

optic-spinal MS in Japanese that is not related to HTLV-1 disease [106].

Rarely, optic nerve inflammation can be part of a paraneoplastic syndrome. ON has been documented in cases involving bronchial carcinoma, oat cell carcinoma, and lymphoma. Pathologic data have shown that inflammation and demyelination, not the carcinomatous or lymphomatous invasion of the optic nerve, cause the decreased vision [107–110].

Pathogenesis and Pathophysiology of ON

Demyelination

Fifty percent of MS patients have clinical evidence of having had ON (at autopsy, almost 100 % have ON), and 20 % of them have it as their presenting sign [111]. The initial event before demyelination is the breakdown of the blood–brain barrier through the inflammation of the vascular endothelium. With the lack of oligodendrocytes in the retina, perivenular retinal sheathing represents this vascular inflammation without demyelination. The venous sheathing occurs as a clinically silent retinal disease before the development of ON. This feature may not be visible on funduscopic examination but may be demonstrable on fluorescein angiography [112]. The basic defect in ON/MS involves demyelination of the optic nerve, which blocks or slows the conduction of axonal transmission or decreases the amplitude of the nerve action potential. Various degrees of visual loss result from this process. The perivenular demyelinating plaques from optic nerves of patients who have acute MS reveal similar pathology to the periventricular plaques found elsewhere in the brain. These plaques show a perivascular cuffing of T and B cells, edema in the myelin nerve sheaths, and subsequent myelin breakdown. In ON the axons of the optic nerve are usually spared, resulting in good clinical recovery. More advanced lesions elsewhere in the CNS white matter often involve axonal degeneration, resulting in physical or mental disability. On histopathology macrophages engulf the degraded myelin products and glial cells proliferate to cause permanent conduction block with no clinical recovery [113, 114].

Cell-Mediated Damage

The neuroimmunologic factors that mediate demyelination of the optic nerve involve cell-mediated cytotoxicity. In one study, 76 % of the patients who had ON were found to have encephalitogenic, myelin basic protein (MBP), cerebroside, and ganglioside antibodies [115]. Patients who had ON/MS and patients who had isolated ON and CSF oligoclonal bands both had encephalitogenic antibodies. Elevated T-cell mediated cytotoxicity against the encephalitogenic peptide is a highly specific marker for demyelination in MS. ON patients who test positive for this antigen have a greater risk of developing CDMS [116]. The increased CSF MBP- and MBP-reactive B cells in patients who had ON could correlate with the process of early myelin breakdown or restoration [117]. Although magnetic resonance imaging (MRI) generally has been accepted as the marker of disease activity in patients who have MS, the concentration of MBP in CSF also has been useful as a marker during acute exacerbations of MS. It is significantly correlated with the visual acuity in patients who have ON, the Kurtzke expanded disability status scale score in patients who have MS, the cerebrospinal leukocyte count, intrathecal immunoglobulin G synthesis, and the cerebrospinal-albumin concentration quotient [117]. Furthermore, the activated T cells recognizing these MBP peptides secreted interferon-gamma (IFN-γ) [118]. The cytokine profile of IFN-γ, interleukin-4, and tumor growth factor-β in patients who had ON was the same as that found in patients who had CDMS [119]. The production of these cytokines is much greater in the CSF than systemically, which underscores the autonomy of the immune responses in the CSF. The up-regulation of these cytokines has been demonstrated in very early MS, as manifested by acute ON associated with more than two MS lesions on MRI of the brain and oligoclonal IgG bands in CSF [118].

The activated IFN-γ-producing T cells in the inflammatory foci of optic nerve sections in rats with acute experimental allergic encephalomyelitis showed elevated levels of calpain expression [119]. Calpain has been shown to degrade axonal and myelin proteins, including MBP, neurofilament proteins, and myelin-associated glycoprotein, and may, therefore, play a role in the pathogenesis of ON in MS [120]. Furthermore, the proinflammatory cytokines tumor necrosis factor (TNF) and lymphotoxin in the CSF were found to be elevated in patients who had ON to the same degree as patients who had CDMS [121].

Anti-MBP and antimyelin phospholipid protein (PLP) antibodies may significantly contribute to the pathophysiology of optic nerve damage [122]. Patients who had isolated ON were found to have significantly more anti-PLP-secreting B cells in the blood than patients who had other neurological diseases; anti-PLP antibody is more specific for demyelinating disease than is anti-MBP antibody [123]. It is also associated with the subtype of MS that has less frequent inflammation in the CSF and central nervous system (CNS) parenchyma, whereas anti-MBP antibody is associated with the more common form of MS that has more frequent prominent inflammatory CSF and CNS features [124]. The increased CNS synthesis of both anti-MBP and anti-PLP antibodies is found in patients who have ON, whether idiopathic or MS related. The synthesis of these antibodies is also not associated with the presence of the human leukocyte antigen (HLA)-DRB1*1501 gene [125].

Genetic Factors

Based on studies in Canada [126] and Finland [127], first-degree relatives have a 25–50 times greater risk of being affected than the general population. Overall, the risk is highest in monozygotic twins with a concordance rate of about 30 % in digyzotic twins and in other siblings less than 10 %, providing strong evidence for genetic factors in MS [128–131]. In siblings the earliest symptoms of the disease tend to cluster by age rather than by year, suggesting that genetic factors influence the onset of the disease [132–134].

Based on association studies using the case–control design testing of specific candidate genes and studying sporadic and familial cases, the only consistently replicated finding has been an association with the HLA-DR2 allele within the major histocompatibility complex (MHC) on chromosome 6. Data from the study by Haines in 1998 [134] strongly indicate that sporadic and familial MS share a common genetic susceptibility. These data also support the hypothesis that a genetically determined immune response plays a primary role in the pathogenesis of MS. Furthermore, the MHC locus probably represents less than half of the entire genetic etiology of MS. Families not segregating the HLA-DR2 allele appear to have no linkage to the MHC and therefore must be influenced by other genes [134].

Based on the study by The Multiple Sclerosis Genetics Group in 2002 [135], the association of DR2 in families with diverse clinical presentations suggests that there exists a common genetic basis to various clinical phenotypes of MS. The MHC genes appear to primarily influence penetrance, whereas other loci modulate specific phenotypes, such as location in the brain or spinal cord, demyelination, and severity of inflammation [136]. Epigenetic factors, such as the selection of different disease-inducing antigens, also influence the location and severity of experimental allergic encephalitis phenotypes induced with different encephalitogenic peptides [137]. It is likely that a similar interplay of genetic and epigenetic factors operates in human MS. HLA-DRB *15.01 is the major MS susceptibility allele at the MHC. This allele is a polymorphism and not a mutation. It is found in about 60 % of MS patients with Northern European descent. The allele explains about 20 % of MS genetic susceptibility and having two copies of HLA-DRB *15.01 increases the risk of MS. Two other alleles, HLA-DRB1*03.01 and HLA-DRB1*13.03, also increase the risk for MS. The HLA-DRB1*15.01 allele lowers the age of onset of MS by about 2 years [138].

The Class I MHC region contributes even more to MS risk than HLA-DRB *15.01 alone

and suggests that the innate immune system is involved in MS pathogenesis. The MHC also has a major protective allele, HLA-A*02.01. Non-HLA MS risk conferring genes also modulate disease expression. Alleles of the IL2α (alpha) and IL7α (alpha) were the first two non-HLA genes identified. Alleles of the IL2 receptor are expressed on regulatory CD4+ T cells. The IL7R receptor allele is the most common polymorphism associated with MS and is not a mutation. It promotes lymphocyte maturation and survival, but the functional significance of this polymorphism is still not well understood [138].

About 40 other non-MHC loci have been proven to contribute to MS susceptibility. Many of which have immunological functions, such as T-helper cell differentiation and lymphocyte trafficking, are involved in vitamin D metabolism and neuronal function. About 50 other loci may also contribute to MS risk [138].

Epidemiologic Factors

Age, sex, and race all play some role as risk factors for the development of MS. The onset of ON at a young age is a predictive factor in the development of MS. The relative risk for MS increases by a factor of 1.7 for each decade less than 54 years of age in adults [139]. There is also a tendency for females to develop MS after ON, such that 69 % of 47 females and 33 % of 20 males developed MS after approximately 15 years since their initial attack of ON [139]. Based on the 2-year data from the ONTT, Caucasians were found to be at higher risk than African Americans to develop MS even after 4 years of follow-up [140].

Regarding environmental factors during early development, a maternal parental influence on the development of MS in offspring seems to be present. When half-siblings are concordant for MS, the shared parent is almost twice as likely to be the mother [141, 142]. Birth month is also a risk factor in the development of MS. More MS patients were born in May and fewer in November in Canada, Denmark, Sweden, and Australia [143].

Regarding environmental factors during adolescence, the place of residence before the age of 15 years is involved in MS pathogenesis. When adolescents migrate from a geographic region of high MS prevalence to a region of low prevalence, or vice versa, they seem to adopt a prevalence similar to that of the region to which they moved. By contrast, when they make the same move after the age of 15 years, they seem to retain the risk of the geographic region from which they moved [144].

Other environmental factors that may play a role in the pathogenesis of MS include EBV infection, vitamin D deficiency, diet, trauma or stress, and tobacco [145].

Visual Prognosis

Young to middle-aged adults, predominately females, who present with ON as the initial manifestation of MS have a better prognosis of non-disabling MS than those who present initially with other MS features [146]. After 1 year of follow-up in the ONTT, 69 % of patients had visual acuity of 20/20 or better, 93 % had 20/40 or better, and 3 % had 20/200. These results were similar in each treatment group [147].

Other factors besides age may also affect visual prognosis. Longer lesions of the optic nerve and involvement of the intracanalicular segment are related to slightly less complete visual recovery [148]. The presence of Uhtohff's phenomenon, transient visual blurring associated with an elevation of body temperature following ON, is most common in patients with other evidence of MS [149]. Scholl et al. [150] reported that these patients were more likely to have an abnormal MRI of the brain and that they were more likely to develop MS. Uhtohff's symptom was present in about 10 % of patients in the ONTT 6 months after the onset of ON. It is important to note that Uhtohff's phenomenon may also occur in healthy patients after ON, in patients with Leber's optic neuropathy and in patients with optic neuropathies from other causes [151]. Uhtohff's symptom results from a reversible conduction block in impulse transmission by demyelinated nerve fibers [151].

Risk of MS in Pediatric ON

Although the risk of developing MS within 15 years in adults after unilateral ON was found to be 50 % in the ONTT [152], the risk of conversion to MS in children is still unclear. According to Lucchinetti et al. [153], the risk of developing MS after childhood ON was estimated by Kaplan–Meyer methods to be 13 % at 10 years, 19 % by 20 years, 22 % by 30 years, and 26 % by 40 years. In another study by Wilejto et al. [154], the 2-year risk was 36 %, whereas the 2-year risk was 17 % in a retrospective study by Bonhomme et al. [155]; the risk of developing MS in children depends upon the age at presentation of the ON, rather than on whether the ON was bilateral or unilateral. Unilateral ON occurred more frequently in older children (OR 1.26, $p<0.0001$). After adjusting for age, the risk of MS was not significantly different between the children with unilateral or bilateral ON (OR = 1.67, $p=0.2$). For every yearly increase in age, the risk of MS increases by 32 % ($p=0.006$). The risk of MS also increases in children with abnormal brain MRI findings at the time of presentation of ON. In a retrospective study of 18 patients Waldman AT et al. [156], the relative risk of MS among children with recurrent ON was 4.0 ($p=0.25$). Larger studies will be needed to confirm this finding. The risk of developing MS in children depends upon the age of presentation of the ON, rather than on whether the ON was bilateral or unilateral. Unilateral ON occurred more frequently in older children (OR 1.26, $p<0.0001$). After adjusting for age, the risk of MS was not significantly different between the children with unilateral or bilateral ON (OR = 1.67, $p=0.2$). For every yearly increase in age, the risk of MS increases by 32 % ($p=0.006$). The risk of MS also increases in children with abnormal brain MRI findings at the time of presentation of ON [156].

Diagnostic Testing

According to the conclusions of the ONTT [157], MRI of the brain is a good predictor of MS and should be considered to assess the risk of future neurologic events of MS and for treatment decision making. A total of 40–70 % of patients who have isolated ON have been reported to have periventricular white matter signal abnormalities on T2-weighted MRI scans (Fig. 1.2). In the ONTT [139], the 2-year risk for developing CDMS (Table 1.1) was 3 % if the patient initially had a normal brain MRI scan and 36 % if the patient initially had two or more lesions within the central white matter. The 4-year risk for having CDMS was 13 % if the MRI scan of the brain initially was normal, 35 % if the MRI scan showed one to two abnormalities, and 50 % if the MRI scan showed three or more abnormalities in the white matter. According to the Optic Neuritis Study Group [140], the 5-year cumulative probability of developing CDMS after ON was 30 % for all treatment groups. Neurological impairment was slight. At 5 years, 16 % of 202 patients who had no brain MRI lesions developed CDMS, whereas 51 % of 89 patients who had three or more MRI lesions did. Presence of previous nonspecific symptoms also was predictive of CDMS. Low-risk factors for CDMS included optic disc

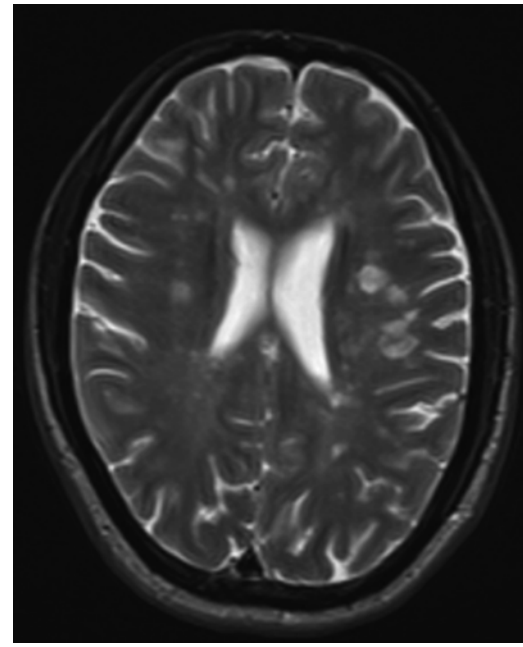

Fig. 1.2 T2-weighted axial MRI of brain showing multiple periventricular white matter hyperintensities, as typically seen in MS

Table 1.1 2010 Revised McDonald multiple sclerosis diagnostic criteria [Reprinted from Polman CH, Reingold SC, Banwell B, et al. Diagnostic criteria for multiple sclerosis: 2010 revisions to the McDonald criteria. Ann Neurol 2011;69(2):292–302. With permission from John Wiley & Sons, Inc]

Clinical Attacks	Lesions	Additional criteria to make diagnosis
≥2	Objective clinical evidence of ≥2 lesions or objective clinical evidence of 1 lesion with reasonable historical evidence of a prior attack	None. Clinical evidence alone will suffice; additional evidence desirable but must be consistent with MS
≥2	Objective clinical evidence of 1 lesion	Dissemination in space; or await further clinical attack implicating a different CNS site
1	Objective clinical evidence of ≥2 lesions	Dissemination in time; or await a second clinical attack
1	Objective clinical evidence of 1 lesion	Dissemination in space; or await further clinical attack implicating a different CNS site AND dissemination in time; or await a second clinical attack
0 (progression from onset)		One year of disease progression, retrospectively or prospectively, AND at least two of the following: 1. Dissemination in the brain based on ≥1T2 lesion in periventricular, juxtacortical, or infratentorial regions 2. Or dissemination in the spinal cord based on ≥2T2 lesions 3. Or positive CSF

swelling, lack of pain, and mild visual acuity loss. The number of MRI lesions was highly correlated with the 5-year risk for CDMS, but a normal brain MRI scan did not preclude the development of CDMS. In a recent study by Brex et al. [158], on patients who first presented with ON, or other isolated syndromes clinically suggestive of MS, CDMS developed in 88 % of patients with abnormal MRI findings at presentation and in 19 % with normal initial MRI results [159]. After the 8-year follow-up of 26 patients who had acute monosymptomatic ON, 54 % of them developed CDMS. Furthermore, patients who presented with ON actually developed much milder MS [147]. Overall, it is believed that most patients who have a history of ON and who are destined to develop MS do so within 7 years of the onset of visual symptoms [160].

The signs of optic nerve inflammation may be visualized on neuroimaging. In some cases of typical ON, diffuse enlargement of the optic nerve can be seen on fat-suppressed MRI scans with and without contrast enhancement on coronal orbital sections (Fig. 1.3) [161]. Gadolinium-enhancement and T2-signal abnormalities correlated with ultrastructural studies showing inflammatory infiltrate and expansion of the extracellular space. Demyelinative lesions seemed to progress from the optic nerve insertion at the globe to the orbital apex [162]. MRI can also detect foci of enhancement along the nerve which represents demyelinative lesions. It is important to note that similar MRI enhancements along the optic nerve can also be seen in patients who have ischemic, infectious, or radiation-induced optic neuropathies, but they are not pathognomonic for a demyelinative process [163].

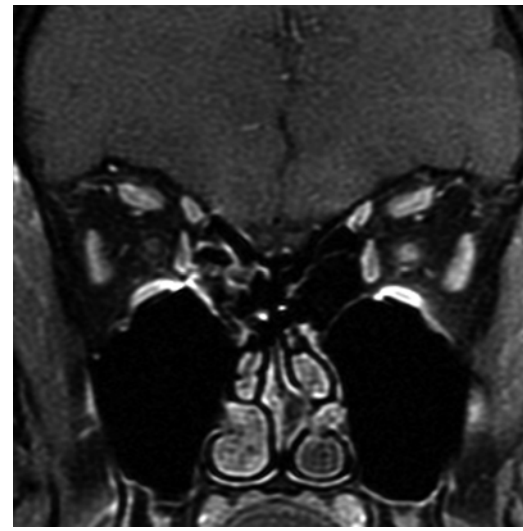

Fig. 1.3 T1-weighted coronal MRI of brain with fat saturation and contrast showing left optic nerve enhancement

Based on the ONTT, ancillary laboratory testing in patients who have typical ON does not yield

any clinically useful information. These included routine blood tests, ANA, fluorescein treponemal antibodies (FTA-ABS), chest X-ray, and CSF analysis (as detailed later). Based on the experience of the ONTT, it was concluded that CSF analysis was not necessary in the routine evaluation of patients who present with a typical profile of acute ON. Most CSF tests added little additional information to MRI results for predicting the 2-year development of CDMS [164]. However, a more recent study showed some predictive value in the assessment of CSF of patients who have MS. Those who had both abnormal MRI and elevated intrathecal IgG synthesis had a 46 % increased risk for developing MS after 4 years, compared with 33 % if they had only an abnormal MRI [165]. A normal initial CSF after ON does not exclude the development of MS in the future. Certain serologic and CSF findings in isolated ON are associated with MS: (1) MS CSF oligoclonal bands, (2) CSF anti-MBP antibody, (3) CSF anti-PLP antibody, and (4) a cytokine profile of activated T cells (interferon-γ, interleukin-4, and tumor growth factor-β) similar to that found in patients who have CDMS. These CSF and serologic factors all have been detected in patients who have isolated ON and who eventually develop CDMS [166]. Based on the Optic Neuritis Study Group assessment, the presence of CSF oligoclonal bands was useful as a predictive factor for developing MS 5 years after ON only when the brain MRI scan was normal [166]. It is generally accepted that an abnormal MRI scan at the time of ON is significantly related to later MS development. In a literature-based meta-analysis by Skov et al. [167], oligoclonal bands have a sensitivity of 73–100 % (mean 88.5 %), a specificity of 41–90 % (mean 57 %), and OR values between 2.75 and 171 (mean 34.2).

Furthermore, a positive ANA did not have any effect on the patient's course or response to any treatment given [3]. Therefore, besides neuroimaging, no further laboratory testing is required for typical ON.

The visual evoked potential (VEP), a measure of afferent visual function, is not useful when ON is suspected. The poor visual acuity during acute disease precludes adequate measurement of the P100 latency. On the other hand, the VEP is useful later on in determining whether the episode of visual loss involved demyelination [168]. The VEP usually reveals a prolonged latency after the resolution of acute ON. This indication of impaired optic nerve conduction persists even after visual acuity returns to 20/20. Only the amplitude of the VEP may be normal [169–171].

Atypical ON

For atypical ON, testing must be performed to rule out other etiologies mimicking MS. MRI of the orbits with fat suppression is indicated for patients who have the following characteristics of atypical ON: (1) older than 45 years, (2) bilateral presentation, (3) a vertical hemianopic visual field defect, (4) progression of the ON for more than 2 weeks, and (5) recent sinusitis. It is imperative to rule out compressive lesions, such as aneurysms and tumors in the intraorbital, intracanalicular, and intracranial areas [172]. Serological and CSF studies should be performed on any patient who presents with signs or symptoms and course of disease that are unlike typical ON and who are suspected of having an underlying systemic or local infection or inflammation. Laboratory tests should include erythrocyte sedimentation rate and ANA for connective tissue disease, rapid plasma reagin and FTA-ABS for syphilis, and serum angiotensin-converting enzyme for sarcoidosis [172].

Techniques for the Early Diagnosis and Monitoring of ON in MS

Retinal Nerve Fiber Layer (RNFL) and Macular Volume Measurements by Optical Coherence Tomography (OCT) in the Assessment and Monitoring of Anterior Visual Pathway Dysfunction in ON

OCT of the RNFL allows direct visualization and quantification of the atrophy of unmyelinated axons in eyes *with* a history of ON. It can be used to study the timing of RNFL changes with visual

function at various recovery stages of ON over a 12-month period. In a study by Costello et al. [173], the earliest significant inter-eye RNFL difference was detected 2 months after ON in the temporal aspect of the RNFL. Inter-eye comparisons revealed RNFL thinning in clinically affected eyes that persisted for more than 24 months. RNFL thinning was detected within 6 months and then stabilized from 7 to 12 months after ON. A threshold RNFL thickness of 75 μm predicted visual recovery after ON. Loss in the mean RNFL thickness has been estimated to occur at a rate of 3.7 μm/year after onset of ON.

In MS patients *without* ON, the time course of RNFL loss has also been delineated by a statistical analysis of the longitudinal study on 593 eyes by Talman et al. [174] which revealed that an average of 2 μm in RNFL thinning occurred each year, the calculated average amount of RNFL loss as part of the normal aging process. This small amount of RNFL thinning in the aging process cannot be directly measured in MS patients because it is below the resolution of Heidelberg Spectralis and Cirrus HD-OCT OCT of 4–6 μm [175]. Phase 2 clinical trials with OCT done for mostly 4–6 months duration did not capture the RNFL thinning that could have been observed after 2 years. Fourier domain OCT techniques should provide better resolution in future clinical studies. Although topographic change analysis and statistical image mapping methods have been validated, no consensus yet has been established on how to obtain and analyze longitudinal OCT data in MS [176].

RNFL thinning can occur in eyes of MS patients not previously affected by ON. RNFL thickness and macular volume were significantly decreased in secondary progressive multiple sclerosis (SPMS), but not in primary progressive multiple sclerosis (PPMS) when compared with controls. Thinning was greatest in the temporal quadrant of the RNFL in SPMS more than in PPMS patients, and even less in RRMS patients when compared with control [177, 178]. Significant global reductions in RNFL and macular volume were detected in SPMS eyes without a history of ON, but not in PPMS eyes compared with controls [177].

Although OCT can predict visual recovery after ON, such that a lower RNFL value is correlated with impaired visual function [179], it has not been shown to have predictive value in the assessment of future risk of MS. The RNFL thickness does not reliably distinguish patients at higher risk of converting to CDMS after ON. The progressive RNFL thinning in CDMS patients is probably related to recurrent subclinical ON events. This RNFL thinning can serve as a marker that can differentiate them from non-MS patients over time [180]. At the CIS stage, OCT does not reveal subclinical retinal axonal loss and does not predict conversion to MS in 6 months [181]. No reliable marker yet exists for conversion to CDMS and it is still uncertain whether conversion even occurs from the CIS stage. Since 28 % of ONTT patients with abnormal brain MRI at baseline did not experience a relapse at 15 years [152], it remains unclear whether CIS represents a separate category from early MS with relapses, or whether it is part of the MS spectrum representing the mildest form of the disease.

Since OCT of the RNFL is reproducible, noninvasive, relatively inexpensive, and has good correlation with visual function, it may have a role to monitor longitudinal axonal loss over time in neuroprotection studies with some limitations in regards to the timing of RNFL loss. In a study by Henderson et al. [182] no significant difference in RNFL thickness or macular volume was observed between patients with progressive MS (PPMS and SPMS) on two occasions with a median interval of 575 days apart and the control group on two occasions with a median interval of 656 days apart. Time domain OCT appeared to have limited ability in detecting significant disease-related retinal axonal loss involving the anterior visual pathways in the progressive forms of MS, especially in this patient cohort with later stages of MS. RNFL loss could hypothetically develop in a nonlinear, nonuniform temporal pattern. Faster RNFL loss probably occurs in earlier RRMS when subclinical inflammatory demyelination is more prominent, especially in the optic nerve, and in the early stages of PPMS when more inflammatory brain lesions appear [183]. For assessment of neuroprotection in patients

presenting in the acute ON stage, Henderson et al. [184] determined that RNFL loss measured by OCT after 6 months was a reasonable outcome measure for proof-of-concept trials. In addition, VEP and other imaging modalities, discussed later in this chapter, may have a role in defining posterior visual pathway involvement when OCT techniques do not detect more anterior disease at a particular stage of MS.

OCT has not been shown definitively to correlate with brain atrophy. In the study by Gordon-Lipkin et al. [185] decreased brain parenchymal fraction was correlated with RNFL loss, based on an MS population in which 50 % had a history of ON prior to enrolling in the study, and this RNFL thinning can occur following ON when no brain atrophy is observed at the onset of MS [186]. It remains unclear whether or not clinically detectable ON determines the severity of RNFL thinning, since PPMS patients appeared to have severe ongoing RNFL thinning regardless of history of ON [178]. It could be hypothesized that early RNFL thinning could predict more rapid brain atrophy, but the exact timing of RNFL thinning in relation to brain atrophy is still unclear.

Furthermore, OCT has not been reliably correlated with more global neurological disability measures. Data regarding the association of the expanded disability status scale (EDSS) and RNFL thickness have been conflicting. Although the Early Treatment Diabetic Retinopathy Study (ETDRS) scores correlate with those of the EDSS [187], MS functional composite (MSFC) scores, and MRI lesion load [188], RNFL thickness may not [177, 188]. Fisher et al. [189] found that increasing neurologic impairment, as measured by the EDSS and by the MSFC, correlated with RNFL thickness, but Pueyo et al. [190] did not. Since retinal axonal loss was detected in MS eyes with a history of ON and in MS eyes without, RNFL correlated with optic nerve functional assessments, including visual acuity, visual fields, OCT, scanning laser polarimetry (GDx), and VEPs, rather than other neurological impairment tests, such as EDSS [190]. In other studies by Albrecht et al. [191] and Siger et al. [192], the correlation between EDSS and RNFL thickness was strong in MS patients *without* ON. It was postulated that the mild RNFL changes from asymptomatic axonal damage or transsynaptic axonal degeneration in unaffected eyes of MS patients were not masked by ON-related RNFL loss.

Regardless of measurement differences in these previous studies, EDSS has limitations in CIS and early MS because it measures mobility and motor functions that are not prominent in the early stages of MS. Because of increasing evidence of cognitive deficits related to memory, information processing, and executive function in patients who present with isolated ON or other clinically isolated syndromes (CISs) [193], tests that include cognitive and visual impairment may be more useful outcome measures to be correlated with OCT RNFL in future clinical trials.

In addition to the RNFL, more advanced OCT techniques can also be applied to quantify macular volume and retinal ganglion cell (RGC) loss. Analogous to the gray matter atrophy in MS brains, neuronal (RGC) loss in the macula occurs with RNFL axonal degeneration. Reduction in average macular volume, corresponding to approximately 34 % loss of neuronal cells by average thickness, is associated with significant RNFL axonal loss [194]. Trip et al. [195, 196] demonstrated a significant decrease in both average RNFL thickness and average macular volume in eyes affected with ON compared to control eyes. Non-ON eyes also showed thinning in both parameters compared to control eyes. Gugleta et al. [197] showed relative thinning of the central macular region compared to the outer macular ring in ON and non-ON eyes. Preferential thinning of the central macular region in eyes with no history of ON could represent RGC loss secondary to subclinical inflammation of the optic nerve and optic tract serving the central visual field. This hypothesis is consistent with the observation by Keltner et al. [10] in that asymptomatic central visual field defects are common in the fellow eyes of MS patients with unilateral history of ON. It was concluded that preferential loss of central relative to peripheral macular thickness in non-ON eyes might indicate primary neurodegenerative processes, such as apoptosis. Longitudinal studies in more MS patients are

needed to further characterize the relationship and timing of RGC degeneration in the inner and outer macular volumes with RNFL thinning.

In addition to being a potential surrogate marker and monitoring tool for MS, OCT can be helpful in the diagnosis of neuromyelitis optica (NMO). OCT has recently been shown to be useful in distinguishing NMO from MS, such that more severe and diffuse retinal damage occurs after ON in NMO than in MS [198]. RNFL loss of greater than 15 μm after ON in a patient not previously diagnosed with MS should prompt consideration of an NMO syndrome [199]. In addition to RNFL thickness, vascular changes, including attenuation of the peripapillary vascular arcade (3/40 MS eyes vs. 22/32 NMO eyes) and focal arteriolar narrowing (0/40 MS eyes vs. 9/32 NMO eyes), have been shown to be a more prevalent funduscopic finding in NMO than in MS patients [198].

High-Contrast Visual Acuity Testing in ON/MS Clinical Trials

The ETDRS visual acuity measurement is correlated with RNFL measurements on OCT and visual field defects. Trip et al. [195] showed that a loss of 1 μm in RNFL predicted a significant decrease in visual acuity of 0.01 log MAR on the ETDRS chart and a 10 % reduction in RNFL significantly correlated with a progression of visual field defects and only macular volume (RGCs) significantly correlated with worsening of color vision on the Farnsworth–Munsell 100-Hue test. Focal reduction of superior and inferior, as opposed to nasal and temporal, RNFL quadrants was associated with worsening of corresponding visual field defects [195]. In Costello et al. [179], visual acuity correlated with RNFL measurements less than or equal to 70 μm. Visual field defects may be a more sensitive measure of visual function than visual acuity in ON.

In 54 ON patients, the largest proportion of patients developed visual field defects between 3 and 6 months after the ON episode and this correlated with RNFL thickness of less than or equal to 75 μm. Eleven percent had decreased RNFL thickness after 3 months and 85 % 6 months after onset of ON. RNFL and macular volume also significantly correlated with visual acuity (ETDRS), low contrast acuity, and visual field mean deviation in all subgroups of MS (RRMS, SPMS, and PPMS) patients [185].

Low-Contrast Letter Acuity and Contrast Sensitivity Testing in ON/MS Clinical Trials

Low-contrast letter acuity and contrast sensitivity have been shown to correlate with RNFL thickness, supporting validity for these visual function tests as secondary clinical outcome measures for MS trials. OCT may also have a role in assessing neuroprotective and other disease-modifying therapies [186].

Despite good visual acuity on ETDRS and Snellen testing after an ON episode, more sensitive testing with low-contrast letter acuity and contrast sensitivity can reveal subtle visual impairment. The Spectralis OCT has been used by Davies et al. [200] to manually segment retinal layers in order to estimate retinal cell ganglion layer volume. They found that lower ganglion cell layer volumes were associated with worse performance on low-contrast letter acuity testing. In eyes affected with ON, low-contrast letter acuity for both 1.25 and 2.5 % contrast level and for contrast sensitivity testing was significantly worse compared with fellow unaffected eyes [189]. For every one-line decrease in low-contrast letter acuity or contrast sensitivity score, the mean RNFL thickness was shown to decrease by 4 μm [189]. The low and high contrast letter acuity both correlate well with the health related quality of life scores in MS [201]. These tests were applied in two recent clinical trials with natalizumab [202] as a prespecified tertiary endpoint, and low-contrast acuity testing was shown to have the capacity to demonstrate treatment effects and may be considered for use in the assessment of visual outcomes in future MS clinical trials.

VEPs in the Early Detection of ON and Cortical Plasticity

The delayed P100 latency of the VEP in unaffected eyes can provide evidence for clinically silent lesions to fulfill diagnostic criteria for MS, especially for PPMS according to the McDonald criteria [203]. VEP has been shown to be more sensitive for detecting clinical and subclinical ON than OCT. The sensitivity of OCT measuring RNFL after ON was 60 %, decreasing further with mild onset and good recovery. VEP sensitivity was superior at 81 %. VEP identified 75 % of subclinically affected eyes while OCT identified less than 20 % [204]. Since MS patients without ON can have RNFL loss secondary to retrograde trans-synaptic RGC degeneration due to MS lesions within the optic radiations [205], future VEP studies will be needed to distinguish subclinical ON in the anterior visual pathway from postgeniculate MS lesions that may also contribute to average global RNFL thinning.

Multifocal VEP (mfVEP) abnormalities correlate topographically, not only with visual field defects, but also with RNFL thickness. In a study by Klistorner et al. [206], patients with acute unilateral ON between 6 and 36 months prior to the study and 25 age-matched controls underwent mfVEP testing. RNFL loss in the upper, temporal, and lower retinal sectors highly correlated with the reduction of mean mfVEP amplitude in corresponding areas of the visual field in all three sectors. The greatest reduction in RNFL was in the temporal sector and in the mean mfVEP amplitude corresponding to the central portion of the visual field.

Although conventional VEP, a more readily available and shorter test to perform, may be used as a screening tool for ON/MS, the mfVEP has been shown to be more sensitive than full-field VEP in detecting small, localized defects [207, 208]. In 26 patients with unilateral ON 73 % of affected eyes were identified as abnormal by amplitude and/or latency by full-field VEP while 89 % was considered abnormal when mfVEP was used [209]. Since early diffuse CNS inflammation occurs in patients with MS, the clinically unaffected eye of patients with unilateral ON may reflect the status of normal-appearing white matter in the CNS, which can be assessed electrophysiologically. In a study by Fraser et al. [210], 36.4 % of 46 patients with ON without a diagnosis of MS and with delayed mfVEP latencies in the unaffected eye progressed to CDMS according to the McDonald criteria over a 1-year period, compared with 0 % of those with normal latencies. Furthermore, the degree of latency prolongation and amplitude decline 12 months after the initial episode and it may be proportional to the risk of MS [206].

mfVEP has also demonstrated posterior visual pathway cortical plasticity. Although recovery from ON is mostly attributed to resolution of acute inflammation, the redistribution of ion channels along the demyelinated membrane and the subsequent remyelination, part of this recovery may result from neural plasticity. In a study by Klistorner et al. [206], 25 patients with acute unilateral ON developed progressive axonal loss as demonstrated by RNFL thinning, while mfVEP amplitude asymmetry decreased supporting continuous functional recovery of more posterior visual pathways between 6 and 12 months after onset of ON. At 12 months the mfVEP amplitude of the ON eye improved by 17.8 %, while the RNFL thickness decreased by 20.8 %, regardless of the degree of ON remyelination. It was concluded that this structural–functional discrepancy at the postinflammatory stage may support the concept of neural plasticity contributing to functional recovery after acute ON.

Imaging of Anterior Visual Pathway Involvement

Although MRI of the brain is used to detect clinically silent demyelinating lesions and to clarify the risk for developing CDMS, MRI of the optic nerve is not routinely used in the diagnosis of ON, but may be useful to rule out other causes of visual loss in atypical cases. Similar to OCT, neuroimaging techniques allow visualization and quantification of MS lesions in vivo.

Fat- and CSF-suppressed MRI imaging sequences have reliably demonstrated optic nerve atrophy [211]. Using fat saturated short echo fast fluid-attenuated inversion recovery (FLAIR) sequences, more severe optic atrophy and smaller optic nerve volume were associated with poor baseline visual acuity and VEP parameters [212]. Studies have also confirmed that initial optic nerve swelling evolves into atrophy [213], and that gadolinium enhancement on fat-suppressed T1-weighted spin echo images is a consistent feature of acute ON [212]. The degree of atrophy correlates with disease duration suggesting ongoing axonal loss in a previously demyelinated lesion [214]. In a study comparing short T1 inversion recovery (STIR), spectral presaturation inversion recovery (SPIR), and SPIR-FLAIR sequences, SPIR-FLAIR has also been demonstrated to be most sensitive in detecting length of the lesion in affected optic nerves [215]. With triple-dose gadolinium, patients with shorter acute optic nerve lesions had a better visual prognosis than those with a longer lesion [211].

Therefore, the initial optic nerve lesion length correlates with the degree of visual impairment, suggesting that acute demyelination is related to conduction block.

Novel quantitative imaging techniques, such as magnetization transfer ratio (MTR) have demonstrated that the mean MTR value was significantly reduced in affected optic nerves associated with poor vision. Using MTR with a two-dimensional gradient echo sequence, this value correlated with visual acuity but not VEP P100 latency [210]. These results are inconsistent with those by Thorpe et al. [216], possibly because this cohort was biased toward those with worse vision, and axonal loss in these optic nerves may have been more severe. In another study by Hickman et al. [217], the mean MTR value in affected optic nerves decreased over time with a nadir after approximately 240 days, consistent with the period of demyelination evolving into axonal degeneration. The mean MTR value then slightly increased, suggestive of possible remyelination. Furthermore, in a study by Trip et al. [218], the MTR correlated with axonal loss on RNFL thinning, suggesting that MTR was also reduced due to axonal loss. The relative proportion of demyelination and axonal loss in relation to the reduced MTR value was unclear in this study.

Using a fat- and CSF-suppressed zonal oblique multislice echo planar imaging (ZOOM-EPI) diffusion-weight imaging (DWI) sequence, the mean apparent diffusion coefficient is significantly increased in optic nerves after ON [218] and correlated with visual acuity and VEP P100 amplitude. This sequencing technique further developed into diffusion tensor imaging (DTI) of the orbital optic nerves [196]. In a study by Trip et al. [196], DTI measurements on patients with incomplete recovery following ON revealed that mean diffusivity was increased and fractional anisotropy was decreased in affected nerves compared to controls. The increase in MD and decrease in FA were not associated with visual acuity, but was significantly correlated with a decrease in VEP P100 amplitude, suggestive of axonal loss.

Therefore, reliable DWI and DTI measurements of the orbital optic nerves using ZOOM-EPI can demonstrate the structural integrity of the axons. These sequencing techniques are now performed not only on 1.5 T MRIs, but also on 3 T and higher MRIs using surface coils along the course of the orbital optic nerves and faster acquisition times for better resolution [219–221].

Imaging of Posterior Visual Pathway Involvement

Spontaneous visual recovery typically occurs within weeks or months after onset of ON, depending on the resolution of inflammation, remyelination, and neuronal plasticity in the subcortical and cortical visual pathways. Various neuroimaging techniques have been applied to determine where recovery occurs along this visual pathway.

DTI tractography, a reconstruction technique that connects adjacent voxels based on the diffusion tensor properties of the tissue, can be used to reconstruct the optic radiations. In a study by Ciccarelli et al. [222], DTI tractography in patients 1 year following a CIS event revealed that the posterior regions of the optic radiations were located more inferolaterally than in controls. The voxel

scale connectivity values were reduced, suggestive of trans-synaptic degeneration, and did not correlate with incidental lesions in the optic radiations which can be found in ON. Such optic radiation damage was recently shown to be associated with ON injury, as measured by RNFL thickness, and was associated with visual dysfunction, based on high and low contrast letter acuity scores [205]. It was also hypothesized that the more inferolateral location of the optic radiations post-ON might also represent cortical plasticity.

MTR and functional MRI (fMRI) studies provide further evidence for trans-synaptic degeneration and cortical plasticity after ON. In a study of 80 patients with isolated ON [223], reduction in gray matter in both visual cortices on MTR significantly correlated with the patients' baseline and 3-month visual acuity. The reduced MTR in the visual cortex following ON could reflect trans-synaptic degeneration corresponding to more anterior optic nerve injury.

fMRI has been used to study cortical plasticity after ON. This technique measures brain activity in vivo based on the blood-oxygenation level dependent (BOLD) effect. Oxygenated hemoglobin has a different MRI signal and can be detected in activated brain regions that have greater oxygen requirements. Decreased activation of the visual cortex compared to controls can be seen in both acute and chronic ON patients [224]. Increased BOLD signal significantly correlates with visual acuity and contrast sensitivity measurements [225]. In a study by Werring et al. [226], the volume of extra-occipital activation involving higher level multimodality sensory processing was correlated with the VEP P100 latency, which might be related to persistent optic nerve demyelination. The lateral occipital areas could be a site for cortical reorganization contributing to visual recovery [224]. fMRI, along with structural MRI and electrophysiologic data from 28 patients with acute unilateral ON suggest that acute visual loss is associated with the degree of inflammation and conduction block in the optic nerve, but not with the pathology occurring in the optic radiations or occipital cortex. After accounting for factors which reduce afferent input, the finding of improved vision with greater fMRI response in 28 patients with unilateral ON in a study by Jenkins et al. [227] suggests that adaptive neuroplasticity may occur in the association cortex of the dorsal stream of higher visual processing. It is still unclear whether other extrastriate cortical regions participate in adaptive plasticity in the acute and chronic stages of ON. This early adaptive neuroplasticity may even predict the outcome of ON independent of tissue damage. Jenkins et al. [227] showed that higher baseline fMRI responses in the lateral occipital complexes were associated with better visual outcome at 12 months, regardless of stimulation of the affected or unaffected eye and independent of any measures of demyelination by VEP and axonal loss by VEP, MRI, and OCT. No acute electrophysiologic or structural measures of the anterior or posterior visual pathways were associated with visual outcome. Therefore, early neuroplasticity in the higher visual areas, not demyelination or axonal loss in the visual pathways, determines visual outcome after ON.

In another study by Korsholm et al. [228], the lateral geniculate nucleus (LGN), which is the main thalamic relay nucleus in the visual pathway, has also been shown to be involved as another site of adaptive neuroplasticity. The *increase* in fMRI signal from the LGN, lateral occipital complexes, V1, and V2 areas of the visual cortex, during stimulation of the *affected* eye occurred with a *decreased* signal in corresponding areas associated with stimulation of the *unaffected* eye. These findings lead to the hypothesis that compensatory neuroplasticity along visual pathways in the affected eye was developing in the first 6 months since onset of ON. Although increasing evidence support compensatory brain reorganization after ON, the precise timing and location of this process require further investigation.

Treatment of Optic Neuritis

Results of the ONTT

Long-Term Visual Outcome after 15 Years in the ONTT

(See section "Visual Field".)

Risk of Development of CDMS After IV Methylprednisolone (IVMP) for ON

According to the ONTT (in patients with ≥2 MRI white matter lesions at baseline) [229], IVMP significantly decreased the risk of development of MS for the first 2 years but this beneficial effect was not maintained at 5, 10, and 15 years [152, 230, 231]. The overall risk of MS was 13 % at 2 years, 29 % at 5 years, 41 % at 10 years, and 50 % at 15 years [196, 230–232]. Most patients developed CDMS within 5 years. The absence or presence of a single white matter lesion on baseline MRI was the most important predictor for conversion to CDMS. The risk of CDMS with one or more lesions was 72 % at 15 years [152]. The ONTT also showed that a history of ON in the fellow eye and mild neurologic symptoms, such as sensory deficits, increased the risk of developing CDMS at 2 years in all patients with ≥1 white matter lesion on MRI. The risk of MS was low at 15 years for patients with a normal brain MRI, no light perception on baseline visual acuity, absence of ocular pain, severe optic disc swelling, disc/peripapillary hemorrhage, or retinal macular exudates [152].

Intravenous Immunoglobulin (IVIg) in ON

In a double-blind, randomized trial by Roed et al., 68 patients with ON were randomized within 4 weeks of onset to undergo IVIg. IVIg had no effect on long-term visual function after acute ON in terms of visual acuity and contrast sensitivity. It also had no effect in reducing latency on VEPs [233]. Although IVIg had been demonstrated to have some therapeutic benefit for other demyelinating diseases, such as chronic inflammatory demyelinating polyneuropathy, Noseworthy et al. recently found that IVIg did not reverse the chronic visual loss in patients with ON [234].

Plasmapheresis in ON

Plasmapheresis is not commonly used for the treatment of ON. In a recent study of ten patients treated with plasma exchange (PE) for acute, severe ON unresponsive to previous high-dose IV glucocorticoids [235], seven patients experienced visual improvement. On follow-up, three patients continued to improve, two were stable, and two experienced worsening of vision. Plasmapheresis may have a role as "rescue therapy" for patients with a severe attack of ON.

Results of the CHAMPS/ CHAMPIONS

About half of the patients, presenting with a monofocal CIS presentation with a positive MRI with at least two white matter lesions greater than 3 mm in diameter, in the CHAMPS (Controlled High-Risk Subjects Avonex Multiple Sclerosis Prevention Study) [231] study had ON. The primary outcome of the study was the development of CDMS with secondary outcome measures based on MRI findings. Patients treated with intramuscular (IM) interferon ß (beta)-1a weekly had a lower cumulative 3-year probability of developing CDMS compared with placebo (35 % vs. 50 %, respectively, $p = 0.002$). The interferon-treated group also had a significant reduction in the volume of T2-weighted lesions, number of new or enlarging T2-weighted lesions, and number of gadolinium-enhancing lesions. Furthermore, all of the different CIS groups benefited from early treatment and had a decreased risk of developing MS [231], especially in those with >9T2-weighted and >1 gadolinium enhancing lesion on baseline MRI, they had a 66 % risk reduction in the development of CDMS. CHAMPIONS (Controlled High Risk Avonex Multiple Sclerosis Prevention Study in Ongoing Neurologic Surveillance) was a 5-year open label continuation of CHAMPS, in which placebo and ongoing treated patients were given IM interferon ß(beta)-1a weekly for 3 years. The probability of developing CDMS was lower in the early treatment group compared with the delayed treatment group (adjusted hazard ratio 0.57, $p = 0.008$). But no significant differences were found in any of the secondary outcome measures, including disease course, annualized relapse rate, disability, and MRI metrics [236].

Results of the ETOMS

In ETOMS (Early Treatment of MS Study) [237], a multicenter, randomized, controlled trial, about one-third of the CIS patients had ON. Clinically isolated syndrome patients with ≥4T2-weighted lesions were randomized to receive either 22 μg of subcutaneous (SQ) interferon ß (beta)-1a (Rebif) weekly or placebo within 3 months of their initial presentation of CIS. At 2 years the interferon-treated group had a significantly lower cumulative probability of developing CDMS compared with the placebo group (34 % vs.45 %, respectively, $p=0.045$). The interferon-treated group also had lower T2-weighted lesion burden, a significantly decreased annualized relapse rate (0.33 vs. 0.43, $p=0.045$), and a longer time to conversion to CDMS (569 days vs. 252 days) compared with the placebo group. But no difference was found in disability measures between the two groups.

Results of the BENEFIT Study

About 40 % of the CIS patients enrolled in the BENEFIT (Betaseron in Newly Emerging MS for Initial Treatment) [238] study presented with ON. This multicenter, randomized, controlled trial enrolled CIS patients with ≥2T2-weighted MRI lesions greater than 3 mm in size within 2 months of initial presentation of CIS and were randomized to either receiving interferon ß (beta)-1b(Betaseron) 250 μg every other day subcutaneously or placebo. Compared to the placebo group, the interferon-treated group had a significant decreased cumulative 2-year probability of developing CDMS (69 % vs. 85 % $p<0.00001$), a longer time to conversion to CDMS, a decreased accumulation of new gadolinium-enhancing lesions, and T2-weighted lesion volume.

In the 5-year extension study of BENEFIT [239], ongoing interferon-treated patients and placebo patients were given interferon ß (beta)-1b(Betaseron) 250 μg every other day subcutaneously for another 2 years. Compared to the delayed treatment group, the early treatment group had a significantly delayed onset of CDMS by 45 % ($p<0.0001$) by McDonald criteria, a significant reduction in new or enlarging T2 lesions ($p=0.0062$), and a greater reduction in relapse rate (hazard ratio of 0.21 vs. 0.27), but no significant reduction in EDSS progression and FAMS-TOI (functional assessment of MS trial outcomes index) after 5 years.

Results of the PreCISe Study

The PreCISe study [240] is a multicenter, randomized, controlled trial which enrolled CIS patients with unifocal presentation with ≥2T2-weighted MRI lesions measuring ≥6 mm and were randomly assigned to receive glatiramer acetate (GA) (Copaxone) 20 mg subcutaneously every day or placebo for up to 3 years. Compared to the placebo group, the glatiramer-treated group had a significantly reduced risk of developing CDMS by 45 % (hazard ratio of 0.55, $p=0.0005$). The time for 25 % of patients to convert to CDMS was prolonged by 115 % (336 for placebo vs. 722 days for glatiramer).

Some Issues Regarding the Treatment of ON to Delay Progression of MS

According to the ONTT, short-term corticosteroids given at the ON stage did not alter the course of this disease [230]. Although the results of CIS clinical trials, as described earlier, favor early treatment to delay conversion to CDMS, these studies have not shown any significant benefit in improving neurological disability, especially in the recent BENEFIT trial in which EDSS was the primary outcome measure. The 5-year data showed no significant delay in time to confirm EDSS progression between delayed and early treatment groups [241]. Clinically isolated syndrome patients with multiple T2 brain lesions at baseline appeared to have benefited the most with early treatment and showed some delay in EDSS after the first 3 years, but not at the end of 5 years [242]. Since about 18 [243] to 28 % [152] of CIS patients will have no or very few relapses, or may not convert to CDMS, whether to treat

CIS patients with current immunomodulatory drugs is still debatable. CIS may be a separate subpopulation different from early RRMS.

Some information about the risk of developing CDMS can be gathered from MRI and CSF parameters. The baseline MRI lesion volume at the CIS stage has been found to be most predictive for the development of CDMS. Baseline MRI findings and its change at earlier time points, based on serial MRIs, are modestly correlated with disability after 20 years. In the study by Fisniku et al. [242], 80 % of CIS patients who had ≤1 brain T2 lesion, compared with 20 % of CIS patients who had a normal baseline brain MRI, developed CDMS within 20 years. Those CIS patients with 1–3T2 lesions had a risk of CDMS that was similar to those with 10 or more lesions. Furthermore, CIS patients who eventually developed SPMS tended to have a greater increase in T2 lesion volume over the first 5 years, compared with those who developed RRMS. Although the above data suggests that baseline MRI lesion volume at the CIS stage can be most predictive for the development of CDMS, MRI alone is not a reliable predictor of disability because outcomes in the natural history of the disease are extremely variable. Although the presence of CSF oligoclonal bands may be predictive of MS risk in CIS patients, as shown in a cohort of 52 CIS patients [244], the new 2010 McDonald dissemination in space criteria for RRMS does not include CSF findings as part of the evaluation; CSF remains useful to exclude alternative diagnoses [245]. According to the revised 2010 McDonald criteria, CIS patients who have at least one asymptomatic *gadolinium-enhancing* lesion and at least one asymptomatic *nonenhancing* lesion are most likely to develop CDMS with a very low false positive rate [245]. However, no specific biomarkers yet exist to clearly distinguish CIS from RRMS patients. It is also important to take into consideration that EDSS, which measures mostly motor dysfunction, does not capture very early MS-related cognitive and visual disabilities. More potent neuroprotective agents, rather than the currently available immunomodulatory drugs, may have a role in the treatment of CIS patients to prevent progression of any possible disease. This potential treatment effect needs to be further investigated in the ON stage because of increasing evidence of cognitive deficits related to memory, information processing, and executive function in patients who present with isolated ON or other CISs [190].

Novel biomarkers are still needed to more accurately and reliably distinguish CIS from RRMS. In addition to MRI parameters, newer studies are incorporating OCT RNFL measurements, CSF and genetic biomarkers, and more sophisticated cognitive testing to see whether these parameters can give information about earlier MS progression in CIS patients. This additional information may help stratify CIS patients for no treatment or for more specific treatments in the future. More potent neuroprotective and/or neuroregenerative agents, rather than the currently available immunomodulatory drugs, may have a role in the treatment of CIS patients to prevent progression of disease.

Neuromyelitis Optica

Epidemiology

NMO is a relatively rare disorder. Population-based studies reveal the prevalence of NMO to be 0.44 per 100,000 and the annual incidence to be 0.05 per 100,000 among Caucasians in the United Kingdom [246]. In another study in the French West Indies and Martinique, the NMO prevalence was 2.5 per 100,000 and the annualized incidence of 0.1 per 100,000 among Afro-Caribbeans [247].

NMO predominately affects women in 80–90 % of cases with a median age of onset in the late 40s, which is about 10 years later than for MS [246]. Most NMO patients are Caucasians living in North America, but in other parts of the world NMO may be more prevalent in Asians and Africans [246]. Although familial cases have been reported, NMO is usually a sporadic disease [248].

Diagnosis

NMO is typically characterized as ON and transverse myelitis which usually present months to

years apart or simultaneously. The spinal cord lesions are often severe and extend over three or more vertebral segments, causing paraparesis or quadriparesis, spinal cord sensory syndromes, and or sphincter dysfunction. Lhermitte's sign and paroxysmal tonic spasms are usually present in about 40 % of patients. The revised diagnostic criteria for NMO involve clinical, neuroimaging, and NMO-IgG criteria have been validated (Table 1.2) [249, 250]. NMO is now recognized as a spectrum of disorders that can include involvement of the brain and neuroendocrine systems in patients with NMO-IgG and who may or may not have had ON and transverse myelitis. NMO pathology may extend into the brainstem causing nausea, vomiting, and hiccups. Up to 40 % of children with +NMO antibody have vomiting and encephalopathy and neurogenic respiratory failure. Endocrinopathies can result from hypothalamic dysfunction, encephalopathy, and the posterior reversible encephalopathy syndrome (PRES) (Table 1.3) [251].

Table 1.2 2006 revised NMO diagnostic criteria

Absolute criteria
1. Optic neuritis
2. Acute myelitis
Supportive criteria
1. Negative brain MRI at disease onset
2. Spinal cord MRI with contiguous T2-weighted signal abnormaltiy over ≥3 vertebral segments
3. NMO-IgG seropositive status

[Reprinted from Wingerchuk DM, Hogancamp WF, O'Brien PC, Weinshenker BG. The clinical courseof neuromyelitis optica (Devic's syndrome). Neurology. 1999 Sep 22;53(5):1107–14. With permission from Elsevier]

ON in NMO may be unilateral, simultaneous, or bilateral sequential. The length of the optic nerve lesions tends to be extensive, as can be seen on MRI of orbits with gadolinium. The optic chiasm may also be affected. Visual loss tends to be more severe in NMO compared with MS, and specific ophthalmoscopic features can help distinguish ON of NMO from MS (Figs. 1.4 and 1.5). These neuro-ophthalmic findings in NMO include: (1) attenuation of the peripapillary vasculature, (2) focal arteriolar narrowing occasionally associated with obscuration of the vessel lumen,

Table 1.3 A comparison of the clinical features distinguishing NMO from MS [Reprinted from Wingerchuk DM, Lennon VA, Lucchinetti CF, et al. The spectrum of neuromyelitis optica. Lancet Neurol 2007; 6:805–815. With permission from Elsevier]

	NMO	MS
Median age of onset	Median 39 years	Median 29 years
Gender	80–90 % female	60–70 % female
Prevalence	Non-Caucasian populations	Geographic distribution
Lesion sites	Mostly optic nerve and spinal cord	Any white matter tract
Attacks	Severe	Milder
Clinical onset and course	Onset with relapse	85 % Relapsing-remitting
	80–90 % Relapsing course	15 % Primary progressive
	10–20 % Monophasic course	Not monophasic
Secondary progressive course	Rare	Common
	NMO	MS
MRI brain	Often normal or non-specific white matter lesions; 10 % hypothalamic, corpus callosal, perventricular, or brainstem lesions	Periventricular white matter lesions
MRI spinal cord	Longitudinal ≥3 vertebral segments central lesions	Short segment peripheral lesions
CSF oligoclonal bands	90 % Absent	Present
Respiratory failure	Frequent (32 %)	Rare
Coexisting autoimmune disorders	Frequent (30 %)	Rare
NMO-IgG	Frequent (62 %)	Absent

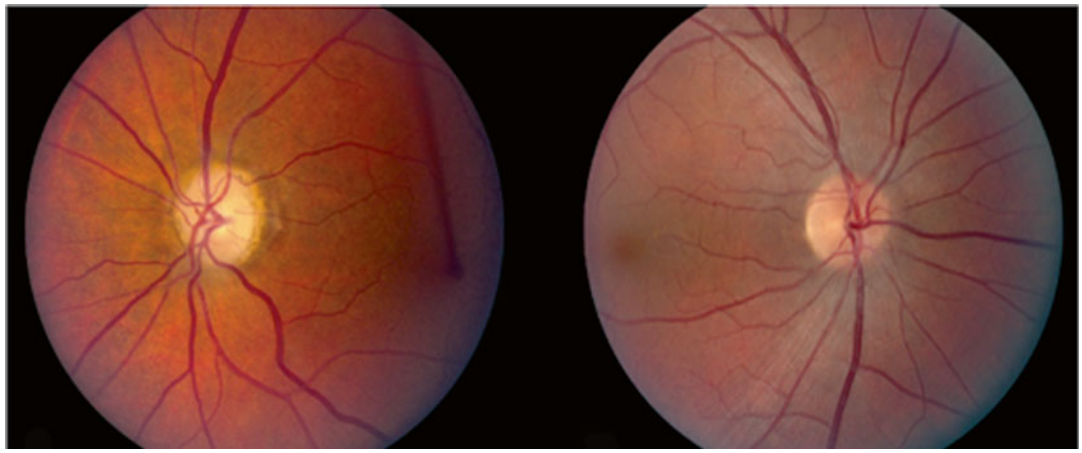

Fig. 1.4 On the *left*, left optic neuritis in an NMO patient. There is diffuse attenuation of blood vessels coming from the disc. Visual acuity was 20/20. Optic disc pallor is severe and diffuse. Only the vein coming from the superior edge of the disc looks normal in size. On the *right*, right optic neuritis in an MS patient. Visual acuity was 20/20. The optic disc pallor is segmental and mild. Blood vessels look normal and RNFL thinning is seen in both the superior and inferior arcuate bundles [Reprinted from Green AJ, Cree BA. Distinctive retinal nerve fibre layer and vascular changes in neuromyelitis optica following optic neuritis. *J Neurol Neurosurg Psychiatry*. 2009 Sep;80(9):1002–1005. With permission from BMJ Publishing Group]

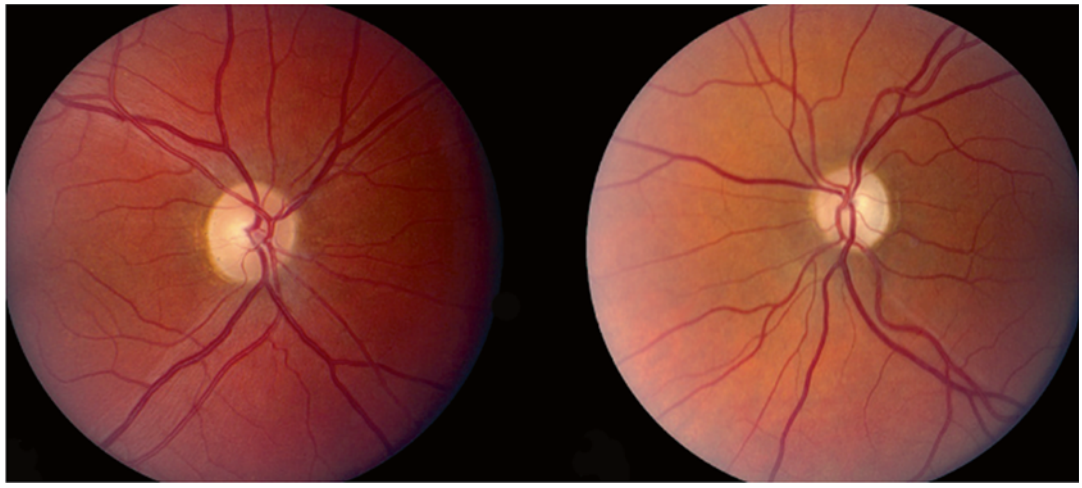

Fig. 1.5 On the *left*, right optic neuritis in NMO patient. Visual acuity is 20/20 and disc pallor is segmental and moderate. The arterioles arising from the superior and inferior nasal edge of the disc are narrowed. On the *right*, left optic neuritis in MS patient. Visual acuity is worse at 20/200 and disc pallor is diffuse with normal appearing vessels [Reprinted from Green AJ, Cree BA. Distinctive retinal nerve fibre layer and vascular changes in neuromyelitis optica following optic neuritis. *J Neurol Neurosurg Psychiatry*. 2009 Sep;80(9):1002–1005. With permission from BMJ Publishing Group]

(3) approximately two times as much RNFL thinning than ON in MS, and (4) diffuse RNFL thinning rather than focally in the maculopapillary bundle, as seen in MS [252].

The ON in NMO is a vasculopathy. Vascular hyalinization causes thickened blood vessel walls and narrowed vessel lumen in retrobulbar optic nerves and spinal cords of NMO patients. Direct inflammatory injury mediated by aquaporin-4 (AQP4) autoantibody leads to sheathing of blood vessels. AQP4 is expressed on the abluminal surface of endothelial cells in retinal arterioles

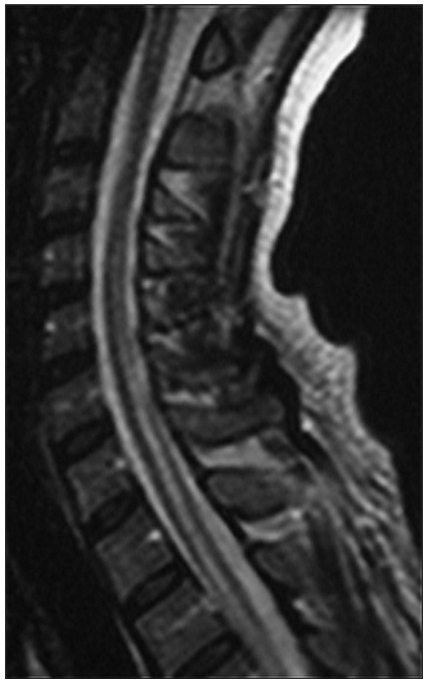

Fig. 1.6 T2 hyperintense signal changes on MRI of spine showing longitudinally extensive myelitis typically located in the central spinal cord spanning ≥3 vertebral segments [Courtesy of Robert Zak]

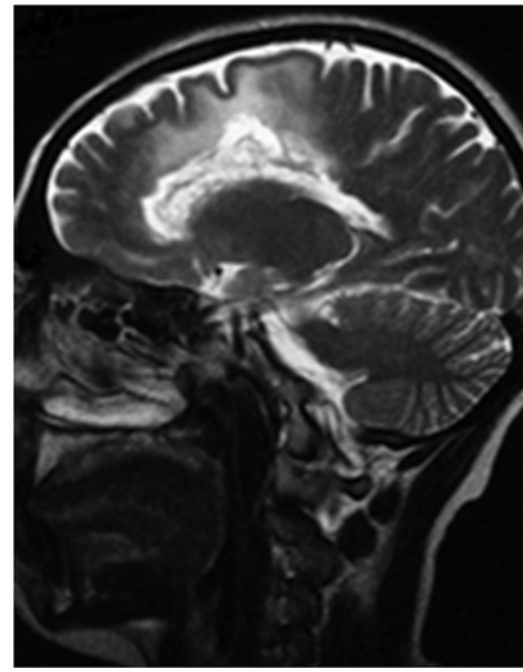

Fig. 1.7 T2-weighted MRI of brain revealing periventricular and corpus callosal hyperintense lesions radiating into white matter [Courtesy of Elli Grange]

and astrocytic end feet of tight junctions of the blood–brain barrier [253]. This autoantibody also plays a role in upregulating the response to injury [254] and is present in the walls of astrocyte-associated and inner retinal arterioles [255].

Unlike ON in MS where the maculopapillar bundles are selectively injured [256, 257], NMO, like glaucoma and nonarteritic ischemic optic neuropathy, is a vascular-mediated optic neuropathy that can cause injury to the arcuate fibers of the RNFL [258, 259].

In the early NMO stages, brain MRI may be normal or show nonspecific white matter lesions. In patients who present with acute ON, MRI of the orbits with gadolinium may show enhancement of one or both optic nerves or optic chiasm. Longitudinal extensive transverse myelitis, affecting the central cord and extending over ≥3 vertebral segments, is the most specific indicator of NMO (Fig. 1.6). These acute lesions are often seen as such during an acute myelitis attack. Their MRI features can evolve over weeks to years so that the longitudinally extensive pattern is no longer evident [249].

At least 60 % of NMO patients accumulate nonspecific white matter lesions over time and up to 10 % meet the radiological criteria for the diagnosis of MS. Brain MRI lesions do not exclude the diagnosis of NMO [260]. Large confluent subcortical white matter lesions can have a "cloud-like" gadolinium enhancement [261]. Unlike the perpendicularly oriented lesions in the corpus callosum seen in MS, NMO lesions are usually oriented linearly and along the axis of the corpus callosum (Fig. 1.7) [262]. T2 signal abnormalities in the hypothalamic, thalamic, or brainstem areas adjacent to the fourth ventricle or aqueduct are seen in about 10 % of patients with NMO (Fig. 1.8) [263–265].

Laboratory Studies

CSF testing reveals elevated white cell counts, occasionally with a neutrophilic predominance (50–1,000 × 10^6 WBC/dL) and high protein of

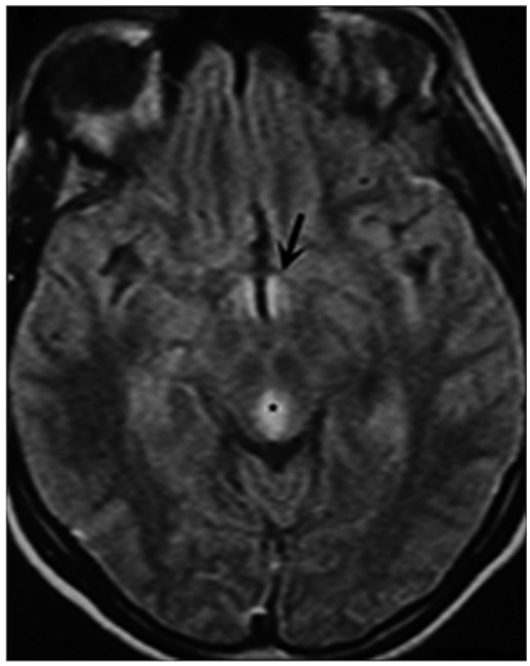

Fig. 1.8 FLAIR sequence on MRI of brain showing NMO lesions in the central brainstem (see *asterisk*) and in the hypothalamus (see *arrow*) [Courtesy of Robert Zak]

100–150 mg/L, unlike the mild lymphocytic pleocytosis (<25 × 10^6 WBC/L). CSF oligoclonal bands are found in 20–30 % of patients with compared to 85 % of patients with MS [249].

The NMO-IgG test should be considered in patients who present with bilateral simultaneous ON; chronic recurrent immune optic neuropathies, especially in those with severe visual deficits and poor recovery; longitudinally extensive transverse myelitis (LETM); PRES syndrome; or a cryptogenic leukodystrophy. The NMO-IgG test by indirect immunofluorescence technique using mouse cerebellum tissue by Lennon et al. was 73 % sensitive and 91 % specific for distinguishing NMO from MS [266]. Retesting initial seronegative patients who are clinically suspicious to have NMO is reasonable. Antibody levels also may rise before a clinical relapse and decrease with immunosuppressive treatment. The antibody is directed against the water channel AQP4 which regulates bidirectional water flux between blood and brain or CSF. It is expressed on astrocytic foot processes and the abluminal surface of blood vessels, not on neurons, oligodendroglia, or choroid epithelium cells. High levels of AQP4 are expressed in the spinal cord (especially the gray matter), optic nerve, brainstem, hypothalamus, and periventricular regions. It is also found in the area postrema and supraoptic nucleus. These high density areas of AQP4 correspond to the lesions seen on MRI in some NMO patients [266].

Approximately 50 % of NMO patients who are seropositive for NMO-IgG also have serum autoantibodies, such as ANA and extractable nuclear antigen, and about one-third have one or more systemic autoimmune diseases, such as thyroiditis and myasthenia gravis. A total of 10–40 % of NMO patients may also meet the clinical criteria for connective tissue diseases, such as Sjogren's syndrome and systemic lupus erythematosus [249, 267]. These patients who present with the clinical symptoms and signs of NMO with a seropositive NMO-Ig most likely have a coexisting autoimmune disease or connective tissue disease [249, 267].

Clinical Course

In a retrospective study of 1,274 patients with ON by Pirko et al. [268], the 10-year conversion rate to MS was 29.8 % and to NMO 12.5 %. Based upon data from several studies [269, 270], the cumulative conversion rate tends to increase most rapidly in the first 10 years, after which it continues to rise, albeit more slowly. More severe visual loss and earlier subsequent relapses occurred in those with NMO than in MS [268].

The course of NMO involves stepwise accumulation of disability because of poor recovery with each relapse. Within 5 years, more than 50 % of relapsing NMO patients have visual acuity of worse than 20/200 or require at least some ambulatory assistance [249, 271].

More than 90 % of patients with NMO have the relapsing form [249]. Predictive factors that may increase the risk of developing the relapsing form of NMO include the following features: (1) first interattack interval of several weeks to

months, (2) female gender, and (3) better motor recovery after the first myelitis event [271]. Patients who are AQP4 seropositive, compared to seronegative status, tend to be women who have a high relapse frequency, a high EDSS, and do not usually have a secondary progressive phase, as typically seen in MS [272]. Patients with the monophasic disorder are often seronegative and the frequency and severity of relapses seem to be lower compared to seropositive patients. A positive NMO IgG status in recurrent ON patients predicts poor visual outcome and a >50 % risk of relapse at 1 year [273].

Pathology and Pathogenesis

The pathology of NMO is distinct from that of MS. Inflammation and demyelination are seen in NMO lesions in the optic nerve and spinal cord. The gray matter and white matter are both affected and necrotic areas with cavitation can be seen in the spinal cord. The inflammatory infiltrates consist of neutrophils and eosinophils and the blood vessels are hyalinized. In active brain NMO lesions, immunoglobulin and complement are deposited in a vasculocentric "rim" and "rosette" pattern. AQP4 immunoreactivity is lost in NMO lesions, whereas AQP4 expression is increased in MS lesions. In another type of NMO affecting the spinal cord extending into the medullary tegmentum and into the area postrema, AQP4 immunoreactivity is lost. Inflammation persists but no demyelination or necrosis is present [274].

NMO-IgG complement-mediated tissue injury is the primary cause of NMO. In vitro studies show that NMO-IgG modulates expression of AQP4 on the astrocyte surface. NMO-IgG is involved in complement-mediated cell membrane injury, cell death, disruption of the blood–brain barrier, and enhancement of granulocyte recruitment [275, 276]. NMO-IgG causes internalization of AQP4 in astrocytes. Loss of AQP4 in the paranodal regions leads to demyelination. NMO-IgG also modulates the glutamate transporter EAAT2 and decreases glutamate reuptake. In vivo studies show that NMO-IgG causes exacerbation of CNS inflammation of experimental autoimmune encephalitis animals [277–281]. Clinical evidence that also supports a humoral immune mechanism in NMO includes: (1) coexisting systemic autoimmune disorders or autoimmune seropositivity and (2) an excellent response to PE [282].

Treatment

For an acute attack of NMO, IVMP 1 g/day × 5 days is the first line treatment. If there is no response, then seven PEs over 2 weeks should be given. Depending on the time interval between attack onset and therapy initiation, approximately 60 % recover. One randomized, double-blinded study evaluated the transition from corticosteroids to PE in patients with either acute transverse myelitis (four patients with initial episode and one patient with recurrence) or myelitis in the context of NMO (two patients) [283]. Patients with inadequate treatment response to steroids were randomized to active or sham exchange. A crossover was made if no recovery or only a mild recovery was seen after a 2-week treatment period. Of the four PE-treated patients with acute transverse myelitis, one patient experienced dramatic improvement, two failed, and one died from a heparin complication. The two patients with NMO experienced significant improvement with PE whereas no effect was observed with sham exchange. Other retrospective studies also have shown benefits in different groups of patients, including 18 Afro-Caribbean patients with transverse myelitis in which six were NMO-IgG positive [284] and two of the NMO-IgG positive patients had severe transverse myelitis [285].

For the prevention of relapses, the combination of azathioprine and prednisone can be used for relapsing NMO patients who do not need immediate induction therapy because they have not a recent severe attack or have been free of relapses for several months. Maintenance azathioprine as monotherapy can be started at 50 mg/day and increased by 50-mg increments weekly up to a maximal dose of 2.5–3 mg/kg/day. Dosage changes are needed if the leukocyte count falls

below 3,000/mm [3] or the platelet count decreases below 100,000/mm [3]. Prednisone is also started at 0.5–1.0 mg/kg/day, usually up to 60–80 mg/day with azathioprine. Prednisone can be tapered off when azathioprine reaches its target dose and when clinical symptoms are stable. Some patients may become steroid dependent and require prednisone 5–15 mg/day to prevent relapses [282]. Some contraindications to this drug are hypersensitivity to the drug itself, pregnancy, and prior exposure to alkylating agents which can lead to increased risk of lymphoma. Some side effects include gastrointestinal problems, rash, drug fever, and hepatotoxicity. This combination of immunosuppressive therapy often leads to a decrease in frequency of attacks and a decrease in NMO-IgG titers.

IVIg is not efficacious for treatment of relapses, but is useful for relapse prevention. In a placebo-controlled, randomized study of 55 patients who underwent IVIg 0.4 g/kg/day for 5 days followed by three single infusions per month for 3 months, or placebo, no visual improvement was observed in the IVIg-treated group [234]. IVIg has been more beneficial for relapse prevention. In a report of two patients with NMO, including a patient who was unresponsive to azathioprine and prednisolone, both patients were relapse free for 5.5 years after 1 year of treatment with monthly infusions of IVIg [286].

For patients who cannot tolerate azathioprine and who do not require immediate-onset therapy, mycophenolate mofetil can be used as an alternative. It suppresses B- and T-cell proliferation but does not affect hemopoiesis and neutrophil count and activity. It also does not cause gastrointestinal side effects as does azathioprine. For patients with thiopurine methyltransferase deficiency, mycophenolate mofetil may be a better treatment choice. The onset of action is not faster than azathioprine. In a retrospective case series of 24 patients with NMO who were treated over a median of 27 months, mycophenolate mofetil was shown to decrease the median annualized relapse rate from 1.3 to 0.09 ($p<0.001$). Disability stabilized or decreased in 22 of 24 patients (91 %) [287].

Mycophenolate mofetil is started at 500 mg twice a day. After 1 week, it is increased to 1,000 mg twice daily. Some contraindications to this drug are pregnancy, hypersensitivity to the drug itself, concurrent use of live attenuated vaccines, bone marrow suppression, and hypoxanthine-guanine phosphoribosyl-transferase deficiency [282].

For treatment-resistant NMO, rituximab, an anti-CD20 monoclonal antibody, depletes B cells, as NMO is a B-cell-mediated disorder. Rituximab may be started in patients who have relapsing NMO despite treatment with other immunosuppressive therapies or in patients who need fast-onset induction therapy because of a recent severe relapse. In a study that included eight patients with worsening NMO, rituximab was given on an off-label, compassionate-use basis after immunomodulatory drugs in six patients, azathioprine in three patients, and mitoxantrone in one patient. Rituximab stabilized the disease for at least several months after its administration. Six of the 8 patients were relapse free after 1 year of follow-up, and the median attack rate decreased from 2.6 to 0 attacks per patient per year. Seven of the 8 patients experienced substantial recovery of neurological function over 1 year of follow-up. The median EDSS score increased from 7.5 to 5.5 [288]. In another prospective open-label study in 30 patients with relapsing NMO or NMO spectrum disorder, 28 patients showed a marked reduction in relapse rate while taking rituximab over 24 months. The relapse rate was reduced significantly by 88 % and 70 % of patients became relapse free over 24 months. Disability either improved or stabilized in 97 % of patients. Anti-AQP4 antibody levels significantly decreased after treatment with rituximab. Additional treatments with rituximab gave sustained efficacy over 24 months. This drug was well tolerated and no clinical significant adverse events lead to discontinuation of rituximab [289].

Rituxan is started at 375 mg/m^2/week for 4 weeks within 2–3 weeks and becomes effective faster than azathioprine or mycophenolate mofetil. If symptoms continue, infusions are repeated every 6–12 months. After treatment for 1 1/2 years, relapse rate is often reduced and disability is stabilized. Contraindications to this drug include type 1 hypersensitivity reactions and

hepatitis B infection (may cause reactivation). Some side effects include infusion reactions, such as fever, chills, rigors, nausea, urticarial, angioedema, bronchospasm, hypotension, headache, dizziness, asthenia, rash, and cardiac arrhythmias [282].

Other alternative treatments for unresponsive patients include mitoxantrone 12 mg/m [2] every 3 months, methotrexate, cyclosporine, cyclophosphamide, ocrelizumab (anti-CD20), and ofatumumab (anti-CD20) [282]. There are no data for guidelines of when to discontinue immunosuppression in patients who are clinically stable for several years.

Five years of relapse-free immunosuppression has been recommended for NMO-IgG seropositive patients who have had an attack, such as an LETM attack, and who are at risk of relapse. Beyond this time frame, adverse side effects, such as malignancies, may arise [290, 291]. Interferon ß (beta)-1b induces an inhibitory effect on the proliferation of leukocytes, antigen presentation, and T-cell migration across the blood–brain barrier and enhances anti-inflammatory cytokine production.

Interferon ß (beta)-1b treatment has been evaluated in several studies which have shown that this form of therapy is not effective in NMO in terms of relapse rate and disability [292, 293]. Furthermore, interferon ß (beta)-1b can exacerbate NMO, as shown in one study of two patients with NMO and anti-AQP4 antibodies who developed extensive brain lesions 2 months after interferon ß (beta)-1b initiation [294]. In another study, a patient developed a dramatic increase of anti-AQP4 antibodies and an increase in relapse rate during the interferon ß (beta)-1b treatment, and then both decreased after the patient was switched to immunosuppressive therapy [295]. These treatment responses to interferon ß (beta)-1b could be explained by the increased effect of type 1 interferon on B-cell activation and differentiation.

GA contains synthetic polypeptides composed of four amino acids resembling MBP. It induces antigen-presenting cells with anti-inflammatory properties and promotes the generation of immunoregulatory T cells that suppress pathogenic T cells. GA has been shown to be effective in only two cases in the literature so far. One patient had a reduction in relapse rate from 0.9/year in the 15-year pretreatment period to 0.25/year after 9 years of GA therapy [296]. Another patient, who was unresponsive to cyclophosphamide, was treated with GA with monthly corticosteroid pulses for a year and had no relapses and no new spinal cord lesions [297].

Paraneoplastic Optic Neuropathies

Paraneoplastic ophthalmologic syndromes are usually retinopathies and rarely optic neuropathies [298–320]. Most paraneoplastic optic neuropathies are associated with small cell lung carcinoma [298–305]. Others are associated with B-cell lymphomas [305, 306], pancreatic glucagonoma [307], neuroblastoma [308, 309], uterine sarcoma [310], breast carcinoma [311, 312], prostate carcinoma [313], nasopharyngeal carcinoma [314], bronchial carcinoma [315], papillary thyroid [299, 316], nonsmall cell lung carcinoma [317, 318], and renal cell carcinoma [299, 319, 320].

The paraneoplastic optic neuropathies, seen often with small cell lung carcinomas and rarely thymomas, are associated with collapsing response-mediating-protein-5 (CRMP-5), a 62-kDa neuronal antigen [321]. CRMP-5 is expressed in adult central and peripheral neurons, including synapses, and in small cell lung carcinomas, and rarely in thymomas. The CRMP family of proteins is believed to mediate growth guidance cues during neurogenesis. Since 1993, Yu et al. have documented 121 cases in their laboratory. CRMP-5 may be as common as PCA-1 (anti-Yo autoantibody), and second in frequency to ANNA-1 (anti-Hu antibody). Anti-CV2 was recognized in 2001 to be the same entity as CRMP-5-IgG by Yu and colleagues [321] and Lennon and colleagues [299].

Retinitis has also been recognized as a possible associated component of paraneoplastic autoimmune ON associated with CRMP-5-IgG [299]. Fifteen of the 172 patients with CRMP-5-IgG paraneoplastic syndromes had ON and 5 of those

15 also had retinitis. These 15 ON patients were 52–74 and were smokers; eight were female. Fourteen developed subacute visual loss and visual field defects. Four of the four tested had abnormal ERGs and vitreous cells were observed in 9 of the 15 ON patients.

CRMP-5-IgG is not specific for paraneoplastic optic neuropathy. Only 16 (9 %) of 172 patients with positive CRMP-5 titers had paraneoplastic optic neuropathy and the remainder had other neurologic impairments [299]. Up to 35 % of patients with positive CRMP-5 titers and small cell lung carcinomas have some neurologic features, such as optic neuropathy/retinitis with vitreous cells, other cranial neuropathies, and subacute chorea, or other basal ganglia disorders [299, 322–324]. Neuro-ophthalmic manifestations include decreased upgaze, nystagmus, cranial neuropathies, and opsoclonus [321, 325]. The presence of CRMP-5 antibody does not predict a specific neurologic syndrome but rather directs the investigation toward an underlying cancer, which is found in up to 90 % of patients [299, 324, 326]. Although neurological symptoms and signs can occur with paraneoplastic ON and retinitis, a patient with isolated CRMP-5 paraneoplastic optic neuropathy and vitritis associated with small cell lung carcinoma has been reported [301].

Paraneoplastic optic neuropathies involve subacute, progressive, usually bilateral visual loss not associated with pain; however, it can present with acute visual loss. The optic disc is normal or edematous and can involve the optic chiasm. Visual field defects include enlarged blind spots, arcuate and altitudinal defects, paracentral scotomas, peripheral constriction, or generalized depression [299]. Fluorescein angiography can show optic nerve head disc leakage and peripheral retinal vascular leakage [299]. Full-field ERG abnormalities have been inconsistently documented. MRI of the brain may be normal appearing or may reveal hyperintense T2 signal changes in subcortical areas, enhancement of optic nerves and spinal cord [299]. On histologic section, mild axonal loss and demyelination can often be seen (Fig. 1.9). Vasculitis, infectious, demyelinating, infiltrative disorders, such as metastases, and direct external compression to the optic nerve should be ruled out. If CRMP-5-IgG in the serum or CSF is present, then a vitreal biopsy is not necessary. A workup for systemic malignancy should be undertaken, including a chest X-ray, a CT scan of chest, and a whole-body positron emission tomography scan, usually from orbits to thighs. If no cancer is detected, these imaging techniques can be repeated at least every 3 months and then later every 6 months, according to Darnell and Posner [327].

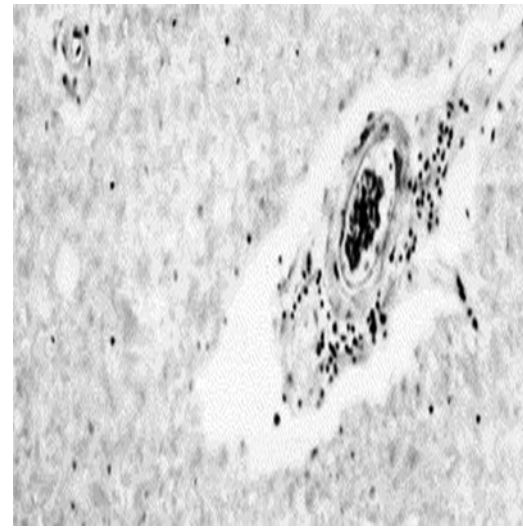

Fig. 1.9 Hematoxylin-phloxine-saffron stain of the right optic nerve showing mild axonal loss and demyelintation in a patient with paraneoplastic optic neuropathy associated with thymoma (magnification 10×)

Treatment of the specific underlying cancer in paraneoplastic optic neuropathy patients and systemic immunosuppressive agents, such as high-dose MP and IVIg, has resulted in variable visual improvement.

Polyneuropathy, Organomegaly, Endocrinopathy, Monoclonal Gammopathy, and Skin Changes (POEMS)

POEMS syndrome is a rare paraneoplastic disorder related to an underlying plasma cell dyscrasia that affects more commonly males in their 50s [328]. Diagnosis of this disorder is based on having three of the major criteria (polyradiculoneuropathy, clonal plasma cell disorder (PCD),

sclerotic bone lesions, elevated vascular endothelial growth factor (VEGF), and the presence of Castleman disease, two of which must include monoclonal PCD and chronic progressive polyneuropathy, and at least one minor criteria (organomegaly, endocrinopathy, characteristic skin changes, papilledema, extravascular volume overload, and thrombocytosis) [328]. Patients present with blurred vision or ocular pain, and occasionally decreased central vision and metamorphopsia. Bilateral optic disc edema is associated with POEMS syndrome in 29–73 % of patients [329–332], which can be occasionally complicated by CME [332, 333] and bilateral serous macular detachment [334]. Enlargement of the blind spot and arcuate field defects can be seen [335, 336].

Fluorescein angiography reveals late optic disc leakage or petaloid leakage in CME. OCT may also detect CME. Elevated serum VEGF levels, interleukin-6, interleukin-1beta, and TNF-α may be measured. Production of proangiogenic and proinflammatory cytokines by abnormal plasma cells is thought to contribute to the development of POEMS syndrome and correlates with disease activity [337, 338]. In addition to increased vascular permeability of the optic nerve and macula from the effects of VEGF, increased intracranial pressure [339] and infiltration of the optic nerve and vasculitis [340] could contribute to visual symptoms.

Intravitreal anti-VEGF agents may be a promising treatment for CME in POEMS syndrome. Systemic POEMS is treated with radiation therapy for bone lesions, chemotherapy, corticosteroids, and autologous stem cell transplantation [328].

Autoimmune-Related Retinopathy and Optic Neuropathy (ARRON) Syndrome

ARRON syndrome can affect only the optic nerve, only the retina, or both simultaneously [341]. Keltner et al. initially described 12 ARRON patients who were mostly females with an average onset of 50 years. They had painless, asymmetric visual loss ranging from 20/20 to no light perception in the more affected eye. Three of the 12 patients had photospias. Optic disc pallor was seen in 11 of 12 patients. Eight of 12 patients had nonspecific retinal changes and 10 of the 11 patients had ERG abnormalities. CME was often seen [341]. Patients with ARRON syndrome often have concurrent systemic autoimmune disorders, such as SLE, which may predispose them to develop this syndrome. The diagnosis of ARRON syndrome is one of exclusion. An underlying malignancy must be ruled out in this clinical setting of progressive visual loss. Various antiretinal antibodies have been characterized, such as alpha-enolase antibodies, 22 kDa neuronal antibodies against the retina and optic nerve [342], and other unidentified proteins [343]. The presence of antiretinal antibodies is not diagnostic, as they can be present in up to 12 % of normal individuals [344].

Treatment of ARRON syndrome is directed at the basic immunologic abnormalities using immunosuppressive treatments, such as corticosteroids, IVIg, and autologous hematopoietic stem cell transplantation [345, 346].

References

1. Kinnunen E. The incidence of optic neuritis and its prognosis for multiple sclerosis. Acta Neurol Scand. 1983;68:371–7.
2. Rodriguez M, Siva A, Cross SA, O'Brien PC, Kurland LJ. Optic neuritis: a population-based study in Olmsted County, Minnesota [see comments]. Neurology. 1995;45:244–50.
3. Cantore WA. Optic neuritis. Pa Med. 1996; 99(Suppl):96–8.
4. Optic Neuritis Study Group. The clinical profile of optic neuritis. Experience of the optic neuritis treatment trial [see comments]. Arch Ophthalmol. 1991;109:1673–8.
5. Beck RW. Optic neuritis. In: Miller NR, Newman NJ, editors. The essentials: Walsh & Hoyt's clinical neuro-ophthalmology. Baltimore, MD: Williams & Wilkins; 1999. p. 599–648.
6. Keltner JL, Johnson CA, Spurr JO, Beck RW. Baseline visual field profile of optic neuritis. The experience of the optic neuritis treatment trial. Optic Neuritis Study Group [see comments]. Arch Ophthalmol. 1993;111:231–4.
7. Fang JP, Lin RH, Donahue SP. Recovery of visual field function in the optic neuritis treatment trial. Am J Ophthalmol. 1999;128(5):566–72.

8. Cleary PA, Beck RW, Bourque LB, Backlund JC, Miskala PH. Visual symptoms after optic neuritis. Results from the optic neuritis treatment trial. J Neuroophthalmol. 1997;17(1):18–23.
9. Keltner JL, Johnson CA, Spurr JO, Beck RW. Comparison of central and peripheral visual field properties in the optic neuritis treatment trial. Am J Ophthalmol. 1999;128(5):543–53.
10. Keltner JL, Johnson CA, Spurr JO, Beck RW. Visual field profile of optic neuritis. One- year follow-up in the optic neuritis treatment trial. Arch Ophthalmol. 1994;112:946–53.
11. Merle H, Olindo S, Donnio A, Beral L, Richer R, Smadja D, et al. Retinal nerve fiber layer thickness and spatial and temporal contrast sensitivity in multiple sclerosis. Eur J Ophthalmol. 2010;20(1):158–66.
12. Trauzettel-Klosinski S. Various stages of optic neuritis assessed bysubjective brightness of flicker. Arch Ophthalmol. 1989;107(1):63–8.
13. Nichols BE, Thompson HS, Stone EM. Evaluation of a significantly shorter version of the Farnsworth-Munsell l00-hue test in patients with three different optic neuropathies. J Neuroophthalmol. 1997;17:1–6.
14. Frisen L, Hoyt WF. Insidious atrophy of retinal nerve fibers in multiple sclerosis. Funduscopic identification in patients with and without visual complaints. Arch Ophthalmol. 1974;92:91–7.
15. Lightman S, McDonald WI, Bird AC, Francis DA, Hoskins A, Batchelor JR. Retinal venous sheathing in optic neuritis. Its significance for the pathogenesis of multiple sclerosis. Brain. 1987;110(pt 2):405–14.
16. Killer HE, Job O. Differential diagnostic considerations on retrobulbar neuritis. Nervenarzt. 1996;67: 815–20.
17. Swartz NG, Beck RW, Savino PJ, Sergott RC, Bosley TM, Lam BL. Pain in anterior ischemic optic neuropathy. J Neuroophthalmol. 1995;15:9–10.
18. Warner JE, Lessell S, Rizzo III JF, Newman NJ. Does optic disc appearance distinguish ischemic optic neuropathy from optic neuritis? Arch Ophthalmol. 1997;115:1408–10.
19. Smith JL, Hoyt WF, Susac JO. Ocular fundus in acute Leber optic neuropathy. Arch Ophthalmol. 1973;90:349–54.
20. Brown MD, Torroni A, Reckord CL, et al. Phylogenetic analysis of Caucasian 11778-positive and 11778-negative Leber's hereditary optic neuropathy patients indicates multiple independent occurrences of the common primary mitochondrial DNA mutations. Hum Mutat. 1995;6:311–25.
21. Selbst RG, Selhorst JB, Harbison JW, et al. Parainfectious optic neuritis: report and review following varicella. Arch Neurol. 1983;40:347–50.
22. Manor RS, Cohen S, Ben-Sira T. Bilateral acute retrobulbar optic neuropathy associated with epidemic keratoconjunctivitis in a compromised host. Arch Ophthalmol. 1986;104:1271–2.
23. Spalton DJ, Murdoch I, Holder GE. Coxsackie B5 papillitis. J Neurol Neurosurg Psychiatry. 1989;52: 1310–1.
24. McKibbin M, Cleland PG, Morgan SJ. Bilateral optic neuritis after hepatitis A. J Neurol Neurosurg Psychiatry. 1995;58(4):508.
25. Achiron LR. Postinfectious hepatitis B optic neuritis. Optom Vis Sci. 1994;71:53–6.
26. Gross JG, Sadun AA, Wiley CA, et al. Severe visual loss related to isolated peripapillary retinal and optic nerve head cytomegalovirus infection. Am J Ophthalmol. 1989;108:691–8.
27. Jones J, Gardner W, Newman T. Severe optic neuritis in infectious mononucleosis. Ann Emerg Med. 1988;17:361–4.
28. Sweeney BJ, Manji H, Gilson RJC, et al. Optic neuritis and HIV-1 infection. J Neurol Neurosurg Psychiatry. 1993;56:705–7.
29. Srivastava SP, Neman HV. Optic neuritis in measles. Br J Ophthalmol. 1963;47:180–1.
30. Strong LE, Henderson JW, Gangitano JL. Bilateral retrobulbar neuritis secondary to mumps. Am J Ophthalmol. 1974;78:331–2.
31. Connolly JH, Hutchinson WM, Allen IV, et al. Carotid artery thrombosis, encephalitis, myelitis and optic neuritis associated with rubella virus infections. Brain. 1975;98:583–94.
32. Purvin V, Hrisomalos N, Dunn D. Varicella optic neuritis. Neurology. 1988;38:501–3.
33. Deane JS, Bibby K. Bilateral optic neuritis following herpes zoster ophthalmicus. Arch Ophthalmol. 1995;113:972–3.
34. Colarizi A, Panico E. Atrofia secondaria del nervo ottico consecutiva a infezione carbonchiosa. Bull Acad Med Roma. 1933;59:399–408.
35. Smallberg GJ, Sherman SH, Pezeshkpour GH, et al. Optic neuropathy due to brain abscess. Am J Ophthalmol. 1976;82:188–92.
36. McLean DR, Russell N, Khan MY. Neurobrucellosis: clinical and therapeutic features. Clin Infect Dis. 1992;15:582–90.
37. Brazis PW, Stokes HR, Ervin FR. Optic neuritis in cat scratch disease. J Clin Neuro Ophthalmol. 1986;6:172–4.
38. Ellsworth J, Marks MI, Vose A. Meningococcal meningitis in children. Can Med Assoc J. 1979; 120(2):155–8.
39. Miller HG, Staton JB, Gibbons JL. Parainfectious encephalomyelitis and related syndromes: a critical review of the neurological complications of certain specific fevers. Q J Med. 1956;25:427–505.
40. Miller BW, Frenkel M. Report of a case of tuberculosis retrobulbar neuritis and osteomyelitis. Am J Ophthalmol. 1971;71:751–6.
41. Bajpai PC, Dikshit SK. Bilateral optic neuritis and encephalitis accompanying typhoid. J Indian Med Assoc. 1958;30:54–7.
42. Vital Durand D, Gerard A, Rousset H. [Neurological manifestations of whipple disease]. Rev Neurol. 2002;158(10C1):988–92 [Article in French].
43. Yen M-Y, Lui J-H. Bilateral optic neuritis following bacille calmette-guerin (BCG) vaccination. J Clin Neuro Ophthalmol. 1991;114:2437–50.

44. Berkman N, Banzarti T, Dhaoui R, et al. Neuropapillite bilaterale avec decollement sereux du neuroepithelium, au decours d'une vaccination contre l'hepatite B. Bull Soc Ophtalmol Fr. 1996;96:187–90.
45. Chayakul V, Ishikawa S, Chotibut S, et al. Convergence insufficiency and optic neuritis due to anti-rabic inoculation. Jpn J Ophthalmol. 1975;19: 307–14.
46. Topaloglu H, Berker M, Kansu T, et al. Optic neuritis and myelitis after booster tetanus toxoid vaccination. Lancet. 1992;339:178–9.
47. Wagener HP. Edema of the optic disks in cases of encephalitis. Am J Med Sci. 1952;223:205–15.
48. Perry HD, Mallen FJ, Grodin RW, et al. Reversible blindness in optic neuritis associated with influenza vaccination. Ann Ophthalmol. 1979;11:545–50.
49. Graham EM, Ellis CJK, Sanders MD, et al. Optic neuropathy in sarcoidosis. J Neurol Neurosurg Psychiatry. 1986;49:756–63.
50. Golnik KC, Newman SA, Wispelway B. Cryptococcal optic neuropathy in the acquired immune deficiency syndrome. J Clin Neuro Ophthalmol. 1991;11:96–103.
51. Gross JG, Sadun AA, Wiley CA, et al. Severe visual loss related to isolated peripapillary retinal and optic nerve head cytomegalovirus infection. Am J Ophthalmol. 1989;108:691–8.
52. Grossniklaus HE, Frank KE, Tomsak RL. Cytomegalovirus retinitis and optic neuritis in acquired immune deficiency syndrome: report of a case. Ophthalmology. 1987;94:1601–4.
53. Litoff D, Catalano RA. Herpes zoster optic neuritis in human immunodeficiency virus infection. Arch Ophthalmol. 1990;108:782–3.
54. Zambrano W, Perez GM, Smith JL. Acute syphilitic blindness in AIDS. J Clin Neuro Ophthalmol. 1987; 7:1–5.
55. Nichols JW, Goodwin JA. Neuro-ophthalmologic complications of AIDS. Semin Ophthalmol. 1992; 7:24–9.
56. Falcone PM, Notis C, Merhige K. Toxoplasmic papillitis as the initial manifestation of acquired immunodeficiency syndrome. Ann Ophthalmol. 1993; 25:56–7.
57. Holland GN, Engstrom Jr RE, Glasgow BJ, et al. Ocular toxoplasmosis in patients with the acquired immunodeficiency syndrome. Am J Ophthalmol. 1988;106:653–7.
58. Larsen M, Toft PB, Bernhard P, Herning M. Bilateral optic neuritis in acute human immunodeficiency virus infection. Acta Ophthalmol Scand. 1998; 76(6):737–8.
59. Newman NJ, Lessell S. Bilateral optic neuropathies with remission in two HIV-positive men. J Clin Neuro Ophthalmol. 1992;12(1):1–5.
60. Jacobson DM, Marx JJ, Dlesk A. Frequency and clinical significance of Lyme seropositivity in patients with isolated optic neuritis. Neurology. 1991;41:706–11.
61. Sanborn GE, Kivlin JD, Stevens M. Optic neuritis secondary to sinus disease. Arch Otolaryngol. 1984;110(12):816–9.
62. Gass JD. Diseases of the optic nerve that may simulate macular disease. Trans Sect Ophthalmol Am Acad Ophthalmol Otolaryngol. 1977;83:763–70.
63. Moreno RJ, Weisman J, Waller S. Neuroretinitis: an unusual presentation of ocular toxoplasmosis. Ann Ophthalmol. 1992;24:68–70.
64. Farthing CF, Howard RS, Thin RN. Papillitis and hepatitis B. Br Med J. 1986;29(2):1712.
65. Knapp A. Optic neuritis after influenza, with changes in the spinal fluid. Arch Ophthalmol. 1916;45:247–9.
66. Arruga J, Valentines J, Mauri F, et al. Neuroretinitis in acquired syphilis. Ophthalmology. 1985;92: 262–70.
67. Audry-Chaboud D, Durnas R, Audry F, et al. Coxsackie B virus neuropapillitis. Rev Otoneuroophthalmol. 1981;53:473–82.
68. Folk JC, Weingeist TA, Corbett JJ, et al. Syphylitic neuroretinitis. Am J Ophthalmol. 1983;95:480.
69. Copeland Jr RA. Lyme uveitis. Int Ophthalmol Clin. 1990;30:291.
70. Barkay S, Garzozi H. Leptospirosis and uveitis. Ann Ophthhalmol. 1984;16:164.
71. Tabbara KF. Brucellosis and nonsyphilitic treponemal uveitis. Int Ophthalmol Clin. 1990;30:294.
72. Jampol LM, Staruch S, Albert DM. Intraocular nocardiosis. Am J Ophthalmol. 1973;76:568.
73. Schlaegel TF, O'Connor GR. Tuberculosis and syphilis. Arch Ophthalmol. 1981;99:2206.
74. Jay WM, Schanzlin DJ, Fritz KJ. Medical therapy of metastatic meningococcal endophthalmitis. Am J Ophthalmol. 1979;87:567.
75. Murray HW, Knox DL, Green WR, et al. Cytomegalovirus retinitis in adults: a manifestation of disseminated viral infection. Am J Med. 1977; 63:574.
76. Pavan-Langston D, Brockhurst RJ. Herpes simplex panuveitis. Arch Ophthalmol. 1969;81:783.
77. Brown RM, Mendis U. Retinal arteritis complicating herpes zoster ophthalmicus. Br J Ophthalmol. 1973;57:344.
78. Krill AE. The retinal disease of rubella. Arch Ophthalmol. 1967;77:445.
79. Font RL, Jenis EH, Tuck KD. Measles maculopathy associated with subacute sclerosing panencephalitis (SSPE). Arch Pathol. 1973;96:168.
80. Shuman JS, Orellana J, Friedman AH, et al. Acquired immunodeficiency syndrome (AIDS). Surv Ophthalmol. 1987;31:384.
81. Gagliuso DJ, Teich SA, Friedman AH, et al. Ocular toxoplasmosis in AIDS patients. Trans Am Ophthalmol Soc. 1990;88:63.
82. Wilkinson CP. Ocular toxocariasis. In: Schachat AP, Murphy RB, Patz A, editors. Retina, vol. 2. St. Louis: CV Mosby; 1989. p. 1421–2.
83. Bird AC, Anderson J, Fuglsang H. Morphology of posterior segment lesions of the eye in patients with onchocerciasis. Br J Ophthalmol. 1976;60:2.

84. Tabbara KF. Endogenous ocular candidiasis. In: Tabbara KF, Hyndiuk RA, editors. Infections of the eye. Boston: Little, Brown; 1986. p. 43–4.
85. Schlaegel TF. Presumed ocular histoplasmosis. In: Tasman W, Jaeger EA, editors. Duane's clinical ophthalmology, vol. 4. Philadelphia, PA: JB Lippincott; 1981. p. 169–72.
86. Shields JA, Wright DM, Augsberger JJ, et al. Cryptococcal chorioretinitis. Am J Ophthalmol. 1980;89:210.
87. Naidoff MA, Green WR. Endogenous Aspergillus endophthalmitis occurring after kidney transplant. Am J Ophthalmol. 1975;79:502.
88. Zakka KA, Foos RY, Brown WJ. Intraocular coccidioidomycosis. Surv Ophthalmol. 1978;22:313.
89. Bond WI, Sanders CV, Joffe L, et al. Presumed blastomycosis endophthalmitis. Ann Ophthalmol. 1982;14:1183.
90. Bullen CL, Liesegang TJ, McDonald TJ, DeRemee RA. Ocular complications of Wegener's granulomatosis. Ophthalmology. 1983;90:279–90.
91. Haynes BF, Fishman ML, Fauci AS, Wolff SM. The ocular manifestations of Wegener's Granulomatosis. Fifteen years experience and review of the literature. Am J Med. 1977;63:131.
92. Baer JC, Raizman MB, Foster CS. Ocular Behcet's disease in the U.S.: clinical presentation and visual outcome in 29 patients. In: Masahiko U, Shigeaki O, Koki A, editors. Proceedings of the 5th international symposium on the immunology and immunopathology of the eye, Tokyo, 13–15 Mar 1990. New York: Elsevier Science; 1990. p. 383
93. Oppenheimer S, Hoffbrand BI. Optic neuritis and myelopathy in SLE. Can J Neurol Sci. 1986;13:129.
94. Svitra PP, Perry H. Vogt-Koyanagi-Harada (Uveomeningitic) syndrome. In: Albert DM, Jakobiec FA, editors. Principles and practice of ophthalmology. Philadelphia, PA: WB Sanders Company; 1994. p. 213–8.
95. Kincaid MC, Green WR. Ocular and orbital involvement in leukaemia. Surv Ophthalmol. 1983;27: 211–32.
96. Qualman SJ, Mendelsohn G, Mann RB, Green WR. Intraocular lymphomas: natural history based on a clinicopathologic study of eight cases and review of the literature. Cancer. 1983;52:878–86.
97. Font RL, Naumann G, Zimmerman LE. Primary malignant melanoma of the skin metastatic to the eye and orbit. Am J Ophthalmol. 1967;63:738–54.
98. Stephens RF, Shields JA. Diagnosis and management of cancer metastatic to the uvea: a study of 70 cases. Ophthalmology. 1979;86:1336–49.
99. Ryan SJ, Maumenee AE. Birdshot retinochoroidopathy. Am J Ophthalmol. 1980;89:31.
100. Kirkham TH, Ffytche TJ, Sanders MD. Placoid pigment epitheliopathy with retinal vasculitis and papillitis. Br J Ophthalmol. 1972;56:875.
101. Dodwell DG, Jampol LM, Rosenburg M, et al. Optic nerve involvement associated with MEWDS. Ophthalmology. 1990;97:862.
102. Fujisawa C, Fujiara H, Hasegawa E, et al. The cases of serpiginous choroiditis [Japanese]. Nippon Ganka Gakkai Zasshi. 1978;82:135.
103. McCluskey PJ, Watson PG, Lightman S, Haybittle J, Restori M, Branley M. Posterior scleritis: clinical features, systemic associations, and outcome in a large series of patients. Ophthalmology. 1999;106:2380–6.
104. Dutton D, Burde RM, Kingele TG. Autoimmune retrobulbar optic neuritis. Am J Ophthalmol. 1982;94:11–7.
105. IJdo JW, Conti-Kelly AM, Greco P, Abedi M, Amos M, Provenzale JM. Anti- phospholipid antibodies in patients with multiple sclerosis and MS-like illnesses: MS or APS? [see comments]. Lupus. 1999;8:109–15.
106. Sakuma R, Fujihara K, Sato N, Mochizuki H, Itoyama Y. Optic-spinal form of multiple sclerosis and antithyroid autoantibodies. J Neurol. 1999;246:449–53.
107. Bennet WM. Bronchial carcinoma presenting with non-metastatic bilateral papillitis. Br Dis Chest. 1986;80:189–90.
108. Boghen D, Sebag M, Michaud J. Paraneoplastic optic neuritis and encephalomyelitis. Report of a case. Arch Neurol. 1988;45:353–6.
109. Coppeto JR, Monteiro ML, Cannarozzi DB. Optic neuropathy associated with chronic lymphomatous meningitis. J Clin Neuro Ophthalmol. 1988;8:39–45.
110. Pillay N, Gilbert D, Ebers GC, Brown JD. Internuclear ophthalmoplegia and "optic neuritis": paraneoplastic effects of bronchial carcinoma. Neurology. 1984;34:788–91.
111. Perkin GD, Rose FC. Optic neuritis and its differential diagnosis. New York: Oxford medical publications, Oxford University Press; 1979.
112. Engell T, Sellebjerg E, Jensen C. Changes in the retinal veins in acute optic neuritis. Acta Neurol Scand. 1999;100:81–3.
113. Traugott U, Raine CS, McFarlin DE. Acute experimental allergic encephalomyelitis in the mouse: immunopathology of the developing lesion. Cell Immunol. 1985;91:240–54.
114. Prineas JW, Barnard RO, Kwon EE, et al. Multiple sclerosis: remyelination of nascent lesions. Ann Neurol. 1993;33:137–51.
115. Frick E. Optic neuritis and multiple sclerosis. Cell-mediated cytotoxicity by peripheral blood lymphocytes against basic protein of myelin, encephalitogenic peptide, cerebrosides and gangliosides. Eur Neurol. 1988;28:120–5.
116. Sellebjerg E, Christiansen M, Nielsen PM, Frederiksen JL. Cerebrospinal fluid measures of disease activity in patients with multiple sclerosis. Mult Scler. 1998;4:475–9.
117. Soderstrom M, Link H, Xu Z, Frederiksson S. Optic neuritis and multiple sclerosis: anti-MBP and anti-MBP peptide antibody-secreting cells are accumulated in CSF. Neurology. 1993;43:1215–22.
118. Navikas V, Link H. Review: cytokines and the pathogenesis of multiple sclerosis. J Neurosci Res. 1996; 45:322–33.

119. Shields DC, Tyor WR, Deibler GE, Banik NL. Increased calpain expression in experimental demyelinating optic neuritis: an immunocytochemical study. Brain Res. 1998;784:299–304.
120. Inuzuka T, Sato S, Baba H, Miyatake T. Neutral protease in cerebrospinal fluid from patients with multiple sclerosis and other neurological diseases. Acta Neurol Scand. 1987;76:18–23.
121. Navikas V, He B, Link J, Haglund M, Soderstrom M, Frederikson S. Augmented expression of tumour necrosis factor-alpha and lymphotoxin in mononuclear cells in multiple sclerosis and optic neuritis. Brain. 1996;119(1):213–23.
122. Potter NT, Bigazzi PE. Acute optic neuritis associated with immunization with the CNS myelin proteolipid protein. Investig Ophthalmol Vis Sci. 1992;33:1717–22.
123. Sellebjerg FT, Frederiksen JL, Olsson T. Anti-myelin basic protein and anti-proteolipid protein antibody-secreting cells in the cerebrospinal fluid of patients with acute optic neuritis. Arch Neurol. 1994;51:1032–6.
124. Warren KG, Catz I, Johnson E, Mielke B. Anti-myelin basic protein and anti-proteolipid protein specific forms of multiple sclerosis. Ann Neurol. 1994;35:280–9.
125. Sellebjerg F, Madsen HO, Frederiksen JL, Ryder LP, Svejgaard A. Acute optic neuritis: myelin basic protein and proteolipid protein antibodies, affinity, and the HLA system. Ann Neurol. 1995;38:943–50.
126. Sadovnik AD, Baird PA, Ward RH. Multiple sclerosis: updated risks for relatives. Am J Med Genet. 1988;29:533–41.
127. Wilkstrom J, Kinnunen E, Porras J. The age-specific prevalence ratio of familial multiple sclerosis. Neuroepidemiology. 1984;3:74–82.
128. Ebers GC, Bulman DE, Sadovnick AD, et al. A population-based study of multiple sclerosis in twins. N Engl J Med. 1986;315:1638–42.
129. Kinnunen E, Koskenvuo M, Kaprio J, Aho K. Multiple sclerosis in a nation-wide series of twins. Neurology. 1987;37:1627–9.
130. Sadovnik AD, Armstrong H, Rice GP, et al. A population-based study of multiple sclerosis in twins: update. Ann Neurol. 1993;33:281–5.
131. Mumford CJ, Wood NW, Kellar-Wood H, et al. The UK study of multiple sclerosis in twins. J Neurol. 1992;239 Suppl 2:62 (abstract).
132. Doolittle TH, Myers RH, Lehrich JR, et al. Multiple sclerosis sibling pairs: clustered onset and familial predisposition. Neurology. 1990;40:1546–52.
133. Bulman DE, Sadovnik AD, Ebers GC. Age of onset in siblings concordant for multiple sclerosis. Brain. 1991;114:937–50.
134. Haines JL, Terwedow HA, Burgess K, Pericak-Vance MA, Rimmler JB, Martin ER, et al. Linkage of the MHC to familial multiple sclerosis suggests genetic heterogeneity. The Multiple Sclerosis Genetics Group. Hum Mol Genet. 1998;7(8):1229–34.
135. Barcellos LF, Oksenberg JR, Green AJ, Bucher P, Rimmler JB, et al. Genetic basis for clinical expression in multiple sclerosis. Brain. 2002;125:150–8.
136. Butterfield RJ, Blankenhorn EP, Roper RJ, Zachary JF, Doerge RW, Teuscher C. Identification of genetic loci controlling the characteristics and severity of brain and spinal cord lesions in experimental allergic encephalomyelitis. Am J Pathol. 2000;157:637–45.
137. Sobel RA. Genetic and epigenetic influence on EAE phenotypes induced with different encephalitogenic peptides. J Neuroimmunol. 2000;108:45–52.
138. Cree B. Multiple sclerosis genetics. Update on multiple sclerosis I: basic science. Lecture conducted from the American Academy of Neurology Meeting: Honolulu, HI; 2011
139. Rizzo JF, Lessell S. Risk of developing multiple sclerosis after uncomplicated optic neuritis: a long-term prospective study. Neurology. 1988;38:185–90.
140. Beck RW, Trobe JD. The optic neuritis treatment trial. Putting the results in perspective. The Optic Neuritis Study Group. J Neuroophthalmol. 1995;15:131–5.
141. Sadovnick AD, Ebers GC, Dyment DA, et al. Evidence for genetic basis of multiple sclerosis. The Canadian Collaborative Study Group. Lancet. 1996;347(9017):1728–30.
142. Ebers GC, Sadovnick AD, Dyment DA, et al. Parent-of-origin effect in multiple sclerosis: observations in half-siblings. Lancet. 2004;363(9423):1773–4.
143. Willer CJ, Dyment DA, Sadovnick AD, et al. Canadian Collaborative Study Group. Timing of birth and risk of multiple sclerosis: population based study. BMJ. 2005;330(7483):120.
144. Dean G, Kurtzke JF. On the risk of multiple sclerosis according to age atimmigration to South Africa. Br Med J. 1971;3(5777):725–9.
145. Burrell AM, Handel AE, Ramagopalan SV, et al. Epigenetic mechanisms in multiple sclerosis and the major histocompatibility complex (MHC). Discov Med. 2011;11(58):187–96.
146. Sorensen TL, Frederikson JL, Bronnum-Hansen H, Petersen HC. Optic neuritis as onset manifestation of multiple sclerosis: a nationwide, long-term survey. Neurology. 1999;53:473–8.
147. Beck RW, Cleary FA. Optic neuritis treatment trial. One-year follow-up results [see comments]. Arch Ophthalmol. 1993;111:773–5.
148. Kupersmith MJ, Alban T, Zeiffer B, Lefton D. Contrast-enhanced MRI in acute optic neuritis: relationship to visual performance. Brain. 2002;125(Pt 4):812–22.
149. Uhthoff W. Untersuchungen uber die bei der multiplen herdsklerose vorkommenden augenstorungen. Arch Psychiatr Nervenkr. 1890;21(55–116):303–410.
150. Scholl GB, Song H-S, Wray SH. Uhthoff's symptom in optic neuritis: relationship to magnetic resonance imaging and development of multiple sclerosis. Ann Neurol. 1991;30:180–4.

151. Nelson D, Jeffreys WH, McDowell F. Effect of induced hyperthermia on some neurological diseases. Arch Neurol Psychiatr. 1958;79:31–9.
152. Optic Neuritis Study Group. Multiple sclerosis risk after optic neuritis: final optic neuritis treatment trial follow-up. Arch Neurol. 2008;65:727–32.
153. Lucchinetti CF, Kiers L, O'Duffy A, et al. Risk factors for developing multiple sclerosis after childhood optic neuritis. Neurology. 1997;49(5):1413–8.
154. Wilejto M, Shroff M, Buncic JR, et al. The clinical features, MRI findings, and outcome of optic neuritis in children. Neurology. 2006;67(2):258–62.
155. Bonhomme GR, Waldman AT, Balcer LJ, et al. Pediatric optic neuritis: brain MRI abnormalities and risk of multiple sclerosis. Neurology. 2009;72: 881–5.
156. Waldman AT, Stull L, Balcer LJ, et al. Age at presentation determines the risk of pediatric multiple sclerosis after unilateral or bilateral optic neuritis (abstract). Presented at the Child Neurology Society Annual Meeting: Louisville, KY; 2009
157. Beck RW, Arrington J, Murragh FR, Cleary PA, Kaufinan DI. Brain magnetic resonance imaging in acute optic neuritis. Experience of the Optic Neuritis Study Group. Arch Neurol. 1993;50:841–6.
158. Brex PA, Ciccarelli O, O'Riordan JI, Sailer M, Thompson AJ, Miller DH. A longitudinal study of abnormalities on MRI and disability from multiple sclerosis. N Engl J Med. 2002;346(3):199–200.
159. Druschky A, Heckmann JG, Claus D, Katalinic A, Druschky KF, Neundorfer B. Progression of optic neuritis to multiple sclerosis: An 8-year follow-up study. Clin Neurol Neurosurg. 1999;101:189–92.
160. Miller DH, Ormerod IE, McDonald WI, MacManus DG, Kendall BE, Kingsley DP. The early risk of multiple sclerosis after optic neuritis. J Neurol Neurosurg Psychiatry. 1988;51:1569–71.
161. Cornblath WT, Quint DJ. MRI of optic nerve enlargement in optic neuritis. Neurology. 1997; 48:821–5.
162. Guy J, Fitzsimmons J, Ellis EA, Beck B, Mancuso A. Intraorbital optic nerve and experimental optic neuritis. Correlation of fat suppression magnetic resonance imaging and electron microscopy. Ophthalmology. 1992;99:720–5.
163. Guy J, Mao J, Bidgood Jr WD, Mancuso A, Quisling RG. Enhancement and demyelination of the intraorbital optic nerve. Fat suppression magnetic resonance imaging. Ophthalmology. 1992;99:713–9.
164. Rolak LA, Beck RW, Paty DW, Tourtellotte WW, Whitaker JN, Rudick RA. Cerebrospinal fluid in acute optic neuritis: experience of the optic neuritis treatment trial. Neurology. 1996;46:368–72.
165. Ghezzi A, Torri V, Zaffaroni M. Isolated optic neuritis and its prognosis for multiple sclerosis: a clinical and paraclinical study with evoked potentials. CSF examination and brain MRI. Ital J Neurol Sci. 1996;17:325–32.
166. Cole SR, Beck RW, Moke PS, Kaufinail DI, Tourtellotte WW. The predictive value of CSF oligoclonal banding for MS 5 years after optic neuritis. Optic Neuritis Study Group. Neurology. 1998;51:885–7.
167. Skov AG, Skov T, Frederiksen JL. Oligoclonal bands predict multiple sclerosis after optic neuritis: a literature survey. Mult Scler. 2011;17(4):404–10.
168. Andersson T, Siden A. An analysis of VEP components in optic neuritis. Electromyogr Clin Neurophysiol. 1995;35:77–85.
169. Halliday AM. Visual evoked potentials in demyelinating disease. Adv Neurol. 1981;31:201–15.
170. Spehlmann R. Evoked potential primer. 1st ed. Boston, MA: Butterworth Publishers; 1985.
171. Frederiksen JL, Petrera J. Serial visual evoked potentials in 90 untreated patients with acute optic neuritis. Surv Ophthalmol. 1999;44 Suppl 1: S54–62.
172. de Seze J. Atypical forms of optic neuritis. Rev Neurol (Paris). 2001;168(10):697–701.
173. Costello F, Hodge W, Pan YI, et al. Retinal nerve fiber layer and future risk of multiple sclerosis. Can J Neurol Sci. 2008;35(4):482–7.
174. Talman LS, Bisker ER, Sackel DJ, et al. Longitudinal study of vision and retinal nerve fiber layer thickness in multiple sclerosis. Ann Neurol. 2010;67:749–60.
175. Wolf-Schnurrbusche UEK, Ceklic L, Brinkmann CK, et al. Macular thickness measurements in healthy eyes using six different optical coherence tomography instruments. Investig Ophthalmol Vis Sci. 2009;50:3432–7.
176. Petzold A, de Boer JF, Schippling S, et al. Optical coherence tomography in multiple sclerosis: a systematic review and meta-analysis. Lancet Neurol. 2010;9:923–32.
177. Henderson AP, Trip SA, Schlottmann PG, et al. An investigation of the retinal nerve fiber layer in progressive multiple sclerosis using optical coherence tomography. Brain. 2008;131(Pt1):277–87.
178. Pulicken M, Balcer LJ, Frohman E, et al. Optical coherence tomography and disease subtype in multiple sclerosis. Neurology. 2007;69:2085–92.
179. Costello F, Hodge W, Lorello GR, et al. Quantifying axonal loss after optic neuritis with optical coherence tomography. Ann Neurol. 2006;59:963–9.
180. Costello F, Pan YI, Eggenberger E, et al. Tracking retinal nerve fiber layer loss after optic neuritis: a prospective study using optical coherence tomography. Mult Scler. 2008;14:893–905.
181. Outteryck O, Zephir H, Defoort S, et al. Optical coherence tomography in clinically isolated syndrome: no evidence of subclinical retinal axonal loss. Arch Neurol. 2009;66(11):1373–7.
182. Henderson AP, Schlottmann PG, Altmann DR, et al. A preliminary longitudinal study of the retinal nerve fiber layer in progressive multiple sclerosis. J Neurol. 2010;257(7):1083–91.
183. Ingle GT, Sastre-Garriga J, Miller DH, et al. Is inflammation important in early PPMS? A longitudinal MRI study. J Neurol Neurosurg Psychiatry. 2005;76:1255–8.

184. Henderson AP, Altmann DR, Trip AS, et al. A serial study of retinal changes following optic neuritis with sample size estimates for acute neuroprotection trials. Brain. 2010;33(9):2592–602.
185. Gordon-Lipkin E, Reich DS, Smith SA, et al. Retinal nerve fiber layer is associated with brain atrophy in multiple sclerosis. Neurology. 2007;69:1603–9.
186. Gout O. Retinal nerve fiber layer is associated with brain atrophy in multiple sclerosis. Neurology. 2008;1:69.
187. Baier ML, Rudick RA, Miller D, et al. Low-contrast letter acuity testing captures visual dysfunction inpatients with multiple sclerosis. Neurology. 2005;64:992–5.
188. Grazioli E, Zivadinov R, Weinstock-Guttman B, et al. Retinal nerve fiber layer thickness is associated with brain MRI outcomes in multiple sclerosis. J Neurol Sci. 2008;268(1–2):12–7.
189. Fisher JB, Markowitz CE, Galetta SL, et al. Relation of visual function to retinal nerve fiber layer thickness in multiple sclerosis. Ophthalmology. 2006; 113:324–32.
190. Pueyo V, Fernandez J, Almarcegui C, et al. Axonal loss in the retinal nerve fiber layer in patients with multiple sclerosis. Mult Scler. 2008;14:609–14.
191. Albrecht P, Froehlich R, Hartung HP, et al. Optical coherence tomography measures axonal loss in multiple sclerosis independently of optic neuritis. J Neurol. 2008;254:1595–6.
192. Siger M, Dziegielewski K, Jasek L, et al. Optical coherence tomography in multiple sclerosis: thickness of the retinal nerve fiber layer as a potential measure of axonal loss and brain atrophy. J Neurol. 2008;255:1555–60.
193. Feuillet L, Reuter F, Audoin B, et al. Early cognitive impairment in patients with clinically isolated syndrome suggestive of multiple sclerosis. Mult Scler. 2007;13(1):124–7.
194. Burkholder BM, Loguidice MJ, Bisker E, et al. Macular volume determined by optical coherence tomography as a measure of neuronal loss in multiple sclerosis. Arch Neurol. 2009;66:1366–72.
195. Trip SA, Jones SJ, Altmann DR, et al. Retinal nerve fiber layer axonal loss and visual dysfunction in optic neuritis. Ann Neurol. 2005;58:383–91.
196. Trip SA, Jones SJ, Li WY, et al. Optic nerve diffusion tensor imaging in optic neuritis. Neuroimage. 2006;30:498–505.
197. Gugleta K, Kochkorov A, Grieshaber M, et al. Pattern of macular thickness changes measured by ocular coherence tomography in patients with multiple sclerosis. Klin Monbl Augenheilkd. 2008;225:408–12.
198. Green AJ, Cree BA. Distinctive retinal nerve fibre layer and vascular changes in neuromyelitis optica following optic neuritis. J Neurol Neurosurg Psychiatry. 2009;80(9):1002–5.
199. Ratchford JN, Quigg ME, Conger A, et al. Optical coherence tomography helps differentiate neuromyelitis optica and MS optic neuropathies. Neurology. 2009;73(4):302308.
200. Davies E, Jacobs D, Wilson J, et al. Ganglion cell layer volume by spectralis optical coherence tomography (OCT) in multiple sclerosis. Platform presentation at the NANOS Annual Meeting, Tucson, Arizona, 2010. http://www.nanosweb.org/i4a/pages/index.cfm?pageID=3513. Accessed 28 Nov 2010.
201. Mowry EM, Daniels AB, Jacobs DA, et al. Vision related quality of life in multiple sclerosis: correlation with new measures of low and high contrast letter acuity. J Neurol Neurosurg Psychiatry. 2009;80:767–72.
202. Balcer LJ, Calabresi PA, Confavreux C, et al. Natalizumab reduces visual loss in patients with relapsing multiple sclerosis. Neurology. 2007;68: 1299–304.
203. Polman CH, Edan G, Filippi M, et al. Diagnostic criteria for multiple sclerosis: 2005 revisions to the McDonald criteria. Ann Neurol. 2005;58:840–6.
204. Naismith RT, Xu J, Shepherd JB, et al. Optical coherence tomography is less sensitive than visual evoked potentials in optic neuritis. Neurology. 2009;73:46–52.
205. Reich DS, Gordon-Lipkin EM, Ozturk A, et al. Damage to the optic radiation in multiple sclerosis is associated with retinal injury and visual disability. Arch Neurol. 2009;66:998–1006.
206. Klistorner A, Nguyen T, Garrick R, Paine M, et al. Multifocal VEP and OCT in optic neuritis: a topographical study of the structure-function relationship. Doc Ophthalmol. 2009;118:129–37.
207. Beck RW, Backlund JC. The course of visual recovery after optic neuritis. Experience of the optic neuritis treatment trial. Ophthalmology. 1994;101:1771–8.
208. Beck RW. What we have learned from the optic neuritis treatment trial. Ophthalmology. 1995;102: 1504–8.
209. Klistorner A, Garrick R, Graham S, et al. Correlation between full-field and multifocal VEP's in optic neuritis. Doc Ophthalmol. 2008;116:19–27.
210. Fraser C, Graham S, Garrick R, et al. Multifocal visual evoked potential latency analysis: predicting progression to multiple sclerosis. Arch Neurol. 2006;63:847–50.
211. Jackson A, Laitt RD, Kassner A, et al. Optic neuritis: MR imaging with combined fat- and water-suppression techniques. Radiology. 1998;206:57–63.
212. Hickman SJ, Brierley CM, Silver NC, et al. Detection of optic nerve atrophy following a single episode of unilateral optic neuritis by MRI using a fat-saturated short-echo fast FLAIR sequence. Neuroradiology. 2001;43:123–8.
213. Hickman SJ, Jones SJ, Altmann DR, et al. A serial MRI study following optic nerve mean area in acute optic neuritis. Brain. 2004;127:2498–505.
214. Inglese M, Bianchi S, Gerevini S, et al. Irreversible disability and tissue loss in multiple sclerosis: a conventional and magnetization transfer magnetic resonance imaging study of the optic nerves. Arch Neurol. 2002;59:20–5.
215. Hickman SJ, Toosy AT, Miszkiel KA, et al. Visual recovery following acute optic neuritis – a clinical,

electrophysiological and magnetic resonance imaging study. J Neurol. 2004;251(8):996–1005.
216. Thorpe JW, Jones SJ, Moseley I, et al. Magnetisation transfer ratios and transverse magnetization decay curves in optic neuritis: correlation with clinical findings and electrophysiology. J Neurol Neurosurg Psychiatry. 1995;59:487–92.
217. Hickman SJ, Toosy AT, Jones SJ, et al. Serial magnetization transfer imaging in acute optic neuritis. Brain. 2004;127(Pt 3):692–700.
218. Trip SA, Jones SJ, Li WY, et al. Optic nerve magnetization transfer imaging and measures of axonal loss and demyelination in optic neuritis. Mult Scler. 2007;13:857–9.
219. Karim S, Poukens V, Demer JL. Demonstration of systematic variation in human intraorbital optic nerve size by quantitative magnetic resonance imaging and histology. Investig Ophthalmol Vis Sci. 2004;45:1047–51.
220. Ueki S, Matsuzawa H, Takagi M, et al. Assessment of axonal degeneration along the human visual pathway using diffusion trace analysis. Am J Ophthalmol. 2006;142:591–6.
221. Weigel M, Lazzaro A, Hennig J, et al. Fast and quantitative high-resolution magnetic resonance imaging of the optic nerve at 3.0 tesla. Invest Radiol. 2006;41:83–6.
222. Ciccarelli O, Hickman SJ, Parker GJ, et al. Optic radiation changes after optic neuritis detected by tractography-based group mapping. Hum Brain Mapp. 2005;25:308–16.
223. Audoin B, Au Duong MV, Ibarrola D, et al. Voxel-based analysis of MTR images: a method to locate gray matter abnormalities in patients at the earliest stage of multiple sclerosis. J Magn Reson Imaging. 2004;20:765–71.
224. Toosy AT, Miszkiel KA, Jones SJ, et al. Adaptive cortical plasticity in higher visual areas after acute optic neuritis. Ann Neurol. 2005;57:622–33.
225. Langkilde AR, Rostrup E, Larsson HB. Functional MRI of the visual cortex and visual testing in patients with previous optic neuritis. Eur J Neurol. 2002; 9:277–86.
226. Werring DJ, Toosy AT, Miller DH, et al. Recovery from optic neuritis is associated with a change in the distribution of cerebral response to visual stimulation: a functional magnetic resonance imaging study. J Neurol Neurosurg Psychiatry. 2000;68:441–9.
227. Jenkins T, Toosy A, Miszkiel K, et al. Dissecting structure-function interactions in acute optic neuritis to investigate neuroplasticity. Hum Brain Mapp. 2010;31:276–86.
228. Korsholm K, Madsen KH, Frederiksen JL, et al. Cortical neuroplasticity in patients recovering from acute optic neuritis. Neuroimage. 2008;42(2):836–44.
229. Beck RW, Trobe JD, Kaufman DI, et al. The effect of corticosteroids for acute optic neuritis on the subsequent development of multiple sclerosis. The Optic Neuritis Study Group. N Engl J Med. 1993;329: 1764–9.
230. Optic Neuritis Study Group. High- and low-risk profiles for the development of multiple sclerosis within 10 years after optic neuritis: experience of the optic neuritis treatment trial. Arch Ophthalmol. 2003;121:944–9.
231. Optic Neuritis Study Group. The 5-year risk of MS after optic neuritis. Experience of the optic neuritis treatment trial. Neurology. 1997;49:1404–13.
232. Beck RW, Chandler DL, Cole SR, et al. Interferon beta-1a for early multiple sclerosis: CHAMPS trial subgroup analyses. Ann Neurol. 2002;51: 481–90.
233. Roed HG, Langkilde A, Sellebjerg F, et al. A double-blind, randomized trial of IV immunoglobulin treatment in acute optic neuritis. Neurology. 2005; 64(5):804–10.
234. Noseworthy JH, O'Brien PC, Petterson TM, et al. A randomized trial of intravenous immunoglobulin in inflammatory demyelinating optic neuritis. Neurology. 2001;56(11):1514–22.
235. Ruprecht K, Klinker E, Dintelmann T, Rieckmann P, Gold R. Plasma exchange for severe optic neuritis: treatment of 10 patients. Neurology. 2004;63(6):1081–3.
236. Kinkel RP, O'Connor P, Murray TJ, et al. IM interferon beta-1a delays definite multiple sclerosis 5 years after a first demyelinating event. Neurology. 2006;66:678–84.
237. Comi G, Barkhof F, Durelli L, et al. Early Treatment of Multiple Sclerosis Study Group. Effect of early interferon treatment on conversion to definite multiple sclerosis: a randomised study. Lancet. 2001;357:1576–1582.
238. O'Connor P. The effects of intramuscular interferon beta-1a in patients at high risk for development of multiple sclerosis: a post hoc analysis of data from CHAMPS. Clin Ther. 2003;25:2865–74.
239. Kappos L, Polman CH, Edan G, et al. Long-term effect of early treatment with interferon beta-1b after a first clinical event suggestive of multiple sclerosis: 5-year active treatment extension of the phase 3 BENEFIT trial. Lancet Neurol. 2009;8:987–97.
240. Comi G, Rodegher M, Moiola L, et al. Effect of glatiramer acetate on conversion to clinically definite multiple sclerosis in patients with clinically isolated syndrome (PreCISe study): a randomised, double-blind, placebo-controlled trial. Lancet. 2009;374:1503–11.
241. Fisniku LK, Brex PA, Altmann DR, et al. Disability and T2 MRI lesions: a 20-year follow-up of patients with relapse onset of multiple sclerosis. Brain. 2008;131:808–17.
242. Kappos L, Polman CH, Freedman MS, et al. Treatment with interferon beta-1b delays conversion to clinically definite and Mc Donald MS in patients with clinically isolated syndromes. Neurology. 2006;67:1242–9.
243. Gilmore CP, Cottrell DA, Scolding NJ, et al. Window of opportunity for no treatment in early multiple sclerosis? Mult Scler. 2010;16(6):756–9.

244. Masjuan J, Alvarez-Cermeno JC, Garcia-Barragan N, et al. Clinically isolated syndromes: a new oligoclonal band test accurately predicts conversion to MS. Neurology. 2006;66:576–8.
245. Polman CH, Reingold SC, Banwell B, et al. Diagnostic criteria for multiple sclerosis: 2010 revisions to the McDonald criteria. Ann Neurol. 2011; 69(2):292–302.
246. Bizzoco E, Lolli F, Repice AM, et al. Prevalence of neuromyelitis optica spectrum disorder and phenotype distribution. J Neurol. 2009;256:1891–8.
247. Cabre P, Heinzlef O, Merle H, et al. MS and neuromyelitis optica in Martinique (French West Indies). Neurology. 2001;56:507–14.
248. Wingerchuk DM, Hogancamp WF, O'Brien PC, Weinshenker BG. The clinical course of neuromyelitis optica (Devic's syndrome). Neurology. 1999; 53(5):1107–14.
249. Yamakawa K, Kuroda H, Fujihara K, et al. Familial neuromyelitis optica (Devic's syndrome) with late onset in Japan. Neurology. 2000;55(2):318–20.
250. Wingerchuk DM, Lennon VA, Pittock SJ, Lucchinetti CF, Weinshenker BG. Revised diagnostic criteria for neuromyelitis optica. Neurology. 2006;66(10): 1485–9.
251. Wingerchuk DM, Lennon VA, Lucchinetti CF, et al. The spectrum of neuromyelitis optica. Lancet Neurol. 2007;6:805–15.
252. Green AJ, Cree BAC. Distinctive retinal nerve fiber layer and vascular changes in neuromyelitis optic following optic neuritis. J Neurol Neurosurg Psychiatry. 2009;80:1002–5.
253. Roemer SF, Parisi JE, Lennon VA, et al. Pattern-specific loss of aquaporin-4 immunoreactivity distinguishes neuromyelitis optica from multiple sclerosis. Brain. 2007;130:1194–205.
254. Aoki-Yoshino K, Uchihara T, Duyckaerts C, et al. Enhanced expression of aquaporin-4 in human brain with inflammatory diseases. Acta Neuropathol. 2005;110:281–8.
255. Wang AG, Yen MY, Fann MJ. The expression of aquaporin-4 in the retina and optic nerve. Immunofluorescence staining of human and mouse retina and optic nerve Presented at the Asian Society of Neuro-Ophthalmology, Taipei, 2008; abstract FP-10.
256. Parisi V, Manni G, Spadero M, et al. Correlation between morphological and functional retinal impairment in multiple sclerosis. Investig Ophthalmol Vis Sci. 1999;40:2520–7.
257. Sepulcre J, Murie-Fernandez M, Salinas-Alaman A, et al. Diagnostic accuracy of retinal abnormalities in predicting disease activity in MS. Neurology. 2007;68:1488–94.
258. Quigley HA, Miller NR, Green WR. The pattern of optic nerve fiber loss in anterior ischemic optic neuropathy. Am J Ophthalmol. 1985;100:769–76.
259. Mok KH, Lee VW, So KF. Retinal nerve fiber loss pattern in high-tension glaucoma by optical coherence tomography. J Glaucoma. 2003;12:255–9.
260. Pittock SJ, Lennon VA, Krecke K, et al. Brain abnormalities in neuromyelitis optica. Arch Neurol. 2006;63:390–6.
261. Ito S, Mori M, Makino T, et al. "Cloud-like enhancement" is a magnetic resonance imaging abnormality specific to neuromyelitis optica. Ann Neurol. 2009;66:425–8.
262. Nakamura M, Misu T, Fujihara K, et al. Occurrence of acute large and edematous callosal lesions in neuromyelitis optica. Mult Scler. 2009;15:695–700.
263. Misu T, Fujihara K, Nakashima I, et al. Intractable hiccup and nausea with periaqueductal lesions in neuromyelitis optica. Neurology. 2005;65:1479–82.
264. Banwell B, Tenembaum S, Lennon VA, et al. Neuromyelitis optica-IgG in childhood inflammatory demyelinating CNS disorders. Neurology. 2008;70:344–52.
265. Poppe AY, Lapierre Y, Melancon D, et al. Neuromyelitis optica with hypothalamic involvement. Mult Scler. 2005;11:617–21.
266. Lennon VA, Wingerchuk DM, Kryzer TJ, et al. A serum autoantibody marker of neuromyelitis optica: distinction from multiple sclerosis. Lancet. 2004; 364:2106–12.
267. O'Riordan JI, Gallagher HL, Thompson AJ, et al. Clinical, CSF, and MRI findings in Devic's neuromyelitis optica. J Neurol Neurosurg Psychiatry. 1996;60:382–7.
268. Pirko I, Blauwet LK, Lesnick TG, et al. The natural history of recurrent optic neuritis. Arch Neurol. 2004;61(9):1401–5.
269. Rodriguez M, Siva A, Cross SA, O'Brien PC, Kurland LT. Optic neuritis: a population-based study in Olmsted County, Minnesota. Neurology. 1995; 45(2):244–50.
270. Francis DA, Compston DA, Batchelor JR, McDonald WI. A reassessment of the risk of multiple sclerosis developing in patients with optic neuritis after extended follow-up. J Neurol Neurosurg Psychiatry. 1987;50(6):758–65.
271. Wingerchuk DM, Weinshenker BG. Neuromyelitis optica: clinical predictors of a relapsing course and survival. Neurology. 2003;60(5):848–53.
272. Siritho S, Nakashima I, Takahashi T, Fujihara K, Prayoonwiwat N. AQP4 antibody-positive Thai cases: clinical features and diagnostic problems. Neurology. 2011;77(9):827–34.
273. Matiello M, Lennon VA, Jacob A, et al. NMO-IgG predicts the outcome of recurrent optic neuritis. Neurology. 2008;70:2197–200.
274. Takahashi T, Fujihara K, Nakashima I, et al. Anti-aquaporin-4 antibody is involved in the pathogenesis of NMO: a study on antibody titer. Brain. 2007;130:1235–43.
275. Hinson SR, Pittock SJ, Lucchinetti CF, et al. Pathogenic potential of IgG binding to water channel extracellular domain in neuromyeltiis optica. Neurology. 2007;69:2221–31.
276. Vincent T, Saikali P, Cayrol R, et al. Functional consequences of neuromyelitis optica-IgG astrocyte

interactions on blood–brain barrier permeability and granulocyte recruitment. J Immunol. 2008;181: 5730–7.
277. Hinson SR, Roemer SF, Lucchinetti CT, et al. Aquaporin-4 binding autoantibodies in patients with neuromyelitis optica impair glutamate transport by down-regulating EAAT2. J Exp Med. 2008; 205:2473–81.
278. Bennett JL, Lam C, Kalluri SR, et al. Intrathecal pathogenic anti-aquaporin-4 antibodies in early neuromyelitis optica. Ann Neurol. 2009;66:617–29.
279. Bradl M, Misu T, Takahashi T, et al. Neuromyelitis optica: pathogenicity of patient immunoglobulin in vivo. Ann Neurol. 2009;66:630–43.
280. Kinoshita M, Nakatsuji Y, Kimura T, et al. Neuromyelitis optica: passive transfer to rats by human immunoglobulin. Biochem Biophys Res Commun. 2009;386:623–7.
281. Saadoun S, Waters P, Bell BA, et al. Intracerebral injection of neuromyelitis optica immunoglobulin G and human complement produces neuromyelitis optica lesions in mice. Brain. 2010;133:349–61.
282. Wingerchuk DM, Weinshenker BG. Neuromyelitis optica. Curr Treat Options Neurol. 2005;7(3): 173–82.
283. Weinshenker BG, O'Brien PC, Petterson TM, et al. A randomized trial of plasma exchange in acute central nervous system inflammatory demyelinating disease. Ann Neurol. 1999;46:878–86.
284. Bonnan M, Valentino R, Olindo S, et al. Plasma exchange in severe spinal attacks associated with neuromyelitis optica spectrum disorder. Mult Scler. 2009;15:487–92.
285. Watanabe S, Nakashima I, Misu T, et al. Therapeutic efficacy of plasma exchange in NMO-IgG-positive patients with neuromyelitis optica. Mult Scler. 2007;13:128–32.
286. Bakker J, Metz L. Devic's neuromyelitis optica treated with intravenous gamma globulin (IVIg). Can J Neurol Sci. 2004;31:265–7.
287. Jacob A, Matiello M, Weinshenker BG, et al. Treatment of neuromyelitis optica with mycophenolate mofetil: retrospective analysis of 24 patients. Arch Neurol. 2009;66(9):1128–33.
288. Cree BA, Lamb S, Morgan K, et al. An open label study of the effects of rituximab in neuromyelitis optica. Neurology. 2005;64:1270–2.
289. Kim SH, Kim W, Li XF, et al. Repeated treatment with rituximab based on the assessment of peripheral cirating memory B cells in patients with relapsing neuromyelitis optica over 2 years. Arch Neurol. 2011;68(11):1412–20.
290. Weinshenker BG, Wingerchuk DM, Vukusic S, et al. Neuromyelitis optica IgG predicts relapse after longitudinally extensive transverse myelitis. Ann Neurol. 2006;59:566–9.
291. Yang Y, Huang DH, Wu WP, Wu L, Chen LF, Wu Q. The role of aquaporin-4 antibodies in Chinese patients with neuromyelitis optica. J Clin Neurosci. 2013;20(1):94–8.
292. Uzawa A, Mori M, Hayakawa S, et al. Different responses to interferon beta-1b treatment in patients with neuromyelitis optica and multiple sclerosis. Eur J Neurol. 2010;17:672–6.
293. Tanaka M, Tanaka K, Komori M. Interferon-beta (1b) treatment in neuromyelitis optica. Eur Neurol. 2009;62:167–70.
294. Shimizu Y, Yokoyama K, Misu T, et al. Development of extensive brain lesions following interferon beta therapy in relapsing neuromyelitis optica and longitudinally extensive myelitis. J Neurol. 2008;255: 305–7.
295. Palace J, Leite MI, Nairne A, et al. Interferon beta treatment in neuromyelitis optica: increase in relapses and aquaporin-4 antibody titers. Arch Neurol. 2010;67:1016–7.
296. Bergamaschi R, Uggetti C, Tonietti S, et al. A case of relapsing neuromyelitis optica treated with glatiramer acetate. J Neurol. 2003;250:359–61.
297. Gartzen K, Limmroth V, Puzki N. Relapsing neuromyelitis optica responsive to glatiramer acetate treatment. Eur J Neurol. 2007;14:e12–3.
298. Bhatti MT, Gres KE, Petitto VB, et al. Cells, cells, and more cells. Surv Ophthalmol. 2007;52(3):315–24.
299. Cross SA, Salomao DR, Parisi JE, et al. Paraneoplastic autoimmune optic neuritis with retinitis defined byCRMP-5-IgG. Ann Neurol. 2003;54(1):38–50.
300. Luiz JE, Lee AG, Keltner JL, et al. Paraneoplastic optic neuropathy and autoantibody production in small-cell carcinoma of the lung. J Neuroophthalmol. 1998;18(3):178–81.
301. Margolin E, Flint A, Trobe JD. High-titer collapsin response-mediating protein-associated (CRMP-5) paraneoplastic optic neuropathy and Vitritis as theonly clinical manifestations in a patient with small cell lung carcinoma. J Neuroophthalmol. 2008; 28(1):17–22.
302. Moss HE, Liu GT, Dalmau J. Glazed (vision) and confused. Surv Ophthalmol. 2010;55(2):169–73.
303. Rosencher L, Maisonobe T, Lavole A, et al. Neurologic paraneoplastic syndrome with anti-CV2/ CRMP5 antibodies revealing a small cell lung cancer. Effectiveness of the lung cancer treatment. Rev Neurol (Paris). 2012;168(4):371–4.
304. Thambisetty MR, Scherzer CR, Yu Z, et al. Paraneoplastic optic neuropathy and cerebellar ataxia with small cell carcinoma of the lung. J Neuroophthalmol. 2001;21(3):164–7.
305. Toribio-García JA, Franco-Benito M, García-Ruiz-de-Morales JM. [Paraneoplastic optic neuritis in an unknown small cell lung carcinoma defined by CRMP-5-IgG]. Arch Soc Esp Oftalmol. 2007; 82(12):777–80.
306. Nakayama-Ichiyama S, Yokote T, Hiraoka N, et al. A paraneoplastic neuromyelitis optica spectrum disorder associated with a mature B-cell neoplasm. Leuk Res. 2011;35(7):e111–3.
307. Lambrecht ER, van der Loos TL, van der Eerden AH. Retrobulbar neuritis as the first sign of the

glucagonoma syndrome. Int Ophthalmol. 1987; 11(1):13–5.
308. Kennedy MJ, Eustace P, O'Briain DS, et al. Paraneoplastic papilloedema in neuroblastoma. Postgrad Med J. 1987;63(744):873–6.
309. Scott JX, Moses PD, Somashekar HR, Sathish Kumar T. Paraneoplastic papilloedema in a child with neuroblastoma. Indian J Cancer. 2005;42(2):102–3.
310. Suzuki T, Obara Y, Sato Y, et al. Cancer-associated retinopathy with presumed vasculitis. Am J Ophthalmol. 1996;122(1):125–7.
311. Antoine JC, Honnorat J, Vocanson C, et al. Posterior uveitis, paraneoplastic encephalomyelitis and autoantibodies reacting with developmental protein of brain and retina. J Neurol Sci. 1993;117(1–2): 215–23.
312. Pulido J, Cross SA, Lennon VA, et al. Bilateral autoimmune optic neuritis and vitreitis related to CRMP-5-IgG: intravitreal triamcinolone acetonide therapy of four eyes. Eye (Lond). 2008;22(9): 1191–3.
313. Carboni G, Forma G, Bond AD, et al. Bilateral paraneoplastic optic neuropathy and unilateral retinal compromise in association with prostate cancer: a differential diagnostic challenge in a patient with unexplained visual loss. Doc Ophthalmol. 2012;125(1):63–70.
314. Hoh ST, Teh M, Chew SJ. Paraneoplastic optic neuropathy in nasopharyngeal carcinoma – report of a case. Singapore Med J. 1991;32(2):170–3.
315. Pillay N, Gilbert JJ, Ebers GC, et al. Internuclear ophthalmoplegia and "optic neuritis": paraneoplastic effects of bronchial carcinoma. Neurology. 1984; 34(6):788–91.
316. Kuroda Y, Miyahara M, Sakemi T, et al. Autopsy report of acute necrotizing opticomyelopathy associated with thyroid cancer. J Neurol Sci. 1991; 120(1):29–32.
317. Asproudis IC, Nikas AN, Psilas KG. Paraneoplastic optic neuropathy in a patient with a non-small cell lung carcinoma: a case report. Eur J Ophthalmol. 2005;15(3):420–3.
318. Murakami Y, Yoshida S, Yoshikawa H, et al. CRMP-5-IgG in patient with paraneoplastic optic neuritis with lung adenocarcinoma. Eye (Lond). 2007;21(6):860–2.
319. Hoogenraad TU, Sanders EACM, Tan KEWP. Paraneoplastic optic neuropathy with histopathological verification of absence of meningeal metastases. Neuroophthalmology. 1989;9:247–50.
320. Srikantha N, Goverdhan S, Evans A. Paraneoplastic optic neuropathy associated with papillary renal cell carcinoma. Br J Ophthalmol. 2010. [Epub ahead of print].
321. Yu Z, Kryzer TJ, Griesmann GE, Kim K, Benarroch EE, Lennon VA. CRMP-5 neuronal autoantibody: marker of lung cancer and thymoma-related autoimmunity. Ann Neurol. 2001;49(2):146–54.
322. Lennon VA, Yu Z, Kryzer TJ, et al. Are the newly discovered paraneoplastic anti-collapsin response-mediator protein 5 antibodies simply anti-CV2 antibodies? Reply Ann Neurol. 2001;50:690–1.
323. Pittock SJ, Kryzer TJ, Lennon VA. Paraneoplastic antibodies coexist and predict cancer, not neurological syndrome. Ann Neurol. 2004;56(5):715–9.
324. Sheorajpanday R, Slabbynck H, Van De Sompel W, et al. Small cell lung carcinoma presenting as collapsing response-mediating protein (CRMP)-5 paraneoplastic optic neuropathy. J Neuroophthalmol. 2006;26(3):168–72.
325. Battaller L, Dalmau JO. Paraneoplastic disorders of the central nervous system: update on diagnostic criteria and treatment. Semin Neurol. 2004;24(4):461–71.
326. Thambisetty MR, Scherzer CR, Yu Z, Lennon VA, Newman NJ. Paraneoplastic optic neuropaty and cerebellar ataxia with small cell carcinoma of the lung. J Neuroophthalmol. 2001;21(3):164–7.
327. Darnell RB, Posner JB. Paraneoplastic syndromes. New York: Oxford University Press; 2011.
328. Dispenzieri A. POEMS syndrome. Blood Rev. 2007;21:285–99.
329. Bolling JP, Brazis PW. Optic disc swelling with peripheral neuropathy, organomegaly, endocrinopathy, monoclonal gammopathy, and skin changes (POEMS syndrome). Am J Ophthalmol. 1990; 109(5):503–10.
330. Brazis PW, Liesegang TJ, Bolling JP, Kashii S, Trachtman M, Burde RM. When do optic disc edema and peripheral neuropathy constitute poetry? Surv Ophthalmol. 1990;35(3):219–25.
331. Casalé Turú A, Cabot Garcia J, Llanas Reus R, Nieto Uresandi MI, Monteagudo Jimenez M, Torremorell Balague D. Papilledema and POEMS syndrome. Ophthalmologica. 1992;205(3):144–8.
332. Chong DY, Comer GM, Trobe JD. Optic disc edema, cystoid macular edema, and elevated vascular endothelial growth factor in a patient with POEMS syndrome. J Neuroophthalmol. 2007;27(3):180–3.
333. Gutierrez-Ortiz C, Castro-Rebollo M, Pareja J, Beckford C, Teus M. Bilateral non-simultaneous optic neuropathy and unilateral macular edema in a patient with POEMS syndrome. Eur J Ophthalmol. 2009;19(1):166–9.
334. Okada K, Yamamoto S, Tsuyama Y, Mizunoya S. Case of POEMS syndrome associated with bilateral macular detachment resolved by autologous peripheral blood stemcell transplantation. Jpn J Ophthalmol. 2007;51(3):237–8.
335. Kaushik M, Pulido JS, Abreu R, Amselem L, Dispenzieri A. Ocular findings in patients with polyneuropathy, organomegaly, endocrinopathy, monoclonal gammopathy, and skin changes syndrome. Ophthalmology. 2011;118(4):778–82.
336. Gutierrez-Ortiz C, Castro-Rebollo M, Pareja J, Beckford C, Teus M. Bilateral non-simultaneous optic neuropathy and unilateral macular edema in a patient with POEMS syndrome. Eur J Ophthalmol. 2009;19(1):166–9.
337. Soubrier M, Dubost JJ, Serre AF, et al. Growth factors in POEMS syndrome: evidence for a marked

increase in circulating vascular endothelial growth factor. Arthritis Rheum. 1997;40(4):786–7.
338. Watanabe O, Arimura K, Kitajima I, Osame M, Maruyama I. Greatly raised vascular endothelial growth factor (VEGF) in POEMS syndrome. Lancet. 1996;347(9002):702.
339. Dai RP, Dong FT, Chu J. [Ocular features of polyneuropathy-organomegaly-endocrinopathy-monoclonal gammopathy-skin changes syndrome]. Zhonghua Yan Ke Za Zhi. 2005;41(10):917–9.
340. Bourdette DN, Rosenberg NL. Infiltrative orbitopathy, optic disk edema, and POEMS. Neurology. 1984;34(4):532–3.
341. Keltner JL, Thirkill CE, Huynh PM. Autoimmune-related retinopathy and optic neuropathy (ARRON) syndrome (Abstract). J Neuroophthalmol. 2002;22: 160–1.
342. Keltner JL, Thurkill CE. The 22 k-Da antigen in optic nerve and retinal diseases. J Neuroophthalmol. 1999;19:71–83.
343. Adamus G, Ren G, Weleber RG. Autoantibodies against retinal proteins in paraneoplastic and autoimmune retinopathy. BMC Ophthalmol. 2004;4:5.
344. Gitlits VM, Toh BH, Sentry JW. Disease association, origin, and clinical relevance of autoantibodies to the glycolytic enzyme enolase. J Investig Med. 2001;49: 138–45.
345. Ferreyra HA, Jayasundera T, Khan NW, et al. Management of autoimmune retinopathies with immunosuppression. Arch Ophthalmol. 2009;127: 390–7.
346. Jampol LM, Fishman GA. Imunosuppression for autoimmune retinopathy. Arch Ophthalmol. 2009; 127:573–5.

Ischemic Optic Neuropathies

2

Jane W. Chan

Nonarteritic Anterior Ischemic Optic Neuropathy (NAION)

Incidence of NAION

NAION is a relatively common disorder. The yearly incidence of NAION is 2.3–10.2 per 100,000 persons over 50 years of age and 0.5 per 100,000 for all ages [1]. Although NAION usually affects patients older than 50 years [2, 3], it may also occasionally occur in younger patients. In a study by Hayreh et al. [3] of 406 patients with NAION, the mean age of affected patients was 60 ± 14 years, with a range of 11–91 years. Eleven percent of the study patients were younger than 45 years, 49 % were between 45 and 64 years, and 40 % were 65 years or older. There is no sex predilection [3, 4]. Caucasians have a smaller cup-to-disc (C/D) ratio compared to that of African Americans. Most patients affected with NAION are, therefore, Caucasians [5].

Symptoms and Signs of NAION

In NAION, acute visual loss is usually painless and may present initially with blurred central vision, a visual field defect, or both. In the Ischemic Optic Neuropathy Decompression Trial (IONDT), 42 % (174 of 418) developed visual loss within 2 h of awakening, 42 % reported that the visual loss occurred later in the day, and the remainder could not recall the time of visual loss [6]. In the IONDT, 10 % (17/167) of patients reported mild retrobulbar or retro-orbital discomfort at the time of visual loss. Pain associated with eye movement, such as that seen in optic neuritis, is not considered a typical feature in NAION [6].

About half the patients in the IONDT had initial visual acuity better than 20/64 and were younger (less than 65 years), with a lower incidence of diabetes and hypertension, and 51 % (213 of 420) had visual acuity worse than 20/64 [6]. The degree of dyschromatopsia and the severity of the afferent papillary defect are usually proportional to the severity of visual acuity loss [7]. An absolute inferior *nasal* field defect is more common than an absolute inferior *altitudinal* defect. The combination of a relative inferior altitudinal defect with an absolute inferior nasal defect is most often observed in NAION [5]. Other types of field defects include central scotomas, arcuate defects, quadrantic defects, generalized constriction of the field, or a combination of these. In a study of 169 patients by Repka et al. [7], 46 % had inferior altitudinal visual field defects, 20 % had central defects, 17 % had superior altitudinal defects, 8 % had inferior arcuate defects, 8 % had inferior quadrantic defects, and 1 % had unclassified defects.

J.W. Chan, M.D. (✉)
Department of Neurology, Neuro-Ophthalmology,
University of Nevada School of Medicine,
975 Kirman Avenue (111), Reno, Nevada 89502, USA
e-mail: worjun@aol.com

J.W. Chan (ed.), *Optic Nerve Disorders: Diagnosis and Management*,
DOI 10.1007/978-1-4614-0691-4_2, © Springer Science+Business Media New York 2014

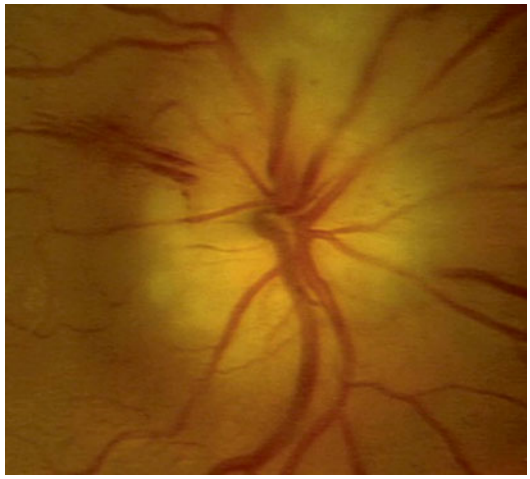

Fig. 2.1 Diffuse hyperemic disc swelling with peripapillary splinter hemorrhages can often be seen in NAION

The optic disc is more often diffusely swollen, rather than segmentally (Fig. 2.1) [8], in which the superior aspect of the disc is more involved than the inferior aspect. This pattern of superior or inferior involvement of the disc may be related to the anatomic division of the circle of Zinn-Haller [9]. The disc edema is pale rather than hyperemic, and flame-shaped hemorrhages may also be seen at or near the disc margin [9].

An absent cup or small cup-to-disc ratio is a major predisposing risk factor for the development of NAION. A smaller physiological optic disc cup represents a smaller scleral canal through which the optic nerve exits the eye. Crowding of the optic nerve fibers in the small scleral canal may lead to impairment of axonal transport and decreased laminar circulation [10].

Arteries in the peripapillary regions are usually focally or diffusely narrowed. In rare instances, hard exudates in the macula rarely may form a hemi-star or, rarely, a complete star figure [3]. After several days or weeks of onset of NAION, focal telangiectatic vessels may develop on the affected disc. It is thought that these changes represent a phenomenon called luxury perfusion, dilation of local blood vessels to allow increased perfusion of the area around the infarcted disc [2].

The optic disc edema usually resolves within 1–2 months after onset. The optic disc then becomes segmentally or diffusely pale. The optic cup rarely enlarges, as in arteritic AION and glaucoma [10].

Course and Prognosis of NAION

Within a week, most patients experience stabilization of their visual deficits, but visual function may continue to worsen over several days to even weeks after the onset of NAION. In the IONDT, 42 % (38 of 89) of the untreated patients also experienced spontaneous improvement of visual acuity by three or more Snellen lines from baseline after 6 months; 44.9 % had little or no change, and 12.4 % experienced worsening of visual acuity by three or more Snellen lines [11]. After 2 years of follow-up, 31 % (27 of 87) of these patients from the IONDT had improvement of three or more lines visual acuity, 47.1 % had little or no change, and 21.8 % experienced worsening of visual acuity by three or more lines [12]. Therefore, the natural history of visual recovery in NAION was better than previously reported in the literature [3, 7, 11].

There are limited data in the literature assessing the extent that visual fields may continue to progress after the onset of NAION. In a study by Arnold et al. [13], 22.2 % (6 of 22) patients had greater than 2 dB increase of mean sensitivity loss, which was measured more than 3 months after onset and may not have captured field loss in the progressive phase of NAION.

Recurrence of NAION in the same eye occurs in less than 5 % [14]. It is thought that optic disc atrophy after NAION could decrease crowding of the nerve fibers and reduce the risk of recurrence. Sequential occurrence of NAION is more common because most patients have small cup-to-disc ratios in both eyes [8]. The risk of fellow-eye involvement is 15 % within 5 years and is associated with poor baseline visual acuity in the first eye and to diabetes, but not associated with age, sex, smoking history, or aspirin use [15]. In a study by Repka et al. [7], 24 % (20 of 83) of patients with NAION had sequential involvement of the fellow eye. The mean time interval between involvement of the first eye and involvement of

the fellow eye was 2.9 years. In the IONDT, 23 % (94 of 420) patients had optic disc pallor in the fellow eye, suggestive of a prior episode of NAION. In a study of 4,431 patients by Beck et al. [16], the 2-year cumulative rate of developing NAION in the fellow eye was 15–20 % at 5 years.

Bilateral simultaneous NAION is rare and is more common in arteritic AION. A subtype of NIAON in juvenile diabetes presents simultaneously in both eyes in up to one-third of patients [17].

Differential Diagnosis of NAION

When atypical features of NAION occur, neuroimaging and other laboratory tests must be performed to rule out alternative diagnoses. Atypical features of NAION include the following: (1) onset at less than 40 years of age, (2) absence of vasculopathic risk factors, (3) no light perception (NLP) on initial presentation, (3) presence of vitreous cells, and (4) progression of visual field defect and persistent disc edema [18].

Other types of focal disc ischemia, mimicking NAION, may occur without disc swelling, as in patients with systemic hypertension. Sudden visual field defects, such as small arcuate or paracentral defects, with preserved visual acuity are associated with small nerve fiber layer hemorrhages at the disc margin. This portion of the disc then becomes pale and atrophied to cause a slight increase in the disc cup to mimic glaucomatous cup enlargement, but visual acuity or field defects do not usually progress, as in glaucoma [19].

The degree of rim pallor, location of rim pallor, and peripapillary retinal artery to vein (A:V) ratio can be useful in distinguishing optic atrophy from NAION or optic neuritis [20]. Disc pallor is often worse in NAION than after optic neuritis. The superior or inferior segment of the disc rim is affected in NAION compared to the temporal-central (papillomacular) or diffuse temporal rim in optic neuritis. The A:V ratio is often lower after NAION compared with that in optic neuritis [20].

Diagnostic Tests of NAION

On fluorescein angiography, optic disc filling is delayed in patients with NAION, but peripapillary choroidal filling is not always delayed [21].

Retinal nerve fiber layer (RNFL) thickness, as measured by a scanning laser polarimeter, the GDx nerve fiber layer analyzer (Laser Diagnostic Technologies, Inc., San Diego, CA), is thinner in AION eyes than in healthy eyes and correlates with visual field defects.

Neuroimaging can be used to help differentiate NAION from optic neuritis. In a retrospective study [22] of 64 patients diagnosed as having either NAION or optic neuritis, the optic nerve was abnormal in the clinically affected eye in 31 of the 32 optic neuritis patients but in only 5 of the 32 NAION patients. The five NAION patients had increased short (T1) inversion recovery signal in the affected optic nerve, and two had enhancement of the optic nerve.

Optical coherence tomography (OCT) has been used to assess RNFL thickness in patients with NAION. RNFL edema can be measured at the onset of NAION and RNFL thickness can be monitored over time in these patients. Although the Stratus OCT tends to provide higher C/D ratios than those estimated by slit lamp evaluation, Contreras et al. found that patients with NAION had a lower cup-to-disc ratios with a higher vertical integrated rim area (VIRA) than those in the normal population. The lower C/D ratio supports the hypothesis that a crowded optic nerve head is involved in the pathogenesis of NAION. Transient hypo- or nonperfusion leads to nerve fiber edema, which could lead to further ischemia, and finally to NAION. The higher VIRA in NAION fellow eyes compared with control eyes in the presence of a similar optic disc size and similar RNFL thicknesses could be explained by the more anterior position of the lamina cribosa in patients with NAION. Measurement technique by OCT may also influence this finding because nerve fibers have more space as they enter the deeper optic cup and some of them may not have been counted by the OCT software [21].

The relationship between the nerve fiber layer count and optic nerve size is still Debatable [22, 23].

Savini et al. found that the RNFL thickness increased significantly with an increase in optic disc size, while others have not confirmed this finding [21]. It is still unclear whether eyes with large optic nerve heads have a thicker RNFL because of more nerve fibers or because of a shorter distance between the circular scan and the optic disc edge, since the RNFL thickness decreases at increasing distances from the optic nervehead [23]. Based on Stratus OCT studies by Contreras et al., mean RNFL thickness was not correlated with disc size [21, 24]. Based on histopathological studies, the normal range of nerve fiber counts in the optic nerve is very wide [23]. No difference in optic disc size between those with NAION and control patients was observed [21].

C/D ratio increases about 50 % after NAION compared with the fellow eye and may be related to RNFL loss after ischemic damage. This finding could also support the hypothesis that cupping in eyes with NAION is more difficult to detect, compared to the cupping in arteritic AION eyes, because of the previously small or absent physiologic cup and the development of optic disc pallor [8, 21].

Bellusci et al. demonstrated that OCT can identify different patterns of RNFL loss related to specific typical visual field defects in NAION. In patients with an inferior altitudinal defect, RNFL loss was limited to the temporal, superior, and nasal optic disc quadrants in both the acute and chronic stages. In those with diffuse field loss, the RNFL was also diffusely decreased in all four quadrants. Those with only a central or cecocentral scotoma had RNFL atrophy in the superior and temporal quadrants, which corresponded to the involvement of axons from the papillomacular bundle [25].

RNFL thinning is also significantly more severe in the superior quadrant in NAION eyes which explains the common finding of an inferior altitudinal defect [26, 27]. DeLeon-Ortega et al. [27] showed that RNFL loss correlated significantly with the corresponding hemifield defect in NAION eyes, but also greater RNFL loss than control eyes even in the sectors corresponding to the relatively unaffected hemifield. RNFL loss in NAION eyes may extend beyond the area that corresponds to the visual field defect. Greater field loss is detected by frequency-doubling perimetry technology compared with standard automated perimetry in patients with NAION with altitudinal defects [28]. Temporal RNFL loss also corresponds to greater central visual acuity loss [26, 27]. Furthermore, OCT can diagnose optic disc edema and monitor RNFL loss over time, especially at onset and at 6 months after NAION, when RNFL loss has reached its plateau and is correlated with central visual acuity and visual field mean deviation [26]. The above findings suggest that OCT may play an important role in monitoring for the neuroprotective effects in clinical trials and for the estimation of visual prognosis. OCT can provide a quantitative measurement of ganglion cell loss in pale optic discs beyond what is seen and measured with other conventional clinical techniques.

Although the RNFL loss extends beyond the area corresponding to the visual field defect in glaucoma and NAION [28], greater RNFL loss occurs in the quadrant corresponding to the unaffected hemifield in glaucoma compared to NAION, while there was no noticeable difference between the two groups in the quadrant corresponding to the affected hemifield. Temporal quadrant RNFL loss, which is clinically correlated with central vision damage, is worse in NAION than in glaucoma [29].

Differentiation of NAION from Primary Open Angle Glaucoma

Greater excavation of the disc, greater thinning of the neuroretinal rim, and more RNFL loss is present in eyes with open-angle glaucoma than in those with either NAION or arteritic AION [30]. Disc rim RNFL may also be another objective measurement to differentiate open-angle glaucoma from NAION [31].

Risk Factors of NAION

In addition to a small cup-to-disc ratio, other common systemic disorders may be risk factors

for the development of NAION. An increased risk of NIAON occurs in 47 % of patients with hypertension and 24 % of patients with diabetes [1].

In a retrospective study based on the Medicare 5 % national database from 1991 to 2007, the risk of developing NAION among those with diabetes mellitus (DM) was 40 %. Male gender increased the risk of developing NAION by 32 %. No other covariate was statistically significantly associated with developing NAION. Among patients greater than 67 years of age, the annual incidence of NAION was 82 per 100,000 persons [32].

In the IONDT, 60 % of patients had one or more vasculopathic risk factors, including hypertension, diabetes, and tobacco use [3]. In an uncontrolled study of 137 patients, smoking was a significant risk factor for NAION in younger patients compared to nonsmokers [33]. Other studies have shown conflicting data in that hypertension was not found to be significantly more prevalent in patients with NAION than in age-matched controls [34]. Carotid artery stenosis or occlusion is not considered a cause of NAION, but rather there is evidence of widespread atherosclerosis affecting both large and small vessels. In a carotid ultrasound study with 15 patients with NAION [35], 11 patients with transient monocular blindness, and 30 age-matched controls, the mean carotid stenosis was not significantly worse in NAION patients (19 %) compared to controls (9 %), but more severe in patients with transient monocular blindness (77 %). Two of the 15 patients with NAION had carotid stenosis greater than 30 %, compared with 5 of 30 controls and 10 of 11 patients with transient monocular blindness.

Pathogenesis of NAION

Mechanical and anatomical factors have also been shown to influence the risk of developing NAION. A small cup-to-disc ratio, or a small disc with little or no physiological cupping, implies a small optic disc diameter and smaller scleral canal. Nerve fibers pass through a restricted space in the lamina cribosa and optic disc. The crowding of nerve fibers in this small canal and axoplasmic stasis associated with disc edema are the two factors thought to contribute to anterior disc ischemia. This compressive ischemia induces further stasis of axoplasmic flow, and a vicious cycle of ischemia ultimately ends in disc infarction [7]. Using digital imaging technology to reconstruct serial histopathological sections of an optic nerve affected by NAION, Tesser et al. [36] have shown that the morphology of the NAION infarct appears to be more consistent with a compartment syndrome causing tissue ischemia than a disease of blood vessels. In addition to a small disc size and small physiological cup, anatomic features in a "disk at risk" include elevation of the disc margins by a thick nerve fiber layer and anomalies of blood vessel branching. The sharp 90° turn of the retinal ganglion cell axons entering the lamina cribosa has also been thought to contribute mechanical stress to decrease axoplasmic flow [37, 38].

Vascular and hemodynamic factors are also thought to contribute to the pathogenesis of NAION. There has been no pathological evidence so far showing occlusion of the posterior ciliary arteries in patients with NAION, but fluorescein angiography has revealed delayed filling of the prelaminar optic disc in the edematous phase before the development of impaired filling associated with atrophy from loss of vasculature [39]. Further studies by Arnold et al. [40] showed that delayed prelaminar optic disc filling, appearing later than choroidal and retinal filling, was seen in 76 % of patients with acute NAION, compared with no delay in normal controls. No consistent delay in adjacent parapapillary choroidal filling was seen compared to normal controls. The delayed optic disc filling in NAION with normal parapapillary choroidal filling is suggestive of impaired perfusion within the paraoptic branches of the short posterior ciliary arteries supplying the optic disc distal to the branching of the choroidal vessels from the short posterior ciliary arteries. Vascular insufficiency in the paraoptic branches of these short posterior ciliary arteries that supply the laminar and prelaminar regions of the optic disc may result in ischemia and infarction [32]. These short posterior ciliary arteries form the circle of Zinn-Haller to supply

the anterior optic nerve in two distinct superior and inferior regions. Hypoperfusion in either of these vascular territories results in corresponding altitudinaldefects [41–43].

Nocturnal hypotension may play a role in the development of NAION. Hayreh et al. [44] showed that a 25.3 % decrease in systolic blood pressure and a 31.2 % decrease in diastolic blood pressure occurred in 52 patients with NAION during 24-h ambulatory blood pressure monitoring. No control patients were monitored, but the age-matched normal population for nocturnal diastolic reduction was only 7–21 %. Patients with worsening field defects from NAION and who were taking antihypertensive medications had even lower nocturnal diastolic reductions. Another study on 24 patients by Landau et al. [45] showed a mean systolic blood pressure reduction of 11 % and a mean diastolic blood pressure reduction of 18 % in patients with NAION, compared to controls, who had 13 % and 18 %, respectively. No significant difference was seen, but a substantially slower rise in blood pressure during the morning was observed in patients with NAION when compared to normal controls. Therefore, the role of nocturnal hypotension in the development of NAION remains unclear at this time.

Vasospasm from ineffective vascular autoregulation and/or structural changes in vessels causing narrowing may result in increased vascular resistance that then leads to reduced perfusion pressure in the optic nerve head [46]. Autoregulatory mechanisms may be impaired by arteriosclerosis, vasospasm, or antihypertensive medications, such as beta-blockers. In studies by Hayreh [47], serotonin-induced vasoconstriction was observed in central retinal arteries and posterior ciliary arteries of monkeys who had atherosclerosis. This abnormal vasoconstriction induced by endogenous serotonin released during platelet aggregation within atherosclerotic plaques was mediated by endothelial-derived vasoactive agents. Hayreh et al. proposed that this vasoconstriction could cause impaired autoregulation to result in hypoperfusion of the optic nerve head. These endogenous vasoactive agents, such as endothelin-1 and calcium ions, have been shown to cause hypoperfusion in the optic nerve head, as measured by laser Doppler flowmetry [48]. The ischemia was reversible with a calcium channel blocker. Another study showed that repeated intravitreal injections of endothelin-1 in rabbits reduced blood flow to the optic nerve head to cause axonal loss [49].

Treatment of NAION

Surgical decompression of the optic nerve and medical treatments, including anticoagulants [50], diphenylhydantoin [51], levodopa [52], sub-Tenon's injections of vasodilators [50], intravenous norepinephrine [53, 54], thrombolytic agents and stellate ganglion blocks [55], corticosteroids [56], aspirin [57], and heparin-induced low-density lipoprotein (LDL)/fibrinogen precipitation or hemodilution [58], have not been proven to be effective. Optic nerve decompression surgery (ONDS) failed to show any long-term benefit in patients with NAION, because the rate of improvement after ONDS was similar to the rate of spontaneous improvement, and this procedure had no influence on the clinical course of NAION [59]. In the IONDT, 23.9 % of patients undergoing surgery had a significantly greater risk of losing three or more lines of Snellen visual acuity at 6 months compared to 12.4 % of the patients without surgery. The IONDT Research Group finally recommended that ONDS should not be performed for acute NAION [10].

Although no proven treatments are available for NAION at this time, aspirin may have a role in decreasing the risk of recurrence of NAION in the second eye after NAION in the first eye. In a retrospective, uncontrolled study by Beck et al. [60], the 2-year cumulative probability of NAION in the second eye was 7 % in the 153 patients taking aspirin and 15 % in the 278 patients not taking aspirin. The 5-year cumulative probabilities in both groups were 17 % and 20 %, respectively. Although the long-term benefit of aspirin to prevent NAION in the second eye was minimal, the short-term, 2-year, benefit of taking aspirin appeared significant. In the follow-up study of the IONDT, NAION in the second eye occurred

in 14.7 % of IONDT patients over approximately 5 years. This rate of recurrence of NAION did not appear to be influenced by aspirin use [13].

In a prospective study of 696 consecutive eyes by Hayreh et al. [61], patients with acute NAION who presented within 2 weeks of onset, when optic disc edema is still present, were treated with prednisone starting at 80 mg a day with a taper over about a month. These patients had an initial visual acuity of 20/70 or worse with moderate to severe visual field defect. The treated group had a 69.8 % ($p=0.001$) visual acuity improvement and a 40.1 % ($p=0.005$) improvement in visual field defect after 6 months from onset of NAION. In both treated and untreated groups, these parameters continued to improve up to about 6 months from onset of NAION and minimally thereafter. Median follow-up of these patients was 3.8 years.

Corticosteroid therapy in acute NAION may decrease optic disc edema by reducing the capillary permeability and fluid leakage, as seen on fluorescein angiography. The patients with NAION treated with prednisone also had faster resolution of optic disc edema than the untreated ones. It is postulated that this faster resolution of optic disc edema leads to less compression of the capillaries in the optic nerve head and then to improved blood flow in the capillaries to provide better circulation in the optic nerve head for the function of the surviving axons and not the hypoxic ones [62].

Intravitreal triamcinolone acetonide for the treatment of NAION has been controversial with one study showing improvement in visual acuity but not in visual field defects [56] and another study showing no change in visual acuity [63]. The injection of triamcinolone acetonide increases the volume of the eyeball leading to a transient increase in intraocular pressure (IOP) for several days to weeks. This increase in IOP may further compromise the optic nerve head circulation [64].

Although the neuroprotective effects of topical brimonidine were promising in animal studies, 0.2 % brimonidine tartrate proved unsuccessful in patients with NAION [65]. In a 3-month double-blind, placebo-controlled, randomized multicenter trial of 36 patients older than 40 years of age with first-eye involvement of NAION within the first week after visual loss, the final visual acuity did not show any statistically significant difference by treatment. Nonsignificant trends for improved visual fields were noted in the brimonidine group. No serious adverse events occurred.

Levodopa and carbidopa have been shown in some studies to be effective in improving visual acuity and visual fields after NAION. In a prospective, randomized, double-blinded, placebo-controlled trial of 20 patients with NAION of 30 months mean duration, the patients treated with levodopa/carbidopa had a mean visual improvement of 7.5 letters from baseline compared with the placebo group. Three patients had a doubling of the visual angle as denoted by a gain of at least 15 letters. Color vision did not significantly change [66]. Although levodopa/carbidopa appears beneficial in the treatment of NAION, another study of 24 patients who were randomized to receive levodopa/carbidopa or placebo showed that the drug had no therapeutic effect on the visual recovery of patients with NAION. Side effects of levodopa, such as dizziness, orthostatic hypotension, vomiting, and cardiac arrhythmia, were observed [67].

Recent interest in using hyperbaric oxygen therapy for ischemic conditions has given rise to the possibility of its application to NAION. Although several studies by Bojic et al. [68–70] have shown promising results in patients with NAION with hyperbaric oxygen, data regarding the benefits of hyperbaric oxygen for NAION have been controversial. In the study of 20 patients by Arnold et al. [71], no significant improvement in visual acuity or visual field after treatment with 100 % oxygen at 2.0 atmospheres of pressure.

Heparin-induced extracorporeal LDL/fibrinogen precipitation (HELP) eliminates selectively fibrinogen, LDL, cholesterol, triglycerides, and LP(a) from blood plasma using extracorporeal circulation. The reduction of fibrinogen and LDL by about 50 % after only one procedure can be safe and more effective than hemodilution in NAION. LDL apheresis was tried successfully in a 64-year-old patient with bilateral sequential

NAION who had hyperlipidemia as his only risk factor. After undergoing three sessions of LDL apheresis, the scotomas reduced in size after each session until it remained stable at 6 months. His best corrected vision improved from 2/10 to 6/10 after the third session of treatment. LDL cholesterol and fibrinogen decreased after the third session from 239 to 31 mg/dL and from 289 to 92 mg/dL, respectively. Whether this man experienced spontaneously visual recovery coincidental with LDL apheresis is unclear [58].

Transvitreal optic neurotomy in the treatment of NAION involves relaxation of the scleral ring of the prelaminar and laminar regions of the optic nerve head to reduce constriction of underperfused nerve fibers. This scleral outlet compartment syndrome is thought to lead to necrosis of edematous nerve fibers. In a report by Soheilian et al. [72], seven patients with severe visual loss of less than 20/800 from NAION underwent transvitreal optic neurotomy. Visual acuity improved in six of seven patients. The mean preoperative visual acuity was 20/2,400 and the mean postoperative visual acuity was 20/250, with an average of ten lines of improvement. Visual fields improved in two patients who had enough visual acuity to undergo perimetry. Other patients with severe visual loss could not perform preoperative or postoperative visual field testing.

Anterior Ischemic Optic Neuropathy (AION) in Other Clinical Settings

Although NAION usually occurs in older patients with vasculopathic risk factors, AION may also occur in various other clinical settings.

Diabetic Papillopathy

Diabetic papillopathy is an atypical form of NAION [73]. In patients with juvenile diabetes, transient unilateral or bilateral optic disc edema often develops with mild or absent visual symptoms. Blind spot enlargement is more commonly seen than an arcuate field defect. Although these field defects may persist, visual acuity usually improves as the disc edema resolves [74–76]. The dilated, telangiectatic vessels on the disc, mimicking neovascularization, disappear as disc edema resolves. The formation of these vessels is thought to be related to the luxury perfusion phenomenon described after typical NAION [77, 78]. Diabetic papillopathy may develop in patients with or without diabetic retinopathy. Typical NAION with true disc neovascularization may also occur in patients with juvenile diabetes [79].

Diabetic papillopathy may also be seen in patients with adult-onset diabetes mellitus. In a study of 19 patients with diabetic papillopathy [79], the mean age of onset was 50 years of age and 33 % had type II diabetes mellitus. Hyperemic disc edema resolved within 3.7 months. Seventy percent of eyes had macular edema and 52 % of eyes had capillary nonperfusion on fluorescein angiography. Eighty-nine percent (34 of 38) of eyes had a final visual acuity of 20/50 or better. Decreased visual acuity was related to macular edema.

Similar to typical NAION, a small C:D ratio is a risk factor for the development of diabetic papillopathy. In a study of 27 eyes with diabetic papillopathy [79], 63 % (17 of 27) had cup-to-disc ratios of 0.1, which was significantly higher than normal controls. Diabetic papillopathy can even precede the development of typical NAION. Telangiectasia can often develop on the disc and may mimic neovascularization. In a report by Sato et al. [80], a 58-year-old woman with diabetes mellitus and small C:D ratios developed bilateral optic disc edema. Her left inferior altitudinal defect and hypoperfusion in the superior segment of the left optic disc on the early phase of the fluorescein angiogram were consistent with left NAION. Her right eye then developed similar findings. Although her vision recovered slightly, the visual field defects remained in both eyes.

NAION Associated with Optic Disc Drusen

NAION has been associated with optic disc drusen, which could cause compression of the optic nerve

fibers and decrease disc circulation [81]. Based on a review of 20 patients who experienced an episode of AION in an eye with optic disc drusen [82], the mean age of the patients was 49.4 years, with a range of 18–69 years. Fifty percent had vascular risk factors. Three patients reported episodes of transient visual loss before their permanent field defects. Sixty-two percent of eyes had 20/60 or better. Seventy-nine percent had an altitudinal or arcuate field defect, and 21 % had a cecocentral scotoma. Final visual acuity was 20/40 or better in 62 % of eyes and 20/200 or worse in 14 % of eyes. Patients with optic disc drusen-related NAION were younger than those with NAION, were more likely to report preceding episodes of transient visual obscuration, and had a better visual acuity outcome. Vascular risk factors, pattern of field defects, and occurrence of a subsequent similar event in the fellow eye were similar to those with NAION not related to optic disc drusen.

Chlamydia in AION

Increasing evidence links *Chlamydia pneumoniae* with atherosclerosis and other vascular disorders. In a retrospective case-controlled study of 71 patients with NAION and 71 controls matched for age and gender [83], patients with NAION had significantly higher IgG antibody titers to *C. pneumoniae*, an IgG titer of 1:128 or greater in 29 patients compared to 15 controls. The odds ratio for patients with an IgG titer of 1:128 or greater was 2.56 with a 95 % confidence interval of 1.2–5.5. Adjustment for hypertension, diabetes mellitus, and myocardial infarction resulted in an odds ratio of 3.48 with a 95 % confidence interval of 1.3–9.6. Although this study suggested that elevated titers of IgG antibodies to *C. pneumoniae* were associated with NAION, another study of 14 patients with NAION revealed that *C. pneumoniae* IgA, IgG, and IgM titers were not significantly different than those of age- and sex-matched controls. No specific *C. pneumoniae* nucleic acid sequences were detected in the AION patients or in the controls [84]. This study did not support the association of AION with previous *C. pneumoniae* infection. *C. pneumoniae* may play a role in initiating atherosclerosis, but its role in mediating specific vascular disorders is still unclear.

Shock-Induced AION

Shock-induced anterior ischemic optic neuropathy (SIAION) is associated with anemia and hypotension [85, 86]. Acute visual loss after spontaneous hemorrhage usually affects patients between 40 and 60 years of age [87]. Bilateral visual loss often occurs within 48 h after the onset of hemorrhage in about half of patients and may present up to 10 days later in 40 % of patients [73]. Unilateral visual loss occurs in about 12 % of patients [87].

A small C:D ratio, or "disk at risk," may be a risk factor for developing SIAION [88, 89]. In a review of fundus photos from 19 patients with SIAION [89], 14 patients had optic disc morphology typical of acute NAION. The affected optic disc was diffusely pallid and edematous and small. Most had small or absent central cups. Peripapillary hemorrhages were occasionally seen. The fellow unaffected eye also often had a small C:D ratio.

After acute spontaneous hemorrhage, about 50 % of patients with NAION experience some visual recovery, but only 10–15 % recover completely [90–95]. In most documented cases of spontaneous hemorrhage, the hemoglobin is less than 5.0 g/dL at the time of visual loss [90–95].

Hypotension and anemia are both risk factors for developing NAION in uremic patients on dialysis. NAION has been reported more often in chronic uremic adult patients (12) than in uremic children (5) on dialysis [96, 97]. Adult uremic patients who developed NAION were usually on dialysis for many years with chronic hypotension that was exacerbated during each dialysis treatment. They presented more often with bilateral, rather than unilateral, acute visual loss during hemodialysis [98, 99]. Neither the type of dialysis, hemo- or peritoneal dialysis, nor sex of the patient seemed to have any influence on the occurrence of NAION [96]. Some visual recovery

may be possible if the hypotension during dialysis is corrected in a timely manner. Two adult uremic patients have been reported to develop NAION in this setting recovered partial vision, such that the visual acuity in one eye of one of the patients improved from NLP for several hours to 20/40 [100].

Patients with end-stage renal disease and long-term hemodialysis who develop calcific uremic arteriolopathy can be at risk for developing NAION. In a report by Korzets et al. [101], two uremic patients presented with hypotension and acute unilateral visual loss. Although they were treated with high-dose steroid therapy, significant vision was not recovered. Their temporal artery biopsies revealed medial calcification. Hypoperfusion to the optic nerve head can result from a combination of hypotension and calcific arteriolopathy in arteries supplying the optic nerve.

Nonarteritic ischemic optic neuropathy may occur during the perioperative period, including cardiopulmonary bypass [102–106], aortofemoral bypass [107], various abdominal procedures [86, 90–95, 108], hip surgery [104], mitral valvulotomy, cholecystectomy [90], parathyroidectomy [109], lumbar spine surgery [107, 110, 111], and after coronary angiography [112]. In a review of 30 patients with perioperative ION [110], 17 were of the anterior type. Nonarteritic ischemic optic neuropathy was associated with hypotension and/or anemia and occurred mostly after coronary bypass surgery. The mean hemoglobin level decreased by 42 % (from 143 to 83 g/L) in four of the patients during the perioperative period. NAION associated with lumbar surgery was thought to result from the deliberate reduction of intraoperative blood pressure to reduce bleeding and the reluctance to transfuse because of the risk of human immunodeficiency virus type 1 transmission from contaminated blood. Twenty-eight of the patients in this study were older than 40 years of age and had the vascular risk factors for AION, such as hypertension, coronary artery disease, diabetes mellitus, and a history of smoking. Bilateral AION occurred in 18 of 30 patients. More than 50 % had visual acuity worse than 20/100 with little or no visual recovery. Most patients presented with optic disc edema at the time of initial visual loss, while others developed delayed disc edema several days later.

In a multicenter case–control study of 80 adult patients with ION from the American Society of Anesthesiologists Postoperative Visual Loss Registry, these patients were compared with 315 adult control subjects without ION after spinal fusion surgery. The risk factors associated with ION after spinal fusion surgery were obesity, male sex, Wilson frame use, longer anesthetic duration, greater estimated blood loss, and decreased percent colloid administration [113].

In a study of six patients with perioperative ION [107], three had the anterior type. Two patients had bilateral AION and one had unilateral AION. Their optic discs were small with little or no central cup. They all had hemoglobin levels less than 80 g/L for 30 min–72 h with decreased mean blood pressure between 24 and 46 % of preoperative levels for more than 15–120 min.

Because 10–15 % of cardiac procedures are currently performed without cardiopulmonary bypass to reduce morbidity, two patients who underwent off-pump cardiac surgery developed postoperative NAION [112]. Potential risk factors in the second patient were severe anemia, new onset atrial fibrillation with rapid ventricular rate, hypotension postoperatively, a small optic disc, uncontrolled diabetes mellitus, and a past medical history of hypertension and coronary artery disease.

NAION has also been reported to occur after large volume liposuction in two patients [114, 115].

NAION and Elevated IOP

It is unclear whether elevated IOP may play a role in the development of NAION. Studies in the past 36 years have revealed conflicting data. Elevated IOP and glaucoma were associated with NAION [116, 117]. In a study by Katz [117], the mean peak diurnal IOP was greater in 16 patients with NAION than in the 15 normal controls. It was suggested that a transient increase of IOP could lead to ischemia of the optic nerve head because of a decrease in perfusion pressure

below a threshold level. In a study by Hayreh et al. [118], the IOP was not elevated in patients with NAION compared to patients with open-angle glaucoma and normal tension glaucoma. In another study of 137 patients with NAION by Chung et al. [33], the mean IOP was 16.2 mmHg, which was similar to the IOP expected in the general population [119]. It is still unclear whether elevated IOP is associated with the development of NAION.

In a review by Williams et al. [120], some patients experienced both AION and posterior ischemic optic neuropathy (PION) from orbital or ocular compression during the face-down position in surgery. Increased IOP and decreased perfusion pressure in the optic nerve head during cervical spine surgery are thought to increase the risk of developing NAION. In a report by Abraham et al. [121], on an uneventful surgery for atlanto-axial dislocation in the prone position, a 32-year-old man developed sudden unilateral painless visual loss immediately postoperatively. He recovered his visual acuity completely in 1 month, but his optic disc pallor, inferior altitudinal defect, and color deficit persisted. No evidence of intraoperative anemia, hypotension, or vasculopathic risk factors was noted. His NAION was thought to be related to surgery in a prolonged prone position with his face on a malpositioned horseshoe headrest, which could potentially increase the IOP and decrease the perfusion pressure of the optic nerve head.

NAION and Chronic Anemias

In addition to hypoperfusion from acute hypotension and hemorrhagic-related anemia, chronic nutritional anemia may be a predisposing factor to NAION. Nonarteritic ION has been reported in severe folate deficiency anemia [122]. It is hypothesized that a low hematocrit can reduce the oxygen-carrying capacity of blood to lead to NAION [123]. A left NAION developed in a 37-year-old man with a hematocrit of 13.9 % and hemoglobin of 4.5, with a mean corpuscular volume of 125, corrected reticulocyte count of 0.5 %, and a folate level of 0.9 ng/mL (normal, greater than 1.8 ng/mL). The C/D ratio was not reported. Very low hemoglobin levels may decrease oxygen delivery to the prelaminar optic nerve to cause NAION. Even mild iron deficiency anemia has been associated with NAION. In a report by Kacer et al. [124], a 50-year-old woman developed unilateral NAION that was related to her underlying iron deficiency anemia with a hemoglobin of 7.3 g/dL and hematocrit of 25 %.

NAION and Coagulopathies

NAION has been associated with coagulopathies, such as antiphospholipid antibody syndrome, protein C and S deficiencies, antithrombin deficiency, tissue plasminogen activator deficiency, heterozygous factor V Leiden mutation, and methyltetrahydrofolate reductase mutations.

In a study by Acheson and Sanders [125], seven patients developed NAION associated with a prothrombotic state. The total number of patients tested was not reported. Two patients had reduced levels of protein C, one of protein S, one of antithrombin III, and one of tissue-plasminogen activator (t-PA). Two others were found to have the lupus anticoagulant. Bilateral visual loss occurred in six of seven patients and recurrent or progressive visual loss occurred in the same eye in four of seven patients. Two patients presented were less than 30 years of age. Many of these patients also had vasculopathic risk factors of hypertension, diabetes, and smoking. A subgroup of patients less than 40 years of age and recurrent episodes of visual loss may have NAION that needs to be treated with anticoagulants.

In the retrospective case-controlled study by Salomon et al. [126], 61 patients with NAION were tested for protein C, protein S, antithrombin III, lupus anticoagulant, Factor V, Factor II, and methyleneterahydrofolate reductase (MTHFR C677T). None of the genetic or acquired thrombophilic markers was a significant risk factor for NAION. Ischemic cardiac disease, hypercholesterolemia, and diabetes mellitus were deemed risk factors for NAION with odds ratios of 2.9 (95 % confidence interval, 1.3–6.4), 2.6 (95 % confidence interval, 1.2–5.5),

and 2.3 (95 % confidence interval, 1.1–4.8). Ischemic cardiac disease and hypercholesterolemia had an additive risk for NAION with a combined odds ratio of 4.5 (95 % confidence interval, 1.4–14.5). This study suggested that prothrombotic factors did not play a significant role in NAION, but vasculopathic factors were more important.

In a study of 25 patients with NAION by Nagy et al. [127], 24 % (6 of 25) had activated protein C resistance secondary to the heterozygous factor V Leiden mutation compared to only 5.9 % in the control group. Odds ratio calculations showed that patients with factor V Leiden mutation were at a significantly increased risk of developing NAION than control patients.

Patients with NAION may also have impairment of homocysteine metabolism [128]. Mild hyperhomocysteinemia is considered an independent risk factor for atherothrombotic disease, such as NAION. In a study by Kawasaki et al. [129], elevated plasma homocysteine was found in 17 % (2 of 12) of patients who had bilateral sequential NAION. Neither of these two patients had hypertension or had a history of smoking. One of them had mild hypercholesterolemia.

Nonarteritic ION can be associated with homozygosity for the C677T MTHFR mutation [130]. In a study of 12 patients with NAION, 58 % had at least one gene mutation in the C677T MTHFR, G1691A V Leiden, or G20210A prothrombin gene, compared with 14 % in the controls. The sample size had a power of 85 % to detect this case–control difference at alpha = 0.05. Of the eight women with NAION, 63 % first experienced visual loss while taking hormone replacement therapy or during pregnancy with estrogen-induced thrombophilia superimposed upon heritable thrombophilia and hypofibrinolysis. In another study by Weger et al. [131], however, hyperhomocysteinemia, not the MTHFR C677T mutation, was found to be associated with NAION.

Nonarteritic ION is also associated with a specific platelet polymorphism located on the glycoprotein Ib alpha gene [132]. In this study of 92 patients with NAION, the B allele of glycoprotein Ib alpha with a variable number of tandem repeats (VNTR) was an independent risk factor for NAION with an odds ratio of 4.25 and a 95 % confidence interval of 1.67–10.82. Fifty-six percent (9 of 16) of patients who had the B allele VNTR developed NAION in the fellow eye compared to only 23.6 % (17 of 72) of controls had second-eye involvement. Recurrence of NAION in the fellow eye occurred earlier in patients who had the specific gene polymorphism. The presence of the B allele VNTR of glycoprotein Ib alpha confers a significant risk for NAION and predisposes affected patients to fellow-eye involvement.

A prothrombotic abnormality should be ruled out in a patient who has any of the possible predisposing factors for NAION: (1) history of primary antiphospholipid antibody syndrome or other hypercoagulable states, (2) family history of clotting disorders, (3) absence of vasculopathic risk factors, (4) age of 40 years or less, (5) recurrent episodes of AION in the same eye or in the fellow eye, (6) history of smoking, and (7) use of estrogen–progestin oral contraceptives or replacement estrogen therapy [133, 134].

Laboratory studies should include complete blood count (CBC) with differential and platelets, sedimentation rate, fibrinogen level, prothrombin time, activated partial thromboplastin time, anticardiolipin IgM and IgG antibodies, lupus anticoagulant, fasting serum level of homocysteine, folate, and vitamin B12. When fasting serum homocysteine is elevated, the folate level is usually low and vitamin B12 level shows no significant change [133].

If prothrombotic abnormalities are present after checking laboratory abnormalities 6 months later, then a hematologist should be consulted for further management [133].

NAION in Migraine

Patients with classical migraines can occasionally develop NAION during a severe headache [132–140]. Vasospasm is believed to play a role in reducing perfusion to the optic nerve head [141]. In previously reported cases, visual acuity usually improved, but visual field did not.

Recurrence of NAION was not observed for up to 2–3 years after the initial attack.

Nonarteritic ION can occur in other disorders presenting with migraine, such as cerebral autosomal dominant arteriopathy with subcortical infarcts and leukoencephalopathy (CADASIL). In a report by Rufa et al. [142], a 60-year-old man with diffuse subcortical leukoencephalopathy, tetraparesis, and a family history of stroke presented with acute right visual loss at the age of 27 years. Re-evaluation at this later age revealed that his right optic disc atrophy was associated with arteriolar narrowing and decreased right visual acuity. Fluorescein angiography of the right eye revealed persistent peripapillary hypofluorescence with a retinal pigment epithelial window defect in the inferior temporal region. Pattern reversal visual evoked potentials were absent in the right. The left P100 latency was delayed and reduced in amplitude. The diagnosis of CADASIL was confirmed by molecular analysis, in which he was shown to be heterozygous for the C406T mutation on exon 3 of the Notch 3 gene. The possibility of CADASIL should be considered in patients with NAION who do not have typical cardiovascular risk factors but do have a family history of stroke.

NAION and Sleep Apnea Syndrome

Sleep apnea syndrome could play an important role in the pathogenesis of NAION. In a 2002 study by Mojon et al. [143], 71 % (12 of 17) patients with NAION had sleep apnea syndrome. Approximately 75 % of patients with NAION experience visual loss upon awakening [144]. It is hypothesized that repetitive prolonged apneas may impair optic nerve head blood flow autoregulation [145]. Impairment of vascular autoregulation in the optic nerve head may be a result of sleep apnea-related arterial blood pressure fluctuations (episodic nocturnal hypertension or hypotension), arteriosclerosis, and even an imbalance between vasodilators, such as nitric oxide, and vasoconstrictors, such as endothelin [134]. Episodic increased intracranial pressure during apnea [146] may also contribute to decreased circulation in the optic nerve head. In a prospective study of 108 patients with sleep apnea syndrome treated with continuous positive airway pressure (CPAP) between 4 months and 6 years, one patient had bilateral sequential NAION and two patients had unilateral NAION despite treatment with CPAP [147]. Larger studies are needed to clarify the role of CPAP in preventing NAION.

Arteritic AION

Incidence of Giant Cell Arteritis (GCA)

The most common vasculitic disorder that causes AION is GCA. AION is also the most common cause of visual loss in patients with GCA [148], comprising 71–83 % of cases [149, 150]. The yearly incidence is 20 per 100,000 persons more than 50 years of age [151, 152]. Because the incidence of GCA increases with age by about 22-fold from 60 to 90 years of age, more patients older than 65 years are affected by GCA than by NAION. The mean age at diagnosis of GCA is about 73 years throughout the world, regardless of country. In these studies, females were affected 2–3 times more often than men [153–158]. Cardiovascular risk factors, early menopause, and smoking, particularly in women, have been reported to be associated with an increased risk of GCA [159, 160]. The incidence of GCA is higher in Caucasians, especially of northern European descent, than in African Americans in the USA [151, 153].

Genetic Background of GCA

A genetic predisposition to GCA has been suggested from case reports of first-degree relatives and monozygotic twins [161–163]. Haplotypes of human leukocyte antigen (HLA) classes I and II, particularly the HLA-DRB1*04 haplotype, and gene polymorphisms for adhesion molecules, cytokines, chemokines, or growth factors. An association of HLA-DRB1*04 haplotype and risk of ocular involvement [164] or resistance to corticosteroids [165, 166] has been suggested.

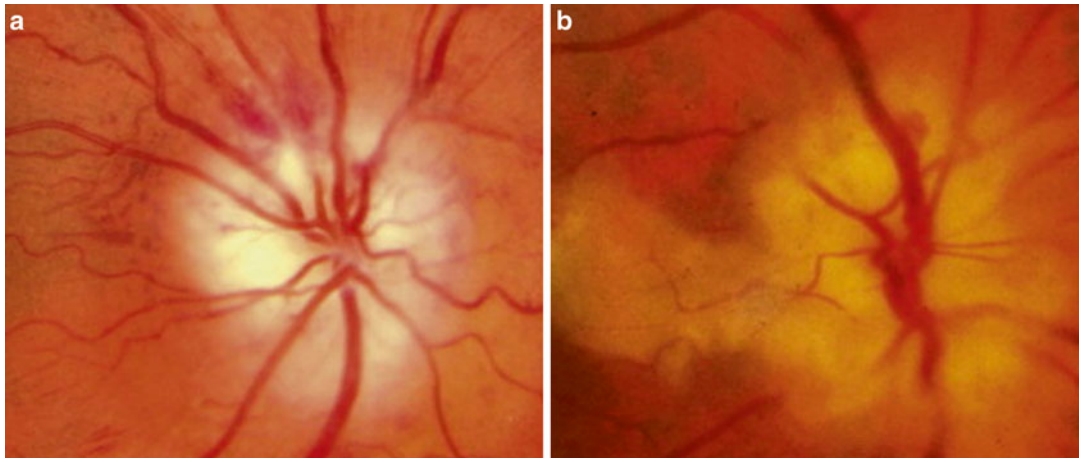

Fig. 2.2 (**a**) Chalky white edematous optic disc in arteritic AION. (**b**) Arteritic AION and cilioretinal artery occlusion

Symptoms and Signs of GCA

Besides advanced age, headache, scalp tenderness, jaw claudication, ear pain, myalgia, arthralgia, fatigue, fever, chills, malaise, anorexia, and weight loss are systemic symptoms associated with GCA [167]. More than 20 % of patients with positive temporal artery biopsies do not have these systemic symptoms [168]. The risk of permanent visual loss in GCA is increased in patients with transient visual loss and/or jaw claudication and decreased in those with elevated liver enzyme levels and/or constitutional symptoms [169].

Visual loss in arteritic AION may occur suddenly or may be preceded by transient monocular visual symptoms in 30 % of cases or by transient diplopia and amaurosis fugax in 2–30 % of cases [169]. These episodes of transient ischemia may lead to ION, central or branch retinal arterial occlusion, choroidal infarction, or a combination of any of these structures.

Visual loss is usually unilateral initially, but if untreated, becomes bilateral within days to weeks in 30 % of cases [169]. The visual loss is much more severe in patients with arteritic AION than in those with NAION. Approximately 54 % of patients with arteritic AION have a visual acuity of count fingers to NLP, compared to 26 % of patients with NAION [169]. In contrast to the hyperemic disc edema in NAION, the optic disc edema in arteritic AION often has a chalky-white appearance that may be complicated by retinal or choroidal ischemia, causing visual loss to be more severe (Fig. 2.2a, b) [5]. Cotton wool spots and flame-shaped intraretinal hemorrhages may also be seen in the peripapillary area. Unlike NAION, arteritic AION may occur in discs of any size.

Visual field defect in patients with arteritic NAION may be altitudinal, arcuate, and even more extensive than those with NAION [169].

Visual loss in arteritic AION is progressive and may affect the fellow eye in 25–50 % of patients within several days or weeks. As the swelling resolves, the disc becomes pale and the retinal arteries become narrowed. In contrast to NAION, cupping and neuroretinal rim loss can eventually develop in arteritic AION. Although these two disc features are also seen in glaucomatous optic neuropathy, arteritic AION is not associated with an enlargement of parapapillary atrophy [170].

Pathophysiology of GCA

The inflammation in arteritic AION affects blood vessels that lack an internal elastic lamina. The short posterior ciliary arteries supplying the retrolaminar and laminar regions of the optic disc

are most commonly affected. Sectors of choroid ischemia may occur concomitantly with arteritic AION. The ophthalmic artery, posterior ciliary arteries, and the intraneural central retinal artery are rarely affected to cause orbital ischemia. The severity of permanent loss in visual acuity and visual field is determined by the extent of infarction [169].

Granuloma formation in GCA is mediated by antigen-specific T cells. Th1 cells are corticosteroid resistant, whereas Th17 cells are explicitly corticosteroid sensitive. This difference in therapeutic responsiveness strongly suggests two independent inflammatory pathways to the disease process that would require other immunotherapies besides corticosteroids. Since high-dose corticosteroids and aspirin only inhibit Th17 cells which produce interferon-gamma (IFN-γ) (gamma), the corticosteroid-resistant Th1-mediated vasculitic inflammation continues for a year or longer (Fig. 2.3).

T cells and macrophages infiltrate into the layers of the arterial to directly or indirectly regulate the process of myofibroblast proliferation and matrix deposition. Multinucleated giant cells and macrophages located at the media–intima border produce not only platelet-derived growth factor (PDGF) but also vascular endothelial growth factor (VEGF) [171]. Both these angiogenic factors appear to play a role in the formation of neocapillaries to support the hyperplastic intima. VEGF production in the arterial wall is correlated with the concentration of IFN-γ (gamma) in the tissue [171]. IFN-γ (gamma) is produced by T lymphocytes in the adventitia of the inflamed artery [172, 173]. These T cells undergo clonal expansion in the artery and continue the disease process by regulating macrophages [173, 174]. Eradication of these T cells eliminates the disease, but IFN-γ (gamma) production has been shown to be relatively resistant to standard corticosteroid treatment [175]. Aspirin has been shown to decrease IFN-γ (gamma) production in the artery.

Arterial medial wall damage is the precursor to intimal hyperplasia. This damage is mediated by oxidative stress in the mitochondria of macrophages. Mitochondrial genes of macrophages have been found to be highly expressed in arteritic lesions [176, 177]. Evidence of reactive oxygen species from macrophages has been detected by antibodies to lipid peroxidation products in damaged smooth muscle membranes. These reactive oxygen intermediates combine with nitrogen intermediates to cause protein nitration of endothelial cells. The exact functional consequences of nitration in medial endothelial cells need to be investigated. With the fragmentation of the internal elastic lamina by metalloproteinases,

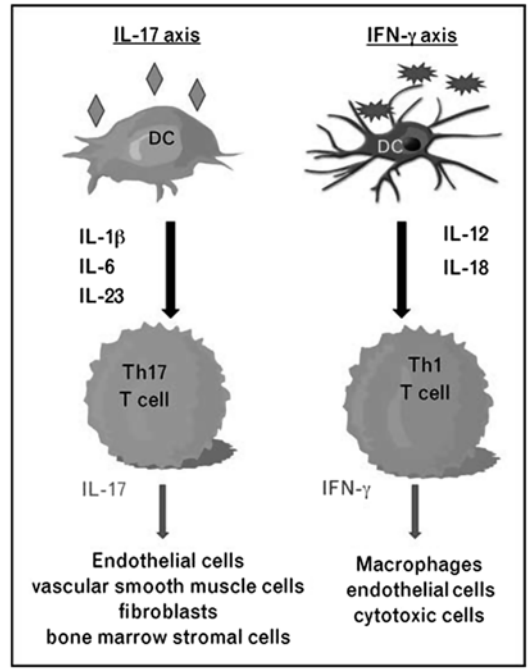

Fig. 2.3 Two separable immune axes participate in giant cell arteritis. Studies in untreated and treated GCA patient have indicated that two separable cytokine networks contribute to the vasculitic immune pathology. Dendritic cells producing IL-1b, IL-6, and IL-23 coax T cells to differentiate into IL-17 producers that modulate the function of endothelial cells, vascular smooth muscle cells, fibroblasts, and bone marrow stromal cells. In an independent immune pathway, dendritic cells release IL-12 to induce the differentiation of IFN-γ (gamma)-producing T cells. The downstream, target cells are macrophages, endothelial cells, and cytotoxic cells. The IL-17 axis is steroid responsive, whereas the IFN-γ (gamma) axis is steroid resistant. The separability of both axes is strongly suggestive for distinct immune instigators. GCA, giant cell arteritis [Reprinted from Weyand, CM, Younge, BR, Goronzy JJ. IFN-γ (gamma) and IL-17: the two faces of T-cell pathology in giant cell arteritis. Curr Opin Rheumatol. 2011;23:43–49. With permission from Wolters Kluwer Health]

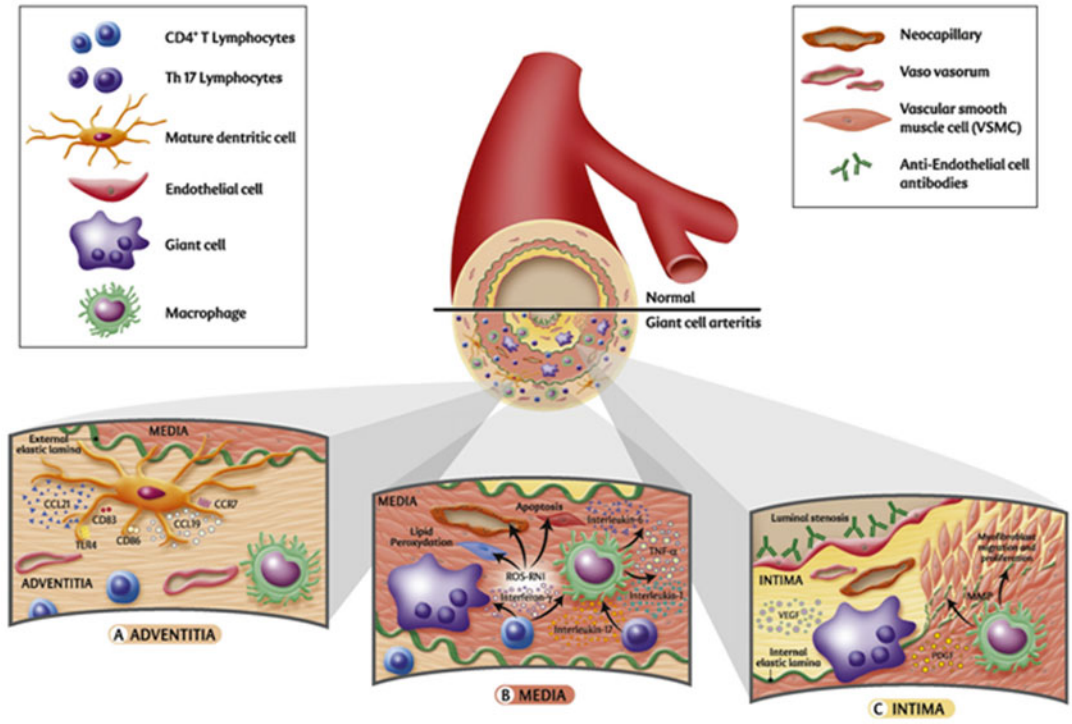

Fig. 2.4 Pathophysiology of GCA. (**a**) DCs are present in the adventitia, and at their surface, they express a number of components of the innate immune system such as TLR that recognize pathogen-associated molecular patterns. After activation by an unknown stimulus, mature DCs express CD83 or CD86, a co-receptor required for their interaction with TLs. They also produce CCR7 and homing chemokines such as CCL18, CCL19, CCL20, and CCL21 and their receptors. CCR7 binds CCL19 and CCL21 in an autocrine mechanism that contributes to DCs being trapped in the arterial wall. Thus, DCs may act as antigen-presenting cells, recruiting and activating CD4+ TLs and infiltrating the external elastic lamina and the intima–media junction. (**b**) TLs undergo clonal expansion. Most are IFN-γ (gamma)-producing Th1 TLs, which promote recruitment and activation of macrophages. However, IL-17-producing TLs, Th17 cells, which can induce proinflammatory cytokine production by macrophages, are also present in small proportions. Activated macrophages produce proinflammatory cytokines such as TNF-α (alpha), IL-1, and IL-6, thus promoting local and systemic inflammation. They can fuse, form giant cells, and participate in the formation of granulomas, which are located close to the internal elastic lamina, at the intima–media junction. Giant cells and medial macrophages release ROS and RNI, which contribute to VSMC and EC lipid peroxidation and apoptosis. (**c**) These cells also express MMPs, PDGF, and VEGF, which lead to the destruction of the internal elastic lamina, the pathological hallmark of GCA and vascular remodeling, with proliferation and migration of medial myofibroblasts and neoangiogenesis. These last events contribute to intimal hyperplasia and luminal stenosis. The role of anti-EC in the pathogenesis of GCA remains poorly understood. *Abbreviations*: *CCL* chemokine (C–C motif) ligand, *CCR* chemokine (C–C motif) receptor, *CD* cluster of differentiation, *DCs* dendritic cells, *ECs* endothelial cells, *IFN-γ* interferon-γ (gamma), *IL* interleukin, *GCA* giant cell arteritis, *MMP* matrix metalloproteinases, *PDGF* platelet-derived growth factor, *RNI* reactive nitrogen intermediates, *ROS* reactive oxygen species, *Th1* T helper 1 cells, *TL* T lymphocytes, *TLR* Toll-like receptor, *TNF-α (alpha)* tumor necrosis factor-α (alpha),*VEGF* vascular endothelial growth factor, *VSMCs* vascular smooth muscle cells [Reprinted from Ly K, Régent A, Tamby MC, Mouthon L, Pathogenesis of giant cell arteritis: More than just an inflammatory condition? Autoimmunity Reviews. 2010; 9:635–645. With permission from Elsevier]

myofibroblasts can migrate into the intimal layer where they proliferate and deposit extracellular matrix. Expansion of the hyperplastic intima is supported by neocapillaries via angiogenic factors derived from specialized macrophages. Hyperproliferation of the intimal layer may then ultimately lead to stenosis and occlusion (Fig. 2.4) [176, 177].

Evidence involving microorganisms as an etiological factor in GCA has been conflicting. Varicella-zoster virus and *C. pneumoniae* have been shown to be associated with GCA based upon DNA polymerase chain reaction (PCR) analysis [178, 179]. Other studies have not supported these data. Haugeberg et al. [180] did not detect *C. pneumoniae* by PCR in any of the 20 histologically proven biopsies of GCA. Regan et al. [181] reevaluated 90 biopsies and found no evidence of the *C. pneumoniae* 16S rRNA gene. In another smaller prospective study by Helweg-Larsen et al. [182], PCR analysis did not detect *C. pneumoniae*, parvovirus B19, or all the eight human herpes viruses [herpes simplex virus (HHV) 1 and -2, Epstein–Barr, cytomegalovirus, varicella-zoster, and HHV-6, -7, -8]. *Burkholderia* has also been recently identified in blood and superficial temporal artery biopsies of GCA patients [183].

Diagnosis of GCA

Clinical criteria for the diagnosis of GCA established by The American College of Rheumatology [184] (Table 2.1) can be unreliable for patients presenting with eye complications. These criteria are used to distinguish GCA from other systemic vasculitides for rheumatologic complaints without serious consequences. These same criteria can pose false-positive and false -negative diagnoses of GCA that would put vision at risk.

Table 2.1 Diagnostic criteria for GCA by the American College of Rheumatology, 1990 [Reprinted from Hunder GG, Bloch DA, Michel BA, et al. The American College of Rheumatology 1990 criteria for the classification of giant cell arteritis. Arthritis Rheum 1990;33(8):1122–8. With permission from John Wiley & Sons, Inc.]

The American College of Rheumatology 1990 criteria for the diagnosis of giant cell arteritis include three or more of the following:
• More than 50 years of age at disease onset
• New onset of localized headache
• Temporal artery tenderness or decreased temporal artery pulse
• Elevated ESR (Westergren) > 50 mm/h
• Biopsy sample including an artery showing necrotizing arteritis characterized by predominance of mononuclear cell infiltrates or a granulomatous process with multinucleated giant cells

Certain specific clinical features in the setting of acute visual loss have been shown to be associated with a positive temporal artery biopsy. According to Liu et al. [150] and Hall et al. [185] headache, jaw claudication, weight loss, malaise, anorexia, polymyalgia rheumatic, and chalky white disc edema were most associated with GCA. In decreasing order of importance, jaw claudication, a C-reactive protein (CRP) > 2.45 mg/L, neck pain, and ESR > 47 mm/h were most predictive of temporal arteritis in a study by Hayreh et al. [167].

An elevated sedimentation rate (ESR) is present in more than 95 % of patients with biopsy-proven GCA. The risk of developing GCA is not correlated with the degree of elevation, and 8–22 % of patients with biopsy-proven GCA have a normal ESR [186–189]. Therefore, patients with symptoms and signs suggestive of GCA with an ESR in the normal range should still undergo a temporal artery biopsy. Because no definitive studies exist on the range of ESR in normal persons, formulas by Miller et al. [190] allow an estimation of the normal ESR. The maximum normal ESR for a man may be calculated by dividing his age by 2. For a woman, the maximum normal ESR is equivalent to her age plus 10 divided by 2 [190]. An elevated ESR is not specific for GCA and may occur in other systemic inflammatory diseases. An elevated ESR with an elevated CRP is considered more sensitive in diagnosing GCA in 97 % of cases. The CRP is more sensitive at 100 % sensitivity than the ESR at 92 % sensitivity in patients with GCA. CRP rises more rapidly in the acute phase of GCA and responds more rapidly to the effects of treatment [167].

Thrombocytosis in which the platelet count is elevated to greater than 400×10^3/L may yield better diagnostic results than the ESR in terms of positive predictive value and negative predictive value in patients suspected of having GCA [191]. In a retrospective study of 91 patients who underwent temporal artery biopsy, the positive predictive value was 87 % and the negative predictive value was 67 % when using the platelet count as a diagnostic test for GCA. Using the ESR for

diagnosis resulted in a positive predictive value of 54 % and a negative predictive value of 55 % [161]. Because corticosteroids have been shown to cause an approximate 25 % reduction in the mean platelet count, this may serve as a marker of response to treatment [192]. Another retrospective comparison of 121 biopsy-confirmed GCA patients with 287 patients with NAION did not confirm these findings [193]. Patients with GCA had significantly higher platelet counts, ESR, CRP, and white blood count (WBC), but lower hemoglobin and hematocrit values compared to the NAION group. The predictive ability of elevated platelet count as a diagnostic marker for GCA was similar to that of ESR or CRP.

Although the pretreatment ESR may be a prognostic indicator for duration of treatment, CRP and interleukin-6 (IL-6) may be more sensitive indicators of disease activity than ESR in GCA patients [194].

The temporal artery biopsy is considered the gold standard for diagnosis of GCA. Its sensitivity in practice is 87.1 % (confidence interval of 95 %, 81.8–91.7 %) in a single temporal artery biopsy [195]. The temporal artery biopsy should be done within 1 week of starting prednisone, but it may be positive up to 1 month later if active disease persists. The rate of a positive temporal artery biopsy is 82 % if on no prednisone and 60 % if on ≤1 week of prednisone [196].

Because skip lesions may lead to false-negative biopsy results in 4–5 % of cases, it is recommended to obtain a biopsy specimen on the clinically affected side measuring at least 3 cm long [185].

In a study by Boyev et al. in 364 bilateral temporal artery biopsies, bilateral simultaneous or sequential temporal artery biopsies improve the diagnostic yield ≥3 % of GCA cases. The likelihood of a correct diagnosis is high since 97 % of cases had the same findings on both biopsies. The authors concluded that it was worthwhile to perform bilateral biopsies because delayed diagnosis/treatment of GCA could lead to permanent blindness and high morbidity, and long-term corticosteroid use in patients without GCA could pose unnecessary adverse side effects [197].

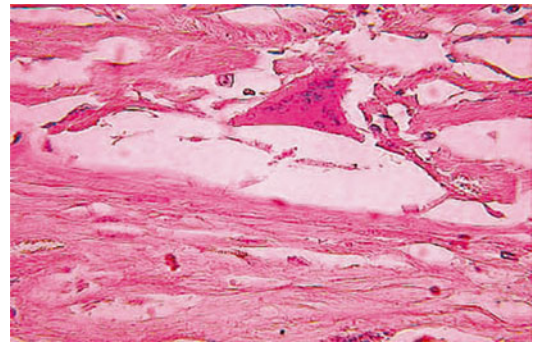

Fig. 2.5 H & E stain of a multinucleate giant cell

On the other hand, a unilateral temporal artery biopsy would be more advantageous for a population with a low clinical suspicion for GCA. It would require less time and would involve lower cost and risks of minor surgical complications than a bilateral biopsy. In a study by Hall et al., a unilateral temporal artery biopsy is associated with a low frequency of subsequent positive contralateral biopsy and no adverse visual or neurological outcomes. The discordance rate was low at 3.4 % in this study cohort [185].

Whether it is done unilaterally or bilaterally, the temporal artery biopsy should be done whether or not the patient has started corticosteroids. In a prospective study of patients with a clinical diagnosis of GCA, 86 % (six of seven) of patients who underwent a temporal artery biopsy after 4 weeks of corticosteroid treatment still had cellular infiltrates characteristic of active GCA [198]. Disruption or loss of the internal elastic lamina may be present up to 6 months after initiation of steroids [196]. If clinical suspicion of GCA is high in a patient with a negative biopsy, a second biopsy should be done [169, 185]. If a patient with negative bilateral biopsies is strongly suspected of having GCA, this patient should be treated despite negative biopsy results. A negative biopsy does not rule out GCA and the diagnosis of GCA is ultimately based on clinical judgment.

The pathological diagnosis of GCA requires the presence of macrophages in the elastica, with or without multinucleated giant cells (Fig. 2.5). Active GCA can have intimal thickening and edema, thrombosis and recanalization, chronic

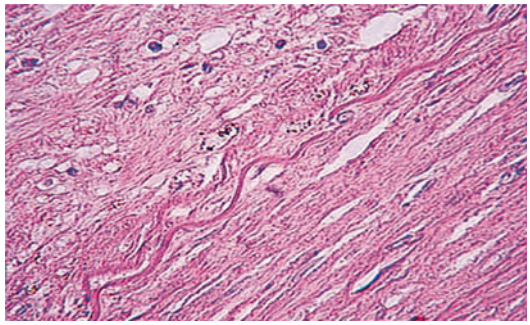

Fig. 2.6 H & E stain of fragmented internal elastica lamina

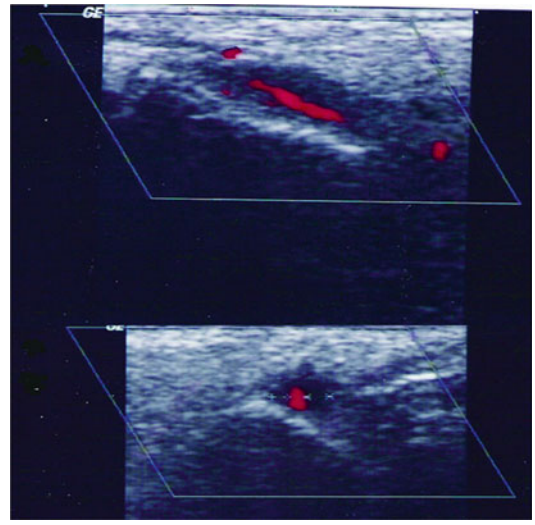

Fig. 2.7 Halo sign on U/S in patient with GCA. Hypoechoic area around the temporal artery in longitudinal view above and in cross-sectional view below [Reprinted from Karahaliou M, Vaiopoulos G, Papaspyrou S, Kanakis MA, Revenas K, Sfikakis PP. Color duplex sonography of temporal arteritis before decision for biopsy: a prospective study in 55 patients with suspected giant cell arteritis. Arthritis Research and Therapy. 2006;8:R116. With permission from Springer Science + Business Media]

inflammation with necrosis, fragmentation and loss of internal elastic lamina (Fig. 2.6), inflammatory infiltrate of lymphocytes, macrophages, and giant cells in all levels of the blood vessel wall; and thickened and scarred media and adventitia [199].

The presence of lymphocytes may result from surgical manipulation during the biopsy or to vasculitis other than GCA. Inflammatory changes may not be continuous along the artery and may result in skip lesions in approximately 8 % of cases [200]. Besides the presence of macrophages in the elastica, another important pathological feature is the reduplication, interruption, and fragmentation of the internal elastic lamina, which can occur in both active and healed GCA. The identification of internal elastic membrane calcification is diagnostically important because the inflammatory process in GCA starts as a foreign-body giant cell attack on calcified parts of the internal elastic membrane [201, 202].

Extensive choroidal hypoperfusion seen on fluorescein angiography is helpful in the diagnosis of GCA. Arteritic AION affects both the posterior ciliary and choroidal vessels compared to NAION, which affects only the posterior ciliary circulation. In patients with AION, a delay of choroidal filling is by more than 15 or 18 s. This delay of choroidal filling associated with acute visual loss and normal optic discs is suggestive of PION caused by GCA [169].

Color duplex sonography has been shown to be a noninvasive and inexpensive imaging technique to help localize inflammation in temporal arteritis and is sometimes used for a directional biopsy to increase the probability to confirm a clinical diagnosis of GCA (Fig. 2.7) [203]. Although it can image the course of the affected superficial temporal artery, seen as a hypoechoic halo effect from edema of the arterial wall [204–206], the procedure is operator and equipment dependent and is not capable of distinguishing inflammatory from atheromatous lesions. The sensitivity of a hypoechoic halo was 40 % and its specificity was 79 % for the diagnosis of GCA confirmed by temporal artery biopsy [207].

Ultrasound biomicroscopy (UBM) gives a higher resolution sonographic image and may play a role in predicting a negative result of a temporal artery biopsy in patients with GCA. In a study by Vianna et al. 2005 on 8 patients with positive temporal artery biopsies compared with 18 patients with negative biopsies, a halo sign and/or intra-arterial filling condensation and enlargement of muscularis media was seen in 8/8 patients with biopsy-proven GCA; 10/18 patients

with negative biopsies had one or both UBM findings. The absence of both UBM findings correlates with a negative temporal artery biopsy and therefore, has a 100 % negative predictive value [208].

Three Tesla magnetic resonance imaging (MRI) can also help localize inflammation in temporal arteritis for a directional biopsy and may be used to investigate other etiologies of visual loss, especially when patients present with atypical symptoms. MRI findings can reveal enhancement of the orbital fat and optic nerve. Optic nerve sheath enhancement represents fibroadipose tissue containing arteries with intimal thickening and mild mural inflammation consisting predominately of lymphocytes and occasional giant cells [209]. Multifocal dural and temporalis muscle enhancement, and perivascular enhancement of the superficial temporal artery, have also been reported in patients with GCA [210].

Magnetic resonance angiography (MRA) or cerebral angiography in GCA may demonstrate irregular narrowing or stenosis of the superficial temporal artery. MRA may be useful when bilateral temporal artery biopsies are normal in a patient highly suspected of having GCA [211–213].

Treatment of GCA

Corticosteroids are the only proven effective therapy for stopping visual loss in patients with GCA. Methylprednisolone at 1 g/day IV for 3–5 days followed by high-dose oral prednisone is considered the treatment of choice to prevent further damage of the affected eye and to prevent visual loss in the fellow eye. Dosage in the range of 1–2 mg/kg/day should be given if oral prednisone alone is used. This therapy should be maintained for about 4 weeks until symptoms subside and serum markers of inflammation normalize. Early high-dose oral or intravenous corticosteroids for at least 2 weeks have been shown to be effective in preventing further visual loss in most patients with GCA [185]. Prednisone can then be slowly tapered over the next 12–18 months with monitoring of the ESR and CRP, but can take up to 1–3 years to achieve a maintenance dose or eventual discontinuation of corticosteroids. Prednisone can be decreased by 10 mg each month, and then more slowly by 5 or 1 mg each month when a dose of 10 or 15 mg is attained [214]. In a prospective study by Hunder et al., it was found that corticosteroids administered daily during the taper had less chance of relapse compared with alternate day dosing [215]. If GCA is highly suspected, steroids should not be delayed until biopsy confirmation has been obtained. The artery remains abnormal for at least 2 weeks after steroids are started [196]. If the patient has a positive temporal artery biopsy, higher doses of corticosteroids should be used during the first 2 months when the risk of new ocular ischemia is highest. A definitive, biopsy-proven diagnosis requires at least 6 months, and usually 12 months, of corticosteroids [216, 217].

Only 4–15 % of patients with arteritic AION experience improvement in visual acuity, but not in visual fields, with treatment [218, 219]. Despite high-dose corticosteroids, progression of visual loss or second-eye involvement can occasionally occur within 5 days of initiation of treatment [220].

After the first 4 weeks of treatment when corticosteroids are tapered, more than 50 % of patients have recurrence of symptoms and elevation of the ESR and CRP as an indication of disease activity that requires an increase of prednisone to the previous dose before relapse [217]. Recurrence of arteritic AION in the same affected eye is rare and may occur without systemic symptoms or elevation of ESR and CRP [220]. In the series by Hayreh and Zimmerman [218], no patients on high-dose prednisone experienced blindness after the first 5 days. However, a higher rate of late visual impairment was noticed during tapering of prednisone with a shift to alternate-day treatment after 3 months.

Although GCA has been considered a self-limiting disease after 1–2 years of treatment [221], studies have demonstrated that GCA can have a protracted course with multiple relapses [189, 190]. In two studies [222, 223], the mean duration of corticosteroid therapy was 5.8 years with a range from 0 to 12.8 years. After 5 years,

43 % of patients were still on therapy, and after 9 years 25 % continued on treatment. Despite adequate control of symptoms by corticosteroids, underlying inflammation may still persist in patients with GCA. Although corticosteroids effectively inhibit nuclear factor-KB pathways to suppress cytokines, such as IL-1, IL-6, and IL-2, contributing to systemic symptoms, interferon-γ production is unaffected and it continues to help maintain the inflammatory infiltrate in the vessel wall. In a retrospective review of 100 patients with biopsy-proven GCA [224], 10 % of patients had ipsilateral recurrence of AION from 3 to 36 months after the initial AION. Although 83 % of patients had elevated acute-phase reactants or new systemic symptoms consistent with GCA, only 17 % developed these clinical premonitory features with enough lead time to allow physicians to prevent recurrence of visual loss.

Acetylsalicylic acid (ASA) may have an anti-inflammatory action in patients with GCA. In a study of a mouse chimera model of GCA [225], ASA predominantly suppresses transcription of interferon-γ. It may be able to inhibit T-cell function and prevent progression of intimal hyperplasia and luminal occlusion. Because ASA can also inhibit platelet aggregation, it has been postulated that it may be used with other anticoagulants, such as clopidogrel, for thrombosis. Thrombosis has been documented in vertebral arteries affected by GCA [226], but an occlusive vasculopathy from intimal proliferation also causes ischemia in GCA. Among the 175 GCA patients in a retrospective study by Nesher et al. [227], patients receiving low-dose aspirin were five times less likely to experience cranial ischemic complications (AION and strokes) by the time of diagnosis. Low-dose aspirin users were also fivefold less likely to develop cranial ischemic complications after prednisone was started. Low-dose aspirin decreased the absolute risk of cranial ischemic complications after GCA was diagnosed from 13 to 3 %. This study suggests that low-dose aspirin significantly reduces the rate of AION and strokes in patients with GCA, despite that the aspirin-treated group had more risk factors for cardiovascular disease. In another retrospective study by Lee et al., adjunctive low-dose aspirin at 81 mg per day lead to fewer ischemic events without an increased risk of bleeding complications in patients with GCA compared to the untreated group [228].

Because of the complications of long-term corticosteroids, such as osteoporosis, steroid-sparing agents can help reduce the maintenance dose of prednisone. Evidence supporting the use of these various agents is limited or inconclusive. Four small prospective and retrospective series describe the use of two immunosuppressive agents in 16 patients with corticosteroid-resistant GCA and 1 patient with corticosteroid-resistant polymyalgia rheumatica [229–232]. Among the patients in these various studies, the add-on agent to corticosteroids was cyclophosphamide, dapsone, or methotrexate. Information regarding diagnostic criteria and measures of disease activity was limited in these small studies. Methotrexate was shown in some studies to be effective as an adjunctive treatment in GCA [233–235]. Some patients were able to reduce their corticosteroid maintenance dose by using supplementary methotrexate. Studies on the combined effect of methotrexate and corticosteroids yielded conflicting results [233, 234]. In a randomized, controlled, double-blind study by Spiera et al. [235], 21 patients with GCA were treated with either high-dose corticosteroids and methotrexate starting at 7.5 mg/week or placebo. Corticosteroids were tapered according to the clinical response, with methotrexate or placebo dose increased by 2.5 mg/week for relapses with a maximum allowable dose of 20 mg/week. After clinical remission and discontinuation of prednisone, methotrexate or placebo was tapered monthly to 0 by 2.5 mg/week. No significant difference was seen between the methotrexate- and placebo-treated patients with regard to the cumulative corticosteroid dose, to the number of weeks to completion of corticosteroids, nor to the number of weeks to taper prednisone to less than 10 mg/day, and the bone mineral density in the lumbar spine or hip at 1 year. No late visual loss occurred in either group. Therefore, this study clearly shows that treatment with methotrexate and corticosteroids is a safe alternative to corticosteroid therapy alone in patients with GCA and is

more effective in controlling disease. Jover et al. [234] also reported that the combination of methotrexate and corticosteroids was more effective than prednisone alone in maintaining disease remission, and that the cumulative mean dose of corticosteroids was lower in the methotrexate group after 2 years. However, these findings were not confirmed in a larger multicenter 1-year study by Hoffman et al. [233], which showed that the addition of methotrexate to a conventional steroid regimen did not improve disease control or reduce steroid dose. The disparity of the foregoing study results could be attributed to differences in study size, inclusion criteria, criteria for determining relapse, and dosage in tapering protocols. To what extent these differences in treatment regimen might have contributed to the different results is not known.

Azathioprine has been shown to be an effective adjunctive treatment in GCA. In a randomized, double-blinded, placebo-controlled study [236], 9 of 16 patients (5 with biopsy-proven GCA) who received azathioprine at an average dose of 1.5–2.7 mg/kg/day completed the 52 weeks of therapy; other patients did not because of medication-related adverse effects. A statistically significant lower mean dose of prednisone was noted in the azathioprine group compared to placebo.

Cyclosporin A was shown in an open, controlled, randomized study to have no additive effect compared with prednisone alone in GCA [237].

For patients who have corticosteroid-resistant GCA, tumor necrosis factor (TNF) blockers have been shown in some case reports to be effective. The inflammatory infiltrate in GCA consists of mostly T lymphocytes, macrophages, and giant cells. Cytokines, such as TNF-α, are released by activated macrophages and T cells. Although increased serum levels of TNF-α have not been demonstrated in patients with GCA, up to 60 % of cells in GCA inflammatory lesions have TNF-α. TNF-α microsatellite polymorphisms have also been associated with GCA [238, 239].

Because TNF-α is one of the major cytokines mediating inflammation in GCA, agents that block this factor have been used in some patients with treatment-resistant GCA. Infliximab is an anti-TNF-α monoclonal antibody used successfully in six patients with GCA who were resistant and/or intolerant to corticosteroids and methotrexate [240]. In a study of four patients who had corticosteroid-related side effects while on this medication from 42 to 54 months and recurrent relapses while tapering to 7.5–12.5 mg/day [238], they received two infusions of infliximab at 3 mg/kg. Three patients had clinical remission with discontinuation of corticosteroids after 5–6 months. Infliximab was well tolerated without any major side effects.

Uthman et al. [241] administered a larger dose of infliximab at 5 mg/kg that was used as monotherapy to successfully control GCA in a 75-year-old woman after her initial course of prednisone. Another TNF blocker is etanercept, which has been used in the treatment of corticosteroid-resistant GCA. In a report by Tan et al. [242], an 80-year-old man with GCA who had been treated with more than 20 mg/day prednisolone was started on etanercept 25 mg po BID. Within 1 month, his symptoms improved. His prednisolone was then reduced to 5 mg/day and his etanercept was decreased to once every 8 days. Etanercept has also been used in treatment-resistant cases of GCA [243].

Visual Prognosis of AION in GCA

Despite treatment, worsening of vision may continue. Recovery of vision is rare and only occurs in less than 15 % of patients [244].

Based on a retrospective study of 114 eyes of biopsy-proven GCA patients who were treated with high-dose corticosteroids [244], 4 % (5 of 114) of eyes with initial visual loss had improvement in visual field and visual acuity of greater than two lines. Ninety-one percent had AION, 10.5 % had central retinal artery occlusion, 10 % had cilioretinal artery occlusion, and 4 % had PION. Seven eyes from six patients had improvement in visual acuity without improvement in visual fields. Eccentric fixation could have accounted for previously higher reported rates of visual recovery after treatment in past clinical studies.

The visual prognosis of AION from GCA is generally poor. A high proportion of patients with permanent visual loss have been shown to have had delayed diagnosis and treatment. In a retrospective review of 146 patients by Font et al. [245], 35 % of patients had systemic symptoms for an average of 10 months before visual loss and 65 % noted premonitory visual symptoms for an average of 8.5 days. Other studies [246–248] also showed a clear relationship between visual improvement and the time to diagnosis and initiation of treatment. If treatment was started within 24 h from onset of symptoms, visual improvement was noted in 58 % of patients, compared with only 6 % in those who had a longer delay in treatment. Early initiation of treatment appears to be the most important factor in successful treatment of visual complications from GCA, because 92 % of the visual losses often occur before the start of therapy [248].

Other Etiologies of Arteritic AION

Although the most common vasculitic disorder causing arteritic AION is GCA, other etiologies include polyarteritis nodosa [249], herpes zoster [250], rheumatoid arthritis [251], antineutrophilic cytoplasmic antibody vasculitis [252], Takayasu's arteritis [253], Behcet's disease [254], Crohn's disease [255], and connective tissue disorders such as systemic lupus erythematosus [256], Wegener's vasculitis [257], and Churg–Strauss angiitis [258]. Rarely, infections, such as *Rickettsia conorii*, can be present with AION [259].

Posterior Ischemic Optic Neuropathy

Incidence of PION

Arteritic and nonarteritic conditions may affect the retrobulbar portion of the optic nerve to cause PION, which is much less common than AION. In a retrospective study of 72 patients with PION [260], 38 of 72 had nonarteritic PION, 6 of 72 had arteritic PION, and 28 of 72 had perioperative PION. Patients with nonarteritic PION had similar vasculopathic risk factors as those with NAION, but they did not have a small cup-to-disc ratio. Patients with arteritic PION were older and had more severe visual loss with less recovery; those with perioperative PION were younger and had bilateral visual loss with poor recovery.

Table 2.2 Diagnostic criteria for PION [Reprinted from Buono LM, Foroozan R. Perioperative posterior ischemic optic neuropathy: review of the literature. Surv Ophthalmol 2005;50(1):15–26. With permission from Elsevier]

• Acute visual acuity loss and/or visual field defect with decreased or absent color defect
• Ipsilateral relative afferent pupillary defect (RAPD) in unilateral involvement or minimally reactive or nonreactive pupils in bilateral involvement
• Normal optic disc and retinal examination at the onset of visual loss
• Exclusion of other identifiable causes of visual loss, such as retinal vascular occlusion, glaucoma, anterior segment trauma, etc.
• Exclusion of other causes of retrobulbar optic neuropathy, such as compression, demyelination, vasculitis, etc.
• Abnormal visual evoked potential
• Normal electroretinogram
• Development of optic disc atrophy or pallor within 4 to 8 weeks of onset of visual loss

Symptoms and Signs of PION

In PION, visual loss is acute and painless, associated with a relative afferent pupillary defect, and a central visual field defect, alone or in combination with other types of field defects. The optic disc in PION usually appears normal, in contrast to disc edema seen in AION. Within 4–6 weeks, the optic disc usually becomes pale. Progressive PION may occasionally lead to gradual visual loss over weeks to months. PION is a diagnosis of exclusion (Table 2.2) [261].

Pathophysiology of PION

The posterior optic nerve is supplied only by the pial capillary plexus from the ophthalmic artery and is separate from the vascular territory of the anterior optic disc which is supplied by the

paraoptic branches of the short posterior ciliary arteries. The pial capillary plexus is relatively poorly vascularized. More posteriorly, the intracanalicular optic nerve is supplied by two independent vascular circles derived from the ophthalmic artery. The intracranial portion of the optic nerve is also supplied by a separate vascular system from branches of the ipsilateral internal carotid, anterior cerebral, and anterior communicating arteries [261].

PION in Systemic Disorders

Retrobulbar optic nerve ischemia has been shown to be related to cardiovascular and cerebrovascular diseases. Carotid artery disease may cause PION as an isolated event or as part of the oculocerebral syndrome in which a hemispheric stroke is associated with an ipsilateral PION. Optic atrophy may develop in the affected eye within 2 months of onset of visual loss. Severe carotid atherosclerosis may also cause NAION in one eye and progressive PION in the fellow eye. Chronic ischemia from ipsilateral carotid occlusive disease can lead to a slowly progressive PION that may be complicated by iris neovascularization [262]. PION is also more commonly a complication of spontaneous rather than traumatic carotid artery Dissection [263].

PION can occur in the clinical setting where a fistula may steal blood away from the intraorbital optic nerve. A posterior-draining dural carotid cavernous sinus fistula fed by the right meningohypophyseal trunk and right middle meningeal artery and an ophthalmic-middle meningeal arterial anastomosis led to the development of a right PION in a 79-year-old woman who presented with acute right visual loss, ocular motor abnormalities, and pulsatile tinnitus [264].

Other inflammatory diseases that can cause PION include GCA, lupus, polyarteritis nodosa, and herpes zoster. Infections have been associated with PION. Inflammation of the medial posterior ciliary artery from herpes zoster ophthalmicus, causing acute visual loss with a deep, steep-sided altitudinal visual field defect, has been associated with PION [265]. Fungal embolization by *Aspergillus fumigatus* to the retrobulbar optic nerve caused acute monocular visual loss in a 35-year-old woman [266].

Although AION has been well described in patients after an episode of classical migraine (migraine with visual aura), PION has been reported in two patients with PION. PION can occur as acute visual loss during or after a migraine, or following an episode of visual aura without headache [267].

An acute isolated PION has been reported as the presenting sign of a ruptured anterior communicating artery aneurysm. Because the ION usually occurs ipsilateral to the subarachnoid hemorrhage, it is hypothesized that the hemorrhage caused a decreased blood supply to the posterior circulation of the optic nerve [268]. In a report by Hara et al. [269], two patients developed disc atrophy with excavation and permanent superior altitudinal defects after the subarachnoid hemorrhage.

PION often is a complication of arachnoiditis affecting the intracranial optic nerves and chiasm in basal meningitis, head injury, intracranial tumor, empty sella syndrome, foreign-body reaction to muslin wrapping, or systemic disease. Ischemia is induced by compression of the optic nerve from vascular occlusion and fibrosis in arachnoiditis. PION is also presumed to occur in lymphoma, sepsis, intranasal corticosteroid injection, intranasal epinephrine-containing anesthetic injection, and amyloidosis [270].

PION has been reported in sickle cell disease in a 52-year-old black man with a history of sickle cell with SS trait [271].

Perioperative PION

Hypotension from anemia or from any decrease in blood flow to the ipsilateral common or internal carotid artery during surgery may cause PION [261]. Most cases of perioperative PION occur with acute blood loss after procedures, such as lumbar spine [272–274], cardiopulmonary bypass [275, 276], radical neck dissection [277–284], and liposuction [285]. The incidence of perioperative PION is estimated to range from 0 to

0.12 % [261]. Of 14,102 cases of spine surgery at the Johns Hopkins Hospital over 20 years, the incidence of PION was 0.028 % (4 cases). More than 50 % of patients with perioperative PION develop visual loss after lower spine surgery after being in the prone position for a prolonged period of time. More than 70 % develop bilateral PION [272].

Most affected patients are in their fifth decade and experience acute visual loss in the postoperative period, less than or equal to 24 h after recovery from anesthesia. Visual acuity may range from 20/70 to NLP. According to a review of the literature by Buono et al. [261], approximately 61 % of patients had bilateral simultaneous visual loss and none had sequential involvement; those with bilateral visual loss experienced the worst visual deficits. About 38 % of patients had some visual recovery, but about 86 % with NLP initially had no visual improvement. Those with better vision initially had more substantial visual recovery. Overall, about half of all eyes had a final visual outcome of hand motion or worse. All patients developed optic disc atrophy. Approximately 66 % of patients had vascular risk factors, such as hypertension, DM, hypercholesterolemia, coronary artery disease, congestive heart failure, cardiac arrhythmia, obesity, and tobacco use. The remainder had no vascular risk factors. The average duration of operation was 8.7 h. The mean decrease of hematocrit was 14.4 % between the preoperative and the perioperative period. The mean decrease of systolic blood pressure was 53 mmHg between the preoperative and the perioperative period. The mean intraoperative estimated blood loss was 3.7 L. If no intraoperative hypotension is documented during the surgery, then anemia is most likely, as evidenced by a mean hemoglobin level that has decreased by 40–50 % in the perioperative period.

Neuroimaging of the optic nerves in the perioperative setting can sometimes show the location of the lesion in PION. In a report of a 61-year-old man with bilateral PION after cardiac bypass surgery, MRI of the orbits with diffusion-weighted and fluid-attenuated inversion recovery sequences can reveal abnormal hyperintensity in both intraorbital optic nerves [286]. Bilateral intraorbital optic nerve enhancement was seen on MRI 8 weeks after coronary bypass grafting in a 57-year-old woman who had hypotensive PION [287].

Histopathology demonstrates that infarction occurs in the intraorbital portion of the optic nerve in patients with perioperative PION. The central axial portion of the optic nerve is usually infarcted, and may be hemorrhagic, with sparing of the nerve periphery. Occasionally, the infarction may extend to the periphery circumferentially, especially in the midorbital section of the optic nerve. The loss of peripheral axons appears to correspond to constricted visual fields [93]. In the report by Nawa et al. [279] on a 67-year-old man with bilateral PION after radical neck dissection complicated by intraoperative hypotension and anemia, histopathology of the optic nerve revealed acellularity of the fibrovascular pial septae, swollen macrophages, some hemorrhage, and loss of myelin. The paracentral pial vessels had a few small thrombi, but no emboli.

Perioperative hemodynamic changes causing decreased oxygen delivery to the optic nerve are thought to cause PION. These hemodynamic factors include hypotension, anemia, increased venous pressure, a prone position during surgery, direct ocular compression, increased cerebrospinal fluid pressure, and embolism. Another factor that may decrease oxygen delivery to the optic nerve is defective vascular autoregulation caused by vascular endothelial dysfunction [288]. It has been shown that normal compensatory vasoconstriction and vasodilation during fluctuating blood pressures does not occur in diabetic patients [288]. This lack of vascular autoregulation during perioperative hypotensive episodes would increase the risk of developing perioperative PION [289]. Anatomic variation of the intraorbital blood supply may also account for a patient's susceptibility to perioperative PION. The arterial supply of the intraorbital optic nerve derives from two separate systems, the peripheral centripetal vessels and the axial centrifugal vessels. The pial plexus is formed by collaterals directly from the ophthalmic artery and from collateral from other intraorbital subdivisions of

the ophthalmic artery. The axial system is formed from branches of the central retinal artery after it penetrates the optic nerve sheath. These branches radiate from the central optic nerve to penetrate the parenchyma. The anastomoses between the peripheral and central vascular systems may vary among patients. Those who lack these anastomoses have a watershed zone that is more susceptible to ischemia during perioperative hemodynamic changes [93].

PION as a Complication of Ocular or Sinus Surgery

See "Traumatic Optic Neuropathy."

PION as a Complication of Radiotherapy

See "Nutritional and Toxic Optic Neuropathies."

Treatment for PION

The visual prognosis for PION is usually poor. No proven effective treatment is available to reverse visual loss [261]. Perioperative correction of hemodynamic abnormalities may be beneficial in certain instances. In a report by Stevens et al. [273], correction of anemia and hypotension led to complete visual recovery in one patient, who received blood transfusions to maintain a hematocrit above 35 % and a blood pressure about 140/80 mmHg by discontinuation of antihypertensive medications. Postoperative visual acuity was 20/70 in the right eye (OD) and 20/200 in the left eye (OS). After transfusion, visual acuity was 20/40 OD and 20/30 OS. Seven months later, his visual acuity improved to 20/20 OU. This report suggests that early transfusion for perioperative anemia can prevent perioperative PION. Specific clinical guidelines for transfusion have been controversial, and the decision to transfuse should be based upon the patient's risk of developing complications of decreased oxygenation [290].

In addition, simultaneous internal jugular vein ligation should be avoided to prevent PION after radical neck dissection. Staging of the neck dissection does not appear to prevent PION [277–284].

References

1. Johnson LN, Arnold AC. Incidence of nonarteritic and arteritic anterior ischemic optic neuropathy. Population-based study in the state of Missouri and Los Angeles County, California. J Neuroophthalmol. 1994;14(1):38–44.
2. Boghen DR, Glaser JS. Ischaemic optic neuropathy. The clinical profile and history. Brain. 1975;98(4): 689–708.
3. Characteristics of patients with nonarteritic anterior ischemic optic neuropathy eligible for the Ischemic Optic Neuropathy Decompression Trial. Arch Ophthalmol. 1996;114(11):1366–74.
4. Repka MX, Savino PJ, Schatz NJ, et al. Clinical profile and long-term implications of anterior ischemic optic neuropathy. Am J Ophthalmol. 1983;96(4): 478–83.
5. Kanski JJ, Bowling B. Clinical ophthalmology: a systematic approach. 7th ed. Philadelphia, PA: Saunders; 2007.
6. Hayreh SS, Zimmerman B. Visual field abnormalities in nonarteritic anterior ischemic optic neuropathy: their pattern and prevalence at initial examination. Arch Ophthalmol. 2005;123(11): 1554–62.
7. Arnold AC. Pathogenesis of nonarteritic anterior ischemic optic neuropathy. J Neuroophthalmol. 2003;23(2):157–63.
8. Danesh-Meyer HV, Savino PJ, Sergott RC. The prevalence of cupping in end-stage arteritic and nonarteritic anterior ischemic optic neuropathy. Ophthalmology. 2001;108(3):593–8.
9. Optic nerve decompression surgery for non-arteritic anterior ischemic optic neuropathy (NAION) is not effective and may be harmful. The Ischemic Optic Neuropathy Decompression Trial Research Group. JAMA. 1995;273(8): 625–32.
10. Ischemic Optic Neuropathy Decompression Trial: twenty-four-month update. Arch Ophthalmol 2000; 118(6):793–8.
11. Arnold AC, Hepler RS. Natural history of nonarteritic anterior ischemic optic neuropathy. J Neuroophthalmol. 1994;14(2):66–9.
12. Hayreh SS. Anterior ischaemic optic neuropathy. Differentiation of arteritic from non-arteritic type and its management. Eye. 1990;4(pt 1):25–41.
13. Newman NJ, Scherer R, Langenberg P, et al. Ischemic Optic Neuropathy Decompression Trial Research Group. The fellow eye in NAION: report from the ischemic optic neuropathy decompression

trial follow-up study. Am J Ophthalmol 2002; 134(3):317–28
14. Beck RW, Hayreh SS, Podhajsky PA, et al. Aspirin therapy in nonarteritic anterior ischemic optic neuropathy. Am J Ophthalmol. 1997;123(2):212–7.
15. Goff MJ, Kerrison JB. Bilateral simultaneous anterior ischemic optic neuropathy in a young, healthy man. Arch Ophthalmol. 2003;121(11):1652–3.
16. Lee AG, Lin DJ, Kaufman M, et al. Atypical features prompting neuroimaging in acute optic neuropathy in adults. Can J Ophthalmol. 2000;35(6):325–30.
17. Miller NR, Newman NJ, editors. Walsh and Hoyt's clinical neuro-ophthalmology. 5th ed. Baltimore, MD: Williams & Wilkins; 1998.
18. Rath EZ, Rehany U, Linn S, et al. Correlation between optic disc atrophy and aetiology: anterior ischaemic optic neuropathy vs. optic neuritis. Eye. 2003;17(9):1019–24.
19. Arnold AC, Badr MA, Hepler RS. Fluorescein angiography in nonischemic optic disc edema. Arch Ophthalmol. 1996;114(3):293–8.
20. Rizzo III JF, Andreoli CM, Rabinov JD. Use of magnetic resonance imaging to differentiate optic neuritis and nonarteritic anterior ischemic optic neuropathy. Ophthalmology. 2002;109(9): 1679–84.
21. Contreras I, Rebolleda G, Noval S, et al. Optic disc evaluation by optical coherence tomography in nonarteritic anterior ischemic optic neuropathy. Investig Ophthalmol Vis Sci. 2007;48(9):4087–92.
22. Jonas JB, Schmidt AM, Müller-Bergh JA, et al. Human optic nerve fiber count and optic disc size. Investig Ophthalmol Vis Sci. 1992;33(6):2012–8.
23. Savini G, Zanini M, Carelli V, et al. Correlation between retinal nerve fibre layer thickness and optic nerve head size: an optical coherence tomography study. Br J Ophthalmol. 2005;89(4):489–92.
24. Chan CKM, Cheng ACO, Leung CKS, et al. Quantitative assessment of optic nerve head morphology and retinal nerve fiber layer in non-arteritic ischemic optic neuropathy with optical coherence tomography and confocal scanning laser ophthalmoscopy. Br J Ophthalmol. 2009;93:731–5.
25. Bellusci C, Savini G, Carbonelli M, Carelli V, Sadun AA, Barboni P. Retinal nerve fiber layer thickness in nonarteritic anterior ischemic optic neuropathy: OCT characterization of the acute and resolving phases. Graefes Arch Clin Exp Ophthalmol. 2008; 246(5):641–7.
26. Contreras I, Noval S, Rebolleda G, Munoz-Negrete FJ. Follow-up of nonarteritic anterior ischemic optic neuropathy with optical coherence tomography. Ophthalmology. 2007;114:2338–44.
27. DeLeon-Ortega J, Carroll KE, Arthur SN, Girkin CA. Correlations between retinal nerve fiber layer and visual field in eyes with nonarteritic anterior ischemic optic neuropathy. Am J Ophthalmol. 2007;143:288–94.
28. Girkin CA, McGwin Jr G, DeLeon-Ortega J. Frequency doubling technology perimetry in nonarteritic ischemic optic neuropathy with altitudinal defects. Br J Opthalmol. 2004;88:1274–9.
29. Horowitz J, Fishelzon-Arev T, Rath EZ, Segev E, Geyer O. Comparison of optic nerve head topography findings in eyes with non-arteritic anterior ischemic optic neuropathy and eyes with glaucoma. Graefes Arch Clin Exp Ophthalmol. 2010; 248(6):845–51.
30. Danesh-Meyer HV, Boland MF, Savino PJ, Miller NR, Subramania PS, Girkin CA, et al. Optic disc morphology in open-angle glaucoma compared with anterior ischemic optic neuropathies. Investig Ophthalmol Vis Sci. 2010;51:2003–10.
31. Suh MH, Kim SH, Park KH, Kim SJ, Kim T, Hwang S, et al. Comparison of the correlations between optic disc rim area and retinal nerve fiber layer thickness in glaucoma and nonarteritic anterior ischemic optic neuropathy. Am J Ophthalmol. 2011;151: 277–86.
32. Lee MS, Grossman D, Arnold AC, Sloan FA. Incidence of nonarteritic anterior ischemic optic neuropathy: increased risk among diabetic patients. Ophthalmology. 2011;118(5):959–63.
33. Chung SM, Gay CA, McCrary III JA. Nonarteritic ischemic optic neuropathy. The impact of tobacco use. Ophthalmology. 1994;101(4):779–82.
34. Jacobson DM, Vierkant RA, Belongia EA. Nonarteritic anterior ischemic optic neuropathy. A case–control study of potential risk factors. Arch Ophthalmol. 1997;115(11):1403–7.
35. Fry CL, Carter JE, Kanter MC, et al. Anterior ischemic optic neuropathy is not associated with carotid artery atherosclerosis. Stroke. 1993;24(4):539–42.
36. Tesser RA, Niendorf ER, Levin LA. The morphology of an infarct in nonarteritic anterior ischemic optic neuropathy. Ophthalmology. 2003;110(10): 2031–5.
37. Beck RW, Savino PJ, Repka MX, Schatz NJ, Sergott RC. Optic disc structure in anterior ischemic optic neuropathy. Ophthalmology. 1984;91(11):1334–7.
38. Feit RH, Tomsak RL, Ellenberger Jr C. Structural factors in the pathogenesis of ischemic optic neuropathy. Am J Ophthalmol. 1984;98(1):105–8.
39. Eagling EM, Sanders MD, Miller SJ. Ischaemic papillopathy. Clinical and fluorescein angio-graphic review of forty cases. Br J Ophthalmol. 1974; 58(12):990–1008.
40. Arnold AC, Hepler RS. Fluorescein angiography in acute nonarteritic anterior ischemic optic neuropathy. Am J Ophthalmol. 1994;117(2):222–30.
41. Knox DL, Kerrison JB, Green WR. Histopathologic studies of ischemic optic neuropathy. Trans Am Ophthalmol Soc. 2000;98:203–20. discussion 221–2.
42. Olver JM, Spalton DJ, McCartney AC. Microvascular study of the retrolaminar optic nerve in man: the possible significance in anterior ischaemic optic neuropathy. Eye. 1990;4(pt 1):7–24.
43. Onda E, Cioffi GA, Bacon DR, Van Buskirk EM. Microvasculature of the human optic nerve. Am J Ophthalmol. 1995;120(1):92–102.

44. Hayreh SS, Podhajsky P, Zimmerman MB. Role of nocturnal arterial hypotension in optic nerve head ischemic disorders. Ophthalmologica. 1999;213(2): 76–96.
45. Landau K, Winterkorn JM, Mailloux LU, et al. 24-hour blood pressure monitoring in patients with anterior ischemic optic neuropathy. Arch Ophthalmol. 1996;114(5):570–5.
46. Hayreh SS, Piegors DJ, Heistad DD. Serotonin-induced constriction of ocular arteries in atherosclerotic monkeys. Implications for ischemic disorders of the retina and optic nerve head. Arch Ophthalmol. 1997;115(2):220–8.
47. Harris A, Ciulla TA, Chung HS, et al. Regulation of retinal and optic nerve blood flow. Arch Ophthalmol. 1998;116(11):1491–5.
48. Strenn K, Matulla B, Wolzt M, et al. Reversal of endothelin-1-induced ocular hemodynamic effects by low-dose nifedipine in humans. Clin Pharmacol Ther. 1998;63(1):54–63.
49. Oku H, Sugiyama T, Kojima S, et al. Experimental optic cup enlargement caused by endothelin-1-induced chronic optic nerve head ischemia. Surv Ophthalmol. 1999;44 suppl 1:S74–84.
50. Arnold AC, Levin LA. Treatment of ischemic optic neuropathy. Semin Ophthalmol. 2002;17(1):39–46.
51. Keltner JL, Becker B, Gay AJ, Podos SM. Effect of diphenylhydantoin in ischemic optic neuritis. Trans Am Ophthalmol Soc. 1972;70:113–30.
52. Johnson LN, Gould TJ, Krohel GB. Effect of levodopa and carbidopa on recovery of visual function in patients with nonarteritic anterior ischemic optic neuropathy of longer than six months' duration. Am J Ophthalmol. 1996;121(1):77–83.
53. Smith JL. Norepinephrine therapy of ischemic optic neuropathy. J Clin Neuro Ophthalmol. 1981;1(4): 289–90.
54. Kollarits CR, McCarthy RW, Corrie WS, et al. Norepinephrine therapy of ischemic optic neuropathy. J Clin Neuro Ophthalmol. 1981;1:283–8.
55. Kajiwara K, Tsubota K, Hara Y. High-dose urokinase thrombolysis and stellate ganglion block for anterior ischemic optic neuropathy. Folia Ophthalmol Jpn. 1990;41:59–64.
56. Kaderli B, Avci R, Yucel A, Guler K, Gelisken O. Intravitreal triamcinolone improves recovery of visual acuity in nonarteritic anterior ischemic optic neuropathy. J Neuroophthalmol. 2007;27(3):164–8.
57. Botelho PJ, Johnson LN, Arnold AC. The effect of aspirin on the visual outcome of nonarteritic anterior ischemic optic neuropathy. Am J Ophthalmol. 1996;121(4):450–1.
58. Maas A, Walzl M, Jesenik F, et al. Application of HELP in nonarteritic anterior ischemic optic neuropathy: a prospective, randomized, controlled study. Graefes Arch Clin Exp Ophthalmol. 1997; 235:14–9.
59. Yee RD, Selky AK, Purvin VA. Outcomes of optic nerve sheath decompression for nonarteritic ischemic optic neuropathy. J Neuroophthalmol. 1994; 14(2):70–6.
60. Beck RW, Hayreh SS, Podhajsky PA, Tan ES, Moke PS. Aspirin therapy in nonarteritic anterior ischemic optic neuropathy. J Ophthalmol. 1997;123(2): 212–7.
61. Hayreh SS, Zimmerman MB. Non-arteritic anterior ischemic optic neuropathy: role of systemic corticosteroid therapy. Graefes Arch Clin Exp Ophthalmol. 2008;246(7):1029–46.
62. Hayreh SS, Zimmerman MB. Optic disc edema in non-arteritic anterior ischemic optic neuropathy. Graefes Arch Clin Exp Ophthalmol. 2007;245(8): 1107–21.
63. Jonas JB, Spandau UH, Harder B, Sauder G. Intravitreal triamcinolone acetonide for treatment of acute nonarteritic anterior ischemic optic neuropathy. Graefes Arch Clin Exp Ophthalmol. 2007; 245(5):749–50.
64. Jonas JB, Sauder G, Budde WM, Spandau UH, Kamppeter BA, Harder B. Triamcinolone acetonide-induced ocular hypertension. J Ocul Pharmacol Ther. 2006;22(4):247–50.
65. Wilhelm B, Ludtke H, Wilhelm H, The BRAION study group. Efficacy and tolerability of 0.2% brimonidine tartrate for the treatment of acute nonarteritic anterior ischemic optic neuropathy (NAION): a 3-month, double-masked, randomized, placebo-controlled trial. Graefes Arch Clin Exp Ophthalmol. 2006;244(5):551–8.
66. Johnson LN, Guy ME, Krohel GB, Madsen RW. Levodopa may improve vision loss in recent onset, nonarteritic anterior ischemic optic neuropathy. Ophthalmology. 2000;107(3):521–6.
67. Simsek T, Eryilmaz T, Acaroglu G. Efficacy of levodopa and carbidopa on visual function in patients with non-arteritic anterior ischaemic optic neuropathy. Int J Clin Pract. 2005;59(3):287–90.
68. Bojic L, Ivanisevic M, Gosovic G. Hyperbaric oxygen therapy in two patients with non-arteritic anterior optic neuropathy who did not respond to prednisone. Undersea Hyperb Med. 2002;29(2):86–92.
69. Bojic L, Cerovski B, Bucan K, et al. Hyperbaric oxygen for the treatment of nonarteritic anterior ischemic optic neuropathy. Acta Med Croatica. 1995;49(3):133–6.
70. Bojic L, Kovacevic H, Andric D, Karaman-Kraljevic K, Cagalj S. The effects of hyperbaric oxygen on visual functions in ischaemic optic neuropathy. Arh Hig Rada Toksikol. 1994;45(1):19–24.
71. Arnold AC, Hepler RS, Lieber M, Alexander JM. Hyperbaric oxygen therapy for nonarteritic anterior ischemic optic neuropathy. Am J Ophthalmol. 1996;122(4):535–41.
72. Soheilian M, Koochek A, Yazdani S, Peyman GA. Transvitreal optic neurotomy for nonarteritic anterior ischemic optic neuropathy. Retina. 2003; 23(5):692–7.
73. Lubow M, Makley Jr TA. Pseudopapilledema of juvenile diabetes mellitus. Arch Ophthalmol. 1971; 85(4):417–22.
74. Barr CC, Glaser JS, Blankenship G. Acute disc swelling in juvenile diabetes. Clinical profile and

natural history of 12 cases. Arch Ophthalmol. 1980;98(12):2185–92.
75. Pavan PR, Aiello LM, Wafai MZ, Briones JC, Sebestyen JG, Bradbury MJ. Optic disc edema in juvenile-onset diabetes. Arch Ophthalmol. 1980; 98(12):2193–5.
76. Hayreh SS, Zahoruk RM. Anterior ischemic optic neuropathy. VI. In juvenile diabetics. Ophthalmologica. 1981;182(1):13–28.
77. Friedland S, Winterkorn JM, Burde RM. Luxury perfusion following anterior ischemic optic neuropathy. J Neuroophthalmol. 1996;16(3):163–71.
78. Ho AC, Maguire AM, Yanuzzi LA, et al. Rapidly progressive optic disc neovascularization after diabetic papillopathy. Am J Ophthalmol. 1995;120: 673–5.
79. Regillo CD, Brown GC, Savino PJ, et al. Diabetic papillopathy. Patient characteristics and fundus findings. Arch Ophthalmol. 1995;113(7):889–95.
80. Sato T, Fujikado T, Hosohata J, Ohji M, Tano Y. Development of bilateral, nonarteritic anterior ischemic optic neuropathy in an eye with diabetic papillopathy. Jpn J Ophthalmol. 2004;48(2):158–62.
81. Munteanu M, Lehaci C. Acute anterior ischemic optic neuropathy in association with optic nerve drusen. Oftalmologia. 2004;48(3):16–9.
82. Purvin V, King R, Kawasaki A, Yee R. Anterior ischemic optic neuropathy in eyes with optic disc drusen. Arch Ophthalmol. 2004;122(1):48–53.
83. Weger M, Haas A, Stanger O, et al. *Chlamydia pneumoniae* seropositivity and the risk of non-arteritic ischemic optic neuropathy. Ophthalmology. 2002; "109(4):749–52.
84. Vecsei PV, Kircher K, Reitner A, Khanakha G, Stanek G. Chlamydia in anterior ischemic optic neuropathy. Ophthalmologica. 2002;216(3):215–20.
85. Drance SM, Morgan RW, Sweeney VP. Shock-induced optic neuropathy: a cause of nonprogressive glaucoma. N Engl J Med. 1973;288(8):392–5.
86. Hayreh SS. Anterior ischemic optic neuropathy. VIII. Clinical features and pathogenesis of post-hemorrhagic amaurosis. Ophthalmology. 1987; 94(11):1488–502.
87. Hollenhorst RW, Wagener HP. Loss of vision after distant hemorrhage. Am J Med Sci. 1950;219: 209–44.
88. Moster ML. Visual loss after coronary artery bypass surgery. Surv Ophthalmol. 1998;42(5):453–7.
89. Foroozan R, Buono LM, Savino PJ. Optic disc structure and shock-induced anterior ischemic optic neuropathy. Ophthalmology. 2003;110(2):327–31.
90. Chisholm IA. Optic neuropathy of recurrent blood loss. Br J Ophthalmol. 1969;53(5):289–95.
91. Lazaro EJ, Cinotti AA, Eichler PN, Khawaja AA. Amaurosis due to massive gastrointestinal hemorrhage. Am J Gastroenterol. 1971;55(1):50–3.
92. Klewin KM, Appen RE, Kaufman PL. Amaurosis and blood loss. Am J Ophthalmol. 1978;86(5): 669–72.
93. Johnson MW, Kincaid MC, Trobe JD. Bilateral retrobulbar optic nerve infarctions after blood loss and hypotension. A clinicopathologic case study. Ophthalmology. 1987;94(12):1577–84.
94. Chan JW. Acute bilateral simultaneous PION after ectopic pregnancy-related hemorrhage. Eye. 2006;20(6):747–8.
95. Presencia AC, Hernandez AM, Guia ED. Amaurosis following blood loss. Ophthalmologica. 1985;191: 119–22.
96. Basile C, Addabbo G, Montanaro A. Anterior ischemic optic neuropathy and dialysis: role of hypotension and anemia. J Nephrol. 2001;14(5):420–3.
97. Chutorian AM, Winterkorn JM, Geffner M. Anterior ischemic optic neuropathy in children: case reports and review of the literature. Pediatr Neurol. 2002; 26(5):358–64.
98. Servilla KS, Groggel GC. Anterior ischemic optic neuropathy as a complication of hemodialysis. Am J Kidney Dis. 1986;8(1):61–3.
99. Hamed LM, Winward KE, Glaser JS, Schatz NJ. Optic neuropathy in uremia. Am J Ophthalmol. 1989;108(1):30–5.
100. Connolly SE, Gordon KB, Horton JC. Salvage of vision after hypotension-induced ischemic optic neuropathy. Am J Ophthalmol. 1994;117(2):235–42.
101. Korzets A, Marashek I, Schwartz A, Rosenblatt I, Herman M, Ori Y. Ischemic optic neuropathy in dialyzed patients: a previously unrecognized manifestation of calcific uremic arteriolopathy. Am J Kidney Dis. 2004;44(6):e93–7.
102. Alpert JN, Pena Y, Leachman DR. Anterior ischemic optic neuropathy after coronary bypass surgery. Tex Med. 1987;83(8):45–7.
103. Larkin DF, Wood AE, Neligan M, Eustace P. Ischaemic optic neuropathy complicating car-diopulmonary bypass. Br J Ophthalmol. 1987;71(5):344–7.
104. Rizzo III JF, Lessell S. Posterior ischemic optic neuropathy during general surgery. Am J Ophthalmol. 1987;103(6):808–11.
105. Shahian DM, Speert PK. Symptomatic visual deficits after open heart operations. Ann Thorac Surg. 1989;48(2):275–9.
106. Tice DA. Ischemic optic neuropathy and cardiac surgery. Ann Thorac Surg. 1987;44(6):677.
107. Brown RH, Schauble JF, Miller NR. Anemia and hypotension as contributors to periopera-tive loss of vision. Anesthesiology. 1994;80(1):222–6.
108. Ballen PH, Fox MJ, Weissman GS. Ischemic optic neuropathy secondary to intestinal hemorrhage. Ann Ophthalmol. 1985;17(8):486–8.
109. Jaben SL, Glaser JS, Daily M. Ischemic optic neuropathy following general surgical procedures. J Clin Neuro Ophthalmol. 1983;3(4):239–44.
110. Katz DM, Trobe JD, Cornblath WT, Kline LB. Ischemic optic neuropathy after lumbar spine surgery. Arch Ophthalmol. 1994;112(7):925–31.
111. Lee AG. Ischemic optic neuropathy following lumbar spine surgery. Case report. J Neurosurg. 1995; 83(2):348–9.
112. Tidow-Kebritchi S, Jay WM. Anterior ischemic optic neuropathy following off-pump cardiac bypass surgery. Semin Ophthalmol. 2003;18(4):166–8.

113. Postoperative Visual Loss Study Group. Risk factors associated with ischemic optic neuropathy after spinal fusion surgery. Anesthesiology. 2012;116(1):15–24.
114. Foroozan R, Varon J. Bilateral anterior ischemic optic neuropathy after liposuction. J Neuroophthalmol. 2004;24(3):211–3.
115. Minagar A, Schatz NJ, Glaser JS. Liposuction and ischemic optic neuropathy. Case report and review of literature. J Neurol Sci. 2000;181(1–2):132–6.
116. Tomsak RL, Remler BF. Anterior ischemic optic neuropathy and increased intraocular pressure. J Clin Neuro Ophthalmol. 1989;9(2):116–8.
117. Katz B. Anterior ischemic optic neuropathy and intraocular pressure. Arch Ophthalmol. 1992; 110(5):596–7.
118. Hayreh SS, Zimmerman MB, Podhajsky P, Alward WL. Nocturnal arterial hypotension and its role in optic nerve head and ocular ischemic disorders. Am J Ophthalmol. 1994;117(5):603–24.
119. Shiose Y. Intraocular pressure: new perspectives. Surv Ophthalmol. 1990;34(6):413–35.
120. Williams EL, Hart Jr WM, Tempelhoff R. Postoperative ischemic optic neuropathy. Anesth Analg. 1995;80(5):1018–29.
121. Abraham M, Sakhuja N, Sinha S, Rastogi S. Unilateral visual loss after cervical spine surgery. J Neurosurg Anesthesiol. 2003;15(4):319–22.
122. Golnik KC, Newman SA. Anterior ischemic optic neuropathy associated with macrocytic anemia. J Clin Neuro Ophthalmol. 1990;10(4):244–7.
123. Foulds WS, Chisholm IA, Stewart JB, Wilson TM. The optic neuropathy of pernicious anemia. Arch Ophthalmol. 1969;82(4):427–32.
124. Kacer B, Hattenbach LO, Horle S, Scharrer I, Kroll P, Koch F. Central retinal vein occlusion and nonarteritic ischemic optic neuropathy in 2 patients with mild iron deficiency anemia. Ophthalmologica. 2001;215(2):128–31.
125. Acheson JF, Sanders MD. Coagulation abnormalities in ischaemic optic neuropathy. Eye. 1994;8(pt 1):89–92.
126. Salomon O, Huna-Baron R, Kurtz S, et al. Analysis of prothrombotic and vascular risk factors in patients with nonarteritic anterior ischemic optic neuropathy. Ophthalmology. 1999;106(4):739–42.
127. Nagy V, Facsko A, Takacs L, et al. Activated protein C resistance in anterior ischaemic optic neuropathy. Acta Ophthalmol Scand. 2004;82(2):140–3.
128. Stanger O, Weger M, Obeid R, et al. Impairment of homocysteine metabolism in patients with retinal vascular occlusion and non-arteritic ischemic optic neuropathy. Clin Chem Lab Med. 2005; 43(10):1020–5.
129. Kawasaki A, Purvin VA, Burgett RA. Hyperhomocysteinemia in young patients with nonarteritic anterior ischaemic optic neuropathy. Br J Ophthalmol. 1999;83(11):1287–90.
130. Glueck CJ, Wang P, Bell H, Rangaraj V, Goldenberg N. Nonarteritic anterior ischemic optic neuropathy: associations with homozygosity for the C677T methylenetetrahydrofolate reductase mutation. J Lab Clin Med. 2004;143(3):184–92.
131. Weger M, Stanger O, Deutschmann H, et al. Hyperhomocysteinaemia, but not MTHFR C677T mutation, as a risk factor for non-arteritic ischaemic optic neuropathy. Br J Ophthalmol. 2001;85(7):803–6.
132. Salomon O, Rosenberg N, Steinberg DM, et al. Nonarteritic anterior ischemic optic neuropathy is associated with a specific platelet polymorphism located on the glycoprotein Ib alpha gene. Ophthalmology. 2004;111(1):184–8.
133. Levine SR. Hypercoagulable states and stroke: a selective review. CNS Spectr. 2005;10(7):567–78.
134. Luescher TF. The endothelium and cardiovascular disease: a complex relationship. N Engl J Med. 1994;330:1081–3.
135. Corbett JJ. Neuro-ophthalmic complications of migraine and cluster headaches. Neurol Clin. 1983;1(4):973–95.
136. Cowan Jr CL, Knox DL. Migraine optic neuropathy. Ann Ophthalmol. 1982;14(2):164–6.
137. Katz B, Bamford CR. Migrainous ischemic optic neuropathy. Neurology. 1985;35(1):112–4.
138. McDonald WI, Sanders MD. Migraine complicated by ischaemic papillopathy. Lancet. 1971;2(7723): 521–3.
139. Victor DI, Welch RB. Bilateral retinal hemorrhages and disk edema in migraine. Am J Ophthalmol. 1977;84(4):555–8.
140. Weinstein JM, Feman SS. Ischemic optic neuropathy in migraine. Arch Ophthalmol. 1982;100(7): 1097–100.
141. Flammer J, Pache M, Resink T. Vasospasm, its role in the pathogenesis of diseases with particular reference to the eye. Prog Retin Eye Res. 2001;20(3):319–49.
142. Rufa A, De Stefano N, Dotti MT, et al. Acute unilateral visual loss as the first symptom of cerebral autosomal dominant arteriopathy with subcortical infarcts and leukoencephalopathy. Arch Neurol. 2004;61(4):577–80.
143. Mojon DS, Hedges III TR, Ehrenberg B, et al. Association between sleep apnea syndrome and nonarteritic anterior ischemic optic neuropathy. Arch Ophthalmol. 2002;120(5):601–5.
144. Hayreh SS, Podhajsky PA, Zimmerman B. Nonarteritic anterior ischemic optic neuropathy: time of onset of visual loss. Am J Ophthalmol. 1997; 124(5):641–7.
145. Hayreh SS. The 1994 Von Sallman lecture. The optic nerve head circulation in health and disease. Exp Eye Res. 1995;61(3):259–72.
146. Purvin VA, Kawasaki A, Yee RD. Papilledema and obstructive sleep apnea syndrome. Arch Ophthalmol. 2000;118(12):1626–30.
147. Behbehani R, Mathews MK, Sergott RC, Savino PJ. Nonarteritic anterior ischemic optic neuropathy in patients with sleep apnea while being treated with continuous positive airway pressure. Am J Ophthalmol. 2005;139(3):518–21.

148. Keltner JL. Giant-cell arteritis. Signs and symptoms. Ophthalmology. 1982;89(10):1101–10.
149. Aiello AL, Sadun AA, Feldon SE. Spontaneous improvement of progressive anterior ischemic optic neuropathy: report of two cases. Arch Ophthalmol. 1992;110(9):1197–9.
150. Liu GT, Glaser JS, Schatz NJ, Smith JL. Visual morbidity in giant cell arteritis. Clinical characteristics and prognosis for vision. Ophthalmology. 1994; 101(11):1779–85.
151. Liu NH, LaBree LD, Feldon SE, Rao NA. The epidemiology of giant cell arteritis: a 12-year retrospective study. Ophthalmology. 2001;108(6):1145–9.
152. Tomsak RL. Giant cell arteritis. Ophthalmology. 2002;109(2):219–20.
153. Kobayashi S, Yano T, Matsumoto Y, et al. Clinical and epidemiologic analysis of giant cell (temporal) arteritis from a nationwide survey in 1988 in Japan: the first government-supported nationwide survey. Arthritis Rheum. 2003;49:594–8.
154. Haugeberg G, Paulsen PQ, Bie RB. Temporal arteritis in Vest Agder County in southern Norway: incidence and clinical findings. J Rheumatol. 2000; 27(11):2624–7.
155. Baldursson O, Steinsson K, Björnsson J, Lie JT. Giant cell arteritis in Iceland. An epidemiologic and histopathologic analysis. Arthritis Rheum. 1994; 37(7):1007–12.
156. Salvarani C, Crowson CS, O'Fallon WM, Hunder GG, Gabriel SE. Reappraisal of the epidemiology of giant cell arteritis in Olmsted County, Minnesota, over a fifty-year period. Arthritis Rheum. 2004;51(2): 264–8.
157. Ramstead CL, Patel AD. Giant cell arteritis in a neuro-ophthalmology clinic in Saskatoon, 1998–2003. Can J Ophthalmol. 2007;42(2):295–8.
158. Salvarani C, Cantini F, Boiardi L, Hunder GG. Polymyalgia rheumatica and giant cell arteritis. N Engl J Med. 2002;347(4):261–71.
159. Larsson K, Mellström D, Nordborg E, Odén A, Nordborg E. Early menopause, low body mass index, and smoking are independent risk factors for developing giant cell arteritis. Ann Rheum Dis. 2006;65(4):529–32. Ann Rheum Dis. 2006;65(8): 1120. Erratum.
160. Duhaut P, Pinede L, Demolombe-Rague S, et al. Giant cell arteritis and cardiovascular risk factors: a multicenter, prospective case–control study. Groupe de Recherche sur l'Artérite à Cellules Géantes. Arthritis Rheum. 1998;41(11):1960–5.
161. Liozon E, Ouattara B, Rhaiem K, et al. Familial aggregation in giant cell arteritis and polymyalgia rheumatica: a comprehensive literature review including 4 new families. Clin Exp Rheumatol. 2009;27(1 Suppl 52):S89–94.
162. Kemp A. Monozygotic twins with temporal arteritis and ophthalmic arteritis. Acta Ophthalmol (Copenh). 1977;55(2):183–90.
163. Wernick R, Davey M, Bonafede P. Familial giant cell arteritis: report of an HLA-typed sibling pair and a review of the literature. Clin Exp Rheumatol. 1994;12(1):63–6.
164. Gonzalez-Gay MA, Garcia-Porrua C, Hajeer AH, Dababneh A, Ollier WE. HLA-DRB1*04 may be a marker of severity in giant cell arteritis. Ann Rheum Dis. 2000;59(7):574–5.
165. Rauzy O, Fort M, Nourhashemi F, et al. Relation between HLA DRB1 alleles and corticosteroid resistance in giant cell arteritis. Ann Rheum Dis. 1998;57(6):380–2.
166. Weyand CM, Hicok KC, Hunder GG, Goronzy JJ. The HLA-DRB1 locus as a genetic component in giant cell arteritis. Mapping of a disease-linked sequence motif to the antigen binding site of the HLA-DR molecule. J Clin Invest. 1992; 90(6):2355–61.
167. Hayreh SS, Podhajsky PA, Raman R, Zimmerman B. Giant cell arteritis: validity and reliability of various diagnostic criteria. Am J Ophthalmol. 1997;123(3):285–96.
168. Gonzalez-Gay MA, Garcia-Porrua C, Miranda-Filloy JA. Giant cell arteritis: diagnosis and therapeutic management. Curr Rheumatol Rep. 2006;8(4):299–302.
169. Hayreh SS, Podhajsky PA, Zimmerman B. Occult giant cell arteritis: ocular manifestations. Am J Ophthalmol. 1998;125(4):521–6.
170. Hayreh SS, Jonas JB. Optic disc morphology after arteritic anterior ischemic optic neuropathy. Ophthalmology. 2001;108(9):1586–94.
171. Kaiser M, Younge B, Bjornsson J, Goronzy JJ, Weyand CM. Formation of new vaso vasorum in vasculitis. Production of angiogenic cytokines by multinucleated giant cells. Am J Pathol. 1999; 155(3):765–74.
172. Wagner AD, Bjornsson J, Bartley GB, Goronzy JJ, Weyand CM. Interferon-gamma-producing T cells in giant cell vasculitis represent a minority of tissue-infiltrating cells and are located distant from the site of pathology. Am J Pathol. 1996;148(6):1925–33.
173. Brack A, Geisler A, Martinez-Taboada VM, et al. Giant cell vasculitis is a T cell-dependent disease. Mol Med. 1997;3(8):530–43.
174. Martinez-Taboada V, Hunder NN, Hunder GG, Weyand CM, Goronzy JJ. Recognition of tissue residing antigen by T cells in vasculitic lesions of giant cell arteritis. J Mol Med. 1996;74(11):695–703.
175. Brack A, Rittner HL, Younge BR, et al. Glucocorticoid-mediated repression of cytokine gene transcription in human arteritis-SCID chimeras. J Clin Invest. 1997;99(12):2842–50.
176. Rittner HL, Kaiser M, Brack A, et al. Tissue-destructive macrophages in giant cell arteritis. Circ Res. 1999;84(9):1050–8.
177. Weyand CM, Goronzy JJ. Pathogenic mechanisms in giant cell arteritis. Cleve Clin J Med. 2002;69 suppl 2:SII28–32.
178. Mitchell BM, Font RL. Detection of varicella zoster virus DNA in some patients with giant cell arteritis. Investig Ophthalmol Vis Sci. 2001;42(11):2572–7.

179. Rimenti G, Blasi F, Cosentini R, et al. Temporal arteritis associated with *Chlamydia pneumoniae* DNA detected in an artery specimen. J Rheumatol. 2000;27(11):2718–20.
180. Haugeberg G, Bie R, Nordbo SA. Temporal arteritis associated with *Chlamydia pneumoniae* DNA detected in an artery specimen. J Rheumatol. 2001;28(7):1738–9.
181. Regan MJ, Wood BJ, Hsieh YH, et al. Temporal arteritis and *Chlamydia pneumoniae*: failure to detect the organism by polymerase chain reaction in ninety cases and ninety controls. Arthritis Rheum. 2002;46(4):1056–60.
182. Helweg-Larsen J, Tarp B, Obel N, Baslund B. No evidence of parvovirus B19, *Chlamydia pneumoniae* or human herpes virus infection in temporal artery biopsies in patients with giant cell arteritis. Rheumatology (Oxf). 2002;41(4):445–9.
183. Katz, B, Koening C, Patel B, Kim C, et al. Identification of Burkholderia in the temporal arteries and blood of patients with giant cell arteritis. Abstract presentation at NANOS meeting, Canada:Vancouver, 2011.
184. Hunder GG, Bloch DA, Michel BA, et al. The American College of Rheumatology 1990 criteria for the classification of giant cell arteritis. Arthritis Rheum. 1990;33(8):1122–8.
185. Hall JK, Volpe NJ, Galetta SL, et al. The role of unilateral temporal artery biopsy. Ophthalmology. 2003;110(3):543–8. discussion 548.
186. Jundt JW, Mock D. Temporal arteritis with normal erythrocyte sedimentation rates presenting as occipital neuralgia. Arthritis Rheum. 1991;34(2):217–9.
187. Salvarani C, Hunder GG. Giant cell arteritis with low erythrocyte sedimentation rate: frequency of occurrence in a population-based study. Arthritis Rheum. 2001;45(2):140–5.
188. Wise CM, Agudelo CA, Chmelewski WL, McKnight KM. Temporal arteritis with low erythrocyte sedimentation rate: a review of five cases. Arthritis Rheum. 1991;34(12):1571–4.
189. Wong RL, Korn JH. Temporal arteritis without an elevated erythrocyte sedimentation rate. Case report and review of the literature. Am J Med. 1986;80(5): 959–64.
190. Miller A, Green M, Robinson D. Simple rule for calculating normal erythrocyte sedimentation rate. Br Med J (Clin Res Ed). 1983;286(6361):266.
191. Foroozan R, Danesh-Meyer H, Savino PJ, et al. Thrombocytosis in patients with biopsy-proven giant cell arteritis. Ophthalmology. 2002;109(7): 1267–71.
192. Gonzalez-Alegre P, Ruiz-Lopez AD, Abarca-Costalago M, Gonzalez-Santos P. Increment of the platelet count in temporal arteritis: response to therapy and ischemic complications. Eur Neurol. 2001;45(1):43–5.
193. Costello F, Zimmerman MB, Podhajsky PA, Hayreh SS. Role of thrombocytosis in diagnosis of giant cell arteritis and differentiation of arteritic from non-arteritic anterior ischemic optic neuropathy. Eur J Ophthalmol. 2004;14(3):245–57.
194. Salvarani C, Cantini F, Boiardi L, Hunder GG. Laboratory investigations useful in giant cell arteritis and Takayasu's arteritis. Clin Exp Rheumatol. 2003;21(6 suppl 32):S23–8.
195. Niederkohr RD, Levin LA. A Bayesian analysis of the true sensitivity of a temporal artery biopsy. Investig Ophthalmol Vis Sci. 2007;48(2):675–80.
196. Hedges 3rd TR, Gieger GL, Albert DM. The clinical value of negative temporal artery biopsy specimens. Arch Ophthalmol. 1983;101(8):1251–4.
197. Boyev LR, Miller NR, Green WR. Efficacy of unilateral versus bilateral temporal artery biopsies for the diagnosis of giant cell arteritis. Am J Ophthalmol. 1999;128(2):211–5.
198. Ray-Chaudhuri N, Kine DA, Tijani SO, et al. Effect of prior steroid treatment on temporal artery biopsy findings in giant cell arteritis. Br J Ophthalmol. 2002;86(5):530–2.
199. Lie JT. Temporal artery biopsy diagnosis of giant cell arteritis: lessons from 1109 biopsies. Anat Pathol. 1996;1:69–97.
200. Poller DN, van Wyk Q, Jeffrey MJ. The importance of skip lesions in temporal arteritis. J Clin Pathol. 2000;53(2):137–9.
201. McDonnell PJ, Moore GW, Miller NR, Hutchins GM, Green WR. Temporal arteritis. A clinicopathologic study. Ophthalmology. 1986;93(4):518–30.
202. Nordborg E, Nordborg C. Giant cell arteritis: strategies in diagnosis and treatment. Curr Opin Rheumatol. 2004;16(1):25–30.
203. Karahaliou M, Vaiopoulos G, Papaspyrou S, et al. Colour duplex sonography of temporal arteries before decision for biopsy: a prospective study in 55 patients with suspected giant cell arteritis. Arthritis Res Ther. 2006;8(4):R116.
204. Ho AC, Sergott RC, Regillo CD, et al. Color Doppler hemodynamics of giant cell arteritis. Arch Ophthalmol. 1994;112(7):938–45.
205. Schmid R, Hermann M, Yannar A, Baumgartner RW. Color duplex ultrasound of the temporal artery: replacement for biopsy in temporal arteritis. Ophthalmologica. 2002;216(1):16–21.
206. Schmidt WA, Kraft HE, Vorpahl K, Volker L, Gromnica-Ihle EJ. Color duplex ultrasonography in the diagnosis of temporal arteritis. N Engl J Med. 1997;337(19):1336–42.
207. Salvarani C, Silingardi M, Ghirarduzzi A, et al. Is duplex ultrasonography useful for the diagnosis of giant-cell arteritis? Ann Intern Med. 2002;137(4): 232–8.
208. Vianna RN, Mansour M, Ozdal PC, et al. The role of ultrasound biomicroscopy in predicting the result of temporal artery biopsy in temporal arteritis patients: a preliminary study. Eur J Ophthalmol. 2005;15(6): 655–9.
209. Morgenstern KE, Ellis BD, Schochet SS, Linberg JV. Bilateral optic nerve sheath enhancement from giant cell arteritis. J Rheumatol. 2003;30(3):625–7.

210. Lee AG, Eggenberger ER, Kaufman DI, Manrique C. Optic nerve enhancement on magnetic resonance imaging in arteritic ischemic optic neuropathy. J Neuroophthalmol. 1999;19(4):235–7.
211. Harada S, Mitsunobu F, Kodama F, et al. Giant cell arteritis associated with rheumatoid arthritis monitored by magnetic resonance angiography. Intern Med. 1999;38(8):675–8.
212. Mitomo T, Funyu T, Takahashi Y, et al. Giant cell arteritis and magnetic resonance angiography. Arthritis Rheum. 1998;41(9):1702.
213. Stanson AW. Imaging findings in extracranial (giant cell) temporal arteritis. Clin Exp Rheumatol. 2000;18(4 suppl 20):S43–8.
214. Ghanchi FD, Dutton GN. Current concepts in giant cell (temporal) arteritis. Surv Ophthalmol. 1997; 42(2):99–123.
215. Hunder GG, Sheps SG, Allen GL, et al. Daily and alternate-day corticosteroid regimens in treatment of giant cell arteritis: comparison in a prospective study. Ann Intern Med. 1975;82:613–8.
216. Zborowska B, Ell J, McGhee-Collett M, Scolyer R, McCluskey PJ. Progressive visual loss in a patient with presumed temporal arteritis despite treatment: how to make the diagnosis. Clin Exp Ophthalmol. 2004;32(3):335–6.
217. Hayreh SS, Zimmerman B. Visual deterioration in giant cell arteritis patients while on high doses of corticosteroid therapy. Ophthalmology. 2003; 110(6):1204–15.
218. Hayreh SS, Zimmerman B. Management of giant cell arteritis. Our 27-year clinical study: new light on old controversies. Ophthalmologica. 2003; 217(4):239–59.
219. Foroozan R, Deramo VA, Buono LM, et al. Recovery of visual function in patients with biopsy-proven giant cell arteritis. Ophthalmology. 2003;110(3):539–42.
220. Kim N, Trobe JD, Flint A, Keoleian G. Late ipsilateral recurrence of ischemic optic neuropathy in giant cell arteritis. J Neuroophthalmol. 2003;23(2):122–6.
221. Hunder GG. Giant cell arteritis and polymyalgia rheumatica. Med Clin N Am. 1997;81(1):195–219.
222. Andersson R, Malmvall BE, Bengtsson BA. Long-term corticosteroid treatment in giant cell arteritis. Acta Med Scand. 1986;220(5):465–9.
223. Bengtsson BA, Malmvall BE. Prognosis of giant cell arteritis including temporal arteritis and polymyalgia rheumatica. A follow-up study on ninety patients treated with corticosteroids. Acta Med Scand. 1981;209(5):337–45.
224. Chan CC, Paine M, O'Day J. Predictors of recurrent ischemic optic neuropathy in giant cell arteritis. J Neuroophthalmol. 2005;25(1):14–7.
225. Weyand CM, Kaiser M, Yang H, Younge B, Goronzy JJ. Therapeutic effects of acetylsalicylic acid in giant cell arteritis. Arthritis Rheum. 2002;46(2):457–66.
226. Ruegg S, Engelter S, Jeanneret C, et al. Bilateral vertebral artery occlusion resulting from giant cell arteritis: report of 3 cases and review of the literature. Medicine (Baltimore). 2003;82(1):1–12.
227. Nesher G, Berkun Y, Mates M, et al. Low-dose aspirin and prevention of cranial ischemic complications in giant cell arteritis. Arthritis Rheum. 2004;50(4):1332–7.
228. Lee MS, Smith SD, Galor A, Hoffman GS. Antiplatelet and anticoagulant therapy in patients with giant cell arteritis. Arthritis Rheum. 2006; 54(10):3306–9.
229. Doury P, Pattin S, Eulry F, Thabaut A. The use of dapsone in the treatment of giant cell arteritis and polymyalgia rheumatica. Arthritis Rheum. 1983;26(5):689–90.
230. Krall PL, Mazanec DJ, Wilke WS. Methotrexate for corticosteroid-resistant polymyalgia rheumatica and giant cell arteritis. Cleve Clin J Med. 1989;56(3):253–7.
231. Spiera RF, Kupersmith M, Paget S, Spiera H. Vision loss in giant cell arteritis patients treated with alternate-day corticosteroids: comment on the article by Hoffman et al. Arthritis Rheum. 2003; 48(4):1159–60.
232. Utsinger PD. Treatment of steroid nonresponsive giant cell arteritis with cytoxan. Arthritis Rheum. 1982;25(suppl):S31.
233. Hoffman GS, Cid MC, Hellmann DB, et al. International network for the study of systemic vasculitides. A multicenter, randomized, double-blind, placebo-controlled trial of adjuvant methotrexate treatment for giant cell arteritis. Arthritis Rheum. 2002;46(5):1309–18.
234. Jover JA, Hernandez-Garcia C, Morado IC, et al. Combined treatment of giant-cell arteritis with methotrexate and prednisone. A randomized, double-blind, placebo-controlled trial. Ann Intern Med. 2001;134(2):106–14.
235. Spiera RF, Mitnick HJ, Kupersmith M, et al. A prospective, double-blind, randomized, placebo controlled trial of methotrexate in the treatment of giant cell arteritis (GCA). Clin Exp Rheumatol. 2001;19(5):495–501.
236. De Silva M, Hazleman BL. Azathioprine in giant cell arteritis/polymyalgia rheumatica: a double-blind study. Ann Rheum Dis. 1986;45(2):136–8.
237. Schaufelberger C, Andersson R, Nordborg E. No additive effect of cyclosporin A compared with glucocorticoid treatment alone in giant cell arteritis: results of an open, controlled, randomized study. Br J Rheumatol. 1998;37(4):464–5.
238. Cantini F, Niccoli L, Salvarani C, Padula A, Olivieri I. Treatment of longstanding active giant cell arteritis with infliximab: report of four cases. Arthritis Rheum. 2001;44(12):2933–5.
239. Airo P, Antonioli CM, Vianelli M, Toniati P. Anti-tumour necrosis factor treatment with infliximab in a case of giant cell arteritis resistant to steroid and immunosuppressive drugs. Rheumatology (Oxf). 2002;41(3):347–9.
240. Andonopoulos AP, Meimaris N, Daoussis D, Bounas A, Giannopoulos G. Experience with infliximab (anti-TNF alpha monoclonal antibody) as monotherapy

for giant cell arteritis. Ann Rheum Dis. 2003; 62(11):1116.
241. Uthman I, Kanj N, Atweh S. Infliximab as monotherapy in giant cell arteritis. Clin Rheumatol. 2006;25(1):109–10.
242. Tan AL, Holdsworth J, Pease C, Emery P, McGonagle D. Successful treatment of resistant giant cell arteritis with etanercept. Ann Rheum Dis. 2003; 62(4):373–4.
243. Martínez-Taboada VM, Rodríguez-Valverde V. A double-blind placebo controlled trial of etanercept in patients with giant cell arteritis and corticosteroid side effects. Ann Rheum Dis. 2008;67(5):625–30.
244. Hayreh SS, Zimmerman B, Kardon RH. Visual improvement with corticosteroid therapy in giant cell arteritis. Report of a large study and review of literature. Acta Ophthalmol Scand. 2002;80(4): 355–67.
245. Font C, Cid MC, Coll-Vinent B, Lopez-Soto A, Grau JM. Clinical features in patients with permanent visual loss due to biopsy-proven giant cell arteritis. Br J Rheumatol. 1997;36(2):251–4.
246. Schmidt D, Vaith P, Hetzel A. Prevention of serious ophthalmic and cerebral complications in temporal arteritis? Clin Exp Rheumatol. 2000;18(4 suppl 20):S61–3.
247. Gonzalez-Gay MA, Blanco R, Rodriguez-Valverde V, et al. Permanent visual loss and cerebrovascular accidents in giant cell arteritis: predictors and response to treatment. Arthritis Rheum. 1998;41(8): 1497–504.
248. Aiello PD, Trautmann JC, McPhee TJ, Kunselman AR, Hunder GG. Visual prognosis in giant cell arteritis. Ophthalmology. 1993;100(4):550–5.
249. Hsu CT, Kerrison JB, Miller NR, Goldberg MF. Choroidal infarction, anterior ischemic optic neuropathy, and central retinal artery occlusion from polyarteritis nodosa. Retina. 2001;21(4):348–51.
250. Salazar R, Russman AN, Nagel MA, et al. Varicella zoster virus ischemic optic neuropathy and subclinical temporal artery involvement. Arch Neurol. 2011;68(4):517–20.
251. Perić S, Cerovski B, Perić P. Anterior ischemic optic neuropathy in patient with rheumatoid arthritis: case report. Coll Antropol. 2001;25(Suppl):67–70.
252. Duran E, Merkel PA, Sweet S, Swan N, Babikian VL. ANCA-associated small vessel vasculitis presenting with ischemic optic neuropathy. Neurology. 2004;62(1):152–3.
253. Nithyanandam S, Mohan A, Sheth U. Anterior ischemic optic neuropathy in a case of Takayasu's arteritis. Oman J Ophthalmol. 2010;3(2):94–5.
254. Kim S, Kang S, Roh YJ. A case of anterior ischemic optic neuropathy associated with Behcet's disease. Eye. 2011;25(3):395–6.
255. Felekis T, Katsanos KH, Zois CD, et al. Anterior ischemic optic neuropathy in a patient with Crohn's disease and aberrant MTHFR and GPIIIa gene variants. J Crohns Colitis. 2010;4(4):471–4.
256. Frigui M, Frikha F, Sellemi D, et al. Optic neuropathy as a presenting feature of systemic lupus erythematosus: two case reports and literature review. Lupus. 2011;20(11):1214–8.
257. Khurma V, Appen R, Wolf MD, Hansen KE. Wegener granulomatosis presenting as bilateral loss of vision. Clin Rheumatol. 2005;11(5):267–9.
258. Hayakawa K, Akatsuka I, Matsukura S, Kawai K, Ohkuma H, Shimamura K. Case of anterior ischemic optic neuropathy accompanied by Churg-Strauss syndrome. Nippon Ganka Gakkai Zasshi. 2004; 108(10):612–7.
259. Khairallah M, Zaouali S, Ben Yahia S, et al. Anterior ischemic optic neuropathy associated with *Rickettsia conorii* infection. J Neuroophthalmol. 2005;25(3): 212–4.
260. Sadda SR, Nee M, Miller NR, Biousse V, Newman NJ, Kouzis A. Clinical spectrum of posterior ischemic optic neuropathy. Am J Ophthalmol. 2001; 132(5):743–50.
261. Buono LM, Foroozan R. Perioperative posterior ischemic optic neuropathy: review of the literature. Surv Ophthalmol. 2005;50(1):15–26.
262. Saul GV, Sarkies NJC. PION due to internal carotid artery occlusion. Neuro-Ophthalmology. 1987;7: 349–53.
263. Tsai RK, Sun CY. Spontaneous dissection of internal carotid artery presenting as isolated posterior ischaemic optic neuropathy. Br J Ophthalmol. 1997; 81(6):513.
264. Hashimoto M, Ohtsuka K, Suzuki Y, Hoyt WF. A case of posterior ischemic optic neuropathy in a posterior-draining dural cavernous sinus fistula. J Neuroophthalmol. 2005;25(3):176–9.
265. Kothe AC, Flanagan J, Trevino RC. True posterior ischemic optic neuropathy associated with herpes zoster ophthalmicus. Optom Vis Sci. 1990; 67(11):845–9.
266. Weinstein JM, Morris GL, ZuRhein GM, Gentry LR. Posterior ischemic optic neuropathy due to *Aspergillus fumigatus*. J Clin Neuro Ophthalmol. 1989;9(1):7–13.
267. Lee AG, Brazis PW, Miller NR. Posterior ischemic optic neuropathy associated with migraine. Headache. 1996;36(8):506–10.
268. Claes C, Milea D, Bodaghi B, Tran TH, LeHoang P, Blanc R. Acute retrobulbar optic neuropathy due to rupture of an anterior communicating artery aneurysm. Acta Ophthalmol Scand. 2006;84(1): 145–6.
269. Hara N, Mukuno K, Ohtaka H, Shimizu K. Ischemic optic neuropathy associated with subarachnoid hemorrhage after rupture. Ophthalmologica. 2003; 217(1):79–84.
270. Taravati P, Lee AG, Bhatti MT, Lewis SB. That's a wrap. Surv Ophthalmol. 2006;51(4):434–44.
271. Perlman JI, Forman S, Gonzalez ER. Retrobulbar ischemic optic neuropathy associated with sickle cell disease. J Neuroophthalmol. 1994;14(1):45–8.

272. Chang SH, Miller NR. The incidence of vision loss due to perioperative ischemic optic neuropathy associated with spine surgery: the Johns Hopkins Hospital experience. Spine. 2005;30(11):1299–302.
273. Stevens WR, Glazer PA, Kelley SD, Lietman TM, Bradford DS. Ophthalmic complications after spinal surgery. Spine. 1997;22(12):1319–24.
274. Cheng MA, Sigurdson W, Tempelhoff R, Lauryssen C. Visual loss after spine surgery: a survey. Neurosurgery. 2000;46(3):625–30.
275. Nuttall GA, Garrity JA, Dearani JA, Abel MD, Schroeder DR, Mullany CJ. Risk factors for ischemic optic neuropathy after cardiopulmonary bypass: a matched case/control study. Anesth Analg. 2001;93(6):1410–6.
276. Sweeney PJ, Breuer AC, Selhorst JB, et al. Ischemic optic neuropathy: a complication of cardiopulmonary bypass surgery. Neurology. 1982;32(5):560–2.
277. Balm AJ, Brown DH, De Vries WA, Snow GB. Blindness: a potential complication of bilateral neck dissection. J Laryngol Otol. 1990;104(2):154–6.
278. Maran AG, Amin M, Wilson JA. Radical neck dissection: a 19-year experience. J Laryngol Otol. 1989;103(8):760–4.
279. Nawa Y, Jaques JD, Miller NR, Palermo RA, Green WR. Bilateral posterior optic neuropathy after bilateral radical neck dissection and hypotension. Graefes Arch Clin Exp Ophthalmol. 1992;230(4):301–8.
280. Schobel GA, Schmidbauer M, Millesi W, Undt G. Posterior ischemic optic neuropathy following bilateral radical neck dissection. Int J Oral Maxillofac Surg. 1995;24(4):283–7.
281. Kirkali P, Kansu T. A case of unilateral posterior ischemic optic neuropathy after radical neck dissection. Ann Ophthalmol. 1990;22(8):297–8.
282. Marks SC, Jaques DA, Hirata RM, Saunders Jr JR. Blindness following bilateral radical neck dissection. Head Neck. 1990;12(4):342–5.
283. Milner GA. A case of blindness after bilateral neck dissection. J Laryngol Otol. 1960;74:880–5.
284. Pazos GA, Leonard DW, Blice J, Thompson DH. Blindness after bilateral neck dissection: case report and review. Am J Otolaryngol. 1999;20(5):340–5.
285. Moura FC, Cunha LP, Monteiro ML. Bilateral visual loss after liposuction: case report and review of the literature. Clinics (Sao Paulo). 2006;61(5):489–91.
286. Purvin V, Kuzma B. Intraorbital optic nerve signal hyperintensity on magnetic resonance imaging sequences in perioperative hypotensive ischemic optic neuropathy. J Neuroophthalmol. 2005;25(3):202–4.
287. Vaphiades MS. Optic nerve enhancement in hypotensive ischemic optic neuropathy. J Neuroophthalmol. 2004;24(3):235–6.
288. McAuley DF, McGurk C, Nugent AG, et al. Vasoconstriction to endothelin-1 is blunted in non-insulin-dependent diabetes: a dose–response study. Clin Sci (Lond). 2000;99:175–9.
289. Dzau VJ. Tissue angiotensin and pathobiology of vascular disease: a unifying hypothesis. Hypertension. 2001;37:1047–52.
290. Practice guidelines for blood component therapy: a report by the American Society of Anesthesiologists Task Force on Blood Component Therapy. Anesthesiology 1996;84(3):732–47.

Papilledema

3

Jane W. Chan

Papilledema

Papilledema is clinically defined as optic disc swelling resulting only from increased intracranial pressure (ICP), as opposed to the optic disc swelling from other etiologies, such as ischemia or inflammation. Cerebrospinal fluid pressure (CSF) equal to or greater than 250 mmH_2O taken in an adult person lying in the lateral recumbent position is considered abnormally elevated. Normal CSF pressure is usually in the range of 100–250 mmH_2O in adults [1, 2].

Symptoms of Papilledema

One of the most common symptoms of increased ICP is headache. It is usually a dull, pulsatile, occipital, or generalized headache. It can occur daily and last for hours. The headache is not related to the ICP changes or other associated symptoms. It may be worsened with Valsalva maneuvers, such as coughing or straining. It is usually associated with neck stiffness, nausea, and vomiting. Occasionally, retrobulbar pain may occur with eye movement. Pain may even radiate to facial dermatomes [3].

J.W. Chan, M.D. (✉)
Department of Neurology, Neuro-Ophthalmology,
University of Nevada School of Medicine,
975 Kirman Avenue (111), Reno, Nevada 89502, USA
e-mail: worjun@aol.com

Transient visual obscurations may involve blurry vision to complete loss of vision and are thought to be related to transient ischemia of the optic nerve [3]. Acute episodes of blurry vision are the most common and usually last less than 30 s and rarely several hours [4]. They may be monocular or binocular and are not related to the degree of ICP or to the severity of papilledema. These visual symptoms are precipitated by postural changes [4]. Positive visual phenomena, such as photopsias and phosphenes, are also transient and are thought to be related to traction of the retrobulbar optic nerve or retina [5].

Pulsatile tinnitus is often unilateral and is eliminated temporarily by compression of the ipsilateral jugular vein and by lowering CSF pressure by a lumbar puncture (LP). High-pressure vascular pulsations are thought to be transmitted by CSF to the venous sinus walls to cause this tinnitus [6].

Signs of Papilledema

The key feature of increased ICP is papilledema and may be classified into the following four different stages: (1) early, (2) fully developed, (3) chronic, and (4) atrophic [5].

A very early sign of papilledema is hyperemia, dilatation of capillaries on the disc surface. The retinal nerve fiber layer (RNFL) also loses its superficial curvilinear light reflexes to become more red. The optic disc usually is swollen, initially in the inferior pole, then at the superior

J.W. Chan (ed.), *Optic Nerve Disorders: Diagnosis and Management*,
DOI 10.1007/978-1-4614-0691-4_3,

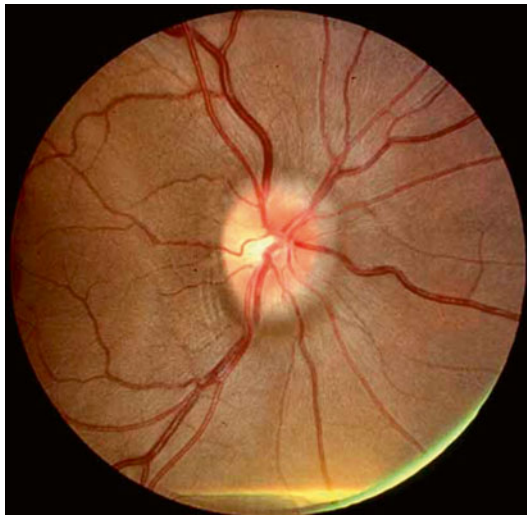

Fig. 3.1 Grade 1 papilledema—temporal disc elevation. [Reprinted with permission from The University of Iowa and EyeRounds.org]

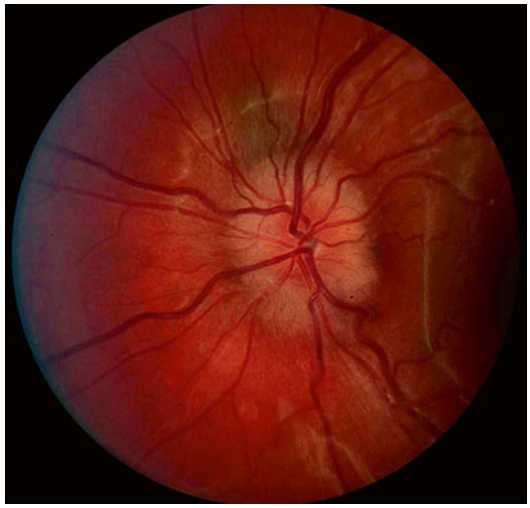

Fig. 3.2 Grade 2 papilledema—circumferential disc elevation. [Reprinted with permission from The University of Iowa and EyeRounds.org]

pole, followed by the temporal and nasal aspects, respectively [6]. Because of the disc swelling, the optic disc margins become blurred (Figs. 3.1 and 3.2). Rupture of a distended capillary within or surrounding the disc may also cause peripapillary nerve fiber layer hemorrhages. These flame-shaped hemorrhages appear as thin streaks of blood on or near the margins of the optic disc. Because of the elevated ICP, spontaneous retinal

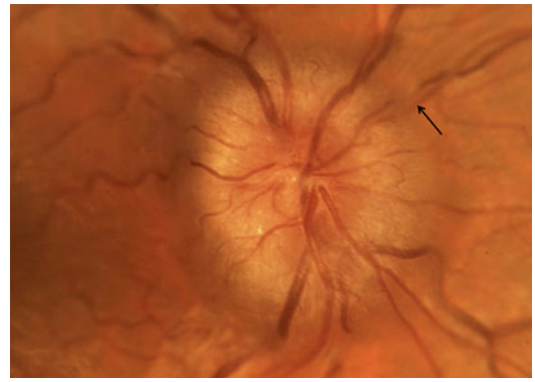

Fig. 3.3 Grade 3 papilledema—obscuration of blood vessels at outside edge of disc. [Reprinted with permission from The University of Iowa and EyeRounds.org]

venous pulsations are absent. CSF pressures of 200 mmH_2O or greater may even inhibit these pulsations. As 20 % of persons with normal CSF pressure have spontaneous venous pulsations, the observation of spontaneous venous pulsations only indicates that the CSF pressure is below 200 mmH_2O at that time and is not always a reliable sign of papilledema [5, 6].

In more fully developed papilledema, peripheral retinal veins become engorged and dark. Closer to the disc, splinter hemorrhages may be seen as edema in the RNFL increases at or adjacent to the disc margin. More flame-shaped hemorrhages may appear as a result of sudden rises of CSF pressure. The surface of the disc then becomes elevated above the retinal surface, and microaneurysms and dilated capillaries appear. The peripapillary surface blood vessels become obscured by more edema in the RNFL (Figs. 3.3–3.5). Focal retinal infarcts, or cotton wool spots and tortuous vessels appear [5, 6].

In severely elevated ICP, circumferential choroidal folds, or Paton's lines, may develop (Fig. 3.6). Choroidal folds may even be the initial presenting sign of increased ICP, according to a study by Griebel and Kosmorsky [7]. Ten of 12 patients had ICPs of greater than 120 mmH_2O, and 8 of 12 were diagnosed with increased intracranial hypertension (IIH). Four patients had increased ICP and choroidal folds in the absence of papilledema. It was hypothesized that the choroidal folds might represent enlargement of the

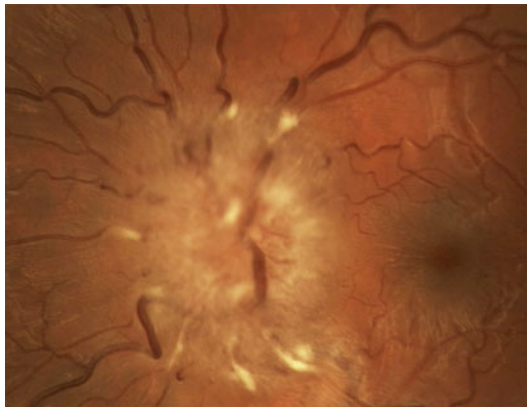

Fig. 3.4 Grade 4 papilledema—obscuration of blood vessels on the disc periphery. [Reprinted with permission from The University of Iowa and EyeRounds.org]

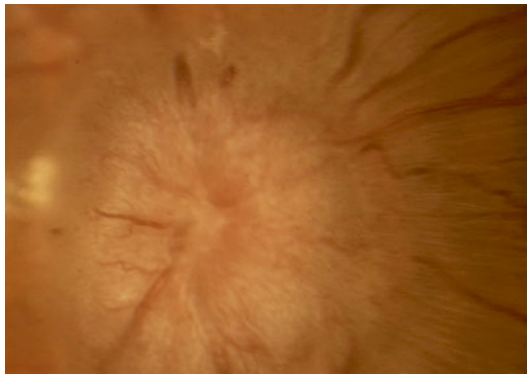

Fig. 3.5 Grade 5 papilledema—grade 4 features with partial or total obscuration of disc vessels. [Reprinted with permission from The University of Iowa and EyeRounds.org]

retrolaminar optic nerve sheath in the absence of axonal swelling. Alternatively, it was proposed that the choroidal folds might persist after resolution of the papilledema. The presence of choroidal folds in isolation might be related to the timing of the evaluation.

Hard exudates and hemorrhages may occur in the peripapillary region and in the macula to cause decreased central vision. Development of macular edema may be a risk factor for permanent visual loss in PTCS. In a study by Talks et al. [8] 44 % (21 of 48) of eyes in 24 patients who had progressive visual deterioration from PTCS requiring optic nerve sheath fenestration developed macular changes, including choroidal

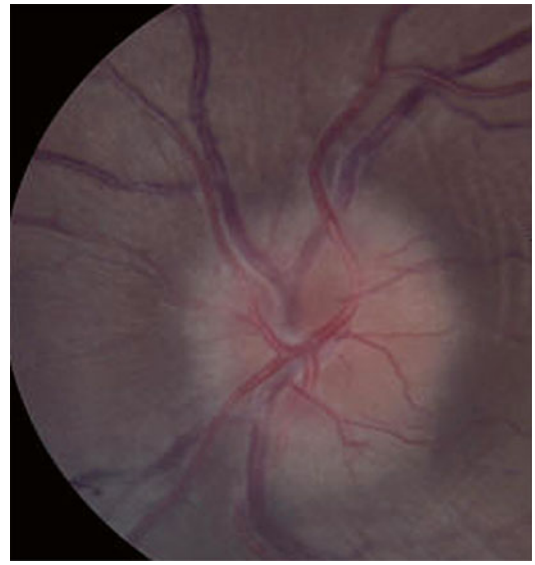

Fig. 3.6 Atrophic papilledema with choroidal folds. [Courtesy of Frank Ingle, M.D.]

folds, Paton's lines, nerve fiber layer hemorrhages, subretinal hemorrhages, macular stars, macular edema, and retinal pigment epithelial changes. These changes probably contributed to the severe visual loss in five eyes, three of which did not improve despite treatment. It was concluded that these macular changes might not have had a significant impact on optic nerve-related visual loss in patients with IIH, but the patients who developed macular edema might be at greater risk for permanent visual loss.

If ICP increases abruptly, severe subhyaloid hemorrhages may occur and occasionally bleed and dissect into the vitreous in about 4 % of patients with papilledema [9]. These intraretinal hemorrhages are often the result of compression of the central retinal vein from the swollen optic disc and usually resolve with treatment of elevated ICP [10].

In chronic papilledema, hemorrhages and exudates slowly resolve, and the optic disc cup is gradually destroyed [6]. The disc may have hard exudates mimicking disc drusen, a sign that the papilledema has been present for several months. Nerve fiber layer atrophy may also appear as slit-like defects on red-free direct ophthalmoscopy [11]. Chronic papilledema may even persist for many years causing significant visual symptoms,

especially in patients with pseudotumor cerebri or with intracranial tumors [12].

If left untreated, chronic papilledema will result in disc pallor with attenuated and sheathed retinal vessels [13, 14]. The nerve fiber layer appears dull, and some patients have persistent pigmentary changes or choroidal folds in the maculae [14, 15].

The duration for each of the stages of papilledema just described varies among individuals. Not all patients with papilledema progress through these stages. Some may begin with fully developed papilledema and then advance to the chronic stage, followed by the atrophic stage when optociliary shunt vessels appear [16–28]. These preexisting veins shunt blood from the retinal to the choroidal venous circulation [19]. The elevated ICP is believed to compress the central retinal vein directly or the optic nerve indirectly to cause these vessels to become enlarged and thereby visible. The optic atrophy resulting from chronic papilledema also causes a selective loss of peripheral axons with sparing of central axons so that central visual acuity is spared [20].

Asymmetric papilledema, when one eye appears to have more severe papilledema than the other, may occur in the Foster Kennedy syndrome [21–24]. Frontal lobe or olfactory groove tumors compress the ipsilateral optic nerve to cause optic atrophy. Meanwhile, growth of the mass causes increased ICP, which then distends the contralateral optic nerve sheath, resulting in papilledema. Previous lesions in the optic chiasm or optic tract can also lead to asymmetric papilledema [21–24]. Patients with temporal hemianopia and atrophy of nasal fibers have band atrophy with sparing of the most upper and lower (temporal) arcuate fibers. During papilledema, the swelling is limited to the superior and inferior regions of the disc. In patients with nasal hemianopia, atrophy of temporal fibers and swelling is limited to the nasal region of the disc [25].

Unilateral papilledema in normal optic discs occurs in approximately 4 % of cases. It is thought to be secondary to varying degrees of communication between the subarachnoid space and optic nerve head through the optic canal [26]. In a report by Krishna et al. [27] a young obese woman presented with headache and a left sixth nerve palsy without optic disc swelling. Her CSF was normal except for an opening pressure of 440 mmH_2O. Magnetic resonance imaging (MRI) of the brain was normal, and her symptoms resolved completely on acetazolamide treatment. Atrophic or anomalous discs may not develop papilledema, except in regions of the disc where some axons are still functioning. Therefore, most cases of unilateral papilledema represent bilateral asymmetric papilledema.

Central vision is affected in papilledema. Visual acuity may range from normal to no light perception. The visual acuity is not related to the degree of papilledema, except for atrophic papilledema in which the vision would be invariably poor. However, contrast sensitivity defects do correlate to the severity of visual loss. Acute loss of central vision is usually a late phenomenon that can be related to local ischemia, such as ischemic optic neuropathy, or retinal vascular occlusions related to a rapid rate of increase in ICP, or to an underlying coagulopathy [28, 29]. Along with loss of visual acuity, visual field defects develop slowly and progressively. Concentric enlargement of the blind spot is the most common defect, followed by isopter constriction and loss of the inferior nasal quadrant of the visual field with a nasal step [30]. Color defects usually involve red-green abnormalities. No afferent pupillary defect is detected in most instances of bilateral papilledema. One-third of patients have horizontal diplopia. One-fifth of these are sixth nerve palsies; the remainder have third nerve palsies, fourth nerve palsies, or hypertropias [5].

Diagnostic Testing

Although papilledema is most often diagnosed by careful ophthalmoscopic examination, some cases of optic disc swelling may not be so apparent. Optical coherence tomography (OCT) can be used as an adjunct to ophthalmoscopy to monitor the severity and evolution of papilledema in PTCS. OCT can also help distinguish papilledema from non-arteritic ischemic optic neuropathy (NAION) or optic neuritis. The retinal pigment

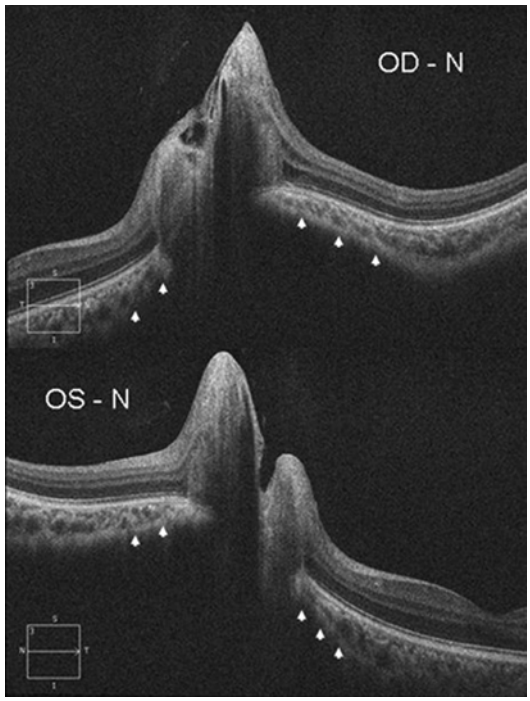

Fig. 3.7 The retinal pigment epithelium/basement membrane (RPE/BM) angle is positive and the sclera is bowed inward (*arrowheads*). The RPE/BM angle and sclera have more inward angulation on the nasal side (N) of the optic canal of each eye. (OD = top and OS = bottom). [Reprinted from Kupersmith MJ, Sibony P, Mandel G, Durbin M, Kardon RH. Optical coherence tomography of the swollen optic nerve head: deformation of the peripapillary retinal pigment epithelium layer in papilledema. Invest Ophthalmol Vis Sci. 2011;52(9):6558–64. With permission from IOVS]

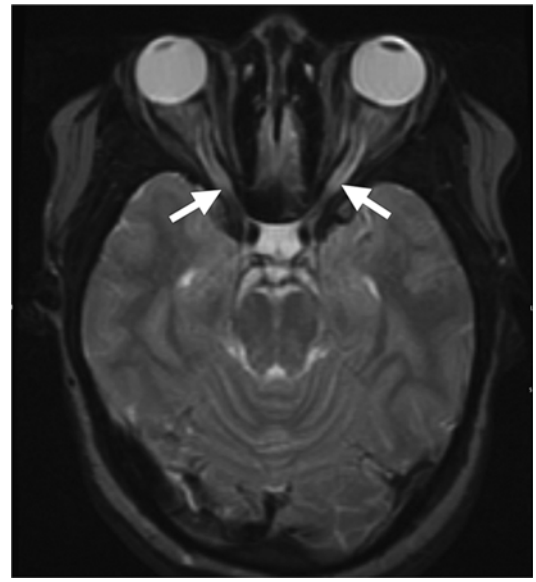

Fig. 3.8 Increased fluid can occasionally be visualized in the optic nerve sheath surrounding the optic nerves on axial MRI of orbits. [Reprinted from Choudhary AK, Donnelly LF, Racadio JM, Strife JL, et al. Diseases Associated with Childood Obesity. AJR 2007;188:1118–30. With permission from American Roentgen Ray Society]

epithelium/basement membrane is often indented inward and this angular deflection is thought to be caused by elevated pressure in the subarachnoid space that does not correspond with the amount of RNFL swelling. This inward displacement of the retinal pigment epithelium/basement membrane reverses as papilledema resolves with treatment (Fig. 3.7) [31]. In a study of 44 eyes in patients with mild papilledema associated with IIH and 44 controls, the RNFL thickness was 75 % greater than in control eyes. The RNFL thickness significantly correlated with Humphrey visual field indices of mean deviation and pattern standard deviation. Regression analysis showed that for every 10 μm of mean RNFL thickness increase at baseline, there was a 0.6 dB decrease in mean deviation at the last follow-up visit. In severe papilledema evolving to disc atrophy, the thinning of the RNFL would be associated with visual loss [32]. Fluorescein angiography may diagnose early papilledema in only some instances [33, 34]. An A- and B-scan ultrasound with a 30° test when indicated can help determine whether the optic disc is truly swollen and if there is increased ICP [35]. A computed tomography (CT) scan of the orbits can delineate calcium deposits to distinguish drusen from papilledema. Increased fluid can occasionally be visualized in the optic nerve sheath surrounding the optic nerve (Fig. 3.8). To evaluate for an intracranial mass or hydrocephalus, CT or MRI of the brain with and without contrast should be done. A LP can then be performed to measure the ICP [6].

Pathology

On histopathology, the optic nerve head with papilledema protrudes into the vitreous, displaces the adjacent retina, and causes folds in the

posterior retinal layers. The compression and displacement of the peripapillary retina are thought to contribute to the enlargement of the blind spot [36, 37]. Peripapillary subretinal fluid can cause hyperopia from elevation of the retina and can also lead to a refractive scotoma or enlarged blind spot [38].

The prelaminar portion of the optic nerve is swollen whereas the postlaminar aspect is not. The papilledema arises from intraaxonal swelling [39]. Increased numbers of mitochondria, disorganized neurofilaments, and accumulation of intracellular membranes also can be seen. Necroses appear from prolonged ischemic of the compressive effects of the angulated nerve fibers exiting the optic nerve head [40, 41].

Possible Mechanisms of Visual Loss Related to Papilledema

Histological evidence and the types of visual field defects seen in PTCS localize the site of the lesion at the optic nerve head. Increased ICP is translated along the subarachnoid space of the optic nerve sheath, which causes an increased pressure gradient across the optic nerve head. This pressure within the optic nerve contributes to axoplasmic stasis. According to Tso et al. [42] both slow and fast axoplasmic transport is disrupted, resulting in intraaxonal edema. Another potential mechanism of visual loss in PTCS is optic disc ischemia. Delays in prelaminar arterial filling are seen on fluorescein angiography in patients with papilledema. The visual field defects occurring in patients with papilledema are also similar to those found in other ischemic optic neuropathies, such as glaucoma and anterior ischemic optic neuropathy. The axoplasmic stasis, intraaxonal edema, and compression of small arterioles lead to optic nerve ischemia [43].

Common Secondary Causes of Increased Intracranial Pressure

Intracranial masses, such as abscesses, arteriovenous malformations, hemorrhages, infarctions, inflammatory masses, and neoplasms, may cause increased ICP by displacement of space in the cranium, produce focal or diffuse cerebral edema, or obstruct CSF flow by blocking CSF drainage. CSF obstruction may be by direct compression of venous sinuses or indirectly by the production of protein that obstruct infiltration through the arachnoid villi by such tumors as carcinomas, lymphomas, leukemias, and leptomeningeal gliomatosis. Infratentorial tumors more often than supratentorial ones cause papilledema. Infratentorial tumors often obstruct the aqueduct or compress the vein of Galen or superior sagittal sinus. Supratentorial tumors usually compress the falx or vein of Galen. Other types of supratentorial tumors located in one of the lateral ventricles or in the nondominant hemisphere may also cause papilledema without any localizing signs. Only 60 % of intracranial tumors cause enough increased ICP to result in papilledema. Other mass lesions include hematomas and abscesses [44].

Aqueductal stenosis is associated with papilledema. The stenosis may be congenital and may or may not be associated with a Chiari malformation. Infants present with macrocephaly, whereas adults present with papilledema, headache, dorsal midbrain syndrome, meningitis, hemorrhage, pituitary compression causing endocrinological dysfunction, seizures, gait ataxia, and CSF rhinorrhea [5].

Among congenital conditions, mucopolysaccharidosis is a common cause of ICP and papilledema. Deposition of mucopolysaccharides in the arachnoid villi inhibits resorption of CSF [5]. Craniosynostosis may also cause decreased venous outflow through the jugular foramina. Approximately 15 % of patients with premature synostosis of the cranial sutures develop papilledema, whereas other types, such as oxycephaly, scaphocephaly, and trigonocephaly, often do not. Papilledema develops in about 40 % of patients with craniofacial dysostosis, such as Crouzon's syndrome and Apert syndrome. Papilledema, if it develops, usually presents before the age of 10 years [45].

By blocking CSF flow in the ventricles or by obstructing CSF absorption into the arachnoid villi, subarachnoid hemorrhage may also cause increased ICP and papilledema. A total of

10–24 % of patients with ruptured intracranial aneurysms develop papilledema within several hours or weeks [46].

By causing diffuse cerebral edema, obstructing the aqueduct, and/or obstructing CSF resorption in the arachnoid villi, meningitis and encephalitis may produce increased ICP and papilledema [47]. About 2.5 % of patients with meningitis develop papilledema [48]. Tuberculous meningitis is the most common cause, followed by cryptococcal meningitis in which the papilledema may be more severe. Papilledema usually resolves with treatment of the infection.

Granulomatous infections, such as syphilis, tuberculosis, and sarcoidosis, may cause nodular masses and fibrosis of the meninges that obstruct CSF flow [48]. About 20 % of patients with viral encephalitis, especially herpes simplex and herpes zoster, have papilledema [49]. California encephalitis, lymphocytic choriomeningitis, infectious mononucleosis, Coxsackie meningo-encephalitis, and poliomyelitis may occasionally present with papilledema [50].

Increased CSF protein produced by spinal cord tumors may obstruct CSF resorption in the arachnoid villi. Spinal cord tumors may grow in the cervical region to compress the cerebellum upward and obstruct CSF flow through the foramen magnum, but more often neurinomas and ependymomas in the thoracic and lumbar regions produce these high amounts of protein or blood products from recurrent hemorrhaging, respectively [5]. Paragangliomas in the lower spinal cord may also lead to PTCS. In a report by Haslbeck et al. [51] a patient with a cauda equina paraganglioma presented with papilledema and a right sixth nerve palsy. CT and MRI of the brain were normal. The CSF opening pressure was 330 mmH_2O with increased erythrocytes of 35,000 cells/mm^3 and elevated CSF protein of 4,500 mg/dL. Although these findings were initially attributed to a traumatic tap, a subsequent spinal MRI revealed a paraganglioma extending from L3 to the filum terminale.

By a similar mechanism, elevated CSF protein in Guillain–Barre syndrome and chronic inflammatory demyelinating polyneuropathy (CIDP) may also lead to papilledema. However, papilledema has been observed in patients with CIDP with only mildly elevated CSF protein [52].

Decreased venous drainage is another common cause of communicating hydrocephalus that may lead to papilledema. The superior sagittal and transverse venous sinuses are most commonly affected. Extraaxial tumors, such as meningiomas, may directly compress the superior sagittal sinus. Acoustic neuromas and metastatic tumors may also compress the transverse sinus. Early papilledema develops in otitis media when complicated by septic thrombosis of the transverse sinus, in which the infection spreads to the mastoid air cells and then to the adjacent lateral sinus. In contrast, papilledema develops late in the course of septic thrombosis of the cavernous sinus. Iatrogenic etiologies, including ligation or occlusion of a jugular vein during surgery or thrombosis of an indwelling catheter, may cause severe papilledema to develop within 2 weeks. It often gradually resolves as collateral veins form to shunt the CSF [53].

Cerebral Venous Sinus Thrombosis

Cerebral venous sinus thrombosis affects women between 20 and 35 years of age. Young women, those during pregnancy, and especially those during puerperium are at highest risk of developing cerebral venous sinus thrombosis [53]. The superior sagittal sinus is involved in 72 % of patients and the lateral sinuses in about 70 % of patients (Fig. 3.9). More than one sinus is affected in greater than 30 % of patients. In 30–40 % of patients, both sinuses and cerebral or cerebellar veins are involved. The slow growth of the thrombus and extensive collateralization of the venous system account for the gradual onset of symptoms over weeks to months [54]. The ischemia from the thrombus causes hemorrhagic infarction in the cortex and adjacent white matter in 10–50 % of patients [55–57]. Patients with cerebral venous thrombosis can present with headache, papilledema, focal neurological deficits, seizures, and mental status changes [58]. The clinical presentation of cerebral venous thrombosis can vary, but four main types have been identified: (1) focal

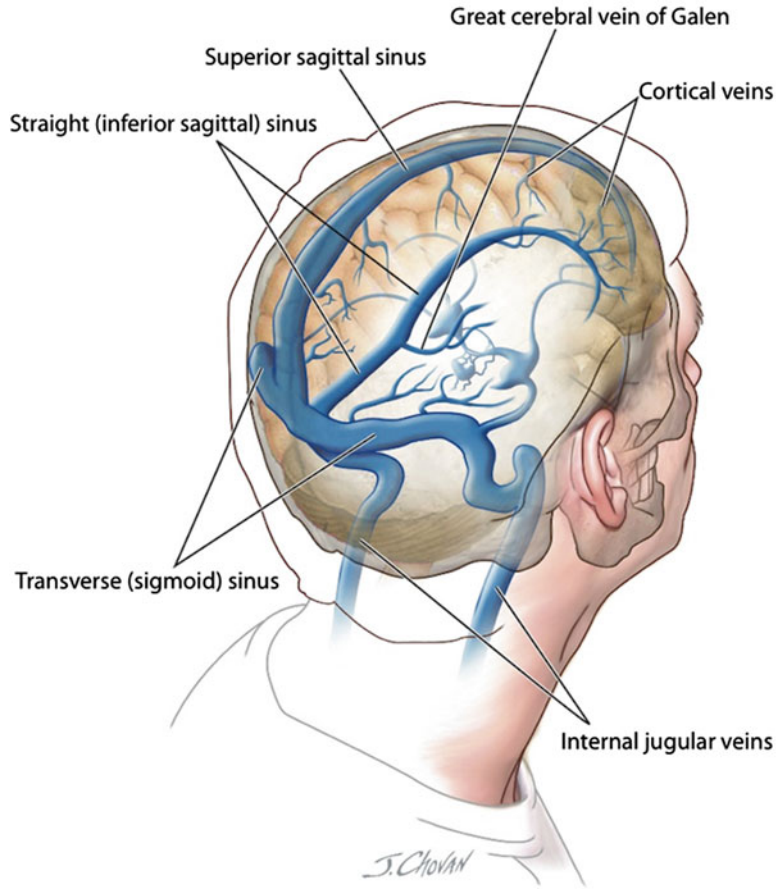

Fig. 3.9 Diagram of the major cerebral venous sinus and veins. [Courtesy of Joe Chovan]

neurological deficits or partial seizures (75 %); (2) isolated increased ICP with headache, papilledema, and sixth nerve palsy (18–38 %); (3) subacute diffuse encephalopathy without any localizing neurological signs to suggest increased ICP; and (4) acute painful ophthalmoplegia with chemosis and proptosis from cavernous sinus thrombosis [59, 60]. In 80 % of patients with cerebral venous thrombosis, a cause or predisposing factor can be identified. There is a wide spectrum of etiologies, such as infection, autoimmune disorders, coagulopathies, and tumors (Table 3.1) [61].

Cerebral venous thrombosis has a good long-term prognosis. Up to 86 % of patients have complete recovery [62]. Mortality ranges from 5.5 to 18 % [62]. The frequency of long-standing epilepsy was low, suggesting that anticonvulsants do not need to be continued in most patients. Only 12 % of patients have a recurrence of cerebral venous thrombosis and 14 % have a different type of venous thrombosis [62].

On CT scan of the brain, the "empty delta sign," representing the opacification of collateral veins in the wall of the superior sagittal sinus after contrast injection, is seen only in 10–20 % of patients (Fig. 3.10). CT scan of the brain is normal in 10–20 % of patients with proven cerebral venous sinus thrombosis [53]. The most reliable diagnostic modality for cerebral venous sinus thrombosis is MRI and MR venogram of the brain, which can show thrombosis, cerebral edema, infarction, hemorrhage, and anatomy of

Table 3.1 Some causes and predisposing factors of cerebral venous sinus thrombosis

• Infection from penetrating head injury, intracranial infection, localized infection elsewhere in the body, and sepsis or systemic infection
• Head injury complication
• Neurosurgery complication
• Stroke and hemorrhage
• Space-occupying lesion
• Infusions from central venous line
• Cardiac disease
• Hormonal and endocrinological causes
• Malignancies
• Red blood cell disorders
• Thrombocytopenia coagulation disorders
• Severe dehydration
• Inflammatory bowel disease
• Connective tissue disorders
• Behçet's disease
• Sarcoidosis
• Nephrotic syndrome
• Drugs (such as L-asparaginase)

[Reprinted from Allroggen H, Abbott RJ. Cerebral venous sinus thrombosis. Postgrad Med J. 2000;76(891):12–5. With permission from BMJ Publishing Group]

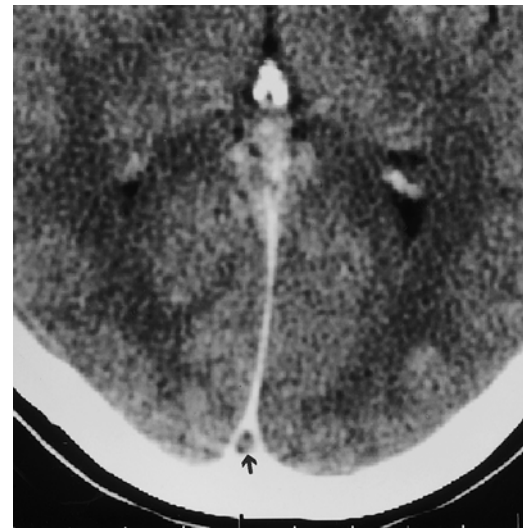

Fig. 3.10 Empty delta sign in a patient with superior sagittal sinus thrombosis. Transverse contrast-enhanced CT image reveals low-attenuating thrombus (*arrow*) within the superior sagittal sinus, surrounded by a triangular area of enhancement. [Reprinted from Lee E JY. The Empty Delta Sign. Radiology 2002;224:778–89. With permission from The Radiological Society of North America (RSNA®)]

the abnormal venous circulation. If the diagnosis is still doubtful, then cerebral angiography may be necessary [53, 56, 57]. Absence or hypoplasia of the anterior aspect of the superior sagittal sinus, which is a normal variant, can simulate thrombosis on MR venogram. Contrast enhancement may also be mistaken for normal contrast material accumulating within the sinus [57]. Compared to MR venogram, CT venography may better visualize sinuses or cortical veins with low flow [63].

CSF abnormalities occur in up to 84 % of patients and include increased ICP, increased protein, presence of red blood cells, and pleocytosis [55]. Meningitis and subarachnoid hemorrhage must be ruled out before the diagnosis of cerebral venous sinus thrombosis can be established. Acquired and inherited coagulation disorders, such as Factor V Leiden mutation if resistance to activated protein C is abnormal, should be evaluated. Activity of protein C and S; antithrombin III; and levels of plasminogen, fibrinogen, and anticardiolipin antibodies should also be performed before starting anticoagulation and 6 months afterwards [64].

Anticoagulants as the treatment of choice for cerebral sinus thrombosis have been controversial. In a Cochrane Database Systematic Review [65], two small trials addressing this issue were selected for analysis. Each trial was a randomized, controlled trial in which anticoagulant therapy was compared with placebo or open control in patients with cerebral venous sinus thrombosis confirmed by MR angiography or intraarterial contrast. The efficacy of intravenous, adjusted-dose unfractionated heparin was examined in one trial of 20 patients. The efficacy of high-dose, body weight-adjusted, subcutaneous, low molecular weight heparin (Nadroparin) was examined in the other study of 59 patients. The pooled relative risk of death associated with anticoagulant therapy was 0.33 [95 % confidence interval (CI), 0.08–1.21] and that of dependency was 0.46 (95 % CI,

0.16–1.31). No new symptomatic intracerebral hemorrhages were observed. One gastrointestinal hemorrhage occurred after anticoagulant treatment. Therefore, anticoagulant treatment for cerebral venous sinus thrombosis seemed safe. It did not reduce the risk of death or dependency, but statistical significance was not attained.

Heparin is started as a continuous intravenous infusion at 1,000 Units/h and is adjusted according to the activated partial thromboplastin time, 1.5–2 times control. It is contraindicated in patients who are actively bleeding or who have hypersensitivity to the drug. Some side effects include hemorrhage and hypersensitivity reactions. Immune-mediated thrombocytopenia occurs in 2–5 % of patients receiving unfractionated heparin. Oral warfarin is usually started after a few days and adjusted to obtain an International Normalized Ratio between 2 and 3. Warfarin may be continued up to 3 months, based upon a study by Einhaupl and Masuhr [66], no recurrence of cerebral venous thrombosis occurred after 3 months of anticoagulant treatment. However, warfarin may need to be continued so long as the risk of cerebral venous thrombosis is present, as in patients with malignancy, inflammatory disease, inherited thrombophilia, etc.

In women who have had a history of cerebral venous thrombosis during pregnancy or a history of recurrent deep venous thrombosis, low molecular weight heparin is usually given for preventative treatment. For women who have postpartum cerebral venous thrombosis, low molecular weight heparin is continued after delivery for up to 1 month for prophylaxis.

Although intravenous and intrasinus thrombolysis have been used in patients who fail heparin, intrasinus infusion with streptokinase or urokinase is faster than the intravenous route. Delivery of the thrombolytic agent, such as tissue plasminogen activator (tPA) or urokinase, locally to the clot requires a lower dose associated with less risk of hemorrhage. Local endovascular urokinase or tPA can also be used in patients with brain edema and hemorrhage [65]. More randomized, controlled data are needed to clarify the details of delivery techniques, choice of drugs, drug dosages, etc.

Pseudotumor Cerebri Syndrome

Symptoms

The most common symptoms of the PTCS, include headache, transient visual obscurations, pulsatile tinnitus, and diplopia. In a review of 82 patients [67], 68 % of patients had specific headache disorders, such as episodic tension headache in 30 % and migraine without aura in 20 %. These patients with PTCS often had headaches unrelated to increased ICP, and these headaches often persist despite normalization of the ICP.

Signs

Papilledema may be absent in some cases of PTCS, especially in obese women and some men with new daily persistent headache (NDPH) syndrome (the acute onset of headache within 3 days that is persistent for 15 days or more each month for at least 3 months) [68]. Conversely, PTCS can be present with papilledema and normal CSF opening pressure [69]. (Please see "Symptoms and Signs of Papilledema.")

Diagnostic Criteria of Pseudotumor Cerebri Syndrome

The diagnostic criteria for PTCS, a term that includes idiopathic and secondary etiologies of increased intracranial hypertension. The idiopathic form of PTCS is outlined in Table 3.2. A patient is considered to have definite PTCS if criteria A–E are fulfilled. The diagnosis is considered probable if criteria A–D are met with bilateral papilledema present, and the measured CSF pressure is lower than that specified for a definitive diagnosis. Papilledema is the hallmark of PTCS and is usually present in the acute presentation of this syndrome. The patient's mental status must be normal (awake and alert). Cranial nerve 6th and 7th palsies can be present but there can be no other unexplained focal neurologic deficits. Regarding neuroimaging, the brain parenchyma

Table 3.2 Diagnostic criteria for pseudotumor cerebri syndrome (idiopathic intracranial hypertension)

1. Required for diagnosis of pseudotumor cerebri syndrome[a]
A. Papilledema
B. Normal neurologic examination except for cranial nerve abnormalities
C. Neuroimaging: Normal brain parenchyma without evidence of hydrocephalus, mass, or structural lesion and no abnormal meningeal enhancement on MRI with and without gadolinium for typical patients (female and obese), and on MRI with and without gadolinium and magnetic resonance venography for others; if MRI is unavailable or contraindicated, contrast-enhanced CT may be used
D. Normal CSF composition
E. Elevated lumbar puncture opening pressure of ≥250 mm CSF in adults and ≥280 mm CSF in children (250 mm CSF if the child is not sedated and not obese) in a properly performed lumbar puncture.
2. Diagnosis of pseudotumor cerebri syndrome without papilledema
In the absence of papilledema, a diagnosis of pseudotumor cerebri syndrome can be made if B–E from above are satisfied, and in addition if the patient has a unilateral or bilateral abducens nerve palsy
In the absence of papilledema or sixth nerve palsy, a diagnosis of pseudotumor cerebri syndrome can be suggested but not made if B–E from above are satisfied, and in addition at least three of the following neuroimaging criteria are satisfied:
i. Empty sella
ii. Flattening of the posterior aspect of the globe
iii. Distention of the perioptic subarachnoid space with or without a tortuous optic nerve
iv. Transverse venous sinus stenosis

[a]A diagnosis of pseudotumor cerebri syndrome is definite if the patient fulfills criteria A–E. The diagnosis is considered probable if criteria A–D are met but the measured CSF pressure is lower than that specified for a definitive diagnosis.

[Reprinted from Friedman DI, Liu GT, Digre KB. Revised diagnostic criteria for the pseudotumor cerebri syndrome in adults and children. Neurology 2013;81: 1159–65. With permission from Wolters Kluwer Health]

must be normal without evidence of hydrocephalus, structural lesions, or meningeal enhancement on MRI with and without gadolinium, for typical obese female patients, and on the MRI with and without gadolinium and magnetic resonance venography (MRV) for all others. If MRI is unavailable or contraindicated, contrast-enhanced CT with or without venography may be used. MRV may show venous narrowing supportive of a diagnosis of PTCS in any patient. It should be performed to detect cerebral venous sinus thrombosis in atypical patients, such as nonobese individuals, women on oral contraceptives, prepubertal children, men, and patients with progressive visual loss despite therapy. Venous sinus occlusion and arteriovenous fistulas may also cause PTCS. After neuroimaging and the exclusion of any contraindications to a lumbar puncture, CSF analysis should be performed in all suspected cases of PTCS to rule out an underlying etiology. The CSF should be normal. The CSF opening pressure is considered abnormal if it is ≥250 mm CSF in adults and ≥280 mm CSF in children (250 mm CSF if the child is not sedated and not obese) [1].

Pseudotumor Cerebri Syndrome Without Papilledema

It is also important to be aware that PTCS can also present without papilledema in 5.7 [1] to 15 % of patients with chronic headache [70]. The diagnostic criteria for the PTCS without papilledema is outlined in Table 2.2. The mean opening pressures are above 250 mmH_2O for the patients with PTCS without papilledema, but they have relatively lower opening pressures compared to those with PTCS with papilledema. This slightly lower CSF opening pressure might explain the lack of optic disc swelling and increased likelihood of normal visual fields. In a study by Corbett et al., even after papilledema resolved in ten PTCS patients, five still had significantly increased ICP [71]. In another study with 353 patients with PTCS, the prevalence of those without papilledema was 5.7 % ($n=20$). The ones without papilledema had photopsias (20 %), spontaneous venous pulsation (75 %), and nonphysiologic visual field constriction (20 %) more often than those with papilledema. The mean CSF opening pressure was lower than those with papilledema at 309 versus 373 cmH_2O. Visual acuities were comparable between the

two groups [72]. Another retrospective study of 281 cases of PTCS also showed a high prevalence of nonphysiologic visual loss (tubular or peripheral constriction) in patients with PTCS without papilledema. These patients also had psychiatric illnesses and psychosocial stressors as comorbidities. The majority of these patients were managed surgically in which 53 % had ONSF, shunt, or both. The authors suggest more careful consideration in the treatment of these patients before offering surgical options [73]. PTCS can also be a chronic, recurrent condition in which papilledema, if present, can completely resolve despite persistent elevated ICP. Other symptoms such as, headache, pulsatile tinnitus, and especially vertigo are common in PTCS without papilledema [70, 72, 74].

Epidemiology/Genetics

PTCS usually affects obese teenage girls and young child-bearing women. The prevalence is about one case per 100,000 women. For women between the ages of 20 and 44 years who are 20 % above ideal body weight, the prevalence is higher, at 19 cases per 100,000 women [75]. The average age of onset ranges from 11 to 58 years, with a mean of about 30 years [75–77].

Men are affected less frequently. The prevalence is 0.3 cases per 100,000 men, but in men who are more than 20 % above their ideal body weight, it increases to 1.5 cases per 100,000 men. The ratio of male to female is approximately 1:4.3 to 1:8 [75].

Regarding racial risk factors for visual loss, black patients with PTCS tended to have more severe visual loss in at least one eye in a study of 450 patients (197 black, 253 nonblack). CSF opening pressure, visual acuity, visual field defects, and degree of papilledema were greater than controls. It was hypothesized that blacks had a more aggressive form of PTCS and required closer visual monitoring [78].

This disorder is rarely familial, and it has not been confirmed by genetic studies whether it is autosomal dominant [75].

Visual Course and Prognosis

The most significant complication of PTCS is blindness or permanent visual impairment from chronic papilledema resulting in optic atrophy. The visual loss is often insidious, and peripheral vision is affected first. Central visual acuity may be affected last in patients with papilledema. In a study of 35 patients with PTCS over a 3-year period [79], visual field assessment was more sensitive than both Snellen visual acuity and Pelli-Robson contrast sensitivity testing. Eighty-seven percent of patients had visual field defects on Goldmann perimetry compared to 82 % on Humphrey perimetry. The most common visual field defects were enlarged blind spots, arcuate defects, nasal steps, and peripheral constriction. In a prospective study of nine patients with PTCS and asymmetric papilledema [80], the eye with greater papilledema tended to have worse visual acuity, contrast sensitivity, and visual field defects. High-grade papilledema might be a risk factor for visual dysfunction. Humphrey automated perimetry and stereophotographs documenting changes in the optic discs over time were most useful in monitoring visual course.

The prognosis of PTCS is usually good. Some patients may remain asymptomatic for years. In about 10 % of patients, it will recur. PTCS may be a self-limiting condition that spontaneously remits before significant damage occurs to the optic nerve [81]. About 25 % of 57 patients in a study by Corbett et al. [71] experienced blindness or severe visual impairment in one or both eyes. These patients with severe visual loss had persistent elevated CSF opening pressures between 220 and 550 mmH_2O on repeat lumbar puncture. Although visual loss is usually gradual, patients with severe papilledema may rapidly become blind. Vision should be monitored closely in patients who have papilledema, decreased visual acuity, and frequent transient obscurations, as they may require surgical intervention.

The presentation and course of PTCS in older affected patients is slightly different. In a study of nine women and five men [82], 64 % were obese, 36 % were asymptomatic, and none presented with headache alone. Twenty-nine percent had

secondary causes of increased ICP, including transverse sinus thrombosis, chronic obstructive pulmonary disease and cor pulmonale, and corticosteroid withdrawal after prolonged administration. After 2 years of follow-up, 12 patients remained in the study. Eight had stable visual fields, three had improved visual fields, and one had worsened field defects. It was concluded that more patients over 44 years of age were more often men, were less often obese, were less symptomatic, and had identifiable causes of elevated ICP in 29 %. The visual prognosis in this age group appeared to be good.

Obesity appears to be correlated with visual outcome. Recent weight gain is associated with later worsening of visual fields [83]. Morbid obesity (body mass index (BMI) greater than 40 kg/m^2) is also associated with a worse visual outcome [84].

Losing weight by diet and exercise is associated with improvement in papilledema, but it is not clear whether this change in funduscopic finding affects ultimate visual outcome [84–86].

Pathogenesis of PTCS

Several theories have been put forth to explain the pathogenesis of PTCS. No clear evidence exists to support Quincke's theory that excess CSF production increases CSF volume in PTCS [87].

Later theories proposed by Foley and Dandy suggested that increased cerebral blood flow could cause elevated ICP [81, 88]. Positron emission tomography of the brain has revealed markedly increased cerebral blood or water volumes but almost no change in cerebral blood flow [88]. Recent brain MRI studies on patients with PTCS have demonstrated increased water apparent diffusion coefficients and increased white matter water signals. Convective transependymal flow may cause interstitial brain edema and increased brain water content [89–93].

A more recent theory suggests that elevated venous pressure could lead to increased resistance to CSF absorption and subsequently increased ICP in pseudotumor cerebri [94, 95]. Several studies have shown that increased sagittal sinus pressure leads to decreased CSF absorption because CSF pressure is not high enough to drive bulk flow of CSF across the meninges [94–96]. Elevated dural sinus pressures measured during intracranial venography have been demonstrated in patients with no obvious evidence of dural sinus obstruction [97]. In contrast, more recent studies have suggested that the increased venous pressure in PTCS may be caused by the elevated ICP and not the reverse. In a prospective study by Farb et al. [98] auto-triggered elliptic-centric-ordered three-dimensional gadolinium-enhanced MR venography (ATECO MRV) showed that 27 of 29 patients with PTCS and only 4 of 59 control patients had substantial bilateral sinovenous stenosis. The sensitivity and specificity of ATECO MRV to identify patients with PTCS was 93 %. It was thought that the idiopathic narrowing of the venous sinuses in patients with PTCS probably represented transverse sinus compression from increased ICP. The increased ICP from PTCS might have exacerbated the underlying venous sinus abnormality and created a flow-limiting stenosis and resultant pressure gradient.

Stenosis of large intracranial venous sinuses can be seen on MRV in almost all patients with PTCS and are considered a reliable radiologic marker of intracranial hypertension with a high specificity of 93 % and sensitivity of 93 % [98].

These venous sinus stenoses may often appear as a smooth narrowing of a sinus segment with or without flow gaps. Segmental hypoplasia or aplasia of one or more central venous sinuses, occasionally extending to an entire transverse sinus, can also be found. Asymmetries in the caliber of the transverse sinuses can also sometimes extend into the ipsilateral jugular veins. Regardless of their appearance on MRV, a venous pressure gradient exists across the stenosis with a potential effect in raising the CSF pressure [97, 99].

Venous sinus stenosis and elevated venous pressure may not be the only mechanism for PTCS. In another postmortem study of 20 transverse sinuses [100], the presence of a large septum may be one of the causes of venographic cryptic stenosis located at the junction of the middle and lateral third of the transverse sinus. The venographic cryptic stenosis was thought to be one of the etiological factors involved in PTCS.

Self-limited venous collapse could also be precipitated by jugular valvular insufficiency. In a study of 20 consecutive patients with PTCS and 20 healthy controls matched for age, gender, and BMI [101], jugular valvular insufficiency was more frequently found in PTCS patients with central venous stenosis compared to controls (70 % vs. 30 %; $P<0.05$). This finding was associated with irregular leaflet structures on B-mode imaging. Bilateral insufficiency was more frequent in patients with PTCS, but it was not significant ($P=0.08$). Sinovenous outflow obstruction was found in 5/6 patients that had undergone contrast-enhanced MR venography and digital subtraction angiography. Since PTCS patients are often obese, an increased abdominal pressure transmitted into the intracranial venous system through an incompetent jugular valve could play a role in triggering the self-limited venous collapse.

Other possible reasons for dural sinus stenosis include preexisting anatomical abnormalities, such as trabeculae/septae, endoluminal giant arachnoid granulations [102], or congenital hypoplasia of central vein segments [103]. Minor variations of central venous diameter, either compression or dilatation, could also be physiologic [102–104].

Tapered transverse sinus narrowing of >50 % in a cohort of 14 PTCS patients and 19 controls was associated with small or absent adjacent bony grooves in the skull. These narrowed transverse venous sinuses were thought to be primary or fixed defects. Some patients with PTCS demonstrated tapered transverse venous sinus stenoses with disproportionately large bony grooves in the skull, suggesting a secondary, or acquired venous sinus narrowing. This study further illustrates the various etiologies of transverse venous sinus stenosis [103].

Because of the increased incidence of PTCS in females, endocrinological dysfunction has been hypothesized to contribute to the development of this disorder. Obesity may cause increased intra-abdominal pressure, leading to increased right heart filling pressure and subsequently increased central venous pressure [105, 106]. Evidence supporting this theory shows that weight loss and bariatric surgery [106, 107] decrease papilledema and lower CSF pressures. Acute weight gain may be related to relapses of PTCS, and obesity-associated sleep apnea may lead to increased ICP [108–110]. In a study by Lampl et al. [111] significantly higher levels of leptin, a protein secreted by adipose cells that influences regulation of energy balance and body weight, were found in obese patients with PTCS. Obesity may also be associated with fat-related cytokines and other inflammatory cytokines. In a study of 26 patients with PTCS compared to 62 controls [112], CSF leptin was significantly higher in patients with PTCS ($P=0.001$) compared to controls after correction for age, gender, and BMI. BMI correlated with serum leptin and CSF leptin in the control group but not in the IIH group. It was thought that obesity in PTCS could be a result of hypothalamic leptin resistance. However, serum and not CSF leptin was found to be elevated in PTCS patients in another small study. In a series of eight PTCS patients and eight controls [113], elevated levels of CSF CCL2 and elevated levels of serum CCL7, CCL8, IL-1 alpha, and leptin were measured by cytokine antibody array in PTCS patients compared with controls. This study demonstrates various cytokines, besides leptin, may play a role in the pathogenesis of PTCS.

In a prospective study of 65 patients [114], plasma levels of ghrelin, a hormone that usually increases during overeating and decreases in obesity, did not differ between patients with PTCS and obese control patients. Ghrelin levels were similar during fasting and after eating. Therefore, this hormone does not play a role in the maintenance of obesity in patients with PTCS.

PTCS could be induced by nonvisceral fat-related mechanisms. In a study of 44 consecutive patients diagnosed with PTCS, 184 women in an obesity clinic of the same medical center were compared with 199 obese women participating in a national health survey in Israel [115]. Waist-to-hip ratio, a measurement of body fat distribution approximately reflecting the upper to lower body fat ratio, was 0.79 in PTCS patients, 0.84 in the national survey group, and 0.91 in the obesity clinic group ($P<0.001$). Comparisons were adjusted for age and BMI. It was concluded that fat tends to accumulate in the lower body compared to other obese women without PTCS of the same age range, unlike fat in the upper body which is associated with hypertension, diabetes,

Table 3.3 Systemic disorders and exogenous agents associated with increased intracranial pressure

Endocrine and metabolic dysfunction
• Addison's disease
• Diabetic ketoacidosis
• Hyperthyroidism/hypothyroidism
• Hypoparathyroidism: primary and secondary
• Obesity, recent weight gain
• OB/GYN-eclampsia, oral progestational agents, menarche, menopause, pregnancy
• Turner's syndrome
Exogenous agents
• Amiodarone
• Amphotericin
• Carbidopa/Levadopa (Sinemet) (?)
• Chordecone
• Cimetidine
• *cis*-Retinoic acid: all-*trans*-retinoic acid (for acute promyelocytic leukemia)
• Corticosteroids: prolonged therapy or withdrawal of either systemic or topical forms
• Cytosine arabinoside
• Cytarabine
• Danazol
• Doxycycline
• Fluoroquinolone
• Growth hormone: chorionic gonadotropin
• Heavy metals: arsenic, lead
• Indomethacin
• Isotretinoin
• Ketoprofen
• Leuprorelin acetate (LH-RH analogue)
• Levonorgestrel implants (Norplant)
• Lithium carbonate
• Minocycline
• Nalidixic acid
• Nitrofurantoin
• Oral contraceptives
• Ofloxacin
• Pancreatic enzyme
• Perhexiline maleate
• Phenothiazine
• Phenytoin
• Stanozol
• Sulfonamides
• Tamoxifen
• Testosterone
• Tetracycline
• Vitamin A
Systemic disorders
• Beçhet's disease
• Guillain–Barre syndrome
• Hematological disorders: antiphospholipid antibody syndrome, anemia, idiopathic thrombocytopenic purpura, thrombophilia
• Hypertension
• Infectious disorders: HIV, Lyme disease, psittacosis, syphilis, viral meningitis, subacute bacterial endocarditis, bacterial meningitis
• Multiple sclerosis
• Neoplastic disorders: leukemia, spinal cord tumors, carcinomatous meningitis
• Polyangiitis overlap syndrome
• Polycystic ovarian syndrome
• Renal disease
• Reye's syndrome
• Sarcoidosis
• Sjogren's syndrome
• Systemic lupus erythematosus

dyslipidemia, and the metabolic syndrome. It was thought that PTCS could be induced by non-visceral fat-related mechanisms.

Patients with PTCS recurrence had significant increases in BMI compared to patients without recurrence in a study of 50 women. Weight gain is considered a risk factor for PTCS recurrence [116].

Obesity may not be the risk factor in all cases of PTCS. In a retrospective series of 10 Asian patients with PTCS, only one patient was obese according to BMI, seven were overweight, and six weighed normal. Awareness of the possibility that obesity may not be a risk factor of PTCS in Asians could help diagnose PTCS earlier in this population [117].

Systemic Disorders, Medications, and Other Risk Factors Associated with PTCS

Various systemic disease have been associated with increased ICP, including systemic lupus erythematosus [118–120], underlying malignancies [121], anemia [122], Addison's disease [123], hyperthyroidism and hypothyroidism [124, 125], and uremia [126–128] (Table 3.3).

Cerebral venous sinus thrombosis leads to increased venous pressure and higher CSF pressures, with clinical findings of papilledema and headache [129]. It may closely mimic the symptoms and signs of PTCS [130]. (Please see "Cerebral Venous Sinus Thrombosis.")

Other venous abnormalities that can elevate intracranial venous pressures include dural arteriovenous fistulae [131] and carotid-cavernous fistulae [132]. A retrospective study by Cognard et al. [131] demonstrated that 9 of 13 patients with intracranial dural arteriovenous fistulas presented with symptoms and signs of PTCS, including headache, papilledema, visual obscurations, and horizontal diplopia from sixth nerve palsy. It was thought that the arteriovenous fistulas impaired venous outflow. Three of the patients had tonsillar herniation following lumbar puncture or lumbar shunting, and one died.

Iatrogenic disruption of venous drainage [133], radical neck dissection [134–136], or catheter-induced subclavian vein thrombosis [137] has also been associated with elevated intracranial venous and CSF pressures. Venous sinus compression by tumors has also been reported [138]. Another series [139] of 22 obese young women with PTCS showed no evidence of cerebral venous thrombosis on MRI and MRV of the brain. It was suggested that MRV be used to evaluate atypical presentations of isolated intracranial hypertension, such as those occurring in nonobese, male, or elderly patients, or when other clinical features suggest the possibility of cerebral venous thrombosis.

Hypercoagulable states that can lead to dural sinus thrombosis or PTCS include malignancies [140], systemic lupus erythematosus [118–120], protein C and S deficiencies [141], antithrombin III deficiency [142], Factor V Leiden mutations [143, 144], anticardiolipin antibodies [145, 146], oral contraceptive use [147], and pregnancy [148]. Idiopathic intracranial hypertension (IIH) appears to be associated with coagulation disorders and polycystic ovarian syndrome. Exogenous estrogens or pregnancy can predispose patients with these underlying disorders to develop PTCS [149]. Immediate treatment involves direct endovascular thrombolytic therapy. Long-term treatment for such hypercoagulable states involves heparin and warfarin anticoagulation [150].

Many systemic disorders and hereditary conditions have been linked to increased ICP. Severe iron deficiency anemia is associated with pseudotumor cerebri. In a series by Biousse et al. [151] six patients with PTCS developed bilateral papilledema associated with peripapillary hemorrhages. Two had retinal cotton wool spot and two had preretinal hemorrhages. All had severe iron deficiency anemia. Their symptoms and signs of PTCS markedly improved after treatment of the anemia. It was suggested that a complete blood count be checked in patients with PTCS, especially without known associated factors, such as obesity or medications, or when therapy to lower ICP does not improve the patient's condition. Although headache in sickle cell disease (SCD) is usually attributable to anemia or cerebrovascular disease, three children, one with SCD-SC, and two with SCD-SS, who presented with headache and bilateral papilledema and enlarged blind spots developed PTCS [152].

Gender and age may also influence the risks of developing PTCS. Although PTCS occurs more commonly in women, men were twice as likely as women to develop severe visual loss in a study by Bruce et al. These men tended to be older, were more likely to have sleep apnea, had less headache, and more visual disturbance at presentation. Therefore, closer monitoring of visual function in men is required because they may not experience or report symptoms of increased ICP [153].

In another study by Fraser et al. [154] men with PTCS were also more likely than controls to have symptoms of testosterone deficiency, as measured by the Androgen Deficiency in Aging Males questionnaire. It was hypothesized that hypogonadism and PTCS were mediated by the effect of low testosterone levels on body fat distribution in men, such that low testosterone levels in men were associated with increased visceral fat.

Sleep apnea is associated with PTCS in men. In a study by Lee et al. [155] 6 of 32 men with PTCS had sleep apnea. Of the six patients, one was treated with acetazolamide alone, four received acetazolamide and continuous positive airway pressure (CPAP), and one was treated

with CPAP alone. All patients had 20/20 or better visual acuity bilaterally, enlarged blind spots, and optic disc swelling bilaterally. Five patients had normal visual fields after treatment, and one patient had residual visual field defects. At the end of follow-up, three patients had normal optic discs, two had improved papilledema, and one had optic disc pallor. Treatment of sleep apnea with CPAP helped improve the symptoms and signs of PTCS in affected men.

Other systemic disorders that have been recently linked to increased ICP include primary aldosteronism; [156] hypothyroidism with myxedema, papilledema, and elevated CSF protein; [157] Crohn's disease; [158] Goldenhar's syndrome; [159] and treatment of spontaneous CSF leaks [160].

Various medications have been associated with increased ICP, including excessive vitamin A [161], the vitamin A derivatives isotretinoin [162, 163], all-*trans*-retinoic acid [164–166], tetracycline/minocycline [167, 168], doxycycline [169], nalidixic acid [170], fluoroquinolones [171, 172], sulfa drugs [173], oral contraceptives [174], danazol [175], corticosteroid withdrawal, especially in children [176], lithium [177, 178], thyroid replacement therapy after thyroidectomy [179], and mesalazine [180] (see Table 3.3).

In a study by Jacobson et al. [181] serum retinol levels in 16 female patients who did not have vitamin A supplementation were significantly higher than in the 70 control patients. It is unclear whether vitamin A metabolism causes increased ICP or if elevated retinol levels represent an epiphenomenon.

In a study of 12 patients [167], 75 % developed increased ICP within 8 weeks of starting minocycline for the treatment of acne. The increased ICP resolved after discontinuing the medication and three patients had residual visual loss.

Another study on recombinant human growth hormone (rhGH) showed that 4 of 3,332 children developed PTCS [182]. Three additional cases of PTCS in children receiving rhGH were also reported by Rogers et al. [183]. Two of the three patients had resolution of papilledema with acetazolamide and with discontinuation of the drug.

Neuroimaging Features of PTCS

Findings of brain CT scans have revealed not only slit-like ventricles in 11 % of patients with PTCS but also enlarged optic nerve sheaths in 47 % and empty sella syndrome in 46 % [184]. Quantitative analysis of ventricular volume has shown no difference between patients with PTCS and age-matched control subjects [185].

No evidence of ventriculomegaly, mass lesion, or venous sinus thrombosis on CT or MRI is required to establish the diagnosis of PTCS. However, some subtle radiologic signs have been associated with PTCS. In a study of 20 patients [186], 80 % had flattening of the posterior sclera, 70 % had an empty sella, 50 % had enhancement of the prelaminar optic nerve, 45 % had distension of the perioptic subarachnoid space, 45 % had vertical tortuosity of the orbital optic nerve, and 30 % had intraocular protrusion of the prelaminar optic nerve. These findings were absent or seen in less than 5 % of the 20 control patients. These radiologic signs are not specific for PTCS, but their presence supports the diagnosis.

Cerebrospinal Fluid Features

To determine the CSF opening pressure in an adult patient, a lumbar puncture performed on the patient in a relaxed, lateral decubitus position is required for establishment of the diagnosis of pseudotumor cerebri. A CSF opening pressure greater than 250 mmH_2O would fulfill one of the modified Dandy criteria mentioned previously [1]. Forty-two percent of asymptomatic obese female patients have opening pressures of greater than 250 mmH_2O [187]. In some cases, papilledema may be seen in patients with an opening pressure of less than 250 mmH_2O. If the diagnosis is uncertain, ICP monitoring with intraparenchymal pressure monitors may be necessary [188].

Management of PTCS

Patients with papilledema, regardless of the cause of the increased ICP, should be followed at regu-

lar intervals to detect the earliest evidence of an optic neuropathy. Central visual loss is usually a late phenomenon. Arcuate scotomas and nasal steps are commonly an early finding. Color defects can occur at any stage. Most visual defects associated with papilledema are reversible if the ICP is lowered before severe visual loss, chronic papilledema, or optic atrophy develops. Monitoring of the best corrected visual acuity at distance and near, color vision testing, visual field testing with kinetic and automated static perimetry, and ophthalmoscopic examination of the optic disc with fundus photos should be done every 1–2 weeks for very unstable patients, or every 1–3 months for moderately stable patients, and up to every 4–12 months for stable patients [189].

Medical Treatment

The two major goals of therapy in PTCS are to prevent visual loss and to treat and prevent headaches. If the patient has mild to moderate (grade 1–2) papilledema, normal visual acuity, and visual fields (except for an enlarged blind spot) without headaches, then weight loss and a low-salt diet can be tried. Weight loss may be beneficial for patients with PTCS, especially if they are supervised by professional dieticians in weight loss programs [189]. In one retrospective series [86], obese women with PTCS who lost weight (mean weight loss of 13.3 ± SD 9.9 pounds) had decreased papilledema and improved visual fields compared to those who did not lose weight (mean weight loss of 0.2 ± SD 0.6 pounds). In a study of 15 patients by Johnson et al. [85] a weight loss of 6 % was associated with a marked improvement of severe papilledema. Although weight loss was correlated with decreased papilledema, visual acuity and visual field were not [84, 85]. Severe obesity with a BMI of greater than 40 kg/m^2 was associated with a worse visual outcome [84].

The mainstay of medical treatment of PTCS is weight loss. The Idiopathic Intracranial Hypertension Treatment Trial is currently an ongoing prospective randomized, double-blinded, placebo-controlled trial to compare the efficacy of acetazolamide (up to 4 g/day) added to a low-sodium, weight reduction diet vs. dieting alone on preventing or restoring visual loss. Patients with mild visual loss (−2 to −5 dB baseline perimetric mean deviation (PMD)) will be recruited. Other goals of this study include identifying proteomic and genetic risk factors for IIH; determining serum and CSF levels of potential mediators of IIH suggested by the genetic analysis; searching for single nucleotide polymorphisms related to obesity that confer risk for the development of IIH; and determining whether leptin, vitamin A, or other adipose-related cytokines are associated with IIH. The primary outcome measure of this study is change in the PMD from baseline to month 6. Other secondary outcome measures include changes in papilledema grade, CSF pressure measurements, visual acuity, contrast sensitivity, OCT imaging, and quality of life measures [190].

Certain medications, such as vitamin A, vitamin A derivatives, and tetracycline, must be avoided as much as possible, but pediatric patients with PTCS receiving all-*trans*-retinoic acid [164–166] as chemotherapy for leukemia should not discontinue their treatment. The secondary PTCS syndrome should be treated.

If headaches develop, then antimigraine medications may be added. The chronic headaches of PTCS are best treated prophylactically. Because many of these agents, such as tricyclic antidepressants, calcium channel blockers, and sodium valproate, may cause weight gain or edema, newer antiepileptic medications may be considered as better alternatives. Short-term weight gain as a side effect may lead to worsening or recurrence of PTCS. Topiramate, an antiepileptic medication with mild carbonic anhydrase inhibition, may prove effective in headache relief and weight loss. Studies on the efficacy of topiramate in decreasing elevated ICP are being studied. For abortive therapy, the triptans and nonsteroidal anti-inflammatory agents may be useful [189].

If the patient develops moderate (grade 3) papilledema with decreased visual acuity and abnormal visual field defects in addition to an enlarged blind spot, acetazolamide 1 g/day may be necessary. To lower the CSF pressure, carbonic anhydrase inhibitors, such as acetazolamide, are the

most effective medications, as shown by Rubin et al. [191] in which 6–57 % of patients experienced a decrease in CSF production. Carbonic anhydrase inhibitors reduce sodium transport across the choroid plexus epithelium and it is believed to decrease production of CSF. Acetazolamide is commonly prescribed at a dose of 500 mg (extended-release) orally daily or twice daily and increased until a daily dose of a maximum of 3 g/day is achieved. Contraindications to acetazolamide include sulfonamide allergy, significant hepatic or renal disease, and chronic angle-closure glaucoma [192]. The side effects of this medication include a metallic taste to carbonated beverages, paresthesias, anorexia, metabolic acidosis, drowsiness, and confusion. Renal calculi and aplastic anemia rarely occur [192]. Acetazolamide is continued until symptoms and signs resolve and then it is slowly tapered off. If clinical features of PTCS recur during tapering, it is continued indefinitely [189].

Alternatively, methazolamide, which may be slightly less effective with a lower incidence of side effects than acetazolamide, may be used. Although less effective than acetazolamide or furosemide, a diuretic with a mild effect on CSF production may also be used in patients who cannot tolerate acetazolamide. For patients who are allergic to sulfa, triamterene and spironolactone may be tried. However, these drugs have no proven effect on CSF production [189].

Furosemide, a loop diuretic with weak carbonic anhydrase activity, has also been reported as an alternative to acetazolamide or as combination therapy [193]. Furosemide is started at 20–80 mg/day and may be increased up to 160 mg/day. It is contraindicated in anuric patients. Some side effects include excessive diuresis leading to dehydration and hypotension, hypokalemia, and hyperchloremia [192].

If the patient has severe (grade 4 or 5) papilledema associated with macular edema, retinal hemorrhages, visual acuity of worse than 20/50, and progressive visual field defects, then acetazolamide may be increased up to 4 g/day. A short course of high-dose corticosteroids can be added for the treatment of acute visual loss from papilledema [194], especially while arranging surgical intervention. Methylprednisolone 250 mg IV four times daily for 5 days, with oral taper at 80 mg over 4–8 weeks with acetazolamide at 500 mg orally twice daily is often used. Common side effects from corticosteroids include weight gain, fluid retention, increased intraocular pressure, and hyperglycemia, which are problematic in patients with PTCS [176, 194].

Serial LPs are not recommended, but patients with severe papilledema and sudden visual loss may need immediate lumbar puncture and drainage of a large volume of CSF until surgical intervention can be arranged [195].

Surgical Treatment

Indications for surgery include the following: (1) progressive visual loss despite maximal medical treatment, (2) severe or sudden visual loss at onset with an afferent pupillary defect or signs of advancing optic nerve dysfunction, and (3) severe papilledema causing macular edema or exudates [195]. The degree of visual worsening despite maximal medical treatment may be defined as the development of loss of greater than two lines of Snellen visual acuity, generalized field constriction of greater than 20°, or the development of a new visual field defect [195].

Optic nerve sheath decompression (ONSD) has been shown to be safe and effective in treating vision in PTCS. Visual acuity is stabilized or improved in 93–97 % of eyes; visual field is stabilized or improved in 85–95 % of eyes [196–198].

ONSD involves cutting a window in the dura and arachnoid of the bulbous portion of the edematous optic nerve sheath. This procedure decreases disc swelling on the operated side, and in some instances the contralateral papilledema also. It is more effective in acute papilledema than in chronic papilledema [199]. The mechanism of ONSD in PTCS remains unclear. It may filter out CSF locally to reduce pressure to allow improvement in peripapillary circulation. It may also globally lower ICP and occasionally relieve headaches in one-third of patients undergoing unilateral ONSD [198, 200]. Lastly, a more likely hypothesis is that postoperative scarring of the arachnoid shifts the pressure gradient posteriorly from the lamina cribrosa to the myelinated portion of the optic

nerve [200, 201] to protect the optic nerve head from elevated CSF pressure. Improvement in blood flow to the optic nerve has been shown in color Doppler studies where blood velocities in the ophthalmic, short ciliary, and central retinal arteries increased after ONSD [198]. In a retrospective study [196] of 158 eyes, 94 % (in 86 patients) who underwent ONSD had stable or improved visual acuity and 88 % had improvement in their visual fields. Only 13 % (8 of 61) patients reported improvement in their headaches following ONSD. Repeat ONSD was performed on nine eyes in six patients for progressive visual loss. All nine eyes had stable or improved visual acuity, and five of eight had stable or improved visual fields. Forty-five percent had benign and transient postoperative complications. The most common complication was diplopia, which spontaneously resolved in 87 % of patients. In a retrospective series of 78 patients who underwent ONSD compared to 20 controls [202], unilateral ONSD significantly decreased the grade of papilledema in both ipsilateral (operated) and contralateral (unoperated) eyes. The reduction of papilledema and stability of the visual field in the contralateral (unoperated) eyes suggested that bilateral ONSF might not be necessary in PTCS patients with bilateral visual loss and papilledema.

In conclusion, ONSD is recommended when medical treatment, such as diuretics and weight loss are not effective in preventing further progressive visual loss. Progression in visual loss involves developing a new visual field defect, a generalized constriction of greater than 20°, or a loss of more than two lines of Snellen acuity. ONSD may not be the treatment of choice for those who have progressive visual loss and intractable headaches, which are better managed by ventriculoperitoneal (VP) or lumboperitoneal (LP) shunting.

The benefits of ONSD are not long term. It does not consistently reduce ICP and, therefore, does not treat the underlying problem of PTCS. More than 80 % of patients with PTCS develop recurrent papilledema within 1 year of the procedure. In a study of 11 ONSDs in 75 eyes of 54 patients with PTCS [203], 32 % of ONSDs failed within 39 months after surgery. Only about 75 % of ONSDs were functioning 6 months after surgery, and the likelihood of a functioning ONSD steadily decreased thereafter such that 66 % of ONSDs were functioning at 12 months, 55 % at 3 years, 38 % at 5 years, and 16 % at 6 years after surgery. Although patients could be treated with a second ONSD after initial failure, eyes that had more than one ONSD rarely stabilized or improved after surgery and were more likely to experience a significant vascular complication than eyes that underwent only one ONSD.

The medial approach to the orbit is preferred, but some surgeons do the lateral approach, which requires an orbitotomy. The advantages of the medial approach include the following: (1) quicker access to the optic nerve, (2) retrobulbar anesthesia may be sufficient, and (3) no skin incision is required. Disadvantages of the medial approach are that (1) the medial rectus must be disinserted, (2) the bulbous portion of the nerve may be difficult to see because of the oblique angle of the approach, (3) the placement of a retractor against the inner surface of the medial rectus muscle may damage its innervation, (4) the potential for papillary dysfunction exists, and (5) adjunctive lateral orbitotomy may still be required to provide better exposure of the optic nerve [204].

The most common complications of ONSD are diplopia from transient lateral rectus palsy and pupillary dilation resulting from sphincter denervation. Transient or prolonged postoperative visual loss is a rare complication [205] (Table 3.4).

CSF diversion procedures include LP shunting and VP shunting to lower the ICP in PTCS. In a review of 134 patients who underwent shunting for PTCS [191] between 1942 and 1979 with a mean follow-up of 11.6 years [191], 14 patients received shunts. Of the six patients who had VP shunts, four had resolution of symptoms within 6 months. One patient developed a shunt obstruction that required revision and another had a shunt infection that required removal. Of the eight patients who had LP shunts, all improved within 1 month. One patient had a shunt infection, and one had severe low-pressure symptoms from overshunting. In a follow-up study by Johnston et al. [206] of 36 patients who had shunts for the treatment of PTCS, 52 % had complications and 48 %

Table 3.4 A comparison of the complications of surgical treatment for pseudotumor cerebri syndrome (PTCS)

Complications of optic nerve sheath fenestration
• Vascular occlusion: central retinal artery occlusion, branch retinal artery occlusion, choroidal infarction
• Hemorrhage in sheath or orbit
• Traumatic optic neuropathy
• Diplopia
• Pupil dilation
• Anterior segment ischemia
• Compressive optic neuropathy from orbital cyst
• Corneal delle formation
• Infection
Complications of lumboperitoneal shunt
• Obstruction
• Infection
• Low-pressure headaches
• Radiculopathy
• Tonsillar herniation
• Syringomyelia
• Subdural hematoma
• Shunt migration

[Reprinted from Binder DK, Horton JC, Lawton MT, McDermott MW. Idiopathic intracranial hypertension. Neurosurgery 2004;54(3):538–51;discussion 551–2. With permission from Wolters Kluwer Health]

had shunts that failed. The lowest revision and complication rates were associated with LP shunts. Two more recent studies also support that shunting is a reasonable treatment for PTCS. In a study of 27 patients with PTCS [207], over a mean of 47 months after shunting, vision improved or remained the same in 14 patients, and headaches improved in all patients. The only serious complication was shunt failure. Fifty-six percent required shunt revision. The average number of revisions per patient was 2.4, with one revision required every 2.6 years. In another study [208] of 30 patients who had LP shunting for PTCS with a mean follow-up of 35 months, 71 % (10 eyes) improved by at least two Snellen chart lines and only one eye had a decrease in vision. Sixty-four percent of eyes with abnormal fields had improvement on Goldmann perimetry. The only complication was frequent shunt obstruction. Twelve patients did not need shunt revision. The other patients had an average of 2.5 revisions per patient, except for the four patients who needed 10 or more revisions.

The most common complication associated with LP shunts is obstruction, which may account for up to 65 % of all revisions. The second most common is secondary intracranial hypotension caused by excessive drainage of CSF via the LP shunt in 15 %. Lumbar radiculopathy accounted for 4.5 % of all revisions. Other less common problems include shunt infections, tonsillar herniation, syringomyelia, and catheter migration [207].

A programmable shunt valve can prevent low-pressure headaches, a complication that is less common in VP shunting than in LP shunting. This low-pressure headache is a consequence of overshunting. The most common symptoms of overshunting are postural headaches, neck pain, vomiting, photophobia, blurred vision, transient visual obscurations, visual field constriction, and sixth nerve palsies [208]. MRI findings of intracranial hypotension include leptomeningeal enhancement, tonsillar herniation, and subdural effusions [209]. Stereotactic surgical techniques have also allowed better outcomes with VP shunts, especially in those who experience repeated LP shunt obstructions. In a study of seven patients who were treated with stereotactic VP shunts for PTCS, five of the seven patients experienced resolution of papilledema and six of the seven had resolution of headaches postoperatively [210].

Despite improvements in the external control of ICP, paradoxical symptoms may occasionally recur. Worsening visual loss, headaches, dizziness, and other increased ICP symptoms may indicate shunt malfunction, but they may also occur with a functioning shunt. After many years of remission of symptoms, patients may develop "shunt dependency," increased ICP when the shunt is removed or even inserted [208].

The advantages of LP shunting over ONSD as the initial surgical treatment for PTCS, as purported by Binder et al. [211] include the following: (1) LP shunting does not pose a direct risk to the eye. Optic nerve or retinal vascular complications occur in 2 % of cases; (2) ONSD in one eye improves papilledema in both eyes, but the results in the contralateral eye are less pronounced; (3) the rate of shunt obstruction is similar to that of ONSD becoming closed from scarring over a sim-

ilar period; (4) LP shunting is more effective than ONSD in treating headaches because ONSD mainly produces a local decrease in pressure within the subarachnoid space behind the optic nerve head [198]. LP shunting treats the underlying problem of increased ICP and, therefore, treats both papilledema and headaches; (5) some patients with PTCS have sixth nerve palsy that resolves after LP shunt but does not after ONSD. A sixth nerve palsy may even be a complication of ONSD; (6) papilledema usually resolves after LP shunting if there is no obstruction, but residual papilledema may persist after ONSD (Table 3.4).

ONSD may be appropriate for patients with PTCS who refuse, cannot undergo, or do not respond to LP shunting. For patients with severe papilledema caused by an inoperable malignant brain tumor, ONSD may serve as a short-term treatment for visual loss. Both immediate ONSD and LP shunting may even be required in patients with PTCS who present with marked papilledema and/or macular edema, decreased central visual acuity, severe visual field defect, and ocular motility deficits [211].

No prospective controlled trials have been done comparing LP shunting versus VP shunting in PTCS. In a retrospective series of 34 patients who underwent CSF diversion for their PTCS, no significant difference was found between the groups that received a VP shunt and those who received an LP shunt in both headache and visual outcome. The rate of complications was 20.5 % and the need for revision was 35 % for all patients who underwent either type of shunt. Patients with LP shunting had more complications and first time revisions than patients with VP shunting [212]. Another study of 25 PTCS patients also confirmed that both types of shunts were effective in controlling all clinical manifestations of PTCS in the immediate postoperative period. But this study showed that failure rates were slightly higher for VP shunts at 14 % compared with 11 % in LP shunts. The revision rates were higher with LP shunts at 60 % compared to 30 % with VP shunts. Therefore, PTCS patients who underwent a VP shunt had less complications and revisions than those who received an LP shunt [213].

Because of the high rate of complications and failures following VP or LP shunting, bariatric surgery may be an effective alternative in severely obese patients with PTCS. However, it is not the treatment of choice in the setting of acute visual loss because its benefit is not apparent until 1 year later. Dramatic decreases in CSF pressure and papilledema have been achieved with gastric stapling [98]. In the study by Sugerman et al. [105] 19 of 24 patients who underwent bariatric surgery experienced resolution of headache and pulsatile tinnitus. Their average weight loss was 45 kg and their BMI decreased to 30 ± 5 kg/m^2. CSF opening pressures were not measured in this series, but a previous study by Sugerman et al. [106] showed that CSF opening pressure decreased from 353 ± 35 to 168 ± 12 mmH_2O in eight patients who underwent similar surgery. The mechanism for lowering increased ICP is unclear. Complications from a gastric bypass, such as a proximal Roux-en-Y procedure, include wound infections, incisional hernias, and stenosis of the gastrojejunal anastomosis. Vitamin deficiencies and osteoporosis are also possible.

In a review of a series of 62 bariatric surgery cases for PTCS [214], Roux-en-Y gastric bypass was the most common bariatric procedure performed. Ninety-two percent (56 of 61) of PTCS patients had resolution of their presenting symptoms postoperatively; 97 % (34 of 35) of PTCS patients who had pre- and post-op funduscopic exams had resolution of their papilledema postoperatively. Ninety-two percent (11 of 12) of patients who had pre- and post-op formal visual field testing had complete or nearly complete resolution of visual field defects. The remaining patient had stabilization of previously progressive visual loss. In 13 patients, the average postoperative ICP decrease was 25 cmH_2O. This study summarized Class IV evidence supporting the use of bariatric surgery for the treatment of PTCS. Prospective, controlled studies are needed.

Because of the increasing evidence of nonthrombotic dural venous sinus stenosis, endovascular stenting has become a more popular option for treatment of PTCS. Most of the data regarding the efficacy of these procedures are derived from uncontrolled case series regarding CSF diversion procedures, venous sinus stenting (Fig. 3.11a, b), and bariatric surgery. The safety and efficacy of these procedures still need to be

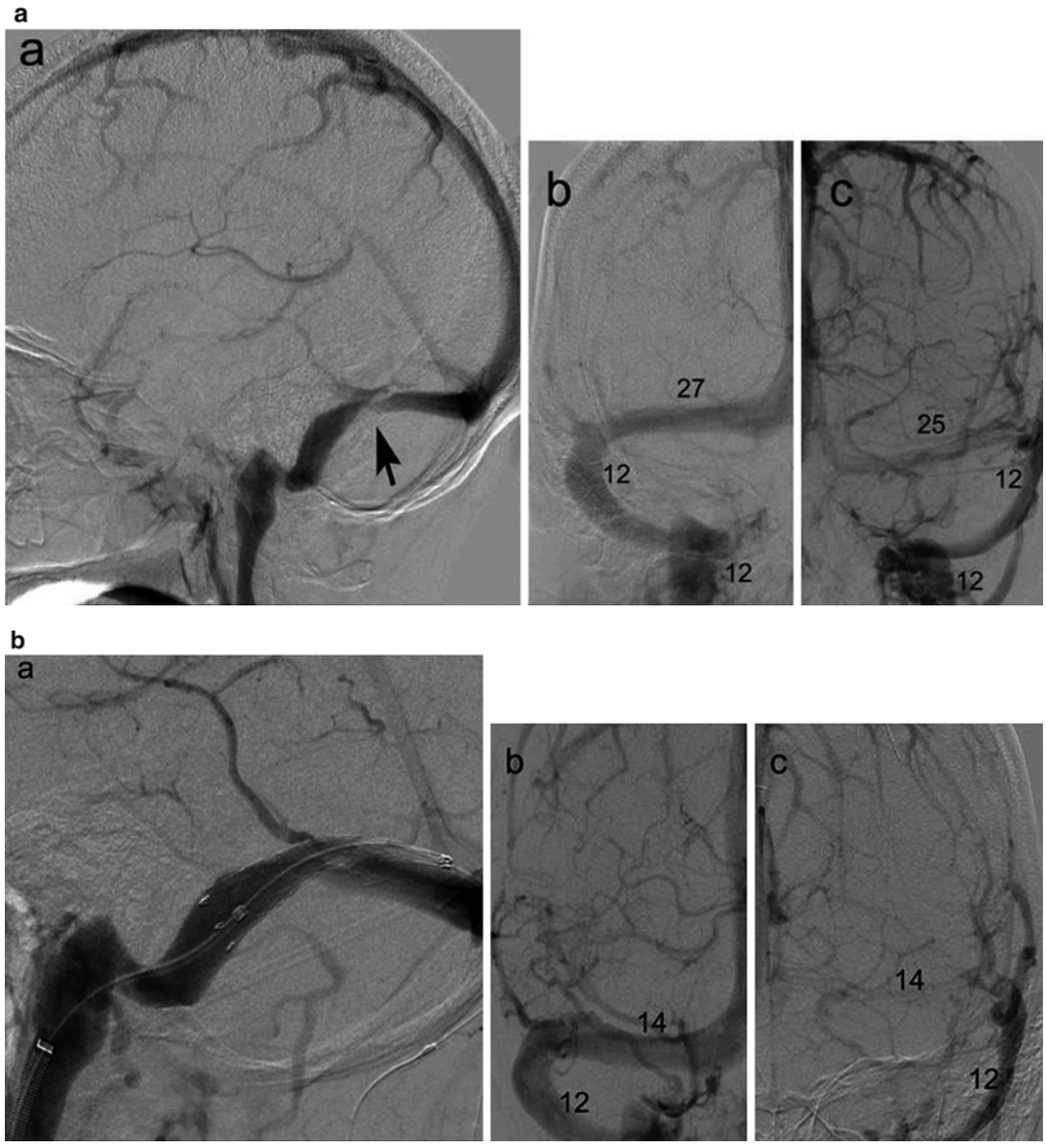

Fig. 3.11 (**a**) Cerebral angiography was performed after induction of general anesthesia, using a coaxial microcatheter supported by a guide catheter positioned in the internal jugular veins from a common femoral puncture. Pressure measurements were taken throughout the venous sinuses using a transducer referenced to zero at the level of the midaxillary line. The pressures measured during angiography were 27 and 25 mmHg in the prestenotic segments of the left and right transverse sinuses, respectively, and 12 mmHg in the poststenotic segments bilaterally. Thus, the right and left transverse sinuses demonstrated a pressure gradient of 12–15 mmHg without any thrombosis. The preoperative right transverse sinus venograms show the stenosis (a, *arrow*). The preoperative left (b) and right (c) transverse sinus venograms show the pressure values (in mmHg). (**b**) Under general anesthesia, a Luminex 10×40 mm stent was placed across the right transverse sinus, reducing the pressure gradient to 2 mmHg bilaterally. The intraoperative venogram shows the stent (a). The postoperative left (b) and right (c) transverse sinus venograms show the pressure values (in mmHg). [Reprinted from Ahmet A, Lee M, Steinberg GK, Marcellus M, Marks MP. Efficacy of endovascular stenting in dural venous sinus stenosis for the treatment of idiopathic intracranial hypertension. Neurosurgical Focus. 2009;27(5):E14. With permission from the American Association of Neurological Surgeons]

investigated in randomized controlled studies to determine their roles in the treatment of PTCS. Venous sinus stenting may be considered for refractory cases of PTCS associated with venous sinus hypertension. In a report by Higgins et al. [215] a woman with refractory PTCS underwent venography and manometry that showed partial obstruction of both transverse sinuses, with raised pressures proximal to the obstructions. Dilation of one of the sinuses with a stent reduced the pressure gradient, with marked improvement in her symptoms. In a later series by Higgins et al. [216] 12 patients with refractory PTCS underwent venography and manometry showing intracranial venous hypertension proximal to stenoses in the lateral sinuses. After venous sinus stenting, intrasinus pressures were variable reduced. Follow-up measurements of CSF opening pressure confirmed a reduction in ICP. There was no consistent relationship between venous pressure reductions and symptom relief. Five patients became asymptomatic, two improved, and five were unchanged. Five of the 12 patients had improved or resolved papilledema. It was suggested that lateral sinus stenting be used as an alternative treatment to neurosurgical intervention in intractable cases. In another study by Ogungbo et al. [217] a 37-year-old woman with IIH had obstruction of the right transverse sinus with high pressure of 40 mmHg proximal to the obstruction and low pressure of 15 mmHg distally, as seen on MRV and cerebral venography. She was treated by transvenous sinus stenting that resolved her symptoms and bilateral papilledema. It still remains unproven whether the stenoses are the cause or the result of elevated ICP [97]. In a study of 13 female patients with PTCS who were being evaluated for sinovenous stent placement, 10 of 13 patients had a pressure gradient across the stenosis between 11 and 50 mmHg, which decreased after unilateral transverse sinus stent placement. This study showed that restoring the patency of stenotic venous sinuses resulted in improvement of headaches and papilledema. No periprocedural complications occurred [218].

In another retrospective analysis of published cases on dural venous sinus stenting, 78 % of PTCS patients had complete relief or improvement of their main presenting symptoms after endovascular stenting. Resolution or improvement of papilledema was seen in 85.1 % of patients. Therefore, endovascular stenting should be considered as a treatment option in PTCS related to venous sinus stenosis [219].

The debate regarding whether venous sinus stenosis is the cause or the result of increased ICP continues. The venous pressure gradient may normalize and the stenosis may decrease or resolve after a single 20 ml of CSF is taken out by lumbar puncture or after continuous CSF diversion procedures such as lumboperitoneal shunt [220–222]. These findings suggest that venous flow changes in PTCS are likely the effect of CSF hypertension, not the cause. But increasing evidence also indicate that the placement of a self-expanding stent at the venous stenosis level is consistently followed by the immediate and long-standing resolution of PTCS symptoms [223–225].

Therefore, an acute CSF decrease in CSF volume by LP or continuous CSF diversion may reduce the stenosis and the related pressure gradient across it. On the other hand, stenting of the segmental venous narrowing at the transverse sinus level may revert to the CSF hypertensive state. These findings indicate that sinus venous stenosis and CSF hypertension in PTCS patients may influence each other in a vicious cycle in which the starting point may only be arbitrarily chosen. The self-limited venous collapse is considered a likely predisposing mechanism of PTCS. The primary inciting event triggering the CSF and venous sinus higher pressure balance shift remains unclear at this time. There is evidence that a central venous hypertension not related to an anatomical or functional stenosis may result from changes in cerebral blood flow autoregulation, leading to a transient or persistent hyperperfusion of the brain [226].

PTCS During Pregnancy

The incidence of PTCS in pregnancy is similar to age-matched nonpregnant controls. Although PTCS can develop or worsen during pregnancy, the risk of fetal loss is the same as that of nonpregnant

age-matched controls. The diagnostic criteria and method of diagnosis are the same as that for the general population. PTCS appears to present during the first two trimesters of pregnancy with typical symptoms and signs. Visual outcome is similar to age-matched nonpregnant women [227].

The pregnant patient with PTCS is managed in a similar manner to the nonpregnant one with some exceptions. Dieting is not as strict, such that weight gain up to less than 20 pounds is acceptable. Acetazolamide is a category C medication in pregnancy (risk cannot be ruled out because data are lacking), but most neuro-ophthalmologists have been prescribing this medication after the first trimester without known teratogenic effects. Acetazolamide use is recommended after 20 weeks of gestation. Until then, corticosteroids may be administered for visual loss [228]. Corticosteroid use has not been associated with birth defects in humans. Thiazide diuretics are not recommended in the second half of pregnancy. ONSD may be the preferred surgical treatment for progressive visual loss because the enlarging uterus may cause peritoneal catheter obstruction in a shunt [229]. Furthermore, cerebral venous thrombosis should always be considered as the etiology of ICP after delivery or after fetal loss [230].

PTCS in Children

PTCS occurs more often in boys and nonobese younger children in the age range between 3 and 11 years [231, 232]. Adolescent girls are more often affected than adolescent boys [233, 234]. The pathogenesis of this disorder is still unclear, but secondary causes of PTCS, such as otitis media, viral infection, medications, and closed head injury, are more commonly seen in about 50 % of cases [235]. Antibiotics used in the treatment of these infections may also play a role. More cases involving medication use, such as recombinant growth hormone and all-t*rans*-retinoic acid, have been documented [232]. Neckstiffness or torticollis, strabismus, lateral rectus palsy, and facial palsy occur more often in children than adults [235, 236]. Irritability, apathy, somnolence, dizziness, and ataxia are other presenting signs of PTCS in children [236]. Headache is less common in children compared to adults. Children with PTCS may even be asymptomatic [237]. New diagnostic criteria for pediatric PTCS have been proposed: (1) symptoms and signs of elevated ICP, (2) prepubertal stage, (3) normal sensorium, (4) with or without reversible cranial nerve palsies, and (5) CSF opening pressure greater than 280 mmH_2O (Table 3.2) [238].

In a retrospective study of 90 children with PTCS less than 18 years of age over a mean follow-up period of 30.65 months, visual outcome, including visual acuity and visual field, was good. The recurrent rate was 23.7 %, and the risk of recurrence was highest within the first 18 months after diagnosis of PTCS [239]. MRI and MRV of the brain should be used to exclude intracranial pathology. Narrowing of transverse venous sinuses may be seen in PTCS. Transverse venous sinus flow gaps may be normal in up to 30 % of cases because of developmentally related variations in the sinuses, such as smaller, nondominant sinuses, absent transverse sinuses, or involution of the occipital sinuses [240]. MRV-related artifacts can also compromise views of sinus flow, making accurate diagnosis challenging [241].

The management of PTCS otherwise is similar to that in adults. Most children have good visual prognosis with medical treatment, and those with visual worsening undergo ONSF and LP shunting [236].

References

1. Friedman DI, Liu GT, Digre KB. Revised diagnostic criteria for the pseudotumor cerebri syndrome in adults and children. Neurology. 2013;81:1159–65.
2. Giuseffi V, Wall M, Siegel PZ, Rojas PB. Symptoms and disease associations in idiopathic intracranial hypertension (pseudotumor cerebri): a case-control study. Neurology. 1991;41(2 pt 1):239–44.
3. Hayreh SS. Optic disc edema in raised intracranial pressure. VI. Associated visual disturbances and their pathogenesis. Arch Ophthalmol. 1977;95(9):1566–79.
4. Cogan DG, Kuwabara T. Papilledema. Exp Eye Res. 1977;25(Suppl):419–33.
5. Kosmorsky G. Pseudotumor cerebri. Neurosurg Clin N Am. 2001;12(4):775–97.
6. Spalton DJ, Hitchings RA, Hunter PA, editors. Atlas of clinical ophthalmology. Philadelphia: JB

Lippincott; 2005. Tan JCH, associate editor; Harry J, pathology advisor.
7. Griebel SR, Kosmorsky GS. Choroidal folds associated with increased intracranial pressure. Am J Ophthalmol. 2000;129(4):513–6.
8. Talks SJ, Mossa F, Elston JS. The contribution of macular changes to visual loss in benign intracranial hypertension. Eye. 1998;12(pt 5):806–8.
9. Keane JR. Papilledema with unusual ocular hemorrhages. Arch Ophthalmol. 1981;99(2):262–3.
10. McCasland BJ, Mendicino ME, Newman NJ. Subretinal haemorrhage in idiopathic intracranial hypertension. Br J Ophthalmol. 1999;83(7):883–4.
11. Hedges III TR, Legge RH, Peli E, Yardley CJ. Retinal nerve fiber layer changes and visual field loss in idiopathic intracranial hypertension. Ophthalmology. 1995;102(8):1242–7.
12. Orcutt JC, Page NG, Sanders MD. Factors affecting visual loss in benign intracranial hypertension. Ophthalmology. 1984;91(11):1303–12.
13. Schreiber S, Bischoff P. Beidseitige opticusatrophie bei pseudotumor cerebri. Klin Mbl Augenheilkd. 1983;182:465–7.
14. Neetens A, Smets RM. Papilledema. Neuro-ophthalmology. 1989;9:81–101.
15. Carter SR, Seiff SR. Macular changes in pseudotumor cerebri before and after optic nerve sheath fenestration. Ophthalmology. 1995;102(6):937–41.
16. Eggers HM, Sanders MD. Acquired optociliary shunt vessels in papilloedema. Br J Ophthalmol. 1980;64(4):267–71.
17. Hedges TR. Papilledema: its recognition and relation to increased intracranial pressure. Surv Ophthalmol. 1975;19(4):201–23.
18. Henkind P, Benjamin JV. Vascular anomalies and neoplasms of the optic nerve head. Trans Ophthalmol Soc U K. 1976;96(3):418–23.
19. Anderson RL, Flaharty PM. Treatment of pseudotumor cerebri by primary and secondary optic nerve sheath decompression. Am J Ophthalmol. 1992; 113(5): 599–601.
20. Levin PS, Newman SA, Quigley HA, Miller NR. A clinicopathologic study of optic neuropathies associated with intracranial mass lesions with quantification of remaining axons. Am J Ophthalmol. 1983;95(3): 295–306.
21. Lepore FE. Unilateral and highly asymmetric papilledema in pseudotumor cerebri. Neurology. 1992; 42(3 pt 1):676–8.
22. Moster ML, Slavin M, Wall M. Unilateral disc edema in a young woman. Surv Ophthalmol. 1995;39(5):409–16.
23. Sher NA, Wirtschafter J, Shapiro SK, See C, Shapiro I. Unilateral papilledema in 'benign' intracranial hypertension (pseudotumor cerebri). JAMA. 1983; 250(17):2346–7.
24. Strominger MB, Weiss GB, Mehler MF. Asymptomatic unilateral papilledema in pseudotumor cerebri. J Clin Neuroophthalmol. 1992;12(4):238–41.
25. Paul TO, Hoyt WF. Funduscopic appearance of papilledema with optic tract atrophy. Arch Ophthalmol. 1976;94(3):467–8.
26. Hayreh SS. Pathogenesis of oedema of the optic disc (papilloedema): a preliminary report. Br J Ophthalmol. 1964;48:522–43.
27. Krishna R, Kosmorsky GS, Wright KW. Pseudotumor cerebri sine papilledema with unilateral sixth nerve palsy. J Neuroophthalmol. 1998;18(1):53–5.
28. Liu GT, Volpe NJ, Schatz NJ, Galetta SL, Farrar JT, Raps EC. Severe sudden visual loss caused by pseudotumor cerebri and lumboperitoneal shunt failure. Am J Ophthalmol. 1996;122(1):129–31.
29. Repka MX, Miller NR, Savino PJ. Pseudotumor cerebri. Am J Ophthalmol. 1984;98(6):741–6.
30. Wall M, Hart Jr WM, Burde RM. Visual field defects in idiopathic intracranial hypertension (pseudotumor cerebri). Am J Ophthalmol. 1983;96(5):654–69.
31. Kupersmith MJ, Sibony P, Mandel G, Durbin M, Kardon RH. Optical coherence tomography of the swollen optic nerve head: deformation of the peripapillary retinal pigment epithelium layer in papilledema. Invest Ophthalmol Vis Sci. 2011;52(9): 6558–64.
32. Rebolleda G, Munoz-Negrete FJ. Follow-up of mild papilledema in idiopathic intracranial hypertension with optical coherence tomography. Invest Ophthalmol Vis Sci. 2009;50:5197–200.
33. Hayreh SS, Hayreh MS. Optic disc edema in raised intracranial pressure. II. Early detection with fluorescein fundus angiography and stereoscopic color photography. Arch Ophthalmol. 1977;95(7):1245–54.
34. Sanders MD, Ffytche TJ. Fluorescein angiography in the diagnosis of drusen of the disc. Trans Ophthalmol Soc U K. 1967;87:457–68.
35. Salgarello T, Tamburrelli C, Falsini B, Giudiceandrea A, Colotto A. Optic nerve diameters and perimetric thresholds in idiopathic intracranial hypertension. Br J Ophthalmol. 1996;80(6):509–14.
36. Zimmerman LE. Histology and general pathology of the optic nerve. Trans Am Acad Ophthalmol Otolaryngol. 1956;60(1):14–30.
37. Reese AB. Peripapillary detachment of the retina accompanying papilledema. Trans Am Ophthalmol Soc. 1930;28:341–51.
38. Corbett JJ, Jacobson DM, Mauer RC, Thompson HS. Enlargement of the blind spot caused by papilledema. Am J Ophthalmol. 1988;105(3):261–5.
39. Ashton N. The eye in malignant hypertension. Trans Am Acad Ophthalmol Otolaryngol. 1972;76(1):17–40.
40. Hayreh SS. Pathogenesis of edema of the optic disc. Doc Ophthalmol. 1968;24(2):289–411.
41. Hayreh SS. Blood supply of the optic nerve head and its role in optic atrophy, glaucoma, and oedema of the optic disc. Br J Ophthalmol. 1969;53(11):721–48.
42. Tso MO, Hayreh SS. Optic disc edema in raised intracranial pressure. IV. Axoplasmic transport in experimental papilledema. Arch Ophthalmol. 1977; 95(8):1458–62.

43. Orcutt JC, Page NG, Sanders MD. Factors affecting visual loss in benign intracranial hypertension. Ophthalmology. 1984;91(11):1303–12.
44. Petrohelos MA, Henderson JW. The ocular findings of intracranial tumor. A study of 358 cases. Trans Am Acad Ophthalmol Otolaryngol. 1950;55:89–98.
45. Bergelsen TI. The premature synostosis of the cranial sutures. Acta Ophthalmol (Copenh). 1958;36 Suppl 51:1–176.
46. Krayenbul H, Yasargil MG. Das hirnaneurysma. Geigy: Basel; 1958.
47. Margolis G, Kilham L. Hydrocephalus in hamsters, ferrets, rats, and mice following inoculations with reovirus type I. II. Pathologic studies. Lab Invest. 1969;21(3):189–98.
48. Hanna LS, Girgis NI, Yassin MMW, et al. Incidence of papilledema and optic atrophy in meningitis. Jpn J Ophthalmol. 1981;25:69–73.
49. Miller JD, Ross CA. Encephalitis. A four-year survey. Lancet. 1968;1(7552):1121–6.
50. Silverstein A. Papilledema with acute viral infections of the brain. Mt Sinai J Med. 1974;41(3):435–43.
51. Haslbeck KM, Eberhardt KE, Nissen U, et al. Intracranial hypertension as a clinical manifestation of cauda equine paraganglioma. Neurology. 1999;52(6):1297–8.
52. Fantin A, Feist RM, Reddy CV. Intracranial hypertension and papilledema in chronic inflammatory demyelinating polyneuropathy. Br J Ophthalmol. 1993;77(3):193.
53. Ameri A, Bousser MG. Cerebral venous thrombosis. Neurol Clin. 1992;10(1):87–111.
54. Bousser MG, Barnett HJM. Cerebral venous thrombosis. In: Bousser MG, Barnett HJM, editors. Stroke: pathophysiology, diagnosis, and management. 2nd ed. New York: Churchill-Livingstone; 1992. p. 517–37.
55. Bousser MG, Chiras J, Bories J, Castaigne P. Cerebral venous thrombosis: a review of 38 cases. Stroke. 1985;16(2):199–213.
56. Buonanno FS. Cerebral sinovenous thrombosis. Curr Treat Options Cardiovasc Med. 2001;3(5):417–27.
57. Provenzale JM, Joseph GJ, Barboriak DP. Dural sinus thrombosis: findings on CT and MR imaging and diagnostic pitfalls. AJR Am J Roentgenol. 1998;170(3):777–83.
58. Biousse V, Tong F, Newman NJ. Cerebral venous thrombosis. Curr Treat Options Neurol. 2003;5(5): 409–20.
59. Villringer A, Mehraein S, Einhaupl KM. Pathophysiological aspects of cerebral sinus venous thrombosis (SVT). J Neuroradiol. 1994;21(2):72–80.
60. Bousser MG, Russell RR. Cerebral venous thrombosis. London: Saunders; 1997.
61. Allroggen H, Abbott RJ. Cerebral venous sinus thrombosis. Postgrad Med J. 2000;76(891):12–5.
62. Preter M, Tzourio C, Ameri A, Bousser MG. Long-term prognosis in cerebral venous thrombosis. Follow-up of 77 patients. Stroke. 1996;27(2):243–6.
63. Ozsvath RR, Casey SO, Lustrin ES, Alberico RA, Hassankhani A, Patel M. Cerebral venography: comparison of CT and MR projection venography. AJR Am J Roentgenol. 1997;169(6):1699–707.
64. Deschiens MA, Conard J, Horellou MH, et al. Coagulation studies, factor V Leiden, and anticardiolipin antibodies in 40 cases of cerebral venous thrombosis. Stroke. 1996;27(10):1724–30.
65. Stam J, De Bruijn SF, De Veber G. Anticoagulation for cerebral sinus thrombosis. Cochrane Database Syst Rev 2002;4:CD002005.
66. de Bruijn SF, Stam J. Randomized, placebo-controlled trial of anticoagulant treatment with low-molecular-weight heparin for cerebral sinus thrombosis. Stroke. 1999;30(3):484–8.
67. Friedman DI, Rausch EA. Headache diagnoses in patients with treated idiopathic intracranial hypertension. Neurology. 2002;58(10):1551–3.
68. Evans RW. New daily persistent headache. Curr Pain Headache Rep. 2003;7(4):303–7.
69. Green JP, Newman NJ, Stowe ZN, Nemeroff CB. "Normal pressure" pseudotumor cerebri. J Neuroophthalmol. 1996;16(4):241–6.
70. Mathew NT, Ravishankar K, Sanin LC. Coexistence of migraine and idiopathic intracranial hypertension without papilledema. Neurology. 1996;46(5):1226–30.
71. Corbett JJ, Savino PJ, Thompson HS, et al. Visual loss in pseudotumor cerebri. Follow-up of 57 patients from five to 41 years and a profile of 14 patients with permanent severe visual loss. Arch Neurol. 1982;39:461–74.
72. Digre KB, Nakamoto BK, Warner JE, et al. A comparison of idiopathic intracranial hypertension with and without papilledema. Headache. 2009;49: 185–93.
73. Ney JJ, Volpe NJ, Liu GT, Balcer LJ, Moster ML, Galetta SL. Ophthalmology. 2009;116(9):1808–13.
74. Bono F, Cristiano D, Mastrandrea C, et al. The upper limit of normal CSF opening pressure is related to bilateral transverse sinus stenosis in headache sufferers. Cephalalgia. 2010;30(2):145–51.
75. Durcan FJ, Corbett JJ, Wall M. The incidence of pseudotumor cerebri. Population studies in Iowa and Louisiana. Arch Neurol. 1988;45(8):875–7.
76. Radhakrishnan K, Sridharan R, Ashok PP, Mousa ME. Pseudotumour cerebri: incidence and pattern in North-Eastern Libya. Eur Neurol. 1986;25(2):117–24.
77. Radhakrishnan K, Thacker AK, Bohlaga NH, Maloo JC, Gerryo SE. Epidemiology of idiopathic intracranial hypertension: a prospective and case-control study. J Neurol Sci. 1993;116(1):18–28.
78. Bruce BB, Preechawat P, Newman NJ, Lynn MJ, Biousse V. Racial differences in idiopathic intracranial hypertension. Neurology. 2008;70(11): 861–7.
79. Rowe FJ, Sarkies NJ. Assessment of visual function in idiopathic intracranial hypertension: a prospective study. Eye. 1998;12(pt 1):111–8.
80. Wall M, White II WN. Asymmetric papilledema in idiopathic intracranial hypertension: prospective interocular comparison of sensory visual function. Invest Ophthalmol Visual Sci. 1998;39(1):134–42.

81. Foley J. Benign forms of intracranial hypertension; toxic and otitic hydrocephalus. Brain. 1955;78(1): 1–41.
82. Bandyopadhyay S, Jacobson DM. Clinical features of late-onset pseudotumor cerebri fulfilling the modified dandy criteria. J Neuroophthalmol. 2002; 22(1):9–11.
83. Wall M, George D. Idiopathic intracranial hypertension. A prospective study of 50 patients. Brain. 1991;114(pt 1A):155–80.
84. Rowe FJ, Sarkies NJ. The relationship between obesity and idiopathic intracranial hypertension. Int J Obes Relat Metab Disord. 1999;23(1):54–9.
85. Johnson LN, Krohel GB, Madsen RW, March Jr GA. The role of weight loss and acetazol-amide in the treatment of idiopathic intracranial hypertension (pseudotumor cerebri). Ophthalmology. 1998;105(12): 2313–7.
86. Kupersmith MJ, Gamell L, Turbin R, Peck V, Spiegel P, Wall M. Effects of weight loss on the course of idiopathic intracranial hypertension in women. Neurology. 1998;50(4):1094–8.
87. Donaldson JO. Pathogenesis of pseudotumor cerebri syndromes. Neurology. 1981;31(7):877–80.
88. Dandy WE. Intracranial pressure without brain tumor: diagnosis and treatment. Ann Surg. 1937;106:492–513.
89. Raichle ME, Grubb Jr RL, Phelps ME, Gado MH, Caronna JJ. Cerebral hemodynamics and metabolism in pseudotumor cerebri. Ann Neurol. 1978;4(2): 104–11.
90. Gideon P, Sorensen PS, Thomsen C, Stahlberg F, Gjerris F, Henriksen O. Increased brain water self-diffusion in patients with idiopathic intracranial hypertension. AJNR Am J Neuroradiol. 1995; 16(2):381–7.
91. Moser FG, Hilal SK, Abrams G, Bello JA, Schipper H, Silver AJ. MR imaging of pseudo-tumor cerebri. AJR Am J Roentgenol. 1988;150(4):903–9.
92. Sorensen PS, Thomsen C, Gjerris F, Henriksen O. Brain water accumulation in pseudotumour cerebri demonstrated by MR-imaging of brain water self-diffusion. Acta Neurochir Suppl (Wien). 1990; 51:363–5.
93. Sorensen PS, Thomsen C, Gjerris F, Schmidt J, Kjaer L, Henriksen O. Increased brain water content in pseudotumour cerebri measured by magnetic resonance imaging of brain water self diffusion. Neurol Res. 1989;11(3):160–4.
94. Johnston I, Paterson A. Benign intracranial hypertension. II. CSF pressure and circulation. Brain. 1974;97(2):301–12.
95. Rottenberg DA, Foley KM, Posner JB. Hypothesis: the pathogenesis of pseudotumor cerebri. Med Hypotheses. 1980;6(9):9138.
96. Janny P, Chazal J, Colnet G, Irthum B, Georget AM. Benign intracranial hypertension and disorders of CSF absorption. Surg Neurol. 1981;15(3):168–74.
97. Karahalios DG, Rekate HL, Khayata MH, Apostolides PJ. Elevated intracranial venous pressure as a universal mechanism in pseudotumor cerebri of varying etiologies. Neurology. 1996;46(1):198–202.
98. Farb RI, Vanek I, Scott JN, et al. Idiopathic intracranial hypertension: the prevalence and morphology of sinovenous stenosis. Neurology. 2003;60(9):1418–24.
99. King JO, Mitchell PJ, Thomson KR, et al. Manometry combined with cervical puncture in idiopathic intracranial hypertension. Neurology. 2002;58:26–30.
100. Sumbranian RM, Tress BM, King JO, Eizenberg N, Mitchell PJ. Transverse sinus septum: a new aetiology of idiopathic intracranial hypertension? Australas Radiol. 2004;48:114.
101. Nedelmann M, Kaps M, Mueller-Forell W. Venous obstruction and jugular valve insufficiency in idiopathic intracranial hypertension. J Neurol. 2009; 256:964–9.
102. Arjona A, Delgado F, Fernandez-Romero E. Intracranial hypertension secondary to giant arachnoid granulations. J Neurol Neurosurg Psychiatry. 2003;74:418.
103. Connor SEJ, Siddiqui MA, Stewart VR, et al. The relationship of transverse sinus stenosis to bony groove dimensions provides an insight into the etiology of idiopathic intracranial hypertension. Neuroradiology. 2008;50:999–1004.
104. Farb RI, Forghani R, Lee SK, et al. The venous distension sign: a diagnostic sign of intracranial hypotension at MR imaging of the brain. AJNR Am J Neuroradiol. 2007;28:1489–93.
105. Sugerman HJ, DeMaria EJ, Felton III WL, Nakatsuka M, Sismanis A. Increased intra-abdominal pressure and cardiac filling pressures in obesity-associated pseudotumor cerebri. Neurology. 1997;49(2):507–11.
106. Sugerman HJ, Felton III WL, Salvant Jr JB, Sismanis A, Kellum JM. Effects of surgically induced weight loss on idiopathic intracranial hypertension in morbid obesity. Neurology. 1995;45(9):1655–9.
107. Sugerman HJ, Felton III WL, Sismanis A, Kellum JM, DeMaria EJ, Sugerman EL. Gastric surgery for pseudotumor cerebri associated with severe obesity. Ann Surg. 1999;229(5):634–40. discussion 640–42.
108. Brockmeier B, Burbach H, Runge M, Altenkirch H. Raised intracranial pressure in chronic respiratory disease. Lancet. 1997;349(9055):883.
109. Jennum P, Borgesen SE. Intracranial pressure and obstructive sleep apnea. Chest. 1989;95(2):279–83.
110. McNamara ME. Idiopathic intracranial hypertension without papilledema: related to sleep apnea? Arch Neurol. 1992;49(1):14.
111. Lampl Y, Eshel Y, Kessler A, et al. Serum leptin level in women with idiopathic intracranial hypertension. J Neurol Neurosurg Psychiatry. 2002; 72(5):642–3.
112. Ball AK, Sinclair AJ, Curnow SJ, et al. Elevated cerebrospinal fluid (CSF) leptin in idiopathic intracranial hypertension (IIH): evidence for hypothalamic leptin resistance? Clin Endocrinol (Oxf). 2009;70(6):863–9.

113. Dhungana S, Sharrack B, Woodroofe N. Cytokines and chemokines in idiopathic intracranial hypertension. Headache. 2009;49(2):282–5.
114. Subramanian PS, Goldenberg-Cohen N, Shukla S, Cheskin LJ, Miller NR. Plasma ghrelin levels are normal in obese patients with idiopathic intracranial hypertension (pseudotumor cerebri). Am J Ophthalmol. 2004;138(1):109–13.
115. Kesler A, Kliper E, Shenkerman G, et al. Idiopathic intracranial hypertension is associated with lower body adiposity. Ophthalmology. 2010;117:169–74.
116. Ko MW, Chang SC, Ridha MA, et al. Weight gain and recurrence in idiopathic intracranial hypertension: a case control study. Neurology. 2011;76:1564–7.
117. Kim TW, Choung HK, Khwarg SI, et al. Eur J Neurol. 2008;15(8):876–9.
118. Carlow TJ, Glaser JS. Pseudotumor cerebri syndrome in systemic lupus erythematosus. JAMA. 1974;228(2):197–200.
119. Li EK, Ho PC. Pseudotumor cerebri in systemic lupus erythematosus. J Rheumatol. 1989;16(1): 113–6.
120. Padeh S, Passwell JH. Systemic lupus erythematosus presenting as idiopathic intracranial hypertension. J Rheumatol. 1996;23(7):1266–8.
121. Waxman J, Wasan H. The architecture of cancer. BMJ. 1992;305(6865):1306–7.
122. Capriles LF. Intracranial hypertension and iron deficiency anemia: report of four cases. Arch Neurol. 1963;9:147–53.
123. Condulis N, Germain G, Charest N, Levy S, Carpenter TO. Pseudotumor cerebri: a presenting manifestation of Addison's disease. Clin Pediatr (Phila). 1997;36(12):711–3.
124. Huseman CA, Torkelson RD. Pseudotumor cerebri following treatment of hypothalamic and primary hypothyroidism. Am J Dis Child. 1984;138(10): 927–31.
125. Raghavan S, DiMartino-Nardi J, Saenger P, Linder B. Pseudotumor cerebri in an infant after L-thyroxine therapy for transient neonatal hypothyroidism. J Pediatr. 1997;130(3):478–80.
126. Chang D, Nagamoto G, Smith WE. Benign intracranial hypertension and chronic renal failure. Cleve Clin J Med. 1992;59(4):419–22.
127. Guy J, Johnston PK, Corbett JJ, Day AL, Glaser JS. Treatment of visual loss in pseudotumor cerebri associated with uremia. Neurology. 1990;40(1):28–32.
128. Noetzel MJ, Rioux SD. Pseudotumor cerebri associated with obstructive nephropathy. Pediatr Neurol. 1986;2(4):238–40.
129. Couban S, Maxner CE. Cerebral venous sinus thrombosis presenting as idiopathic intracranial hypertension. Can Med Assoc J. 1991;145(6):657–9.
130. Biousse V, Ameri A, Bousser MG. Isolated intracranial hypertension as the only sign of cerebral venous thrombosis. Neurology. 1999;53(7):1537–42.
131. Cognard C, Casasco A, Toevi M, Houdart E, Chiras J, Merland JJ. Dural arteriovenous fistulas as a cause of intracranial hypertension due to impairment of cranial venous outflow. J Neurol Neurosurg Psychiatry. 1998;65(3):308–16.
132. Halbach VV, Higashida RT, Hieshima GB. Interventional neuroradiology. AJR Am J Roentgenol. 1989;153(3):467–76.
133. Vijayan N. Headache following removal of acoustic neuroma. Headache. 1995;35(10):639.
134. Kiers L, King JO. Increased intracranial pressure following bilateral neck dissection and radiotherapy. Aust N Z J Surg. 1991;61(6):459–61.
135. Lam BL, Schatz NJ, Glaser JS, Bowen BC. Pseudotumor cerebri from cranial venous obstruction. Ophthalmology. 1992;99(5):706–12.
136. Sklar FH, Beyer Jr CW, Ramanathan M, Cooper PR, Clark WK. Cerebrospinal fluid dynamics in patients with pseudotumor cerebri. Neurosurgery. 1979;5(2): 208–16.
137. Birdwell BG, Yeager R, Whitsett TL. Pseudotumor cerebri. A complication of catheter-induced subclavian vein thrombosis. Arch Intern Med. 1994;154(7):808–11.
138. Marr WG, Chambers JW. Occlusion of the cerebral dural sinuses by tumor simulating pseudotumor cerebri. Am J Ophthalmol. 1966;61(1):45–9.
139. Lee AG, Brazis PW. Magnetic resonance venography in idiopathic pseudotumor cerebri. J Neuroophthalmol. 2000;20(1):12–3.
140. Wasan H, Mansi JL, Benjamin S, Powles R, Cunningham D. Myeloma and benign intracranial hypertension. BMJ. 1992;304(6828):685.
141. Pasquale LR, Moster ML, Schmaier A. Dural sinus thrombosis with abnormalities of protein S and fibrinogen. Arch Ophthalmol. 1990;108(5):644.
142. Sussman J, Leach M, Greaves M, Malia R, Davies-Jones GA. Potentially prothrombotic abnormalities of coagulation in benign intracranial hypertension. J Neurol Neurosurg Psychiatry. 1997;62(3):229–33.
143. Ludemann P, Nabavi DG, Junker R, et al. Factor V Leiden mutation is a risk factor for cerebral venous thrombosis: a case-control study of 55 patients. Stroke. 1998;29(12):2507–10.
144. Weih M, Vetter B, Ziemer S, et al. Increased rate of factor V Leiden mutation in patients with cerebral venous thrombosis. J Neurol. 1998;245(3):149–52.
145. Leker RR, Steiner I. Anticardiolipin antibodies are frequently present in patients with idiopathic intracranial hypertension. Arch Neurol. 1998;55(6): 817–20.
146. Mokri B, Jack Jr CR, Petty GW. Pseudotumor syndrome associated with cerebral venous sinus occlusion and antiphospholipid antibodies. Stroke. 1993;24(3):469–72.
147. Walsh FB, Clark DB, Thompson RS, Nicholson DH. Oral contraceptives and neuroophthalmologic interest. Arch Ophthalmol. 1965;74(5):628–40.
148. Cantu C, Barinagarrementeria F. Cerebral venous thrombosis associated with pregnancy and puerperium. Review of 67 cases. Stroke. 1993;24(12):1880–4.

149. Glueck CJ, Iyengar S, Goldenberg N, Smith LS, Wang P. Idiopathic intracranial hypertension: associations with coagulation disorders and polycystic ovary syndrome. J Lab Clin Med. 2003;142(1):35–45.
150. Bousser MG. Cerebral venous thrombosis: diagnosis and management. J Neurol. 2000;247(4):252–8.
151. Biousse V, Rucker JC, Vignal C, Crassard I, Katz BJ, Newman NJ. Anemia and papilledema. Am J Ophthalmol. 2003;135(4):437–46.
152. Henry M, Driscoll MC, Miller M, Chang T, Minniti CP. Pseudotumor cerebri in children with sickle cell disease: a case series. Pediatrics. 2004;113(3 pt 1):e265–9.
153. Bruce BB, Kedar S, Van Stavern GP, et al. Idiopathic intracranial hypertension in men. Neurology. 2009;72:304–9.
154. Fraser JA, Bruce BB, Rucker J, et al. Risk factors for idiopathic intracranial hypertension in men: a case-control study. J Neurol Sci. 2010;290(1–2):86. doi:10.1016/j.jns.2009.11.001.
155. Lee AG, Golnik K, Kardon R, Wall M, Eggenberger E, Yedavally S. Sleep apnea and intracranial hypertension in men. Ophthalmology. 2002;109(3):482–5.
156. Weber KT, Singh KD, Hey JC. Idiopathic intracranial hypertension with primary aldosteronism: report of 2 cases. Am J Med Sci. 2002;324(1):45–50.
157. Frost N, Lee MS, Sweeney P. Myxedema, papilledema, and elevated CSF protein. Neurology. 2004;63(4):754–5.
158. Villain MA, Pageaux GP, Veyrac M, Arnaud B, Harris A, Greenfield DS. Effect of acetazolamide on ocular hemodynamics in pseudotumor cerebri associated with inflammatory bowel disease. Am J Ophthalmol. 2002;134(5):778–80.
159. Tillman O, Kaiser HJ, Killer HE. Pseudotumor cerebri in a patient with Goldenhar's and Duane's syndromes. Ophthalmologica. 2002;216(4):296–9.
160. Mokri B. Intracranial hypertension after treatment of spontaneous cerebrospinal fluid leaks. Mayo Clin Proc. 2002;77(11):1241–6.
161. Morrice G. Papilledema and hypervitaminosis A. JAMA. 1970;213(8):1344.
162. Roytman M, Frumkin A, Bohn TG. Pseudotumor cerebri caused by isotretinoin. Cutis. 1988;42(5):399–400.
163. Spector RH, Carlisle J. Pseudotumor cerebri caused by a synthetic vitamin A preparation. Neurology. 1984;34(11):1509–11.
164. Naderi S, Nukala S, Marruenda F, Kudarvalli P, Koduri PR. Pseudotumour cerebri in acute promyelocytic leukemia: improvement despite continued ATRA therapy. Ann Hematol. 1999;78(7):333–4.
165. Visani G, Bontempo G, Manfroi S, Pazzaglia A, D'Alessandro R, Tura S. All-*trans*-retinoic acid and pseudotumor cerebri in a young adult with acute promyelocytic leukemia: a possible disease association. Haematologica. 1996;81(2):152–4.
166. Visani G, Manfroi S, Tosi P, Martinelli G. All-t*rans*-retinoic acid and pseudotumor cerebri. Leuk Lymphoma. 1996;23(5–6):437–42.
167. Chiu AM, Chuenkongkaew WL, Cornblath WT, et al. Minocycline treatment and pseudotumor cerebri syndrome. Am J Ophthalmol. 1998;126(1):116–21.
168. Giles CL, Soble AR. Intracranial hypertension and tetracycline therapy. Am J Ophthalmol. 1971;72(5):981–2.
169. Friedman DI, Gordon LK, Egan RA, et al. Doxycycline and intracranial hypertension. Neurology. 2004;62(12):2297–9.
170. Cohen DN. Intracranial hypertension and papilledema associated with nalidixic acid therapy. Am J Ophthalmol. 1973;76(5):680–2.
171. Getenet JC, Croisile B, Vighetto A, et al. Idiopathic intracranial hypertension after ofloxacin treatment. Acta Neurol Scand. 1993;87(6):503–4.
172. Winrow AP, Supramaniam G. Benign intracranial hypertension after ciprofloxacin administration. Arch Dis Child. 1990;65(10):1165–6.
173. Ch'ien LT. Intracranial hypertension and sulfamethoxazole. N Engl J Med. 1976;283:47.
174. Sunku AJ, O'Duffy AE, Swanson JW. Benign intracranial hypertension associated with levonorgestrel implants. Ann Neurol. 1993;34:299.
175. Hamed LM, Glaser JS, Schatz NJ, Perez TH. Pseudotumor cerebri induced by danazol. Am J Ophthalmol. 1989;107(2):105–10.
176. Neville BGR, Wilson J. Benign intracranial hypertension following corticosteroid withdrawal in childhood. Br Med J. 1970;3:554–6.
177. Levine SH, Puchalski C. Pseudotumor cerebri associated with lithium therapy in two patients. J Clin Psychiatry. 1990;51(6):251–3.
178. Saul RF, Hamburger HA, Selhorst JB. Pseudotumor cerebri secondary to lithium carbonate. JAMA. 1985;253(19):2869–70.
179. Serratrice J, Granel B, Conrath J, et al. Benign intracranial hypertension and thyreostimulin suppression hormonotherapy. Am J Ophthalmol. 2002;134(6):910–1.
180. Rosa N, Giamundo A, Jura A, Iaccarino G, Romano A. Mesalazine-associated benign intracranial hypertension in a patient with ulcerative colitis. Am J Ophthalmol. 2003;136(1):212–3.
181. Jacobson DM, Berg R, Wall M, Digre KB, Corbett JJ, Ellefson RD. Serum vitamin A concentration is elevated in idiopathic intracranial hypertension. Neurology. 1999;53(5):1114–8.
182. Crock PA, McKenzie JD, Nicoll AM, et al. Benign intracranial hypertension and recombinant growth hormone therapy in Australia and New Zealand. Acta Paediatr. 1998;87(4):381–6.
183. Rogers AH, Rogers GL, Bremer DL, McGregor ML. Pseudotumor cerebri in children receiving recombinant human growth hormone. Ophthalmology. 1999;106(6):1186–9. discussion 1189–90.
184. Wessel K, Thron A, Linden D, Petersen D, Dichgans J. Pseudotumor cerebri: clinical and neuroradiological findings. Eur Arch Psychiatry Neurol Sci. 1987;237(1):54–60.

185. Jacobson DM, Karanjia PN, Olson KA, Warner JJ. Computed tomography ventricular size has no predictive value in diagnosing pseudotumor cerebri. Neurology. 1990;40(9):1454–5.
186. Brodsky MC, Vaphiades M. Magnetic resonance imaging in pseudotumor cerebri. Ophthalmology. 1998;105(9):1686–93.
187. Hannerz J, Greitz D, Ericson K. Is there a relationship between obesity and intracranial hypertension? Int J Obes Relat Metab Disord. 1995;19(4):240–4.
188. Czosnyka M, Pickard JD. Monitoring and interpretation of intracranial pressure. J Neurol Neurosurg Psychiatry. 2004;75(6):813–21.
189. Friedman DI, Jacobson DM. Idiopathic intracranial hypertension. J Neuroophthalmol. 2004;24(2):138–45.
190. Wall, M., NORDIC Idiopathic Intracranial Hypertension Treatment Trial (IIHTT): NORDIC clinical trials. http://www.nordicclinicaltrials.com/nordic/?wicket:bookmarkablePage=:org.slr.nordic.webapp.cms.DisplayCmsPage&id=8. Accessed 22 Aug 2013.
191. Rubin RC, Henderson ES, Ommaya AK, Walker MD, Rall DP. The production of cerebrospinal fluid in man and its modification by acetazolamide. J Neurosurg. 1966;25(4):430–6.
192. Physicians' desk reference. 58th ed. Montvale, NJ: Thomson PDR; 2004. p. 1208–9. Diamox.
193. Schoeman JF. Childhood pseudotumor cerebri: clinical and intracranial pressure response to acetazolamide and furosemide treatment in a case series. J Child Neurol. 1994;9(2):130–4.
194. Liu GT, Glaser JS, Schatz NJ. High-dose methylprednisolone and acetazolamide for visual loss in pseudotumor cerebri. Am J Ophthalmol. 1994; 118(1):88–96.
195. Corbett JJ, Thompson HS. The rational management of idiopathic intracranial hypertension. Arch Neurol. 1989;46(10):1049–51.
196. Banta JT, Farris BK. Pseudotumor cerebri and optic nerve sheath decompression. Ophthalmology. 2000;107(10):1907–12.
197. Kelman SE, Heaps R, Wolf A, Elman MJ. Optic nerve decompression surgery improves visual function in patients with pseudotumor cerebri. Neurosurgery. 1992;30(3):391–5.
198. Sergott RC. Optic nerve sheath decompression: neuropathologic, clinical, and hemodynamic results and rationale. Trans Am Ophthalmol Soc. 1991;89:675–720.
199. Spoor TC, Ramocki JM, Madion MP, Wilkinson MJ. Treatment of pseudotumor cerebri by primary and secondary optic nerve sheath decompression. Am J Ophthalmol. 1991;112(2):177–85.
200. Keltner JL. Optic nerve sheath decompression. How does it work? Has its time come? Arch Ophthalmol. 1988;106(10):1365–9.
201. Hamed LM, Tse DT, Glaser JS, Byrne SF, Schatz NJ. Neuroimaging of the optic nerve after fenestration for management of pseudotumor cerebri. Arch Ophthalmol. 1992;110(5):636–9.
202. Alsuhaibani A, Carter KD, Nerad JA, et al. Effect of optic nerve sheath fenestration on papilledema of the operated and the contralateral nonoperated eyes in idiopathic intracranial hypertension. Ophthalmology. 2011;118:412–4.
203. Spoor TC, McHenry JG. Long-term effectiveness of optic nerve sheath decompression for pseudotumor cerebri. Arch Ophthalmol. 1993;111(5): 632–5.
204. Pelton RW, Patel BC. Superomedial lid crease approach to the medial intraconal space: a new technique for access to the optic nerve and central space. Ophthal Plast Reconstr Surg. 2001;17(4): 241–53.
205. Plotnik JL, Kosmorsky GS. Operative complications of optic nerve sheath decompression. Ophthalmology. 1993;100(5):683–90.
206. Johnston I, Besser M, Morgan MK. Cerebrospinal fluid diversion in the treatment of benign intracranial hypertension. J Neurosurg. 1988;69(2):195–202.
207. Eggenberger ER, Miller NR, Vitale S. Lumboperitoneal shunt for the treatment of pseudotumor cerebri. Neurology. 1996;46(6):1524–30.
208. Burgett RA, Purvin VA, Kawasaki A. Lumboperitoneal shunting for pseudotumor cerebri. Neurology. 1997;49(3):734–9.
209. Hart A, David K, Powell M. The treatment of "acquired tonsillar herniation" in pseudotumour cerebri. Br J Neurosurg. 2000;14(6):563–5.
210. Tulipan N, Lavin PJ, Copeland M. Stereotactic ventriculoperitoneal shunt for idiopathic intracranial hypertension: technical note. Neurosurgery. 1998; 43(1):175–6.
211. Binder DK, Horton JC, Lawton MT, McDermott MW. Idiopathic intracranial hypertension. Neurosurgery. 2004;54(3):538–51. discussion 551–2.
212. Tarnaris A, Toma AK, Watkins LD. Is there a difference in outcomes of patients with idiopathic intracranial hypertension with the choice of cerebrospinal fluid diversion site: a single centre experience. Clin Neurol Neurosurg. 2011;113(6):477–9.
213. Abubaker K, Ali A, Raza K, et al. Idiopathic intracranial hypertension: lumboperitoneal shunts versus ventriculoperitoneal shunts—case series and literature review. Br J Neurosurg. 2011;25(1):94–9.
214. Fridley J, Foroozan R, Sherman V, et al. Bariatric surgery for the treatment of idiopathic intracranial hypertension. J Neurosurg. 2011;114(1):34–9.
215. Higgins JN, Pickard JD. Lateral sinus stenoses in idiopathic intracranial hypertension resolving after CSF diversion. Neurology. 2004;62(10):1907–8.
216. Higgins JN, Cousins C, Owler BK, Sarkies N, Pickard JD. Idiopathic intracranial hypertension: 12 cases treated by venous sinus stenting. J Neurol Neurosurg Psychiatry. 2003;74(12):1662–6.
217. Ogungbo B, Roy D, Gholkar A, Mendelow AD. Endovascular stenting of the transverse sinus in a patient presenting with benign intracranial hypertension. Br J Neurosurg. 2003;17(6):565–8.

218. Bussiere M, Falero R, Nicolle D, et al. Unilateral transverse sinus stenting of patients with idiopathic intracranial hypertension. AJNR Am J Neuroradiol. 2010;31(4):645–50.
219. Arac A, Lee M, Steinberg GK, et al. Efficacy of endovascular stenting in dural venous sinus stenosis for the treatment of idiopathic intracranial hypertension. Neurosurg Focus. 2009;27(5):E14.
220. De Simone R, Marano E, Fiorillo C, et al. Sudden reopening of collapsed transverse sinuses and longstanding clinical remission after a single lumbar puncture in a case of idiopathic intracranial hypertension: pathogenetic implications. Neurol Sci. 2005;25:342–4.
221. Scoffings DJ, Pickard JD, Higgins JNP. Resolution of transverse sinus stenoses immediately after CSF withdrawal in idiopathic intracranial hypertension. J Neurol Neurosurg Psychiatry. 2007;78:911–2.
222. Lee SW, Gates P, Morris P, et al. Idiopathic intracranial hypertension: immediate resolution of venous sinus "obstruction" after reducing cerebrospinal fluid pressure to <10 cm H_2O. J Clin Neurosci. 2009;16:1690–2.
223. Rohr A, Dorner L, Stingele R, et al. Reversibility of venous sinus obstruction in idiopathic intracranial hypertension. AJNR Am J Neuroradiol. 2007;28:656.
224. Stienen A, Weinzierl M, Ludolph A, et al. Obstruction of cerebral venous sinus secondary to idiopathic intracranial hypertension. Eur J Neurol. 2008;15:1416–8.
225. Bono F, Giliberto C, Mastrandrea C, et al. Transverse sinus stenosis persist after normalization of the CSF pressure in IIH. Neurology. 2005;65:1090–3.
226. Bateman GA. Vascular hydraulics associated with idiopathic and secondary intracranial hypertension. Am J Neuroradiol. 2002;23:1180–6.
227. Cinciripini GS, Donahue S, Borchert MS. Idiopathic intracranial hypertension in prepubertal pediatric patients: characteristics, treatment, and outcome. Am J Ophthalmol. 1999;127(2):178–82.
228. Huna-Baron R, Kupersmith MJ. Idiopathic intracranial hypertension in pregnancy. J Neurol. 2002; 249(8):1078–81.
229. Shapiro S, Yee R, Brown H. Surgical management of pseudotumor cerebri in pregnancy: case report. Neurosurgery. 1995;37(4):829–31.
230. McDonnell GV, Patterson VH, McKinstry S. Cerebral venous thrombosis occurring during an ectopic pregnancy and complicated by intracranial hypertension. Br J Clin Pract. 1997;51(3):194–7.
231. Balcer LJ, Liu GT, Forman S, et al. Idiopathic intracranial hypertension: relation of age and obesity in children. Neurology. 1999;52(4):870–2.
232. Rangwala LM, Liu GT. Pediatric idiopathic intracranial hypertension. Surv Ophthalmol. 2007;52(6): 597–617.
233. Gordon K. Pediatric pseudotumor cerebri: descriptive epidemiology. Can J Neurol Sci. 1997;24(3): 219–21.
234. Scott IU, Siatkowski RM, Eneyni M, Brodsky MC, Lam BL. Idiopathic intracranial hypertension in children and adolescents. Am J Ophthalmol. 1997; 124(2):253–5.
235. Phillips PH, Repka MX, Lambert SR. Pseudotumor cerebri in children. J AAPOS. 1998;2(1):33–8.
236. Baker RS, Baumann RJ, Buncic JR. Idiopathic intracranial hypertension (pseudotumor cerebri) in pediatric patients. Pediatr Neurol. 1989;5(1):5–11.
237. Weig SG. Asymptomatic idiopathic intracranial hypertension in young children. J Child Neurol. 2002;17(3):239–41.
238. Avery RA, Shah SS, Licht DJ, et al. Reference range for cerebrospinal fluid opening pressure in children. N Engl J Med. 2010;363(9):891–3.
239. Soiberman U, Stolovitch C, Balcer LJ, Regenbogen M, Constantini S, Kesler A. Idiopathic intracranial hypertension in children: visual outcome and risk of recurrence. Childs Nerv Syst. 2011;27(11):1913–8.
240. Ayanzen RH, Bird CR, Keller PJ, McCully FJ, Theobald MR, Heiserman JE. Cerebral MR venography: normal anatomy and potential diagnostic pitfalls. AJNR Am J Neuroradiol. 2000;21(1):74–8.
241. Widjaja E, Griffiths PD. Intracranial MR venography in children: normal anatomy and variations. AJNR Am J Neuroradiol. 2004;25(9):1557–62.

Compressive and Infiltrative Optic Neuropathies

4

Jane W. Chan

Compression of the Anterior Visual Pathway (Optic Nerve and Chiasm) from Intrinsic Optic Nerve Tumors

Optic Nerve Sheath Meningiomas

Epidemiology

In contrast to the meningiomas from intracranial extension or the ectopic orbital ones, primary optic nerve sheath meningioma (ONSM) arise from the intraorbital optic nerve sheath and grow circumferentially around the optic nerve to result in an optic neuropathy by interfering with axonal transport and pial blood supply to the nerve. They constitute 1–2 % of all meningiomas and account for one-third of all primary optic nerve tumors. They are also the second most common optic nerve tumor after glioma [1]. Only 10 % of ONSM arise from the orbit, compared to 90 % from intracranial extension. More than 90 % of ONSM develop in the orbital optic nerve rather than in the canalicular portion [2].

The mean age of presentation is 40.8 years, according to data from 256 patients [3]. These ONSMs are usually unilateral and occur more frequently among females in a 1:2 male-to-female ratio. Bilateral and multifocal ONSMs occurred in younger patients with neurofibromatosis type II (NF-2) [4], who presented at a mean age of 12.8 years [2], compared to intracranial meningiomas, which occur around 50 years of age.

Symptoms and Signs

The most common presenting symptom of ONSM is a gradual decrease in visual acuity, which may progress to being moderate or severe, with 15–50 % of patients having better than 20/40 vision [5]. Transient visual obscurations may also be the presenting symptom, which may be gaze evoked, postural, or spontaneous [6]. Visual field defects often include peripheral constriction; central, centrocecal, and paracentral scotomas; altitudinal defects; and enlarged blind spots [5, 7]. Generalized constriction appears to be more frequently seen in patients with canalicular tumors [8]. Proptosis is often mild to moderate and is seen less frequently in patients with canalicular lesions, because they often present with visual loss when the tumor is quite small. Extraocular motility restriction is greatest in attempted upgaze [9]. Approximately half of affected patients have orbital pain and generalized headache [5].

On funduscopic examination, the optic disc is usually either atrophic or swollen [6–8]. Patients with more posterior or intracanalicular ONSMs who present with slower progressive visual loss without proptosis or disc edema, however, may present with normal optic discs. As optic nerve compression progresses, the degree of optic atrophy increases [7, 10, 11]. Optociliary vessels

J.W. Chan, M.D. (✉)
Department of Neurology, Neuro-Ophthalmology,
University of Nevada School of Medicine,
975 Kirman Avenue (111), Reno, Nevada 89502, USA
e-mail: worjun@aol.com

J.W. Chan (ed.), *Optic Nerve Disorders: Diagnosis and Management*,
DOI 10.1007/978-1-4614-0691-4_4, © Springer Science+Business Media New York 2014

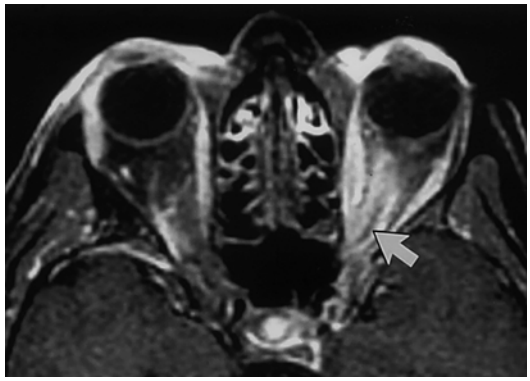

Fig. 4.1 Optic nerve sheath meningioma. Axial contrast-enhanced, fat-suppressed T1-weighted spin-echo MRI of orbits shows left optic nerve sheath meningioma. Optic nerve sheath meningiomas appear as a circumferential thickening of the optic nerve (*arrow*) that enhances and the optic nerve appears as a central linear hypointensity, producing the tram-track sign. [Reprinted from Kanamalia U. The optic nerve tram-track sign. Radiology 2003;227: 718–719. With permission from The Radiological Society of North America]

shunting blood from the retinal to choroidal circulation are seen in 15–33 % of patients and are associated with optic disc edema or atrophy [6–8]. When the compressed optic nerve obstructs flow in the central retinal vein, vestigial retinociliary anastomoses from earlier embryonic development reestablish the flow of retinal venous blood to vortex veins [12]. These optociliary shunt vessels are seldom seen, and they usually appear years after symptoms begin and may involute as optic atrophy is fully developed. These vessels are useful in the diagnosis of ONSMs but are not pathognomonic [6–8].

Neuroimaging Features

Neuroimaging commonly shows diffuse, tubular enlargement of the optic nerve. This appearance may be confused with optic gliomas, but kinking of the optic nerve (a classic neuroimaging sign of optic gliomas) is not seen in ONSMs. On computed tomography (CT) scan, calcification along the length of the optic nerve may be seen in 20–50 % of patients and is sometimes referred to as a "tram-track sign" (Fig. 4.1) [7, 13]. On magnetic resonance imaging (MRI) of the orbits, the tumor is isointense with brain on T1- and T2-weighted images and enhances homogeneously with gadolinium. T1-weighted fat suppression images with gadolinium help delineate the tumor surface adjacent to the orbital fat. This technique demonstrates the tram-tracking sign by enhancing the contrast between the tumor and perineural subarachnoid space [14].

Other processes mimicking the appearance of ONSMs on neuroimaging include idiopathic orbital inflammatory syndrome (sclerosing type), perioptic neuritis [15], sarcoid infiltration or other inflammatory infiltration of the optic nerve [16], metastases to the optic nerve [17], malignant optic nerve glioma of adulthood, optic nerve glioma in childhood, orbital schwannoma, cavernous hemangioma, lymphangioma, hemangiopericytoma, and optic nerve hemangioblastoma [18, 19].

Histopathology

ONSMs arise from meningothelial cells located uniformly as arachnoid villi along the canalicular and intraorbital regions of the optic nerves. ONSMs are believed to arise from the meningothelial "cap cells" of these arachnoid villi.

Three histological types are seen in ONSMs. In the meningothelial pattern, polygonal cells are arranged in sheets separated by vascular trabeculae. The cells have marginated chromatin and pseudo-inclusions, which are invaginated cell and nuclear membranes. Mitoses are uncommon. In the fibroblastic pattern, spindle-shaped cells in parallel configuration are interlaced with bundles of intercellular collagen and reticulin. In the transitional pattern, a mixture of features of the previous two histological types is seen. Spindle or oval cells are arranged in a concentric whorl formation. Psammoma bodies are more commonly seen in this type than in the meningothelial pattern. These bodies develop from hyalinization and deposition of calcium salts in the degenerated central whorls. The calcium formed in these areas accounts for the "tram-track sign" [20].

ONSMs extend along subarachnoid spaces and are encapsulated by intact arachnoid and dura. They commonly invade the optic nerve along its septae, around the spaces surrounding the central retinal vessels [21], and even through the dura and into surrounding orbital tissues [14, 22].

If ONSMs are adjacent to bone, the tumor can extend into the haversian canal system to cause hyperostosis and bone proliferation [23]. ONSMs can also extend posteriorly through the optic canal to the middle cranial fossa but often do not invade the brain [24]. In contrast to meningiomas of the optic chiasm, ONSMs rarely extend into the optic chiasm to the contralateral optic nerve [2].

ONSMs are often indolent for many months to years, and pregnancy may accelerate their growth so they become clinically apparent [22]. The tumor grows within the subarachnoid space to encase the optic nerve. This compression results in impairment of axonal transport, disc edema, optociliary shunt vessels, and eventually demyelination [25]. Continued compression of the pial blood supply leads to optic atrophy.

Prognosis and Treatment

ONSMs are benign tumors that are slow growing over a period of many years. They typically remain unilateral and rarely extend intracranially. Monocular visual loss, rather than morbidity and mortality, is the primary concern. Many patients maintain good vision for up to 18 years. The mortality rate is very low [26, 27].

Observation is recommended when the ONSM is confined to the orbit and when visual function is good. Serial visual acuity, visual fields, pupillary exam, and color vision testing should be done every 4–6 months initially. If the tumor is stable, visual function testing should then be done every 12 months. MRI can be performed once a year. In a retrospective review of 42 patients with unilateral ONSM followed over a mean of 6.2 years [26], 8 of 16 had a visual acuity of 20/100 or better and 6 had a visual acuity of 20/30 or better; three patients had slight improvement. Visual fields remained stable in four patients and improved in the three patients who also had slightly better visual acuity. In another study by Egan and Lessell [26], 54 % of 16 patients with ONSMs maintained visual acuity of 20/30 or better during a mean follow-up of 10 years. In a study by Saeed et al. [27], 35 % of patients with ONSMs maintained visual acuity of 20/50 or better during a mean follow-up period of 5.2 years. Because of the benign course of ONSMs, radiation therapy is not necessary in all patients with ONSM and is reserved for those patients whose visual function declines under observation.

In patients with worsening visual acuity, visual field defects, or intracranial extension documented on MRI of the brain, radiotherapy is the treatment of choice to preserve vision and prevent further growth of the tumor. Optic nerve sheath biopsy is rarely required because the diagnosis of ONSM can usually be made by typical radiographic features, but it may be done for atypical presentations of ONSM before radiotherapy is started. Stereotactic and three-dimensional conformal fractionated radiotherapy can deliver radiation more precisely with less risk of complications. It is recommended that 28 daily fractions of 1.8–2 Gy per fraction up to a total of 50.4–56 Gy is administered over 5–6 weeks. Several studies have shown that visual acuity may improve in 36–58 % of patients, and visual function can remain stable in 42–50 % [28–30].

The risk of complications is determined by the delivery method and use of fractions greater than 1.9 Gy. In a retrospective series of 15 patients with primary ONSM [29], transient problems included local erythema that occurred in 5 patients and local alopecia in 11 patients. Late complications at mean follow-up of 37 months included functional hyperprolactinemia in one patient and partial hypophyseal insufficiency in another patient. In another retrospective study by Narayan et al. [30], mild corneal inflammation was found early in one patient, and most other patients had transient alopecia. At a mean of 51 months of follow-up, one patient had dry eye syndrome, two patients had iritis, and one patient had grade 2 radiation retinopathy that did not affect vision. Visually significant radiation retinopathy has been reported in a patient who received 48–54 Gy to the optic nerve head and 27–48 Gy to the posterior retina. Visual acuity progressively worsened from 20/15 at 22 months posttreatment to 20/300 at 4 years posttreatment [31]. Furthermore, radiation optic neuropathy has been seen in patients receiving single doses between 8 and 12 Gy or total doses of more than 50 Gy [32, 33]. Therefore, stereotactic and three-dimensional,

conformal, low-dose, fractionated radiotherapy for ONSMs appears to improve visual outcome.

Surgery often leads to a poor visual outcome and is reserved for specific circumstances. If significant intracranial extension of the tumor occurs, then surgery is the treatment of choice to prevent involvement of the other eye. If the affected eye is proptotic and blind, then surgery is recommended for cosmetic improvement. To decrease the risk of intracranial extensions or contralateral extension, resection of the tumor and the optic nerve with no salvageable vision would be reasonable. A variety of surgical procedures, including en bloc excision of tumor with optic nerve, total excision of tumor, tumor debulking, and optic nerve sheath decompression have been described in case series reports. These procedures invariably lead to visual loss if disruption of the pial vasculature that supplies the intraorbital optic nerve is involved. Other surgical complications include bleeding, risk of infection, risks associated with anesthesia, ophthalmoplegia, and ptosis. In a retrospective study of 47 patients by Saeed et al. [27], en bloc excision of tumor resulted in no detectable recurrence, in contrast to tumor debulking, which was associated with later recurrence. Poor visual outcomes were observed after optic nerve sheath decompression, probably because the pial vasculature was disrupted. In another study in 15 eyes of 11 patients with tumors confined to the optic canal [34], however, decompression of the canal via craniotomy and without tumor resection led to long-term stable or improved vision.

In contrast to ONSMs that arise secondarily as a result of direct spread from the planum sphenoidale or tuberculum sellae into the optic canal, some meningiomas may rarely arise from extradural ectopic nests of meningeal tissue. In contrast to ONSMs, these tumors separate from the optic nerve dura and can be completely resected without damage to the optic nerve. Visual prognosis in such cases is relatively good [6, 7].

Hydroxyurea has been a chemotherapy option for patients with unresectable recurrent intracranial meningiomas [35]. It has recently been used as an alternative primary treatment for ONSM, as reported in one patient. In the study by Paus et al. [36], hydroxyurea was administered to a 46-year-old patient with primary ONSM compressing the optic nerve to cause visual acuity of 20/400. After 20 mg/kg/day oral hydroxyurea for 10 months, his visual acuity improved to 20/25. No detectable change in the size of his tumor was seen on MRI. His vision remained Stable 18 months thereafter. The side effects of oral hydroxyurea include myelosuppression, gastrointestinal symptoms, blackening of nails, skin rash, and hair loss. In patients who have progressive disease despite radiation therapy, hydroxyurea may be another treatment option. Although meningioma tumor cells have been found to have estrogen and progesterone receptors, hormonal therapy has not been successful. Chemotherapy with progesterone-receptor antagonists, such as RU-486, caused 10 % tumor shrinkage in 5 of 14 patients with unresectable meningiomas; visual fields improved in only 1 patient during follow-up of 3–31 months. Three patients experienced progression of their tumors [37].

In children, ONSMs may be more aggressive and require more frequent follow-up and neuroimaging. In a study of 88 patients with ONSMs [27], two of six children had NF-2, two of six had cafe-au-lait spots, and three of six developed intracranial extension of the tumor.

A suspected diagnosis of ONSM requires further investigation for NF-2. If NF-2 is associated with ONSM, orbital surgery is recommended when tumor progression is seen on MRI or when the affected eye develops proptosis or pain. If the ONSM presents as an isolated finding in the orbit associated with good vision, then observation for any visual or radiographic progression is recommended. Excision of the optic nerve and even the optic chiasm is preferred if intracranial involvement is documented. Postoperative visual function in these cases is usually poor. As no prior experience has been published for radiation therapy in childhood ONSM, it is not advocated in the pediatric population. Therefore, observation and surgery, when necessary, are the main management strategies for childhood ONSMs [38].

Compression of the Optic Nerve from Orbital Lesions

Graves' Ophthalmopathy and Optic Nerve Compression

Epidemiology

In a study of 120 patients (103 females) more than 15 years of age, the male incidence of thyroid ophthalmopathy was 3 in 100,000 and the female incidence was 16 in 100,000. Graves' ophthalmopathy usually presents bimodally at 20 and 60 years of age [39]. Graves' disease and thyroid ophthalmopathy are associated with HLA-DR, B8, and DW haplotypes. A familial tendency also occurs in about 30 % of patients, as shown in twin studies [40]. The strongest risk factor for the development of thyroid ophthalmopathy is hyperthyroidism. Smoking has been shown to be a risk factor for the development and progression of this disorder. Thyroid ophthalmopathy is also more severe in women and with advancing age, especially in men [41].

Symptoms and Signs

Graves' ophthalmopathy is an immune-mediated inflammatory disorder of the orbit associated with diplopia, ophthalmoparesis, and infiltration of extraocular muscles. The compressive optic neuropathy occurs in less than 5 % of patients with thyroid disease [42]. In patients with advanced thyroid ophthalmopathy who undergo orbital decompression, optic neuropathy occurs in up to 50 % of patients [43]. The likelihood of developing a compressive optic neuropathy from Graves' ophthalmopathy is most significantly correlated with the presence of extraocular motility deficits and periorbital edema at the orbital apex [43]. Unilateral congestive manifestations, such as proptosis, periorbital edema, conjunctival chemosis, and motility limitation, often precede the bilateral, symmetric, gradual visual loss. Most patients have a subtle and insidious onset of visual loss [44]. Some patients may experience more acute visual loss. Other signs of compressive optic neuropathy include afferent pupillary defect and color deficits. The most common visual field defects are central scotomas, arcuate or altitudinal defects, paracentral scotomas, and generalized constriction [45]. In a study of 36 eyes in patients with dysthyroid optic neuropathy [44], 33 % of patients had mild to marked optic disc edema with visual acuities of 20/60 or worse. Fifty percent of patients had normal optic discs and about 17 % had pale discs. Horizontal or vertical folds or striae can occasionally be seen at the posterior pole adjacent to the optic disc [46–48]. Less commonly, optic disc edema with peripapillary hemorrhages may be present in patients who experience more acute visual loss.

Thyroid ophthalmopathy is a distinct autoimmune disorder from Graves' hyperthyroidism. The severity of the ophthalmopathy does not correlate with the thyroid function or levels of thyroid-stimulating antibodies [49, 50]. Most patients develop eye symptoms within 18 months of onset of hyperthyroidism, but the ophthalmopathy can precede or follow thyroid dysfunction at any time. Thirty-five percent of patients develop thyroid ophthalmopathy more than 6 months after being diagnosed with hyperthyroidism, whereas only 7 % develop thyroid ophthalmopathy more than 6 months before having hyperthyroidism. It is estimated that about 40 % of all patients with hyperthyroidism will develop thyroid ophthalmopathy at some time [51, 52]. Furthermore, the treatment for Graves' hyperthyroidism does not seem to significantly affect the onset or course of Graves' ophthalmopathy [53].

Diagnostic Testing

Orbital CT scan usually reveals enlargement of the nontendinous portion of the extraocular muscles and can exclude tumors or other orbital pathology as a cause of exophthalmos. In addition to extraocular muscle enlargement and sparing of the tendons (Fig. 4.2), orbital CT scans can demonstrate proptosis, lacrimal gland enlargement, and eyelid soft tissue edema. Low density areas in the eye muscles could represent glycosaminoglycan deposition or fatty infiltration in more chronic cases [54]. MRI of the orbits with short tau inversion recovery (STIR) and gadolinium sequences may also demonstrate greater detail of the enlarged muscles in the apex of the

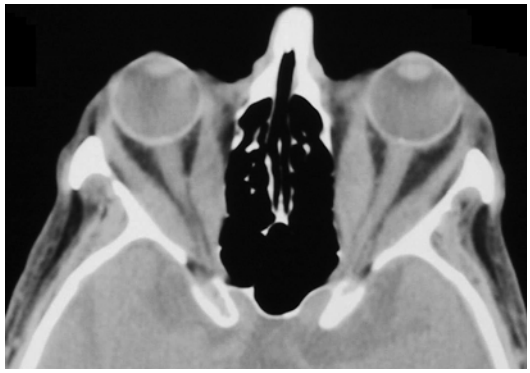

Fig. 4.2 Thyroid ophthalmopathy. Axial CT scan of orbits shows enlarged extraocular muscles with sparing of the tendons in thyroid ophthalmopathy, which distinguishes this disorder from orbital pseudotumor where the tendons are involved

orbit to mimic an orbital apex tumor, especially on axial sections. STIR sequences can detect high water content in tissues representing inflammation or active disease. The signal intensity of enlarged muscles is low on T1-weighted imaging and appears isointense to fat on T2-weighted imaging. The surrounding enlarged muscles can be seen apposing the optic nerve in the orbital apex in patients with optic neuropathy [42, 43].

Pathology

In early thyroid ophthalmopathy, the nontendinous portion of the extraocular muscles has interstitial edema and an inflammatory infiltrate, consisting of B cells more than T cells [55]. These inflammatory stimuli cause endomysial fibroblasts to produce mucopolysaccharide, such as hyaluronic acid [56]. The muscle fibers themselves later become edematous and inflamed. In later stages of severe thyroid ophthalmopathy, the fatty infiltrated and fibrosed muscle causes a restrictive myopathy. The inflammation and increase in orbital fat contribute to a mechanical compression of the optic nerve [57]. The optic nerve is not stretched, because the degree of exophthalmos is not correlated with the severity of optic neuropathy [42]. Histopathological specimens of compressed optic nerves show a decrease in neurofilaments in the axons [56] that is consistent with a compressive optic neuropathy. CT studies have shown that increased extraocular muscle volume is associated with optic neuropathy [43, 50], and improvement of the optic neuropathy appears to correlate with a decrease in extraocular muscle enlargement at the apex of the muscle cone [42].

Pathophysiology

Although activating autoantibodies to thyrotropin receptor (TSHR) are the primary cause of hyperthyroidism in Graves' disease, thyroid eye disease (TED) can present independent of Graves' disease. The level of TSHR autoantibodies correlates with the severity of TED, but there is currently no evidence that these autoantibodies cause ophthalmopathy. Other pathogenic mechanisms, such as environmental factors, and some genes, such as human leukocyte antigen (HLA), cytotoxic T-lymphocyte-antigen 4 (CTLA-4), CD40, and PTPN22, appear to be involved [58, 59].

The active phase of TED is characterized by infiltration of orbital tissues by T lymphocytes, mast cells, and B lymphocytes. It is unclear whether the primary cause of TED is antigen dependent or independent. The production of TSHR autoantibodies suggests that both humoral and cell-mediated immune mechanisms are involved [60]. Fibrocytes from the bone marrow may infiltrate orbital tissues in TED and mediate inflammation and fibrosis, whereas they are absent in healthy orbital tissues [61]. Fibrocytes demonstrate an increased expression of TSHR, comparable with the levels on thyroid epithelial cells. The binding of thyrotropin to TSHR can result in the upregulation of tumor necrosis factor alpha (TNF-α) and interleukin-6 (IL-6) cytokine production. Autoantibodies against both the TSHR and insulin-like growth factor-1 receptor (IGF-1R) [62], which are present on the cell surface of fibroblasts, are involved in the expression of inflammatory cytokines, such as CD34 and CD40 [63]. Thyrotropin receptor signaling overlaps with that of IGF-1R and together may comprise a functional complex in thyroid and orbital tissue.

Management

Corticosteroids

Visual loss from compressive optic neuropathy is an emergent ocular complication of TED.

Corticosteroids are considered the treatment of first choice. In a randomized study of 15 patients with active Graves' ophthalmopathy [64], 82 % of patients who underwent surgery did not respond because of persistent visual loss and chemosis; these patients then required further immunosuppressive therapy. Only 45 % of the patients who underwent intravenous (IV) methylprednisolone pulses for 2 weeks followed by oral prednisone for 4 months did not improve in visual acuity and needed decompressive surgery. When patients failed their initial therapy and were switched to the other treatment arm, visual acuity usually improved. In a prospective, single-blinded, randomized study of 82 patients with Graves' ophtahlmopathy [65], 87.8 % of patients who underwent orbital radiotherapy and IV corticosteroids compared to 63.4 % of patients who had orbital radiotherapy and oral corticosteroids experienced decreased proptosis. Although diplopia improved in both groups, there was no statistically significant difference between the two groups. Compressive optic neuropathy improved in 11 of 14 patients who received IV corticosteroids. The rate of side effects with IV corticosteroids was lower than that with oral corticosteroids [65, 66]. Steroid-sparing agents, such as cyclosporine, are often used for long-term immunosuppression [67]. Prospective studies are currently underway to determine the optimal dose of intravenous corticosteroids in patients with moderate-to-severe TED.

Radiation therapy

If vision improves with corticosteroids, radiation therapy may be considered as a steroid-sparing modality. A total dose of 2,000 cGy is administered in ten fractions over 2 weeks. Improvement in periorbital edema, extraocular motility, and optic neuropathy may be seen from weeks to months after the radiation treatment. Radiation therapy does not affect proptosis and does not prevent progression of the disease [53]. It has been shown that the combination of orbital radiotherapy and high-dose systemic corticosteroids provides a more favorable response in severe Graves' ophthalmopathy than orbital radiotherapy alone [65].

Surgery

When medical therapy fails, posterior orbital decompression surgery should be considered. Studies have shown that surgery involving at least two walls, the orbital floor and medial wall, or in more severe cases, three walls, the orbital floor, medial wall, and lateral wall, is effective in improving vision [68]. In a study of 48 eyes that had transantral orbital decompression after failing corticosteroids, 77 % had improved visual acuity, 17 % were stable, and 6 % worsened [69]. The most common complication is diplopia [70, 71]. In a study of 17 patients with Graves' ophthalmopathy who were not responsive to medical treatment [72], endonasal endoscopic orbital decompression improved visual acuity, decreased proptosis, and intraocular pressure. Postoperative diplopia was managed by eye muscle surgery or by application of prisms. In another study by Shepard et al. [73], endoscopic medial decompression with a lateral decompression with preservation of the medial orbital strut between the ethmoid cavity and the orbital floor could minimize the risk of diplopia.

Advancement in the knowledge of the immunopathogenesis of TED and in the development of more specifically targeted immunotherapies may lead to a paradigm shift in the conventional management of TED, as outlined above. The diagnosis and treatment of the disease in its earliest stages may alter the course of the disease. Antioxidants, anticytokines, T-cell depletion therapies, B-cell depletion therapies, and anti-IGF-1R antibodies are possible treatments to be considered for earlier treatment to delay the course of TED and to prevent complications, such as compressive optic neuropathy.

Antioxidants

In a randomized, double-blinded, placebo-controlled study of 159 patients with mild Graves' orbitopathy, a comparison of the effects of antioxidant therapy, anti-inflammatory therapy, and placebo was studied. Oxygen free radicals and cytokines play a pathogenic role in Graves' orbitopathy. Selenium (100 μg twice daily), pentoxifylline (600 mg twice daily), or placebo (twice daily) was given to patients over a 6-month period.

Selenium significantly improved mild TED in terms of quality of life outcome measures, reduced progression of the orbital inflammation, and improvement in clinical activity score (CAS). These clinical improvements were sustained after 1 year of follow-up [74].

Anticytokine Therapies

Anticytokine therapies against TNF-α, such as etanercept and infliximab, have short-term effectiveness in TED patients, as shown in several case reports [75, 76]. No randomized, double-blinded, placebo-controlled trials have yet been performed. The side effects of infection and neoplasm must be considered in these therapies. Other anticytokine therapies, including IL-6 receptor (IL-6) blockers and IL-1 inhibitors have been shown to be beneficial in rheumatoid arthritis (RA) and other autoimmune disorders, but these agents have not yet been studied in TED patients [77, 78].

T-cell Depletion Therapies

T-cell depletion is a potential treatment strategy for TED. Anti-CD3 antibodies binding to the T-cell receptor (TCR) complex have been used to downregulate pathogenic CD4+ T-cell activity in type 1 diabetes mellitus [79]. CTLA-4 is a regulator of T-lymphocyte activation, which inhibits T-cell responses. Antibodies against CTLA-4 may interrupt T-cell activation by blocking its interaction with CD80 and CD86 on antigen-presenting cells. This treatment has been promising in autoimmune disorders, such as RA and MS [80, 81]. Other potential therapeutic targets of T-cell activation, which have not yet been explored in TED patients include the CD40-CD40L, CD80, and CD86 pathways.

B-Cell Depletion Therapies

Rituximab (RTX) is an anti-CD 20 chimeric humanized monoclonal antibody that depletes mature B cells. Plasma cells are not directly affected by RTX since they do not express CD20. This depletion of B cells in TED may subsequently alter antigen presentation and cytokine production. In addition, studies have shown that B cell-deficient mice are unable to generate T cell responses following immunization with TSHR, indicating their critical role in the initiation of autoimmune thyroid disease [82, 83]. Although plasma cells and antibody production are not directly affected, antibody-mediated responses are decreased by blocking cytokine production and antigen presentation.

In a study of ten patients with Graves' orbitopathy [84], RTX was administered twice intravenously at 1,000 mg on days 1, 15, and 20 with methylprednisolone, administered weekly intravenously at 500 mg for 16 weeks. Rituxan had no significant effect on thyroid autoantibodies. The production of IL-6 and its soluble receptor (sIL-6R) was unchanged in response to RTX. Rituxan may exert its effect on TED by inhibiting B cell antigen presentation rather than affecting humorally or cytokine-mediated responses.

In a retrospective, interventional case series of six patients [85] with severe, progressive Graves' orbitopathy unresponsive to corticosteroids, rapid and sustained resolution of orbital inflammation and dysthyroid optic neuropathy followed treatment with RTX. Proptosis and strabismus did not improve.

In a study of nine patients [86] with active TED treated with RTX, CAS scores significantly improved. Response to this therapy was related to initial peripheral B-cell depletion. No recurrence of disease was noted at 1 year follow-up, despite return of peripheral B-cell levels after 4–5 months.

In a prospective, open-label study of 12 patients [87] with TED and CAS of 4 or greater, rituximab (1,000 mg) was administered on days 1 and 15. After follow-up over 1 year, these patients had significantly reduced CAS scores that appeared to be associated with rituximab infusion. The variable natural history of TED makes it difficult to assess the intrinsic efficacy of rituximab. Further investigation of rituximab for TED in a larger controlled clinical trial is needed.

Idiopathic Orbital Inflammatory Pseudotumor

Epidemiology

Idiopathic orbital inflammatory pseudotumor may also cause compression of the proximal

optic nerve and secondary optic disc edema. It is a nongranulomatous process limited to the orbit with no identifiable cause. Its incidence is approximately 9 % of all orbital mass lesions. There is no sexual predilection, but it often occurs between 40 and 60 years of age [88].

Symptoms and Signs

Acute, recurrent, or chronic orbital pain; conjunctival redness; diplopia; and decreased vision are the most common symptoms. In contrast to thyroid ophthalmopathy, pain in idiopathic orbital pseudotumor is often unilateral and is more acute and worsens with eye movements. Patients usually present with signs of unilateral proptosis, ptosis, ocular motility deficits in the field of the inflamed muscle, and good vision. If the inflammation worsens, then a compressive optic neuropathy may develop and manifest as decreased visual acuity, visual field defects, afferent pupillary defect, color deficits, and optic disc edema [88]. In contrast, eyelid retraction and restrictive eye movements with impaired vision are more often seen in thyroid ophthalmopathy [52].

Diagnostic Testing

To screen for inflammatory/autoimmune systemic disorders that may cause orbital inflammatory pseudotumor, serum syphilis serology, antinuclear antibody, angiotensin-converting enzyme (ACE), antineutrophilic cytoplasmic antibody levels, and a chest X-ray should be performed. Orbital CT scan commonly reveals a thickened posterior sclera, uvea, and lacrimal gland [88]. The extraocular muscles and tendons are also enlarged (Fig. 4.3). Perioptic infiltration leads to optic nerve sheath enlargement. Inflammatory infiltrates also extend into the orbital fat. Because orbital inflammatory pseudotumor may involve single or multiple muscles and may be well circumscribed, it can mimic an orbital tumor [89]. On MRI, orbital inflammatory pseudotumor is often isointense to muscle on T1-weighted images and isointense to orbital fat on T2-weighted images [90]. If the orbital inflammation occurs in a patient who has a history of malignancy or if it is recurrent or atypical in appearance, then a biopsy should be considered for definitive diagnosis. Otherwise, the diagnosis of idiopathic orbital inflammatory pseudotumor is one of exclusion [89].

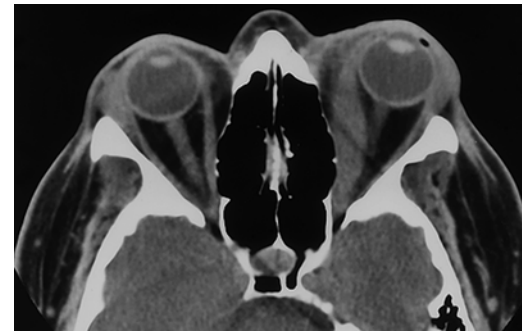

Fig. 4.3 Orbital inflammatory pseudotumor. Axial CT scan of orbits shows orbital inflammatory pseudotumor. The left medial rectus muscle is enlarged with involvement of its tendon

Histopathology

The inflammation is often localized to the ocular muscles, lacrimal glands, and orbital vessels. Idiopathic orbital inflammatory pseudotumor can be quite variable in presentation, either with numerous types of cells or with predominantly collagen and a few cells. The major hallmark features include the following: (1) cellular polymorphism, consisting of lymphocytes, plasma cells, histiocytes, and eosinophils; (2) lymphoid follicles with germinal centers; (3) absence of atypia; and (4) ancillary evidence of inflammation, such as plasmacytoid cells and capillary proliferation with swollen, enlarged endothelial cells [88].

Management

Prednisone 80–100 mg daily is the initial treatment of choice. If vision does not respond or if the inflammatory pseudotumor recurs during taper, low-dose radiation may then be administered [88]. In contrast to thyroid ophthalmopathy, which may respond to steroids slowly, idiopathic orbital pseudotumor responds immediately and resolves completely. In patients who are refractory to corticosteroids and who do not have other identifiable disorder, cyclophosphamide or cyclosporine may be used as adjunctive therapy. Orbital radiation therapy may also be considered as an alternative treatment.

Sellar and Suprasellar Compressive Lesions on Optic Nerve and Chiasm

See Table 4.1 [91].

Pituitary Adenoma

Epidemiology

Of all the masses that present within the pituitary sella, pituitary adenomas are the most common type of tumors, which may account for 10–20 % of all intracranial tumors [91]. There is no sexual predilection, but they are most common in adults during 30–40 years of age. These tumors are not hereditary, for they are associated with multiple endocrine adenomatosis, an autosomal dominant disorder.

Symptoms and Signs

Bilateral visual field defects, especially bitemporal ones, are the hallmark of a chiasmal lesion, such as a pituitary adenoma. The pituitary adenoma can compress the distal optic nerve on one side near its junction with the optic chiasm and also compress the inferior nasal fibers from the contralateral eye before continuing posteriorly into the chiasm. This type of structural compression produces an anterior chiasmal syndrome or distal optic nerve syndrome. Damage to the distal optic nerve causes an ipsilateral decrease in visual acuity with a color defect, relative afferent pupillary defect, and possible temporal field loss. Eventually the optic disc becomes pale. Damage to the contralateral inferior nasal fibers causes a superior temporal field defect without evidence of an optic neuropathy. Rarely does a pituitary adenoma compress a postfixed chiasm to cause monocular visual loss. The decreased central visual acuity is often associated with central or arcuate scotomas [92, 93].

Neuroimaging

MRI of the brain allows visualization of tumors up to less than 1.0 cm in diameter. Pituitary adenomas can invade the dura or bone and may infiltrate surrounding structures. Locally invasive pituitary adenomas are often histologically benign. Macroadenomas, defined as greater than 1.0 cm in diameter, are usually the type that grows large enough to affect the visual pathways (Fig. 4.4). These benign tumors may extend superiorly to contact and/or compress the optic chiasm. Compression of the chiasm inferiorly results in bilateral superior temporal quadrantanopsia. As the tumor enlarges, the field defect progresses to a complete bitemporal hemianopsia.

Table 4.1 Types of sellar and suprasellar compressive lesions in relation to age [Reprinted from Richardson GS. Pituitary tumors. In: Samuels MA, Feske SK, editors. Office practice of neurology. Philadelphia: Churchill Livingstone; 2003:1060–1067. With permission from Elsevier]

Age group	More common	Less common
Pediatric to young adult	• Chiasmal-hypothalamic glioma	• Arachnoid cyst
	• Craniopharyngioma	• Arteriovenous malformation
		• Dermoid cyst
		• Empty sella syndrome
		• Ganglioglioma
		• Germ cell tumors
		• Pituitary adenoma
		• Rathke's cyst
Middle-aged to older adult	• Aneurysm (internal carotid)	• Malignant optic glioma
	• Craniopharyngioma	• Metastases to chiasm, sella, or suprasellar region
	• Meningioma	• Spheno-ethmoidal mucocele
	• Pituitary adenoma	
	• Pituitary apoplexy	

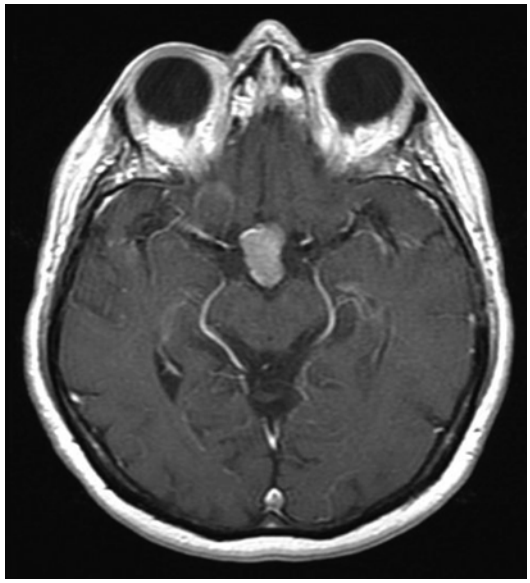

Fig. 4.4 Axial contrast-enhanced T1-weighted MRI of the brain revealed pituitary adenoma

If the optic chiasm is prefixed, pituitary tumors compress the optic tract and posterior chiasm. If the optic chiasm is postfixed, pituitary tumors affect the optic nerve and anterior chiasm [94, 95].

In a study of 27 patients with pituitary macroadenomas [96], 9 patients demonstrated unilateral optic nerve hyperintensity lesions on T2-weighted MRI, whereas 5 patients revealed bilateral signal intensity abnormality of the optic nerve at the site of compression and in the ventral aspect of the tumor. Abnormal hyperintensity of the optic nerves ventral to the pituitary macroadenoma was associated with the degree of visual acuity impairment. Recovery of visual acuity was also correlated to disease duration. MRI of the optic nerves may play a role in monitoring and managing visual outcome.

Pathology

Pituitary adenomas can be either secretory or nonsecretory. Null cell adenomas or nonsecreting adenomas are more common and demonstrate no clinical or immunohistochemical evidence of hormone secretion. Secretory adenomas are less common and produce one or more anterior pituitary hormones, including prolactin, growth hormone, adrenocorticopic hormone, follicle-stimulating hormone, or luteinizing hormone. Pituitary carcinomas are exceedingly rare and usually require distant metastases to establish this diagnosis [91].

On histology, pituitary adenomas appear as a sheet of follicular, trabecular, or cystic components with foci of hemorrhage or necrosis, but no mitoses. The tumor has a pseudocapsule that facilitates surgical separation from the adjacent normal gland [91].

Management

The most commonly used medical therapy is oral dopamine (D2) receptor agonists, such as bromocriptine, cabergoline, and quinagolide, in managing prolactinomas. These medications limit prolactin secretion and reduce prolactinoma size. Reduction of tumor size and improvement of visual fields may occur within hours of starting treatment, but poor response to this treatment requires surgical resection. In macroprolactinomas that are greater than 10 mm in diameter, bromocriptine has been reported to maintain remission for 5 years in 5–15 % of patients. Cabergoline and quinagolide have fewer side effects than bromocriptine, which can cause nausea and orthostatic hypotension. In microprolactinomas that are less than 10 mm in diameter, the use of D2 agonists has been controversial because their natural history is still incompletely defined [91].

If the tumor is not a prolactinoma, then surgery would be the initial treatment of choice for pituitary adenomas. According to a study on 53 patients who underwent transphenoidal surgery, visual field defects improved in 89 % of the patients and visual acuity improved in 82 % [96]. In a retrospective analysis of 35 patients by Randeva et al. [97], transphenoidal surgery for pituitary apoplexy resulted in significantly greater improvement in visual acuity and fields when it was performed within 8 days compared to surgery after this time period. In a report of 15 patients by McFadzean et al. [98], high-dose steroids along with radiotherapy followed by surgical resection resulted in postoperative visual acuity improvement in 10 of 15 patients; only 2 were unchanged.

Radiotherapy is an alternative when surgery is not an appropriate initial step. Postoperative radiation is used for certain tumor histologies for which remission and recurrence rates after operative resection can be reduced with combined therapy. Although postoperative radiation is still used to treat residual tumor after resection of pituitary adenoma, it is no longer routinely given to patients after resection of nonsecretory adenomas or to those in whom endocrine measures are normal. The improved resolution on MRI and newer endocrine measures allow a more expectant management approach in which radiation is reserved for patients with evidence of tumor growth or endocrinologic evidence of recurrent hypersecretion [91].

Pituitary Apoplexy

Epidemiology

The incidence of pituitary apoplexy ranges from 5 to 16.6 % in patients with a preexisting pituitary adenoma. It affects males to females in a ratio of about 1–9 [99].

Symptoms and Signs

Pituitary apoplexy, infarction, and hemorrhage of the pituitary gland is a neuro-ophthalmic emergency. Pituitary apoplexy is characterized by sudden onset of severe headaches with vomiting, other signs of meningeal irritation, and visual loss. In studies by Muller-Jensen and Ludecke [99] and Ahmed et al. [100], a decrease in visual acuity and central scotoma, affecting one eye more than the other, was commonly seen. The classical bitemporal field defect was absent in 50 % of those with perimetry. Compressive ischemic damage from the preexisting tumor can occur in the intracranial portions of the optic nerves, the optic chiasm, and the optic tracts [94]. Third nerve palsies as part of an external ophthalmoplegia occur in more than 50 % of patients as a consequence of compressive ischemia from tumor or hemorrhage in the cavernous sinus, subarachnoid space, or brainstem [101].

Pathogenesis

The high metabolic demand of the normal pituitary gland, along with the tenuous blood supply through a portal (double-capillary) vascular system, predisposes the gland to infarction in situations where the blood supply is compromised. Pituitary apoplexy may occur in the setting of pituitary tumor growth, leading to high metabolic demand and increased pressure within the sella, causing a critical reduction in blood flow. Apoplexy may also occur in pregnant women at the time of delivery (Sheehan's syndrome). The physiological hypertrophy of the gland associated with pregnancy produces predisposing conditions analogous to those seen with pituitary tumors. At delivery, transient hypotension may precipitate the crisis, resulting in infarction. With a normal gland and no erosion in the sella, the neuro-ophthalmic manifestations, other than a headache, may be subtle or absent, and Sheehan's syndrome may be unrecognized until hypopituitarism becomes evident after delivery with failure of lactation or postpartum amenorrhea [91].

Neuroimaging

MRI is more sensitive than CT in detecting pituitary apoplexy. MRI reveals a macroadenoma with heterogeneous signals representing hemorrhage (Fig. 4.5) whereas routine CT shows an unenhancing, hyperdense sellar mass. Lumbar puncture should also be performed to rule out subarachnoid hemorrhage. If cerebrospinal fluid (CSF) red blood cells are present, a cerebral angiogram should be done to screen for a ruptured aneurysm in the sellar region if the CT and MRI results are inconclusive [91].

Treatment

Because most patients have hypopituitarism, high-dose corticosteroids should be administered. The patient needs to be stabilized with appropriate hormonal replacement therapy by an endocrinologist and then needs to be evaluated for transphenoidal tumor Resection [98]. Although some patients spontaneously improve, those who undergo surgery within 1 week usually experience improvement in their visual acuity, visual fields, and ocular motility problems.

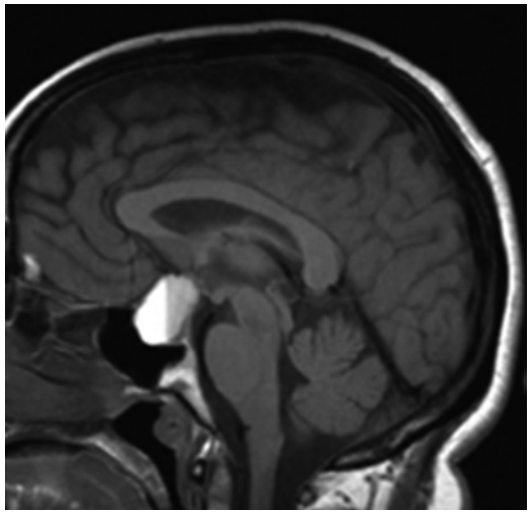

Fig. 4.5 Pituitary apoplexy. Sagittal T1 weighted MRI of brain without contrast shows pituitary apoplexy. Note the fluid level within the tumor indicative of the apoplectic tumor

Suprasellar Meningioma

Epidemiology

Suprasellar meningiomas represent 3–10 % of all meningiomas [102]. Women are more commonly affected than men, and most patients are between 30 and 60 years of age [102].

Symptoms and Signs

Most patients present with suprasellar meningiomas present with painless, asymmetric progressive loss of visual acuity [102]. These tumors tend to cause asymmetric compression of the optic nerves [103]. Some patients may present with unilateral visual symptoms representing an optic neuropathy but actually also have a milder contralateral optic neuropathy with only signs of slightly decreased visual acuity, decreased color vision, and visual field defects [104].

Visual field defects may include arcuate defects, altitudinal defects, central scotomas, and peripheral constriction [104]. Less often seen is the distal optic nerve syndrome in which the patient has unilateral visual loss and a junctional scotoma, a superior temporal field defect in the contralateral, asymptomatic eye [103]. In patients with postfixed optic chiasms, suprasellar meningiomas may grow between the optic nerves to compress them against the internal carotid arteries [105]. Compression of the temporal fibers of the intracranial areas of both optic nerves results in binasal visual field defects. If the optic chiasm is compressed, asymmetric bitemporal visual field defects usually occur. When suprasellar meningiomas extend posteriorly or when the optic chiasm is prefixed, damage to the optic tract results in a homonymous hemianopia. A pure optic tract syndrome is very rare, and the optic tract lesion is often associated with an additional optic neuropathy. Optic disc swelling, as part of a Foster-Kennedy syndrome or a cavernous sinus syndrome, is seen more commonly in suprasellar meningiomas that arise from the anterior clinoid process [103].

On funduscopic examination, optic atrophy is often seen. Sometimes optic nerves may appear normal. Based on the study of 18 patients by Chicani and Miller [106], 17 % of patients had normal optic discs, 39 % had bilateral optic disc pallor, and 44 % had one normal disc and one pale disc. If suprasellar meningiomas become large to produce increased intracranial pressure, then papilledema may develop with unilateral or bilateral sixth nerve palsies.

Neuroimaging

The MRI features of a suprasellar meningioma include the suprasellar epicenter, tapered dural base, and bright enhancement with gadolinium that differentiates it from a pituitary adenoma. Magnetic resonance angiography (MRA) or cerebral angiography often reveals a tumor blush that is characteristic of a meningioma, but this may also occur in pituitary adenomas [107].

Pathology

Suprasellar meningiomas often arise from arachnoid granulations overlying the dura of the tuberculum sellae and continue to compress and displace, rather than invade adjacent brain. Some can also arise from the diaphragma sellae [108, 109]. Meningiomas from the tuberculum sellae and diaphragma sellae are located in the retrochiasmatic region and can grow to compress the visual pathways [88]. Meningiomas are

commonly a combination of the transitional form, composed of whorls and psammoma bodies, and the syncytial type, composed of sheets of polygonal cells. The fibroblastic type of meningioma consists of spindle cells with collagen. The more aggressive variants include the papillary, angioblastic, and anaplastic types [110].

Course and Visual Prognosis

The visual prognosis in patients with suprasellar meningiomas is influenced by the duration of visual symptoms before tumor resection, tumor size, and preoperative visual function. In a recent study of 18 patients with suprasellar meningiomas, Chicani and Miller [106] showed that about 80 % of eyes in patients treated within 1 year of onset of symptoms improved or remained stable after surgery, whereas 70 % of eyes in patients treated more than 1 year after symptom onset either worsened or remained stable. After 10 years or more of postoperative follow-up, 72 % of patients had visual acuity of 20/40 or better in at least one eye. Previous studies, such as those of Gregorious et al. [111] and Rosenberg and Miller [104], have shown that a shorter duration of visual symptoms is associated with better preoperative visual function and smaller tumor size. Tumors restricted to the tuberculum sellae had a better outcome than those that extended to other areas. The average postoperative mortality in most reported series of suprasellar meningiomas was 10 % [104].

Management

The treatment of choice for suprasellar meningiomas, regardless of size, is surgical resection, but recurrence is common even after total tumor removal and after 10 years or more. The recurrence rates for suprasellar meningiomas range from 5 % to greater than 30 % [112–116]. Radiation therapy, such as three-dimensional conformal fractionated radiation therapy and stereotactic radiosurgery, should be started shortly after surgery to attain the best visual outcome [117–121]. It has been recommended that postoperative patients with complete resection still be monitored on a long-term basis with serial eye examinations and neuroimaging for any recurrences to allow the opportunity for early and aggressive treatment. Patients with incomplete resection of their suprasellar meningiomas should undergo postoperative radiation therapy [106].

In older patients with minimal visual loss over a long period of time, observation may be appropriate because meningiomas are benign and slow growing. Chemotherapy with progesterone-receptor antagonists, such as RU-486, and interferon-alpha has been unsuccessful in the past. For malignant meningiomas, novel angiogenesis inhibitors are being studied [122].

Craniopharyngioma

Epidemiology

Craniopharyngiomas are suprasellar tumors that commonly manifest in childhood. Craniopharyngiomas are the most common brain tumors of nonglial origin in children, representing about 3–6 % of all childhood tumors. The age of incidence is bimodal, occurring more commonly in patients less than 18 years of age and less often between 50 and 70 years [126].

Symptoms and Signs

Children and adolescents often develop symptoms and signs of increased intracranial pressure and hypothalamic-pituitary defects, such as growth failure, obesity, diabetes insipidus, slow sexual development, heat dysregulation, spontaneous pain, and vasomotor disturbances [127]. Most develop visual loss and may not be detected until they have secondary strabismus or other symptoms [128].

Adults with craniopharyngiomas develop gradual progressive visual loss and mental status changes [129]. In a retrospective study of 74 patients by Baskin and Wilson [129], 88 % of men over 18 years of age presented with impotence and 82 % of women over 18 years of age presented with either primary or secondary amenorrhea, often with galactorrhea. Compression of the tumor onto the hypothalamus or pituitary stalk most commonly leads to deficiencies in growth hormone, gonadotropin, cortisol, and thyroid-stimulating hormone and in elevated serum prolactin levels [130, 131].

Most patients with craniopharyngiomas develop visual field defects. In the series by Baskin

and Wilson, 72 % had field defects, including bitemporal hemianopia, homonymous hemianopia, and bilateral optic nerve defects [129]. Similar to other suprasellar tumors, craniopharyngiomas cause progressive unilateral or bilateral decrease in visual acuity associated with other evidence of optic neuropathy. The visual field defects are variable and may include central scotomas, cecocentral scotomas, paracentral scotomas, arcuate scotomas, and nasal or binasal defects [132]. If the tumor is compressing the optic nerves from below or from either side in a patient with a postfixed chiasm, then a unilateral or bilateral optic neuropathy develops. A "junctional or anterior chiasmal syndrome" is occasionally formed by a unilateral distal optic neuropathy associated with a superior temporal field defect in the asymptomatic contralateral eye. Bitemporal field defects occur in 25–50 % of patients with craniopharyngiomas from compression of the optic chiasm [108]. These field defects may occur with normal visual function or decreased visual acuity and color vision. If the tumor compresses the optic tract, an incomplete and incongruous homonymous hemianopia may be seen [129].

At the time of diagnosis, the fundus may be normal. As the tumor directly compresses the anterior visual system or displaces the nerves against the internal carotid or anterior cerebral arteries, optic atrophy gradually develops. Papilledema is most often seen in children and adolescents when the tumor has extended into the third ventricle [133].

Ocular motility deficits may appear when craniopharyngiomas cause increased intracranial pressure and compress the subarachnoid portions of the nerves or the brainstem [134]. Seesaw nystagmus is probably a result of compression of the mesencephalon, especially the nucleus of Cajal or its connections [135].

Neuroimaging

CT scans typically show a cystic-appearing lobulated suprasellar mass with a solid mural nodule. Nodular or rim calcification is seen in almost all children with craniopharyngiomas and in about half of all adults. Cystic contents are usually higher in attenuation than the CSF. With contrast administration, nodular or rim enhancement is usually present. The MRI signal characteristics of craniopharyngiomas vary depending on the tumor composition of cystic and solid components. MRI of the brain usually reveals a cyst that is hypointense on T1- and hyperintense on T2-weighted sequences. The increased signal intensity on T1-weighted images represents high protein concentration and/or degraded blood products. With contrast administration, craniopharyngiomas enhance heterogeneously [136]. An MRI with sagittal views and a CT with coronal views should be done for optimal imaging before surgery.

Pathology

Craniopharyngiomas are cystic, calcified benign tumors and are thought to arise from the vestigial nests of squamous cells that are often found at the junction of the lower infundibular stem and the pars distalis of the adenohypophysis. The failure of complete involution of the hypophyseal pharyngeal duct tract leads to the development of the craniopharyngioma [137]. The tumors vary from small, solid, well-circumscribed nodules to large multinodular cysts that invade the sella turcica and displace adjacent brain structures. The cysts are filled with a turbid fluid containing cholesterin crystals. The three histological types of craniopharyngioma are (1) mucoid epithelial cysts lined with ciliated columnar and mucus-secreting cells, (2) squamous epitheliomas consisting of islands of squamous epithelium with cystic degeneration (Fig. 4.6), and (3) adamentinomas consisting of epithelial masses forming a reticulum of teeth-like structures [138].

Management

Patients usually undergo primary total resection or limited surgery of the tumor followed by radiation therapy. Postoperative damage to the optic chiasm, vasculature, and hypothalamus appears to be higher in patients undergoing total resection. Patients undergoing incomplete resection of the tumor followed by radiation therapy often have better survival rates and lower rates of endocrine deficits and neovascular and hypothalamic injury [139]. Tumor recurrence is usually treated with radiation therapy because further surgery is associated with tumor spread and recurrence and increased morbidity

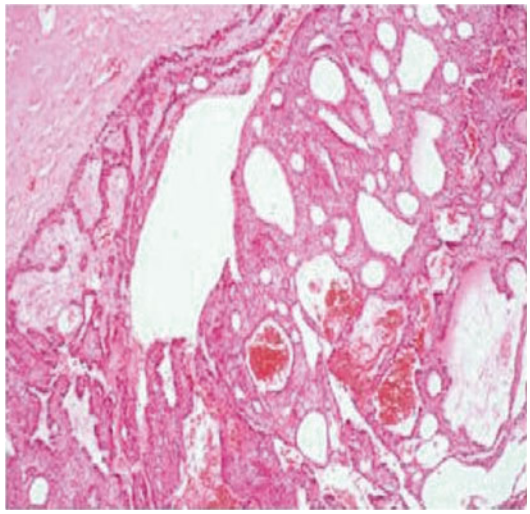

Fig. 4.6 H&E stain showing nests of squamous cells merging into columnar cells surrounding cystic spaces (magnification 10×) [Courtesy of Mitch A. Cohn]

and mortality. Radiation optic neuropathy and cerebral radionecrosis and other complications are becoming more rare because of three-dimensional conformal radiation therapy, stereotactic radiosurgery, stereotactic radiotherapy, and intensity modulated radiation therapy [139].

Postoperative visual prognosis for patients with craniopharyngioma depends mostly on the severity of visual damage that has occurred before treatment and the extent of manipulation of the optic nerves and chiasm at the time of surgery. In the study of 22 patients with resected craniopharyngiomas [140], children (50 %) more often presented with optic atrophy than adults (30 %). Visual loss may be difficult to detect in children until severe stages. Postoperative visual acuity was 20/40 or better in 67 % and worse than 20/40 in 33 %.

Sphenoid Wing Meningioma

Epidemiology

Meningiomas en plaque of the sphenoid wing constitutes about 4 % of all meningiomas [123]. They affect women three to six times more often than men during the ages of 40–50 years [123].

Symptoms and Signs

Slow tumor infiltration of the orbit causes a slowly progressive unilateral proptosis as the most common initial symptom, but optic neuropathy is the most common cranial nerve palsy [124].

Vision is correlated with the location of the tumor in which intraconal or extraconal involvement is associated with worse visual acuity. Optic nerve compression usually occurs late and is related to compression of the orbital portion of the optic nerve. In a retrospective study of 67 patients with meningiomas en plaque originating from the sphenoid wing [125], 28 presented with decreased visual acuity, 7 with blindness, and 24 with visual field defects. Temporal hemianopias, superior temporal defects, and inferior temporal defects were most common. Other less common defects included central scotomas, peripheral constriction, and superior nasal defects. Optic disc pallor was seen in ten patients, and disc edema was observed in three patients.

Neuroimaging

This slow-growing tumor infiltrates the sphenoid bone and the dura. The hyperostosis of the sphenoid wing and optic canal is best seen on high-resolution CT scan. MRI scan demonstrates the extent of infiltration of the dura mater and intracranial extension (Fig. 4.7) [122].

Pathology

(Please see section "Pathology" in section "Suprasellar Meningioma".)

Management

The treatment for sphenoid wing meningiomas is early surgical resection to prevent recurrence. Aggressive resection of the cavernous sinus and superior orbital fissure infiltrated by tumor is not recommended because of the high risk of morbidity. Radiation therapy is reserved for recurrences or subtotal resections. As recurrence rates range between 4 and 20 % in patients with complete excision and up to 50 % in those with subtotal resection, long-term monitoring of this tumor is needed over a 10- to 20-year period [125].

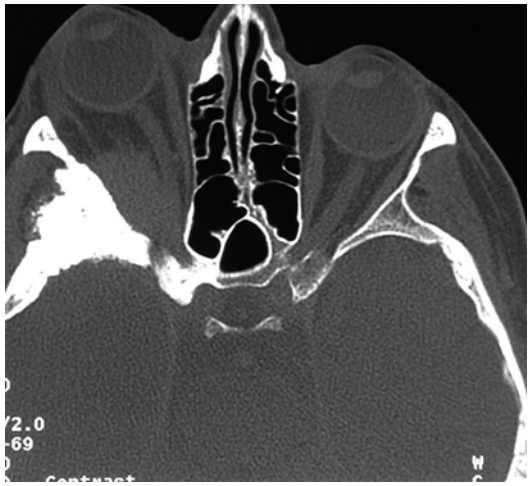

Fig. 4.7 Sphenoid wing meningioma. Orbital CT reveals displacement and compression of the posterior intraorbital and intracannalicular segments of the right optic nerve by a sphenoid meningioma with a significant intraosseous component [Reprinted from Acheson JF. Optic nerve disorders: role of canal and nerve sheath decompression surgery. Eye (Lond). 2004 Nov;18(11):1169–74. With permission from Nature Publishing Group]

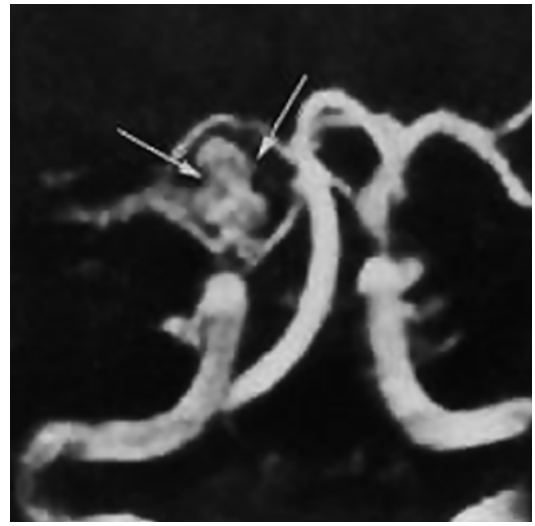

Fig. 4.8 Anterior communicating artery aneurysm. Coronal reformatted images from a CT cerebral angiogram demonstrates a 5 mm aneurysm (*straight arrow*) of the anterior communicating artery (*arrowhead*) that points anteriosuperiorly [Courtesy of J.A. Hirsch]

Internal Carotid or Anterior Communicating Artery Aneurysm

Internal carotid aneurysms can compress the intracranial portion of the optic nerve to cause a gradually progressive unilateral or bilateral optic neuropathy. It may present as an "unexplained" optic neuropathy in some cases. Visual acuity decreases very slowly. Visual field defects reflecting nerve fiber bundle defects are most common. In 25 % of patients, a central scotoma or absolute central visual field is seen. Affected optic discs are excavated, mimicking glaucomatous change. A coronal MRI scan can help confirm compression of the affected optic nerve [141].

Almost one-third of all intracranial aneurysms are located at the anterior communicating artery and present with subarachnoid hemorrhage. Unruptured aneurysms may cause slowly progressive or sudden onset visual loss associated with headache or ocular pain. The midline location of the anterior communicating artery may cause compression of one or both optic nerves, in addition to the optic chiasm and optic tract [142–145]. Local compression of the optic nerves is uncommon, but 6 of 78 patients with anterior communicating aneurysms had signs of optic neuropathy [146]. In a study by Peiris and Ross Russell [147], an unruptured anterior communicating artery aneurysm produced a unilateral optic neuropathy in two of five patients, a bilateral optic neuropathy in the third patient, a unilateral optic neuropathy with a chiasmal syndrome in the fourth patient, and a unilateral optic neuropathy and optic tract syndrome in the last patient. Anterior communicating artery aneurysms (Fig. 4.8) can present as a progressive bilateral optic neuropathy or as a sudden unilateral optic neuropathy [148]. Based on pathological studies by Chan et al. [149], leakage of the anterior communicating artery aneurysm into the optic nerve parenchyma can lead to acute monocular visual loss.

Carotid-Ophthalmic Artery Aneurysm

Most carotid-ophthalmic artery aneurysms arise from the junction of the internal carotid artery and ophthalmic arteries and rarely from the distal

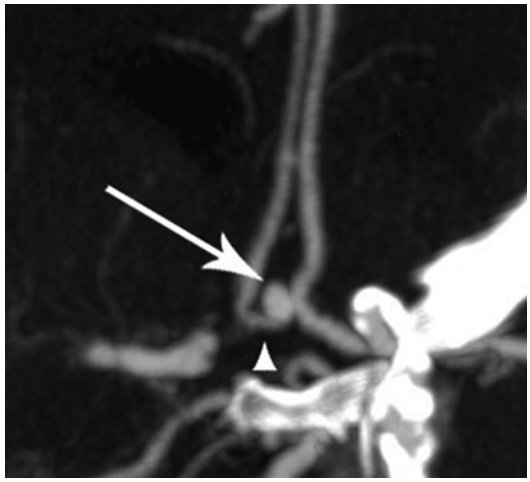

Fig. 4.9 Ophthalmic artery aneurysm. MR cerebral angiography reveals an aneurysm (*arrow*) arising from the internal carotid artery at the site of origin of the ophthalmic artery [Reprinted from Dutton, JJ. CT and MR Imaging of Visual System Lesions. In: Dutton, JJ. Radiology of the Orbit and Visual Pathways. New York NY: Elsevier; 2011: 46–54. With permission from Elsevier]

portion of the ophthalmic artery itself [149, 150]. Aneurysms that are located intracranially, or in the intraorbital area of the vessel, may enlarge the optic canal to cause ipsilateral compressive optic neuropathy [151]. Most patients present with gradual progressive unilateral visual acuity and visual field loss. Aneurysms that arise within the orbit may be asymptomatic [152] or may compress the adjacent optic nerve to cause sudden, fluctuating, or progressive visual loss. Rarely are acute monocular visual loss and proptosis seen from orbital hemorrhage [153]. Direct penetration of the optic nerve by a carotid-ophthalmic artery aneurysm has been documented on MRI [154]. Cerebral angiography revealed the aneurysm to be 12 mm x 7 mm directed superomedially into the optic nerve. Even splitting of the optic nerve has been reported [155].

Aneurysms of the ophthalmic artery itself are very rare (Fig. 4.9). In a report by Yanaka et al. [156], a ruptured ophthalmic artery aneurysm caused only headache [156], while an unruptured one completely penetrated the optic chiasm to cause rapid visual loss to count fingers and a nasal hemianopsia in the left eye and an upper temporal quadrant hemianopsia in the right eye. Intraoperative findings revealed complete penetration of the optic chiasm by the fundus of the aneurysm. The patient recovered his visual acuity, but visual deficits persisted [157].

Sphenoid Sinus Mucocele

Patients with sphenoid sinus mucoceles often present with fronto-orbital pain, visual loss, and cranial nerve palsies involving III or VI [158–161]. Most patients with sphenoid sinus mucoceles develop slowly progressive cranial neuropathies. When the lesion compresses one or both optic nerves, patients may have slowly progressive visual loss [158, 162–164]. Occasionally sudden visual acuity and visual field loss can occur mimicking retrobulbar optic neuritis, especially when the patient has associated ocular pain and no evidence of an orbital mass on neuroimaging studies [163, 165–167].

On neuroimaging, the sphenoid sinus mucocele appears as a cystic lesion of high intensity in the sphenoid sinus. Compression of the optic nerve may be seen as a ring of hyperintensity on STIR images, demonstrating possible CSF in the dilated perioptic subarachnoid space or compressive edema. This ring of hyperintensity usually disappears after surgical decompression of the mucocele [167]. On CT, sphenoid sinus mucoceles appear as a homogeneous space-occupying lesion in the sphenoid sinus (Fig. 4.10).

Sphenoid sinus mucoceles may expand to displace one or both optic nerves or the optic chiasm, in addition to displacing the cavernous portion of the internal carotid artery, the planum sphenoidal, and pituitary gland; eroding the clivus and spread to the superior orbital fissure and invading the posterior orbit [168]. The mucocele may involve the orbit to cause an acute restrictive ophthalmoplegia and even proptosis [169].

Prompt transphenoidal microsurgical decompression of the sphenoid sinus mucocele and antibiotic therapy are necessary to recover good vision [169]. If surgery is delayed more than 7–10 days, the visual prognosis becomes poor [170].

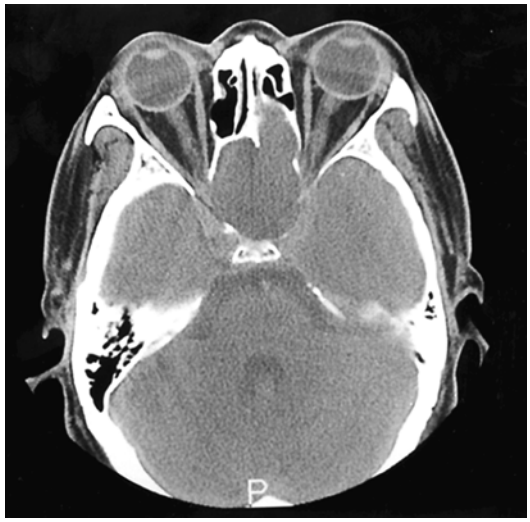

Fig. 4.10 Sphenoid sinus mucocele. Axial CT of the orbits reveals a homogeneous space-occupying lesion in the sphenoid sinus (sphenoid sinus mucocele) [Reprinted from Hiratsuka Y, Hotta Y, Yui A, Nakayasu K, Kanai A. Rhinogenic optic neuropathy caused bilateral loss of light perception. Br J Ophthalmol 1998;82(1):99–100. With permission from BMJ Publishing Group Ltd]

Fibrous Dysplasia

Epidemiology

Fibrous dysplasia is a nonhereditary, nonmalignant skeletal developmental anomaly of the bone-forming mesenchyme that manifests as a defect in osteoblastic differentiation and maturation. The exact incidence of this bone disorder is unknown. It manifests most often between 3 and 15 years of age. Between 10 and 50 % of patients have the craniofacial form in which abnormal bone growth in the optic canal can cause a progressive, compressive optic neuropathy [171–175].

Symptoms and Signs

Most patients with craniofacial fibrous dysplasia involving the sphenoid bone present with a compressive optic neuropathy, manifesting as acute or gradual visual loss associated with an afferent pupillary defect, and a central scotoma or cecocentral scotoma. The optic disc may appear normal [176–179].

Neuroimaging

Clinical features and neuroimaging can help establish the diagnosis of fibrous dysplasia. CT demonstrates the extent of the disease in the craniofacial region. The expansion of the affected bone and matrix of the lesion with subtle, nondisplaced fractures can be seen. Areas of granulation tissue of the lesion may be seen as decreased density in the sphenoid body or root of the lesser wing on CT scan that can erode into the medial wall of the optic canal [180]. MRI is useful in showing malignant change or extension of the tumor into the optic canal to compress the nerve [181].

Pathology

Fibrous dysplasia consists of scattered areas of immature woven trabeculae surrounded by a matrix of fibrous tissue. The trabeculae are immature and not lined with osteoblasts. The fibrous stroma is disorganized and replaces the normal marrow. This bone disorder has been attributed to mutations on a G-protein subunit causing abnormal osteoblastic function and, therefore, the formation of abnormal bone matrix [171].

Management

In cases of acute visual loss, several reports have shown that administration of systemic corticosteroids can help improve vision transiently before the patient undergoes surgery [176, 179]. Optic nerve decompression is a controversial treatment modality in traumatic optic neuropathy and in the prophylaxis of compressive optic neuropathy in fibrous dysplasia. It is less controversial for the treatment of optic nerve compression in fibrous dysplasia. Progressive visual loss and sudden visual loss in patients with sphenoidal fibrous dysplasia are considered absolute indications for undergoing optic nerve decompression. This procedure must be done within 1 week from the onset of visual symptoms to reverse visual loss [182]. Optic nerve decompressive surgery should be considered as prophylaxis in the following situations: (1) patients presenting within 2–3 weeks of rapid visual loss; (2) children and adolescents with no visual loss but radiographic evidence of optic canal stenosis; or (3) adult patients with no visual loss, radiographic evidence of optic canal stenosis, and evidence of continued active fibrous dysplasia. The recurrence

Table 4.2 Some cause of infiltrative optic neuropathies [Based on data from refs. [188, 326]

Infiltration from primary tumors
• Optic glioma: benign or malignant
• Ganglioglioma
Infiltration from secondary tumors
• Metastatic carcinoma
• Anterior extension of retrobulbar optic nerve tumors: optic nerve sheath meningioma
• Lymphoreticular tumors: lymphoma, leukemia, myeloma, and others
• Tumors of the sensory retina and medullary epithelium: retinoblastoma, medulloepithelioma
• Vascular tumors of the retina: capillary hemangioma, cavernous hemangioma, racemose hemangioma
• Glial tumors of the retina: astrocytic hamartoma
• Melanocytic tumors: melanocytoma, malignant melanoma, combined hamartoma of the retina and retinal pigment epithelium
Infiltration from infections and inflammations
• Sarcoidosis
• Idiopathic perioptic neuritis
• Parasites
• Viruses
• Fungi

rate after optic nerve decompression for fibrous dysplasia has not been widely reported. Regrowth of the tumor is less likely as more walls of the optic canal are decompressed [182].

Infiltrative Optic Neuropathies

See Table 4.2 [13, 16, 183–326].

Primary Tumors Infiltrating the Optic Nerve

Benign Anterior Visual Pathway Gliomas

Optic Gliomas Associated with Neurofibromatosis Type I (NF-1)

NF1, an autosomal dominant disorder, is the most common phakomatosis, occurring in 1 of 5,000 [183]. The NF1 gene is located on chromosome 17, encoding a 2818 amino acid protein with a GTPase activator protein domain that functions as a tumor suppressor gene [183]. The gene product, neurofibromin, causes aggregation of melanoblast precursors or Schwann cells during neural crest migration that lead to various hamartomatous and neoplastic lesions, such as malignant schwannomas [184]. The activation of the rapamycin (mTOR) pathway is mediated by the phosphorylation and inactivation of the TSC2-encoded protein tuberin. This activated rapamycin pathway is involved in the development of NF1 related pilocytic astrocytomas [183].

Optic gliomas are relatively uncommon, accounting for less than 5 % of all intracranial pediatric tumors and less than 4 % of all intrinsic optic nerve tumors that present primarily among children in the first decade of life [185]. Optic nerve gliomas usually occur at 9 years of age, and chiasmal gliomas often occur at 7 years of age. Hypothalamic gliomas, causing a diencephalic syndrome, often present at 1 year of age. Based on data from 1,278 cases, approximately 75 % of gliomas involve the chiasm, whereas 25 % are confined to only the optic nerve. The prevalence of NF-1 in patients with gliomas of the anterior visual pathway ranges from 10 to 70 % [185]. This estimate is influenced by the age of the population investigated because the stigmata of NF-1 becomes more apparent with increasing age [186]. As 36 % of optic gliomas related to NF-1 are diagnosed in children over 6 years of age, these children with NF-1 should undergo yearly eye examinations. According to the retrospective study on 54 NF-1 patients by Thiagalingam et al. [187], yearly eye examinations should be extended in patients with NF-1 up to at least 17 years of age, and those with known chiasmal gliomas should be monitored into adulthood. Another study also reports that late-onset tumors can develop as late as the third decade of life and are more likely to progress after diagnosis compared to tumors developing earlier in life. In the study by Listernick et al. [188], 15–19 % of children with NF-1 who underwent CT or MRI had anterior pathway gliomas. Only 20 % of these children with gliomas had visual symptoms. Bilateral optic gliomas are more common in patients with NF-1 [189], whereas chiasmal gliomas are more often seen in non-NF-1 patients [190, 191]. Patients with NF-1 commonly have

Table 4.3 Diagnostic criteria for neurofibromatosis type I [Reprinted from Anonymous. National Institutes of Health Consensus Development Conference Statement: neurofibromatosis. Bethesda, MD, USA, July 13–15,1987. Neurofibromatosis 1988;1(3):172–178. With permission from The National Institutes of Health]

Diagnosis of neurofibromatosis type I (NF-1) requires two or more of the following features:
• Six or more cafe-au-lait spots with diameters greater than 0.5 mm before puberty or 1.5 cm after puberty
• Two or more neurofibromas or a single plexiform neurofibroma
• Freckling in the axillary or inguinal regions
• Optic pathway tumor
• Lisch nodules (iris hamartomas)
• Dysplasia of the sphenoid bone or dysplasia/thinning of the long bone cortex
• A first-degree relative diagnosed with NF-1

optic gliomas that grow circumferentially around the nerve. The tumor then breaks through the pia mater and grows within the subarachnoid space to compress the optic nerve. In patients without NF-1, optic gliomas usually grow intraneurally to cause expansion within the optic nerve [192].

Symptoms and Signs

Although the symptoms and signs of anterior visual pathway gliomas primarily depend on the location of the tumor, children with optic gliomas are asymptomatic and their tumor is diagnosed upon neuroimaging for screening of neurofibromatosis or other unrelated reasons [188, 193]. The prevalence of radiographically identified optic nerve gliomas in children with NF-1 is approximately 15 % in referral centers. Systemic clinical features for the diagnosis of NF1 are summarized in Table 4.3 [194]. Visual loss in at least one eye occurs in 62 % of children with NF-1 when the tumor involves the postchiasmal structures and 32 % when the lesion involves the chiasm and/or optic nerves [195, 196]. Visual loss in the better eye is less likely regardless of the association with NF-1 or the extent of the tumor [197]. In a study by Balcer et al. [196], 28 % of children with NF-1 and gliomas developed visual loss more than 1 year after diagnosis. Most children with NF-1 who had poor vision had their visual loss at the time of diagnosis [189, 196]. In a recent series of 54 patients by Thiagalingam et al. [187], optic pathway gliomas presented in older children between 7 and 15 years of age; 17 of the 56 children were diagnosed after 6 years of age, 22 had tumor progression within 1 year of diagnosis, and 6 showed progression after 1 year. Visual acuity range is variable in which more than half may present with 20/300 or worse [185]. Seventy-five percent or more of patients may have a relative afferent pupillary defect [198]. Proptosis is a common sign in patients with intraorbital optic gliomas, especially in children [199, 200]. Gradual visual loss may be attributed to enlargement of optic gliomas from neoplastic growth, arachnoidal hyperplasia, and gradual cyst degeneration with accumulation of mucopolysaccharide material; all may contribute to separation of longitudinal axon bundles and nerve fiber compression. Rapid visual loss might occur with cystic degeneration or hemorrhage. Vision may occasionally be spared despite extensive proliferation and compression because some nerve fibers may survive for long periods of time; it was observed that visual acuity did not correlate with tumor growth [185, 201]. Hoyt et al. [202] described two patients with radiologic evidence of tumor enlargement maintained stable vision over an 8-year interval. Four additional patients had progressive visual loss despite radiologic demonstration of stability in tumor size after radiotherapy. Spontaneous visual improvement or decrease in tumor size might occur by resorption of mucinous material or variations in hydration [202].

Visual field defects are common in patients with anterior visual pathway gliomas regardless of tumor location. Central and cecocentral scotomas, arcuate defects, altitudinal defects, and peripheral constriction all reflect injury of optic nerve fiber bundles [203]. If the glioma extends into the chiasm, then junctional scotomas and bitemporal hemianopsias may be observed.

On funduscopic examination, optic atrophy may be seen in two-thirds of patients and optic disc edema in one-third of patients, according to data from 383 patients [185]. Optic disc edema has been observed in 48 % of patients with intraorbital optic gliomas and in 22 % of those with

chiasmal tumors [185]. Optociliary shunt vessels, which are commonly seen in patients with optic nerve meningiomas, occur much less often in patients with optic gliomas. Retinal vascular occlusion [204], venous stasis retinopathy with iris neovascular glaucoma [205], or anterior segment ischemia [206] is rarely associated with orbital gliomas.

Ophthalmoplegia is less common in optic gliomas, occurring in 27 % of patients with intraorbital tumors and 21 % with chiasmal gliomas [185]. Gliomas expanding into the orbital apex may compress the extraocular muscles or ocular motor nerves.

Patients with chiasmal gliomas may also be asymptomatic [189, 193], but the symptomatic ones usually present with bilateral visual loss that does not correlate with tumor size. Because the tumor may affect a combination of optic nerve, optic tract, and chiasm, visual field defects may include central scotomas and bitemporal hemianopias with superimposed homonymous hemianopsias [207]. Optic atrophy may reflect more anterior optic pathway injury, whereas optic disc edema may suggest obstructive hydrocephalus or extensive tumor invasion of the optic nerve.

In contrast to optic gliomas, proptosis is less common with chiasmal gliomas. Intracranial-associated symptoms and signs are more prevalent. Based on data from 155 patients, about 28 % of patients with chiasmal glioma presented with headache [185]. Seizures occurred in 13 % of patients with chiasmal tumor involving the midbrain [208]. According to a study by De Sousa et al. [209], 47 % of patients with intracranial gliomas had increased CSF protein. Elevated CSF pressure was present in 85 % of patients with chiasmal gliomas in a study of 13 patients by Borit et al. [210].

Similar to optic gliomas, ophthalmoplegias in patients with chiasmal gliomas may be the result of exophytic tumor expansion compressing ocular motor nerves; increased intracranial pressure may also cause a sixth nerve palsy [185].

Nystagmus was observed in 23 % of patients based on data from 264 patients [185]. Nystagmus may suggest intracranial extension of gliomas, especially in infants who have rapid vertical or horizontal pendular oscillations of small amplitude associated with head movements that may mimic the features of spasmus nutans (a benign, spontaneously remitting disorder consisting of asymmetric nystagmus, head nodding, and anomalous head positioning) [211].

Hypothalamic invasion by exophytic gliomas may cause hypopituitarism. This diencephalic syndrome is most often seen in affected children who appear emaciated despite normal food intake and linear growth [212]. Up to 50–70 % of affected children under 10 years of age may present with precocious puberty, growth failure, diabetes insipidus, and obesity [213].

Neuroimaging

On high-resolution CT, an optic nerve glioma appears as a well-demarcated fusiform enlargement of the optic nerve [214] and increased tortuosity of the nerve, representing elongation of the optic nerve from secondary axial growth and downward deflection [215]. The tumor is isodense with the brain and enhances variably with contrast. Optic nerve gliomas often have less enhancement than ONSM. Localized low-density areas in the central aspects of the tumor are thought to represent cystic degeneration with accumulation of mucin [13]. The perineural pattern of growth leads to a diffuse enlargement of the optic nerve and appears on CT as a low-density thickened dura surrounding a compressed optic nerve, which is seen as a thin central core of higher density. Calcification is rarely seen and was noted in 14 % of cases by Hoyt et al. [201].

CT scan of a chiasmal glioma usually reveals a well-circumscribed enlargement of the optic chiasm or a round, globular suprasellar mass of variable size [216]. Tubular enlargement of the intracranial optic nerves or optic tracts may occasionally be seen on CT. Similar to optic gliomas, chiasmal gliomas variably enhance, and may have regions of lower density, possibly representing cystic degeneration. In contrast to optic gliomas, calcification is more commonly seen in chiasmal gliomas.

MRI offers greater resolution and sensitivity in visualization of anterior visual pathway gliomas. These tumors appear isointense or slightly hypointense relative to the brain on T1-weighted sequences and hyperintense on T2-weighted

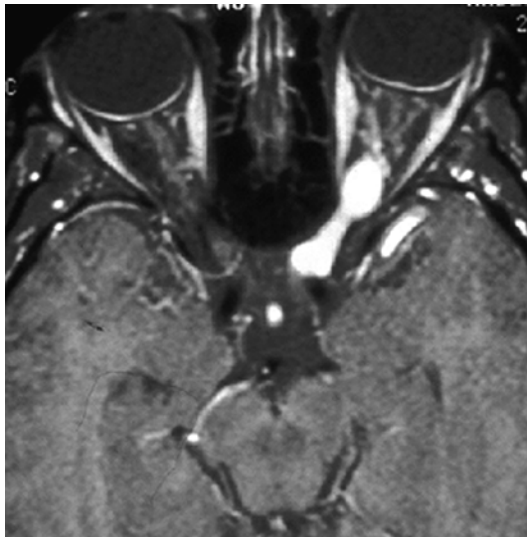

Fig. 4.11 Optic nerve glioma in neurofibromatosis type 1. Axial contrast-enhanced T1-weighted MRI of brain reveals extension of a left optic nerve glioma into the chiasm [Reprinted from Miller NR. Primary tumours of the optic nerve and its sheath. Eye 2004;18(11):1026–37. With permission from Nature Publishing Group]

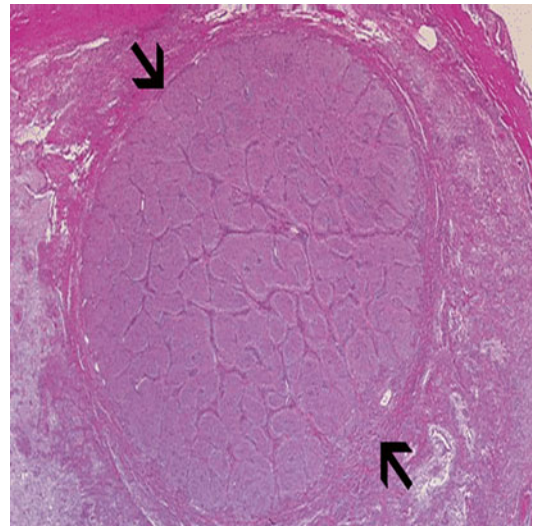

Fig. 4.12 Cross-section at low magnification of the optic nerve showing a pilocytic astrocytoma in between the dural sheath (*arrowhead*) and the optic nerve (*arrows*)

sequences (Fig. 4.11) [217]. Tumor enhancement is also variable. Intracranial growth and extension along the optic tracts are best visualized on postcontrast T1- and T2-weighted sequences. Visualization of a glioma in the orbital optic nerve requires proton density or fluid-attenuated inversion recovery sequences. With this MRI technique, the perineural pattern of arachnoidal gliomatosis would appear as solid tissue rather than water, as seen on T1- and T2-weighted sequences [218, 219].

The following neuroimaging features of anterior visual pathway gliomas are more commonly associated with NF-1: (1) bilateral optic nerve gliomas [189], (2) circumferential or perineural growth pattern [218, 219], (3) elongation and downward "kinking" of the intraorbital optic nerve [220], and (4) posterior extension of the optic chiasmal glioma into both optic tracts and often into the lateral geniculate nuclei and temporal lobes [216]. Hyperintense T2-weighted signal lesions, which are thought to be hamartomas located in the globus pallidus, cerebellum, internal capsule, and brainstem, may also be seen in 75 % of patients with NF-1 [221].

Histopathology

Most optic gliomas are benign, World Health Organization grade I pilocytic astrocytomas, characterized by proliferating neoplastic astrocytic cells in which some cells may develop Rosenthal fibers, enlarged eosinophilic processes surrounded by hyalinized connective tissue [222]. Vascular proliferation and atypia are commonly seen.

In neurofibromatosis, orbital gliomas commonly develop proliferation of arachnoid cells that extend from the nerve through the pia mater into the arachnoid and subarachnoid space. This arachnoid hyperplasia causes reactive proliferation of fibrovascular tissue and meningothelial cells along with neoplastic astrocytes [223]. The arachnoid cell proliferation may also extend beyond the tumor to mimic extension and may even histologically mimic ONSM [223].

Perineural, or circumferential, growth of optic gliomas is seen more often in patients with neurofibromatosis. Proliferating astrocytes enlarge the pia-subarachnoid space to form nests of astrocytes and fibrovascular arachnoidal trabeculae, with mucinous and microcystic degeneration [192]. This circumferential growth compresses the optic nerve (Fig. 4.12). Occasionally, tumor

may also grow into the optic nerve without the cystic changes.

In contrast, the intraneural growth pattern of optic gliomas is predominantly seen in patients without neurofibromatosis [192]. The optic nerve is enlarged by expansion of fibrovascular trabeculae by astrocytic proliferation. Cystic degeneration is rare. The enlargement of the tumor in the optic nerve also obliterates the subarachnoid space [192].

Growth of optic gliomas is often unpredictable and often decreases or halts after reaching a plateau [223]. Proliferation of neoplastic cells, reactive arachnoidal proliferation, and accumulation of extracellular, periodic acid-Schiff-positive mucoid substance secreted by astrocytes all lead to gradual enlargement of the tumor [223]. Sudden enlargement can lead to cystic degeneration or intralesional hemorrhage [224]. Eventually, compression from the tumor leads to demyelination, a disruption of the nerve fibers that results in visual loss [225].

Course and Prognosis

Most untreated gliomas of the anterior visual pathways are slow-growing tumors associated with good long-term survival and good vision [185]. In a review of more than 300 patients from published case series, only 21 % of those with untreated or partially resected optic gliomas had recurrence or progression during a mean follow-up period of 10 years [210]. Of 62 patients with unilateral optic gliomas who were either untreated or underwent partial resection, only 12 (19 %) developed tumor growth during a mean follow-up period of 7 years [226]. The estimated mortality rate during a mean follow-up period of 10 years was 5 % [226]. Most recurrences occurred during the first few years of follow-up. Growth and recurrence of these tumors is followed by a period of stabilization after reaching a plateau. Despite the benign course of optic gliomas, intraparenchymal and leptomeningeal metastases have been documented in some rare cases [227, 228].

Compared to patients with optic gliomas, those with optic chiasmal gliomas have a worse prognosis for survival. The overall mortality rate is determined by the presence or absence of intraparenchymal extension of the tumor. In a study by Miller et al. [199], gliomas limited to the optic chiasm were associated with a better prognosis for survival than those involving the hypothalamus or third ventricle. In a review of more than 300 patients from published case series by Dutton [185], the 10-year mortality rate of patients with untreated or partially resected gliomas limited to the optic chiasm was about 17 %. The 11-year mortality rate of patients with similar tumors that extended into the hypothalamus or third ventricle was approximately 52 %.

The prognosis for survival and rates of recurrence are also influenced by the presence or absence of neurofibromatosis. Most studies show that the presence of NF-1 improves the overall prognosis [189, 208]. The results from these series may have been biased by case ascertainment. Optic gliomas are more prevalent in patients with NF-1, and these tumors are associated with a better prognosis. More optic gliomas are reported in asymptomatic NF-1 patients because they undergo routine neuroimaging screening compared to those without NF-1 who are not screened. On the contrary, the presence of NF-1 may pose an increased risk of developing other NF-1-related central nervous system (CNS) tumors that can contribute to an overall poor prognosis of survival. In a study of 28 patients with optic chiasmal gliomas [220], two of the nine patients with NF-1 died as a result of their chiasmal gliomas and the remainder died of complications related to their additional tumors.

Occasionally, spontaneous visual improvement [229] and regression of tumor mass [230] may be observed in patients with anterior visual pathway gliomas. Sudden unpredictable changes in tumor size are thought to be related to acute cystic degeneration, regression of vascular engorgement, and/or intraparenchymal hemorrhage [230].

Management

Monitoring of Optic Gliomas

In patients with NF-1, ophthalmologic monitoring for optic pathway gliomas is recommended every 3 months after diagnosis, every 6 months at 18 months, and then yearly thereafter. MRI of the brain is recommended about every 6 months

for the first 2 years and then yearly thereafter [222]. Although previous studies have documented a mean age at presentation of optic pathway gliomas of around 4 years [188, 231, 232], 17 of 54 patients with NF-1 were diagnosed with optic pathway gliomas after age 6 [187]. The late-onset tumors in this study were more likely to progress following diagnosis than their counterparts, which presented early in life. Eighty-eight percent of these tumors displayed evidence of ophthalmologic progression, and 50 % exhibited radiographic growth [233]. This study suggests that monitoring children with NF-1 up to at least 17 years of age may be necessary to diagnose later-onset optic pathway gliomas [233].

The management of optic gliomas is controversial. The natural history of these tumors is unclear at this time, as incidences of visual loss, hydrocephalus, and other clinical features vary dramatically among studies. Assessment of treatment efficacy is confounded by unpredictable growth of these tumors. Several studies have shown spontaneous tumor regression after radiographically documented tumor regression [234, 235].

Surgery

There are no studies to support the efficacy of surgical resection of optic gliomas to prevent extension into the chiasm. Biopsy of lesions confined to the visual pathways is not necessary in patients with NF-1. Optic nerve gliomas may even spontaneously regress, as reported in at least 36 patients with or without NF-1. For patients with NF-1 who have hypothalamic extension of the optic glioma, biopsy is controversial because of the risk of further visual loss and hypothalamic dysfunction [216]. For patients with hypothalamic lesions without NF-1, however, biopsy may be reasonable because the risk for malignancy is higher in these patients. Surgical resection of chiasmal/hypothalamic gliomas also remains uncertain. In the series by Wisoff et al. [237], 10 of 16 patients experienced no further growth of the tumor after surgery at a mean follow-up period of 27 months. Three infants died of tumor recurrence. None of the patients had postoperative decrease in vision or diabetes insipidus. Postoperative hypopituitarism was not reported.

Other relative indications for surgical intervention are primarily for alleviating ocular complications. Surgical resection of a blind, painful eye may offer symptomatic relief for the patient. Ophthalmic plastic surgical procedures would be considered appropriate to reduce proptosis because of cosmetic reasons and/or severe corneal exposure injury [237].

Although the clinical and radiologic features of optic gliomas are sufficiently characteristic to obviate the need for a biopsy, some patients have large exophytic tumors that may mimic other suprasellar tumors of childhood, such as germinoma or craniopharyngioma [184]. It may be unclear in such cases whether the tumor is intrinsically associated with the optic chiasm or whether it is a suprasellar/hypothalamic lesion extending into the chiasm. Limited excisional biopsy of an exophytic component is not likely to cause further visual loss. No evidence supports that partial resection of these tumors is associated with any significant improvement over observation in terms of rate of recurrence [238]. In patients with infiltrative tumors of the optic chiasm, diagnostic biopsy can injure the anterior visual pathway and cause further visual loss.

Up to 40 % of patients who have chiasmal gliomas with large exophytic masses develop or present with hydrocephalus [183, 208]. Intraventricular shunt placement is recommended. Although metastatic seeding of the peritoneum following shunt placement rarely occurs, it is not a contraindication [239, 240].

Ascites is a rare complication following placement of a ventriculoperitoneal shunt. In the study by West et al. [240], each of three children had a shunt for chiasmal glioma complicated by hydrocephalus and developed ascites without malignant cells. The ascites resolved after their shunt was revised to a ventriculo-atrial system.

Radiation Therapy

For chiasmatic–hypothalamic gliomas, 80 % of patients treated with radiation therapy at 4,500–5,500 cGy experienced stabilization or tumor

shrinkage as seen on radiologic studies [195]. The efficacy of radiation therapy on visual outcome and tumor progression is uncertain. In studies by Glaser and Hoyt [202, 236], visual outcome was not correlated with radiation therapy in 20 patients. No difference was noted in the disease-free survival rate between the patients who had radiation therapy and those who did not. Even tumor shrinkage on CT scan was not correlated with clinical progression in 16 patients after radiation therapy [216].

The cognitive and endocrinological side effects of radiation therapy occur most often in children less than 5 years of age when chiasmal gliomas are usually diagnosed [242]. Other complications of radiation include malignancies in patients with NF-1, moyamoya disease, and aneurysms [243, 244]. In the study by Tao et al. [245], long-term follow-up of 29 children with irradiated chiasmal gliomas reported a 10-year survival of 89 %. Tumor shrinkage was noted years after radiation. Vision improved in 24 %, worsened in 17 %, remained stable in 48 %, and was not evaluated in 10 %. As a complication of radiation therapy, cognitive impairment was found in 71 % and hypopituitarism in 72 %.

Chemotherapy

No evidence supports the use of chemotherapy in gliomas confined to the optic nerve [246]. Less than 10 % of all diencephalic gliomas in patients with NF-1 will require treatment on the basis of progressive visual loss or radiographic enlargement [246].

Because radiation therapy is not an effective long-term treatment modality for all patients, especially in young children who experience cognitive and endocrinological complications, chemotherapy is a useful alternative for those who have progressive tumors. The combination of carboplatin and vincristine has been shown to be less toxic than radiation and more efficacious than other chemotherapeutic combinations. In a prospective study by Packer [246] in which patients with recurrent or progressive low-grade gliomas received carboplatin and vincristine, 56 % of patients with progressive, newly diagnosed lesions had an initial radiographic response, including complete tumor shrinkage. Progression-free survival, as measured radiographically, was about 74 % for children less than 5 years of age, and about 39 % for children greater than 5 years of age. Therefore, the combination of carboplatin and vincristine is considered, at this time, the preferred treatment for progressive chiasmal or hypothalamic gliomas.

Malignant Anterior Visual Pathway Gliomas

Epidemiology

Malignant anterior visual pathway gliomas often occur in adults with onset at approximately 50 years of age [185]. Men are more commonly affected than women in an approximate ratio of 2:1 [247–249]. In contrast to the benign anterior visual pathway gliomas, these malignant tumors are not associated with NF-1.

Symptoms and Signs

Bilateral and asymmetric visual loss is rapidly progressive over an average of 8.7 weeks [185]. It is commonly associated with retro-orbital pain. These visual symptoms can mimic acute optic neuritis. Based upon a meta-analysis of previous case series of patients with malignant optic gliomas [185], the levels of initial visual acuity of the more affected eye included the following: 5 % had normal visual acuity, 24 % had 20/30 to 20/100, 14 % had 20/200 to 20/400, 38 % had counting fingers to light perception, and 19 % had no light perception. The final visual acuity of the more affected eye revealed that 14 % had hand motion to light perception and 86 % had no light perception. As the tumor extended into the optic chiasm in the early stages, visual loss started in the fellow eye within 5–6 weeks and then progressed to blindness.

In the same meta-analysis of previous case series [185], 94 % of the patients had visual field defects. These field defects included any combination of the following: (1) central, arcuate, or altitudinal scotomas if the optic nerve is affected; or (2) bitemporal hemianopias and junctional scotomas, if the optic chiasm is involved.

The optic disc may appear normal in the early stages. As the tumor infiltrates the optic nerve, the disc may become hyperemic and edematous, often with central retinal artery or vein occlusion [247, 249]. If the tumor remains in the more posterior aspects of the anterior visual pathway, the disc usually becomes pale without edema. If the tumor extends intracranially, then papilledema from increased intracranial pressure may be seen. In the same meta-analysis of previous case series of patients with malignant optic gliomas, normal optic discs were observed in 25 %, disc edema in 43 %, optic atrophy in 31 %, proptosis in 23 %, and ophthalmoplegia in 19 % [185]. The expansive effects of the tumor are thought to cause compression on individual cranial nerve palsies or cause mechanical limitation on the movement of the orbit itself. Convergence and other gaze abnormalities are rare [250].

Malignant gliomas commonly involve the temporal lobes, hypothalamus, and third ventricle to cause seizures, encephalopathy, hemiparesis, and hypothalamic dysfunction. These neurological signs occurred in 35 % of patients in the meta-analysis of previous case series [185].

Neuroimaging

The CT and MRI findings are nonspecific. These malignant tumors often cause enlargement of the chiasm and at least one contiguous optic nerve that enhances after administration of contrast [251–254]. The optic chiasm is affected in nearly all cases, either initially or later as the tumor grows [185]. In the later stages of tumor growth, contiguous infiltration of the anterior visual pathways and exophytic extension from the optic chiasm into the adjacent temporal lobes and hypothalamus/third ventricle may be seen (Table 4.4) [185].

Based on the radiologic presentation of infiltration of the optic chiasm and other anterior visual pathways, the differential diagnosis of an adult malignant optic glioma would include malignancies, such as lymphoma; infections, such as fungi; and inflammatory disorders, such as sarcoidosis. If the tumor extends into the sellar areas, craniopharyngiomas or malignant pituitary adenomas could be considered [185].

Table 4.4 Frequency (from most frequent to least frequent) and site of malignant optic gliomas based on a meta-analysis of 31 previously reported patients in the literature. In some patients, multiple sites were involved [Reprinted from Dutton JJ. Gliomas of the anterior visual pathway. Surv Ophthalmol 1994;38(5):427–452. With permission from Elsevier]

1. Chiasm and hypothalamus
2. Chiasm and optic tracts
3. Chiasm and third ventricle
4. Chiasm and orbital optic nerve
5. Chiasm and temporal lobe
6. Chiasm and basal ganglia

Pathology

Malignant anterior visual pathway gliomas are characterized as having cellular pleomorphism, numerous mitotic figures, necrosis, and hemorrhage, as seen in anaplastic astrocytomas and glioblastoma multiforme 247, 249, 255. Neoplastic cells envelop the optic nerve beneath the pia mater, causing impairment of capillary perfusion, progressive vascular occlusion, and demyelination. Tumor usually spreads below the pia mater along the visual pathways or directly within the substance of the brain to other locations [257].

Prognosis and Treatment

Malignant optic gliomas cause rapidly deteriorating vision and death within a year in middle-aged men [247]. In a review of 39 reported cases of adult malignant optic glioma by Dario et al. [255], no statistically significant difference between the survival of patients with only optic involvement and patients with extraoptic involvement was observed. Patients treated with radiation therapy had more favorable survival curves, with a median of 5.5 months, compared to those who were not treated, with a median survival of 3 months. No statistically significant difference was seen in those who received radiation therapy and chemotherapy (median survival, 6 months) and those who did not (median survival, 3 months). Although complete resection of the tumor is not feasible, biopsy of the optic nerve with poorest vision or partial resection of the tumor is usually possible. No statistically significant difference

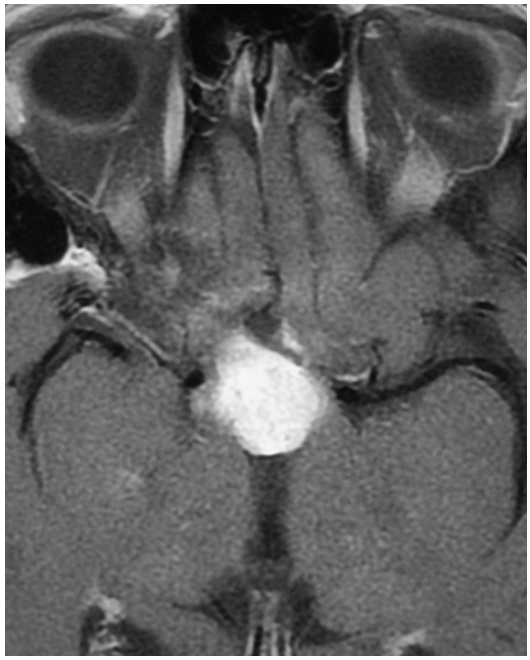

Fig. 4.13 Ganglioglioma of the optic nerve. Axial contrast-enhanced T1-weighted MRI of brain reveals a right ganglioglioma of the right optic nerve extending into the optic chiasm [Reprinted from Gaillard, F Ed. Ganglioglioma of the optic nerve. http://radiopaedia.org/cases/ganglioglioma-of-the-optic-nerve; Accessed February 3, 2012. With permission from Radiopaedia.org]

was seen in patients who underwent biopsy of the tumor versus partial resection of the tumor.

Ganglioglioma of the Optic Nerve

Gangliogliomas are composed of mature ganglion cells and mature glial cells that usually grow in the floor of the third ventricle, but may rarely arise within the optic chiasm or intracranial portions of the optic nerves. Gangliogliomas have been reported to infiltrate one or both optic nerves [256]. Vision worsened gradually or suddenly. Lu et al. [257] described a 38-year-old man who developed acute right visual loss with right orbital pain and headaches. MRI of the orbits with contrast revealed an enhancing fusiform dilation of the optic nerve and can even extend into the chiasm (Fig. 4.13).

On histopathology, gangliogliomas have neoplastic astrocytic proliferation. The glial and neuronal components are well differentiated to the degree that they may mimic pleomorphic fibrillary astrocytomas [258].

Most gangliogliomas have a natural course similar to that of low-grade astrocytomas and have a good prognosis. If chiasmatic infiltration is present, the survival rate may be slightly lower. Some tumors may have malignant features often occurring in the glial component of the tumor, and metastases may occur [258].

Secondary Tumors Infiltrating the Optic Nerve

Leptomeningeal Metastases to the Optic Nerve

Meningeal metastasis can infiltrate the optic nerve to cause visual loss [259]. Malignant cells invade the subarachnoid space of the optic nerve with minimal invasion of the optic nerve parenchyma. In some instances, the infiltrative process becomes compressive as the malignant cells grow and expand into the subarachnoid space around the optic nerve. Approximately 30–40 % of patients with carcinomatous meningitis develop visual loss [260, 261], whereas other studies have found 15 % of cases affecting the optic nerves [262].

Symptoms and Signs

Visual loss in patients with meningeal carcinomatosis commonly occurs after the diagnosis of the primary lesion (lung or breast) has been established. The visual loss may be an isolated finding [263] or may occur with other signs of chronic meningitis [264]. Patients with carcinomatous infiltrative optic neuropathy often present with painless acute or subacute visual loss in one or both eyes. Blindness may even occur within several days.

An afferent pupillary defect, decreased color vision, and visual field defects, such as a central scotoma or nerve fiber bundle defect, may be the initial signs of an infiltrative optic neuropathy. The optic disc usually appears normal at the

onset of visual loss. Only after about 6–8 weeks does the optic disc show atrophy [263, 264].

Diagnostic Testing

On MRI of the brain with gadolinium, enlargement and enhancement of the orbital and canalicular segments of the optic nerve may be seen. Dural metastases appear as curvilinear contrast enhancement patterns beneath the inner table of the skull. In contrast, leptomeningeal tumor appears as contrast-enhanced areas that follow gyral convolutions and may also be seen as nodular deposits on the leptomeninges. The diagnosis of meningeal carcinomatosis also requires CSF cytology; approximately 20 mL or more CSF is often needed to detect malignant cells [265].

Management

Aggressive therapy with intrathecal chemotherapeutic agents, such as methotrexate, can improve symptomatology in some patients with leptomeningeal metastases, and may even occasionally prolong their median survival period for 8 months [265]. If bulky meningeal metastases are associated with leptomeningeal ones, then local radiation therapy can be added [266].

Other Metastases to the Optic Disc

In addition to metastases by CSF circulation within the subarachnoid space, tumor may spread to the optic nerve by the adjacent choroid or retina, by the vascular supply to the optic nerve, or by orbital metastases invading intraocularly [267]. Isolated metastases to the optic nerve are extremely rare and occur in 1.3 % with histologically proven carcinoma metastatic to the eye and orbit [268] and in 4 % with intraocular metastases referred to a tertiary cancer center [269]. Bilateral optic nerve metastases occur in approximately 18 % of patients [270]. Breast and lung carcinomas are the most common metastatic tumors to the optic nerve and uvea. In a study of 29 cases of isolated optic nerve metastasis by Arnold et al. [271], the primary cancers consisted of 27 % breast cancer (4 cases), 27 % lung cancer (4 cases), 27 % stomach cancer (4 cases), 20 % sarcoma (3 cases), and 6 % pancreas (1 case). Other types of cancers that have been reported to spread to the optic nerve include prostatic, esophageal, uterine, ovarian vaginal, hepatic, renal, adrenal, thyroid, and lip carcinomas. Melanomas from the skin have also been reported to metastasize to the optic nerve and optic nerve sheath.

Symptoms and Signs

Visual loss usually progresses over several months. The optic disc is swollen and may have a yellow-white mass of tumor cells [272]. Vitreous tumor cells and hyperemia of uninvolved nerve can also be seen. Compression of venous outflow by the mass of tumor cells may cause retinal venous engorgement and central retinal vein obstruction. If the mass becomes necrotic, then hemorrhage into the optic nerve can occur. Associated choroidal metastases appear as yellow subretinal lesions with a serous detachment of the sensory retina in about 75 % of cases [267].

The differential diagnosis of optic disc metastasis includes primary optic nerve tumors, such as astrocytoma, melanocytoma, and capillary hemangioma; optic nerve granulomas, including sarcoid and juvenile xanthogranuloma; and optic nerve macroaneurysm. Metastasis involving the optic nerve posterior to the lamina cribrosa may mimic retrobulbar neuritis. When metastases extend into the optic nerve posteriorly into the lamina cribosa, the disc may appear normal, mildly hyperemic, or pale, mimicking retrobulbar optic neuritis. The optic disc may also be swollen from increased intracranial pressure from CNS metastases [267].

Diagnostic Testing

On fluorescein angiography, the optic disc tumor may be hypofluorescent in the early phases of the study. Leakage of dye occurs in the hyperemic areas of the optic disc. If retinal venous flow is compressed by the tumor, then a delay in venous filling may be seen [267].

If the diagnosis is uncertain and the patient has no prior history of cancer, then a systemic workup is needed to search for the primary lesion and to exclude other possible etiologies. Neuroimaging with CT, MRI, and ultrasonography may be needed to delineate the intraocular

lesion. Lumbar puncture may be necessary to evaluate for any intracranial involvement. Cytology of vitreous or CSF may be required to obtain a histological diagnosis [246].

Management

Treatment options include observation, radiation therapy, chemotherapy, and enucleation. Observation may be indicated in patients with good visual acuity, especially those who are improving on chemotherapy. External beam radiation may be appropriate if vision is impaired. In adults, about 30–35 Gy can be given in divided doses over 3–4 weeks. For patients with metastatic optic disc tumors with good visual acuity, chemotherapy to control the tumor growth is recommended. If visual acuity is decreased, external beam radiation may be needed. Secondary optic atrophy may be a complication of radiation therapy. Enucleation would be reserved for those patients with a blind and painful eye [267].

Prognosis

The prognosis of patients with metastases to the optic nerve is poor. The mean survival of patients with metastatic carcinoma was 9 months after onset of ocular symptoms [247]. The prognosis for survival is likely influenced by the course of the primary malignancy. In a series of 300 patients with ocular metastases, the mean survival of patients with breast carcinoma was 18 months compared with 8 months for patients with lung carcinoma and 5 months for patients with cutaneous melanoma [268].

Lymphomatous Infiltration of the Optic Nerve

Epidemiology

Infiltration of the optic nerve occurs in 0.5 % of patients with non-Hodgkin's lymphoma (NHL) [273]. Infiltration of the optic nerve in Hodgkin's disease is even less common. In both NHL and Hodgkin's lymphoma, the infiltration of optic nerves arises from extension of CNS tumor. In primary CNS lymphoma (PCNSL), the incidence of ocular involvement is as high as 20–25 % at the time of diagnosis. The true incidence of isolated ocular lymphoma is difficult to ascertain because a significant proportion of patients are not accurately diagnosed until they present with subsequent CNS disease. Nevertheless, ocular lymphoma with or without CNS disease affects up to 500 patients per year and is a very rare condition. The average age of onset for isolated ocular lymphoma is in the late fifties to sixties. Women are affected twice as frequently as men [274].

Symptoms and Signs

Visual symptoms usually present after the diagnosis of lymphoma, but visual loss may occasionally be the initial presenting sign [275, 276]. The location and extent of the lymphoma determines whether the visual loss is slowly progressive [277] or acute [278]. In patients with ocular lymphoma as part of the spectrum of PCNSL or in isolation, the visual symptoms are identical to those of idiopathic vitreitis or uveitis. A lymphomatous infiltrative optic neuropathy (Fig. 4.11) can even present in patients thought to be in clinical remission. The most common presentations are floaters, which may enlarge in size to gradually obscure vision. Blurry vision and scotomas are also occasionally present. Bilateral involvement occurs in more than 80 % of patients. Those who appear to have unilateral symptoms at onset often have bilateral disease on examination or develop it during the course of their illness. About 50 % of patients with ocular lymphoma have no visual symptoms when cells and flare are seen on slit lamp examination. Further funduscopic exam often reveals subretinal deposits of ymphoma and even retinal detachment (Fig. 4.14) [279].

Diagnostic Testing

On cytological evaluation of a vitrectomy specimen, the presence of malignant lymphocytes establishes the diagnosis [280]. Most of these cells are B-cell tumors that stain with B-cell immunohistochemistry markers. Although some reactive T cells are seen, flow cytometry or molecular analysis of the vitreous specimen can confirm the diagnosis and rule out an inflammatory reaction, as seen in idiopathic vitritis [280]. Further testing for elevated levels of interleukin-10

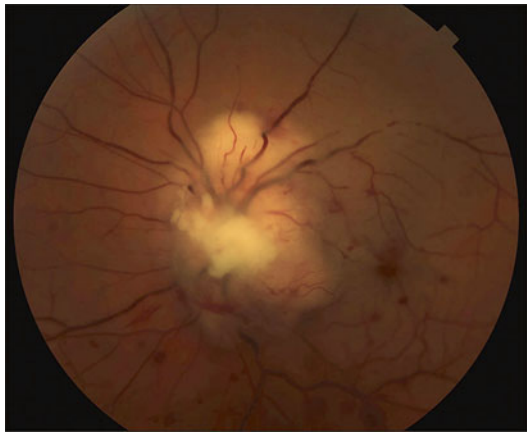

Fig. 4.14 Optic nerve infiltration by diffuse large B-cell lymphoma. Direct infiltration of optic nerve is seen as an elevated mass protruding into the vitreous. Central retinal venous and arterial occlusions are also associated with diffuse retinal vein engorgement, scattered retinal hemorrhages, and box-carring of the retinal arterioles [Reprinted from Dorrepaal SJ, Margolin E. Rapid optic nerve infiltration by diffuse large B-cell lymphoma. Arch Ophthalmol 2009;127(11):1493. With permission from American Medical Association.]

(IL-10), IL-6, and interleukin-12 (IL-12) may provide supportive evidence, in addition to cytological results, of ocular lymphoma. Vitreous IL-10 is elevated in ocular lymphoma, but not in idiopathic vitritis, which is associated with elevated levels of IL-6 and IL-12. Monitoring of the levels of IL-10 may also be helpful in measuring therapeutic response in patients with ocular lymphoma [281].

Neuroimaging

Infiltration of the optic nerve by lymphoma is seen as an enlarged high-density enhancing lesion on CT scan. On MRI, the infiltrated optic nerve can be seen as an enhancing lesion that is iso-, hyper-, or hypointense on T1-weighted imaging and hyperintense on T2-weighted imaging [278].

Management

Prior use of corticosteroids can be cytotoxic to malignant lymphocytes and may cause transient remission of the ocular lymphoma, which often recurs when corticosteroids are discontinued for weeks to sometimes months. Most patients become refractory to repeated courses of corticosteroids [274].

When the CNS is involved, survival without treatment is very limited such that most patients survive for only a few weeks. Radiotherapy, corticosteroids, and vitrectomy can induce remission but do not substantially improve long-term survival [274].

Leukemic Infiltration of the Optic Nerve

Epidemiology

Based on a study by Allen and Straatsma [282], half of the patients who died of leukemia had ocular involvement. The acute form of leukemias affected the eye four times more often than the chronic form. About 90 % of cases with optic nerve involvement occur in patients with the acute forms of leukemia [282, 283]. By the time the optic nerve head is infiltrated by leukemic cells, the disease is often active in the bone marrow [283].

Symptoms and Signs

In contrast to the good visual function observed with other types of optic disc edema, this infiltrative-related disc edema is associated with decreased visual acuity, variable visual field defects, and a relative afferent pupillary defect unless the infiltration is bilateral and symmetric. It is often associated with peripapillary and peripheral retinal hemorrhages [283]. Leukemic cells may also infiltrate the optic disc to form a circumscribed, white elevated lesion associated with yellow deposits and peripapillary hemorrhage (Fig. 4.15) [284]. Subretinal fluid may also develop secondary to retinal pigment epithelial damage [285–287]. The visual acuity in such patients is relatively preserved, unless the infiltration or associated edema and hemorrhage extends into the macula [288]. In addition, optic disc swelling and neovascularization may occur as a local phenomenon in the setting of diffuse retinopathy of acute leukemia [289].

The differential diagnosis of optic disc edema in patients with leukemia includes leukemic infiltration of the CNS with secondary increased intracranial pressure, pseudotumor cerebri related to prolonged corticosteroid use, tumor infiltration

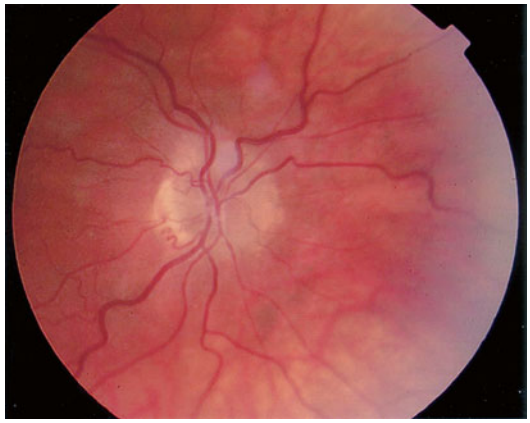

Fig. 4.15 Direct infiltration of the optic nerve head by leukemic cells in acute leukemia [Reprinted from Sharma T, Grewal J, Gupta S, Murray PI. Ophthalmic manifestations of acute leukaemias: the ophthalmologist's role. Eye 2004 Jul;18(7):663–672. With permission from Nature Publishing Group]

of the optic nerve resulting in ischemic papillitis, and perivascular tumor infiltration leading to venous engorgement [284].

Although most infiltrative optic neuropathies are attributed to acute leukemias, chronic leukemias may cause more slowly progressive and less severe visual loss. The optic disc edema is similar to that seen in patients with acute leukemias but without the retinal changes [290].

Similar to lymphomatous infiltrative optic neuropathies, MRI demonstrates abnormal enhancement in optic nerves infiltrated by leukemia. This lesion is iso-, hyper-, or hypointense on T1-weighted imaging and hyperintense on T2-weighted imaging [281].

Pathology

Leukemic infiltration of the optic nerve via the pial septae causes optic disc swelling. This edematous appearance may mimic papilledema caused by increased intracranial pressure. The leukemic cell infiltration proximal to the optic nerve just posterior to the lamina cribrosa contributes to the disruption of axoplasmic flow and compression of nerve fibers to cause disc edema [284–286]. Hemorrhagic necrosis and tumor cells can be seen in the edematous disc and in the retrolaminar interneuronal spaces [290].

Management

Early, aggressive radiation therapy is the most effective treatment of incipient optic nerve head infiltration by leukemia. In a study by Rosenthal et al. [286], four eyes with leukemic infiltration were treated with 2,000 rads external beam radiation over a 1- to 2-week period. Visual function rapidly returned to normal or near normal, and the disc edema resolved. On histopathological examination of these eyes, tumor cells were absent in the prelaminar and retrolaminar regions of the optic nerve.

Myelomatous and Other Lymphoreticular Tumor Infiltration into the Optic Nerve

Multiple myeloma, lymphomatoid granulomatosis, and Langerhans' cell histiocytosis may cause an infiltrative and/or compressive optic neuropathy [291]. Bourdette and Rosenberg [292] described a patient with polyneuropathy, organomegaly, endocrinopathy, monoclonal gammopathy, and skin changes who developed an infiltrative orbitopathy and had blind spot enlargement that improved after corticosteroid treatment. Another report [293] described a patient who developed an optic neuropathy and a chiasmal syndrome resulting from infiltration from reactive lymphohistiocytosis secondary to phenytoin use. Vision improved after treatment with corticosteroids and radiation therapy [293, 294].

Inflammatory Infiltrative Optic Neuropathies

Sarcoidosis

Epidemiology

Sarcoidosis is a relatively common disorder, occurring as often as 82 cases per 10,000 persons in the United States. It affects blacks more severely, and they have twice the frequency of ocular involvement as Caucasians. Most symptomatic patients are between 20 and 40 years of age.

Sarcoidosis is the most common inflammatory etiology of infiltrative optic neuropathies. About 1–5 % of patients with systemic sarcoidosis have

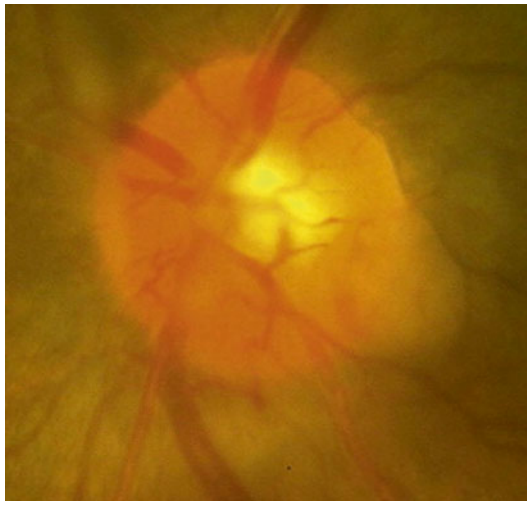

Fig. 4.16 Sarcoid infiltration of the optic nerve head [Reprinted from Kanski JJ. Optic Nerve Head. In: Kanski JJ. Signs in Ophthalmology: Causes and Differential Diagnosis. New York, NY: Elsevier; 2010;264–302. With permission from Elsevier]

optic nerve involvement [295]. Optic nerve dysfunction occurs in patients with neurosarcoidosis. Coexisting uveitis may obscure optic nerve involvement. In a study of 68 patients with neurosarcoidosis reported by Zajicek et al. [296], the optic nerve or chiasm was affected in 38 %. Of these patients, 69 % had unilateral optic nerve involvement and 31 % had bilateral involvement.

Symptoms and Signs

Sarcoidosis may cause an ischemic optic neuropathy, papilledema from a compressive process, or an anterior or retrobulbar optic neuritis from a granulomatous infiltrative process [297]. Visual acuity loss is associated with decreased color vision, visual field defect, and a relative afferent pupillary defect, unless the involvement is bilateral and symmetric. An isolated infiltrative optic neuropathy can manifest initially, or it may occur with other signs of hypothalamic dysfunction, hypothalamic hypopituitarism, or both [297]. Sarcoidosis also causes perioptic neuritis.

On funduscopic examination, the optic disc is usually elevated diffusely or sectorially with nodules (Fig. 4.16). This yellow-white cauliflower-like formation over the disc can also be clearly seen on ultrasonography. Surface disc blood vessels appear dilated, and peripapillary hemorrhages may be seen. Pressure from the lesion can cause a branch retinal vein obstruction. Noncaseating granulomas usually infiltrate the optic disc unilaterally. Although it is not often associated with anterior uveitis, posterior uveitis and retinal phlebitis occur in 80 % of cases [298]. Sarcoidosis may affect the posterior retrobulbar or intracanalicular portion of the optic nerve to cause gradual visual loss and a normal optic disc that gradually becomes pale. Visual acuity ranges from 20/20 to hand motions [16].

Although sarcoid-related disc edema in the setting of progressive visual loss commonly occurs in association with ocular inflammation, it may be difficult to distinguish it from compressive optic neuropathies, such as ONSM. A retrobulbar presentation of sarcoidosis can also mimic optic neuritis. Atypical features of peripapillary hemorrhages or the persistent dependence of visual function on steroids may help differentiate sarcoid optic neuropathy [299].

Diagnostic Testing

The diagnosis is usually confirmed by other systemic clinical, radiographic, and laboratory evidence of sarcoidosis. Laboratory tests supporting the diagnosis of sarcoidosis include an elevated ACE level and histological evidence of sarcoidosis by biopsy. Sensitivity of serum ACE is 84 % and the specificity is 95 %. The combined use of ACE levels and gallium scans can also increase specificity [300]. Furthermore, abnormal uptake on gallium scanning may represent areas suitable for biopsy. Affected conjunctival or lacrimal glands may also be biopsied. Epithelioid and giant cell infiltration forming noncaseating granulomas can be seen on biopsy of the optic nerve.[301]

On CSF analysis, the CSF protein is elevated in 73 % of patients with neurosarcoidosis; the lymphocytic count is elevated; CSF glucose levels are usually normal; CSF oligoclonal bands are present in 55 %; and CSF ACE levels are elevated in up to 50 % of patients [296]. The optic neuropathy may be subclinical in some cases. In patients with neurosarcoidosis, 48 % (23 of 50) patients had visual evoked potential (VEP)

abnormalities, but none had visual symptoms. Fluorescein angiography shows early hypofluorescence and then hyperfluorescence from leakage of disc blood vessels within the lesion [295].

On MRI, the enlargement and contrast enhancement of the orbital portion of the optic nerve are nonspecific for sarcoidosis. The posterior orbital portion of the optic nerve often reveals enlargement and contrast enhancement on MRI and CT, and the optic foramen is often enlarged. Sarcoidosis may extend even more posteriorly to infiltrate the basal meninges, the intracranial portion of the optic nerve, and the optic chiasm [296].

Pathology

Histologically, the optic nerve can be infiltrated by noncaseating granulomas consisting of epithelioid and inflammatory foreign-body giant cells. Asteroids, star-shaped acidophilic bodies, and Schaumann bodies, ovoid, basophilic, birefringent calcium oxalate crystals, may be found within or surrounded by the epithelioid or giant cells [301].

Management

Corticosteroids are the main treatment of sarcoidosis. Oral prednisone at 40–80 mg daily is recommended for neurosarcoidosis. Higher pulse treatments are required when patients are unresponsive. Steroid-sparing agents, such as cyclosporine, azathioprine, methotrexate, and cyclophosphamide, may be required for long-term immunosuppression [302].

Idiopathic Perioptic Neuritis

Epidemiology

Perioptic neuritis affects older patients with a range from 24 to 60 years of age, in which 36 % are older than 50 years of age, compared to optic neuritis, in which 15 % are older than 50 years of age. The exact prevalence of this rare disorder is not known at this time [303, 304].

Symptoms and Signs

Perioptic neuritis may manifest as orbital or ocular pain, decreased vision, and a normal or swollen optic disc that may mimic acute optic neuritis. It is usually an isolated, idiopathic disorder that involves inflammation of the optic nerve sheath [303]. In contrast to optic neuritis that affects central vision, paracentral or arcuate defects are more commonly seen in perioptic neuritis. Although vision often spontaneously recovers in optic neuritis, visual loss often progresses over weeks in perioptic neuritis [304].

Diagnostic Testing

If vitreous cells or retinal infiltrates are seen, then screening for sarcoidosis, syphilis, Lyme disease, and tuberculosis is necessary on serum and CSF. CSF results for these disorders would reveal a normal opening pressure and a mild pleocytosis [303].

In perioptic neuritis, MRI enhancement of the optic nerve with occasional streaks of enhancement of the orbital fat with or without extraocular muscle enhancement can be seen [304]. Enhancement of the lesion on T_1-fat-suppressed imaging is nonspecific but is also highly suggestive of this disorder [305].

Pathology

On histopathology, lymphocytic infiltration and fibrotic thickening of the optic nerve sheath with foci of degenerating collagen can be seen [306]. Granulomatous inflammation in the nerve sheath, vasculitis in the nerve sheath, and optic nerve demyelination or infarction have also been reported [306, 307].

Management

In contrast to patients with optic neuritis, those with perioptic neuritis often experience recurrence of visual loss and are not predisposed to developing a demyelinating disease. In contrast to the corticosteroid treatment protocol of the ONTT for patients with optic neuritis, oral prednisone is given at 80 mg daily [304]. Other steroid-sparing agents may need to be administered on a long-term basis to prevent irreversible visual loss and to induce remission in some patients.

Infectious Infiltrative Optic Neuropathies

Tuberculosis

Epidemiology

Mycobacterium tuberculosis is an obligate aerobe and facultative intracellular parasite that can

survive in mononuclear phagocytes and is able to invade local lymph nodes to spread by hematogenous routes. Since 1985, the incidence of tuberculosis has increased in association with the acquired immunodeficiency syndrome (AIDS), affecting adults 25–40 years of age and during a later peak about 70 years of age [308].

Symptoms and Signs

As a granulomatous inflammatory disease, tuberculosis causes a papillitis more often than it infiltrates the optic nerve [308]. Lana-Peixoto et al. [309] reported an intrinsic tuberculoma of the left intracranial optic nerve on autopsy of a 1.5-year-old child with tuberculous meningitis and disseminated military tuberculosis. In a report by Iraci et al. [310], a 25-year-old man with severe visual loss, diabetes insipidus, and sexual impotence from tuberculous meningitis had a tuberculoma encasing and growing into the anterior optic pathways. Biopsy confirmed the diagnosis, and antituberculous treatment led to recovery of vision in one eye.

Neuroimaging

MRI of the brain often reveals basilar meningeal enhancement and communicating or non-communicating hydrocephalus. Tuberculomas in the brain parenchyma and optic pathways appear as multiple ring-enhancing nodular lesions that represent caseating granulomas. Old tuberculomas often calcify [311].

The primary diagnostic and screening test for tuberculosis is the tuberculin skin test with purified protein derivative and is positive in 50–80 % of cases. CSF analysis reveals a lymphocytic predominance with elevated protein and decreased glucose. CSF acid-fast bacillus smear is positive in about one-fourth of cases. CSF culture is positive in about one-third of cases. CSF polymerase chain reaction testing is not sensitive but is specific [312].

Pathology

Small white tubercles are scattered mainly over the basal meninges. The tuberculomas can both encase and invade the optic nerve to cause an infiltrative and compressive optic neuropathy. They consist of a central core of caseation surrounded by epithelioid cells, giant cells, lymphocytes, plasma cells, and connective tissue. An exudate, consisting of fibrin, lymphocytes, plasma cells, and other monocytes, also obliterates the pontine and interpenduncular cisterns and can spread to the optic chiasm and cranial nerves via the subarachnoid space [313].

Management

The treatment of tuberculosis requires early treatment. If resistance to isoniazid and rifampin is suspected, then pyrazinamide and ethambutol should be added. Pyridoxine is added to prevent peripheral neuropathy from isoniazid neurotoxicity. Prednisone or dexamethasone for edema from tuberculous meningitis improves morbidity and mortality. An infectious disease specialist should also be consulted for management [313].

Cryptococcosis

Epidemiology

Cryptococcus neoformans is an opportunistic fungus that often infects those with underlying illness or immunodeficiency, such as AIDS. Since the development of antiretroviral therapy and fluconazole prophylaxis, the incidence of cryptococcal meningitis has decreased. Without these medications, cryptococcal meningitis is one of the most common CNS complications of immunocompromised patients in the developing world [314]. It affects adults more commonly than children.

Symptoms and Signs

Visual loss may be either acute and severe, occurring in less than 24 h, or gradually progressive. Patients may begin with mild visual loss and then progress to severe visual impairment over weeks to months. In a study by Rex et al. [315], the predictive factors for either acute or gradual visual loss were the presence of papilledema, an elevated CSF opening pressure, and a positive CSF India ink preparation. Medications that reduced intracranial pressure most consistently improved vision in patients who had gradually progressive visual loss. Corticosteroids did not significantly improve visual outcome.

In a study of 80 human immunodeficiency virus (HIV) seropositive patients with cryptococcal infection [316], 32.5 % (26 of 80) patients developed papilledema. Visual loss and sixth nerve palsy occurred in 9 %, and optic atrophy was observed in 2.5 % of patients. Among the 62 patients treated with oral conazoles, optic nerve-related visual loss was less frequent compared to the 18 patients treated with amphotericin B or a combination of amphotericin B and conazoles. Although direct invasion of intraocular structures by *Cryptococcal neoformans* was a rare complication in this study, direct invasion of the optic nerve by the organism has been demonstrated so far in at least 40 patients [315].

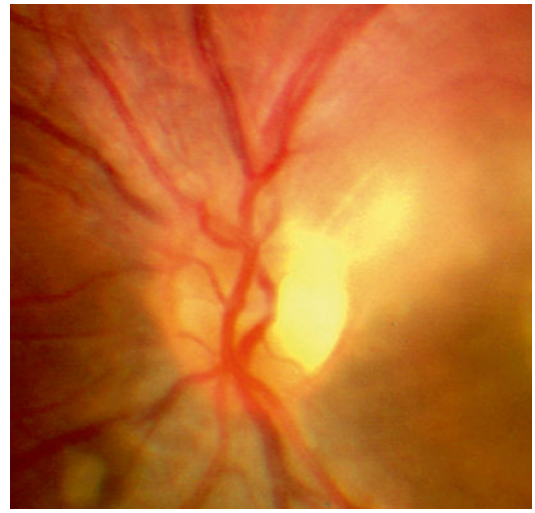

Fig. 4.17 Optic nerve head infiltrated by toxoplasmosis [Reprinted from Kanski JJ. Optic Nerve Head. In: Kanski JJ. Signs in Ophthalmology: Causes and Differential Diagnosis. New York, NY: Elsevier; 2010;264–302. With permission from Elsevier]

Pathology

Cryptococcal organisms can infiltrate the optic nerve to cause visual loss over several days. In a pathological study of a patient with AIDS who developed cryptococcal meningitis [317], focal necrosis of the right intracanalicular optic nerve and the left intraorbital optic nerve adjacent to the optic canal was thought to have caused sudden bilateral visual loss. The meninges surrounding the optic nerve, chiasm, and tracts were filled with cryptococcal organisms. Blood vessels supplying the optic chiasm were normal. Generalized cerebral edema and vacuolization of periventricular white matter were also observed. The visual loss from cryptococcosis can also occur more gradually over a period of months. Cryptococcal organisms in the optic nerve sheath have been shown to be present at the time of sheath fenestration. Despite the visual loss that can occur from papilledema in cryptococcal meningitis, it was concluded that the poor visual outcome after this procedure could have been related to the direct invasion of cryptococcal organisms into the optic nerve [318–321].

Diagnostic Testing

MRI of the brain reveals basilar meningeal enhancement and gelatinous-appearing pseudocysts extending along enlarged perivascular spaces, especially in the basal ganglia [322].

CSF analysis reveals a lymphocytic predominance, but polymorphonuclear cells may be present; protein is usually 50–1,000 mg/dL, and glucose is often less than 40 mg/dL. A definite diagnosis of cryptococcal meningitis is established by a positive CSF culture for *C. neoformans*, a positive CSF India ink stain, or a reactive CSF cryptococcal antigen test [323].

Management

For acute therapy of cryptococcal meningitis, intravenous amphotericin B with oral flucytosine for at least 2 weeks is followed by oral fluconazole to complete a 10-week course until the CSF is sterile. After this 10-week course, if CSF is still not sterile, maintenance therapy with a lower dose of fluconazole should be started. If the patient has AIDS, then antiretroviral therapy needs to be started. An infectious disease specialist should also be consulted for management [324].

Other Infectious Etiologies

Although toxoplasmosis and cytomegalovirus commonly cause a posterior uveitis, rare evidence shows that these organisms can primarily affect the optic nerve. In a retrospective study of 13 patients with toxoplasmosis affecting the optic nerve head [325], patients with primary toxoplasmic involvement of the optic nerve head (Fig. 4.17) who were treated had a final visual acuity of 20/25 or better. Visual field defects were

arcuate or altitudinal. This anterior toxoplasmic optic neuropathy is difficult to diagnose because there is typically no associated vitritis or chorioretinitis. Cytomegalovirus infiltration of the optic nerve is an unusual manifestation. Only one case report documents the presence of cytomegalovirus invasion of the optic nerve head in a 51-year-old immunocompromised patient suffering from lymphoma. No lymphoma cells were seen in the optic nerve [326].

References

1. Cushing H, Eisenhardt L. Meningiomas: their classification, rational behavior, life history, and surgical end results. Springfield: Thomas; 1938.
2. Wilson WB. Meningiomas of the anterior visual system. Surv Ophthalmol. 1981;26(3):109–27.
3. Dutton JJ. Optic nerve sheath meningiomas. Surv Ophthalmol. 1992;37(3):167–83.
4. Cunliffe IA, Moffat DA, Hardy DG, Moore AT. Bilateral optic nerve sheath meningiomas in a patient with neurofibromatosis type 2. Br J Ophthalmol. 1992;76(5):310–2.
5. Sarkies NJ. Optic nerve sheath meningioma: diagnostic features and therapeutic alternatives. Eye. 1987;1(pt 5):597–602.
6. Wright JE, McNab AA, McDonald WI. Primary optic nerve sheath meningioma. Br J Ophthalmol. 1989;73(12):960–6.
7. Sibony PA, Krauss HR, Kennerdell JS, Maroon JC, Slamovits TL. Optic nerve sheath meningiomas. Clinical manifestations. Ophthalmology. 1984; 91(11):1313–26.
8. Trobe JD, Glaser JS, Post JD, Page LK. Bilateral optic canal meningiomas: a case report. Neurosurgery. 1978;3(1):68–74.
9. Alper MG. Management of primary optic nerve meningiomas. Current status: therapy in controversy. J Clin Neuro Ophthalmol. 1981;1(2):101–17.
10. Hart Jr WM, Burde RM, Klingele TG, Perlmutter JC. Bilateral optic nerve sheath meningio-mas. Arch Ophthalmol. 1980;98(1):149–51.
11. Liano H, Garcia-Alix C, Lousa M, Marquez M, Nombela L, de Miguel J. Bilateral optic nerve meningioma. Eur Neurol. 1982;21(2):102–6.
12. Mark LE, Kennerdell JS, Maroon JC, Rosen-baum AE, Heinz R, Johnson BL. Microsurgical removal of a primary intraorbital meningioma. Am J Ophthalmol. 1978;86(5):704–9.
13. Jakobiec FA, Depot MJ, Kennerdell JS, et al. Combined clinical and computed tomographic diagnosis of orbital glioma and meningioma. Ophthalmology. 1984;91(2):137–55.
14. Tien RD, Chu PK, Hesselink JR, Szumowski J. Intra- and para-orbital lesions: value of fat-suppression MR imaging with paramagnetic contrast enhancement. AJNR Am J Neuroradiol. 1991;12(2): 245–53.
15. Dutton JJ, Anderson RL. Idiopathic inflammatory perioptic neuritis simulating optic nerve sheath meningioma. Am J Ophthalmol. 1985;100(3): 424–30.
16. Ing EB, Garrity JA, Cross SA, Ebersold MJ. Sarcoid masquerading as optic nerve sheath meningioma. Mayo Clin Proc. 1997;72(1):38–43.
17. Liauw L, Vielvoye GJ, de Keizer RJ, van Duinen SG. Optic nerve glioma mimicking an optic nerve meningioma. Clin Neurol Neurosurg. 1996;98(3): 258–61.
18. Nerad JA, Kersten RC, Anderson RL. Hemangioblastoma of the optic nerve. Report of a case and review of literature. Ophthalmology. 1988; 95(3):398–402.
19. Rubio A, Meyers SP, Powers JM, Nelson CN, de Papp EW. Hemangioblastoma of the optic nerve. Hum Pathol. 1994;25(11):1249–51.
20. Kleihues P, Burger PC, Scheithauer BW. The new WHO classification of brain tumours. Brain Pathol. 1993;3(3):255–68.
21. Samples JR, Robertson DM, Taylor JZ, Waller RR. Optic nerve meningioma. Ophthalmology. 1983;90(12):1591–4.
22. Wright JE. Primary optic nerve meningiomas: clinical presentation and management. Trans Sect Ophthalmol Am Acad Ophthalmol Otolaryngol. 1977;83(4 pt 1):617–25.
23. Als E. Intraorbital meningiomas encasing the optic nerve. A report of two cases. Acta Ophthalmol (Copenh). 1969;47(4):900–3.
24. Spencer WH. Primary neoplasms of the optic nerve and its sheaths: clinical features and current concepts of pathogenetic mechanisms. Trans Am Ophthalmol Soc. 1972;70:490–528.
25. Kayan A, Earl CJ. Compressive lesions of the optic nerves and chiasm. Pattern of recovery of vision following surgical treatment. Brain. 1975; 98(1):13–28.
26. Egan RA, Lessell S. A contribution to the natural history of optic nerve sheath meningiomas. Arch Ophthalmol. 2002;120(11):1505–8.
27. Saeed P, Rootman J, Nugent RA, White VA, Mackenzie IR, Koornneef L. Optic nerve sheath meningiomas. Ophthalmology. 2003;110(10):2019–30.
28. Andrews DW, Faroozan R, Yang BP, et al. Fractionated stereotactic radiotherapy for the treatment of optic nerve sheath meningiomas: preliminary observations of 33 optic nerves in 30 patients with historical comparison to observation with or without prior surgery. Neurosurgery. 2002;51(4): 890–902.
29. Pitz S, Becker G, Schiefer U, et al. Stereotactic fractionated irradiation of optic nerve sheath meningioma: a new treatment alternative. Br J Ophthalmol. 2002;86(11):1265–8.
30. Narayan S, Cornblath WT, Sandler HM, Elner V, Hayman JA. Preliminary visual outcomes after

three-dimensional conformal radiation therapy for optic nerve sheath meningioma. Int J Radiat Oncol Biol Phys. 2003;56(2):537–43.
31. Subramanian PS, Bressler NM, Miller NR. Radiation retinopathy after fractionated stereotactic radiotherapy for optic nerve sheath meningioma. Ophthalmology. 2004;111(3):565–7.
32. Girkin CA, Comey CH, Lunsford LD, Goodman ML, Kline LB. Radiation optic neuropathy after stereotactic radiosurgery. Ophthalmology. 1997; 104(10):1634–43.
33. Stafford SL, Pollock BE, Leavitt JA, et al. A study on the radiation tolerance of the optic nerves and chiasm after stereotactic radiosurgery. Int J Radiat Oncol Biol Phys. 2003;55(5):1177–81.
34. Guyer DR, Miller NR, Long DM, Allen GS. Visual function following optic canal decompression via craniotomy. J Neurosurg. 1985;62(5):631–8.
35. Schrell UM, Rittig MG, Anders M, et al. Hydroxyurea for treatment of unresectable and recurrent meningiomas. II. Decrease in the size of meningiomas in patients treated with hydroxyurea. J Neurosurg. 1997;86(5):840–4.
36. Paus S, Klockgether T, Urbach H, Schlegel U. Meningioma of the optic nerve sheath: treatment with hydroxyurea. J Neurol Neurosurg Psychiatry. 2003;74(9):1348–50.
37. Grunberg SM, Weiss MH, Spitz IM, Ahmadi J, Sadun A, Russell CA, et al. Treatment of unresectable meningiomas with the antiprogesterone agent mifepristone. J Neurosurg. 1991;74(6):861–6.
38. Shields JA. Optic nerve and meningeal tumors. In: Shields JA, editor. Diagnosis and management of orbital tumors. Philadelphia, PA: Saunders; 1989. p. 170–91.
39. Bartley GB, Fatourechi V, Kadrmas EF, et al. The incidence of Graves' ophthalmopathy in Olmsted County, Minnesota. Am J Ophthalmol. 1995;120: 511–7.
40. Friedman JM, Fialkow PJ. The genetics of Graves' disease. Clin Endocrinol Metab. 1978;7(1):47–65.
41. Feldon SE, Muramatsu S, Weiner JM. Clinical classification of Graves' ophthalmopathy. Identification of risk factors for optic neuropathy. Arch Ophthalmol. 1984;102(10):1469–72.
42. Kennerdell JS, Rosenbaum AE, El-Hoshy MH. Apical optic nerve compression of dysthyroid optic neuropathy on computed tomography. Arch Ophthalmol. 1981;99(5):807–9.
43. Barrett L, Glatt HJ, Burde RM, Gado MH. Optic nerve dysfunction in thyroid eye disease: CT. Radiology. 1988;167(2):503–7.
44. Trobe JD, Glaser JS, Laflamme P. Dysthyroid optic neuropathy. Clinical profile and rationale for management. Arch Ophthalmol. 1978;96(7):1199–209.
45. Glaser JS. The orbit and neuro-ophthalmology. Semin Neurol. 1986;6(2):124–34.
46. Newell FW. Choroidal folds. The seventh Harry Searls Gradle Memorial lecture. Am J Ophthalmol. 1973;75(6):930–42.
47. Cangemi FE, Trempe CL, Walsh JB. Choroidal folds. Am J Ophthalmol. 1978;86(3):380–7.
48. De La Paz MA, Boniuk M. Fundus manifestations of orbital disease and treatment of orbital disease. Surv Ophthalmol. 1995;40(1):3–21.
49. McKenzie JM, McCullagh EP. Observations against a causal relationship between the longacting thyroid stimulator and ophthalmopathy in Graves' disease. J Clin Endocrinol Metab. 1968;28(8):1177–82.
50. Atta HR, McCreath G, McKillop JH, et al. Ophthalmopathy in early thyrotoxicosis: relationship to thyroid receptor antibodies and effects of treatment. Scott Med J. 1990;35(2):41–4.
51. Wiersinga WM, Smit T, van der Gaag R, Koornneef L. Temporal relationship between onset of Graves' ophthalmopathy and onset of thyroidal Graves' disease. J Endocrinol Invest. 1988;11(8):615–9.
52. Sergott RC, Glaser JS. Graves' ophthalmopathy. A clinical and immunologic review. Surv Ophthalmol. 1981;26(1):1–21.
53. Sridama V, DeGroot LJ. Treatment of Graves' disease and the course of ophthalmopathy. Am J Med. 1989;87(1):70–3.
54. Hallin ES, Feldon SE. Graves' ophthalmopathy: I. Simple CT estimates of extraocular muscle volume. Br J Ophthalmol. 1988;72(9):674–7.
55. Jacobson DH, Gorman CA. Endocrine ophthalmopathy: current ideas concerning etiology, pathogenesis, and treatment. Endocr Rev. 1984;5(2):200–20.
56. Hufnagel TJ, Hickey WF, Cobbs WH, Jakobiec FA, Iwamoto T, Eagle RC. Immunohisto-chemical and ultrastructural studies on the exenterated orbital tissues of a patient with Graves' disease. Ophthalmology. 1984;91(11):1411–9.
57. Jakobiec FA, Font RL. Orbit. In: Spencer WH, editor. Ophthalmic pathology, vol. 3. 3rd ed. Philadelphia, PA: Saunders; 1986. p. 462–601.
58. Han S, Zhang S, Zhang W, et al. CTLA4 polymorphisms and ophthalmopathy in Graves' disease patients: association study and meta-analysis. Hum Immunol. 2006;67(8):618–26.
59. Tomer Y. Genetic susceptibility to autoimmune thyroid disease: past, present, and future. Thyroid. 2010;20(7):715–25.
60. Prabhakar BS, Bahn RS, Smith TJ. Current perspective on the pathogenesis of Graves' disease and ophthalmopathy. Endocr Rev. 2003;24(6):802–35.
61. Douglas RS, Afifiyan NF, Hwang CJ, et al. Increased generation of fibrocytes in thyroid-associated ophthalmopathy. J Clin Endocrinol Metab. 2010; 95(1):430–8.
62. Tsui S, Naik V, Hoa N, et al. Evidence for an association between thyroid-stimulating hormone and insulin-like growth factor 1 receptors: a tale of two antigens implicated in Graves' disease. J Immunol. 2008;181(6):4397–405.
63. Pritchard J, Han R, Horst N, Cruikshank WW, Smith TJ. Immunoglobulin activation of T cell chemoattractant expression in fibroblasts from patients with Graves' disease is mediated through the insulin-like

growth factor I receptor pathway. J Immunol. 2003; 170(12):6348–54.
64. Wakelkamp IM, Baldeschi L, Saeed P, Mourits MP, Prummel MF, Wiersinga WM. Surgical or medical decompression as a first-line treatment of optic neuropathy in Graves' ophthalmopathy? A randomized controlled trial. Clin Endocrinol (Oxf). 2005;63(3): 323–8.
65. Marcocci C, Bartalena L, Tanda ML, et al. Comparison of the effectiveness and tolerability of intravenous or oral glucocorticoids associated with orbital radiotherapy in the management of severe Graves' ophthalmopathy: results of a prospective, single-blind, randomized study. J Clin Endocrinol Metab. 2001;86(8):3562–7.
66. Marcocci C, Bartalena L, Bogazzi F, Bruno-Bossio G, Lepri A, Pinchera A. Orbital radiotherapy combined with high dose systemic glucocorticoids for Graves' ophthalmopathy is more effective than radiotherapy alone: results of a prospective randomized study. J Endocrinol Invest. 1991;14(10): 853–60.
67. Krassas GE, Gogakos A, Boboridis K. Corticosteroids in the medical treatment of thyroid ophthalmopathy: when and how? Somatostatin analogues: where we stand today. Pediatr Endocrinol Rev. 2010;7 Suppl 2:204–9.
68. Carter KD, Frueh BR, Hessburg TP, Musch DC. Long-term efficacy of orbital decompression for compressive optic neuropathy of Graves' eye disease. Ophthalmology. 1991;98(9):1435–42.
69. Hallin ES, Feldon SE, Luttrell J. Graves' ophthalmopathy: III. Effect of transantral orbital decompression on optic neuropathy. Br J Ophthalmol. 1988;72(9):683–7.
70. Shorr N, Neuhaus RW, Baylis HI. Ocular motility problems after orbital decompression for dysthyroid ophthalmopathy. Ophthalmology. 1982;89(4):323–8.
71. Young JD. Ocular complications of transantral decompression for thyrotrophic exophthalmos. Proc R Soc Med. 1971;64(9):929–31.
72. Stiglmayer N, Mladina R, Tomic M, Tojagic M, Juri J, Bubas N, et al. Endonasal endoscopic orbital decompression in patients with Graves' ophthalmopathy. Croat Med J. 2004;45(3):318–22.
73. Shepard KG, Levin PS, Terris DJ. Balanced orbital decompression for Graves' ophthal-mopathy. Laryngoscope. 1998;108(11 pt 1):1648–53.
74. Marcocci C, Kahaly GJ, Krassas GE, et al. Selenium and the course of mild Graves' orbitopathy. N Engl J Med. 2011;364(20):1920–31.
75. Durrani OM, Reuser TQ, Murray PI. Infliximab: a novel treatment for sight-threatening thyroid associated ophthalmopathy. Orbit. 2005;24(2):117–9.
76. Komorowski J, Jankiewicz-Wika J, Siejka A, et al. Monoclonal anti-TNF-alpha antibody (infliximab) in the treatment of patient with thyroid associated ophthalmopathy. Klin Oczna. 2007;109(10–12):457–60.
77. Murakami M, Nishimoto N. The value of blocking IL-6 outside of rheumatoid arthritis: current perspective. Curr Opin Rheumatol. 2011;23(3):273–7.
78. Goldbach-Mansky R. Blocking interleukin-1 in rheumatic diseases. Ann N Y Acad Sci. 2009;1182: 111–23.
79. Herold KC, Hagopian W, Auger JA, et al. Anti-CD3 monoclonal antibody in new-onset type 1 diabetes mellitus. N Engl J Med. 2002;346(22):1692–8.
80. Viglietta V, Bourcier K, Buckle GJ, et al. CTLA4 Ig treatment in patients with multiple sclerosis: an open-label, phase 1 clinical trial. Neurology. 2008; 71(12):917–24.
81. Kremer JM, Genant HK, Moreland LW, et al. Results of a two-year follow-up study of patients with rheumatoid arthritis who received a combination of abatacept and methotrexate. Arthritis Rheum. 2008; 58(4):953–63.
82. Naik V, Khadavi N, Naik MN, et al. Biologic therapeutics in thyroid-associated ophthalmopathy: translating disease mechanism into therapy. Thyroid. 2008;18(9):967–71.
83. Tuscano JM, Harris GS, Tedder TF. B lymphocytes contribute to autoimmune disease pathogenesis: current trends and clinical implications. Autoimmun Rev. 2003;2(2):101–8.
84. Vannucchi G, Campi I, Bonomi M, et al. Rituximab treatment in patients with active Graves' orbitopathy: effects on pro-inflammatory and humoral immune reactions. Clin Exp Immunol. 2010;161(3):436–43.
85. Khanna D, Chong KK, Afifiyan NF, et al. Rituximab treatment of patients with severe, corticosteroid-resistant thyroid-associated ophthalmopathy. Ophthalmology. 2010;117(1):133e2–139.
86. Salvi M, Vannucchi G, Campi I, Beck-Peccoz P. Rituximab in the treatment of thyroid eye disease: science fiction? Orbit. 2009;28(4):251–5.
87. Silkiss RZ, Reier A, Coleman M, Lauer SA. Rituximab for thyroid eye disease. Ophthal Plast Reconstr Surg. 2010;26(5):310–4.
88. Jacobiec FA, Jones IS. Orbital inflammations. In: Jones IS, Jakobiec FA, editors. Disease of the orbit. Hagerstown: Harper and Row; 1979. p. 301–410.
89. Curtin HD. Pseudotumor. Radiol Clin N Am. 1987;25(3):583–99.
90. Atlas SW, Grossman RI, Savino PJ, et al. Surface-coil MR of orbital pseudotumor. AJR Am J Roentgenol. 1987;148(4):803–8.
91. Richardson GS. Pituitary tumors. In: Samuels MA, Feske SK, editors. Office practice of neurology. Philadelphia, PA: Churchill Livingstone; 2003. p. 1060–7.
92. Trobe JD. Chromophobe adenoma presenting with a hemianopic temporal arcuate scotoma. Am J Ophthalmol. 1974;77(3):388–92.
93. Hoyt WF, Rios-Montenegro EN, Behrens MM, Eckelhoff RJ. Homonymous hemioptic hypoplasia. Fundoscopic features in standard and red-free illumination in three patients with congenital hemiplegia. Br J Ophthalmol. 1972;56(7):537–45.
94. Gittinger Jr JW. Tumors of the pituitary gland. In: Miller NR, Newman NJ, editors. Walsh and Hoyt's clinical neuro-ophthalmology. 5th ed. Baltimore, MD: Williams & Wilkins; 1999. p. 21412222.

95. Tokumaru AM, Sakata I, Terada H, Kosuda S, Nawashiro H, Yoshii M. Optic nerve hyperintensity on T2-weighted images among patients with pituitary macroadenoma: correlation with visual impairment. AJNR Am J Neuroradiol. 2006;27(2):250–1.
96. Peter M, De Tribolet N. Visual outcome after transsphenoidal surgery for pituitary adenomas. Br J Neurosurg. 1995;9(2):151–7.
97. Randeva HS, Schoebel J, Byrne J, Esiri M, Adams CB, Wass JA. Classical pituitary apoplexy: clinical features, management and outcome. Clin Endocrinol (Oxf). 1999;51(2):181–8.
98. McFadzean RM, Doyle D, Rampling R, Teasdale E, Teasdale G. Pituitary apoplexy and its effect on vision. Neurosurgery. 1991;29(5):669–75.
99. Muller-Jensen A, Ludecke D. Clinical aspects of spontaneous necrosis of pituitary tumors (pituitary apoplexy). J Neurol. 1981;224(4):267–71.
100. Ahmed M, Rifai A, Al-Jurf M, Akhtar M, Woodhouse N. Classical pituitary apoplexy presentation and a follow-up of 13 patients. Horm Res. 1989;31(3): 125–32.
101. Cardoso ER, Peterson EW. Pituitary apoplexy: a review. Neurosurgery. 1984;14(3):363–73.
102. Symon L, Rosenstein J. Surgical management of suprasellar meningioma. Part 1: the influence of tumor size, duration of symptoms, and microsurgery on surgical outcome in 101 consecutivecases. J Neurosurg. 1984;61(4):633–41.
103. Huber A. Eye signs and symptoms in brain tumors. 3rd ed. St. Louis: Mosby; 1976.
104. Rosenberg LF, Miller NR. Visual results after microsurgical removal of meningiomas involving the anterior visual system. Arch Ophthalmol. 1984;102(7): 1019–23.
105. O'Connell JE, Du Boulay EP. Binasal hemianopia. J Neurol Neurosurg Psychiatry. 1973;36(5):697–709.
106. Chicani CF, Miller NR. Visual outcome in surgically treated suprasellar meningiomas. J Neuroophthalmol. 2003;23(1):3–10.
107. Weisberg LA, Numuguchi Y. Neuroimaging in neuroendocrine diseases. Neurol Clin. 1986;4(4): 783–800.
108. Demailly P, Guiot G. [Meningioma of the sellar diaphragm]. Bull Soc Ophtalmol Fr. 1970;70(2): 191–6.
109. Guiot G, Montrieul B, Goutelle A, Comoy J, Langie S. Retro-chiasmatic suprasellar meningiomas. Neurochirurgie. 1970;16(4):273–85.
110. Boulos PT, Dumont AS, Mandell JW, Jane Sr JA. Meningiomas of the orbit: contemporary considerations. Neurosurg Focus. 2001;10(5):E5.
111. Gregorius FK, Hepler RS, Stern WE. Loss and recovery of vision with suprasellar meningiomas. J Neurosurg. 1975;42(1):69–75.
112. Rosenstein J, Symon L. Surgical management of suprasellar meningioma. Part 2: prognosis for visual function following craniotomy. J Neurosurg. 1984; 61(4):642–8.
113. Jaaskelainen J. Seemingly complete removal of histologically benign intracranial meningioma: late recurrence rate and factors predicting recurrence in 657 patients. A multivariate analysis. Surg Neurol. 1986;26(5):461–9.
114. Kajiwara K, Fudaba H, Tsuha M, Ueda H, Mitani T, Nishizaki T, et al. Analysis of recurrences of meningiomas following neurosurgical resection. No Shinkei Geka. 1989;17(12):1125–31.
115. Marks SM, Whitwell HL, Lye RH. Recurrence of meningiomas after operation. Surg Neurol. 1986; 25(5):436–40.
116. Mirimanoff RO, Dosoretz DE, Linggood RM, Ojemann RG, Martuza RL. Meningioma: analysis of recurrence and progression following neurosurgical Resection. J Neurosurg. 1985;62(1):18–24.
117. Carella RJ, Ransohoff J, Newall J. Role of radiation therapy in the management of meningioma. Neurosurgery. 1982;10(3):332–9.
118. Goldsmith BJ, Wara WM, Wilson CB, Larson DA. Postoperative irradiation for subtotally resected meningiomas. A retrospective analysis of 140 patients treated from 1967 to 1990. J Neurosurg. 1994;80(2):195–201.
119. Lunsford LD. Contemporary management of meningiomas: radiation therapy as an adjuvant and radiosurgery as an alternative to surgical removal? J Neurosurg. 1994;80(2):187–90.
120. Miralbell R, Linggood RM, de la Monte S, Convery K, Munzenrider JE, Mirimanoff RO. The role of radiotherapy in the treatment of subtotally resected benign meningiomas. J Neuro-Oncol. 1992;13(2): 157–64.
121. Wilson CB. Meningiomas: genetics, malignancy, and the role of radiation in induction and treatment. The Richard C. Schneider Lecture. J Neurosurg. 1994;81(5):666–75.
122. De Monte F. Current management of meningiomas. Oncology (Williston Park). 1995;9(1):83–91. 96.
123. De Jesus O, Toledo MM. Surgical management of meningioma en plaque of the sphenoid ridge. Surg Neurol. 2001;55(5):265–9.
124. Morita A, Coffey RJ, Foote RL, Schiff D, Gorman D. Risk of injury to cranial nerves after gamma knife radiosurgery for skull base meningiomas: experience in 88 patients. J Neurosurg. 1999;90(1):42–9.
125. Schick U, Bleyen J, Bani A, Hassler W. Management of meningiomas en plaque of the sphenoid wing. J Neurosurg. 2006;104(2):208–14.
126. Bartlett JR. Craniopharyngiomas. An analysis of some aspects of symptomatology, radiology and histology. Brain. 1971;94(4):725–32.
127. Cabezudo JM, Vaquero J, Areitio E, Martinez R, de Sola RG, Bravo G. Craniopharyngiomas: a critical approach to treatment. J Neurosurg. 1981;55(3): 371–5.
128. Onodera J, Kanno C, Okuyama S. Childhood exotropia with craniopharyngioma: report of a case analysis of 13 patients with childhood craniopharyngioma. Folia Ophthalmol Jpn. 1993;44:214–8.
129. Baskin DS, Wilson CB. Surgical management of craniopharyngiomas. A review of 74 cases. J Neurosurg. 1986;65(1):22–7.

130. Barreca T, Perria C, Franceschini R, et al. Diurnal prolactin changes in human cerebro-spinal fluid. Clin Endocrinol (Oxf). 1984;20(6):649–55.
131. Cusimano MD, Kovacs K, Bilbao JM, Tucker WS, Singer W. Suprasellar craniopharyngioma associated with hyperprolactinemia, pituitary lactotroph hyperplasia, and microprolactinoma. J Neurosurg. 1988;69(4):620–3.
132. Cherninkova S, Tzekov H, Karakostov V. Comparative ophthalmologic studies on children and adults with craniopharyngiomas. Ophthalmologica. 1990;201(4):201–5.
133. Matson DD, Crigler Jr JF. Management of craniopharyngioma in childhood. J Neurosurg. 1969; 30(4):377–90.
134. Waga S, Morikawa A, Sakakura M. Craniopharyngioma with midbrain involvement. Arch Neurol. 1979;36(5):319–20.
135. Inagaki M, Suzuki T, Nakano N, Sekimoto S, Ishikawa H, Kitano S. Analysis of two types of see-saw nystagmus. Nippon Ganka Gakkai Zasshi. 1983;87(7):498–506.
136. Osborne AG. Miscellaneous tumors, cysts, and metastases. In: Osborne AG, editor. Diagnostic neuroradiology. St. Louis: Mosby-Year Book; 1994. p. 626–65.
137. Arseni C, Maretsis M. Craniopharyngioma. Neurochirurgia (Stuttg). 1972;15(1):25–32.
138. Adamson TE, Wiestler OD, Kleihues P, Yasargil MG. Correlation of clinical and pathological features in surgically treated craniopharyngiomas. J Neurosurg. 1990;73(1):12–7.
139. Kalapurakal JA. Radiation therapy in the management of pediatric craniopharyngiomas: a review. Childs Nerv Syst. 2005;21(8–9):808–16.
140. Repka MX, Miller NR, Miller M. Visual outcome after surgical removal of craniopharyngiomas. Ophthalmology. 1989;96(2):195–9.
141. Jacobson DM. Symptomatic compression of the optic nerve by the carotid artery: clinical profile of 18 patients with 24 affected eyes identified by magnetic resonance imaging. Ophthalmology. 1999; 106(10):1994–2004.
142. Caprioli J, Fagadau W, Lesser R. Acute monocular visual loss secondary to anterior communicating artery aneurysm in a patient with sickle cell disease. Ann Ophthalmol. 1983;15(9):873–6.
143. Chan JW, Hoyt WF, Ellis WG, Gress D. Pathogenesis of acute monocular blindness from leaking anterior communicating artery aneurysms: report of six cases. Neurology. 1997;48(3):680–3.
144. Date I, Akioka T, Ohmoto T. Penetration of the optic chiasm by a ruptured anterior communicating artery aneurysm. J Neurosurg. 1997;87(2):324–6.
145. Durston JH, Parsons-Smith BG. Blindness due to aneurysm of anterior communicating artery. With recovery following carotid ligation. Br J Ophthalmol. 1970;54(3):170–6.
146. Hook O, Norlen G. Aneurysms of the anterior communicating artery. Acta Neurol Scand. 1964;40:219–40.
147. Peiris JB, Ross Russell RW. Giant aneurysms of the carotid system presenting as visual field defect. J Neurol Neurosurg Psychiatry. 1980;43(12): 1053–64.
148. Norwood EG, Kline LB, Chandra-Sekar B, Harsh III GR. Aneurysmal compression of the anterior visual pathways. Neurology. 1986;36(8):1035–41.
149. Cunningham RD, Sewell JJ. Aneurysm of the ophthalmic artery with drusen of the optic nerve head. Am J Ophthalmol. 1971;72(4):743–5.
150. Stern WH, Ernest JT. Intracranial ophthalmic artery aneurysm. Am J Ophthalmol. 1975;80(2):203–6.
151. Parkinson D, Jain KK, Johnston JB. Saccular aneurysm of the ophthalmic artery: report of an unusual case. Can J Surg. 1961;4:229–32.
152. Kikuchi K, Kowada M. Case report: saccular aneurysm of the intraorbital ophthalmic artery. Br J Radiol. 1994;67(803):1134–5.
153. Rubinstein MK, Wilson G, Levin DC. Intraorbital aneurysms of the ophthalmic artery. Report of a unique case and review of the literature. Arch Ophthalmol. 1968;80(1):42–4.
154. Jea A, Baskaya MK, Morcos JJ. Penetration of the optic nerve by an internal carotid artery-ophthalmic artery aneurysm: case report and literature review. Neurosurgery. 2003;53(4):996–9.
155. Beatty RA. Splitting of the optic nerve by a carotid-ophthalmic artery aneurysm. J Neurosurg. 1986; 65(4):560–2.
156. Yanaka K, Matsumaru Y, Kamezaki T, Nose T. Ruptured aneurysm of the ophthalmic artery trunk demonstrated by three-dimensional rotational angiography: case report. Neurosurgery. 2002;51(4): 1066–9.
157. Fujita A, Tamaki N, Yasuo K, Nagashima T, Ehara K. Complete penetration of the optic chiasm by an unruptured aneurysm of the ophthalmic segment: case report. Surg Neurol. 2002;57(2):130–4.
158. Barat JL, Marchal JC, Bracard S, Auque J, Lepoire J. Mucoceles of the sphenoidal sinus. Report of six cases and review of the literature. J Neuroradiol. 1990;17(2):135–51.
159. Hamard H, Sales MJ, Labetoulle C, Chodkiewicz JP, Roux F. Mucoceles of the sphenoid sinus and their ophthalmological manifestations. J Fr Ophtalmol. 1985;8(10):645–52.
160. Bregeat P. Ophthalmic manifestations of sphenoidal mucoceles. Ann Ophthalmol. 1977;9(3):259–66.
161. Kosling S, Hintner M, Brandt S, Schulz T, Bloching M. Mucoceles of the sphenoid sinus. Eur J Radiol. 2004;51(1):1–5.
162. Chen HJ, Kao LY, Lui CC. Mucocele of the sphenoid sinus with the apex orbitae syndrome. Surg Neurol. 1986;25(1):101–4.
163. Moriyama H, Hesaka H, Tachibana T, Honda Y. Mucoceles of ethmoid and sphenoid sinus with visual disturbance. Arch Otolaryngol Head Neck Surg. 1992;118(2):142–6.
164. Pompili A, Mastrostefano R, Caroli F, et al. Mucocele of neurosurgical interest: clinical consid-

erations on five cases. Acta Neurochir (Wien). 1990;102(3–4):114–21.
165. Casteels I, De Loof E, Brock P, et al. Sudden blindness in a child: presenting symptom of a sphenoid sinus mucocele. Br J Ophthalmol. 1992;76(8):502–4.
166. el-Fiki ME, Abdel-Fattah HM, el-Deeb AK. Sphenoid sinus mucopyocele with marked intracranial extension: a more common phenomenon in the Third World? Surg Neurol. 1993;39(2):115–9.
167. Yamaguchi K, Ohnuma I, Takahashi S, et al. Magnetic resonance imaging in acute optic neuropathy by sphenoidal mucocele. Int Ophthalmol. 1997; 21(1):9–11.
168. Valvassori GE, Putterman AM. Ophthalmological and radiological findings in sphenoidal mucoceles. Arch Ophthalmol. 1973;90(6):456–9.
169. Hejazi N, Witzmann A, Hassler W. Ocular manifestations of sphenoid mucoceles: clinical features and neurosurgical management of three cases and review of the literature. Surg Neurol. 2001;56(5):338–43.
170. Johnson LN, Hepler RS, Yee RD, Batzdorf U. Sphenoid sinus mucocele (anterior clinoid variant) mimicking diabetic ophthalmoplegia and retrobulbar neuritis. Am J Ophthalmol. 1986;102(1):111–5.
171. Finney HL, Roberts TS. Fibrous dysplasia of the skull with progressive cranial nerve involvement. Surg Neurol. 1976;6(6):341–3.
172. Jackson IT, Hide TA, Gomuwka PK, Laws Jr ER, Langford K. Treatment of cranio-orbital fibrous dysplasia. J Maxillofac Surg. 1982;10(3):138–41.
173. Liakos GM, Walker CB, Carruth JA. Ocular complications in craniofacial fibrous dysplasia. Br J Ophthalmol. 1979;63(9):611–6.
174. Mochimatsu Y, Kuwana N, Fujino H. Experience in optic canal decompression in fibrous dysplasia. Neurol Med Chir (Tokyo). 1983;23(3):227–32.
175. Saito K, Suzuki Y, Nehashi K, Sugita K. Unilateral extradural approach for bilateral optic canal release in a patient with fibrous dysplasia. Surg Neurol. 1990;34(2):124–8.
176. Arroyo JG, Lessell S, Montgomery WW. Steroid-induced visual recovery in fibrous dysplasia. J Clin Neuro Ophthalmol. 1991;11(4):259–61.
177. Bocca G, de Vries J, Cruysberg JR, Boers GH, Monnens LA. Optic neuropathy in McCune-Albright syndrome: an indication for aggressive treatment. Acta Paediatr. 1998;87(5):599–600.
178. Mahapatra AK, Gupta PK, Ravi RR. Craniofacial surgery and optic canal decompression in adult fibrous dysplasia. Neurol India. 2003;51(1):123–4.
179. Messaoud R, Zaouali S, Ladjimi A, et al. Compressive optic neuropathy caused by fibrous dysplasia. J Fr Ophtalmol. 2003;26(6):631–6.
180. Chen YR, Wong FH, Hsueh C, Lo LJ. Computed tomography characteristics of non-syndromic craniofacial fibrous dysplasia. Chang Gung Med J. 2002;25(1):1–8.
181. Shah ZK, Peh WC, Koh WL, Shek TW. Magnetic resonance imaging appearances of fibrous dysplasia. Br J Radiol. 2005;78(936):1104–5.
182. Chen YR, Breidahl A, Chang CN. Optic nerve decompression in fibrous dysplasia: indications, efficacy, and safety. Plast Reconstr Surg. 1997;99(1): 22–30.
183. Stumpf DA, Alksne JF, Annegers JF. Neurofibromatosis. Conference statement. National Institutes of Health Consensus Development Conference. Arch Neurol. 1988;45:575–8.
184. Gutmann DH, Collins FS. Recent progress toward understanding the molecular biology of von Recklinghausen neurofibromatosis. Ann Neurol. 1992;31(5):555–61.
185. Dutton JJ. Gliomas of the anterior visual pathway. Surv Ophthalmol. 1994;38(5):427–52.
186. Lubs ML, Bauer MS, Formas ME, Djokic B. Lisch nodules in neurofibromatosis type 1. N Engl J Med. 1991;324(18):1264–6.
187. Thiagalingam S, Flaherty M, Billson F, North K. Neurofibromatosis type 1 and optic pathway gliomas: follow-up of 54 patients. Ophthalmology. 2004;111(3):568–77.
188. Listernick R, Charrow J, Greenwald M, Mets M. Natural history of optic pathway tumors in children with neurofibromatosis type 1: a longitudinal study. J Pediatr. 1994;125(1):63–6.
189. Listernick R, Darling C, Greenwald M, Strauss L, Charrow J. Optic pathway tumors in children: the effect of neurofibromatosis type 1 on clinical manifestations and natural history. J Pediatr. 1995; 127(5):718–22.
190. Deliganis AV, Geyer JR, Berger MS. Prognostic significance of type 1 neurofibromatosis (von Recklinghausen disease) in childhood optic glioma. Neurosurgery. 1996;38(6):1114–8.
191. Packer RJ, Bilaniuk LT, Cohen BH, et al. Intracranial visual pathway gliomas in children with neurofibromatosis. Neurofibromatosis. 1988;1(4):212–22.
192. Stern J, Jakobiec FA, Housepian EM. The architecture of optic nerve gliomas with and without neurofibromatosis. Arch Ophthalmol. 1980;98(3):505–11.
193. Lewis RA, Gerson LP, Axelson KA, Riccardi VM, Whitford RP. von Recklinghausen neurofibromatosis. II. Incidence of optic gliomata. Ophthalmology. 1984;91(8):929–35.
194. Anonymous. National Institutes of Health Consensus Development Conference Statement: neurofibromatosis. Bethesda, MD, USA, July 13–15, 1987. Neurofibromatosis. 1988;1(3):172–178.
195. Garvey M, Packer RJ. An integrated approach to the treatment of chiasmatic-hypothalamic gliomas. J Neuro-Oncol. 1996;28(2–3):167–83.
196. Balcer LJ, Liu GT, Heller G, et al. Visual loss in children with neurofibromatosis type 1 and optic pathway gliomas: relation to tumor location by magnetic resonance imaging. Am J Ophthalmol. 2001; 131(4):442–5.
197. Gayre GS, Scott IU, Feuer W, Saunders TG, Siatkowski RM. Long-term visual outcome in patients with anterior visual pathway gliomas. J Neuroophthalmol. 2001;21(1):1–7.

198. Brand WN, Hoover SV. Optic glioma in children. Review of 16 cases given megavoltage radiation therapy. Childs Brain. 1979;5(5):459–66.
199. Miller NR, Iliff WJ, Green WR. Evaluation and management of gliomas of the anterior visual pathways. Brain. 1974;97(4):743–54.
200. Wright JE, McNab AA, McDonald WI. Optic nerve glioma and the management of optic nerve tumours in the young. Br J Ophthalmol. 1989;73(12):967–74.
201. Hoyt WF, Fletcher WA, Imes RK. Chiasmal gliomas. Appearance and long-term changes demonstrated by computerized tomography. Prog Exp Tumor Res. 1987;30:113–21.
202. Hoyt WF, Baghdassarian SA. Optic glioma of childhood. Natural history and rationale for conservative management. Br J Ophthalmol. 1969;53(12):793–8.
203. Myles ST, Murphy SB. Gliomas of the optic nerve and chiasm. Can J Ophthalmol. 1973;8(4):508–14.
204. Hovland KR, Ellis PP. Hemorrhagic glaucoma with optic nerve glioma. Arch Ophthalmol. 1966;75(6):806–9.
205. Buchanan TA, Hoyt WF. Optic nerve glioma and neovascular glaucoma: report of a case. Br J Ophthalmol. 1982;66(2):96–8.
206. Donaldson DD. Atlas of external diseases of the eye: anterior chamber, iris, and ciliary body. St. Louis: Mosby; 1973.
207. Rush JA, Younge BR, Campbell RJ, MacCarty CS. Optic glioma. Long-term follow-up of 85 histopathologically verified cases. Ophthalmology. 1982;89(11):1213–9.
208. Davis PC, Hoffman Jr JC, Weidenheim KM. Large hypothalamic and optic chiasm gliomas in infants: difficulties in distinction. AJNR Am J Neuroradiol. 1984;5(5):579–85.
209. De Sousa AL, Kalsbeck JE, Mealey Jr J, Ellis FD, Muller J. Optic chiasmatic glioma in children. Am J Ophthalmol. 1979;87(3):376–81.
210. Borit A, Richardson Jr EP. The biological and clinical behaviour of pilocytic astrocytomas of the optic pathways. Brain. 1982;105(pt 1):161–87.
211. Albright AL, Sclabassi RJ, Slamovits TL, Bergman I. *Spasmus nutans* associated with optic gliomas in infants. J Pediatr. 1984;105(5):778–80.
212. DeSousa AL, Kalsbeck JE, Mealey Jr J, Fitzgerald J. Diencephalic syndrome and its relation to opticochiasmatic glioma: review of twelve cases. Neurosurgery. 1979;4(3):207–9.
213. Laue L, Comite F, Hench K, Loriaux DL, Cutler Jr GB, Pescovitz OH. Precocious puberty associated with neurofibromatosis and optic gliomas. Treatment with luteinizing hormone releasing hormone analogue. Am J Dis Child. 1985;139(11):1097–100.
214. Kingsley DP, Kendall BE. CT of the adverse effects of therapeutic radiation of the central nervous system. AJNR Am J Neuroradiol. 1981;2(5):453–60.
215. Imes RK, Hoyt WF. Magnetic resonance imaging signs of optic nerve gliomas in neuro-fibromatosis 1. Am J Ophthalmol. 1991;111(6):729–34.
216. Fletcher WA, Imes RK, Hoyt WF. Chiasmal gliomas: appearance and long-term changes demonstrated by computerized tomography. J Neurosurg. 1986;65(2):154–9.
217. Haik BG, Saint Louis L, Bierly J, et al. Magnetic resonance imaging in the evaluation of optic nerve gliomas. Ophthalmology. 1987;94(6):709–17.
218. Brodsky MC. The "pseudo-CSF" signal of orbital optic glioma on magnetic resonance imaging: a signature of neurofibromatosis. Surv Ophthalmol. 1993;38(2):213–8.
219. Seiff SR, Brodsky MC, MacDonald G, Berg BO, Howes Jr EL, Hoyt WF. Orbital optic glioma in neurofibromatosis. Magnetic resonance diagnosis of perineural arachnoidal gliomatosis. Arch Ophthalmol. 1987;105(12):1689–92.
220. Imes RK, Hoyt WF. Childhood chiasmal gliomas: update on the fate of patients in the 1969 San Francisco Study. Br J Ophthalmol. 1986;70(3):179–82.
221. Duffner PK, Cohen ME, Myers MH, Heise HW. Survival of children with brain tumors: SEER Program, 1973–1980. Neurology. 1986;36(5):597–601.
222. Rootman J. Diseases of the orbit: a multidisciplinary approach. London: Lippincott; 1988.
223. Marquardt MD, Zimmerman LE. Histopathology of meningiomas and gliomas of the optic nerve. Hum Pathol. 1982;13(3):226–35.
224. Wilson WB, Finkel RS, McCleary L, Dreisbach JN, Rak K. Large cystic optic glioma. Neurology. 1990;40(12):1898–900.
225. Goodman SJ, Rosenbaum AL, Hasso A, Itabashi H. Large optic nerve glioma with normal vision. Arch Ophthalmol. 1975;93(10):991–5.
226. North American Study Group for Optic Glioma. Tumor spread in unilateral optic glioma: study report no. 2. Neurofibromatosis. 1989;2:195.
227. Bruggers CS, Friedman HS, Phillips PC, et al. Leptomeningeal dissemination of optic pathway gliomas in three children. Am J Ophthalmol. 1991;111(6):719–23.
228. Poussaint TY, Barnes PD, Nichols K, et al. Diencephalic syndrome: clinical features and imaging findings. AJNR Am J Neuroradiol. 1997;18(8):1499–505.
229. Liu GT, Lessell S. Spontaneous visual improvement in chiasmal gliomas. Am J Ophthalmol. 1992;114(2):193–201.
230. Parazzini C, Triulzi F, Bianchini E, et al. Spontaneous involution of optic pathway lesions in neurofibromatosis type 1: serial contrast MR evaluation. AJNR Am J Neuroradiol. 1995;16(8):1711–8.
231. Listernick R, Louis DN, Packer RJ, Gutmann DH. Optic pathway gliomas in children with neurofibromatosis 1: consensus statement from the NF1 Optic Pathway Glioma Task Force. Ann Neurol. 1997;41(2):143–9.
232. Listernick R, Charrow J, Greenwald MJ, Esterly NB. Optic gliomas in children with neurofibromatosis type 1. J Pediatr. 1989;114(5):788–92.

233. Listernick R, Ferner RE, Piersall L, Sharif S, Gutmann DH, Charrow J. Late-onset optic pathway tumors in children with neurofibromatosis 1. Neurology. 2004;63(10):1944–6.
234. Schmandt SM, Packer RJ. Treatment of low-grade pediatric gliomas. Curr Opin Oncol. 2000;12(3): 194–8.
235. Parsa CF, Hoyt CS, Lesser RL, et al. Spontaneous regression of optic gliomas: thirteen cases documented by serial neuroimaging. Arch Ophthalmol. 2001;119(4):516–29.
236. Glaser JS, Hoyt WF, Corbett J. Visual morbidity with chiasmal glioma. Long-term studies of visual fields in untreated and irradiated cases. Arch Ophthalmol. 1971;85(1):3–12.
237. Wisoff JH, Boyett JM, Berger MS, et al. Current neurosurgical management and the impact of the extent of resection in the treatment of malignant gliomas of childhood: a report of the Children's Cancer Group trial no. CCG-945. J Neurosurg. 1998; 89(1):52–9.
238. Janss AJ, Grundy R, Cnaan A, et al. Optic pathway and hypothalamic/chiasmatic gliomas in children younger than age 5 years with a 6-year follow-up. Cancer. 1995;75(4):1051–9.
239. Saving KL, Kimler BF, Vats TS. Intraperitoneal bleomycin for ventriculoperitoneal spread of a hypothalamic astrocytoma. Cancer Drug Deliv. 1986;3(3): 205–10.
240. Trigg ME, Swanson JD, Letellier MA. Metastasis of an optic glioma through a ventriculoperitoneal shunt. Cancer. 1983;52(4):599–601.
241. West GA, Berger MS, Geyer JR. Childhood optic pathway tumors associated with ascites following ventriculoperitoneal shunt placement. Pediatr Neurosurg. 1994;21(4):254–8.
242. Constine LS, Woolf PD, Cann D, et al. Hypothalamic-pituitary dysfunction after radiation for brain tumors. N Engl J Med. 1993;328(2):87–94.
243. Cappelli C, Grill J, Raquin M, et al. Long-term follow up of 69 patients treated for optic pathway tumours before the chemotherapy era. Arch Dis Child. 1998;79(4):334–48.
244. Grill J, Couanet D, Cappelli C, et al. Radiation-induced cerebral vasculopathy in children with neurofibromatosis and optic pathway glioma. Ann Neurol. 1999;45(3):393–6.
245. Tao ML, Barnes PD, Billett AL, et al. Childhood optic chiasm gliomas: radiographic response following radiotherapy and long-term clinical outcome. Int J Radiat Oncol Biol Phys. 1997;39(3):579–87.
246. Packer RJ. Chemotherapy: low-grade gliomas of the hypothalamus and thalamus. Pediatr Neurosurg. 2000;32(5):259–63.
247. Hoyt WF, Meshel LG, Lessell S, Schatz NJ, Suckling RD. Malignant optic glioma of adulthood. Brain. 1973;96(1):121–32.
248. Harper CG, Stewart-Wynne EG. Malignant optic gliomas in adults. Arch Neurol. 1978;35(11):731–5.
249. Spoor TC, Kennerdell JS, Martinez AJ, Zorub D. Malignant gliomas of the optic nerve pathways. Am J Ophthalmol. 1980;89(2):284–92.
250. Hamilton AM, Garner A, Tripathi RC, Sanders MD. Malignant optic nerve glioma. Report of a case with electron microscope study. Br J Ophthalmol. 1973;57(4):253–64.
251. Albers GW, Hoyt WF, Forno LS, Shratter LA. Treatment response in malignant optic glioma of adulthood. Neurology. 1988;38(7):1071–4.
252. Brodovsky S, ten Hove MW, Pinkerton RM, Ludwin SK, Smith RM. An enhancing optic nerve lesion: malignant glioma of adulthood. Can J Ophthalmol. 1997;32(6):409–13.
253. Hufnagel TJ, Kim JH, Lesser R, et al. Malignant glioma of the optic chiasm eight years after radiotherapy for prolactinoma. Arch Ophthalmol. 1988; 106(12):1701–5.
254. Millar WS, Tartaglino LM, Sergott RC, Friedman DP, Flanders AE. MR of malignant optic glioma of adulthood. AJNR Am J Neuroradiol. 1995;16(8): 1673–6.
255. Dario A, Iadini A, Cerati M, Marra A. Malignant optic glioma of adulthood. Case report and review of the literature. Acta Neurol Scand. 1999;100(5): 350–3.
256. Gritzman MC, Snyckers FD, Proctor NS. Ganglioglioma of the optic nerve. A case report. S Afr Med J. 1983;63(22):863–5.
257. Lu WY, Goldman M, Young B, Davis DG. Optic nerve ganglioglioma. Case report. J Neurosurg. 1993;78(6):979–82.
258. Wahl RW, Dillard Jr SH. Multiple ganglioneuromas of the central nervous system. Arch Pathol. 1972;94(2):158–64.
259. Terry TL, Dunphy EB. Metastatic carcinoma in both optic nerves simulating retrobulbar neuritis. Arch Ophthalmol. 1993;10:611–4.
260. Katz JL, Valsamis MP, Jampel RS. Ocular signs in diffuse carcinomatous meningitis. Am J Ophthalmol. 1961;52:681–90.
261. Fischer-Williams M, Bosanquet FD, Daniel PM. Carcinomatosis of the meninges; a report of three cases. Brain. 1955;78(1):42–58.
262. Little JR, Dale AJ, Okazaki H. Meningeal carcinomatosis. Clinical manifestations. Arch Neurol. 1974;30(2):138–43.
263. Olson ME, Chernik NL, Posner JB. Leptomeningeal metastasis from systemic cancer: a report of 47 cases. Trans Am Neurol Assoc. 1971;96:291–3.
264. Susac JO, Smith JL, Powell JO. Carcinomatous optic neuropathy. Am J Ophthalmol. 1973;76(5): 672–9.
265. Appen RE, de Venecia G, Selliken JH, Giles LT. Meningeal carcinomatosis with blindness. Am J Ophthalmol. 1978;86(5):661–5.
266. Samuels MA, Feske SK. Office practice of neurology. 2nd ed. Philadelphia, PA: Churchill Livingstone; 2003.

267. Shields JA, Shields CL. Intraocular tumors: a text and atlas. Philadelphia, PA: Saunders; 1992.
268. Ferry AP, Font RL. Carcinoma metastatic to the eye and orbit. I. A clinicopathologic study of 227 cases. Arch Ophthalmol. 1974;92(4):276–86.
269. Shields JA, Shields CL, Singh AD. Metastatic neoplasms in the optic disc: the 1999 Bjerrum Lecture: part 2. Arch Ophthalmol. 2000;118(2):217–24.
270. Mack HG, Jakobiec FA. Isolated metastases to the retina or optic nerve. Int Ophthalmol Clin. 1997; 37(4):251–60.
271. Arnold AC, Hepler RS, Foos RY. Isolated metastasis to the optic nerve. Surv Ophthalmol. 1981;26: 75–83.
272. Spalton DJ, Hitchings RA, Hunter PA, editors; Tan JCH, associate editor; Harry J, pathology advisor. Atlas of clinical ophthalmology. Philadelphia; Edinburgh: Elsevier Mosby; 2005.
273. Lester EP, Ultman JE. Lymphoma. In: William WJ, Beutlar E, Erslev AJ, editors. Hematology. New York: McGraw Hill; 1990. p. 53–6.
274. Akpek EK, Ahmed I, Hochberg FH, et al. Intraocular central nervous system lymphoma: clinical features, diagnosis, and outcomes. Ophthalmology. 1999;106(9):1805–10.
275. Peterson K, Gordon KB, Heinemann MH, DeAngelis LM. The clinical spectrum of ocular lymphoma. Cancer. 1993;72(3):843–9.
276. Davis JL, Miller DM, Ruiz P. Diagnostic testing of vitrectomy specimens. Am J Ophthalmol. 2005; 140(5):822–9.
277. Akpek EK, Foster CS. Primary intraocular lymphoma with a low interleukin 10 to inter-leukin 6 ratio and heterogeneous IgH genearrangement. Arch Ophthalmol. 2000;118(5):731–2.
278. Lanska DJ, Lanska MJ, Tomsak RL. Unilateral optic neuropathy in non-Hodgkin's lymphoma. Neurology. 1987;37(9):1563–4.
279. Miller NR, Iliff WJ. Visual loss as the initial symptom in Hodgkin disease. Arch Ophthalmol. 1975;93(11):1158–61.
280. Zaman AG, Graham EM, Sanders MD. Anterior visual system involvement in non-Hodgkin's lymphoma. Br J Ophthalmol. 1993;77(3):184–7.
281. Kline LB, Garcia JH, Harsh III GR. Lymphomatous optic neuropathy. Arch Ophthalmol. 1984;102(11): 1655–7.
282. Allen RA, Straatsma BR. Ocular involvement in leukemia and allied disorders. Arch Ophthalmol. 1961;66:490–508.
283. Rosenthal AR, Egbert PR, Wilbur JR, Probert JC. Leukemic involvement of the optic nerve. Trans Pac Coast Oto Ophthalmol Soc Annu Meet. 1974;55: 137–58.
284. Ellis W, Little HL. Leukemic infiltration of the optic nerve head. Am J Ophthalmol. 1973;75(5):867–71.
285. Nikaido H, Mishima H, Ono H, Choshi K, Dohy H. Leukemic involvement of the optic nerve. Am J Ophthalmol. 1988;105(3):294–8.
286. Rosenthal AR. Ocular manifestations of leukemia. A review. Ophthalmology. 1983;90(8):899–905.
287. Kincaid MC, Green WR. Ocular and orbital involvement in leukemia. Surv Ophthalmol. 1983;27(4): 211–32.
288. Brown GC, Shields JA, Augsburger JJ, Serota FT, Koch P. Leukemic optic neuropathy. Int Ophthalmol. 1981;3(2):111–6.
289. Wiznia RA, Rose A, Levy AL. Occlusive microvascular retinopathy with optic disc and retinal neovascularization in acute lymphocytic leukemia. Retina. 1994;14(3):253–5.
290. Cramer SC, Glaspy JA, Efird JT, Louis DN. Chronic lymphocytic leukemia and the central nervous system: a clinical and pathological study. Neurology. 1996;46(1):19–25.
291. Clarke E. Cranial and intracranial myelomas. Brain. 1954;77(1):61–81.
292. Bourdette DN, Rosenberg NL. Infiltrative orbitopathy, optic disk edema, and POEMS. Neurology. 1984;34(4):532–3.
293. Galetta SL, Stadtmauer EA, Hicks DG, Raps EC, Plock G, Oberholtzer JC. Reactive lymphohistiocytosis with recurrence in the optic chiasm. J Clin Neuro Ophthalmol. 1991;11(1):25–30.
294. Anthony JJ. Malignant lymphoma associated with hydantoin drugs. Arch Neurol. 1970;22(5):450–4.
295. Laties AM, Scheie HG. Sarcoid granuloma of the optic disk: evolution of multiple small tumors. Trans Am Ophthalmol Soc. 1970;68:219–33.
296. Zajicek JP, Scolding NJ, Foster O, et al. Central nervous system sarcoidosis: diagnosis and management. Q J Med. 1999;92(2):103–17.
297. Mayers M. Ocular sarcoidosis. Int Ophthalmol Clin. 1990;30(4):257–63.
298. Beardsley TL, Brown SV, Sydnor CF, Grimson BS, Klintworth GK. Eleven cases of sarcoidosis of the optic nerve. Am J Ophthalmol. 1984;97(1):62–77.
299. Graham EM, Ellis CJ, Sanders MD, McDonald WI. Optic neuropathy in sarcoidosis. J Neurol Neurosurg Psychiatry. 1986;49(7):756–63.
300. Power WJ, Neves RA, Rodriguez A, Pedroza-Seres M, Foster CS. The value of combined serum angiotensin-converting enzyme and gallium scan in diagnosing ocular sarcoidosis. Ophthalmology. 1995;102(12):2007–11.
301. Gass JD, Olson CL. Sarcoidosis with optic nerve and retinal involvement. A clinicopathologic case report. Trans Am Acad Ophthalmol Otolaryngol. 1973;77(6):OP739–50.
302. Johns CJ, Michele TM. The clinical management of sarcoidosis. A 50-year experience at the Johns Hopkins Hospital. Medicine (Baltimore). 1999;78(2):65–111.
303. Kennerdell JS, Dresner SC. The nonspecific orbital inflammatory syndromes. Surv Ophthalmol. 1984; 29(2):93–103.
304. Purvin V, Kawasaki A, Jacobson DM. Optic perineuritis: clinical and radiographic features. Arch Ophthalmol. 2001;119(9):1299–306.

305. Fay AM, Kane SA, Kazim M, Millar WS, Odel JG. Magnetic resonance imaging of optic perineuritis. J Neuroophthalmol. 1997;17(4):247–9.
306. Margo CE, Levy MH, Beck RW. Bilateral idiopathic inflammation of the optic nerve sheaths. Light and electron microscopic findings. Ophthalmology. 1989;96(2):200–6.
307. Rush JA, Kennerdell JS, Martinez AJ. Primary idiopathic inflammation of the optic nerve. Am J Ophthalmol. 1982;93(3):312–6.
308. Schlernitzauer DA, Hodges III FJ, Bagan M. Tuberculoma of the left optic nerve and chiasm. Arch Ophthalmol. 1971;85(1):75–8.
309. Lana-Peixoto MA, Bambirra EA, Pittella JE. Optic nerve tuberculoma. A case report. Arch Neurol. 1980;37(3):186–7.
310. Iraci G, Giordano R, Gerosa M, Pardatscher K, Tomazzoli L. Tuberculoma of the anterior optic pathways. J Neurosurg. 1980;52(1):129–33.
311. Gupta RK, Gupta S, Singh D, Sharma B, Kohli A, Gujral RB. MR imaging and angiography in tuberculous meningitis. Neuroradiology. 1994;36(2): 87–92.
312. Kox LF, Kuijper S, Kolk AH. Early diagnosis of tuberculous meningitis by polymerase chain reaction. Neurology. 1995;45(12):2228–32.
313. Ranglione WC, O'Brien RJ. Tuberculosis. In: Fauci AS, Braunwald E, Isselbacher KJ, et al., editors. Harrison's principles of internal medicine. 14th ed. New York: McGraw-Hill; 1998. p. 156–67.
314. Subsai K, Kanoksri S, Siwaporn C, Helen L. Neurological complications in AIDS patients: the 1-year retrospective study in Chiang Mai University. Thailand. Eur J Neurol. 2004;11(11):755–9.
315. Rex JH, Larsen RA, Dismukes WE, Cloud GA, Bennett JE. Catastrophic visual loss due to *Cryptococcus neoformans* meningitis. Medicine (Baltimore). 1993;72(4):207–24.
316. Kestelyn P, Taelman H, Bogaerts J, et al. Ophthalmic manifestations of infections with *Cryptococcus neoformans* in patients with the acquired immunodeficiency syndrome. Am J Ophthalmol. 1993;116(6): 721–7.
317. Cohen DB, Glasgow BJ. Bilateral optic nerve cryptococcosis in sudden blindness in patients with acquired immune deficiency syndrome. Ophthalmology. 1993;100(11):1689–94.
318. Kupfer C, McCrane E. A possible cause of decreased vision in cryptococcal meningitis. Invest Ophthalmol. 1974;13(10):801–4.
319. Maslin J, Morand JJ, Menard G, Camparo P. [Cryptococcosis]. Med Trop (Mars). 2002;62(5): 480–3.
320. Ofner S, Baker RS. Visual loss in cryptococcal meningitis. J Clin Neuro Ophthalmol. 1987;7(1):45–8.
321. Tan CT. Intracranial hypertension causing visual failure in cryptococcus meningitis. J Neurol Neurosurg Psychiatry. 1988;51(7):944–6.
322. Mathews VP, Alo PL, Glass JD, Kumar AJ, McArthur JC. AIDS-related CNS cryptococcosis: radiologic-pathologic correlation. Am J Neuroradiol. 1992;13(5):1477–86.
323. Brown RW, Clarke RJ, Gonzales MF. Cytologic detection of *Cryptococcus neoformans* in cerebrospinal fluid. Rapid screening methods. Acta Cytol. 1985;29(2):151–3.
324. Sugar AM, Stern JJ, Dupont B. Overview: treatment of cryptococcal meningitis. Rev Infect Dis. 1990;12 suppl 3:S338–48.
325. Banta JT, Davis JL, Lam BL. Presumed toxoplasmosic anterior optic neuropathy. Ocul Immunol Inflamm. 2002;10(3):201–11.
326. Marmor MF, Egbert PR, Egbert BM, Marmor JB. Optic nerve head involvement with cytomegalovirus in an adult with lymphoma. Arch Ophthalmol. 1978;96(7):1252–4.

Traumatic Optic Neuropathies

5

Jane W. Chan

Traumatic Optic Neuropathy as a Complication of Head Injury

Epidemiology

Traumatic optic neuropathy may be a result of severe head trauma or may be associated with little or no evidence of head injury. Traumatic optic neuropathy occurs in approximately 0.5–5 % of closed head injuries [1] and in 2.5 % of patients with maxillofacial trauma and midface fractures [2]. Loss of consciousness is associated with traumatic optic neuropathy in 40–70 % of cases [3, 4]. In closed head injuries, the site of injury causing blindness is often the forehead or supraorbital ridge, less commonly the temporal region. Patients from 20 to 40 years of age represent the major trauma population who experience traumatic optic neuropathy [5].

The prevalence of severe initial visual loss ranges from about 43 to 56 %. Visual loss may present with no light perception (NLP) to 20/20 with an associated visual field defect. More severe visual loss is usually associated with optic canal fracture. In some studies, 43 % (6/14) [6, 7] to 56 % (13/23) [8] of patients presented with light perception or NLP following traumatic optic neuropathy.

J.W. Chan, M.D. (✉)
Department of Neurology, Neuro-Ophthalmology,
University of Nevada School of Medicine,
975 Kirman Avenue (111), Reno, Nevada 89502, USA
e-mail: worjun@aol.com

Deceleration injury directed to the ipsilateral forehead or to the midface region from motor vehicle and bicycle accidents is the most common cause of traumatic optic neuropathy in 17–63 % of cases [9]. The second most common cause of traumatic optic neuropathy is motorcycle accidents followed by falls in as many as 50 % of cases [9]. Other situations that may cause traumatic optic neuropathy include assault, gunshot wounds, falling objects, skateboarding, and even very minor head injuries. Iatrogenic injury may occur during endoscopic sinus surgery and orbital surgery [9].

Basic Anatomy of the Optic Nerve

To better understand the location and mechanisms of optic nerve injury, the anatomic relationships are reviewed.

Optic Nerve Head

The axons of the retinal ganglion cells (RGCs) converge on the posterior pole of the globe at the optic disc. The intraocular portion of the optic nerve is approximately 1 mm long and is the shortest portion of the nerve. It can be divided into prelaminar and laminar segments. In the prelaminar portion, the optic disc, which is oval shaped and approximately 1.5 mm horizontally × 1.75 mm vertically, consists of unmyelinated axons of the RGCs, astrocytes, capillary-associated cells, and fibroblasts. The central retinal artery and vein traverse centrally from the disc. These axons emerge

J.W. Chan (ed.), *Optic Nerve Disorders: Diagnosis and Management*,
DOI 10.1007/978-1-4614-0691-4_5, © Springer Science+Business Media New York 2014

from the globe as fascicles and pass through the lamina cribrosa to the choroid and sclera in the laminar portion of the optic nerve head [10].

The size of the scleral canal and the angle of exit of the canal from the eye may cause variations in the appearance of the optic disc. A larger scleral canal leads to a larger physiological cup size. A smaller scleral canal causes a small or absent physiological cup and gives the appearance of a crowded optic nervehead [10].

The ophthalmic artery arises from the ophthalmic branch of the internal carotid artery. It passes anteriorly through the optic canal alongside the optic nerve, which is covered with dura. In the orbit, the ophthalmic artery gives rise to the central retinal artery, which enters the optic nerve sheath, approximately 10 mm behind the globe, and extends anteriorly to emerge from the center of the optic disc. The central retinal artery does not directly supply blood to the optic disc. Much of it is derived from the choroidal feeder vessels, short posterior arteries, and some from the pial arterial network, which all contribute to the circle of Zinn-Haller, a perineural arteriolar anastomosis that encircles the optic nerve head. The retrolaminar portion of the optic nerve is supplied by anastomosing branches of the central retinal artery and the pial arteries. The laminar and prelaminar portions of the nerve are mainly supplied by branches of the posterior ciliary arteries (Figs. 5.1 and 5.2). Only a small fraction of the blood supply to the optic nerve head comes from choroidal branches of the posterior ciliary arteries that extend to the optic nerve head [10].

The central retinal vein drains most of the optic nerve head. During chronic compression of the intraorbital optic nerve or after central retinal vein occlusion, optociliary shunt vessels (preexisting anastomosis between superficial disc veins and choroidal veins) may enlarge and shunt venous blood from the retina to the choroids. Eventually, it drains into the vortex veins leading to the superior and inferior ophthalmic veins [10].

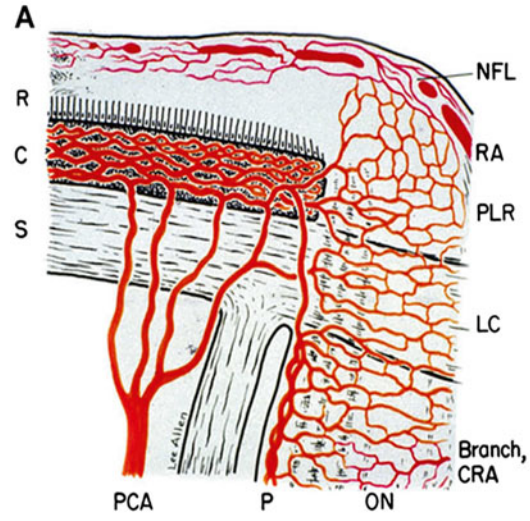

Fig. 5.1 Diagram of the blood supply of the optic nerve head. *Abbreviations*: *A* arachnoid, *C* choroid, *CRA* central retinal artery, *Col. Br.* Collateral branches, *CRV* central retinal vein, *D* dura, *LC* lamina cribrosa, *NFL* surface nerve fiber layer of the disc, *OD* optic disc, *ON* optic nerve; *P* pia, *PCA* posterior ciliary artery, *PR* and *PLR* prelaminar region, *R* retina, *RA* retinal arteriole, *S* sclera, *SAS* subarachnoid space [Reprinted from http://www.medicine.uiowa.edu/eye/AION-part1/. Accessed September 1, 2013. With permission from Sohan S. Hayreh, M.D.]

Orbital Optic Nerve

From the posterior aspect of the globe, the orbital segment of the optic nerve extends to the orbital apex. It is approximately 25 mm long and has a sinuous course that allows free movement of the globe and protects the nerve from injury when there is orbital proptosis [1]. The width of the orbital optic nerve is about 3–4 mm in diameter, twice as wide, mainly because of the myelin produced by oligodendrocytes and its encasement with meninges. Myelination of the axons of RGCs extends from the point where they exit the globe to the point where they synapse in the lateral geniculate nucleus. The myelinated optic nerve is encased with all three layers of the meninges (the dura, arachnoid, and pia mater). The outermost layer is the dura, which is composed of collagen and is continuous with the sclera. At the orbital apex, the dura fuses with the periosteum and with the annulus of Zinn. Underneath the dura is the arachnoid. Arachnoid trabeculae connect this layer with the dura and the underlying pia mater, where capillaries traverse as they enter into the substance of the optic nerve. The subarachnoid space, filled with cerebrospinal fluid (CSF), is continuous with the intracranial portion [10].

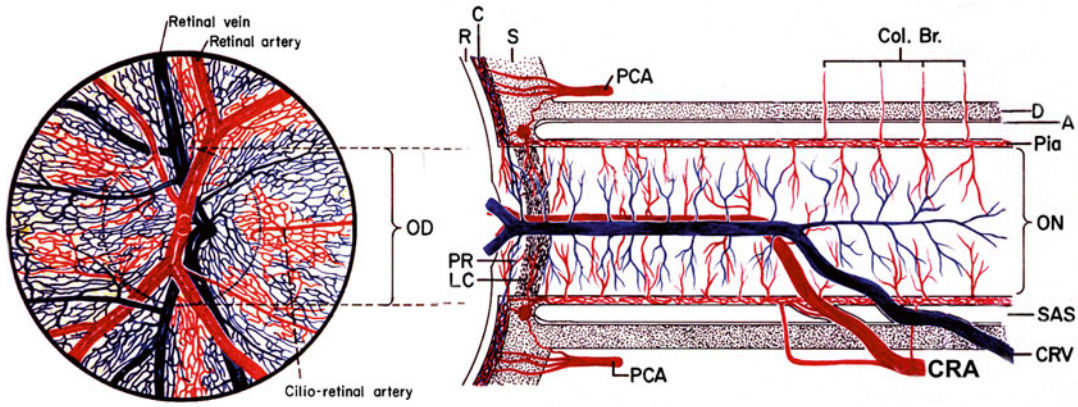

Fig. 5.2 Diagram of the blood supply to the optic nerve. *Abbreviations*: *A* arachnoid, *C* choroid, *CRA* central retinal artery, *Col. Br.* Collateral branches, *CRV* central retinal vein, *D* dura, *LC* lamina cribrosa, *NFL* surface nerve fiber layer of the disc, *OD* optic disc, *ON* optic nerve; *P* pia, *PCA* posterior ciliary artery, *PR* and *PLR* prelaminar region, *R* retina, *RA* retinal arteriole, *S* sclera, *SAS* subarachnoid space [Reprinted from http://www.medicine.uiowa.edu/eye/AION-part1/. Accessed September 1, 2013. With permission from Sohan S. Hayreh, M.D.]

As the optic nerve passes posteriorly toward the optic canal, it is surrounded by orbital fascia, fat, nerves, and vessels. Most of the blood supply to the orbital optic nerve derives from capillaries from the surrounding pial plexus. In the posterior orbit, the optic nerve is crossed superolaterally by the nasociliary branch of the trigeminal nerve, ophthalmic artery, superior ophthalmic vein, and superior division of the oculomotor nerve. The superior rectus, levator palpebrae muscles, trochlear nerve, and frontal branches of the trigeminal nerve are located superior to the optic nerve in the roof of the orbit. Inferior to the optic nerve at the floor of the orbit lie the inferior and medial recti muscles and the inferior division of the oculomotor nerve. Between the optic nerve and the lateral wall of the orbit are the lateral rectus muscle and abducens nerve. Between the lateral rectus muscle and the optic nerve is the ciliary ganglion, parasympathetic postganglionic neurons innervating the constrictor pupillary and ciliary muscles [10].

Regarding the blood supply of the optic nerve, the anterior orbital optic nerve is surrounded by four posterior ciliary arteries that are branches of the ophthalmic artery. In the middle of the orbit, the ophthalmic artery traverses inferolaterally to the optic nerve until it crosses under (or occasionally over) it. In 6 % of cases, the ophthalmic artery can lie medially to the optic nerve as they both reach the orbital apex and pass through the annulus of Zinn, a tendon from the origin of insertion of the four recti muscles [11]. The medial location of the ophthalmic artery is predisposed to injury during a trans-sinus approach for optic nerve decompression [11].

Intracanalicular Optic Nerve

The optic nerve, ophthalmic artery, and sympathetic fibers from the carotid plexus all enter the optic foramen of the optic canal in the apex of the orbital roof. The ophthalmic artery enters the optic canal inferior and lateral to the optic nerve. The length of the optic canal is about 10 mm. It is formed by the two lesser wings of the sphenoid bone. Its thinner medial wall separates the optic nerve from the sphenoid and posterior ethmoid sinuses. In about 4 % of patients the optic nerve may have areas covered only by the nerve sheath and sinus mucosa, without any bony covering between the intracanalicular optic nerve and the adjacent paranasal sinus. These sinuses may eventually enlarge into the optic canals producing pneumosinus dilatans. This finding is often seen with an adjacent optic nerve sheath meningioma [10]. Because the dura of the optic nerve is fused with the periosteum of the optic canal, impact forces that deform bone may be more easily transmitted to the intracanalicular portion of the optic nerve. The intracanalicular optic nerve is also susceptible to injury under the fixed edge of the falciform dural

fold at the edge of the optic canal. The tightly fixed optic nerve within the optic canal is also predisposed to compression from small lesions, arising within the optic canal or at either of its openings, that may be difficult to visualize on thin-section computed tomography (CT) or magnetic resonance imaging (MRI) scanning [10].

Intracranial Optic Nerve

The intracranial optic nerve is covered by a firm fold of dura as it exits the optic canal. The distance between the two optic nerves at this point is about 13 mm, and they extend posteriorly, superiorly, and medially to join at the optic chiasm. The length of the intracranial optic nerve varies from 3 mm to as long as 16 mm, but is usually about 10 mm. If the intracranial optic nerve is shorter than about 12 mm, the optic chiasm is prefixed, in which it is located more anteriorly and superiorly to the sella turcica. If the intracranial optic nerve is longer than 18 mm, the optic chiasm is postfixed, in which it is located more posteriorly to the dorsum sellae. The variation in the length of the optic nerve affects the types of visual field defects caused by tumor in the suprasellar region [10].

Dorsal to the optic nerve is the olfactory tract at the ventral surface of the frontal lobes. Ventral to the optic nerve are the anterior cerebral and anterior communicating arteries. The internal carotid artery from the cavernous sinus may sometimes emerge laterally to the optic nerve. The optic nerve is also adjacent to the internal carotid artery where it bifurcates into the anterior cerebral and middle cerebral arteries and to the proximal portion of the posterior communicating artery. The intracranial optic nerve is supplied by the ophthalmic artery from the internal carotid artery. These anatomic relationships predispose the optic nerve to be injured by traumatic aneurysms of the internal carotid, ophthalmic, and anterior cerebral arteries [10].

Localization of Direct Optic Nerve Injuries from Head Trauma

Direct injury to the optic nerve needs to be distinguished from indirect injury. Direct injury arises from penetrating trauma, such as from orbital fractures associated with midfacial fractures. The most common optic nerve injuries involve posterior indirect injuries, followed by chiasmal, and direct injuries. Direct traumatic optic neuropathy is less common because the laxity of the intraorbital optic nerve allows for both absorption and deflection of the penetrating object. The resilience of the dura to penetration also offers further protection.

If an object penetrates into the orbit, the optic nerve may be directly injured by complete or partial transaction of the nerve, contusion of the nerve, or by compression from hemorrhage or foreign-body impingement [12]. Optic nerve transection occurs as a complication of midfacial trauma and orbital fracture. Visual loss is NLP caused by transection of the optic nerve, perhaps from a bony fragment seen on CT scan.

If orbital hemorrhage is present, an orbital compartment syndrome may occur. An enlarged optic nerve sheath may also be seen on CT. Orbital hemorrhage may be diffuse or localized in the orbit. It is often accompanied by proptosis and ophthalmoplegia. Increased orbital pressure causes injury to the optic nerve, which may be decreased by elevating the head and administering acetazolamide to lower intraocular pressure. If not, lateral canthotomy and drainage of the orbital hemorrhage may be necessary [12].

Orbital emphysema can also occur in the setting of paranasal sinus injury. Thin fractures of the bone lining the orbital wall may produce a ball-valve effect so that air accumulates in the orbit to cause proptosis and compression of the optic nerve. Drainage of air by insertion of a needle into the retroorbital space may resolve this condition [12].

Optic nerve avulsion is often caused by sudden rotation or anterior displacement of the globe with a finger or object to result in optic nerve injury at the lamina cribosa [12]. Funduscopic findings are commonly seen and include peripapillary vitreous hemorrhage, partial or complete optic nerve head avulsion, optic disc swelling, venous congestion, central retinal artery nonperfusion, and retinal edema. In partial and complete avulsion of the optic nerve head, a ring of hemorrhage is formed

around the optic disc. The site of avulsion is seen as a dark crescentic area over the disc. If injury occurs at the orbital optic nerve anterior to the point at which the central retinal artery enters and the central retinal vein exits, arterial and venous obstruction and disc swelling may be seen.

Optic nerve swelling without retinal changes can also occur from hemorrhages in the optic nerve sheath posterior to the origin of the central retinal vessels. Prompt treatment of an optic nerve sheath hematoma may lead to visual recovery. An expanded nerve sheath causing proptosis and a central retinal artery or vein occlusion could indicate the presence of an optic nerve sheath hematoma, especially in the setting of a progressive optic neuropathy. Drainage by sheath fenestration usually restores vision [13, 14].

Localization of Indirect Optic Nerve Injuries from Head Injury

The most common optic nerve injuries involve posterior indirect injuries, followed by chiasmal, and direct injuries [15]. Posterior indirect injury is the most common type of traumatic optic neuropathy and is usually a result of a frontal or midfacial trauma that also may be trivial. The intracranial portion of the nerve is relatively fixed within the bony canal. The orbital bone transfers force from the forehead and brow to the orbital apex [16, 17]. The intracanalicular portion of the optic nerve is the most common site of indirect optic nerve injury [18]. Visual loss is usually immediate, and less often delayed or progressive, with variable visual field defects associated with an afferent pupillary defect and/or dyschromatopsia. Often no ophthalmoscopic signs of injury are seen initially. Injury to the distal optic nerve in the orbit, optic canal, or intracranial cavity usually leads to disc atrophy and pallor after 3–5 weeks. If head trauma with loss of consciousness produces increased intracranial pressure, papilledema may be seen. Optic canal fracture on CT often does not correlate with the severity of the optic neuropathy. It is also imperative to distinguish a preexisting optic neuropathy, which can be observed as optic atrophy in a patient with acute head trauma [9].

The intracranial portion of the optic nerve is least likely to have traumatic damage. Chiasmal injury is uncommon and is usually the result of severe closed head injury or an abrupt traction on the globe. The tethering of the optic nerve within the optic canal may prevent transmission of force to the chiasm. According to a review of 18 cases of autoenucleation [19, 20], 33 % of the optic nerve transections occurred at the anterior chiasm, whereas 55 % of them occurred at the orbital apex. This review and other studies [21, 22] suggest that strong and abrupt tractional forces on the globe are required to cause tears in the optic nerve with chiasmal injury. Clinical findings may include normal central visual acuity, variable visual field defects, such as bitemporal hemianopsia and defects from unilateral lesions of von Willebrand's knee. Anosmia, diabetes insipidus, or other endocrinological disorders, fractures of the skull base, cerebrospinal leakage, meningitis, thalamic injury, and other neurological deficits may also be seen. No treatment is yet available [19].

Diagnosis

Traumatic optic neuropathy is a clinical diagnosis. It usually occurs after head trauma with or without loss of consciousness. Decreased best corrected visual acuity and a relative afferent pupillary defect (RAPD), without other ocular pathology that could account for the visual loss, would support the diagnosis of traumatic optic neuropathy affecting the posterior orbital, intracanalicular, or intracranial portion of the optic nerve. These patients usually have 20/400 or less in the affected eye [15]. More subtle optic nerve injury, which is thought to occur in less than 10 % of cases [4], may present as delayed visual loss.

Examination of the ocular adnexa is important to identify orbital rim fractures and periorbital swelling, which can mimic proptosis. Resistance to retropulsion of the globe and increased intraocular pressure measured by tonometry can help detect retroorbital hemorrhage. Retraction of the swollen eyelids is needed to look for evidence of penetrating ocular injury. Blunt injury to the iris

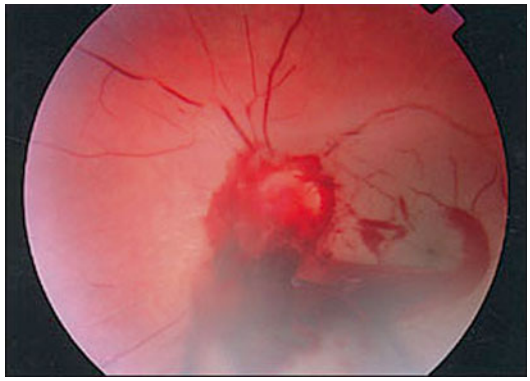

Fig. 5.3 Optic nerve avulsion [Courtesy of Henry Kahn]

can cause hyphema, angle recession, and even lens dislocation [15].

On fundoscopy, a ring of hemorrhage at the site of injury is indicative of partial or complete avulsion of the optic nerve head (Fig. 5.3) [23]. Injury between the globe and where the central retinal vessels enter the optic nerve can cause venous obstruction and traumatic anterior ischemic optic neuropathy [13, 24]. Hemorrhage in the optic nerve sheath posterior to the origin of the central retinal vessels may produce only optic disc swelling [25]. Papilledema from increased intracranial pressure may even be superimposed on traumatic optic neuropathy [26]. Decreased visual acuity with an afferent pupillary defect without intraocular pathology is usually indicative of intracanalicular or intracranial optic nerve injury.

If the patient is unconscious or if the RAPD is absent in bilateral cases, visual evoked potentials (VEP) may help in confirming the suspicion of traumatic optic neuropathy, especially in comatose patients. In unilateral traumatic optic neuropathy, flash VEP amplitudes that are at least 50 % of the normal eye are critical for a good visual outcome [27]. An absent VEP response indicates that visual loss is complete, and recovery of vision is unlikely [28]. An absent electroretinogram (ERG) is associated with a poor potential for visual recovery [29].

Localization of the injury by visual field testing is limited. There is no pathognomonic visual field loss diagnostic of optic nerve injury. Altitudinal visual field defects; central, paracentral, and centrocecal scotomas; and generalized field constriction have been reported [3, 30–32]. Humphrey visual field testing or confrontational testing at the bedside is useful in documenting degree of visual recovery. Optical coherence tomography (OCT) is able to assess and monitor axonal loss after traumatic optic neuropathy [33]. Based upon earlier work by Lundstrom and Frisen [34], serial fundus photography showed that trauma to the intracranial optic nerve caused gradual disappearance of the retinal nerve fiber layer (RNFL) during weeks 4–8. Similar RNFL changes can be seen with the use of OCT.

Early transient increase followed by progressive loss of the retinal nerve fiber layer in traumatic optic neuropathy can be documented by the GDx NFL scanning laser polarimeter nerve fiber analyzer (Laser Diagnostic Technologies, San Diego, CA, USA). In a study by Miyahara et al. [35], the early increase in RNFL represented transient edema of the nerve fibers. Nerve fiber atrophy was completed by day 90 following the injury and was correlated with enlargement of the optic disc. A scanning laser polarimeter nerve fiber analyzer may be used to quantitate the severity of optic nerve damage and the effectiveness of therapy in traumatic optic neuropathy.

Neuroimaging may also help in localizing the site of optic nerve injury. CT scan with 1.5-mm axial sections allows good reformation along any axis and allows sufficient resolution to image optic nerve position orbital hematoma, orbital edema, intrasheath hematoma, nonorganic foreign bodies, and bony fractures (Fig. 5.4). Optic canal fractures are seen on CT scans in approximately 36–67 % of cases [36]. The force from trauma is transferred to the sphenoid and then to the optic nerve as it traverses the optic canal [37]. After metallic foreign bodies are ruled out by CT scan, MRI is more sensitive for detecting chiasmal injury and subtle intraneural or intrasheath hemorrhage, distinguishing it from epidural hemorrhage [4, 38]. MRI of the orbit may reveal focal edema of the optic nerve or optic nerve sheath enhancement with gadolinium. On T2-weighted images, the hyperintense signal from CSF surrounding the injured optic nerve may be absent

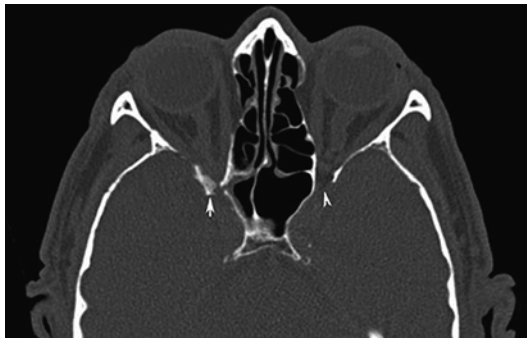

Fig. 5.4 Axial CT scan reveals a fracture in the posterior lateral wall of the right orbit. This fracture fragment is compressing the right optic nerve at the optic canal (*arrow*). The left optic canal is normal (*arrow head*) [Courtesy of Henry Kahn]

when compared with the normal nerve. MRI may distinguish intrasheath from intraneural hemorrhage. MRI is also superior to CT in delineating chiasmal injury [39–41].

Color Doppler imaging may help to differentiate extrinsic optic nerve compression caused by orbital hemorrhage from other causes of optic neuropathy. The B-scan portion of this imaging technique may also help identify optic nerve sheath hematoma [42, 43]. The color Doppler portion may help in evaluating perfusion to the optic nerve head [44, 45].

Visual Prognosis

In the natural history of indirect posterior optic nerve injuries, recovery is never complete. Subtle visual field, color vision, and pupillary defects persist despite complete recovery of visual acuity by Snellen measurements. Most patients develop optic atrophy. Spontaneous improvement from case series ranged from 20 to 71 % [6, 46, 47]. In Lessell's series [6], the extent of visual loss did not correlate with the potential for spontaneous recovery. The variation in extent and rate of recovery and response to treatment could be related to the pathogenesis of traumatic optic neuropathy in various clinical circumstances. For direct optic nerve injuries, the possibility of visual recovery is much less, but recovery of vision has occurred in such cases.

In indirect traumatic optic neuropathy, four features were significant in predicting no recovery of visual acuity: (1) the presence of blood in the posterior ethmoidal cells, (2) loss of consciousness associated with traumatic optic neuropathy, (3) absence of recovery after 48 h of corticosteroid treatment, and (4) age of patient over 40 years [48]. Patients who have the foregoing four poor prognostic factors could be considered for optic canal decompression. In this study, 87 % of patients who had improved visual outcome experienced visual recovery within 48 h of the initiation of corticosteroid treatment. Another sign of favorable recovery is optic nerve swelling after blunt trauma has been associated with a favorable prognosis for visual recovery. Brodsky et al. [49] reported three patients who had partial recovery of vision.

Pathology

Based on 174 postmortem examinations by Crompton [18] on patients who died after closed head trauma, optic nerve dural sheath hemorrhages were found in 83 % of patients. Interstitial optic nerve hemorrhages occurred in 36 % of these patients; two-thirds had the hemorrhage within the optic canal. Tears and ischemic lesions occurred in 44 % of patients; in 81 %, these involved the intracanalicular optic nerve, and in 54 % these affected the intracranial optic nerves.

From a case series of patients who had blunt head trauma, more than 50 % of patients who had traumatic optic neuropathy were found to have sphenoid bone fractures on CT scan. Laser interferometry studies done by Anderson et al. [17] showed that forces applied to the frontal bone during a deceleration injury are transmitted to and concentrated in the optic canal. Elastic deformation of the sphenoid bone allows transfer of the force into the intracanalicular portion of the optic nerve. The firm attachment of the dural sheath to the optic nerve in the optic canal is thought to predispose it to shearing forces, resulting in tearing

of axons and vessels that leads to contusion necrosis. The development and location of a fracture depends upon the elasticity of the bone, in that thicker bone is more inelastic and more likely to fracture. Direct injury to the optic nerve from displaced bony fragments in the optic canal is uncommon.

Shearing forces from blunt head trauma can displace the intracranial optic nerve upward against the falciform dural fold that overlies the intracranial end of the optic canal, resulting in direct or indirect injury. A frontal blow is transmitted posteriorly along the orbital walls to the sphenoid bone and the optic canal. A deceleration injury would allow the globe and the majority of the intraorbital contents to continue forward, whereas the intracanalicular optic nerve would remain immobile because of its tethering at the orbital apex and optic canal. The deceleration would be a shearing force to the optic nerve. Direct optic nerve injury from partial or complete avulsion from the globe usually does not sever the nerve and often leads to permanent injury to just a portion of the nerve [17].

Although optic canal decompression is performed based upon the hypothesis that edema inside the bony canal may lead to more swelling and ischemia of the optic nerve, there is not much evidence that optic nerve edema within the optic canal plays a significant role in causing traumatic posterior optic neuropathy. Vascular changes in and around the optic nerve may play a more important role than just the swelling of the nerve itself. Decreased perfusion pressure to the optic nerve within the optic canal during increased intracranial pressure can also decrease blood flow to the optic nerve causing ischemia [5].

Pathogenesis

Forces from shearing injury cause tears to the microvasculature that are seen as hemorrhage in the optic nerve and its sheaths on pathology. Indirect trauma to the axons may also cause a focal area of impaired axonal transport. This functional separation of the nerve into a proximal and distal segment usually occurs within 6–24 h of injury [50]. The distal segment that is separated from the soma undergoes Wallerian degeneration. The proximal segment that is connected with the soma swells to produce a retraction ball. The soma may then undergo apoptosis, as shown in the studies of optic nerves after ischemic optic neuropathy, with experimental glaucoma, and after trauma [51–53].

Apoptosis is programmed cell death involving active cellular processes through final common pathways. Injured RGCs release extracellular glutamate that induces excitotoxicity. High glutamate concentrations activate N-methyl-D-aspartate (NMDA) receptors that allow entry of excessive calcium into the cell. It has been shown that optic nerve crush leads to an increase in extracellular vitreal glutamate, but the steps by which axotomy induces excitotoxic damage to ganglion cells is still being studied [54]. This abnormally high concentration of calcium leads to inappropriate activation of cascades of proteases, nucleases, and lipases that attack cellular constituents, leading to the generation of highly reactive free radicals. The final stage of apoptosis, execution, occurs through the activation and function of caspases, aspartate-specific cysteine proteins. There are at least ten homologs of the initially described caspase, interleukin-1-beta-converting enzyme [55]. The predominant caspase involved in cell death appears to be CPP32 (caspase-3). Caspase inhibitors may be a possible therapeutic target (see section “Management”).

Intracellular calcium also activates inducible nitric oxide synthase (NOS) to cause increased production of nitric oxide, a highly reactive free radical used for the signaling and regulation of various physiological processes that also induces apoptosis. Free radicals from various sources cause intracellular degeneration and activate the early steps of the apoptotic cascade [56–59]. RGCs do not have NOS [60]. NOS-mediated excitotoxic cell damage relies on the abundant amounts of inducible NOS expressed in reactive astrocytes. In situ hybridization shows intense NOS mRNA signals in the ganglion cell layer and inner nuclear layer, indicative of neuronal NOS proteins being transported through axons into the terminals in the inner nuclear layer. Neuronal

NOS appears to play a role in RGC excitotoxicity mediated via the NMDA receptor [61].

In addition, the excess calcium can also directly cause mitochondrial failure, causing depletion of energy and the generation of more free radicals. Partial ischemia and reperfusion of transiently ischemic areas may generate further oxygen free radicals [62]. The release of these oxygen free radicals leads to peroxidation of lipids in the RGC membrane [63].

Bradykinin and kallidin initiate the release of arachidonic acid from neurons. Through a series of steps, arachidonic acid is transformed into various types of prostaglandins and oxygen free radicals are released. Peroxidation of lipids in the cell membrane may lead to decreased vascular autoregulation and increasing cellular/tissue edema. This type of edema within the optic canal may then produce a compartment syndrome causing more ischemia to the optic nerve. Loss of regulation of calcium homeostasis leads to shifting of extracellular calcium to the intracellular space by voltage- and receptor-gated calcium channels. The excess intracellular calcium leads to cell death [63].

Besides ischemia, inflammation contributes to further neural damage. Mediators of inflammation are released to attract polymorphonuclear lymphocytes and macrophages. Within the first 2 days after injury, polymorphonuclear lymphocytes predominate to cause immediate tissue damage. They are then replaced by macrophages by about 7 days after injury. These macrophages are thought to contribute to delayed tissue damage, as in delayed posttraumatic demyelination. Macrophages release glial promoting factors. This astroglial response after spinal cord injury may inhibit axonal regeneration processes. Inhibition of macrophage responses has been shown to decrease reactive gliosis, as shown in spinal cord injury studies [62, 63].

Management

Treatment of traumatic optic neuropathy with high-dose methylprednisolone was widely accepted when the second National Acute Spinal Cord Injury Study (NASCIS-2) study was published in 1990. The beneficial effects of this medication were extrapolated from those shown in the treatment of acute spinal cord injury in the NASCIS-2 study [64]. In NASCIS 2 [64], a multicenter, randomized, double-blind, placebo-controlled study in patients with acute spinal cord injury, patients were randomly assigned to receive placebo, naloxone, or methylprednisolone within 12 h of spinal injury. Methylprednisolone was given as an initial dose of 30 mg/kg followed by a continuous infusion of 5.4 mg/kg/h. Compared with placebo, treatment with methylprednisolone within 8 h of injury resulted in a significant improvement in motor and sensory function. However, these effects of methylprednisolone in the treatment of spinal cord trauma do not seem to extend to the treatment of optic nerve trauma.

The International Optic Nerve Trauma Study in 1999 [65] showed that neither corticosteroid treatment nor optic canal decompression changed the visual outcome of patients with traumatic optic neuropathy. It was clinically reasonable to consider treatment on an individual patient basis. In this prospective observational study, visual outcomes were compared with patients following observation alone, high-dose steroids given within 7 days of the injury, and optic canal decompression with or without corticosteroids performed within 7 days of the injury. The initial visual acuity of NLP predicted a poor outcome in all groups. No clear benefit was demonstrated for patients undergoing high-dose steroid therapy or canal decompression surgery compared to observation alone. The 57 % improvement of three Snellen lines or more in the untreated group suggested that spontaneous visual recovery also played a role in visual outcome. Some studies [66, 67] have even shown that methylprednisolone exacerbated axonal loss after optic nerve crush injury in rodent models.

In another study by Ohlsson et al. [68], however, methylprednisolone showed no effect on RGC survival, macrophage activity at the site of injury, axonal degeneration/regeneration, or visual function. These results could explain the lack of efficacy demonstrated in the International Optic Nerve Trauma Study, in which there was no

clear benefit for either corticosteroids or optic canal decompression. No randomized, double-blind clinical studies to date provide evidence that methylprednisolone is more effective than observation in the treatment of optic nerve trauma.

The Corticosteroid Randomization After Significant Head Injury trial published in 2004 [69] showed that high-dose methylprednisolone for 48 h after severe head trauma was associated with a higher risk of death from all causes 2 weeks after trauma in the corticosteroid-treated patients (21 % vs. 18 % mortality, $P=0.0001$) [70]. Although not all patients with traumatic optic neuropathy have severe head trauma, a higher mortality rate is associated with treating traumatic optic neuropathy with high-dose corticosteroids. This finding must be included in the informed consent for patients receiving this type of treatment.

Not only is there no clinical evidence for the efficacy of high-dose corticosteroids in the treatment of traumatic optic neuropathy, but there have been several animal studies showing that this treatment is toxic to the injured optic nerve. In the study by Steinsapir et al. [66], methylprednisolone exacerbated axonal loss following crush injury in the rat optic nerve. The authors concluded that clinical studies of traumatic optic neuropathy in the future should also examine the possibility that corticosteroid treatment may have an adverse effect on visual outcome following optic nerve trauma.

Optic nerve crush injury leads to death of RGCs, both as a direct result of the primary injury and via secondary degeneration induced by neurotoxins secreted by dying RGCs. Studies have shown that if optic nerve crush is preceded by an unrelated injury to another part of the central nervous system, for example, the spinal cord, the ensuing T cell-mediated protective autoimmunity results in a significant increase in RGC survival. In another study by Ben Simon et al. [71], head trauma in rats was associated with a neuroprotective effect on optic nerve injury. This neuroprotective effect was inhibited by the administration of high-dose methylprednisolone (30 mg/kg) but not by low-dose methylprednisolone (1 mg/kg). Therefore, corticosteroids may paradoxically interfere with adaptive mechanisms that limit the extent of secondary injury.

Surgical decompression of the optic canal for intracanalicular traumatic optic neuropathy has a limited role in the management of traumatic optic neuropathy. This treatment is based on the hypothesis that swelling in the optic canal may lead to a compartment syndrome. The increasing edema would decrease tissue perfusion to cause more post-injury ischemia to the optic nerve. This procedure is thought to decrease edematous pressure in the optic canal to reverse ischemia and axonal conduction block, which can result in irreversible axonal degeneration [72, 73]. In the International Optic Nerve Trauma Study in 1999 [65], no clear benefit was demonstrated for patients who were given high-dose corticosteroids within 7 days of injury compared to those who underwent optic canal decompression within 7 days of injury with or without corticosteroids. About 57 % of the untreated group experienced a spontaneous improvement of visual acuity of three lines or more. The initial visual acuity of NLP predicted a poor prognosis. According to a review by McCann and Seiff [74], 28 % of patients with traumatic optic neuropathy have some spontaneous improvement in vision. Based on combined unmatched uncontrolled human studies, vision improves in approximately 50 % of patients treated with corticosteroids, 57 % of patients treated with optic nerve decompression, and 62 % of patients treated with corticosteroids and optic nerve decompression [74]. Most patients with a response to corticosteroids will have improved 1 week after initiating treatment [75]. Of patients treated with corticosteroids who did not improve after 3 weeks of observation, 51 % still benefit from surgery [74, 75]. The final visual outcome was not correlated with the interval between injury and surgical intervention [5, 74–77]. The high rate of spontaneous recovery biases clinical studies on the treatment of traumatic optic neuropathy. Since the early 1980s, the rates of spontaneous visual improvement for untreated cases of traumatic optic neuropathy reportedly ranged from 0 to 67 % [46, 78]. Rates of visual improvement after ONSD ranged from 0 to 76 % [79, 80]. Identifying biological markers and having better knowledge of the natural history of traumatic optic neuropathy will help guide the role of

ONSD. Therefore, optic canal decompression surgery has a limited role in the management of traumatic optic neuropathy. This procedure is appropriate for conscious patients with delayed visual loss or whose vision does not improve in the first 4 days. The flash VEP must be at least 50 % of the normal eye or the afferent pupillary defect should be less than 2.1 log units [81].

In children and adolescents, traumatic optic neuropathy is caused by mechanisms similar to those that cause it in adults. In a retrospective review of 40 children [82], treatment did not improve visual outcome. The severity of visual loss and rate and degree of improvement are also similar. The most common causes were motor vehicle accidents (62 %) and sports injuries (22 %). Trauma was blunt in 78 % of cases and penetrating in 22 %. Improvement was more likely when vision was 20/200 or better at presentation, regardless of treatment. Patients with NLP acuity at presentation rarely experienced significant visual improvement despite treatment. Severe initial visual loss with baseline NLP and the presence of a fracture in the optic canal on CT scan were poor prognostic signs, predictive of poor visual outcome. Three patients in this series had an improvement of at least two Snellen lines from a baseline of NLP after treatment.

New Perspectives in the Protection, Repair, and Restoration of the Injured Optic Nerve

Peripheral Nerve Grafts

In rat optic nerve transection models, peripheral nerve grafts have been used to bridge the lesion where RGC axons can form synapses at their targets in the superior colliculus. This connection re-establishes the pupillary light reflex [83–86].

Stem Cell Transplantation

Optic nerve regeneration may offer hope for visual restoration that can occur in glaucoma and other optic neuropathies involving the irreversible loss of RGCs. To replace RGCs, stem cells capable of differentiating into RGCs need to be identified. They need to be transplanted into the eye and integrated into the retina without being rejected. Both embryonic and adult-derived stem cells and precursor cells have been applied to experimental glaucoma models. Most studies confirm that stem cell treatment prolongs RGC survival by providing neurotrophic factors.

Műller cells in the ciliary body and within the retina serve as progenitor cells that can differentiate and integrate into the retina. In adult mice, optic nerve injury by transection or crush injury upregulates cell proliferation and necessary trophic expression in the ciliary body and retina. These Műller cells and reactive astrocytes themselves proliferate and may serve as a source of regenerative cells. An in vitro spontaneously immortalized Műller cell line (M1O-M1) has been shown to have stem cell characteristics and can migrate and differentiate into various retinal cell types [87, 88]. When transplanted into eyes with experimental glaucoma, the migration of these cells into the RGC layer can be promoted by modifying the extracellular matrix with chondroitinase ABC and by controlling microglial reactivity with anti-inflammatory agents [89, 90].

In order to identify whether these progenitor cells have actually become RGCs, several proteins serve as RGC differentiation markers, such as B-3 tubulin, gamma-synuclein, and especially brain-specific homeobox/POU domain protein 3 (Brn 3) [91–94].

The environment, along with neurotrophic factors, must allow axon regrowth to occur since glial scars in the CNS, such as the one created by optic nerve transection, play a major part in hindering neural repair. In experimental models of optic nerve regeneration, microglial inhibitors, such as the immunoglobulin-derived tripeptide Thr-Lys-Pro, permit axons to sprout from the optic nerve stump into the peripheral nerve graft in vitro [95]. Epidermal growth factor receptor (EGFR) inhibitors, such as EGFR tryosine kinase inhibitor, prevent transduction of mechanical signals on glial cells. They inhibit astrocyte activation and subsequent RGC loss in experimental glaucoma [96].

Overexpression of the *bcl-2* gene can also create an environment permissive to axon regrowth. In young mice with immature astrocytes, overexpression of *bcl-2* gene itself is sufficient to facilitate optic nerve regeneration. In adult mice alpha-aminoadipate, a glutamate analogue toxic to astrocytes, but not to neurons, is required to produce similar results [97]. Instead of gene overexpression, lithium has also been shown to induce bcl-2 expression and stimulate RGC axon outgrowth in vitro and in vivo. Administration of both lithium and alpha-aminoadipate stimulates optic nerve regeneration in adult mice [98]. Since activated optic nerve head astrocytes secrete matrix metalloproteinases (MMPs) that can lead to the breakdown of the extracellular matrix necessary for the anchorage of RGCs, MMP inhibitor GM6001 prevents this process to create an environment permissive for RGCs to flourish [99].

After transplantation and differentiation, axon regrowth must form functional synapses with retinal interneurons and their target neurons in the brain, preserving the retinotopic organization of the visual pathway. To promote axon regrowth from both surviving and transplanted RGCs or their precursors, growth factors are required to enhance RGC survival. Intravitreal injection of ciliary neurotrophic factor (CNTF) promotes RGC axon regrowth directly and indirectly via increased expression of endogenous CNTF by astrocytes [100]. Intravitreal injection of an adeno-associated virus (AAV) to deliver fibroblast growth factor-2 (FGF-2) to RGCs leads to increased axon regrowth after axotomy [101]. Medium from Műller cell cultures have increased neurotrophic factor concentrations that can enhance RGC survival and axon regrowth in vitro [102]. Retinoic acid agonists have also been shown to promote neural regrowth in spinal cord injury models [103].

Regarding the use of stem cells for optic nerve regeneration, neural tube-derived embryonic stem cells from chicken have been transplanted into the site of transacted optic nerves. The expression of MMP-2 and MMP-14 by optic nerve head astrocytes helps in breakdown of extracellular matrix proteins, such as chondroitins. Various innate trophic factors are also secreted by these astrocytes to promote regrowth of RGC axons across the lesion to targets in the brain [104].

Transplanted olfactory ensheathing cells have also been shown to penetrate glial scars, possibly by secreting MMPs or by altering the biochemical microenvironment to permit axonal sprouting but not restoration of normal optic nerve structure [105].

Nanotechnology strategies involve the use of amphiphilic carbon nanofibers with neurotrophic factors to create a channel so that progenitor cells can differentiate into RGCs. These self-assembling nanofibers act as astrocytes and can grow around the cells to provide a higher density of neurotrophic growth factors, compared to in vivo or other cell culture techniques [106]. Peptide amphiphile molecules (peptides with a hydrophilic tail and a hydrophobic head group) self-assemble into a network of nanofiber scaffolds only in specific physiologic conditions. The surface of the nanofibers consists of hydrophilic head groups that engage in cell signaling by acting as ligands for cell surface receptors. When they are placed in physiological concentrations of cations, such as calcium, they are triggered to self-assemble into nanofibers that hold the water molecules in place, macroscopically forming a gel-like substrate. Neural retinal cells can be encapsulated in these gels mixing cell culture suspensions with peptide amphiphile solutions by trapping the cells in the interior of the gels. Since the functional peptide sequence forms the outer surface of the nanofibers, the encapsulated cells can engage in cell signaling in three dimensions. The encapsulated cells can differentiate faster into mature neuronal or retinal phenotypes without astrocyte development compared to conventional cell culture methods. This technique with amphiphile peptide substrates has the potential for limiting the effects of reactive gliosis or scarring if applied in vivo. The combination of donor cells and peptide amphiphile substrates can be injected stereotactically to form the nanofiber network in situ in vivo and provide functional cellular signaling to both donor and host cells, while limiting the effects of reactive gliosis. This nanofiber system is currently being investigated for degenerative retinal disorders, such as age-related macular degeneration [106].

After transplanted progenitor cells connect to the target neurons, RGC differentiation and functional vision must be demonstrated. Standard and multifocal ERGs, VEPs, and behavioral tests, such as the detection of orientation, startle and tracking of moving objects, have been used in laboratory animal models [107].

Neuroprotection

The strategies promoting RGC survival include the following approaches: (1) supplying RGCs with exogenous neurotrophic factors, (2) inducing more endogenous expression of neurotrophic factors, (3) upregulating Trk or inactivating p75 receptors, (4) increasing bcl-2/blc-x expression, and, (5) using pharmacological agents that may have neuroprotective properties.

Exogenous neurotrophic factors can prolong RGC survival in vitro and in vivo when injected into the vitreous or optic nerve lesion site. These factors include brain-derived neurotrophic factor (BDNF), CNTF, neurotrophic factor-4, FGF-2, and neurturin [108].

These neurotrophic factors directly injected into the eye have only a transient effect. Various methods to achieve sustained increased endogenous expression of neurotrophic factors include transfection of growth factor genes into RGCs with viral vectors, cell-based delivery approaches, and physical methods. In order to prolong the effects of growth factors to sustain RGC survival in glaucoma and axotomy models, AAV encoding BDNF, CNTF, or glial-derived neurotrophic factor (GDNF) can be injected into the vitreous [109–115]. Another method involves using combined intravitreal application of Ad-GDNF and Ad.X1AP, an X-linked caspase inhibitor of apoptosis, to the optic nerve stump in in vitro transaction molders [116–119].

Stem cell transplantation is another approach to provide sustained secretion of neurotrophic factors in the retina. Mesenchymal stem cells, oligodendrocyte precursor cells, and neural stem and precursor cells promote RGC survival in experimental glaucoma [120–122].

Olfactory ensheathing cells can also be injected into the retina of healthy rate eyes. They secrete neurotrophic factors and membrane adhesion factors while migrating within the retina and along the RGC axon layer into the optic nerve head to ensheathe RGCs with their cytoplasm [123].

Regarding physical methods to enhance RGC survival, transcorneal electrical stimulation has been found to increase calcium influx into retinal Műller cells that then produce more insulin-like growth factor [124, 125].

Other strategies to upregulate Trk or inactivate p75 receptors have been demonstrated in experimental models in order to enhance the effect of exogenous growth factor application and to promote RGC survival. Upregulation of the receptor TrkB by gene transfer enhances BDNF-induced RGC survival after axotomy [126]. In a rodent axotomy model, retinal expression of the proform of NGF was found to be upregulated after axotomy [127]. The proform of NGF has been shown to induce RGC death by activation of p75 receptors with subsequent TNF-alpha expression by Muller cells [128]. The administration of both selective TrkA antagonists and p75 NTR antagonists enhanced survival of RGC in this animal model [127].

Overexpression of the retinal antiapoptotic protein bcl-2 in transgenic mice with transected optic nerves has been shown to enhance RGC survival. The effect of bcl-2 is mediated through an increase in intracellular calcium signaling and activation of CREB and ERK [129].

Other exogenous agents that can activate the bcl-2 pathway to promote RGC survival include N-Berta-alanyl-5-s-glutathionyl-3,4-dihydroxyphenylalanine (5s-GAD), cilostazol, citicoline, lithium, and ROCK inhibitors.

Other pharmacologic agents that enhance RGC survival include erythropoietin and nipradilol. Other agents reduce RGC apoptosis by interfering with the glutamate excitotoxic cascade. One such drug is riluzole, a glutamate release inhibitor, that has been shown to be neuroprotective in a rat ischemia model [54].

NMDA receptor antagonists and polyamine site blockers are neuroprotective in experimental

glaucoma models. Memantine, a low-affinity, no competitive NMDa antagonist, failed to demonstrate a beneficial effect over placebo in a phase III glaucoma clinical trial [130]. Memantine, used in the treatment of Alzheimer's dementia, has been investigated as a potential neuroprotective agent in glaucoma and other optic neuropathies [131]. Although it has been shown to decrease the atrophy of the lateral geniculate nucleus in monkeys with experimental unilateral glaucoma when treated with memantine [132, 133]. These experimental animal models suggested benefit from memantine; a phase III clinical trial of memantine in patients with open angle glaucoma revealed no treatment benefit between the memantine-treated group and placebo group. A slightly slower progression of the disease was observed in patients receiving a higher dose of memantine than in those on a lower dose. This result could have been related to the memantine affecting only a small proportion of RGCs with a particular density of NMDA receptors, while apoptosis might have been triggered by different mechanisms in other RGCs [130].

Other noncompetitive NMDA receptor antagonists, such as amantadine, or agents blocking the polyamine site of the NMDA receptor, such as eliprodil and ifenprodil, also decrease RGC apoptosis in retinal ischemia in vitro [134–137]. These agents have not been investigated in clinical trials. L-Kynurenine, a precursor to an endogenous NMDA receptor antagonist kynurenic acid, is another agent that protects against NMDA-mediated toxicity in animal models [137].

Flavonoids, such as black and green tea, coffee, dark chocolate, and red wine, act as free radical scavengers and have antioxidant properties. Epigallocatechin gallate, a flavonoid in green tea, reduces retinal degeneration when injected into the vitreous in a model of oxidative stress [138]. Gingko biloba extract also has polyphenolic flavonoids that protect mitochondria from oxidative stress and it has shown to improve the visual fields in some patients with NTG [139]. Resveratrol is another polyphenol in grapes and wine that has antiapoptotic effects when applied to trabecular meshwork cells in vitro [140].

Idebenone and coenzyme Q also have neuroprotective effects in animal models and in humans.

Traumatic Optic Neuropathy as a Complication of Ocular Surgery

Surgical procedures in and around the optic nerve are becoming important causes of direct and indirect optic nerve trauma.

Optic Nerve Injury Related to Periorbital Injections

Anesthetic injections at the orbital apex may cause direct optic nerve injury [141–144]. Katsev et al. [145] recommended that the needle introduced beyond the orbital rim for both intraconal and periconal injections be no longer than 31 mm to avoid damage to the optic nerve. MRI of the orbit often reveals localized edema of the optic nerve or optic nerve sheath enhancement with gadolinium. The hyperintense signal from CSF around the injured optic nerve may be absent on T2-weighted imaging when compared with the normal nerve. Optic nerve injury has been reported with other procedures with a blunt cannula and in sub-Tenon's injection [144].

An MRI of the orbits with T1 fat saturation and gadolinium is recommended for any optic neuropathy occurring within the first 24 h of periocular injection. If findings of needle injury are present, then a trial of high-dose corticosteroids should be considered, although corticosteroids have not been proven to be efficacious. In treatment with corticosteroids, in three of four patients [141–143], only one patient had partial visual recovery [5–7].

Optic Nerve Injury After Cataract Surgery

Cataract surgery is one of the most common ocular surgeries, and visual loss is a rare complication. Nonarteritic ischemic optic neuropathy (NAION) following uncomplicated cataract surgery with either periocular anesthesia or general anesthesia has been reported [146–150]. In a retrospective study by McCulley et al. [151], 2 of 5,787 patients developed ischemic optic neuropathy within

6 weeks of cataract surgery, but 1 had previous NAION in the other eye 21 months earlier. In another study by McCulley et al. [152], all 18 cases of NAION in the 17 patients occurred within 6 months of surgery. These data help confirm that intraocular lens surgery is associated with the occurrence of NAION.

Visual loss may present with optic disc edema as an anterior ischemic optic neuropathy or with a normal disc as a posterior ischemic optic neuropathy [147, 148]. NAION after cataract surgery may occur within several hours to 4–6 weeks postoperatively. It has been shown that if ischemic optic neuropathy occurs in one eye after cataract surgery, the risk of recurrence in the other eye may be as high as 30–50 % with subsequent surgery [146, 150]. It has been postulated that an increase in intraocular pressure during the postoperative period may contribute to the development of NAION. In a study of 11 patients with NAION after cataract extraction, Hayreh [147] postulated that the typical increase in intraocular pressure after surgery along with a decrease in systemic blood pressure during general anesthesia lead to decreased perfusion of the optic nerve head and ischemia. The type of anesthesia during surgery was not specified in this case series. There are also other studies that document affected patients with normal intraocular pressures in the perioperative period [146, 153].

Most patients experience spontaneous improvement in visual acuity. Corticosteroids have not been shown to be effective. Most clinicians monitor the intraocular pressure in the perioperative period to help prevent the first ischemic event. Because the risk of NAION to the other eye is high, subsequent contralateral cataract extraction is not recommended [147].

Optic Nerve Injury After Vitrectomy

Ischemic optic neuropathy after vitrectomy to relieve vitreous traction in macular holes is related to surgical manipulation and to local anesthesia. After a pars plana vitrectomy, the cortical vitreous is peeled off the retina, at least around the hole. Aspiration of the cortical vitreous around the optic nerve head may occasionally extend to the equator. This suctioning process of the posterior hyaloid may shear peripapillary axons. Near the nasal edge of the disc, an air-fluid exchange is performed that can cause direct pressure to the optic nerve. At the end of the procedure, the eyes are usually filled with long-acting gas, such as perfluoropropane or sulfur hexafluoride. Patients are then required to position themselves face down for at least 20 h per day for about 2 weeks. Because the intraocular pressure may rise in the immediate postoperative period to cause optic nerve head ischemia, topical medications or oral acetazolamide are given to patients to help prevent this complication [154–159].

Postoperatively, patients may develop visual field defects. In a study by Melberg et al. [158], 3 of 157 patients had temporal visual field defects after vitrectomy. In two of three patients, the visual field defects were beyond the central 30° of fixation and could only be detected by Goldmann perimetry. These absolute defects could not be attributed to retinal detachment or schisis. As all patients underwent general anesthesia, injury to the optic nerve was unlikely. It was hypothesized that direct trauma to the optic nerve during aspiration of the air-fluid exchange procedure caused these field defects. In another study [157], eight patients experienced visual loss after vitrectomy and all had retrobulbar injections, seven of eight patients had fluid-air exchange with long-acting gas, four of eight patients developed afferent pupillary defects, and four of eight developed inferotemporal field defects. Five of eight had optic disc pallor without associated disc edema. No branch retinal vein or branch retinal artery occlusions occurred. The few retinal detachments did not explain the visual field defects. It was postulated that direct trauma to the optic nerve occurred, either by mechanical pressure from the suction catheter tip during air-fluid exchange or by injury from the needle during retrobulbar injection. Indirect trauma secondary to suction on the posterior hyaloid or shearing of peripapillary axons was another possibility. Although increased intraocular pressure may cause ischemic optic neuropathy, no increase in intraocular pressure was noted during the surgery. In another study, Boldt et al. [154] suggested that direct compression forming the gas

bubble itself could cause enough pressure to damage the nerve fiber layer. The retina may also have toxic injury from the gas bubble itself. Other studies confirm the common finding of temporal field defects with vitrectomies for macular holes [155, 156]. The incidence of inferotemporal or temporal visual field defects ranges from 1.9 to 20.5 %. In the study by Paques et al. [159], 10 % of patients had arcuate defects.

Optic Nerve Injury After Trabeculectomy

Visual loss after trabeculectomy is not common. Patients who seem to be at highest risk for significant visual loss after trabeculectomy are those who have advanced glaucoma with preexisting severe visual loss. These high-risk patients often have a field defect that splits fixation or extends within 5° of fixation. Other patients with postoperative hypotony may be predisposed to ischemic optic neuropathy. In a study of 508 eyes of 440 patients [160], only four cases (less than 1 %) of visual loss were observed. These four patients had preoperative visual field defects that split fixation, a finding consistent with a study by Kolker [161]. Three of these patients also had postoperative hypotony in which the intraocular pressures ranged from 0 to 2 mmHg on postoperative day 1. The low pressures persisted for 1 week in two eyes and for 1 month in one eye. Disc edema was not observed, but another study by Kawasaki and Purvin [162] described two patients who developed unilateral optic disc edema after trabeculectomy with intraocular pressures in the low-normal range. Because they did not have severe glaucoma, they did not experience visual field defects. Therefore, intraocular pressures that are too low might predispose to optic nerve injury.

Optic Nerve Injury After Blepharoplasty

Optic nerve injury is uncommon after blepharoplasty. Blindness is estimated at 0.04 % [163]. Visual loss is most likely caused by compression of the optic nerve or of the central retinal artery by a retrobulbar hematoma. The visual loss is reversible with prompt treatment. In a report by Kelly and May [164], a patient developed unilateral blindness from a retrobulbar hemorrhage after lower eyelid blepharoplasty. No blood flow was seen in the retinal arterioles, but after immediate lateral cantholysis and drainage, the patient regained retinal perfusion and recovered normal vision within 72 h. Other similar cases of optic nerve dysfunction secondary to compression by a retrobulbar hematoma after blepharoplasty have been reported with documented abnormal VEPs and normal ERG [165, 166].

Optic Nerve Injury After Endoscopic Sinus Surgery

Posterior ischemic optic neuropathy following intranasal anesthetic injection has been thought to be related to submucosal injection of an anesthetic with epinephrine, causing vasospasm [167].

Traumatic optic neuropathy can rarely be seen after endoscopic sinus surgery. The lack of orientation to surgical landmarks predisposes the surgeon to this complication [168]. The optic nerve canal indents the lateral wall of the sphenoid sinus, an important surgical landmark. Onodi cells usually cover the sphenoid sinus, but can also surround the optic nerve to cause confusion in surgical anatomy. The CT scan cannot reliably identify these cells to help prevent this problem [169].

References

1. Steinsapir KD, Goldberg RA. Traumatic optic neuropathy. Surv Ophthalmol. 1994;38(6):487–518.
2. Al-Qurainy IA, Stassen LF, Dutton GN, Moos KF, el-Attar A. The characteristics of midfacial fractures and the association with ocular injury: a prospective study. Br J Oral Maxillofac Surg. 1991;29(5):291–301.
3. Edmund J, Godfretsen E. Unilateral optic atrophy following head injury. Acta Ophthalmol (Copenh). 1963;41:693–7.
4. Seiff SR. High dose corticosteroids for treatment of vision loss due to indirect injury to the optic nerve. Ophthalmic Surg. 1990;21(6):389–95.

5. Levin LA, Joseph MP, Rizzo III JF, Lessell S. Optic canal decompression in indirect optic nerve trauma. Ophthalmology. 1994;101(3):566–9.
6. Lessell S. Indirect optic nerve trauma. Arch Ophthalmol. 1989;107(3):382–6.
7. Spoor TC. Treatment of optic neuropathy with megadose corticosteroids. Arch Ophthalmol. 1986; 104(11):1585.
8. Mauriello JA, DeLuca J, Krieger A, Schulder M, Frohman L. Management of traumatic optic neuropathy: a study of 23 patients. Br J Ophthalmol. 1992;76(6):349–52.
9. Steinsapir KD, Goldberg RA. Traumatic optic neuropathies. In: Miller NR, Newman NJ, editors. Walsh and Hoyt's clinical neuro-ophthalmology. 5th ed. Baltimore, MD: Williams & Wilkins; 1998. p. 715–40.
10. Sadun AA. Anatomy and physiology of the optic nerve. In: Miller NR, Newman NJ, editors. Walsh and Hoyt's clinical neuro-ophthalmology. 5th ed. Baltimore, MD: Williams & Wilkins; 1998. p. 57–83.
11. Lang J. Clinical anatomy of the nose, nasal cavity, and paranasal sinuses. Stuttgart: Thieme Verlag; 1989. p. 85–98. 125–8.
12. Bilyk JR, Joseph MP. Traumatic optic neuropathy. Semin Ophthalmol. 1994;9(3):200–11.
13. Hupp SL, Buckley EG, Byrne SF, Tenzel RR, Glaser JS, Schatz NS. Posttraumatic venous obstructive retinopathy associated with enlarged optic nerve sheath. Arch Ophthalmol. 1984;102(2):254–6.
14. Guy J, Sherwood M, Day AL. Surgical treatment of progressive visual loss in traumatic optic neuropathy. Report of two cases. J Neurosurg. 1989;70(5): 799–801.
15. Lessell S. Traumatic optic neuropathy and visual system injury. In: Shingleton BJ, Hersh PS, Kenyon KR, editors. Eye trauma. St. Louis: Mosby; 1991. p. 371–9.
16. Gross CE, DeKock JR, Panje WR, Hershkowitz N, Newman J. Evidence for orbital deformation that may contribute to monocular blindness following minor frontal head trauma. J Neurosurg. 1981;55(6): 963–6.
17. Anderson RL, Panje WR, Gross CE. Optic nerve blindness following blunt forehead trauma. Ophthalmology. 1982;89(5):445–55.
18. Crompton MR. Visual lesions in closed head injury. Brain. 1970;93(4):785–92.
19. Frenkel RE, Spoor TC. Diagnosis and management of traumatic optic neuropathies. Adv Ophthalmic Plast Reconstr Surg. 1987;6:71–90.
20. Krauss HR, Yee RD, Foos RY. Autoenucleation. Surv Ophthalmol. 1984;29(3):179–87.
21. Goodhart SP. Avulsion of both eyeballs and extraction of teeth: self-mutilation in chronic encephalitis. Am J Med Sci. 1933;185:674–84.
22. Coppez H, Surle S. Pseudo-corps estrangers de l'oeil. Arch Ophthalmol. 1929;46:449–57.
23. Park JH, Frenkel M, Dobbie JG, Choromokos E. Evulsion of the optic nerve. Am J Ophthalmol. 1971;72(5):969–71.
24. Hedges III TR, Gragoudas ES. Traumatic anterior ischemic optic neuropathy. Ann Ophthalmol. 1981; 13(5):625–8.
25. Crowe NW, Nickles TP, Troost BT, Elster AD. Intrachiasmal hemorrhage: a cause of delayed posttraumatic blindness. Neurology. 1989;39(6):863–5.
26. Manor RS, Cohen S, Svetliza E, Ben SI. Papilledema in traumatic lesion of optic nerve with amaurosis. J Clin Neuro Ophthalmol. 1986;6(2):100–5.
27. Holmes MD, Sires BS. Flash visual evoked potentials predict visual outcome in traumatic optic neuropathy. Ophthalmic Plast Reconstr Surg. 2004; 20(5):342–6.
28. Cornelius CP, Altenmuller E, Ehrenfeld M. The use of flash visual evoked potentials in the early diagnosis of suspected optic nerve lesions due to craniofacial trauma. J Craniomaxillofac Surg. 1996;24(1): 1–11.
29. Jayle GE, Tassy AF. Prognostic value of the electroretinogram in severe recent ocular trauma. Br J Ophthalmol. 1970;54(1):51–8.
30. Hooper RS. Orbital complications of head injury. Br J Surg. 1951;39(154):126–38.
31. Hughes B. Indirect injury of the optic nerves and chiasma. Bull Johns Hopkins Hosp. 1962;111: 98–126.
32. Turner JWA. Indirect injury of the optic nerves. Brain. 1943;66:140–51.
33. Medeiros FA, Sample PA, Zangwill LM, Bowd C, Aihara M, Weinreb RN. Corneal thickness as a risk factor for visual field loss in patients with preperimetric glaucomatous optic neuropathy. Am J Ophthalmol. 2003;136(5):805–13.
34. Lundstrom M, Frisen L. Evolution of descending optic atrophy. A case report. Acta Ophthalmol (Copenh). 1975;53(5):738–46.
35. Miyahara T, Kurimoto Y, Kurokawa T, Kuroda T, Yoshimura N. Alterations in retinal nerve fiber layer thickness following indirect traumatic optic neuropathy detected by nerve fiber analyzer, GDx-N. Am J Ophthalmol. 2003;136(2):361–4.
36. Keane JR, Baloh RW. Posttraumatic cranial neuropathies. Neurol Clin. 1992;10(4):849–67.
37. Wang ML, Seiff SR, Drasner K. A comparison of visual outcome in open-globe repair: succinylcholine with D-tubocurarine vs nondepolarizing agents. Ophthalmic Surg. 1992;23(11):746–51.
38. Seiff SR, Berger MS, Guyon J, Pitts LH. Computed tomographic evaluation of the optic canal in sudden traumatic blindness. Am J Ophthalmol. 1984;98(6): 751–5.
39. Tang RA, Kramer LA, Schiffman J, Woon C, Hayman LA, Pardo G. Chiasmal trauma: clinical and imaging considerations. Surv Ophthalmol. 1994; 38(4):381–3.
40. Moffit B, Duffy K, Lufkin R, Frazee J, Vinuela F, Bentson J. MR imaging of intrachiasmatic hemorrhage. J Comput Assist Tomogr. 1988;12(3):535–6.
41. Levin LA, Rubin PA. Advances in orbital imaging. Int Ophthalmol Clin. 1992;32(3):1–25.

42. Kline LB, McCluskey MM, Skalka HW. Imaging techniques in optic nerve evulsion. J Clin Neuro Ophthalmol. 1988;8(4):281–2.
43. Talwar D, Kumar A, Verma L, Tewari HK, Khosla PK. Ultrasonography in optic nerve head avulsion. Acta Ophthalmol (Copenh). 1991;69(1):121–3.
44. Guthoff RF, Berger RW, Winkler P, Helmke K, Chumbley LC. Doppler ultrasonography of the ophthalmic and central retinal vessels. Arch Ophthalmol. 1991;109(4):532–6.
45. Erickson SJ, Hendrix LE, Massaro BM, et al. Color Doppler flow imaging of the normal and abnormal orbit. Radiology. 1989;173(2):511–6.
46. Millesi W, Hollmann K, Funder J. Traumatic lesion of the optic nerve. Acta Neurochir (Wien). 1988; 93(1–2):50–4.
47. Tang R, Li H, Regner V. Traumatic optic neuropathy: analysis of 37 cases. Philadelphia, PA: Lippincott; 1986.
48. Carta A, Ferrigno L, Salvo M, Bianchi-Marzoli S, Boschi A, Carta F. Visual prognosis after indirect traumatic optic neuropathy. J Neurol Neurosurg Psychiatry. 2003;74(2):246–8.
49. Brodsky MC, Wald KJ, Chen S, Weiter JJ. Protracted posttraumatic optic disc swelling. Ophthalmology. 1995;102(11):1628–31.
50. Povlishock JT, Becker DP, Cheng CL, Vaughan GW. Axonal change in minor head injury. J Neuropathol Exp Neurol. 1983;42(3):225–42.
51. Buchi ER. Cell death in the rat retina after a pressure-induced ischaemia-reperfusion insult: an electron microscopic study. I. Ganglion cell layer and inner nuclear layer. Exp Eye Res. 1992;55(4):605–13.
52. Garcia-Valenzuela E, Gorczyca W, Darzynkiewicz Z, Sharma SC. Apoptosis in adult retinal ganglion cells after axotomy. J Neurobiol. 1994;25(4):431–8.
53. Levin LA, Louhab A. Apoptosis of retinal ganglion cells in anterior ischemic optic neuropathy. Arch Ophthalmol. 1996;114(4):488–91.
54. Vorwerk CK, Zurakowski D, McDermott LM, Mawrin C, Dreyer EB. Effects of axonal injury on ganglion cell survival and glutamate homeostasis. Brain Res Bull. 2004;62(6):485–90.
55. Solary E, Eymin B, Droin N, Haugg M. Proteases, proteolysis, and apoptosis. Cell Biol Toxicol. 1998; 14(2):121–32.
56. Dugan LL, Sensi SL, Canzoniero LM, et al. Mitochondrial production of reactive oxygen species in cortical neurons following exposure to methyl-d-aspartate. J Neurosci. 1995;15(10):6377–88.
57. Fehsel K, Kroncke KD, Meyer KL, Huber H, Wahn V, Kolb-Bachofen V. Nitric oxide induces apoptosis in mouse thymocytes. J Immunol. 1995;155(6): 2858–65.
58. Greenlund LJ, Korsmeyer SJ, Johnson Jr EM. Role of BCL-2 in the survival and function of developing and mature sympathetic neurons. Neuron. 1995; 15(3):649–61.
59. Messmer UK, Ankarcrona M, Nicotera P, Brune B. p53 expression in nitric oxide-induced apoptosis. FEBS Lett. 1994;355(1):23–6.
60. Lau KC, So KF, Tay D, Leung MC. NADPH-diaphorase neurons in the retina of the hamster. J Comp Neurol. 1994;350(4):550–8.
61. Kuehn MH, Fingert JH, Kwon YH. Retinal ganglion cell death in glaucoma: mechanisms and neuroprotective strategies. Ophthalmol Clin N Am. 2005; 18(3):383–95.
62. Kanellopoulos GK, Xu XM, Hsu CY, Lu X, Sundt TM, Kouchoukos NT. White matter injury in spinal cord ischemia: protection by AMPA/ kainite glutamate receptor antagonism. Stroke. 2000;31(8):1945–52.
63. Schuettauf F, Naskar R, Vorwerk CK, Zurakowski D, Dreyer EB. Ganglion cell loss after optic nerve crush mediated through AMPA-kainate and NMDA receptors. Investig Ophthalmol Vis Sci. 2000;41(13): 4313–6.
64. Bracken MB, Shepard MJ, Collins WF, et al. A randomized, controlled trial of methylprednisolone or naloxone in the treatment of acute spinal cord injury. Results of the Second National Acute Spinal Cord Injury Study. N Engl J Med. 1990;322(20):1405–11.
65. Levin LA, Beck RW, Joseph MP, Seiff S, Kraker R. The treatment of traumatic optic neuropathy: the International Optic Nerve Trauma Study. Ophthalmology. 1999;106(7):1268–77.
66. Steinsapir KD, Goldberg RA, Sinha S, Hovda DA. Methylprednisolone exacerbates axonal loss following optic nerve trauma in rats. Restor Neurol Neurosci. 2000;17(4):157–63.
67. Steinsapir KD, Seiff SR, Goldberg RA. Traumatic optic neuropathy: where do we stand? Ophthalmic Plast Reconstr Surg. 2002;18(3):232–4.
68. Ohlsson M, Westerlund U, Langmoen IA, Svensson M. Methylprednisolone treatment does not influence axonal regeneration or degeneration following optic nerve injury in the adult rat. J Neuroophthalmol. 2004;24(1):11–8.
69. Roberts I, Yates D, Sandercock P, et al. CRASH trial collaborators. Effect of intravenous corticosteroids on death within 14 days in 10,008 adults with clinically significant head injury (MRC CRASH trial): randomized placebo-controlled trial. Lancet. 2004;364(9442):1321–8.
70. Bracken MB. CRASH (corticosteroid randomization after significant head injury trial): landmark and storm warning. Neurosurgery. 2005;57(6):1300–2.
71. Ben Simon GJ, Hovda DA, Harris NG, Gomez-Pinilla F, Goldberg RA. Traumatic brain injury induced neuroprotection of retinal ganglion cells to optic nerve crush. J Neurotrauma. 2006;7 :1072–82.
72. Kayan A, Earl CJ. Compressive lesions of the optic nerves and chiasm. Pattern of recovery of vision following surgical treatment. Brain. 1975;98(1): 13–28.
73. McDonald WI. The symptomatology of tumours of the anterior visual pathways. Can J Neurol Sci. 1982;9(4):381–90.
74. McCann JD, Seiff S. Traumatic neuropathies of the optic nerve, optic chiasm, and ocular motor nerves. Curr Opin Ophthalmol. 1994;5(6):3–10.

75. Fujitani T, Inoue K, Takahashi T, Ikushima K, Asai T. Indirect traumatic optic neuropathy: visual outcome of operative and nonoperative cases. Jpn J Ophthalmol. 1986;30(1):125–34.
76. Mahapatra AK, Tandon DA. Traumatic optic neuropathy in children: a prospective study. Pediatr Neurosurg. 1993;19(1):34–9.
77. Girard BC, Bouzas EA, Lamas G, Soudant J. Visual improvement after transethmoid-sphenoid decompression in optic nerve injuries. J Clin Neuro Ophthalmol. 1992;12(3):142–8.
78. Chou PI, Sadun AA, Chen YC, Su WY, Lin SZ, Lee CC. Clinical experiences in the management of traumatic optic neuropathy. Neuro Ophthalmol. 1996; 16(6):325–36.
79. Nau HE, Gerhard L, Foerster M, Nahser HC, Reinhardt V, Joka T. Optic nerve trauma: clinical, electrophysiological and histological remarks. Acta Neurochir (Wien). 1987;89(1–2):16–27.
80. Spoor TC, Hartel WC, Lensink DB, Wilkinson MJ. Treatment of traumatic optic neuropathy with corticosteroids. Am J Ophthalmol 1990;110(6):665–9. Erratum in. Am J Ophthalmol. 1991;111(4):526.
81. Steinsapir KD, Goldberg RA. Traumatic optic neuropathy: an evolving understanding. Am J Ophthalmol. 2011;151(6):928–33.
82. Goldenberg-Cohen N, Miller NR, Repka MX. Traumatic optic neuropathy in children and adolescents. J AAPOS. 2004;8(1):20–7.
83. Vidal-Sanz M, Bray GM, Villegas-Pérez MP, Thanos S, Aguayo AJ. Axonal regeneration and synapse formation in the superior colliculus by retinal ganglion cells in the adult rat. J Neurosci. 1987;7(9):2894–909.
84. Whiteley SJ, Sauvé Y, Avilés-Trigueros M, Vidal-Sanz M, Lund RD. Extent and duration of recovered pupillary light reflex following retinal ganglion cell axon regeneration through peripheral nerve grafts directed to the pretectum in adult rats. Exp Neurol. 1998;154(2):560–72.
85. Avilés-Trigueros M, Sauvé Y, Lund RD, Vidal-Sanz M. Selective innervation of retinorecipient brainstem nuclei by retinal ganglion cell axons regenerating through peripheral nerve grafts in adult rats. J Neurosci. 2000;20(1):361–74.
86. Vidal-Sanz M, Avilés-Trigueros M, Whiteley SJ, Sauvé Y, Lund RD. Reinnervation of the pretectum in adult rats by regenerated retinal ganglion cell axons: anatomical and functional studies. Prog Brain Res. 2002;137:443–52.
87. Limb GA, Salt TE, Munro PM, Moss SE, Khaw PT. In vitro characterization of a spontaneously immortalized human Müller cell line (MIO-M1). Investig Ophthalmol Vis Sci. 2002;43(3):864–9.
88. Lawrence JM, Singhal S, Bhatia B, et al. MIO-M1 cells and similar muller glial cell lines derived from adult human retina exhibit neural stem cell characteristics. Stem Cells. 2007;25(8):2033–43.
89. Bull ND, Limb GA, Martin KR. Human Müller stem cell (MIO-M1) transplantation in a rat model of glaucoma: survival, differentiation, and integration. Investig Ophthalmol Vis Sci. 2008;49(8):3449–56.
90. Singhal S, Lawrence JM, Bhatia B, et al. Chondroitin sulfate proteoglycans and microglia prevent migration and integration of grafted Müller stem cells into degenerating retina. Stem Cells. 2008;26(4): 1074–82.
91. Wang SW, Mu X, Bowers WJ, et al. Brn3b/Brn3c double knockout mice reveal an unsuspected role for Brn3c in retinal ganglion cell axon outgrowth. Development. 2002;129(2):467–77.
92. Quina LA, Pak W, Lanier J, et al. Brn3a-expressing retinal ganglion cells project specifically to thalamocortical and collicular visual pathways. J Neurosci. 2005;25(50):11595–604.
93. Surgucheva I, Weisman AD, Goldberg JL, Shnyra A, Surguchov A. Gamma-synuclein as a marker of retinal ganglion cells. Mol Vis. 2008;14:1540–8.
94. Pan L, Deng M, Xie X, Gan L. ISL1 and BRN3B co-regulate the differentiation of murine retinal ganglion cells. Development. 2008;135(11):1981–90.
95. Thanos S, Mey J, Wild M. Treatment of the adult retina with microglia-suppressing factors retards axotomy-induced neuronal degradation and enhances axonal regeneration in vivo and in vitro. J Neurosci. 1993;13(2):455–66.
96. Liu B, Chen H, Johns TG, Neufeld AH. Epidermal growth factor receptor activation: an upstream signal for transition of quiescent astrocytes into reactive astrocytes after neural injury. J Neurosci. 2006; 26(28):7532–40.
97. Cho KS, Yang L, Lu B, et al. Re-establishing the regenerative potential of central nervous system axons in postnatal mice. J Cell Sci. 2005;118(Pt 5):863–72.
98. Cho KS, Chen DF. Promoting optic nerve regeneration in adult mice with pharmaceutical approach. Neurochem Res. 2008;33(10):2126–33.
99. Manabe S, Gu Z, Lipton SA. Activation of matrix metalloproteinase-9 via neuronal nitric oxide synthase contributes to NMDA-induced retinal ganglion cell death. Investig Ophthalmol Vis Sci. 2005;46(12): 4747–53.
100. Müller A, Hauk TG, Leibinger M, Marienfeld R, Fischer D. Exogenous CNTF stimulates axon regeneration of retinal ganglion cells partially via endogenous CNTF. Mol Cell Neurosci. 2009;41(2):233–46.
101. Sapieha PS, Peltier M, Rendahl KG, Manning WC, Di Polo A. Fibroblast growth factor-2 gene delivery stimulates axon growth by adult retinal ganglion cells after acute optic nerve injury. Mol Cell Neurosci. 2003;24(3):656–72.
102. de Melo Reis RA, Cabral-da-Silva MC, de Mello FG, Taylor JS. Müller glia factors induce survival and neuritogenesis of peripheral and central neurons. Brain Res. 2008;1205:1–11.
103. Agudo M, Yip P, Davies M, et al. A retinoic acid receptor beta agonist (CD2019) overcomes inhibition of axonal outgrowth via phosphoinositide 3-kinase signalling in the injured adult spinal cord. Neurobiol Dis. 2010;37(1):147–55.
104. Charalambous P, Hurst LA, Thanos S. Engrafted chicken neural tube-derived stem cells support the innate propensity for axonal regeneration within the

rat optic nerve. Investig Ophthalmol Vis Sci. 2008;49(8):3513–24.
105. Li Y, Sauvé Y, Li D, Lund RD, Raisman G. Transplanted olfactory ensheathing cells promote regeneration of cut adult rat optic nerve axons. J Neurosci. 2003;23(21):7783–8.
106. Silva GA. Nanotechnology applications and approaches for neuroregeneration and drug delivery to the central nervous system. Ann N Y Acad Sci. 2010;1199:221–30.
107. Coffey PJ, Girman S, Wang SM, et al. Long-term preservation of cortically dependent visual function in RCS rats by transplantation. Nat Neurosci. 2002; 5(1):53–6.
108. Parrilla-Reverter G, Agudo M, Sobrado-Calvo P, Salinas-Navarro M, Villegas-Pérez MP, Vidal-Sanz M. Effects of different neurotrophic factors on the survival of retinal ganglion cells after a complete intraorbital nerve crush injury: a quantitative in vivo study. Exp Eye Res. 2009;89(1):32–41.
109. Weise J, Isenmann S, Klöcker N, et al. Adenovirus-mediated expression of ciliary neurotrophic factor (CNTF) rescues axotomized rat retinal ganglion cells but does not support axonal regeneration in vivo. Neurobiol Dis. 2000;7(3):212–23.
110. Schmeer C, Straten G, Kügler S, Gravel C, Bähr M, Isenmann S. Dose-dependent rescue of axotomized rat retinal ganglion cells by adenovirus-mediated expression of glial cell-line derived neurotrophic factor in vivo. Eur J Neurosci. 2002;15(4):637–43.
111. van Adel BA, Kostic C, Déglon N, Ball AK, Arsenijevic Y. Delivery of ciliary neurotrophic factor via lentiviral-mediated transfer protects axotomized retinal ganglion cells for an extended period of time. Hum Gene Ther. 2003;14(2):103–15.
112. Martin KR, Quigley HA, Zack DJ, et al. Gene therapy with brain-derived neurotrophic factor as a protection: retinal ganglion cells in a rat glaucoma model. Investig Ophthalmol Vis Sci. 2003;44(10): 4357–65.
113. Leaver SG, Cui Q, Plant GW, et al. AAV-mediated expression of CNTF promotes long-term survival and regeneration of adult rat retinal ganglion cells. Gene Ther. 2006;13(18):1328–41.
114. Leaver SG, Cui Q, Bernard O, Harvey AR. Cooperative effects of bcl-2 and AAV-mediated expression of CNTF on retinal ganglion cell survival and axonal regeneration in adult transgenic mice. Eur J Neurosci. 2006;24(12):3323–32.
115. Pease ME, Zack DJ, Berlinicke C, et al. Effect of CNTF on retinal ganglion cell survival in experimental glaucoma. Investig Ophthalmol Vis Sci. 2009;50(5):2194–200.
116. Ju WK, Lee MY, Hofmann HD, Kirsch M, Chun MH. Expression of CNTF in Müller cells of the rat retina after pressure-induced ischemia. Neuroreport. 1999;10(2):419–22.
117. Honjo M, Tanihara H, Kido N, Inatani M, Okazaki K, Honda Y. Expression of ciliary neurotrophic factor activated by retinal Müller cells in eyes with NMDA- and kainic acid-induced neuronal death. Investig Ophthalmol Vis Sci. 2000;41(2):552–60.
118. van Adel BA, Arnold JM, Phipps J, Doering LC, Ball AK. Ciliary neurotrophic factor protects retinal ganglion cells from axotomy-induced apoptosis via modulation of retinal glia in vivo. J Neurobiol. 2005;63(3):215–34.
119. Müller A, Hauk TG, Fischer D. Astrocyte-derived CNTF switches mature RGCs to a regenerative state following inflammatory stimulation. Brain. 2007;130(Pt 12):3308–20.
120. Yu S, Tanabe T, Dezawa M, Ishikawa H, Yoshimura N. Effects of bone marrow stromal cell injection in an experimental glaucoma model. Biochem Biophys Res Commun. 2006;344(4):1071–9.
121. Bull ND, Irvine KA, Franklin RJ, Martin KR. Transplanted oligodendrocyte precursor cells reduce neurodegeneration in a model of glaucoma. Investig Ophthalmol Vis Sci. 2009;50(9):4244–53.
122. Hill AJ, Zwart I, Samaranayake AN, et al. Rat neurosphere cells protect axotomized rat retinal ganglion cells and facilitate their regeneration. J Neurotrauma. 2009;26(7):1147–56.
123. Li Y, Li D, Khaw PT, Raisman G. Transplanted olfactory ensheathing cells incorporated into the optic nerve head ensheathe retinal ganglion cell axons: possible relevance to glaucoma. Neurosci Lett. 2008;440(3):251–4.
124. Morimoto T, Miyoshi T, Matsuda S, et al. Transcorneal electrical stimulation rescues axotomized retinal ganglion cells by activating endogenous retinal IGF-1 system. Investig Ophthalmol Vis Sci. 2005;46(6):2147–55.
125. Sato T, Fujikado T, Morimoto T, Matsushita K, Harada T, Tano Y. Effect of electrical stimulation on IGF-1 transcription by L-type calcium channels in cultured retinal Müller cells. Jpn J Ophthalmol. 2008;52(3):217–23.
126. Cheng L, Sapieha P, Kittlerova P, Hauswirth WW, Di Polo A. TrkB gene transfer protects retinal ganglion cells from axotomy-induced death in vivo. J Neurosci. 2002;22(10):3977–86.
127. Lebrun-Julien F, Morquette B, Douillette A, Saragovi HU, Di Polo A. Inhibition of p75(NTR) in glia potentiates TrkA-mediated survival of injured retinal ganglion cells. Mol Cell Neurosci. 2009; 40(4):410–20.
128. Lebrun-Julien F, Bertrand MJ, De Backer O, et al. ProNGF induces TNF-alpha-dependent death of retinal ganglion cells through a p75NTR non-cell-autonomous signaling pathway. Proc Natl Acad Sci U S A. 2010;107(8):3817–22.
129. Jiao J, Huang X, Feit-Leithman RA, et al. Bcl-2 enhances Ca(2+) signaling to support the intrinsic regenerative capacity of CNS axons. EMBO J. 2005;24(5):1068–78.
130. Osborne NN. Recent clinical findings with memantine should not mean that the idea of neuroprotection in glaucoma is abandoned. Acta Ophthalmol. 2009; 87(4):450–4.

131. Seki M, Lipton SA. Targeting excitotoxic/free radical signaling pathways for therapeutic intervention in glaucoma. Prog Brain Res. 2008;173: 495–510.
132. Hare WA, WoldeMussie E, Weinreb RN, et al. Efficacy and safety of memantine treatment for reduction of changes associated with experimental glaucoma in monkey, II: structural measures. Investig Ophthalmol Vis Sci. 2004;45(8):2640–51.
133. Hare WA, WoldeMussie E, Lai RK, et al. Efficacy and safety of memantine treatment for reduction of changes associated with experimental glaucoma in monkey, I: functional measures. Invest Ophthalmol Vis Sci 2004 Aug;45(8):2625–39. Erratum in. Investig Ophthalmol Vis Sci. 2004;45(9):2878.
134. Kapin MA, Doshi R, Scatton B, DeSantis LM, Chandler ML. Neuroprotective effects of eliprodil in retinal excitotoxicity and ischemia. Investig Ophthalmol Vis Sci. 1999;40(6):1177–82.
135. Pang IH, Wexler EM, Nawy S, DeSantis L, Kapin MA. Protection by eliprodil against excitotoxicity in cultured rat retinal ganglion cells. Investig Ophthalmol Vis Sci. 1999;40(6):1170–6.
136. Guo L, Salt TE, Maass A, et al. Assessment of neuroprotective effects of glutamate modulation on glaucoma-related retinal ganglion cell apoptosis in vivo. Investig Ophthalmol Vis Sci. 2006;47(2): 626–33.
137. Vorwerk CK, Kreutz MR, Dreyer EB, Sabel BA. Systemic L-kynurenine administration partially protects against NMDA, but not kainate-induced degeneration of retinal ganglion cells, and reduces visual discrimination deficits in adults rats. Investig Ophthalmol Vis Sci. 1996;37(12):2382–92.
138. Zhang B, Osborne NN. Oxidative-induced retinal degeneration is attenuated by epigallocatechin gallate. Brain Res. 2006;1124(1):176–87.
139. Quaranta L, Bettelli S, Uva MG, Semeraro F, Turano R, Gandolfo E. Effect of Ginkgo biloba extract on preexisting visual field damage in normal tension glaucoma. Ophthalmology. 2003;110(2):359–62.
140. Luna C, Li G, Liton PB, et al. Resveratrol prevents the expression of glaucoma markers induced by chronic oxidative stress in trabecular meshwork cells. Food Chem Toxicol. 2009;47(1):198–204.
141. Devoto MH, Kersten RC, Zalta AH, Kulwin DR. Optic nerve injury after retrobulbar anesthesia. Arch Ophthalmol. 1997;115(5):687–8.
142. Dorey SE, Gillespie IH, Barton F, MacSweeney E. Magnetic resonance image changes following optic nerve trauma from peribulbar anaesthetic. Br J Ophthalmol. 1998;82(5):586–7.
143. Horton JC, Hoyt WF, Foreman DS, Cohen JA. Confirmation by magnetic resonance imaging of optic nerve injury after retrobulbar anesthesia. Arch Ophthalmol. 1996;114(3):351–3.
144. Kim SK, Golden MA, Bradbury MJ, Rizzo JF. First description of optic neuropathy secondary to sub-Tenon's anesthesia in cataract surgery. Investig Ophthalmol Vis Sci. 2000;41(4):S314.
145. Katsev DA, Drews RC, Rose BT. An anatomic study of retrobulbar needle path length. Ophthalmology. 1989;96(8):1221–4.
146. Carroll FD. Optic nerve complications of cataract extraction. Trans Am Acad Ophthalmol Otolaryngol. 1973;77(5):OP623–9.
147. Hayreh SS. Anterior ischemic optic neuropathy. IV. Occurrence after cataract extraction. Arch Ophthalmol. 1980;98(8):1410–6.
148. Luscavage LE, Volpe NJ, Liss R. Posterior ischemic optic neuropathy after uncomplicated cataract extraction. Am J Ophthalmol. 2001;132(3):408–9.
149. Michaels DD, Zugsmith GS. Optic neuropathy following cataract extraction. Ann Ophthalmol. 1973;5(3):303–6.
150. Serrano LA, Behrens MM, Carroll FD. Post-cataract extraction ischemic optic neuropathy. Arch Ophthalmol. 1982;100(7):1177–8.
151. McCulley TJ, Lam BL, Feuer WJ. Incidence of nonarteritic anterior ischemic optic neuropathy associated with cataract extraction. Ophthalmology. 2001; 108(7):1275–8.
152. McCulley TJ, Lam BL, Feuer WJ. Nonarteritic anterior ischemic optic neuropathy and surgery of the anterior segment: temporal relationship analysis. Am J Ophthalmol. 2003;136(6):1171–2.
153. Hattenhauer MG, Leavitt JA, Hodge DO, Grill R, Gray DT. Incidence of nonarteritic anterior ischemic optic neuropathy. Am J Ophthalmol. 1997;123(1):103–7.
154. Boldt HC, Munden PM, Folk JC, Mehaffey MG. Visual field defects after macular hole surgery. Am J Ophthalmol. 1996;122(3):371–81.
155. Ezra E, Arden GB, Riordan-Eva P, Aylward GW, Gregor ZJ. Visual field loss following vitrectomy for stage 2 and 3 macular holes. Br J Ophthalmol. 1996;80(6):519–25.
156. Hutton WL, Fuller DG, Snyder WB, Fellman RL, Swanson WH. Visual field defects after macular hole surgery. A new finding. Ophthalmology. 1996; 103(12):2152–8.
157. Kerrison JB, Haller JA, Elman M, Miller NR. Visual field loss following vitreous surgery. Arch Ophthalmol. 1996;114(5):564–9.
158. Melberg NS, Thomas MA. Visual field loss after pars plana vitrectomy with air/fluid exchange. Am J Ophthalmol. 1995;120(3):386–8.
159. Paques M, Massin P, Santiago PY, Spielmann AC, Gaudric A. Visual field loss after vitrec-tomy for full-thickness macular holes. Am J Ophthalmol. 1997;124(1):88–94.
160. Costa VP, Smith M, Spaeth GL, Gandham S, Markovitz B. Loss of visual acuity after trabeculectomy. Ophthalmology. 1993;100(5):599–612.
161. Kolker AE. Visual prognosis in advanced glaucoma: a comparison of medical and surgical therapy for retention of vision in 101 eyes with advanced glaucoma. Trans Am Ophthalmol Soc. 1977;75:539–55.
162. Kawasaki A, Purvin V. Unilateral optic disc edema following trabeculectomy. J Neuroophthalmol. 1998; 18(2):121–3.

163. DeMere M, Wood T, Austin W. Eye complications with blepharoplasty or other eyelid surgery. A national survey. Plast Reconstr Surg. 1974;53(6):634–7.
164. Kelly PW, May DR. Central retinal artery occlusion following cosmetic blepharoplasty. Br J Ophthalmol. 1980;64(12):918–22.
165. Anderson RL. Bilateral visual loss after blepharoplasty. Arch Ophthalmol. 1981;99(12):2205.
166. Goldberg RA, Marmor MF, Shorr N, Christen-bury JD. Blindness following blepharoplasty: two case reports, and a discussion of management. Ophthalmic Surg. 1990;21(2):85–9.
167. Savino PJ, Burde RM, Mills RP. Visual loss following intranasal anesthetic injection. J Clin Neuro Ophthalmol. 1990;10(2):140–4.
168. Bolger WE, Keyes AS, Lanza DC. Use of the superior meatus and superior turbinate in the endoscopic approach to the sphenoid sinus. Otolaryngol Head Neck Surg. 1999;120(3):308–13.
169. Driben JS, Bolger WE, Robles HA, Cable B, Zinreich SJ. The reliability of computerized tomographic detection of the Onodi (spheno-ethmoid) cell. Am J Rhinol. 1998;12(2):105–11.

Nutritional and Toxic Optic Neuropathies

6

Michelle Y. Wang, Alfredo A. Sadun, and Jane W. Chan

Introduction

Mitochondrial optic neuropathies (MON) are increasingly recognized as a major spectrum of optic neuropathies resulting from different hereditary and acquired etiologies. The clinical presentation of MON is characterized by a slowly progressive bilateral central visual loss, dyschromatopsia, central or cecocentral scotomas, and loss of high spatial frequency contrast sensitivity [1]. Patients often describe the visual loss as a central haze or dark cloud. Ophthalmoscopic features during the acute or subacute stage may reveal a hyperemic optic disc and peripapillary retinal nerve fiber layer (RNFL) swelling [2]. Temporal pallor of the optic disc gradually develops. No relative afferent pupillary defect is present because of symmetric optic nerve involvement. Clinical features such as poor visual acuity, dyschromatopsia, and central visual field loss can all be explained by selective damage to the papillomacular bundle (PMB). The fibers of the PMB are most susceptible to this type of metabolic insult due to their long unmyelinated segment in the retina and their small caliber. Leber's hereditary optic neuropathy (LHON) and autosomal dominant optic atrophy (DOA) are two well-documented examples of hereditary MONs. Details regarding hereditary optic neuropathies are discussed in the chapter on hereditary optic neuropathies (Chap. 7). Acquired MONs can be categorized into four classes based on etiology: (1) nutritional, (2) drug induced, (3) toxic, and (4) combined metabolic optic neuropathies. In all instances, MON begins with dysfunction of mitochondrial oxidative phosphorylation and results in impaired function of the PMB.

M.Y. Wang, M.D. (✉) • A.A. Sadun, M.D., Ph.D.
Department of Ophthalmology, Doheny Eye Institute,
1450 San Pablo Street, Los Angeles,
California 90033, USA
e-mail: michelle.wang@med.usc.edu; asadun@usc.edu

J.W. Chan, M.D.
Department of Neurology, Neuro-Ophthalmology,
University of Nevada School of Medicine,
975 Kirman Avenue (111), Reno, Nevada 89502, USA
e-mail: worjun@aol.com

Symptoms

Nutritional and toxic optic neuropathies usually present simultaneously and bilaterally. Symptoms are progressive with symmetrical visual loss without pain. Some patients may initially only observe dyschromatopsia. If one eye is severely affected while the other eye has completely normal findings, then the diagnosis of nutritional/toxic optic neuropathy is questionable. The patient will describe a bilateral gradual progressive blurriness, followed by cloudiness at the point of fixation [3].

Signs

Nutritional and toxic optic neuropathies are characterized by slowly progressive, symmetric, and painless vision loss, usually resulting in visual

J.W. Chan (ed.), *Optic Nerve Disorders: Diagnosis and Management*,
DOI 10.1007/978-1-4614-0691-4_6, © Springer Science+Business Media New York 2014

acuity of 20/200 or better. Exceptions are methanol and ethylene glycol poisoning which present with more rapid visual loss, resulting in complete or nearly complete blindness. As visual acuity decreases, a protan defect first develops. Because of the symmetric and bilateral visual impairment, a relative afferent pupillary defect is often not present. The pupillary light response may be bilaterally sluggish or absent. The pupils are often dilated in completely or nearly blind patients. The most common visual field defects seen in nutritional and toxic optic neuropathies are central and cecocentral scotomas. In nutritional optic neuropathies, the optic disc may be normal or mildly hyperemic in the early stages. Peripapillary splinter hemorrhages may occasionally be seen. Over a period of several months to years, PMB atrophy and temporal optic disc pallor are followed by diffuse optic atrophy. In the early stages of toxic optic neuropathies, the optic discs usually appear normal. Disc edema and hyperemia are seen more often in acute intoxications such as methanol or ethylene glycol poisoning. The severity and course of development of PMB and temporal disc atrophy varies according to the type of toxin. For example, optic discs initially appear relatively normal in ethambutol toxicity and then become atrophic if the usage is prolonged; whereas optic disc edema and flame-shaped hemorrhages are the initial presentation in amiodarone toxicity [3].

Evaluation of Nutritional and Toxic Optic Neuropathy

Evaluation of any patient suspected of having a nutritional or toxic optic neuropathy should include a detailed history of when a drug or toxin was ingested, family history, and dietary history. In toxic optic neuropathies, the visual loss may be acute, subacute, or most often, chronic. The onset of visual symptoms occurring during or immediately after exposure to the specific toxin and the occurrence of similar illnesses in coworkers or others exposed to the same drug or chemical may help establish the etiology of the visual loss [3].

In addition to the history and examination, magnetic resonance imaging (MRI) of the brain and orbits with gadolinium is required to rule out compressive and ischemic lesions, since bilateral central visual loss can occur from bilateral anterior chiasmal or occipital lesions. MRI of the optic nerves and optic chiasm with and without gadolinium and diffusion tensor imaging may be needed to assess for signs of inflammation and/or demyelination [3, 4]. Visual field testing by static or kinetic techniques is essential. Although central or cecocentral scotomas are more common in affected patients, bitemporal defects or peripheral field constriction may occasionally occur in patients with ethambutol or amiodarone toxicity, respectively. In any patient with bilateral central scotomas, laboratory investigation for B12 deficiency and folate deficiency must be performed [3].

In diagnosing B12 (cobalamin) deficiency, serum B12 levels may be misleading because it may bind to transcobalamins that may lead to falsely normal serum B12 levels, such as in hepatic disorders. Falsely low serum levels may be seen in folate deficiency or during pregnancy. Serum methylmalonate and homocysteine levels should be measured for a more accurate determination of B12 deficiency. These precursors of the cobalamin-dependent pathway are elevated in at least 85 % of patients with B12 deficiency. Although these elevated levels of metabolites are not specific for B12 deficiency, they are useful in establishing the diagnosis of B12 deficiency when the serum B12 level is in the low to normal range (200–350 pg/mL) [5].

In order to determine the cause of the B12 deficiency, antiparietal cell antibodies, which are present in about 85 % of patients with autoimmune atrophic gastritis and anti-intrinsic factor antibodies, which are more specific than sensitive, should be measured. A Schilling test to look for B12 malabsorption syndrome can also be performed by a gastroenterologist [5].

A complete blood cell count and examination of the peripheral blood smear for any macrocytosis, macro-ovalocytes, and hypersegmented neutrophils is also required to establish the diagnosis of megaloblastic anemia, since B12 deficiency is associated with this disorder [5].

Other laboratory tests in the workup of a nutritional or toxic optic neuropathy include red blood cell folate levels, Venereal Disease

Table 6.1 Differential diagnosis of nutritional and toxic optic neuropathies [Adapted from Miller NR, Newman NJ (eds). Walsh and Hoyt's Clinical Neuro-ophthalmology, 5th edition, vol. l. Baltimore, MD: Lippincott Williams and Wilkins; 2004. With permission from Wolters Kluwer Health]

• Arteritic ischemic optic neuropathy (giant cell arteritis)
• Nonartec ischemic optic neuropathy
• Infiltrative optic neuropathy (sarcoidosis)
• Infectious optic neuropathy (syphilis, Lyme, toxoplasmosis, herpes zoster)
• Optic neuritis from demyelinating disease
• Postradiation optic neuropathy
• Hereditary optic neuropathy (Leber's hereditary optic neuropathy, dominant optic neuropathy)
• Compressive optic neuropathy (orbital pseudotumor, thyroid eye disease)
• Autoimmune optic neuropathy (lupus)

Research Laboratory, vitamin assays, serum protein concentrations, serum chemistry, urinalysis, and heavy metal screening, especially for lead, thallium, and mercury. Identification of the suspected toxin and its metabolite should be performed in the serum and urine (Table 6.1) [5].

Nutritional Optic Neuropathy

Vitamin deficiencies are now rare in the United States and in Western Europe. They are most likely to occur with general malnutrition, as a complication of another disease, such as malabsorption or alcoholism; as a consequence of therapy, such as hemodialysis or total parenteral nutrition; or as a result of an inborn error of metabolism. Vitamin deficiencies, including vitamin B12, vitamin B1, vitamin B2, and folic acid, cause central visual loss, dyschromatopsia, cecocentral scotomas, and a selective loss of the PMB as seen in MON [6].

Vitamin B12 Deficiency Optic Neuropathy

Optic neuropathy is a rare but important manifestation of vitamin B12 deficiency. Since Bastianelli reported an association between optic atrophy and pernicious anemia in 1897 [3], many cases of pernicious anemia associated with vitamin B12 deficiency optic neuropathy have been reported in the literature [7–11]. The optic neuropathy may be the initial manifestation in a patient when no other neurologic signs of B12 deficiency, such as peripheral neuropathy and dementia, are evident. The prevalence of vitamin B12 deficiency has been reported as high as 20 % in industrialized countries [12]. Vitamin B12 optic neuropathy has been reported in a case with microcytic anemia, as opposed to megaloblastic anemia that is typically seen in pernicious anemia [13, 14]. In addition to pernicious anemia, vitamin B12 deficiency may be a consequence of gastrointestinal surgery [15–17] or infection with the fish tapeworm *Diphyllobothrium latum* [18].

Pathophysiology

Vitamin B12 deficiency and its complications are more often seen in pernicious anemia, an autoimmune disorder resulting from antiparietal cell antibodies and anti-intrinsic factor antibodies that inhibit the production of intrinsic factor that is required for absorption of vitamin B12 in the ileum. Pernicious anemia most often occurs in middle-aged or elderly Caucasians. Optic neuropathy may be the initial feature of pernicious anemia, preceding the development of megaloblastic anemia and even lower cervical and upper thoracic posterior column demyelination and leukoencephalopathy. Patients with pernicious anemia and no visual symptoms may have abnormal visual evoked potentials (VEPs) suggestive of subclinical optic nerve and/or optic chiasm lesions [3].

Vitamin B12 deficiency leads to elevated levels of methylmalonyl CoA that interferes with fatty acid synthesis resulting in abnormal myelin formation [19, 20]. This subclinical optic neuropathy can be detected by delayed P100 latencies. B12 deficiency is also postulated to alter oxidative metabolism. It causes decreased levels of succinyl CoA, an integral component of Kreb's cycle. It is thought that impaired oxidative metabolism leads to elevated levels of methyltetrahydrofolate (MTHF), required for converting

homocysteine to methionine. As a kainate receptor agonist, MTHF causes excessive depolarization [21, 22] and depletion of adenosine triphosphate (ATP) [23, 24].

Since the smaller retinal ganglion cells [25] with axons constituting the PMB have a higher energy-to-volume ratio than the larger and more peripheral cells [1, 26, 27] the PMB would be most affected by ATP deficiency. This vulnerability may explain the development of a cecocentral scotoma in B12 deficiency optic neuropathy. ATP deficiency also plays a central role in the pathophysiology of a wide spectrum of MON such as LHON, tobacco–alcohol amblyopia (TAA), and other toxic optic neuropathies [6].

Diagnosis

The diagnostic evaluation of suspected vitamin B12 deficiency consists of checking serum cobalamin level, serum methylmalonate, and homocysteine levels. Although not specific for cobalamin deficiency, the metabolites, methylmalonate and homocysteine, can help establish a diagnosis of cobalamin deficiency when serum cobalamin level is in the low to normal range (200–350 pg/mL) [5]. Vitamin B12 levels below 100 pg/mL often produce neurologic manifestations. Antiparietal cell antibodies are more sensitive, whereas anti-intrinsic factor antibodies are more specific. They may both be used to identify patients with autoimmune atrophic gastritis. The cause of the vitamin B12 deficiency should then be evaluated by the Schilling test to determine the degree of cobalamin malabsorption. Because cobalamin deficiency is associated with megaloblastic anemia, complete blood cell count and examination of peripheral blood smear should be performed to look for macrocytosis with macro-ovalocytes and hypersegmented neutrophils [5].

Management

The treatment of vitamin B12 deficiency is cyanocobalamin 1,000 μg (intramuscularly) IM three times weekly for the first 2 weeks, followed by a maintenance therapy of 500–1,000 μg IM monthly. This replacement therapy is lifelong in most circumstances. Some patients who discontinue maintenance therapy may experience recurrence of neurologic symptoms. Reversal of symptoms and signs is greater with early and aggressive therapy. High-dose folate therapy corrects the megaloblastic anemia caused by cobalamin deficiency, but it does not improve and may even worsen the neurologic disease [5].

Folic Acid Deficiency Optic Neuropathy

Like B12, folate is involved in methionine metabolism. Folate, in the form of MTHF, donates a methyl group to homocysteine to form methionine and tetrahydrofolate. Tetrahydrofolate helps metabolize formate. Therefore, folate deficiency will lead to the accumulation of formate (a blocker of oxidative phosphorylation), which is also a toxic metabolite from methanol, causing optic neuropathy [28]. Folic acid deficiency causes other neurological manifestations, such as polyneuropathy and even subacute combined degeneration of the spinal cord. Although folate deficiency often occurs with other nutrient deficiencies, isolated folic acid deficiency optic neuropathy has been reported [29–32]. In this report, six patients with low folate levels but normal B12 levels developed bilateral visual loss, color defects, and central or cecocentral scotomas with optic discs that were normal, temporally pale, or diffusely pale [29]. Measurement of erythrocyte folate, rather than serum folate, was found to be more sensitive in the early diagnosis of this disorder. With folate replacement therapy, their vision improved within 4–12 weeks of symptom onset. A recent report of optic neuropathy among prisoners in Papua New Guinea was also linked to isolated folate deficiency [33].

Thiamine/B1 Deficiency Optic Neuropathy

Several studies have shown that isolated thiamine deficiency can cause optic neuropathy. Some children maintained on a ketogenic diet for seizure control [34] developed bilateral visual loss with cecocentral scotomas, low serum transketolase

(an indication of thiamine deficiency) but with normal B12 and folate levels. After replacement therapy, their vision recovered. In 1943, Carroll reported five patients with tobacco amblyopia who recovered vision within 6 weeks of supplementation of vitamin B1 [35]. In another case report of a patient with ulcerative colitis who developed no light perception and oculomotor palsy, thiamine replacement therapy resulted in visual recovery within a few days [36]. Thiamine deficiency optic neuropathy has also been associated with Wernicke's encephalopathy in a patient with chronic diarrhea [37].

Vitamin E Deficiency Optic Neuropathy

Vitamin E deficiency causes progressive ataxia, arreflexia, ophthalmoplegia, and pigmentary retinopathy. Optic neuropathy has been reported in a patient with cholestatic liver disease [38] and vitamin E deficiency with normal B12 and folate levels. He developed optic disc pallor and pigmentary retinopathy. VEPs were bilaterally extinguished and the electroretinogram was abnormal.

Zinc Deficiency Optic Neuropathy

Zinc is required for the metabolism of vitamin A in the eye [39, 40]. Zinc also plays an important role in stabilizing microtubules for axonal transport. Zinc deficiency causes defective rapid axonal transport in vitro which may also contribute to the development of optic neuropathy.

Although zinc deficiency may cause abnormal rod function, it has been associated with optic neuropathy in acrodermatitis enteropathica, an autosomal recessive defect in intestinal zinc absorption. Patients with acrodermatitis enteropathica have been documented with optic atrophy [41].

Further evidence linking zinc deficiency with optic neuropathy has indirectly been shown in the chelation of zinc by ethambutol which may cause optic neuropathy. In a study of 84 patients with ethambutol toxicity, those with lower zinc levels (less than 0.7 mg/L) had a higher incidence of optic neuropathy than those with serum levels greater than 1 mg/L [42].

Malabsorption Syndrome/ Diet-Related Optic Neuropathy

Biliopancreatic bypass surgery to induce a malabsorption syndrome to treat morbid obesity can be complicated by hypocalcemia with metabolic bone disease, a marked steatorrhea, and protein malnutrition [43] to cause a combined vitamin A deficiency and nutritional optic neuropathy. The most common nutritional deficits are seen with thiamine, vitamin B12, folate, vitamin D, vitamin E, and copper. Patients can experience various neurological findings ranging from encephalopathy, myelopathy, polyneuropathy to optic neuropathy [44, 45]. Visual function returned to normal after oral vitamin and mineral supplementation. Subacute sensory ataxia and optic neuropathy due to isolated thiamine deficiency after partial gastrectomy has also been reported [46]. Similarly, zinc deficiency-induced dermatitis and optic neuropathy has been reported after bariatric surgery [47].

Individuals with severe eating disorders are at risk for various forms of nutritional optic neuropathy [48]. Similarly, patients following a strict vegan diet who consume no animal products are at risk of multivitamin deficiencies, resulting in blurred vision and painful sensorimotor neuropathy [49, 50]. Autistic children with severe food selectivity and highly stereotyped diets may exclude animal products in their diets, resulting in vitamin B12 optic neuropathy [51]. Therefore, it is important to obtain a detailed dietary history in order to minimize and reverse nutritional visual loss.

Drug-Induced Optic Neuropathy

Drugs can injure the optic nerve by interfering with mitochondrial oxidative phosphorylation, thereby producing a classic clinical picture of MON. Drugs proven to cause MON by blocking

oxidative phosphorylation include ethambutol, chloramphenicol, linezolid, erythromycin, streptomycin, and antiretroviral drugs [28, 52, 53]. Other drugs that can cause optic neuropathy, which are not as much associated with mitochondrial dysfunction, include amiodarone, infliximab, clioquinol, dapsone, quinine, pheniprazine, suramin, and isoniazid [52, 54].

Ethambutol-Associated Optic Neuropathy

Worldwide, there are approximately 9.2 million new cases of tuberculosis (TB) each year, and about 55 % of these patients take ethambutol to prevent or delay the emergence of drug resistance [55]. As a consequence, ethambutol is the most common cause of toxic optic neuropathy accounting for 100,000 new cases each year [56].

Ethambutol, used in the treatment of Mycobacterium tuberculosis, is metabolized to a chelating agent that may impair the function of metal-containing mitochondrial enzymes, such as the copper-containing cytochrome c oxidase of complex IV and the iron-containing NADH:Q oxidoreductase of complex I. Due to the similarity between mammalian mitochondrial DNA and bacterial ribosomes, ethambutol also disrupts oxidative phosphorylation and mitochondrial function by interfering with iron-containing complex I and copper-containing complex IV [53]. Copper is a required cofactor for cytochrome c oxidase, an essential component in the electron transport chain. Ethambutol may reduce the level of copper, thereby interfering with oxidative phosphorylation. Replacing copper leads to improved retinal ganglion cell survivability in in vivo models of ethambutol optic neuropathy [57]. It is interesting that copper deficiency due to malabsorption from bariatric surgery has also been associated with visual loss from optic neuropathy [44, 58]. Other studies suggest that zinc might also play a role in ethambutol toxicity [57, 59], and individuals with reduced serum zinc level may be more susceptible to ethambutol ocular toxicity [42, 60]. A study using cell cultures demonstrated that the chelating effect of ethambutol may inhibit lysosomal activation, resulting in accumulation of zinc in lysosomes with increased lysosomal membrane permeability and cell death [61].

Ethambutol ocular toxicity has been well documented in the literature shortly after its introduction in the 1960s [62–78]. The frequency of visual impairment has been reported in 50 % of patients at a dose of 60–100 mg/kg/day, 5–6 % at 25 mg/kg/day, and 1 % at ≤15 mg/kg/day [79]. Visual loss is typically insidious and symmetrical, occurring typically 2–8 months after initiation of therapy. Central visual field loss is typical [72, 73] (Figs. 6.1a, b), but other patterns such as bitemporal defects have been described [80–82] and neuroimaging may be required because these findings suggest chiasmal involvement. Age, hypertension, and renal disease have been reported as risk factors [83]. The standard treatment regimen for newly diagnosed cases of TB consists of an initial phase lasting 2 months, followed by a continuation phase of 4–6 months. The initial phase usually includes isoniazid, rifampicin, pyrazinamide, and ethambutol. Ethambutol toxicity is duration and dose dependent. The recommended single daily dose for the initial phase in adults is 15–20 mg/kg body weight for 2 months or 20–35 mg/kg body weight three times a week [84]. The dose is as efficacious when given three times weekly as when given daily with the potential advantage of better compliance, reduced cost, and less ocular toxicity [85]. Typically, toxic levels of ethambutol occur when dosage is not adjusted according to the patient's weight or renal function. However, visual loss has been reported in 1 % of patients taking even the recommended dose [86, 87].

The Centers for Disease Control has a dosing table for adults based on estimated body weight [88]. The World Health Organization has recommended a daily dose of 20 mg/kg (range 15–25 mg/kg) for children of all ages with drug-susceptible TB [89]. A higher range of daily dose (20–30 mg/kg) should be considered only for drug-resistant TB [90].

Optic neuropathy is rare with treatment of less than 2 months and often reversible with early withdrawal. However, irreversible dam-

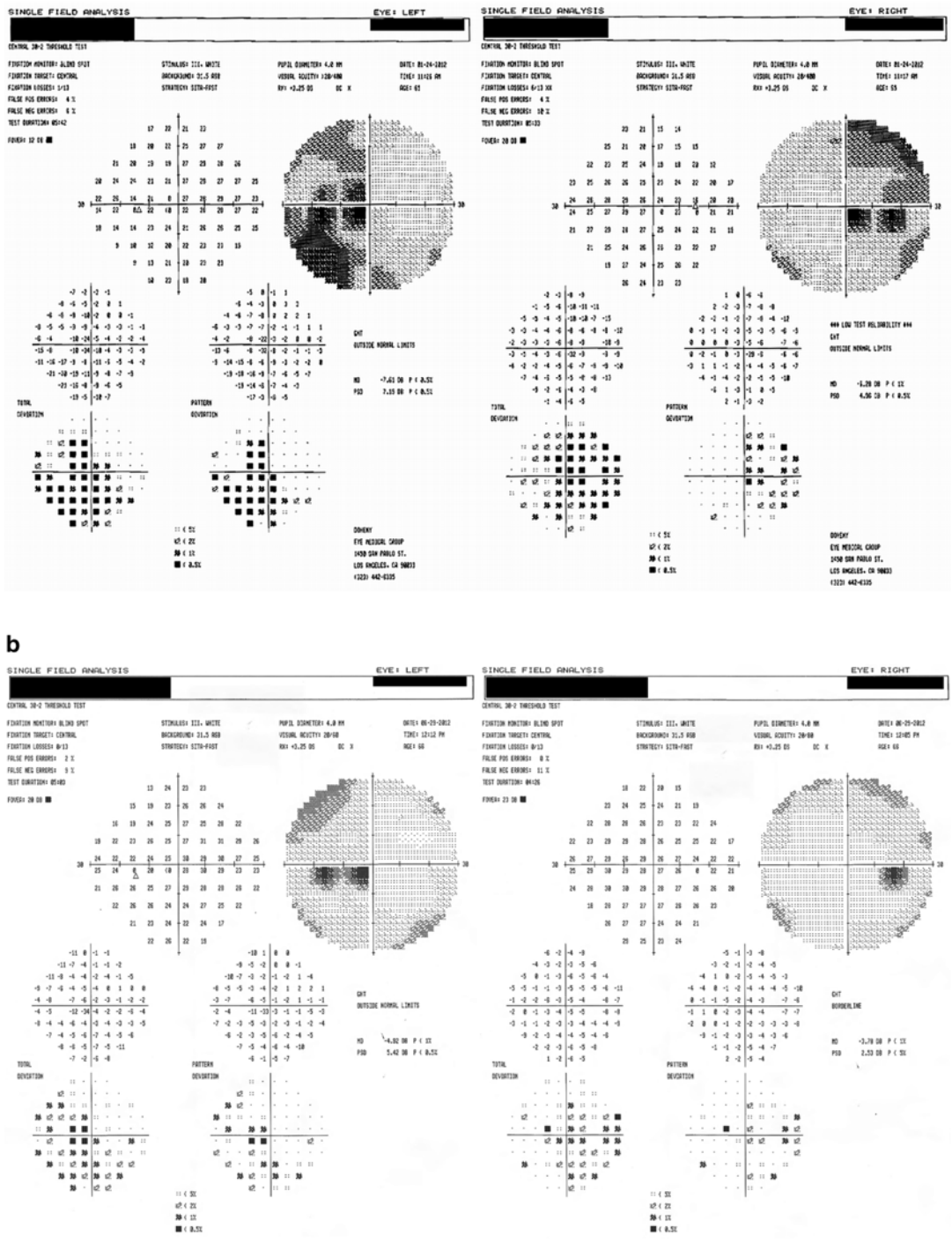

Fig. 6.1 Ethambutol optic neuropathy. (**a**) A 65-year-old woman developed vision of 20/400, right eye, and 20/800, left eye, after beginning ethambutol at a dose of 26.5 mg/kg/day for *Mycobacterium avium*. Humphrey 30–2 central threshold visual fields show bilateral cecocentral scotomas with temporal field depression. (**b**) 3 months after cessation of ethambutol, visual acuity was 20/60, right eye, and 20/80, left eye, with improvement in visual fields. One year later vision was 20/30 bilaterally

age may occur especially if treatment exceeds 6 months [91, 92]. After cessation of ethambutol, visual impairment often worsens over a period of months, followed by stabilization and gradual improvement over the next 6 months. While vision may improve after cessation of the drug, it is not unusual to have permanent visual deficits [93, 94]. Since ethambutol is renally excreted, patients with impaired renal function are at greater risk for toxicity [95]. Most cases of visual loss in patients on recommended doses occur in those with poor renal function [92].

It is important to individualize the treatment regimen and monitor patients closely for early signs of optic neuropathy. Patients should be educated to withdraw the drug at the onset of any visual symptoms. There is no consensus on the standard of treatment for ethambutol ocular toxicity or specific screening and monitoring recommendations for asymptomatic patients. A baseline ophthalmologic examination including visual acuity, color vision, and visual fields should be performed prior to initiation of ethambutol and repeated at the onset of visual symptoms [96]. During the treatment phase, asymptomatic patients taking the recommended doses may be monitored every 1–3 months [97]. Monthly monitoring may be necessary for patients with increased risks for toxicity such as diabetes, chronic renal failure, renal TB, alcoholism, old or young age, or coexisting ocular deficits [98]. Contrast sensitivity and multifocal electroretinogram (ERG) also may be helpful tests to detect subclinical changes [99]. Pattern visual evoked responses may demonstrate an increased mean latency of the P_{100} wave [100] and optical coherence tomography assists in monitoring RNFL thickness [101].

Chloramphenicol-Associated Optic Neuropathy

Chloramphenicol was used to treat cystic fibrosis in children until 1970 when its ocular toxicity was recognized [102]. Chloramphenicol inhibits bacterial protein synthesis by binding to the 50S ribosomal subunit (common to both bacteria and mitochondria), thereby inhibiting mitochondrial protein synthesis as well [103]. The incidence and severity of optic neuropathy is dose dependent. Transmission electron microscopy of bone marrow cells of patients taking chloramphenicol has shown swollen mitochondria with disrupted cristae and an abnormally high level of intramitochondrial iron deposits, confirming the toxic effect of the drug [104].

The clinical findings of chloramphenicol optic neuropathy are characterized by hyperemic optic discs with blurred margins, swelling of the PMB, and central scotomas [105]. Selective damage to the PMB and tortuous peripapillary retinal vessels was often seen. Prompt cessation of the drug and treatment with vitamin B complex usually leads to substantial recovery of visual function.

Linezolid-Associated Optic Neuropathy

Linezolid is used in the treatment of methicillin-resistant Staphylococcus, vancomycin-resistant Enterococcus, nosocomial pneumonia, and complicated skin infections. Linezolid inhibits protein synthesis by binding to 23S rRNA of the bacterial 50S ribosomal subunit and inhibiting formation of the 70S initiation complex. As mitochondrial ribosomes are similar to those of bacteria, protein synthesis in mitochondria also is disrupted.

Linezolid is generally well tolerated when used up to 28 days. Both optic and peripheral neuropathies have been reported in patients taking linezolid for longer periods [106]. Linezolid reaches inhibitory concentrations for most gram-positive pathogens within 4 h after a single oral dose of 600 mg [107]. Toxicity has been associated with off label extended therapy of 5–50 months [108–110]. Full visual recovery has been reported in some cases after discontinuing the drug [111]; however, the peripheral neuropathy is usually irreversible. The initial optic disc edema and peripapillary RNFL thickness resolves after cessation of the drug [111]. In a rat model, linezolid has been shown to induce a dose- and

time-dependent decrease in the activity of mitochondrial complex I and complex IV [112].

Most reports of linezolid toxic optic neuropathy described patients with initial visual acuity of 20/200 or worse, improving to 20/30, or better after discontinuation of the drug. Color defects, visual field defects, and optic disc pallor also improved [113–117]. It is recommended that, if patients are to receive this antibiotic for greater than 28 days, they should be monitored with baseline and monthly eye examinations thereafter. Visual acuity, visual field, color vision, and dilated fundoscopy should be performed.

Other Antibiotics

Erythromycin also binds to the 23S rRNA of the 50S ribosomal subunit, impairing protein synthesis in bacteria and mitochondria. Erythromycin-induced mitochondrial dysfunction has also been noted to be dose dependent [118]. Similarly, streptomycin, an aminoglycoside, better known for toxicities involving the eighth cranial nerve and peripheral nerves, also may cause optic neuropathy [119].

Genetic Mitochondrial Dysfunction Predisposes Patients to Greater Toxicity

Preexisting dysfunction in mitochondrial metabolism from genetic causes such as LHON and autosomal DOA likely makes patients more vulnerable to drug-induced MON.

The nucleoside analog azidothymidine, also known as zidovudine, is an important component of highly active anti-retroviral therapy (HAART), in the treatment of human immunodeficiency virus. It belongs to a class of drugs known as nucleoside reverse transcriptase inhibitors that function by interfering with viral DNA replication. This class of drugs is used not only by retroviral reverse transcriptase, but also by the mitochondrial DNA polymerase gamma [120]. Therefore, all nucleoside analog reverse transcriptase inhibitors may induce mitochondrial toxicity by inhibiting mitochondrial polymerase gamma and mitochondrial DNA (mtDNA) replication [121, 122].

Case reports of profound visual loss and color deficiencies in LHON patients harboring either the 11,778 or 14,484 mutations after initiation of HAART have been reported, suggesting that antiretroviral therapy may be associated with increased risk in genetically predisposed patients [123, 124]. Ethambutol and erythromycin have also been suggested to trigger LHON [125–127]. Similarly, ethambutol has been linked to visual loss in a patient with DOA with an OPA1 mutation [128]. If possible, these drugs should be avoided in patients harboring genetic mitochondrial defects.

Toxic Optic Neuropathy

Methanol-Associated Optic Neuropathy

Methanol, used as an industrial solvent and in automotive antifreeze, is one of the most common causes of toxic optic neuropathy. Methanol is catabolized to formaldehyde in the liver by alcohol dehydrogenase and catalase. Formaldehyde is then metabolized to formic acid by the liver and red blood cell aldehyde dehydrogenases (ADH) [129]. Formate interferes with mitochondrial pathways and blocks ATP production by inhibiting cytochrome oxidase [130, 131] which then can cause impaired axonal transport and loss of membrane polarity and conduction [132]. Disrupted saltatory conduction leads to visual loss, and the axonal compression from retrobulbar disc swelling might also obstruct anterograde axoplasmic flow.

Postmortem histopathologic findings from four revealed that formate toxicity was selective for the retrolaminar optic nerve and the centrum semiovale [133]. Since cytochrome oxidase activity is lower in white matter than in gray matter [134], oligodendroglia of the optic nerve and cerebral white matter could be more vulnerable to formate toxicity than neurons of the retina or cerebral cortex [132].

The symptoms of methanol intoxication are usually delayed for 12–18 h. During this latent period, methanol is oxidized to the more toxic formate which then causes a metabolic acidosis, a hallmark of methanol intoxication. The degree of acidosis reflects the severity of the intoxication. Drowsiness, headache, nausea, vomiting, abdominal pain, and blurry vision are common presenting symptoms and may be followed by blindness, coma, and cardiac arrest if intoxication is severe [135]. Permanent visual loss may occur within hours to days after ingestion of methanol.

Patients intoxicated with methanol present with varying levels of visual loss, even with total permanent blindness. Central and cecocentral scotomas are usually present in patients with partial visual loss. In the early stages, the optic discs may be edematous and hyperemic with peripapillary retinal edema. Pupillary responses are often sluggish and no response to light is indicative of a poor prognosis. The optic discs gradually become pale with glaucomatous-like cupping and retinal arteries may appear attenuated [3]. The visual outcomes in methanol poisoning vary [136]. Patients may present with transient or permanent visual disturbances [137–140]. Blurred or snowfield vision may improve within 2 weeks after treatment. New visual disturbances, however, may still develop subsequently [141]. Prolonged acidosis was shown to be a poor prognostic factor [142, 143].

A serum methanol level greater than 20 mg/dL with a large anion gap, a high serum formate level, and a decreased serum bicarbonate level confirms the diagnosis of methanol intoxication. Peak levels of serum methanol occur 60–90 min after ingestion but this may not correlate with the level of toxicity and is therefore not a reliable prognostic indicator [144].

Either fomepizole or ethanol should be given to interfere with the metabolism of methanol, along with hemodialysis to remove the toxin, and bicarbonate administered to restore acid–base balance. Ethanol is metabolized by ADH and serves as a competitive substrate. The enzyme has 10–20 times greater affinity for ethanol than methanol. Alternatively, fomepizole, an inhibitor of ADH, has been shown to be safe and effective with fewer adverse effects [145]. If treatment is delayed beyond the first several hours of ingestion of methanol, permanent visual damage may occur [3]. Intravenous pulse steroids have been tried in a few cases, with encouraging results [146, 147]. One case suggested that intravenous erythropoietin may be an effective adjuvant with other therapies including steroid, vitamin B12, B6, and folic acid to treat methanol optic neuropathy [148].

Ethylene Glycol-Associated Optic Neuropathy

Ingestion of ethylene glycol, an active ingredient in automobile antifreeze, causes toxic symptoms similar to those of methanol, including nausea, vomiting, abdominal pain, coma, and cardiac arrest. Unlike the complications of methanol intoxication, renal failure is more likely to occur from ethylene glycol poisoning while visual loss is less likely [149]. The optic discs may initially appear normal to be followed by optic atrophy. Unlike the visual findings in methanol toxicity, papilledema from increased intracranial pressure may be associated with nystagmus and ophthalmoplegia [3].

The presence of oxalate crystals in the urine confirms the diagnosis of ethylene glycol intoxication. Glycolate, a metabolite of ethylene glycol, causes a metabolic acidosis and a large anion gap. Therefore, treatment is similar to that for methanol intoxication including bicarbonate, ethanol, and hemodialysis [149].

Toluene-Associated Optic Neuropathy

Toluene is a colorless liquid found in glues, paints, and industrial products. Toluene inhalation can also lead to toxic optic neuropathy [150]. In a study of 15 patients with bilateral optic neuropathy secondary to toluene toxicity, the pattern visual evoked cortical potentials (PVECP) were nonrecordable in both eyes of 11 cases.

The P100 peak latency was prolonged in both eyes of three cases, and only one case showed a normal P100 peak latency [151]. The visual prognosis and the PVECP changes were identical in both eyes of all patients. Changes in visual field defects were not mentioned in this study.

Toluene inhalation causes a central nervous system (CNS) white matter disorder resulting in not only visual loss, but also ataxia, corticospinal deficits, and dementia. Toxicity results in an increase in very long chain fatty acids. Axonal swelling and thinning of the myelin sheaths of peripheral nerves have been demonstrated on histopathologic studies [152].

Combined Nutritional and Toxic Optic Neuropathies

Cuban Epidemic of Optic Neuropathy (CEON)

An epidemic of optic and peripheral neuropathy affected about 50,000 malnourished Cubans in the early 1990s [153]. This outbreak was associated with poor nutrition specifically chronic vitamin B12 and folate deficiency, in addition to chronic, but mild formate toxicity from rum. Regulation of commercial rum in Cuba in 1992 led to greater consumption of inadequately aged home-brewed rum. Field study testing revealed the presence of low levels (1 %) of methanol within the noncommercial rum, which resulted in the accumulation of formate from methanol metabolism. Formate is inadequately detoxified by folate. Additionally, improper preparation of cassava can leave cyanide residuals leading to cyanide poisoning. The CEON is therefore an acquired mitochondrial dysfunction due to several mechanisms that block oxidative phosphorylation: (1) formate accumulation from chronic low dose methanol consumption, (2) folate deficiency, and (3) exposure to cyanide from cassava, cigar, or cigarette smoke [154].

The clinical profile for CEON was typical of MON, presenting with symmetric cecocentral scotomas. The fundus examination showed marked thinning of the PMB, forming a wedge defect bordered by swollen nerve fibers. In addition to optic neuropathy, many Cubans also had peripheral neuropathy, ataxia, and hearing loss. Prompt administration of cyanocobalamin (3 mg) and folate (250 mg) per day resulted in some visual recovery in a significant number of patients [26]. In a 4-month follow-up study of 13 patients with CEON, the average visual acuity recovered from 20/400 to 20/50 and average color vision on the American Optical Color test plates improved from 2/8 to 7/8 following vitamin therapy [26].

In a study by Román [155], the 50,862 reported cases were analyzed further to reveal not only optic neuropathy, but sensorineural deafness, peripheral painful sensory neuropathy, and dorsolateral myeloneuropathy. These clinical features were similar to those seen in Strachan syndrome and beriberi, both disorders resulting from a deficiency of micronutrients [156, 157]. Most Cubans significantly improved in their neurological symptoms after multi-B vitamin and folate supplements. Less than 0.1 % of them had any sequelae.

Formate accumulation from folic acid deficiency and methanol ingestion can cause oxidative phosphorylation defects [158]. In a study of 34 affected Cubans with 65 controls by Gay et al. [158], dietary factors were associated with the occurrence of epidemic neuropathy in Cuba. Smoking and alcohol consumption augmented the adverse effects of dietary deficiencies. The Cubans had a diet consisting of low calories, insufficient protein, fat, and micronutrients, but with a disproportionate excess of sugar.

Some have suggested the presence of LHON mutations which could have further predisposed some Cubans to develop an optic neuropathy. Johns et al. [159] described mitochondrial DNA mutations in two of nine Cubans with optic neuropathy and peripheral neuropathy. They had LHON mutations at nucleotide position 9,438 and 9,738 which are not primary mutations for LHON and probably represent nonpathological polymorphisms or variants [159]. The stresses of poor diet, smoking, alcohol, and other environmental factors could have precipitated the clinical manifestation of LHON in a few genetically predisposed patients [160, 161].

Tobacco–Alcohol Amblyopia

The nutritional optic neuropathy in Cuba was also influenced by other environmental factors. Lincoff et al. [162] and Tucker and Hedges [163] described a clinical syndrome in some Cuban patients involving thiamine and B12 deficient optic neuropathy, plus glossitis, cheilitis, and cheilosis associated with cigarette smoking and alcohol consumption.

TAA is a metabolic optic neuropathy which some investigators take issue with the term and even with the concept [164]. While uncommon in the United States, it is frequent in some Asian or African countries. It typically affects men with a history of heavy tobacco and alcohol use [165, 166]. The mechanism by which tobacco causes optic nerve toxicity is unclear, but it is believed that cyanide in tobacco smoke in combination with vitamin B12 deficiency related to alcohol heavy consumption may play a role in optic nerve damage [167]. Studies have shown that tobacco-derived compounds, including reactive oxygen species and cyanide, interfere with mitochondrial oxidative phosphorylation [168], damage mtDNA [169], and induce changes in mitochondrial morphology [170].

Subacute progressive, symmetric, painless bilateral visual loss, dyschromatopsia, and central or cecocentral scotomas are characteristic symptoms [171–173]. Tortuous small retinal vessels, or telangiectasia, may be seen. The optic discs initially appear normal but temporal pallor usually develops later [173].

TAA occurs most commonly in pipe smokers, cigar smokers, and users of chewing or snuffing tobacco. Nicotine may not play a role in its pathogenesis [174]. The change in tobacco intake habits from snuffing and chewing in the nineteenth and early twentieth centuries to smoking could have contributed to the decrease in its prevalence [175]. While tobacco toxicity is often accompanied by vitamin B12 deficiency, cases in which no nutritional deficiencies were detected have also been associated with tobacco–alcohol toxicity [176, 177]. However, many cases of TAA later proved to be due to underlying genetic problems, such as LHON [178].

The treatment for TAA is cessation of smoking and drinking. Early hydroxycobalamin administration may also be helpful for visual recovery [177].

Some clinical features of TAA are similar to those of LHON. However, the prodromal symptoms of weight loss, polyuria, fatigue, and other neurological manifestations, such as myelopathy and peripheral neuropathy appeared more consistently in CEON and with TAA. Cogwheel smooth pursuit and visual recovery with vitamin supplementation also distinguished this epidemic disorder from LHON [179].

Other Epidemics of Combined Nutritional/Toxic Optic Neuropathies

Similar epidemics of combined optic neuropathy have also been studied in other parts of the world including Strachan syndrome in the Caribbean [180]; syndromes involving Canadian prisoners of war during World War II [181], prisoners of war from Thailand [182], prisoners of war from the Korean war [183]; tropical ataxic neuropathy in Nigeria [184]; and syndromes involving "Konzo" in the Democratic Republic of Congo [185], Mozambique [186] and Tanzania [187].

In Jamaica, Strachan's syndrome was historically associated with poor nutrition during periods of hardship [188], Bilateral visual loss with central or cecocentral scotomas and temporal optic disc pallor was also associated with a painful sensory ataxic peripheral neuropathy and muscle atrophy. Gastric achlorhydria and malabsorption of B12 was often found. Treatment with vitamin B after many years of visual loss did not promote recovery.

A Strachan-like syndrome was also discovered in Nigeria in the 1970s by Osuntokun and Osuntokun [189]. However, these 360 Nigerians with a form of tropical amblyopia presented with gradual or rapid visual loss, color defects, and, notably peripheral constriction, rather than central scotomas. It was hypothesized that peripheral retinal damage might have contributed to the peripherally constricted visual fields, but 41 % of affected persons had marked bilateral temporal disc pallor, similar to that seen in nutritional amblyopia.

Cyanide from cassava beans, a staple food in Nigeria, was thought to have contributed to this disorder. Elevated levels of cyanocobalamin, plasma thiocyanate, cyanide, and urinary thiocyanate were all suggestive of this cyanide exposure. A balanced diet helped improve vision, whereas returning to the cassava diet worsened vision.

Similar to CEON, an outbreak in Tanzania reported in 1988 was characterized by bilateral, simultaneous, painless, visual loss over 2–12 weeks, impaired color vision, and loss of PMB fibers accompanied by central or cecocentral scotomas and a peripheral neuropathy [190–192]. Vitamin B deficiency was found in this population. Low folate status and indoor pollution were additional risk factors for what was termed, the "endemic optic neuropathy in Tanzania" [193].

One hundred and five cases of acute optic neuropathy were also identified in Mogadishu, the Somalian capital [194]. Typical symptoms included bilateral loss of vision with central or cecocentral scotomas and diminished color vision. The optic disc was initially hyperemic, but pallor occurred after a month. Similar to the endemic in Tanzania, the Somalian patients also experienced peripheral neuropathy.

In general, removal of the toxin sometimes leads to some reversal of the optic neuropathy. Oral maintenance replacement therapy of thiamine 100 mg/day, folic acid of 1 mg/day, and vitamin B12 of 1,000 mg/day may be appropriate for those with additional folate deficiency. Folate treatment itself only reverses the megaloblastic anemia caused by cobalamin deficiency and does not improve the optic neuropathy. Discontinuation of smoking and alcohol along with a well-balanced diet emphasizing green vegetables and fruit is critical for recovery in nutritional optic neuropathy [5].

Non-mitochondrial Optic Neuropathies (Non-MOPs)

Amiodarone- and Digoxin-Associated Optic Neuropathy

Amiodarone-induced optic neuropathy has been a controversial topic in the neuro-ophthalmology literature [195]. The underlying pathophysiology is unclear, but one theory is that it is due to the selective accumulation of intracytoplasmic inclusions in the optic nerve axons, thereby leading to optic disc edema, congestion, and decreased axoplasmic flow [196]. An increased incidence (1.79 %) of nonarteritic anterior ischemic optic neuropathy (NAION) serves as the most compelling evidence for amiodarone-induced optic neuropathy [197]. This incidence is higher than the incidence (0.3 %) of NAION found in the general age-matched population. However, this comparison may contain inherent selection bias, as patients on amiodarone have medical problems such as cardiac arrhythmias, hypertension, and other risk factors for NAION which become confounders.

Amiodarone-induced optic neuropathy is characterized by an insidious onset, slow progression, and bilateral visual loss which are associated with optic disc swelling that tends to stabilize within several months of discontinuation of the medication [198]. However, in a review of 55 patients with amiodarone-optic neuropathy, Johnson et al. [199] found that only 51 % of patients presented with painless bilateral simultaneous optic disc edema, and 35 % of patients had acute unilateral disc edema. Johnson et al. opined that the spectrum of amiodarone-associated optic neuropathy could be categorized into five clinical types: (1) insidious onset, (2) acute onset, (3) retrobulbar, (4) increased intracranial pressure, and (5) delayed-progressive onset. They found that the most common form of amiodarone-associated optic neuropathy presented insidiously in 43 % of patients. The second most common type presented with an acute unilateral or bilateral visual loss in 28 % of patients. About 13 % of patients presented with a retrobulbar optic neuropathy in which the visual loss was insidious or acute and in one or both eyes simultaneously. About 8 % of patients taking amiodarone develop increased intracranial pressure greater than 200 mmH_2O. In 8 % of patients, amidoarone-associated optic neuropathy had a delayed-progressive onset. Amiodarone-associated optic neuropathy with a dose ranging from 100 mg to 1,200 mg/day occurred within 12 months of initiation in 88 % of the cases. These patients reported visual loss before any appearance

of optic disc edema and developed disc edema days to weeks after amiodarone was withdrawn, likely because the long half-life of amiodarone is about 3 months [200, 201].

In this same study, nearly 20 % with amiodarone-associated optic neuropathy had 20/200 or worse on presentation [199]. While 40 % experienced some improvement in visual acuity, half of the patients had no change in visual acuity after stopping the drug. In general, this incidence is similar to that of NAION cases. Ten percent had further worsening of their visual acuity after drug withdrawal. Optic atrophy was the common end stage for all patients with corresponding persistent field defects, similar to those seen in NAION. The final outcome of visual acuity in patients seen by this group with amiodarone-associated optic neuropathy was 20/30 compared to 20/60 in patients with NAION [202]. Others have argued that many purported amiodarone cases were simply NAION in patients whose risk factors already predisposed them to the disease [203].

Amiodarone, like other amphiphilic drugs, binds to polar lipids and accumulates within lysosomes [204]. As the fenestrated peripapillary choroidal capillaries are permeable to amiodarone, the choroidal interstitial fluid containing amiodarone may allow drug-induced phospholipidosis, in which membrane-bound bodies with multilamellar inclusion bodies accumulate in astrocytes and even ganglion cell axons in the optic nerve head. Histopathologic study has shown intracytoplasmic lamellar inclusions in large axons of the optic nerve. The accumulation of these inclusions may impair axoplasmic flow to cause optic disc edema.

Amiodarone toxicity to the optic nerve may be dose related with reports varying in range from 200 to 1,200 mg/day. Decreasing the dose of amiodarone may improve the optic disc edema and discontinuation of the drug occasionally may be associated with gradual recovery. Since the half-life of amiodarone is over 3 months, amiodarone-related optic disc edema lasts months compared to the disc edema of NAION that resolves within a few weeks. Unlike the usually persistent field defects of NAION, the mild peripheral field defects may improve in amiodarone-related optic neuropathy. Concurrent use of digoxin with amiodarone may increase the known side effects of digoxin, such as dyschromatopsia, visual disturbances, and visual field defects.

There are some clinical features that may help distinguish amiodarone-induced optic neuropathy from AION [205]. True amiodarone-induced optic neuropathy is probably characterized by an insidious onset of bilateral and symmetrical visual loss with slow progression and occurring within weeks of starting the medications [198]. The optic disc may not have the classic disc-at-risk appearance, and disc edema is typically bilateral which tends to stabilize and then regress months after discontinuation of the medication. On the other hand, NAION is characterized by an acute, unilateral visual loss that is rarely progressive. The fellow optic disc often has a small cup-to-disc ratio, and the unilateral disc edema resolves after a few weeks followed by disc pallor (Table 6.2).

Table 6.2 A comparison of neuro-ophthalmic features between NAION and amiodarone-related optic neuropathy [Adapted from Johnson LN, Krohel GB, Thomas ER. The clinical spectrum of amiodarone-associated optic neuropathy. J Natl Med Assoc. 2004;96:1477–91. With permission from Elsevier]

Features	NAION	Amiodarone optic neuropathy
Medication use	Absent	Within 12 months of initiating amiodarone (median of 4 months)
Gender preference	Male = female	Male > female
Incidence	2.3–10.2/100,000 and >50 years of age	About 2 % in patients treated with amiodarone
Ocular laterality at presentation	Unilateral	65 % bilateral and 35 % unilateral
Visual acuity on presentation	20/20: no light perception	20/20 to 20/200
Optic nerve cup-to-disc ratio	Small (<0.2) cup-to-disc ratio	Any cup-to-disc ratio
Increased intracranial pressure	Absent	Occasional
Duration of disc edema after NAION attack/ after drug withdrawal	2–4 weeks	1–8 months (median of 3 months)

Since the association of amiodarone optic neuropathy remains controversial, and since this medication may be life saving, the decision to discontinue amiodarone in the treatment of life-threatening cardiac arrhythmias is best made by the cardiologist [195, 206]. Nevertheless, it is prudent to perform a careful fundus examination in patients taking amiodarone and to consider alternative antiarrhythmic therapy if there are examination findings consistent with the disease. A baseline ophthalmic examination every 6 months may be appropriate [207].

It is not unusual to find published case reports claiming to describe a new toxic optic neuropathy. Such a collection of anecdotal cases or case series may suggest an association. But establishing an agent to be causal requires a higher standard. The following postulates for establishing toxic optic neuropathy are proposed:

1. A strong scientific rationale should explain why there is an optic neuropathy. Some scientific evidence should support why retinal ganglion cells or their axons are vulnerable.
2. A clinical dose–response curve or association should be present, such that higher doses should make the optic neuropathy worse and more likely, and vice versa.
3. Longer duration of exposure should be a risk factor, such that longer periods of exposure or a higher total dosage should increase the risk, and vice versa.
4. At least some recovery should occur after discontinuation of the toxin.
5. Asymmetry of symptoms and signs should be the exception and explicable. Toxins do not preferentially affect one optic nerve over the other.

Therefore, the more postulates satisfied, the greater the likelihood that the toxin caused the optic neuropathy.

Disulfiram-Associated Optic Neuropathy

Disulfiram, used in the treatment of chronic alcoholism, interferes with the metabolism of acetaldehyde, a metabolite of ethanol. Optic neuropathy has been reported in a few patients with chronic disulfiram use [208]. The mechanism of toxicity on the optic nerve is unknown. Visual loss is usually subacute or chronic and symmetric with central or cecocentral scotomas. The optic discs are often normal initially and later become pale. The optic neuropathy usually recovers completely in 1–5 months after discontinuing disulfiram [3].

Interferon-Alpha-Associated Optic Neuropathy

Interferon-alpha (IFN-α), a glycoprotein produced in response to viral infections, serves as intracellular signaling to enhance expression of specific genes, to enhance and induce lymphocytes to kill target cells, and to inhibit virus replication in infected cells [209]. Since IFN-α has anticytokine, antiviral, immunomodulatory, and antiproliferative activities, it has been used to treat chronic hepatitis B and C, cancer, and essential thrombocytosis [209]. It has been postulated that IFN-α can produce autoantibodies and subsequently cause deposition of immune complexes in the small arteries of the optic nerve. IFN-α can stimulate other cytokines that may lead to an inflammatory reaction of the blood vessels that might subsequently induce ischemia [210–212].

NAION is an uncommon complication of IFN-α treatment [213–223]. Two patients undergoing treatment with IFN-α developed bilateral simultaneous optic neuropathy within 3 months of starting this medication [224]. In one patient, the bilateral optic disc edema and nerve fiber layer hemorrhages were associated with inferior nerve fiber bundle defects. Despite treatment with aspirin 300 mg/day after cessation of IFN-α in one patient, visual acuities and field defects remained unchanged. In the other patient who was treated with IV methylprednisolone 1 g/day for 3 days with prednisone taper after IFN-α was discontinued, visual acuities improved but visual field defects persisted. NAION may occur within 1 week to 3 months after starting IFN-α treatment in patients who do not have underlying vasculopathic risk factors for NAION [210, 225, 226]. The two patients reported by Purvin [211] developed sudden bilateral, sequential visual loss with

disc-related field defects and segmental optic disc edema, which are all features characteristic of NAION. The degree of optic disc pallor may depend on the severity of ischemia. Underlying anemia may decrease perfusion to the optic nerve to cause pallid optic disc edema [225]. Some improvement may be seen after discontinuation of IFN-α treatment [227]. Cessation of interferon therapy should be considered after weighing the risks and benefits of treatment and the extent of optic neuropathy.

Infliximab-Associated Optic Neuropathy

Infliximab is a chimeric antibody of the IgG class that inhibits tumor necrosis factor-α (TNF-α) and is given intravenously for the treatment of rheumatoid arthritis, Crohn's disease, psoriatic arthritis, ankylosing spondylitis, and uveitis. The inhibition of TNF-α has been suggested to induce some demyelinating disorders [228] and exacerbate multiple sclerosis [229, 230]. High TNF-α levels have been found in MS plaques and mononuclear cells of patients with MS [231]. It has also been shown that the infusion of TNF-α in animals models of MS leads to worsening of their demyelinating disease [232].

Infliximab has been associated with the development of retrobulbaroptic neuritis [233–240]. Two women in their fiftieth decade were documented to have developed retrobulbar optic neuritis after treatment with infliximab for rheumatoid arthritis or Crohn's disease [233, 241]. Their vision improved to baseline after discontinuation of the drug. Although these patients did not have underlying MS, it was postulated that TNF-α inhibition may have increased their risk for a demyelinating event.

The Safety Assessment of Biologic Therapy (SABER) study was conducted to evaluate the incidence of optic neuritis in patients using anti-TNF-α therapy (etanercept, infliximab, or adalimumab) or nonbiologic disease-modifying antirheumatic drugs (DMARDs) [242]. The incidence of optic neuritis among new anti-TNF users was 10.4 cases per 100,000 person-years. The incidence was similar among anti-TNF and DMARD groups.

In addition to retrobulbar demyelinating optic neuritis, infliximab has rarely been associated with NAION [243, 244]. Unlike patients with infliximab-associated retrobulbar optic neuritis, these patients did not recover their vision after pulse methylprednisolone.

Treatment with infliximab may also be complicated by a toxic optic neuropathy. After receiving three doses of infliximab for rheumatoid arthritis, three patients in their fiftieth and sixtieth decade developed acute bilateral disc edema with central, cecocentral scotomas, or inferior defects. Despite high-dose steroids, their vision did not improve. It was thought that the three cumulative doses of infliximab contributed to the development of their bilateral toxic optic neuropathy [243]. However, given the small number of cases and their similarity to NAION, these may have been incidental cases of NAION and not toxic optic neuropathy.

Clomiphene Citrate-Associated Optic Neuropathy

Hormonal agents such as clomiphene citrate are often used in the treatment of infertility and can increase the risk of hypercoagulable complications. Visual disturbances occur in up to 10 % [245] of patients treated with clomiphene citrate. Optic neuritis has been reported during treatment with clomiphene [246]. These patients were reported to develop transient blurry vision or "spots" in their vision. NAION was reported in a 31-year-old woman with primary infertility after receiving a 5-day course of clomiphene citrate 50 mg orally each morning [247]. She developed acute unilateral visual loss upon awakening with 20/200, an afferent pupillary defect, decreased red saturation, and an inferior altitudinal defect. The involved optic disc was edematous and hyperemic with venous dilation and splinter hemorrhages. Two months later, her right visual acuity was 20/50 and she had right optic disc pallor. This too may have been, despite the young age, an incidental case of NAION.

Tamoxifen-Associated Optic Neuropathy

Tamoxifen modulates estrogen receptor α activity and is often used as either an adjuvant or as monotherapy in breast cancer treatment. The overall incidence of ocular toxicity is about 1–2 % [79]. While retinopathy and keratopathy are well documented, optic neuropathy rarely occurs [248, 249]. In a prospective study of 65 women with breast cancer who had a normal baseline eye examination and were started on oral tamoxifen of 20 mg/day, 12 % developed ocular toxicity in which seven had a keratopathy, three had bilateral pigmentary retinopathy, and one had bilateral optic neuritis [250]. The patient with optic nerve involvement had residual optic nerve pallor and decreased vision. The keratopathic changes were reversible with discontinuation of the drug. Yearly eye examinations were recommended for patients on long-term tamoxifen.

Sildenafil (Viagra)- and Tadalafil (Cialis)-Associated Optic Neuropathy

Sildenafil and tadalafil are usually used in the treatment of erectile dysfunction (ED) in men. Both have been associated with the development of NAION. Both are selective phosphodiesterase-5 (PDE-5) inhibitors that facilitate the nitric oxide cyclic guanosine monophosphate (cGMP) pathway to relax smooth muscle in the corpus cavernosum, allowing inflow of blood during sexual stimulation. It is also hypothesized that the partial inhibition of phosphodiesterase-6 on the outer retinal photoreceptors causes a transient bluish tinge and increased light sensitivity to be noted by some patients. These mild and transient retinal phenomena are not associated with the optic neuropathy. There are 50 cases of PDE-5 associated NAION documented in the literature, though half of these are not well documented as true optic neuropathies [251–256].

The mean age of the sildenafil cases was 60.3 years and the Food and Drug Administration (FDA) acknowledges that most of these patients also had underlying anatomic or vascular risk factors for the development of NAION including a disc at risk, age over 50, diabetes, hypertension, coronary artery disease, hyperlipidemia, and smoking [257]. It is important to note that even though most of those case reports argue an association between PDE-5 inhibitors and NAION, the causal relationship has not been established conclusively. Nevertheless, the FDA recommends that physicians should advise patients to stop using PDE-5 inhibitors and seek medical attention in the event of sudden loss of vision in one or both eyes. Furthermore, physicians should discuss with the patients the increased risk of NAION in the fellow eye if the patients had already experienced NAION in one eye.

In the reported cases of sildenafil associated with NAION by Pomeranz et al. [258], the patients ranged from 42 to 69 years old and four of the five men had no cardiovascular risk factors. Four of the men experienced acute loss of visual acuity approximately 45 min to 12 h after drug intake. The dose of sildenafil ranged from 50 to 100 mg. One man had taken 50 mg of sildenafil each week and his visual fields gradually worsened over a 15-month period. The visual disturbances occurred after the first dose in one patient, and after two or three doses in another patient. Two of the men had been using sildenafil irregularly for about 2 years. Visual changes usually occurred unilaterally and were accompanied by headache in one patient and by intraocular pain in another. All of these men had small cup-to-disc ratios. Three of the four men had persistent reduction in visual acuity. In another report by Akash et al. [259], a 54-year-old man developed permanent blindness in his left eye from NAION combined with a cilioretinal artery obstruction in what was probably an overdose of sildenafil.

Small physiologic cups are more common in patients with NAION, and it is believed that crowding of nerve fibers through a small scleral canal predisposes this ischemic event [260–262]. The close temporal relationship between the use of sildenafil and NAION in patients with small cup-to-disc ratio in the unaffected eye in the absence of other vascular risk factors also suggests a possible causal relationship [263–266].

Nitric oxide induced by sildenafil is unlikely to be toxic to the optic nerve and retinal ganglion cells even though inhibition of nitric oxide synthetase reduced retinal ganglion cell damage in animals with glaucomatous optic neuropathy [267]. However, nitric oxide is also a potent vasodilator and thus may increase pulsatile ocular blood flow [268]. Alterations in the perfusion of branches of the posterior ciliary artery that supply the optic nerve head have been implicated in NAION. Hayreh proposes that nocturnal hypotension often provokes NAION in patients with a small cup-to-disc ratio, and sildenafil could accentuate physiologic nocturnal hypotension through vasodilation. However, in a study of 15 young healthy males with a mean age of 39 years who underwent ocular blood flow measurements after oral ingestion of sildenafil 100 mg, none developed permanent or transient visual loss, and no significant change in the optic nerve rim or foveolar choroidal blood flow was observed after treatment with sildenafil [269]. However, in older patients especially those with hypertension or diabetes that reduce autoregulation, sildenafil may induce hypotension and NAION. These are precisely the patients with erectile dysfunction not likely to use such treatment.

Tadalafil, another related drug for erectile dysfunction specific for cGMP PDE-5 inhibitor has also been associated with NAION [270–272]. Bollinger et al. [271] reported a 67-year-old man who experienced an episode of transient, inferior blurring of the visual field within 2 h after each of the four doses of tadalafil taken several days apart. Three days later he took the fifth dose and developed a permanent right inferior visual field defect. He had right optic disc edema and his normal left optic disc had a small cup-to-disc ratio. This well-documented case with visual field loss after repeated ingestion of tadalafil suggests that PDE-5 inhibitors can provoke NAION in predisposed cases. Vardenafil, another PDE-5 inhibitor used for erectile dysfunction, has also been reported to cause NAION [273].

Radiation-Induced Optic Neuropathy

Radiation-induced optic neuropathy is an ischemic process, usually presenting as a posterior ischemic optic neuropathy, about 18 months after radiotherapy and after cumulative doses of radiation greater than 50 Gy or single doses greater than 10 Gy. It is often seen as a complication of radiation therapy to the paranasal sinus and skull base regions, and postoperatively for pituitary adenomas, parasellar meningiomas, frontal and temporal gliomas, craniopharyngiomas, intraocular tumors, and nasopharyngeal carcinoma [274–280].

Advancement in neuroimaging and technology has allowed for improvement in the accuracy of radiation dose calculations and precision in delivery. Intensity-modulated radiotherapy and conformal dose distribution have been shown to reduce radiation doses and spare the optic structures [281–283]. It is important to understand each modality of radiation and delivery systems in order to be aware of the risks leading to radiation optic neuropathy. Conventional radiotherapy delivers a radiation beam along a single treatment arc. In contrast, conformal radiotherapy delivers radiation beams in multiple arcs at various angles to maximize radiation delivery to the tumor while minimizing impact on surrounding normal tissues. Both conventional and conformal radiotherapy can be delivered in fractionated doses to allow the healthy tissue time to repair with less risk of optic neuropathy.

Stereotactic radiosurgery delivers a high dose of radiation during a single session. It can also be delivered in fractionated doses that can especially be helpful for lesions near critical structures that cannot tolerate high doses [284]. GammaKnife utilizes a stereotactic localization frame to concentrate radiation and localize lesions. However, conformality is achieved at the expense of dose homogeneity, increasing the risk of optic neuropathy. CyberKnife allows for comparable conformal plans without requiring the invasive stereotactic head frame used with GammaKnife [285]. In general, single doses less than 10 Gy are safe to the anterior visual pathway [285, 286].

However, the safety range may vary depending on individual tolerance. Andrews et al. [288] and Metellus et al. [289] did not report any case of optic neuropathy with a total dose of 50.4 Gy. In a retrospective review of 219 patients, no cases of radiation optic neuropathy were reported when the dose was under 50 Gy. The 10-year risks following doses of 50–60 Gy and 61–78 Gy were 5 % and 30 %, respectively [275]. The tolerable dose ranges widely. No report of radiation optic neuropathy was documented with total doses slightly above the recommended dose ranging from 50–64 Gy or less than 59 Gy [287, 290]. Young et al. [294] conducted topographic correlation of dosimetric measurements with contrast MRI and reported that the tolerance level to radiation of the human optic nerve is 50–55 Gy. However, radiation optic neuropathy was also reported when radiotherapy doses fell within the recommended dose [291]. In particular, in contrast to patients irradiated for paranasal and oral cavity tumors, patients irradiated for pituitary tumors could develop optic neuropathy after doses as low as 42–50 Gy, possibly due to prior optic nerve compression and vascular compromise that lowered the optic nerve threshold to injury [275, 293].

In addition to the radiation dose, the time–dose fractionation is important. In general, a total radiation dose less than 50 Gy and a radiation fraction size less than 2 Gy are considered safe. When the total dose is greater than 60 Gy, the dose per fraction is more important than the total dose in producing an optic neuropathy [293]. In a study of 131 patients, the 15-year actuarial risk of developing an optic neuropathy after doses of 60 Gy or greater was 11 % when treatment was administered in fraction sizes of less than 1.9 Gy, compared with 47 % when given in fraction sizes of 1.9 Gy or greater. Hyperfractionation has also been shown to have a lower risk compared to once-daily radiotherapy [284, 292].

Previous or concurrent treatment with chemotherapy, such as methotrexate, ara-C, vincristine, and other multiple drug combinations, can increase the risk of developing radiation-induced optic neuropathy. Chemotherapeutic agents may be directly toxic to the optic nerve [293, 294]. Radiation may alter cellular structures, such as the blood–brain barrier permeability, or arachnoid granulations, to change the pharmacokinetics of drug distribution and clearance. For example, concurrently administered methotrexate or postradiation therapy is more toxic when it is given before radiation treatment. Radiation is thought to increase blood–brain barrier permeability so that more methotrexate enters the CNS [295, 296]. Therefore, the toxic effects of these chemotherapeutic drugs can potentiate the adverse effects of radiation and vice versa [297]. Preexisting medical disorders, such as diabetes; and endocrinologic disturbances from Cushing's syndrome, and growth hormone-producing tumors, are additional risk factors [298].

Radiation dose per fraction, total dose, total duration of treatment, volume of tissue irradiated, and the type of radiation (proton, electron, or neutron) can also affect the risk of developing radiation-induced optic neuropathy [299, 300]. When the total dose, fraction size, or volume increases, the frequency of complications increases, and the latency to the onset of complications is decreased [301, 302].

Radiation-induced optic neuropathy is a form of late delayed radiation neurotoxicity that affects the white matter months to years after exposure of the anterior visual pathways to ionizing radiation [303]. It is thought that radiation damages the DNA of normal tissues to initiate free radical-mediated damage of the vascular endothelium and glial cells in the white matter [304–315]. The number of vascular endothelial cells is reduced in experimentally radiated rat brains depending on the dose and the time of exposure [311]. In a case-controlled study by Levin et al. [312], histologic features were studied in optic nerves of 16 enucleated eyes from patients with uveal melanoma treated with proton beam irradiation, 6 from normal eyes, and 5 from eyes with nonradiated uveal melanomas. An increase in radiation dosage to the optic nerve was associated with a decrease in the number of endothelial cells. Endothelial cell counts did not correlate with age, gender, visual acuity, or time interval after radiation treatment. In another study of 34 patients with late delayed radiation-induced injury using

proton magnetic resonance spectroscopy [313], *N*-acetyl aspartate (NAA)/creatine and NAA/choline ratios were decreased in areas with worsening brain injury. Since choline was not elevated in the areas of mild to moderate brain injury, demyelination or glial hyperplasia was not a likely primary mechanism of late delayed radiation-induced injury. Unlike other types of ischemia, the ischemia in radiation-induced optic neuropathy involves a gradual decrease in the oxygen gradient from normal tissue to damaged tissue. This gradual oxygen gradient is not conducive to cellular repair. On histology, radiation-injured optic nerves show obliterative endarteritis, endothelial hyperplasia, and fibrinoid necrosis replacing axonal and myelin loss [314, 315].

Radiation-induced optic neuropathy presents with an acute onset of monocular visual loss which progresses over weeks to months. Second eye involvement may follow rapidly or within months. Bilateral sequential visual loss is more common and it is usually painless [302]. Visual symptoms can occur as soon as 3 months or as long as 8 years after radiation therapy, but the majority of cases usually develop about 18 months after treatment is completed, though the latency is variable [276, 302, 316]. Visual acuity also varies widely but severe loss of vision to the level of no light perception occurs in 45 % of cases with up to 85 % of cases having 20/200 or worse [276, 279]. The visual field may show altitudinal defects or central scotomas. If the distal optic nerve is affected, then a junctional scotoma with an optic neuropathy and a contralateral temporal hemianopsia may be seen. Visual loss is usually irreversible; however, spontaneous improvement as much as three or more lines has been reported in patients who have radiation papillopathy [317].

The retrobulbar portion of the optic nerve is the most common site affected from radiation damage. The optic disc may initially appear normal and then become pale over 6–8 weeks. After orbital or intraocular radiation, radiation papillopathy, affecting the optic nerve anterior to the lamina cribrosa may be seen. In such case, the optic disc is swollen, associated with radiation retinopathy, subretinal fluid, peripapillary exudates, and cotton wool spots. The optic disc eventually becomes pale.

The differential diagnosis of radiation-induced optic neuropathy includes recurrence of the primary malignancy, an arachnoiditis, a new radiation-induced parasellar tumor, and a secondary empty sella syndrome with optic nerve and chiasmal prolapse [318–320]. Unlike radiation optic neuropathy, tumor recurrence typically has a slower course of visual loss. Radiation retinopathy and other causes of profound visual loss unrelated to the radiation therapy should also be considered.

MRI of the brain and orbits with gadolinium and T1-weighted fat saturation of the orbits is the diagnostic procedure of choice to differentiate tumor recurrence from radiation-induced optic neuropathy [321–323]. On T1-weighted enhanced images, the injured optic nerves, the optic chiasm, and even the optic tracts may occasionally enhance. This enhancement usually resolves in 3 months followed by optic atrophy. Radiation injury to the anterior visual pathways cannot always be detected in the early stages. In a postmortem study of a 38-year-old man who was treated with interstitial brachytherapy (iridium-192 at 47 Gy) followed by limited-field irradiation of 45 Gy, the extent of injury measured by MRI scan underestimated the damage seen on histology [324].

Treatment for radiation-induced optic neuropathy has been controversial. Corticosteroids and anticoagulants have offered little success. Corticosteroids are unlikely to be useful since radiation injury does not involve vasogenic edema or inflammation. Heparin and warfarin have been shown to increase blood flow to the irradiated tissues [325, 326]. But these drugs have not been shown to be beneficial in improving the vision of patients with radiation optic neuropathy. Radiation optic neuropathy has also been reported to occur, despite anticoagulation treatment during radiation and during the time of visual loss [327, 328].

There is some evidence that hyperbaric oxygen therapy can help in radiation-induced optic neuropathy [317, 329, 330]. It alters the oxygen gradient so that capillary angiogenesis is possible. In a review by Borruat et al. [329] patients

receiving hyperbaric oxygen therapy with greater than or equal to 2.4 atmospheres experienced the best visual outcome compared to those who received no treatment and to those who received only 2.0 atmospheres. These reports suggested that hyperbaric oxygen therapy should be started as early as possible after the onset of visual loss. Treatment should consist of 30 sessions and 90 min each so that patients are breathing 100 % oxygen at a minimum pressure of 2.4 atmospheres. But the results of hyperbaric oxygen therapy are variable [331]. Therefore, hyperbaric oxygen may be attempted in selected cases but, even so, the prognosis remains poor [332].

There is clinical evidence for some management strategies to help improve visual outcome. If one eye has been affected, serial eye examinations should be performed over the 10–20 month period after treatment to monitor for any signs of recurrence in the fellow eye, since bilateral sequential involvement is not uncommon. Serial MRIs of the brain and orbits should be performed over the 20-month period after radiation therapy is completed. As some patients may have MRI signs of radiation injury before loss of vision, subclinical evidence of radiation necrosis on MRI can be treated with prophylactic hyperbaric oxygen therapy [302]. Pattern visual evoked potentials may also play a role in detecting early radiation-induced optic neuropathy even when the eye examination is normal. In a prospective study of 28 patients who underwent radiation therapy for uveal melanomas, 18 % of patients with posterior pole melanomas had clinical signs of an optic neuropathy, but 50 % developed abnormal VEPs, suggesting that subclinical radiation optic neuropathy developed in some patients and radiation-induced optic nerve injury might be more frequent than clinically expected [333].

The optic nerve, by virtue of its unusual anatomy and physiology, is often the site of injury from a variety of metabolic and toxic insults, resulting in severe visual loss. Therefore, it remains important to consider and treat optic neuropathies early. Furthermore, the optic nerve can be the "canary in the coal mine" that alerts the prudent physicians to the potential of serious disease.

References

1. Sadun AA, Win PH, Ross-Cisneros FN, Walker SO, Carelli V. Leber's hereditary optic neuropathy differentially affects smaller axons in the optic nerve. Trans Am Ophthalmol Soc. 2000;98:223–35.
2. Carelli V, Ross-Cisneros F, Sadun AA. Mitochondrial dysfunction as a cause of optic neuropathies. Prog Retin Eye Res. 2004;23:53–89.
3. Miller NR, Newman NJ. editors. Walsh and Hoyt's clinical neuro-ophthalmology, 5th edition, vol. l. Baltimore: Williams and Wilkins; 1998.
4. Biousse V, Newman NJ. Neuro-ophthalmology of mitochondrial diseases. Curr Opin Neurol. 2003;16:35–43.
5. Johnnson RT, Griffin JW, McArthur JC, editors. Current therapy in neurologic disease. 6th ed. St. Louis, MO: Mosby; 2002. p. 363–5.
6. Carelli V, Ross-Cisneros FN, Sadun AA. Optic nerve degeneration and mitochondrial dysfunction: genetic and acquired optic neuropathies. Neurochem Int. 2002;40:573–84.
7. Cohen H. Optic atrophy as the presenting sign in pernicious anaemia. Lancet. 1936;2:1202.
8. Hamilton EA, Ellis PP, Sheets F. Visual impairment due to optic neuropathy in pernicious anemia: report of a case and review of the literature. Blood. 1959;14:378–85.
9. Foulds SW, Chisholm AI, Stewart BJ, Wilson MT. The optic neuropathy of pernicious anemia. Arch Ophthalmol. 1969;82:427–32.
10. Chavala SH, Kosmorsky GS, Lee MK, Lee MS. Optic neuropathy in vitamin B12 deficiency. Eur J Intern Med. 2005;16:447–8.
11. Healton EB, Savage DG, Brust JC, Garrett TJ, Lindenbaum J. Neurologic aspects of cobalamin deficiency. Medicine (Baltimore). 1991;70:229–45.
12. Andrès E, Loukili NH, Noel E, Kaltenbach G, Abdelgheni MB, Perrin AE, et al. Vitamin B12 (cobalamin) deficiency in elderly patients. CMAJ. 2004;171:251–9.
13. Chavala SH, Kosmorsky GS, Lee MK, Lee MS. Optic neuropathy in vitamin B12 deficiency. Eur J Intern Med. 2005;16:447–8.
14. Larner AJ. Visual failure caused by vitamin B12 deficiency optic neuropathy. Int J Clin Pract. 2004;58:977–8.
15. Stambolian D, Behrens M. Optic neuropathy with vitamin B12 deficiency. Am J Ophthalmol. 1977;83:465–8.
16. Areekul S, Roongpisuthipong C, Churdchu K, Thanomsak W. Optic neuropathy in a patient with vitamin B12 deficiency: a case report. J Med Assoc Thai. 1992;75:715–8.
17. Moschos M, Droutsas D. A man who lost weight and his sight. Lancet. 1998;351:1174.
18. Björkenheim B. Optic neuropathy caused by vitamin-B12 deficiency in carriers of the fish tapeworm, Diphyllobothriumlatum. Lancet. 1966;1:688–90.

19. Agamanolis DP, Chester EM, Victor M, Kark JA, Hines JD, Harris JW. Neuropathology of experimental vitamin B12 deficiency in monkeys. Neurology. 1976;26:905–14.
20. Dang CV. Tobacco-alcohol amblyopia: a proposed biochemical basis for pathogenesis. Med Hypotheses. 1981;7:1317–28.
21. Choi DW. Glutamate neurotoxicity and diseases of the nervous system. Neuron. 1988;1:623–34.
22. Hampton CK, Garcia C, Redburn DA. Localization of kainic acid-sensitive cells in mammalian retina. J Neurosci Res. 1981;6:99–111.
23. Ingvar M. Cerebral blood flow and metabolic rate during seizures. Relationship to epileptic brain damage. Ann N Y Acad Sci. 1986;462:194–206.
24. Raley-Susman KM, Miller KR, Owicki JC, Sapolsky RM. Effects of excitotoxin exposure on metabolic rate of primary hippocampal cultures: application of silicon microphysiometry to neurobiology. J Neurosci. 1992;12:773–80.
25. Schiller PH, Logothetis NK, Charles ER. Functions of the colour-opponent and broad-band channels of the visual system. Nature. 1990;343:68–70.
26. Sadun AA, Martone JF, Muci-Mendoza R, Reyes L, DuBois L, Silva JC, Roman G, Caballero B. Epidemic optic neuropathy in Cuba. Eye findings. Arch Ophthalmol. 1994;112:691–9.
27. Pan BX, Ross-Cisneros FN, Carelli V, Rue KS, Salomao SR, Moraes-Filho MN, et al. Mathematically modeling the involvement of axons in Leber's hereditary optic neuropathy. Invest Ophthalmol Vis Sci. 2012;53:7608–17.
28. McMartin KE, Ambre JJ, Tephly TR. Methanol poisoning in human subjects. Role for formic acid accumulation in metabolic acidosis. Am J Med. 1980;8:414–8.
29. Golnik KC, Schaible ER. Folate-responsive optic neuropathy. J Neuroophthalmol. 1994;14:163–9.
30. Hsu CT, Miller NR, Wray ML. Optic neuropathy from folic acid deficiency without alcohol abuse. Ophthalmologica. 2002;216:65–7.
31. de Silva P, Jayamanne G, Bolton R. Folic acid deficiency optic neuropathy: a case report. J Med Case Rep. 2008;2:299.
32. Knox DL, Chen MF, Guilarte TR, Dang CV, Burnette J. Nutritional amblyopia. Folic acid, vitamin B-12, and other vitamins. Retina. 1982;2:288–93.
33. Tousignant B, Brian G, Venn BJ, Gould C, McKay R, Williams S. Optic neuropathy among a prison population in Papua New Guinea. Ophthalmic Epidemiol. 2013;20:4–12.
34. Lessell S. Nutritional disorders: ophthalmological aspects. Bull Soc Belge Ophtalmol. 1983;208 Pt 1:469–72.
35. Carroll FD. The Etiology and Treatment of Tobacco-Alcohol Amblyopia. Trans Am Ophthalmol Soc. 1943;41:385–431.
36. van Noort BA, Bos PJ, Klopping C, Wilmink JM. Optic neuropathy from thiamine deficiency in a patient with ulcerative colitis. Doc Ophthalmol. 1987;67:45–51.
37. Yeh WY, Lian LM, Chang A, Cheng CK. Thiamine-deficient optic neuropathy associated with Wernicke's encephalopathy in patients with chronic diarrhea. J Formos Med Assoc. 2013;112:165–70.
38. Larsen PD, Mock DM, O'Connor PS. Vitamin E deficiency associated with vision loss and bulbar weakness. Ann Neurol. 1985;18:725–7.
39. Solomons NW, Russell RM. The interaction of vitamin A and zinc: implications for human nutrition. Am J Clin Nutr. 1980;33:2031–40.
40. Russell RM, Cox ME, Solomons N. Zinc and the special senses. Ann Intern Med. 1983;99:227–39.
41. Karcioglu ZA. Zinc in the eye. Surv Ophthalmol. 1982;27:114–22.
42. De Palma P, Franco F, Bragliani G, Michetti L, Marescotti A, Pirazzoli G, et al. The incidence of optic neuropathy in 84 patients treated with Ethambutol. Metab Pediatr Syst Ophthalmol. 1989;2:80–2.
43. Scopinaro N, Gianetta E, Civalleri D, Bonalumi U, Bachi V. Two years of clinical experience with bilio-pancreatic bypass for obesity. Am J Clin Nutr. 1980;33:506–14.
44. Becker DA, Balcer LJ, Galetta SL. The Neurological Complications of Nutritional Deficiency following Bariatric Surgery. J Obes. 2012;2012:608534.
45. Juhasz-Pocsine K, Rudnicki SA, Archer RL, Harik SI. Neurologic complications of gastric bypass surgery for morbid obesity. Neurology. 2007;68:1843–50.
46. Spinazzi M, Angelini C, Patrini C. Subacute sensory ataxia and optic neuropathy with thiamine deficiency. Nat Rev Neurol. 2010;6:288–93.
47. Ramos-Leví AM, Sánchez-Pernaute A, Rubio Herrera MA. Dermatitis and optic neuropathy due to zinc deficiency after malabsortive bariatric surgery. Nutr Hosp. 2013;28:1345–7.
48. Mroczkowski MM, Redgrave GW, Miller NR, McCoy AN, Guarda AS. Reversible vision loss secondary to malnutrition in a woman with severe anorexia nervosa, purging type, and alcohol abuse. Int J Eat Disord. 2011;44:281–3.
49. Nightingale LM, Paviour DC. Nutritional optic and peripheral neuropathy: a case report. Cases J. 2009;2:7762.
50. Milea D, Cassoux N, LeHoang P. Blindness in a strict vegan. N Engl J Med. 2000;342:897–8.
51. Pineles SL, Avery RA, Liu GT. Vitamin B12 optic neuropathy in autism. Pediatrics. 2010;126:e967–70.
52. Sobel RS, Yanuzzi LA. Optic nerve toxicity. A classification. In: Singerman I, Jampol LM, editors. Retinal and choroidal manifestations of disease. Baltimore: Williams & Wilkins; 1991. p. 226–50.
53. Kozak SF, Inderlied CB, Hsu HY, Heller KB, Sadun AA. The role of copper on ethambutol's antimicrobial action and implications for ethambutol-induced optic neuropathy. Diagn Microbiol Infect Dis. 1998;30:83–7.

54. Chan JW, Castellanos A. Infliximab and anterior optic neuropathy: case report and review of the literature. Graefes Arch Clin Exp Ophthalmol. 2010; 248:283–7.
55. World Health Organization. Global tuberculosis control: surveillance, planning, financing: WHO report 2008. WHO/HTM/TB/2008.393. Geneva: World Health Organization; 2008.
56. Sadun AA, Wang MY. Ethambutol optic neuropathy: how we can prevent 100,000 new cases of blindness each year. J Neuroophthalmol. 2008;28:265–8.
57. Yoon YH, Jung KH, Sadun AA, Shin HC, Koh JY. Ethambutol-induced vacuolar changes and neuronal loss in rat retinal cell culture: mediation by endogenous zinc. Toxicol Appl Pharmacol. 2000;162:107–14.
58. Pineles SL, Wilson CA, Balcer LJ, Slater R, Galetta SL. Combined optic neuropathy and myelopathy secondary to copper deficiency. Surv Ophthalmol. 2010;55:386–92.
59. Leopold IH. Zinc deficiency and visual impairment. Am J Ophthalmol. 1978;85:871–5.
60. Delacoux E, Moreau Y, Godefroy A, Evstigneef T. Prevention of ocular toxicity of ethambutol: Study of zincaemia and chromatic analysis. J Fr Ophtalmol. 1978;1:191–6.
61. Chung H, Yoon YH, Hwang JJ, Cho KS, Koh JY, Kim JG. Ethambutol-induced toxicity is mediated by zinc and lysosomal membrane permeabilization in cultured retinal cells. Toxicol Appl Pharmacol. 2009;235:163–70.
62. Carr RE, Henkind P. Ocular manifestations of ethambutol, Toxic amblyopia after administration of an experimental antituberculous drug. Arch Ophthalmol. 1962;67:566–71.
63. Citron K. Ethambutol. A review with special reference to ocular toxicity. Tubercle. 1969;50(Suppl):32–6.
64. Leibold JE. Drugs having a toxic effect on the optic nerve. Int Ophthalmol Clin. 1971;11:137–57.
65. Bronte Stewart J, Pettigrew AR, Foulds WS. Toxic optic neuropathy and its experimental production. Trans Ophthalmol Soc U K. 1976;96:355–8.
66. Yoshikawa T, Nagami P. Adverse drug interactions in TB therapy: Risks and recommendations. Geriatrics. 1982;37:61–8.
67. Fledelius HC, Petrera JE, Skjødt K, Trojaborg W. Ocular ethambutol toxicity. Acta Ophthalmol. 1987;65:251–5.
68. Kahana LM. Toxic ocular effects of ethambutol. Can Med Assoc J. 1987;137:212–6.
69. Smith JL. Should ethambutol be barred? J Clin Neuroophthalmol. 1987;7:84–6.
70. Kahana LM. Ethambutol and the eye. Lancet. 1988;2:627.
71. Rahman M, Nizam R. Ethambutol toxic neuroretinopathy in Bangladesh. Pak J Ophthalmol. 1989;5: 37–40.
72. Kumar A, Sandramouli S, Verma L, Tewari HK, Khosla PK. Ocular ethambutol toxicity: Is it reversible? J Clin Neuroophthalmol. 1993;13:15–7.
73. Choi SY, Hwang JM. Optic neuropathy associated with Ethambutol in Koreans. Korean J Ophthalmol. 1997;11:106–10.
74. Murray FJ. U.S. Public Health Service experience with ethambutol. International Congress of Chemother, Vienna 1967;6:33–382.
75. Alvarez KL, Krop LC. Ethambutol-induced ocular toxicity revisited. Ann Pharmacother. 1993;27:102–3.
76. Thomas RJ. Neurotoxicity of antibacterial therapy. South Med J. 1994;87:869–74.
77. Chuenkongkaew W, Samsen P, Thanasombatsakul N. Ethambutol and optic neuropathy. J Med Assoc Thai. 2003;86:622–5.
78. Chan RY, Kwok AK. Ocular toxicity of ethambutol. Hong Kong Med J. 2006;12:56–60.
79. Santaella RM, Fraunfelder FW. Ocular adverse effects associated with systemic medications : recognition and management. Drugs. 2007;67:75–93.
80. Asayama T. Two cases of bitemporalhemianopsia due to ethambutol. Jpn J Clin Ophthalmol. 1969;23: 1209–12.
81. Kho RC, Al-Obailan M, Arnold AC. Bitemporal visual field defects in ethambutol-induced optic neuropathy. J Neuroophthalmol. 2011;31:121–6.
82. Lim SA. Ethambutol-associated optic neuropathy. Ann Acad Med Singapore. 2006;35:274–8.
83. Chen HY, Lai SW, Muo CH, Chen PC, Wang IJ. Ethambutol-induced optic neuropathy: a nationwide population-based study from Taiwan. Br J Ophthalmol. 2012;96:1368–71.
84. World Health Organization. Treatment of tuberculosis: guidelines for national programmes. 3rd ed. Geneva: World Health Organization; 2003. WHO/CDS/TB/2003.313.
85. Griffith DE, Brown-Elliott BA, Shepherd S, McLarty J, Griffith L, Wallace Jr RJ. Ethambutol ocular toxicity in treatment regimens for Mycobacterium avium complex lung disease. Am J Respir Crit Care Med. 2005;172:250–3.
86. Barron GJ, Tepper L, Iovine G. Ocular toxicity from Ethambutol. Am J Ophthalmol. 1974;77:256–60.
87. Citron KM, Thomas GO. Ocular toxicity from Ethambutol. Thorax. 1986;41:737–9.
88. Blumberg HM, Burman WJ, Chaisson RE, Daley CL, Etkind SC, Friedman LN, American Thoracic Society, Centers for Disease Control and Prevention and the Infectious Diseases Society, et al. American Thoracic Society/Centers for Disease Control and Prevention/Infectious Diseases Society of America: treatment of tuberculosis. Am J Respir Crit Care Med. 2003;167:603–62.
89. World Health Organization. Ethambutol efficacy and toxicity. Literature review and recommendation for daily and intermittent dosage in children. Geneva, Switzerland: WHO; 2006.
90. Donald PR, Maher D, Maritz JS, Qazi S. Ethambutol dosage for the treatment of children: literature review and recommendations. Int J Tuberc Lung Dis. 2006;10:1318–30.

91. Kim U, Hwang JM. Early stage ethambutol optic neuropathy: retinal nerve fiber layer and optical coherence tomography. Eur J Ophthalmol. 2009;19: 466–9.
92. Talbert Estlin KA, Sadun AA. Risk factors for ethambutol optic toxicity. Int Ophthalmol. 2010;30:63–72.
93. Tsai RK, Lee YH. Reversibility of Ethambutol optic neuropathy. J Ocul Pharmacol Ther. 1997;13:473–7.
94. Woung LC, Jou JR, Liaw SL. Visual function in recovered Ethambutol optic neuropathy. J Ocul Pharmacol Ther. 1995;11:411–9.
95. De Vita EG, Miao M, Sadun AA. Optic neuropathy in ethambutol treated renal tuberculosis. J Clin Neuroophthalmol. 1987;7:77–83.
96. Wang MY, Sadun AA. Drug-related mitochondrial optic neuropathies. J Neuroophthalmol. 2013;33: 172–8.
97. Cornblath WT, Clavert PC. Best catch from NANOSNET. II. Monitoring for Ethambutol optic nerve toxicity. J Neuroophthal. 2002;22:124–5.
98. Fraunfelder FW, Sadun AA, Wood T. Update on ethambutol optic neuropathy. Expert Opin Drug Saf. 2006;5:615–8.
99. Kandel H, Adhikari P, Shrestha GS, Ruokonen EL, Shah DN. Visual function in patients on ethambutol therapy for tuberculosis. J Ocul Pharmacol Ther. 2012;28:174–8.
100. Menon V, Jain D, Saxena R, Sood R. Prospective evaluation of visual function for early detection of ethambutol toxicity. Br J Ophthalmol. 2009;93: 1251–4.
101. Chai SJ, Foroozan R. Decreased retinal nerve fibre layer thickness detected by optical coherence tomography in patients with ethambutol-induced optic neuropathy. Br J Ophthalmol. 2007;91:895–7.
102. Harley RD, Huang NN, Macri CH, Green WR. Optic neuritis and optic atrophy following chloramphenicol in cystic fibrosis patients. Trans Am Acad Ophthalmol Otolaryngol. 1970;74:1011–31.
103. Gilman AG, Goodman LS, Rail TW, Murad F, editors. Goodman and Gilman's the pharmacological basis of therapeutics. 7th ed. New York, NY: Macmillan; 1985. p. 1179–83.
104. Smith U, Smith DS, Yunis AA. Chloramphenicol-related changes in mitochondrial ultrastructure. J Cell Sci. 1970;7:501–21.
105. Godel V, Nemet P, Lazar M. Chloramphenicol optic neuropathy. Arch Ophthalmol. 1980;98:1417–21.
106. Birmingham MC, Rayner CR, Meagher AK, Flavin SM, Batts DH, Schentag JJ. Linezolid for the treatment of multidrug-resistant, gram-positive infections: experience from a compassionate-use program. Clin Infect Dis. 2003;36:159–68.
107. Fiscella RG, Lai WW, Buerk B, Khan M, Rodvold KA, Pulido JS, Labib S, Shapiro MJ, Blair NP. Aqueous and vitreous penetration of linezolid (Zyvox) after oral administration. Ophthalmology. 2004;111:1191–5.
108. Rucker JC, Hamilton SR, Bardenstein D, Isada CM, Lee MS. Linezolid-associated toxic optic neuropathy. Neurology. 2006;66:595–8.
109. McKinley SH, Foroozan R. Optic neuropathy associated with linezolid treatment. J Neuroophthalmol. 2005;25:18–21.
110. Saijo T, Hayashi K, Yamada H, Wakakura M. Linezolid-induced optic neuropathy. Am J Ophthalmol. 2005;139:1114–6.
111. Javaheri M, Khurana RN, O'hearn TM, Lai MM, Sadun AA. Linezolid-induced optic neuropathy: a mitochondrial disorder? Br J Ophthalmol. 2007;91:111–5.
112. De Vriese AS, Coster RV, Smet J, Seneca S, Lovering A, Van Haute LL, et al. Linezolid-induced inhibition of mitochondrial protein synthesis. Clin Infect Dis. 2006;42:1111–7.
113. Physicians' Desk Reference, 5th ed. Montvale: Thomson PDR, Linezolid; 2004. p. 2808–15.
114. Lee E, Burger S, Shah J, Melton C, Mullen M, Warren F, Press R. Linezolid-associated toxic optic neuropathy: a report of 2 cases. Clin Infect Dis. 2003;37:1389–91.
115. Corallo CE, Paull AE. Linezolid-induced neuropathy. Med J Aust. 2002;177:332.
116. Rho JP, Sia IG, Crum BA, Dekutoski MB, Trousdale RT. Linezolid-associated peripheral neuropathy. Mayo Clin Proc. 2004;79:927–30.
117. Spellberg B, Yoo T, Bayer AS. Reversal of linezolid-associated cytopenias, but not peripheral neuropathy, by administration of vitamin B6. J Antimicrob Chemother. 2004;54:832–5.
118. Yu-Wai-Man P, Griffiths PG, Chinnery PF. Mitochondrial optic neuropathies - disease mechanisms and therapeutic strategies. Prog Retin Eye Res. 2011;30:81–114.
119. Walker GF. Blindness during streptomycin and chloramphenicol therapy. Br J Ophthalmol. 1961;45: 555–9.
120. Lewis W, Dalakas MC. Mitochondrial toxicity of antiviral drugs. Nat Med. 1995;1:417–22.
121. Samuels DC. Mitochondrial AZT, metabolism. IUBMB Life. 2006;58:403–8.
122. Scruggs ER, Dirks Naylor AJ. Mechanisms of zidovudine-induced mitochondrial toxicity and myopathy. Pharmacology. 2008;82:83–8.
123. Shaikh S, Ta C, Basham AA, Mansour S. Leber hereditary optic neuropathy associated with antiretroviral therapy for human immunodeficiency virus infection. Am J Ophthalmol. 2001;131:143–5.
124. Mackey DA, Fingert JH, Luzhansky JZ, McCluskey PJ, Howell N, Hall AJ, et al. Leber's hereditary optic neuropathy triggered by antiretroviral therapy for human immunodeficiency virus. Eye (Lond). 2003;17:312–7.
125. Ikeda A, Ikeda T, Ikeda N, Kawakami Y, Mimura O. Leber's hereditary optic neuropathy precipitated by ethambutol. Jpn J Ophthalmol. 2006;50:280–3.
126. Seo JH, Hwang JM, Park SS. Antituberculosis medication as a possible epigenetic factor of Leber's

hereditary optic neuropathy. Clin Experiment Ophthalmol. 2010;38:363–6.
127. Luca CC, Lam BL, Moraes CT. Erythromycin as a potential precipitating agent in the onset of Leber's hereditary optic neuropathy. Mitochondrion. 2004;4:31–6.
128. Guillet V, Chevrollier A, Cassereau J, Letournel F, Gueguen N, Richard L, et al. Ethambutol-induced optic neuropathy linked to OPA1 mutation and mitochondrial toxicity. Mitochondrion. 2010;10:115–24.
129. Tephly TR, Makar AB, McMartin KE. Methanol: its metabolism and toxicity. In: Majchrowicz E, Noble EP, editors. Biochemistry and pharmacology of ethanol, vol. 1. New York: Plenum; 1979. p. 145–62.
130. Eells JT, Henry MM, Lewandowski MF, Seme MT, Murray TG. Development and characterization of a rodent model of methanol-induced retinal and optic nerve toxicity. Neurotoxicology. 2000;21:321–30.
131. Nicholls P. Formate as an inhibitor of cytochrome c oxidase. Biochem Biophys Res Commun. 1975;67:610–6.
132. Guyton AC. Textbook of medical physiology. Philadelphia: WB Saunders; 1981.
133. Sharpe JA, Hostovsky M, Bilbao JM, Rewcastle NB. Methanol optic neuropathy: a histopathological study. Neurology. 1982;32:1093–100.
134. Wyndham RA. Experimental demyelination of the central nervous system II: respiratory enzyme systems of the brain in poisoning with cyanide and with azide. Aust J Exp Biol Med Sci. 1941;19:243–8.
135. Hsu HH, Chen CY, Chen FH, Lee CC, Chou TY, Zimmerman RA. Optic atrophy and cerebral infarcts caused by methanol intoxication: MRI. Neuroradiology. 1997;39:192–4.
136. Sanaei-Zadeh H, Zamani N, Shadnia S. Outcomes of visual disturbances after methanol poisoning. Clin Toxicol (Phila). 2011;49:102–7.
137. Ingemansson SO. Clinical observations on ten cases of methanol poisoning with particular reference to ocular manifestations. Acta Ophthalmol (Copenh). 1984;62:15–24.
138. Onder F, Ilker S, Kansu T, Tatar T, Kural G. Acute blindness and putaminal necrosis in methanol intoxication. Int Ophthalmol. 1998–1999;22:81–4.
139. Stelmach MZ, O'Day J. Partly reversible visual failure with methanol toxicity. Aust N Z J Ophthalmol. 1992;20:57–64.
140. McKellar MJ, Hidajat RR, Elder MJ. Acute ocular methanol toxicity: clinical and electrophysiological features. Aust N Z J Ophthalmol. 1997;25:225–30.
141. Paasma R, Hovda KE, Jacobsen D. Methanol poisoning and long term sequelae – a six years follow-up after a large methanol outbreak. BMC Clin Pharmacol. 2009;27:5.
142. Liu JJ, Daya MR, Carrasquillo O, Kales SN. Prognostic factors in patients with methanol poisoning. J Toxicol Clin Toxicol. 1998;36:175–81.
143. Dethlefs R, Naraqi S. Ocular manifestations and complications of acute methyl alcohol intoxication. Med J Aust. 1978;2:483–5.
144. Sharma P, Sharma R. Toxic optic neuropathy. Indian J Ophthalmol. 2011;59:137–41.
145. Brent J, McMartin K, Phillips S, Aaron C, Kulig K. Fomepizole for the treatment of methanol poisoning. N Engl J Med. 2001;344:424–9.
146. Sodhi PK, Goyal JL, Mehta DK. Methanol-induced optic neuropathy: treatment with intravenous high dose steroids. Int J Clin Pract. 2001;55:599–602.
147. Shukla M, Shikoh I, Saleem A. Intravenous methylprednisolone could salvage vision in methyl alcohol poisoning. Indian J Ophthalmol. 2006;54:68–9.
148. Pakravan M, Sanjari N. Erythropoietin treatment for methanol optic neuropathy. J Neuroophthalmol. 2012;32:325–8.
149. Jacobsen D, McMartin KE. Methanol and ethylene glycol poisonings. Mechanism of toxicity, clinical course, diagnosis and treatment. Med Toxicol. 1986;1:309–34.
150. Gupta SR, Palmer CA, Curé JK, Balos LL, Lincoff NS, Kline LB. Toluene optic neurotoxicity: magnetic resonance imaging and pathologic features. Hum Pathol. 2011;42:295–8.
151. Kiyokawa M, Mizota A, Takasoh M, Adachi-Usami E. Pattern visual evoked cortical potentials in patients with toxic optic neuropathy caused by toluene abuse. Jpn J Ophthalmol. 1999;43:438–42.
152. Hormes JT, Filley CM, Rosenberg NL. Neurologic sequelae of chronic solvent vapor abuse. Neurology. 1986;36:698–702.
153. Sadun AA, Martone JF. Cuba: response of medical science to a crisis of optic and peripheral neuropathy. Int Ophthalmol. 1994–1995;18:373–8.
154. Sadun AA. Acquired mitochondrial impairment as a cause of optic nerve disease. Trans Am Ophthalmol Soc. 1998;96:881–923.
155. Román GC. An epidemic in Cuba of optic neuropathy, sensorineural deafness, peripheral sensory neuropathy and dorsolateral myeloneuropathy. J Neurol Sci. 1994;127:11–28.
156. Macias-Matos C, Rodriguez-Ojea A, Chi N, Jimenez S, Zulueta D, Bates CJ. Biochemical evidence of thiamine depletion during the Cuban neuropathy epidemic, 1992–1993. Am J Clin Nutr. 1996;64:347–53.
157. Thomas PK, Plant GT, Baxter P, Bates C, Santiago LR. An epidemic of optic neuropathy and painful sensory neuropathy in Cuba: clinical aspects. J Neurol. 1995;242:629–38.
158. Gay J, Porrata C, Hernandez M, Clua AM, Arguelles JM, Cabrera A, et al. Dietary factors in epidemic neuropathy on the Isle of Youth, Cuba. Bull Pan Am Health Organ. 1995;29:25–36.
159. Johns DR, Sadun AA. Cuban epidemic optic neuropathy. Mitochondrial DNA analysis. J Neuroophthalmol. 1994;14:130–4.
160. Mojon DS, Kaufmann P, Odel JG, Lincoff NS, Marquez-Fernandez M, Santiesteban R, et al. Clinical course of a cohort in the Cuban epidemic optic and peripheral neuropathy. Neurology. 1997;48:19–22.

161. Santiesteban-Freixas R, Mendoza-Santiesteban CE, Columbie-Garbey Y, Quevedo AG, Garcia AG, Rodríguez RC. Cuban epidemic optic neuropathy and its relationship to toxic and hereditary optic neuropathy. Semin Ophthalmol. 2010;25:112–22.
162. Lincoff NS, Odel JG, Hirano M. 'Outbreak' of optic and peripheral neuropathy in Cuba? JAMA. 1993;270:511–8.
163. Tucker K, Hedges TR. Food shortages and an epidemic of optic and peripheral neuropathy in Cuba. Nutr Rev. 1993;51:349–57.
164. Grzybowski A. Mitochondrial optic neuropathies: additional facts and concepts. Clin Experiment Ophthalmol. 2013 Jun 18. doi: 10.1111/ceo.12148. [Epub ahead of print]
165. Solberg Y, Rosner M, Belkin M. The association between cigarette smoking and ocular diseases. Surv Ophthalmol. 1998;42:535–47.
166. Carroll FD. Nutritional amblyopia. Arch Ophthalmol. 1966;76:406–11.
167. Smiddy WE, Green WR. Nutritional amblyopia. A histopathologic study with retrospective clinical correlation. Graefes Arch Clin Exp Ophthalmol. 1987;225:321–4.
168. Pryor WA, Arbour NC, Upham B, Church DF. The inhibitory effect of extracts of cigarette tar on electron transport of mitochondria. Free Radic Biol Med. 1992;12:365–72.
169. Ballinger SW, Bouder TG, Davis GS, Judice SA, Nicklas JA, Albertini RJ. Mitochondrial genome damage associated with cigarette smoking. Cancer Res. 1996;56:5692–7.
170. Kennedy JR, Elliott AM. Cigarette smoke: the effect of residue on mitochondrial structure. Science. 1970;168:1097–8.
171. Dunphy EB. Alcohol and tobacco amblyopia: a historical survey. XXXI DeSchweinitz lecture. Am J Ophthalmol. 1969;68:569–78.
172. Pearce JM. Neurological aspects of alcoholism. Br J Hosp Med. 1977;18:132. 134, 136–7.
173. Samples JR, Younge BR. Tobacco-alcohol amblyopia. J Clin Neuro Ophthalmol. 1981;1:213–8.
174. Harrington DO. Amblyopia due to tobacco, alcohol and nutritional deficiency. Differential diagnosis with special reference to the character of the visual field defect. Am J Ophthalmol. 1962;53:967–72.
175. Grzybowski A, Holder GE. Tobacco optic neuropathy (TON) – the historical and present concept of the disease. Acta Ophthalmol. 2011;89:495–9.
176. Syed S, Lioutas V. Tobacco-alcohol amblyopia: a diagnostic dilemma. J Neurol Sci. 2013;327:41–5.
177. Rizzo 3rd JF, Lessell S. Tobacco amblyopia. Am J Ophthalmol. 1993;116:84–7.
178. Cullom ME, Heher KL, Miller NR, Savino PJ, Johns DR. Leber's hereditary optic neuropathy masquerading as tobacco-alcohol amblyopia. Arch Ophthalmol. 1993;111:1482–5.
179. Newman NJ, Torroni A, Brown MD, Lott MT, Fernandez MM, Wallace DC. Epidemic neuropathy in Cuba not associated with mitochondrial DNA mutations found in Leber's hereditary optic neuropathy patients. Cuba Neuropathy Field Investigation Team. Am J Ophthalmol. 1994;118:158–68.
180. Strachan H. On a form of multiple neuritis prevalent in the West Indies. Practitioner. 1897;59:477–84.
181. Fisher C. Residual neuropathological changes in Canadians held prisoners of war by the Japanese (Strachan's disease). Can Serv Med J. 1955; 11:157–99.
182. Gill GV, Bell DR. Persisting nutritional neuropathy amongst former war prisoners. J Neurol Neurosurg Psychiatry. 1982;45:861–5.
183. King Jr JH, Passmore JW. Nutritional amblyopia: a study of American prisoners of war in Korea. Am J Ophthalmol. 1955;39:173–86.
184. Osuntokun BO. Cassava diet, chronic cyanide intoxication and neuropathy in Nigerian Africans. World Rev Nutr Diet. 1981;36:141–73.
185. Carton H, Kazadi K, Kabeya O, Billiau A, Maertens K. Epidemic spastic paraparesis in Bandundu (Zaire). J Neurol Neurosurg Psychiatry. 1986; 49:620–7.
186. Ministry of Health, Mozambique. Mantakassa: an epidemic of spastic paraparesis associated with chronic cyanide intoxication in a cassava staple area of Mozambique. Epidemiology and clinical laboratory findings in patients. Bull World Health Organ. 1984; 62:477–484.
187. Howlett WP, Brubaker GR, Mlingi N, Rosling H. Konzo, an epidemic upper motor neuron disease studied in Tanzania. Brain. 1990;113:223–35.
188. Montgomery RD, Cruickshank EK, Robertson WB, McNemeney WH. Clinical and pathological observations on Jamaican neuropathy: a report on 206 cases. Brain. 1964;87:425–62.
189. Osuntokun BO, Osuntokun O. Tropical amblyopia in Nigerians. Am J Ophthalmol. 1971;72:708–16.
190. Bowman RW, Wedner S, Bowman RF, Masanja H, Bunce C, Wood ML, et al. Optic neuropathy endemic in secondary school children in Dar es Salaam Tanzania. Br J Ophthalmol. 2010;94:146–9.
191. Plant GT, Mtanda AT, Arden GB, Johnson GJ. An epidemic of optic neuropathy in Tanzania: characterization of the visual disorder and associated peripheral neuropathy. J Neurol Sci. 1997;145: 127–40.
192. Johnson GJ, Mtanda AT, Kinabo NN, Sangawe JLF, Masesa DE, Negral AD. Optic nerve and macular atrophy of unknown origin in Tanzania. Arch Publ Health. 1993;51:561–71.
193. Hodson KE, Bowman RJ, Mafwiri M, Wood M, Mhoro V, Cox SE. Low folate status and indoor pollution are risk factors for endemic optic neuropathy in Tanzania. Br J Ophthalmol. 2011;95:1361–4.
194. Dalmar AA, Hodson KE, Plant GT. Epidemic optic neuropathy is evident in the Somalian population. J Neuroophthalmol. 2011;31:127–30.

195. Chen D, Hedges TR. Amiodarone optic neuropathy – review. Semin Ophthalmol. 2003;18:169–73.
196. Fraunfelder FT, Fraunfelder FW. Drug-induced ocular side effects. Boston, MA: Butterworth-Heinemann; 2001.
197. Feiner LA, Younge BR, Kazmier FJ, Stricker BH, Fraunfelder FT. Optic neuropathy and amiodarone therapy. Mayo Clin Proc. 1987;62:702–17.
198. Macaluso DC, Shults WT, Fraunfelder FT. Features of amiodarone-induced optic neuropathy. Am J Ophthalmol. 1999;127:610–2.
199. Johnson LN, Krohel GB, Thomas ER. The clinical spectrum of amiodarone-associated optic neuropathy. J Natl Med Assoc. 2004;96:1477–91.
200. Pollak PT, Bouillon T, Shafer SL. Population pharmacokinetics of long-term oral amiodarone therapy. Clin Pharmacol Ther. 2000;67:642–52.
201. Singh BN. Amiodarone: the expanding antiarrhythmic role and how to follow a patient on chronic therapy. Clin Cardiol. 1997;20:608–18.
202. Characteristics of patients with nonarteritic anterior ischemic optic neuropathy eligible for the ischemic optic neuropathy decompression trial. Arch Ophthalmol. 1996;114:1366–74.
203. Sadun AA. Discussion of claims of the purported clinical spectrum of Amiodarone associated optic neuropathy; 2004 Oct; New Orleans: American Academy of Ophthalmology.
204. Somani P. Basic and clinical pharmacology of amiodarone: relationship of antiarrhythmic effects, dose and drug concentrations to intracellular inclusion bodies. J Clin Pharmacol. 1989;29:405–12.
205. Sadun AA, Gurkan S, Patel V. Hereditary, nutritional, and toxic optic atrophies. In: Yanoff M, Duker JS, editors. Ophthalmology. 3rd ed. Edinburgh: Mosby Elsevier; 2008.
206. Mindel JS. Amiodarone toxic optic neuropathy: reasons for doubting its existence [lecture]. North American Neuro-Ophthalmology Society Annual Meeting; 2006 Feb 25–Mar 2; Tucson, AZ.
207. Li J, Tripathi RC, Tripathi BJ. Drug-induced ocular disorders. Drug Saf. 2008;31:127–41.
208. Orakzai A, Guerin M, Beatty S. Disulfiram-induced transient optic and peripheral neuropathy: a case report. Ir J Med Sci. 2007;176:319–21.
209. Baron S, Tyring SK, Fleischmann Jr WR, Coppenhaver DH, Niesel DW, Klimpel GR, Stanton GJ, Hughes TK. The interferons. Mechanisms of action and clinical applications. JAMA. 1991;266:1375–83.
210. Lohmann CP, Kroher G, Bogenrieder T, Spiegel D, Preuner J. Severe loss of vision during adjuvant interferon alfa-2b treatment for malignant melanoma. Lancet. 1999;353:1326.
211. Purvin VA. Anterior ischemic optic neuropathy secondary to interferon alfa. Arch Ophthalmol. 1995;113:1041–4.
212. Taylor JL, Grossberg SE. The effects of interferon-alpha on the production and action of other cytokines. Semin Oncol. 1998;25:23–9.
213. Rue KS, Hirsch LK, Sadun AA. Impending anterior ischemic optic neuropathy with elements of retinal vein occlusion in a patient on interferon for polycythemia vera. Clin Ophthalmol. 2012;6:1763–5.
214. Selcukbiricik F, Tural D, Senel TE, Sarıca A, Soyluk O, Serdengecti S. Bilateral ischemic optic neuropathy developed under interferon therapy. Case Rep Ophthalmol Med. 2012;2012:102739.
215. Seddik H, Tamzaourte M, Rouibaa F, Fadlouallah M, Benkirane A. Irreversible anterior ischemic optic neuropathy complicating interferon alpha and ribaverin therapy. Int J Hepatol. 2011;2011:814242.
216. Knyazer B, Lifshitz T, Marcus M, Kratz A, Zlotnik A, Levy J. Anterior ischemic optic neuropathy in a patient with hepatitis C treated with interferon-alpha and ribavirin. Isr Med Assoc J. 2011;13:251–3.
217. Fraunfelder FW, Fraunfelder FT. Interferon alfa-associated anterior ischemic optic neuropathy. Ophthalmology. 2011;118:408–11.e1-2.
218. Berg KT, Nelson B, Harrison AR, McLoon LK, Lee MS. Pegylated interferon alpha-associated optic neuropathy. J Neuroophthalmol. 2010;30:117–22.
219. Wei YH, Wang IH, Woung LC, Jou JR. Anterior ischemic optic neuropathy associated with pegylated interferon therapy for chronic hepatitis C. Ocul Immunol Inflamm. 2009;17:191–4.
220. Kabbaj N, Sentissi S, Mohammadi M, Benaïssa A, Amrani N. Anterior ischemic optic neuropathy complicating interferon alpha and ribavirin therapy in patients with chronic hepatitisC. Gastroenterol Clin Biol. 2009;33:115–7.
221. Rodney AJ, Gombos DS, Pagliaro LC, Tannir NM. Ischemic optic neuropathy associated with low-dose interferon alfa: report of two cases. Am J Clin Oncol. 2009;32:86–7.
222. Chan JW. Bilateral non-arteritic ischemic optic neuropathy associated with pegylated interferon for chronic hepatitis C. Eye (Lond). 2007;21:877–8.
223. Norcia F, Di Maria A, Prandini F, Redaelli C. Natural interferon therapy: optic nerve ischemic damage? Ophthalmologica. 1999;213:339–40.
224. Vardizer Y, Linhart Y, Loewenstein A, Garzozi H, Mazawi N, Kesler A. Interferon-alpha-associated bilateral simultaneous ischemic optic neuropathy. J Neuroophthalmol. 2003;23:256–9.
225. Foroozan R. Unilateral pallid optic disc swelling and anemia associated with interferon alpha treatment. J Neuroophthalmol. 2004;24:98–9.
226. Gabler B, Kroher G, Bogenrieder T, Spiegel D, Preuner J, Lohmann CP. [Severe, bilateral vision loss in malignant melanoma of the skin. Anterior ischemic optic neuropathy with irreversible vision and visual field loss in adjuvant interferon alfa-2b therapy]. Ophthalmologe. 2001;98:672–3.
227. Gupta R, Singh S, Tang R, Blackwell TA, Schiffman JS. Anterior ischemic optic neuropathy caused by interferon alpha therapy. Am J Med. 2002;112:683–4.

228. Seror R, Richez C, Sordet C, Rist S, Gossec L, Direz G, et al. Pattern of demyelination occurring during anti-TNF-α therapy: a French national survey. Rheumatology (Oxford). 2013;52:868–74.
229. The Lenercept Multiple Sclerosis Study Group and the University of British Columbia MS/MRI Analysis Group. TNF neutralization in MS: results of a randomized, placebo-controlled multicenter study. Neurology. 1999;53:457–65.
230. Van Oosten BW, Barkhof F, Truyen L, et al. Increased MRI activity and immune activation in two multiple sclerosis patients treated with the monoclonal anti-tumor necrosis factor antibody cA2. Neurology. 1996;47:1531–4.
231. Głabiński A, Mirecka M, Pokoca L. Tumor necrosis factor alpha but not lymphotoxin is overproduced by blood mononuclear cells in multiple sclerosis. Acta Neurol Scand. 1995;91:276–9.
232. Probert L, Akassoglou K, Pasparakis M, Kontogeorgos G, Kollias G. Spontaneous inflammatory demyelinating disease in transgenic mice showing central nervous system-specific expression of tumor necrosis factor alpha. Proc Natl Acad Sci U S A. 1995;92:11294–8.
233. Foroozan R, Buono LM, Sergott RC, Savino PJ. Retrobulbar optic neuritis associated with infliximab. Arch Ophthalmol. 2002;120:985–7.
234. Bidaguren A, Müller-Thyssen A, Blanco A, Mendicute J, Ubeda M. [Retrobulbar optic neuritis associated with Infliximab]. Arch Soc Esp Oftalmol. 2007;82:109–12.
235. Hejazi R, Colombel JF, Peyrin-Biroulet L. Retrobulbar optic neuritis during infliximab treatment for ulcerative colitis. Gastroenterol Clin Biol. 2008;32:162–3.
236. Mumoli N, Niccoli G, Scazzeri F, Picchietti S, Greco A, Cei M. Infliximab-induced retrobulbar optic neuritis. QJM. 2007;100:531.
237. Pikkel J. Possible link between infliximab and optic neuritis. Isr Med Assoc J. 2008;10:477–8.
238. Simsek I, Erdem H, Pay S, Sobaci G, Dinc A. Optic neuritis occurring with anti-tumour necrosis factor alpha therapy. Ann Rheum Dis. 2007;66:1255–8.
239. Strong BY, Erny BC, Herzenberg H, Razzeca KJ. Retrobulbar optic neuritis associated with infliximab in a patient with Crohn disease. Ann Intern Med. 2004;140:W34.
240. Tran TH, Milea D, Cassoux N, Bodaghi B, Bourgeois P, LeHoang P. [Optic neuritis associated with infliximab]. J Fr Ophtalmol. 2005;28:201–4.
241. Mejico LJ. Infliximab-associated retrobulbar optic neuritis. Arch Ophthalmol. 2004;122:793–4.
242. Winthrop KL, Chen L, Fraunfelder FW, Ku JH, Varley CD, Suhler E, et al. Initiation of anti-TNF therapy and the risk of optic neuritis: from the safety assessment of biologic ThERapy (SABER) study. Am J Ophthalmol. 2013;155:183–9.e1.
243. ten Tusscher MP, Jacobs PJ, Busch MJ, de Graaf L, Diemont WL. Bilateral anterior toxic optic neuropathy and the use of infliximab. BMJ. 2003;326:579.
244. Chan JW, Castellanos A. Infliximab and anterior optic neuropathy: case report and review of the literature. Graefes Arch Clin Exp Ophthalmol. 2010;248:283–7.
245. Roch 2nd LM, Gordon DL, Barr AB, Paulsen CA. Visual changes associated with clomiphene citrate therapy. Arch Ophthalmol. 1967;77:14–7.
246. Padron Rivas VF, Sanchez Sanchez A, Lerida Arias MT, Carvajal Garcia-Pardo A. [Optic neuritis appearing during treatment with clomiphene]. Aten Primaria. 1994;14:912–3.
247. Lawton AW. Optic neuropathy associated with clomiphene citrate therapy. Fertil Steril. 1994;61:390–1.
248. Pugesgaard T, Von Eyben FE. Bilateral optic neuritis evolved during tamoxifen treatment. Cancer. 1986;58:383–6.
249. Colley SM, Elston JS. Tamoxifen optic neuropathy. Clin Experiment Ophthalmol. 2004;32:105–6.
250. Noureddin BN, Seoud M, Bashshur Z, Salem Z, Shamseddin A, Khalil A. Ocular toxicity in low-dose tamoxifen: a prospective study. Eye (Lond). 1999;13:729–33.
251. Tarantini A, Faraoni A, Menchini F, Lanzetta P. Bilateral simultaneous nonarteritic anterior ischemic optic neuropathy after ingestion of sildenafil for erectile dysfunction. Case Rep Med. 2012;2012:747658.
252. O'Malley P. Viagra and vision loss: what is known and unknown. Clin Nurse Spec. 2006;20:227–8.
253. Calvet C, Martin K, Robert G, Moore N, Eftekhari P, Farghal H, et al. Treatment of erectile dysfunction by phosphodiesterase-5 inhibitors and nonarteritic anterior ischemic optic neuropathy (NAION). Prog Urol. 2007;17:920–7.
254. Felekis T, Asproudis I, Katsanos K, Tsianos E. A case of nonarteritic anterior ischemic optic neuropathy of a male with family history of the disease after receiving sildenafil. Clin Ophthalmol. 2011;5:1443–5.
255. Moschos MM, Margetis I. Bilateral simultaneous anterior ischemic optic neuropathy associated with sildenafil. Case Rep Ophthalmol. 2011;2:262–5.
256. Goldstein I, Lue TF, Padma-Nathan H, Rosen RC, Steers WD, Wicker PA. Oral sildenafil in the treatment of erectile dysfunction. Sildenafil Study Group. N Engl J Med. 1998;338:1397–404.
257. Lee AG, Newman NJ. Erectile dysfunction drugs and nonarteritic anterior ischemic optic neuropathy. Am J Ophthalmol. 2005;140:707–8.
258. Pomeranz HD, Smith KH, Hart Jr WM, Egan RA. Sildenafil-associated nonarteritic anterior ischemic optic neuropathy. Ophthalmology. 2002;109:584–7.
259. Akash R, Hrishikesh D, Amith P, Sabah S. Case report: association of combined nonarteritic anterior ischemic optic neuropathy (NAION) and obstruction of cilioretinal artery with overdose of Viagra. J Ocul Pharmacol Ther. 2005;21:315–7.
260. Beck RW, Servais GE, Hayreh SS. Anterior ischemic optic neuropathy. IX. Cup-to-disc ratio and its

role in pathogenesis. Ophthalmology. 1987;94:1503–8.
261. Burde RM. Optic disk risk factors for nonarteritic anterior ischemic optic neuropathy. Am J Ophthalmol. 1993;116:759–64.
262. Doro S, Lessell S. Cup-disc ratio and ischemic optic neuropathy. Arch Ophthalmol. 1985;103:1143–4.
263. Boshier A, Pambakian N, Shakir SA. A case of non-arteritic ischemic optic neuropathy (NAION) in a male patient taking sildenafil. Int J Clin Pharmacol Ther. 2002;40:422–3.
264. Cunningham AV, Smith KH. Anterior ischemic optic neuropathy associated with viagra. J Neuroophthalmol. 2001;21:22–5.
265. Dheer S, Rekhi GS, Merlyn S. Sildenafil associated anterior ischaemic optic neuropathy. J Assoc Physicians India. 2002;50:265.
266. Egan R, Pomeranz H. Sildenafil (Viagra) associated anterior ischemic optic neuropathy. Arch Ophthalmol. 2000;118:291–2.
267. Neufeld AH, Sawada A, Becker B. Inhibition of nitric-oxide synthase 2 by aminoguanidine provides neuroprotection of retinal ganglion cells in a rat model of chronic glaucoma. Proc Natl Acad Sci U S A. 1999;96:9944–8.
268. Sponsel WE, Paris G, Sandoval SS, Sanford DK, Harrison JM, Elliott WR, et al. Sildenafil and ocular perfusion. N Engl J Med. 2000;342:1680.
269. Grunwald JE, Siu KK, Jacob SS, Dupont J. Effect of sildenafil citrate (Viagra) on the ocular circulation. Am J Ophthalmol. 2001;131:751–5.
270. Bollinger K, Lee MS. Recurrent visual field defect and ischemic optic neuropathy associated with tadalafilrechallenge. Arch Ophthalmol. 2005;123:400–1.
271. Escaravage Jr GK, Wright Jr JD, Givre SJ. Tadalafil associated with anterior ischemic optic neuropathy. Arch Ophthalmol. 2005;123:399–400.
272. Peter NM, Singh MV, Fox PD. Tadalafil-associated anterior ischaemic optic neuropathy. Eye. 2005;19:715–7.
273. Azzouni F, Abu samra K. Are phosphodiesterase type 5 inhibitors associated with vision-threatening adverse events? A critical analysis and review of the literature. J Sex Med. 2011;8:2894–903.
274. Jiang GL, Tucker SL, Guttenberger R, Peters LJ, Morrison WH, Garden AS, et al. Radiation-induced injury to the visual pathway. Radiother Oncol. 1994;30:17–25.
275. Kline LB, Kim JY, Ceballos R. Radiation optic neuropathy. Ophthalmology. 1985;92:1118–26.
276. Millar JL, Spry NA, Lamb DS, Delahunt J. Blindness in patients after external beam irradiation for pituitary adenomas: two cases occurring after small daily fractional doses. Clin Oncol (R Coll Radiol). 1991;3:291–4.
277. Regine WF, Kramer S. Pediatric craniopharyngiomas: long term results of combined treatment with surgery and radiation. Int J Radiat Oncol Biol Phys. 1992;24:611–7.
278. Roden D, Bosley TM, Fowble B, Clark J, Savino PJ, Sergott RC, et al. Delayed radiation injury to the retrobulbar optic nerves and chiasm. Clinical syndrome and treatment with hyperbaric oxygen and corticosteroids. Ophthalmology. 1990;97:346–51.
279. Schoenthaler R, Albright NW, Wara WM, Phillips TL, Wilson CB, Larson DA. Re-irradiation of pituitary adenoma. Int J Radiat Oncol Biol Phys. 1992;24:307–14.
280. Zhao Z, Lan Y, Bai S, Shen J, Xiao S, Lv R, et al. Late-onset radiation-induced optic neuropathy after radiotherapy for nasopharyngeal carcinoma. J Clin Neurosci. 2013;20:702–6.
281. Mock U, Georg D, Bogner J, Auberger T, Pötter R. Treatment planning comparison of conventional, 3D conformal, and intensity-modulated photon (IMRT) and proton therapy for paranasal sinus carcinoma. Int J Radiat Oncol Biol Phys. 2004;58:147–54.
282. Claus F, De Gersem W, De Wagter C, Van Severen R, Vanhoutte I, Duthoy W, et al. An implementation strategy for IMRT of ethmoid sinus cancer with bilateral sparing of the optic pathways. Int J Radiat Oncol Biol Phys. 2001;51:318–31.
283. Bhandare N, Monroe AT, Morris CG, Bhatti MT, Mendenhall WM. Does altered fractionation influence the risk of radiation-induced optic neuropathy? Int J Radiat Oncol Biol Phys. 2005;62:1070–7.
284. Danesh-Meyer HV. Radiation-induced optic neuropathy. J Clin Neurosci. 2008;15:95–100.
285. Ove R, Kelman S, Amin PP, Chin LS. Preservation of visual fields after peri-sellar gamma-knife radiosurgery. Int J Cancer. 2000;90:343–50.
286. Leber KA, Berglöff J, Pendl G. Dose–response tolerance of the visual pathways and cranial nerves of the cavernous sinus to stereotactic radiosurgery. J Neurosurg. 1998;88:43–50.
287. Abouaf L, Girard N, Lefort T, D'Hombres A, Tilikete C, Vighetto A, et al. Standard-fractionated radiotherapy for optic nerve sheath meningioma: visual outcome is predicted by mean eye dose. Int J Radiat Oncol Biol Phys. 2012;82:1268–77.
288. Andrews DW, Faroozan R, Yang BP, Hudes RS, Werner-Wasik M, Kim SM, et al. Fractionated stereotactic radiotherapy for the treatment of optic nerve sheath meningiomas: preliminary observations of 33 optic nerves in 30 patients with historical comparison to observation with or without prior surgery. Neurosurgery. 2002;51(4):890–902.
289. Metellus P, Kapoor S, Kharkar S, Batra S, Jackson JF, Kleinberg L, et al. Fractionated conformal radiotherapy for management of optic nerve sheath meningiomas: long-term outcomes of tumor control and visual function at a single institution. Int J Radiat Oncol Biol Phys. 2011;80(1):185–92.
290. Parsons JT, Bova FJ, Fitzgerald CR, Mendenhall WM, Million RR. Radiation optic neuropathy after megavoltage external-beam irradiation: analysis of time-dose factors. Int J Radiat Oncol Biol Phys. 1994;30:755–63.

291. Siddiqui JD, Loeffler JS, Murphy MA. Radiation optic neuropathy after proton beam therapy for optic nerve sheath meningioma. J Neuroophthalmol. 2013;33:165–8.
292. Mendenhall WM, Riggs CE, Amdur RJ, Hinerman RW, Villaret DB. Altered fractionation and/or adjuvant chemotherapy in definitive irradiation of squamous cell carcinoma of the head and neck. Laryngoscope. 2003;113:546–51.
293. Sanderson PA, Kuwabara T, Cogan DG. Optic neuropathy presumably caused by vincristine therapy. Am J Ophthalmol. 1976;81:146–50.
294. Griffin JD, Garnick MB. Eye toxicity of cancer chemotherapy: a review of the literature. Cancer. 1981;48:1539–49.
295. Geyer JR, Taylor EM, Milstein JM, Shaw CM, Hubbard BA, Geraci JP, et al. Radiation, methotrexate, and white matter necrosis: laboratory evidence for neural radioprotection with preirradiation methotrexate. Int J Radiat Oncol Biol Phys. 1988;15: 373–5.
296. Balsom WR, Bleyer WA, Robison LL, Heyn RM, Meadows AT, Sitarz A, et al. Intellectual function in long-term survivors of childhood acute lymphoblastic leukemia: protective effect of pre-irradiation methotrexate? A Childrens Cancer Study Group study. Med Pediatr Oncol. 1991;19:486–92.
297. Fishman ML, Bean SC, Cogan DG. Optic atrophy following prophylactic chemotherapy and cranial radiation for acute lymphocytic leukemia. Am J Ophthalmol. 1976;82:571–6.
298. Lessell S. Friendly fire: neurogenic visual loss from radiation therapy. J Neuroophthalmol. 2004;24: 243–50.
299. Marks LB, Spencer DP. The influence of volume on the tolerance of the brain to radiosurgery. J Neurosurg. 1991;75:177–80.
300. Marks JE, Wong J. The risk of cerebral radionecrosis in relation to dose, time and fractionation. A follow-up study. Prog Exp Tumor Res. 1985;29:210–8.
301. Safdari H, Fuentes JM, Dubois JB, Alirezai M, Castan P, Vlahovitch B. Radiation necrosis of the brain: time of onset and incidence related to total dose and fractionation of radiation. Neuroradiology. 1985;27:44–7.
302. Schultheiss TE, Higgins EM, El-Mahdi AM. The latent period in clinical radiation myelopathy. Int J Radiat Oncol Biol Phys. 1984;10:1109–15.
303. Lampert PW, Davis RL. Delayed effects of radiation on the human central nervous system: “early” and “late” delayed reactions. Neurology. 1964;14:912–7.
304. Hopewell JW, van der Kogel AJ. Pathophysiological mechanisms leading to the development of late radiation-induced damage to the central nervous system. Front Radiat Ther Oncol. 1999;33:265–75.
305. Myers R, Rogers MA, Hornsey S. A reappraisal of the roles of glial and vascular elements in the development of white matter necrosis in irradiated rat spinal cord. Br J Cancer Suppl. 1986;7:221–3.
306. van der Kogel AJ. Radiation-induced damage in the central nervous system: an interpretation of target cell responses. Br J Cancer Suppl. 1986;7:207–17.
307. Omary RA, Berr SS, Kamiryo T, Lanzino G, Kassell NF, Lee KS, et al. 1995 AUR Memorial Award. Gamma knife irradiation-induced changes in the normal rat brain studied with 1H magnetic resonance spectroscopy and imaging. Acad Radiol. 1995;2:1043–51.
308. Levin LA, Gragoudas ES, Lessell S. Endothelial cell loss in irradiated optic nerves. Ophthalmology. 2000;107:370–4.
309. Chan YL, Yeung DK, Leung SF, Cao G. Proton magnetic resonance spectroscopy of late delayed radiation-induced injury of the brain. J Magn Reson Imaging. 1999;10:130–7.
310. Crompton MR, Layton DD. Delayed radionecrosis of the brain following therapeutic x-radiation of the pituitary. Brain. 1961;84:85–101.
311. Ross HS, Rosenberg S, Friedman AH. Delayed radiation necrosis of the optic nerve. Am J Ophthalmol. 1973;76:683–6.
312. Borruat FX, Schatz NJ, Glaser JS. [Post-actinic retrobulbar optic neuropathy]. Klin Monbl Augenheilkd. 1996;208:381–4.
313. Guy J, Schatz NJ. Hyperbaric oxygen in the treatment of radiation-induced optic neuropathy. Ophthalmology. 1986;93:1083–8.
314. Brown GC, Shields JA, Sanborn G, Augsburger JJ, Savino PJ, Schatz NJ. Radiation optic neuropathy. Ophthalmology. 1982;89:1489–93.
315. Arnold AC. Radiation optic neuropathy. Presented at the 21st Annual Meeting of the North American Neuro-Ophthalmology Society; 1995 Feb 23; Tucson, AZ.
316. Schatz NJ, Lichtenstein S, Corbett JJ. Delayed radiation necrosis of the optic nerves and chiasm. In: Glaser JS, Smith JL, editors. Neuro-ophthalmology Symposium of the University of Miami and the Bascom Palmer Eye Institute, vol. 8. St. Louis: CV Mosby; 1978. p. 131–9.
317. Kim IK, Lane AM, Egan KM, Munzenrider J, Gragoudas ES. Natural history of radiation papillopathy after proton beam irradiation of parapapillary melanoma. Ophthalmology. 2010;117:1617–22.
318. Kaufman M, Swartz BE, Mandelkern M, Ropchan J, Gee M, Blahd WH. Diagnosis of delayed cerebral radiation necrosis following proton beam therapy. Arch Neurol. 1990;47:474–6.
319. Spaziante R, de Divitiis E, Stella L, Cappabianca P, Genovese L. The empty sella. Surg Neurol. 1981; 16:418–26.
320. Bernstein M, Laperriere N. Radiation-induced tumors of the nervous system. In: Gutin PH, Leibel SA, Sheline GE, editors. Radiation injury to the central nervous system. New York: Raven; 1991.

321. Guy J, Mancuso A, Beck R, Moster ML, Sedwick LA, Quisling RG, Rhoton Jr AL, Protzko EE, Schiffman J. Radiation-induced optic neuropathy: a magnetic resonance imaging study. J Neurosurg. 1991;74:426–32.
322. Hudgins PA, Newman NJ, Dillon WP, Hoffman Jr JC. Radiation-induced optic neuropathy: characteristic appearances on gadolinium-enhanced MR. AJNR Am J Neuroradiol. 1992;13:235–8.
323. McClellan RL, el Gammal T, Kline LB. Early bilateral radiation-induced optic neuropathy with follow-up MRI. Neuroradiology. 1995;37:131–3.
324. Oppenheimer JH, Levy ML, Sinha U, el-Kadi H, Apuzzo ML, Luxton G, et al. Radionecrosis secondary to interstitial brachytherapy: correlation of magnetic resonance imaging and histopathology. Neurosurgery. 1992;31:336–43.
325. Glantz MJ, Burger PC, Friedman AH, Radtke RA, Massey EW, Schold Jr SC. Treatment of radiation-induced nervous system injury with heparin and warfarin. Neurology. 1994;44:2020–7.
326. Rizzoli HV, Pagnanelli DM. Treatment of delayed radionecrosis of the brain: a clinical observation. J Neurosurg. 1984;60:589–94.
327. Danesh-Meyer HV, Savino PJ, Sergott RC. Visual loss despite anticoagulation in radiation-induced optic neuropathy. Clin Experiment Ophthalmol. 2004;32:333–5.
328. Landau K, Killer HE. Radiation damage. Neurology. 1996;46:889.
329. Borruat FX, Schatz NJ, Glaser JS, Feun LG, Matos L. Visual recovery from radiation-induced optic neuropathy. The role of hyperbaric oxygen therapy. J Clin Neuroophthalmol. 1993;13:98–101.
330. Hammerlund C. The physiological effects of hyperbaric oxygen. In: Kindwall EP, editor. Hyperbaric medicine practice. Flagstaff: Best publishing Company; 1995.
331. Miller NR. Radiation-induced optic neuropathy: still no treatment. Clin Experiment Ophthalmol. 2004; 32:233–5.
332. Levy RL, Miller NR. Hyperbaric oxygen therapy for radiation-induced optic neuropathy. Ann Acad Med Singapore. 2006;35:151–7.
333. Kellner U, Bornfeld N, Foerster MH. Radiation-induced optic neuropathy following brachytherapy of uveal melanomas. Graefes Arch Clin Exp Ophthalmol. 1993;231:267–70.

Hereditary Optic Neuropathies

7

Michelle Y. Wang, Alfredo A. Sadun,
and Jane W. Chan

Introduction

A large number of optic neuropathies involve the selective degeneration of retinal ganglion cells (RGCs), resulting in similar clinical presentations and outcomes. Mitochondrial dysfunction, either hereditary or acquired, has been shown to be the common pathophysiology underlying this spectrum of disorders (Fig. 7.1) [1, 2] Leber's hereditary optic neuropathy (LHON) and dominant optic atrophy (DOA), also known as Kjer's optic neuropathy, are examples of hereditary mitochondrial disorders. Acquired mitochondrial disorders frequently have a metabolic origin, which can be categorized into four classes based on etiology: (1) nutritional, (2) drug induced, (3) toxic, and (4) combined optic neuropathies. These diseases will be further discussed in the chapter on metabolic and toxic optic neuropathies (Chap. 6). Understanding the pathophysiology of hereditary and acquired mitochondrial optic neuropathies (MONs) can help us better evaluate and manage these diseases.

M.Y. Wang, M.D. (✉) • A.A. Sadun, M.D., Ph.D.
Department of Ophthalmology, Doheny Eye Institute,
1450 San Pablo St, Suite 5802, Los Angeles,
CA 90033, USA
e-mail: michelle.wang@med.usc.edu; asadun@usc.edu

J.W. Chan, M.D.
Department of Neurology, Neuro-Ophthalmology,
University of Nevada School of Medicine,
975 Kirman Avenue (111), Reno,
Nevada 89502, USA
e-mail: worjun@aol.com

Mitochondria: The Common Pathway

Mitochondria are cytoplasmic organelles that carry their own circular mitochondrial DNA (mtDNA) and provide most of the Adenosine-5′-triphosphate (ATP) required by cells. In oxidative phosphorylation, electrons are transferred down a chain of complexes as protons are translocated across the inner membrane to establish an electrochemical gradient. The energy stored in electron transport is coupled to the synthesis of ATP. In the process, some reactive oxygen species (ROS) are generated as a by-product. Mitochondrial dysfunction causes chronic impairment of energy production and further accumulation of ROS, which can in turn damage the mitochondria. ROS can act as intracellular messengers signaling depolarization of the inner mitochondrial membrane. This alteration of the membrane potential can lead to the opening of mitochondrial permeability transition pores (MPTP) upon reaching a threshold, allowing for leakage of cytochrome c into the cytosol where it forms the apoptosome, a key element triggering the apoptotic cascade [3]. It is important to note that, in LHON, all the mtDNA mutations affect complex I, which has been shown to be associated with the opening of MPTP and the activation of apoptosis [4]. In DOA, the dynamin-like protein encoded by the OPA1

J.W. Chan (ed.), *Optic Nerve Disorders: Diagnosis and Management*,
DOI 10.1007/978-1-4614-0691-4_7, © Springer Science+Business Media New York 2014

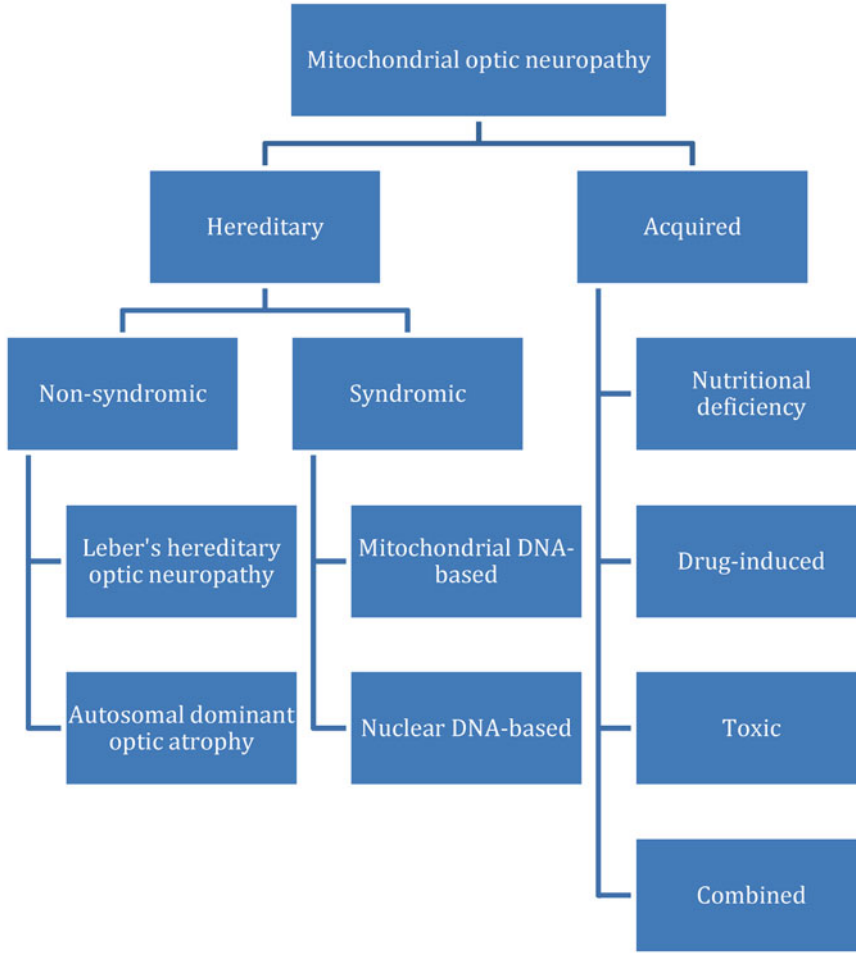

Fig. 7.1 Mitochondrial dysfunction plays a central role in the pathogenesis of many optic nerve diseases, either hereditary or acquired. Mitochondrial optic neuropathies are now recognized as a spectrum of conditions leading to optic atrophy through similar pathophysiology

gene also appears to be involved in mitochondrial fission/fusion and apoptosis. Hence, mitochondrial dysfunction not only leads to the immediate effects of energy depletion, but can also trigger apoptosis, representing the final pathway shared by a myriad of MONs.

Papillomacular Bundle Selectivity

Each time an axon undergoes action potential propagation, sodium/potassium pumps must restore the resting membrane potential. This step requires large quantities of ATP. Not surprisingly, mitochondria, the primary source of ATP, accumulate where they are most needed specifically at the nodes of Ranvier, and in the unmyelinated retinal nerve fiber layer (RNFL), and in the lamina cribrosa zones along the axons. Hence, the unmyelinated regions, which are extremely energy dependent, are the likely "choke points" that are most susceptible to metabolic crises and energy depletion.

The hallmark of a MON is the preferential involvement of the small fibers of the papillomacular bundle (PMB) [5]. Axonal transport is highly energy dependent and the mitochondria themselves need to be transported from the neuronal

somata in the retina to the synaptic terminals located relatively far away.

Therefore, RGCs with their long axons are particularly vulnerable [6]. Defective mitochondrial function compromises efficient axonal transport, including the transport of the mitochondria themselves. Given that a high surface area to volume ratio favors energy consumption over energy production, RGC axons of the PMB are particularly vulnerable because of their narrow caliber. The small PMB axons are also anatomically constrained for mitochondrial transport [7]. In addition, the lack of myelination inside the eye and the fast firing rate upon stimulation make these RGC axons particularly susceptible. As a part of a compensatory mechanism, mitochondria accumulate within RGC axons. These axonal changes can be detected by optical coherence tomography (OCT) [8]. Optic disc pallor usually appears during the later stages, indicating irreversible axonal loss. Consistent with the clinical findings [9], a quantitative histopathologic study demonstrated that the axonal loss in LHON spreads as a wavefront with PMB fibers being preferentially affected early and the fibers in the superonasal region mostly spared [10].

Screening

The PMB is invariably affected first in all MONs. The best screening tests for this spectrum of diseases are those that measure the functions of the PMB. These tests include visual acuity, color vision, contrast sensitivity, central visual fields, and pattern visual evoked potentials (VEPs). The red Amsler grid is also an excellent screening test.

Clinical Presentations

MONs generally share the following six main clinical features (Fig. 7.2): (1) fairly symmetric visual loss, (2) loss of high spatial frequency contrast sensitivity, (3) early and profound loss of color vision, (4) central or centrocecal visual field defects, (5) temporal pallor of the optic discs in the later stages, and (6) preferential loss of the PMB.

Minor variations exist between these optic neuropathies, especially in regard to the age of onset, rate of progression, risk factors, severity and extent of visual loss, and reversibility of the damage, which may all help distinguish one condition from another.

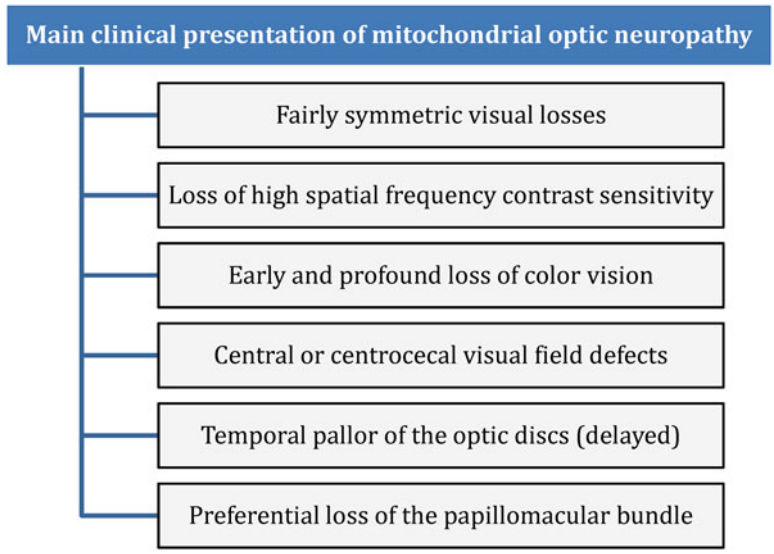

Fig. 7.2 The hallmarks of mitochondrial optic neuropathy of various etiologies are strikingly similar as they share a common pathophysiology pathway

Nonsyndromic Optic Neuropathy in Mitochondrial Diseases

Leber's Hereditary Optic Neuropathy

LHON is a maternally inherited disease with variable penetrance causing acute or subacute painless bilateral sequential central visual loss primarily in young males [11]. The disease was first described in 1871 by Theodor Leber, but the pathogenesis remained unclear until 1988 when Wallace and colleagues discovered a point mutation in the mitochondrial DNA (mtDNA) affecting nucleotide position 11778/ND4 [12]. More mtDNA mutations were later found. Over 95 % of LHON cases involve one of the three primary mtDNA mutations at positions 11778/ND4, 3460/ND1, and 14484/ND6, all of which affect complex I ND subunits of the respiratory chain [13–15]. Many less common pathogenic mutations have also been identified. The mitochondria may carry only wild type, only LHON mutant mtDNA (homoplasmy), or a mixture of mutant and wild-type mtDNA (heteroplasmy). High loads of mutant heteroplasmy, or more often, homoplasmic mutant mtDNA, predispose the subjects to the greatest risk for blindness.

Epidemiology

LHON is the most common mitochondrial disease [16] and the reported prevalence ranges from 1:30,000 in Northeast England, 1:39,000 in Netherlands, to 1:50,000 in Finland [17–19]. These numbers may be underestimated, as many patients remain undiagnosed. Furthermore, most individuals harboring mtDNA mutations are asymptomatic as carriers. Penetrance varies greatly between families and within the same pedigree [20]. The likelihood of visual loss has also been reported to be greater if the mother is affected even within the same pedigree. Only about 50 % of males and about 10 % of females who have one of the three primary mutations actually develop optic neuropathy [21–23]. The clinical severity of this genetic disorder also relates to its penetrance. This incomplete and variable penetrance in homoplasmic LHON and male preponderance suggest that additional factors such as heteroplasmy, environmental factors, mtDNA background, and nuclear modifying genes may play a role in changing the phenotypic expression of LHON.

Molecular Genetics and Genetic Heterogeneity of LHON

LHON is transmitted by mitochondrial, non-Mendelian inheritance. Patients inherit their mtDNA from the mother's oocyte. Because mitochondria are maternally inherited [24], no male-to-male transmission can occur in a LHON pedigree.

Three mtDNA mutations account for 95 % of LHON cases. Thirteen percent of cases are from the G3460A mutation, 69 % of cases are from the G11778A mutation, and 14 % of cases are from the T14484C mutation [25]. The G11778A mutation produces substitution in the ND4 subunit of complex I. Mutations at n 3460 and 14484 produce A52T and M64V substitutions in the ND1 and ND6 subunits of complex I, respectively [25].

Mutations of LHON are classified as primary or secondary mutations. The primary ones are found in multiple LHON families and the highly conserved amino acids are usually altered. The G11778A, T14484C, and G3460A mutations are the most common primary ones [14, 26]. Other more rare primary mutations include G14459A, G15257A, T14596A, C14498T, G13730A, C14482G, and A14495G [14, 27].

The most common and second most severe mutation of LHON is 11778. It accounts for more than 50 % of European cases and 95 % of Asian cases [12, 28]. The mutation has arisen repeatedly in different mtDNA lineages [29] and is occasionally found with other LHON mutations [30]. It is frequently heteroplasmic [31] and is about 82 % penetrant in males. The spontaneous visual recovery rate is only 4 % [21, 28].

The 3460 mutation accounts for about 35 % of European LHON [32]. It has been observed in several mtDNA lineages and occasionally occurs with other LHON mutations. It is usually homoplasmic and is expressed in 69 % of males. The spontaneous visual recovery rate is 22 % [30, 31].

The third primary mutation is 14484. This mutation accounts for about 20 % of European

LHON patients [33]. It is commonly associated with specific mtDNA lineages, often in association with 13708, 15257, or 3394. It has been homoplasmic in every case but one. It has a penetrance in males of 82 %. The spontaneous visual recovery rate is 37 % [33]. The dependence on homoplasmy and the high rate of spontaneous recovery is more suggestive that this mutation is milder.

The 14459 mutation is rare but gives rise to the most severe phenotype [34]. Variable clinical manifestations can range from being normal, to having late-onset optic atrophy, to having early-onset dystonia accompanied by bilateral basal ganglia degeneration. When the mutation approaches homoplasmy, the penetrance is high, with 48 % of maternal relatives with pediatric dystonia, 10 % with only visual loss, and 3 % with both visual loss and dystonia [34, 35].

The mildest primary mutation is 15257. It occurs in up to 15 % of LHON patients but also in 0.3 % of the general population [36]. The mutation has been observed on the same mtDNA lineage, usually together with the 13708 and 14484 mutations in all but one case [37]. This mutation is consistently homoplasmic and has a penetrance in males of 72 %. The probability of spontaneous visual recovery is 28 % [33]. This may be more of a modifying mutation than one that produces LHON in isolation.

Secondary mutations are found at a lower prevalence in control populations and may represent polymorphisms. These secondary mutations often occur in association with a primary mutation or other secondary mutations. A less highly conserved amino acid is mutated. Secondary pathogenic mutations in LHON include G13708A, A4917G, T4216C, G9804A, G9438A, and G15257A [30].

Studies have shown that the nonsynonymous population polymorphisms found in mtDNA haplogroups J_{1c} and J_{2b} increase the penetrance of LHON mutations in 11778/ND4 and 14484/ND6 [38, 39]. Linkage analysis has identified two loci on chromosome X, suggesting chromosome X may play a role in modifying the expression of LHON in males, thereby accounting for the gender prevalence [40]. However, another study has failed to demonstrate excessive skewed inactivation of the X-chromosome in affected females [41], suggesting that there might be multiple modifying genes or factors that remain unidentified.

Risk Factors

The primary etiology of LHON is an mtDNA mutation which, in itself, is not sufficient to lead to visual loss. Tobacco smoking and alcohol consumption have been found in a large Brazilian LHON pedigree to be the two strongest risk factors for LHON [42]. A subsequent multicenter study of 402 LHON patients also found a significant risk for tobacco and alcohol use [43]. Smoke in general, and not necessarily in the form of tobacco smoking, may trigger LHON. A case was reportedly to be triggered by a large tire fire [44]. Other agents that interfere with mitochondrial respiratory function have also been documented in the literature such as ethambutol, chloramphenicol, linezolid, aminoglycosides, and antiretroviral therapy [45–49].

These environmental toxins may reduce the oxidative phosphorylation capacity in patients who already have the genetic predisposition for developing LHON. Cullom et al. [50] found that 2 of 12 patients previously diagnosed as having tobacco–alcohol amblyopia, based on a classical clinical presentation, tested positive for known LHON mutations, one patient for the 11778 mutation and one for the 3460 mutation. The fact that only a few patients who abuse tobacco and alcohol develop optic neuropathy suggests an element of individual susceptibility. Therefore, a patient with an LHON-associated mitochondrial mutation would be predisposed for this particular susceptibility.

Clinical Presentations

LHON typically affects young men between the ages of 15 and 35 years. It is characterized by rapid painless central visual loss in one eye with dyschromatopsia and peripapillary optic disc changes. The fellow eye usually follows a similar course within days to weeks, but simultaneous involvement can also occur. Rarely, monocular involvement has been reported. Visual loss is usually profound, worse than 20/400, but can vary from 20/25 to hand motion vision and stabilizes

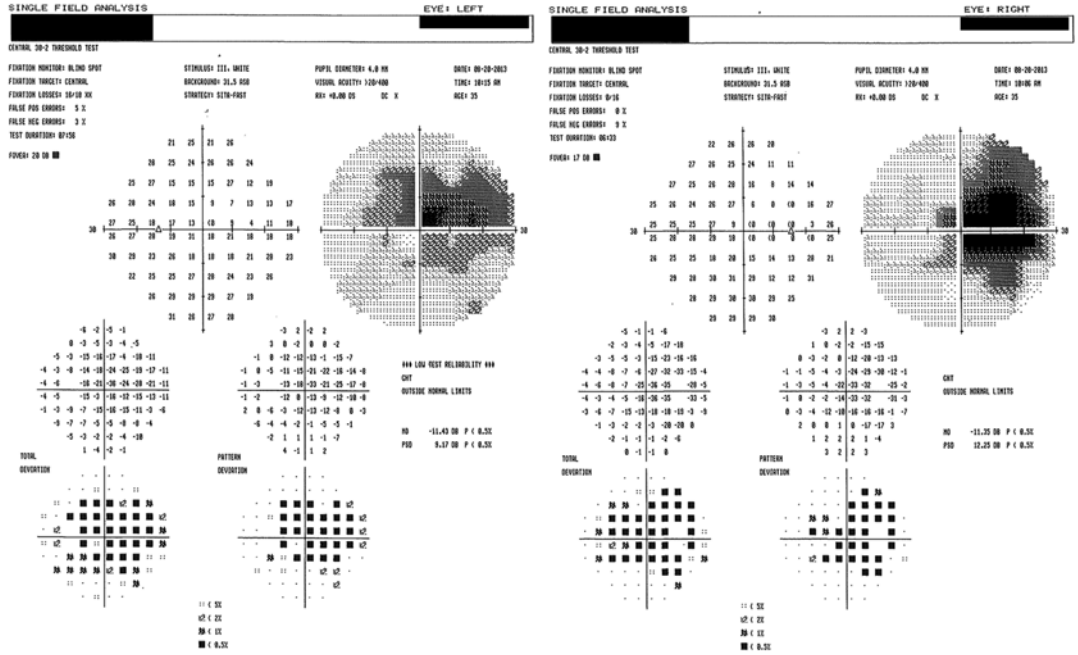

Fig. 7.3 The Humphrey visual field of a LHON patient demonstrating bilateral cecocentral scotoma in both eyes

within a few months [51]. Severe dyschromatopsia is an early clinical feature following visual loss. The visual field typically demonstrates a large absolute central or centrocecal scotoma that usually starts nasal to the blind spot (Fig. 7.3) and later extends to involve both sides of the vertical meridian. As time progresses, loss of the PMB with corresponding atrophy of the temporal optic nerve, which eventually extends to involve the other quadrants, leads to diffuse optic atrophy. The typical clinical outcome is permanent central visual loss with optic atrophy within 6 months. Lack of pain and no visual recovery may help distinguish LHON from other optic neuropathies such as optic neuritis, which also tend to affect patients in the same age group. Patients with the onset of clinical symptoms and signs before 10 years of age have a more benign prognosis [52, 53].

The 11778/ND4 mutation carries the worst prognosis as over 75 % of patients affected with this mutation became legally blind in both eyes [2]. Spontaneous recovery occasionally may occur with a younger age of onset. The 14484/ND6 mutation has the most favorable outcome [54]. Remyelination of denuded axons might partially explain the late visual recovery observed in these patients [55].

After the initial loss of vision, LHON patients may continue to lose residual vision by an ongoing low grade degenerative process. Most remarkably, despite severe visual loss in most cases, pupillary light responses remain relatively preserved. The intrinsically photosensitive retinal ganglion cells (ipRGCs) are a new class of RGCs most recently discovered [56, 57]. These cells contain melanopsin, a photopigment that directly detects irradiance independently of rods and cones, regulates circadian rhythm, and conducts nonimage-forming visual functions, such as the pupillary light reflex. A selective sparing of ipRGCs in LHON and DOA has recently been demonstrated [58, 59], providing an explanation for the preservation of the pupillary response in patients with LHON. This class of cells, physiologically distinct from regular RGCs, appears to be more resistant to neurodegeneration, possibly due to lower firing rate, larger axons, or the absorption of ROS by melanopsin [60].

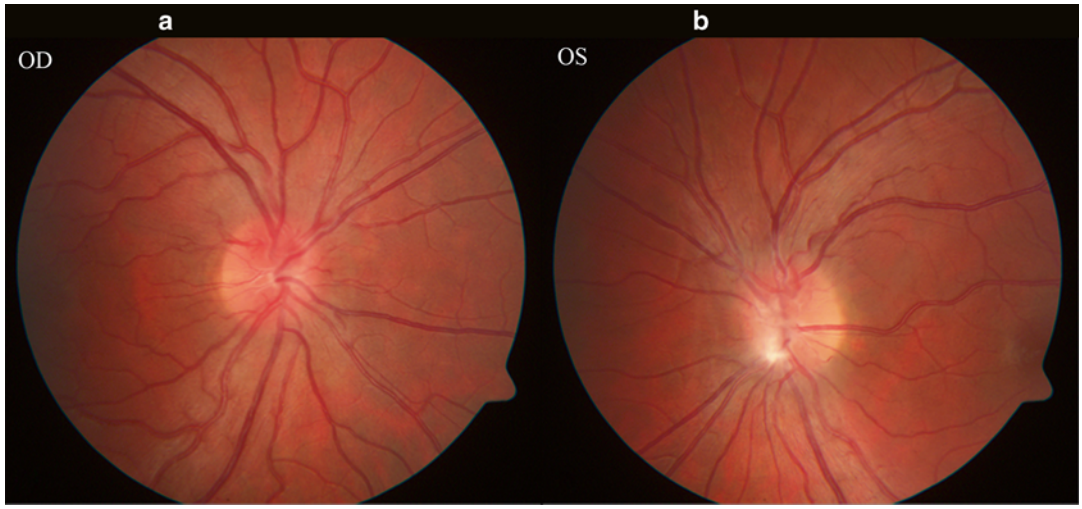

Fig. 7.4 Optic disc photos of a LHON patient demonstrating peripapillary telangiectasia and RNFL swelling around the disc left eye (**b**) greater than the right eye (**a**)

Asymptomatic carriers of LHON may also demonstrate subclinical features such as subtle dyschromatopsia, reduced spatial contrast sensitivity, temporal processing deficits, and an abnormal fundus appearance characterized by focal edema in the arcuate bundle and mild visual field changes [61–65]. In a large Brazilian family with the 11778/ND4 mutation, 15 % of the asymptomatic carriers revealed microangiopathy and swelling of the RNFL [66].

Presymptomatic at-risk patients may show color defects on Farnsworth–Munsell 100-hue test and even mild abnormalities in the pattern-reversal visual evoked responses [67].

Funduscopic Features

In the acute stage of visual loss in LHON, the optic disc appears hyperemic with occasional peripapillary microangiography. Obscuration of the disc margin and transient telangiectagia may also occur. During this acute/subacute stage, a classic triad of signs can be seen in many cases (Fig. 7.4): (1) circumpapillary telangiectatic microangiopathy; (2) RNFL swelling around the disc (pseudoedema), and (3) absence of leakage on fluorescein angiography (in contrast to true disc edema).

Only 58 % of patients with the 11778 mutation show telangiectatic vessels in the acute phase [28] and 33 % with the 14484 mutation [68]. The telangiectatic vessels and pseudoedema of the disc resolve over several months. Optic atrophy develops with the most severe atrophy in the PMB nerve fiber layer. Microangiopathy is uncommon after 6 months [68]. Optic atrophy has been reported to be seen as early as 1 month from the onset of visual symptoms, but it is universally seen by 6 months. Nonglaucomatous cupping of the optic disc and arteriolar attenuation may also develop. Eventually, as the vision stabilizes, temporal pallor of the optic disc results, reflecting preferential axonal loss in the PMB [69].

The optic nerve head (ONH) size may play a role in the pathogenesis of LHON. In 1993, Burde proposed that the disc at risk, a common risk factor seen in nonarteritic anterior ischemic optic neuropathy, may also lead to the optic neuropathy in LHON, as axoplasmic stasis and swelling may further compress the vessels and nerve fibers [70]. Ramos et al. documented that the ONH is larger in LHON carriers than in LHON patients, suggesting that less crowding of RGC axons may play a protective role in the carriers [71]. Furthermore, even among the affected LHON patients, larger optic discs also correlate with visual recovery and better visual outcome, suggesting that this anatomic feature

also influence the final visual outcome in the affected patients. In a separate study, small optic discs were found in cases with acute onset [52]. Therefore, these findings could be relevant in the prognosis of affected patients and in the surveillance and management of LHON carriers.

The characteristic funduscopic findings are not always present in affected persons with LHON who present with visual loss. Abnormal funduscopic findings may also be seen in presymptomatic patients and in asymptomatic maternal relatives who carry mitochondrial mutations associated with this disease. Swelling in the peripapillary RNFL; increased tortuosity of capillaries, medium arteries, and venules; and arteriovenous shunting have been reported in presymptomatic individuals and asymptomatic carriers [72, 73].

Histopathology

Histopathologic studies have demonstrated a dramatic loss of RGCs and their axons with the centrally located, small-caliber fibers of the PMB being the target tissue [74]. The larger axons in the periphery are most spared. Histopathological investigations have also demonstrated a selective loss of the P-cell population and their corresponding smaller RGCs, and a relative preservation of the M cells in the optic nerve [74]. These findings correlate with the fundus changes of early PMB loss, dyschromatopsia, central scotoma, and preservation of the pupillary light response in LHON patients.

Some ultrastructural studies of the muscle from affected patients have demonstrated enlarged, subsarcolemmal mitochondria, proliferation of cristae, and paracrystalline inclusions [74, 75]. In a patient from the Queensland 1 pedigree with mtDNA 4160 and 14484 mutations, electron-dense calcium mitochondrial inclusions within ganglion cells were observed [76].

Differential Diagnosis

A comprehensive history is the key in distinguishing this condition from the other optic neuropathies. LHON patients often can provide a history of visual loss in family members from the maternal side. The optic nerve is usually singularly involved. The absence of systemic or constitutional symptoms is also helpful. In DOA, visual loss occurs at a younger age and progresses slowly over many years. The final vision is usually better than that of LHON, leveling off at 20/100 or 20/200. The tempo of visual loss is another distinguishing feature. LHON patients usually present with subacute visual loss, unlike compressive optic neuropathies and chronic papilledema from idiopathic intracranial hypertension in which the visual loss affects both eyes and progresses much more slowly. In contrast, ischemic optic neuropathies usually cause sudden visual loss and present with peripapillary hemorrhages. The differential diagnosis of painless subacute visual loss in young adults also includes infiltrative or inflammatory optic neuropathies. An infiltrative optic neuropathy is usually characterized by the thickened appearance of the optic disc and disc leakage on fluorescein angiography. MRI imaging may reveal infiltrative or inflammatory lesions of the optic nerve of brain. Nutritional and toxic etiologies may be elicited by a careful history.

Diagnosis

A careful clinical history, especially family history; ophthalmologic testing, and psychophysical testing are all required for the diagnosis of LHON. On fluorescein angiography, there is absence of dye leakage at the optic disc, reflecting pseudoedema only.

OCT evaluation allows for in vivo visualization of LHON, which may be helpful in characterizing the different stages of the disease and quantifying the amount of swelling in the presymptomatic stage. Barboni et al. documented the temporal sequence of RNFL changes on OCT during the clinical course of LHON (Fig. 7.5) [77].

In the acute phase, OCT findings often demonstrate RNFL thickness increase in the temporal and inferior quadrants, which may represent stasis of axonal transport and a compensatory increase in the number of mitochondria in the RNFL. The RNFL can take as long as 3 months to reach its maximum thickness. Eventually, the RNFL in the temporal and inferior quadrants becomes thinner from progressive atrophy. At 3 months, the

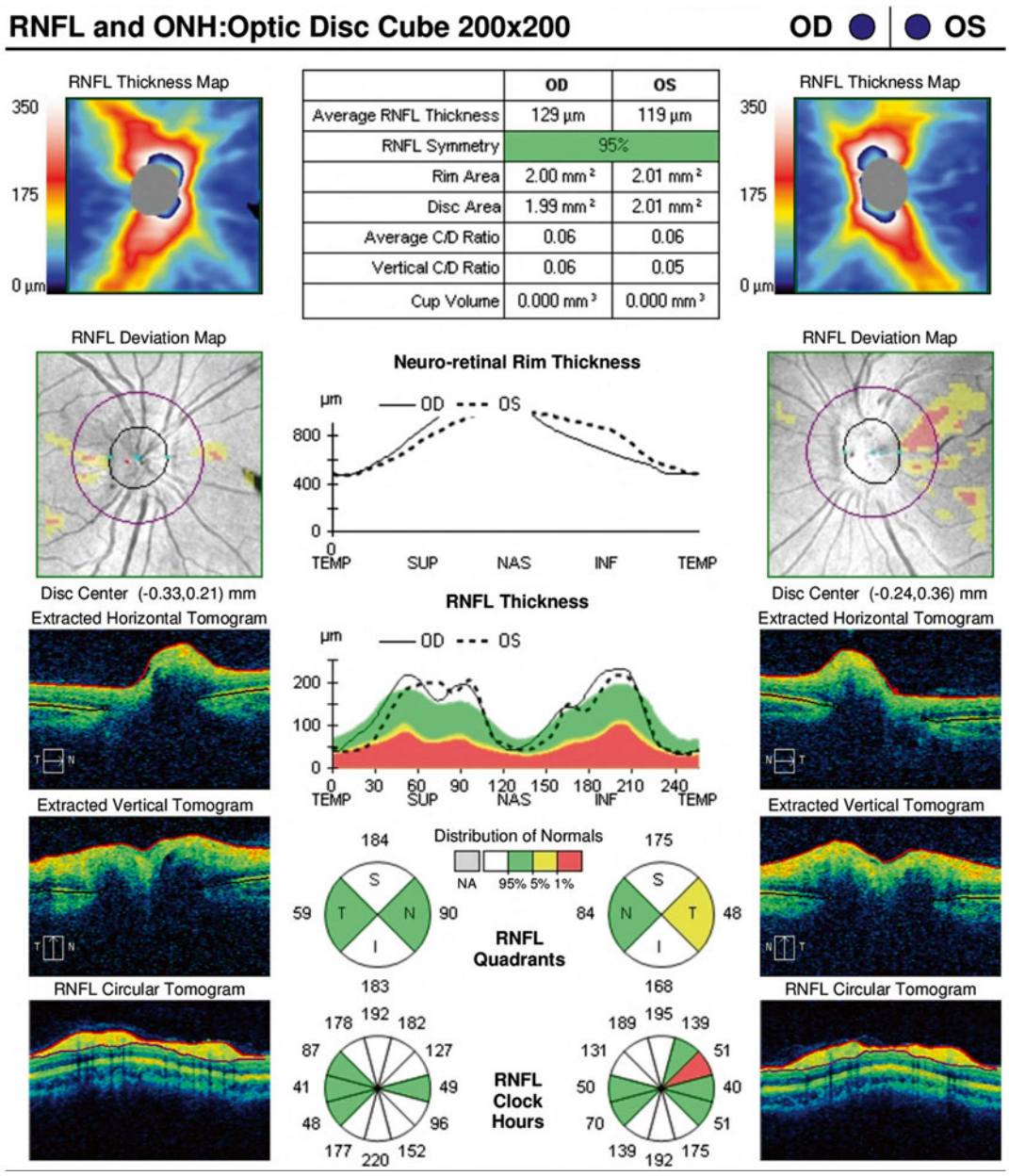

Fig. 7.5 The OCT RNFL analysis of a LHON patient with left eye involvement followed by right eye, demonstrating increased RNFL in superior and inferior quadrants. Note that the temporal quadrant of the first eye already shows some atrophy

thickening is more evident in the superior and nasal quadrants. The OCT finding is consistent with the early preferential involvement of the PMB and with the previously unrecognized early involvement of the inferior quadrant.

In contrast to the rapid decline seen on examination, OCT shows that there is a sequence of structural changes that may progress over 3 months, allowing for a wider therapeutic window of opportunity. In the chronic phase, severe loss of

fibers can be observed in all quadrants, with the nasal fibers being relatively spared [78].

In the asymptomatic carriers, the RNFL of the temporal and, to a lesser extent, the inferior quadrant is thickened, representing the preferential involvement of the PMB in subclinical LHON [79]. The RNFL thickness in LHON carriers also demonstrates higher variability than normal subjects, reflecting the dynamic nature of LHON [80]. The variable RNFL swelling may be due to the opposing forces between the metabolic injury produced by complex I dysfunction and the compensatory response by the RGCs and their axons. Further longitudinal follow-up studies of unaffected carriers are needed to identify the predictive signs of conversion for timely treatment.

The diagnosis of LHON can be confirmed by genetic testing, revealing one of the three point mutations in the mtDNA. However, a negative genetic testing cannot rule out LHON, as 5 % of cases are not due to the three common LHON mutations [81]. If the clinical suspicion remains strong, or if there is evidence of maternal transmission of blindness, a complete mtDNA sequence analysis may be considered.

Systemic Associations with LHON

In the majority of cases, visual dysfunction is the only manifestation in LHON. However, rare associations with multiple sclerosis (MS) and cardiac conduction abnormalities have been reported [82, 83].

The onset of visual loss may occasionally be associated with headache or ocular discomfort in 24 % of patients [68]. Patients with LHON, particularly those with the 11778 mutation, may have symptoms and signs consistent with MS at the time of onset of progressive visual loss [84–86]. Uhthoff's phenomenon has also been reported [87]. Most of these patients are female who have cerebrospinal fluid (CSF) and MRI abnormalities consistent with MS. Five percent of LHON patients with the 11778 mutation have a relative with MS [85]. Primary LHON mutations occur in some MS patients with severely affected optic nerves, but not in patients with MS as a whole [86]. Both disorders, LHON and MS, are thought to occur coincidentally because the prevalence of both diseases is no greater than that of each alone. An underlying LHON mutation may also worsen the prognosis of optic neuritis in patients with MS.

Up to 9 % of patients with LHON have associated cardiac pre-excitation syndromes. Among Finnish patients, pre-excitation syndromes, including Wolff–Parkinson–White and Lown–Ganong–Levine, are common [88]. Prolongation of the corrected QT interval has also been observed in an African-American family with the 11778 mutation [83].

Some pedigrees of LHON have a "Leber's plus" syndrome with more severe neurological abnormalities: (1) optic neuropathy, movement disorders, spastic paraparesis, psychiatric abnormalities, skeletal changes, and acute infantile encephalopathic episodes; (2) optic neuropathy, dystonia, and basal ganglia lesions on neuroimaging; (3) optic neuropathy and myelopathy; and (4) optic neuropathy and fatal encephalopathy in early childhood [34, 83, 89, 90].

Funalot et al. [91] reported three unrelated patients with LHON harboring mtDNA mutations at position 3460 of the mtND1 gene and positions 14459 and 14484 of the mtND6 gene. In addition to visual loss, each patient developed a complicated neurological syndrome resembling Leigh syndrome. Features included gaze palsy, hearing loss, spastic ataxia, cerebellar ataxia, rigidity, hyperreflexia, and multiple hyperintensities in the brainstem [92].

Management

In general, LHON carriers, individuals who have not lost vision, should be advised not to smoke or drink. For affected LHON, the peripheral vision usually remains relatively intact and referral to a low vision specialist may be helpful. Since male patients will not pass on the mutation to all of their children, whereas all female patients will. Genetic counseling of patients and their families is simple yet extremely important. There is no proven treatment to prevent or reverse LHON. It is important to discuss the natural course and poor visual prognosis with patients. They should be advised against smoking tobacco and exposure

to any smoke, including fires. Minimizing the use of alcohol and engaging in a healthy diet incorporating vitamin B and high-quality proteins may be helpful.

Some investigators have used pharmaceutical agents, such as the second generation quinone, idebenone, a short-chain derivative of CoQ_{10}, or the third generation EPI-743 (experimental redox agent) to supplement the defective respiratory chain [93–95]. Others have investigated gene therapy to either bypass or provide functional replacement of the dysfunctional complex I [96]. By providing an alternative pathway, these strategies may restore electron flow, improve energy production, and reduce ROS accumulation.

Vitamins

Anecdotal reports on the therapeutic use of vitamins especially vitamins B2, B12, C, and E have not been proven effective for LHON. However, B12 deficiency may precipitate visual loss in LHON [97]. Therefore, supplemental vitamin B12 may be helpful in genetically predisposed individuals.

Brimonidine

Topical brimonidine, an α-2 agonist, has been hypothesized to promote anti-apoptotic cell signaling by up-regulating Bcl-2 and inhibiting the MPTP opening, thereby preventing mitochondria-induced apoptosis [98]. Topical brimonidine has been shown to have stabilizing effects on RGC survival in animal models of optic nerve injury [99–101]. However, it failed in a small clinical trial to prevent the involvement of the fellow eye in LHON [102].

Antioxidant Agents

The goal of most novel treatments in LHON is to reduce the excessive production of ROS. Antioxidants such as exogenous glutathione; Trolox, a derivative of vitamin E; and decylubiquinone, a coenzyme Q-10 analog, have shown a modest protective effect in vitro [103, 104].

Coenzyme Q10

Coenzyme Q10 (CoQ_{10}; ubiquinone) plays a pivotal role in the mitochondrial respiratory chain. It is a cofactor that transports electrons from complexes I and II to complex III. Some have proposed its use in the therapy of mitochondrial diseases by bypassing the defective complex I. Therefore, coenzyme Q could restore electron flow in the respiratory chain, provide electrons to the chain, or increase mitochondrial antioxidant defenses. Anecdotal successful reports of CoQ_{10} treatment in LHON have been published [105]. However, a few case reports of supplemental use of CoQ_{10} have been unsuccessful because of possible poor drug delivery in that it cannot cross the lipid membranes into the mitochondria [106].

Idebenone

Idebenone is a short chain analog of CoQ_{10} that has decreased hydrophobicity. In vitro, it can compete with natural CoQ_{10} to mediate electron transfer. It has been reported that idebenone has higher delivery to into the mitochondria and higher efficiency to cross the blood–brain barrier [106]. Idebenone has been used to treat other mitochondrial disorders such as Friedreich's ataxia (FA), MELAS, and Wolfram syndrome [107–110]. The first promising result for LHON was shown in 1992 [111] followed by a few more successful case reports [112–115].

Mashima et al. evaluated the effectiveness of idebenone combined with vitamin B2 and vitamin C in the treatment of 28 Japanese patients with LHON [112]. The visual recovery was significantly earlier for treated patients carrying the 11778/ND4 mutation and was limited to small openings that appeared in the paracentral visual field, suggesting that administration of idebenone and vitamins may speed up the recovery process.

Eng et al. reported a case series of seven LHON patients, treated with idebenone alone (450 mg/day). Most eyes showed recovery of visual acuity, color vision, and visual fields. One 11778/ND4 LHON patient improved from counting-fingers vision in both eyes to visual acuities of 20/20 and 20/30 with associated reduction of the central scotomas from a diameter of 20° to less than 5°.

In the Rescue of Hereditary Optic Disease Outpatient Study (RHODOS), the first multicenter

double-blind, randomized, placebo-controlled trial published in 2011, 85 patients with LHON harboring one of the three common mutations were treated with idebenone 900 mg/day for 24 weeks [93]. Even though the study did not reach statistical significance for the primary outcomes in the treatment analysis, there is evidence supporting that patients with discordant visual acuities (defined as patients with a difference in logMAR >0.2 between eyes) are the most likely to benefit from idebenone treatment. The post hoc subgroup analysis suggests that this particular group may have the greatest potential reserve, and timely treatment may prevent further visual loss. Idebenone has also been shown to be safe and well tolerated by the patients.

In the same year, Carelli et al. reported a retrospective evaluation of a large series of 103 LHON patients treated with idebenone (270–675 mg/day) within 1 year of onset for 12–80 months with a 5-year follow-up [94]. The treated group showed an increased frequency of recovery of visual acuity. Early therapy was the most predictive factor for visual recovery which also delayed second eye involvement; however, the final visual outcome of the second eye was not better. The 11778/ND4 patients were the best responders. There was insufficient data to verify the treatment response for the 3460/ND1 and the 14484/ND6 groups that had spontaneous recovery in the non-treated arm. Therefore, both RHODOS and this retrospective study suggest that early and prolonged idebenone treatment may improve the frequency of visual recovery and change the natural course of LHON. These two studies also demonstrate that the window for treatment may be within 1 year of onset of symptoms and signs.

EPI-743

EPI-743, a third-generation quinone, is a member of a new class of drugs called *digital biochemical information transfer and sensing* compounds (D-BITS) [116]. It is a small orally bioavailable molecule that readily crosses into the central nervous system (CNS) [117]. It regulates metabolism and programmed cell death. It has been shown to replenish reduced glutathione, an important part of the cellular antioxidant defense systems [103, 118]. UnlikeCoQ_{10} and idebenone, it is a parabenzoquinone analog that has different groups on the quinone ring and a shorter side chain of three isoprene units (vs. 10 in CoQ10.) [119]. This mechanism allows EPI-743 to have antioxidant protective effect in cell culture 1,000-fold greater compared with CoQ10 and idebenone. An open-label multicenter trial to evaluate its effect as a therapeutic agent for mitochondrial disorders has shown promising results [119, 120].

Sadun et al. have evaluated the efficacy of EPI-743 in LHON patients in an open-label clinical trial [95]. Five LHON patients received EPI-743 orally, three times daily (100–400 mg/dose), for 6–18 months. In this study, EPI-743 significantly changed the natural course of LHON and demonstrated disease arrest and reversal in 80 % of treated patients. This study suggests that EPI-743 may be an effective treatment for LHON.

Other Drugs Activating Mitochondrial Biogenesis and Anti-apoptotic Agents

Experimental drugs inhibiting the apoptosis in RGCs during the acute phase or activating mitochondrial biogenesis in unaffected carriers have been proposed as alternative therapeutic strategies. Drugs, such as cyclosporine, may abort the apoptotic cascade by inhibiting MPTP and may be beneficial in the very early stages of LHON [121].

The induction of mitochondrial biogenesis through pharmacological modulation has shown promising results in mitochondrial disorders. A complex I defective LHON cybrid cell study by Giordano et al. investigated the role of estrogens in LHON to potentially provide an explanation for the male prevalence in this disorder [122]. Patients treated with 17β-oestradiol had reduced production of ROS, lower apoptotic rates, coordinated activation of mitochondrial biogenesis, and significant improvement in energetic competence. The estrogen receptor β was localized to the mitochondrial network of human RGCs and unmyelinated axons of RNFL. Bezafibrate, a peroxisome proliferator-activated receptor pan agonist, was shown to enhance oxidative phosphorylation capacity and conservation of ATP [123].

Gene Therapy

Gene therapy has been proposed to bypass the dysfunctional complex I in LHON. It is important to emphasize that these approaches are still experimental, requiring more evidence to prove their efficacy and safety in humans.

LHON is caused by mutations affecting the mtDNA-encoded subunits of complex I. The nuclear allotropic expression of mtDNA-encoded gene is the most studied gene therapy approach for LHON. It is an alternative approach for correcting mutations in mitochondrial protein-coding genes by expressing these genes in the nucleus with an additional terminal targeting sequence for mitochondrial import [124, 125]. The nuclear-encoded wild-type ND subunit is expressed in the cell cytoplasm and transported to the mitochondria where it is co-assembled in complex I. The wild-type ND subunits are presumed to compete with the mitochondrial-encoded mutant ND subunit producing an artificial heteroplasmy. A mouse model of LHON has been produced by this study group with intravitreal injection of an adeno-associated virus (AAV) vector carrying mutant 11778/ND4 human recoded gene. The impaired RGCs are then rescued through the delivery of an AAV vector containing wild-type ND4 into the mitochondria of RGCs and axons of optic nerve [126, 127]. Human clinical trials using this approach in LHON patients are ongoing [96, 128]. However, another study showed that the allotopically expressed protein was not internalized in mitochondria and the results were due to selection of mtDNA revertants [129]. The debate on the benefits and limitations of allotropic expression of mitochondrial genes continues [130].

Other studies have attempted direct delivery of mtDNA into the mitochondria. One study imported the whole mtDNA molecules complexed with recombinant human mitochondrial transcription factor A (rhTFAM), the major mtDNA nucleoid coating protein [131]. This has led to the activation of mitochondrial biogenesis. Another study used an AAV vector containing the human mtDNA-encoded ND4 subunit gene fused with the adeno-associated capsid VP2 with a mitochondrial targeting sequence (MTS) [132]. This approach led to mitochondrial internalization of the AAV vector and rescue of the pathologic phenotype both in vitro and in a mouse model. These studies represent breakthroughs in providing approaches to introduce mtDNA molecules or AAV vector containing mtDNA genes directly within mitochondria, but more studies are required to elucidate the exact underlying delivery mechanism.

Recently, a mouse model of LHON reproducing genetic, biochemical, psychophysical, and histological features of the disease has been established, allowing further testing of potential therapies. Lin et al. have successfully created a reliable mouse model of LHON with human mtDNA ND6 P25L mutation which exhibited all the hallmarks of human LHON, including loss of central small caliber optic nerve fibers with sparing of larger peripheral fibers, neuronal accumulation of abnormal mitochondria, axonal swelling followed by degeneration, and demyelination [133]. They showed that these mice became blind by psychophysical measures and electrophysiologic testing. These mice had mild impairments of ATP but severe increases of ROS induced by their mitochondrial dysfunction. This is the first reliable animal model created for studying mtDNA in LHON.

A functional replacement for defective complex I has been proposed as an alternative strategy. The alternative NADH dehydrogenase (Ndi1) from yeast mitochondria has shown to restore NADH oxidase deficiencies, electron transfer pathway, and suppress ROS overproduction from defective complex I [134]. Yeast NDI1 has been shown to improve oxidative phosphorylation capacity and increase protection against oxidative stress and cell death in cells carrying the G11778A mutation in vitro [135]. Recently, Marella et al. brought this approach in vivo and injected the adeno-associated virus (AAV, type 5) carrying the mitochondrially targeted NDI1 gene (rAAV5-NDI1) into the rat model of LHON to achieve full expression of Ndi1 protein in the optic nerve and RGCs. In the mitochondria, the Ndi1 protein shuttles electrons to ubiquinone, bypassing complex I and restoring the electron transport chain. Delivering the NDI1 gene

restores vision to the normal level [136]. Another group that has successfully created a murine model of LHON has delivered gene therapy through the vitreous [137]. These studies provide hope that there is a window of opportunity for gene therapy to be applied before cell loss.

Dominant Optic Atrophy of Kjer's

Dominant optic atrophy (DOA), also known as Kjer's optic neuropathy, is an insidious, slowly progressive optic neuropathy with an onset in the first decade of life. The prevalence of DOA is 1:50,000–1:10,000 in Denmark [138]. A mutation in the nuclear OPA1 gene was identified to be the genetic basis in 60 % of cases [139, 140], and the majority of cases have been mapped to chromosome 3q28–q29 [141], The OPA1 gene encodes for a mitochondrial dynamin-related GTPase protein, which has an important role in the mitochondrial fission/fusion, control, and regulation of apoptosis [142]. The most common mutation patterns are missense and nonsense mutations, deletions, and insertions. The resultant protein is truncated and probably rapidly degraded. As in LHON, the penetrance is low, suggesting that environmental factors may also play a role in the phenotypic expression of DOA.

Clinical Presentations

DOA typically affects children before the age of 10, who are often unaware of the problem. Patients usually present with slowly progressive bilateral and symmetrical visual loss and often with centrocecal scotomas (Fig. 7.6). Dyschromatopsia almost always occurs, with blue–yellow and red–green disturbances being the most common [143]. The field of tritanopes is more contracted to blue isopters than to red [144]. The severity of the color defect does not correlate with the degree of loss in visual acuity [143, 145–147]. Visual acuity usually ranges between 20/40 and 20/200, but the clinical expression may vary depending on the

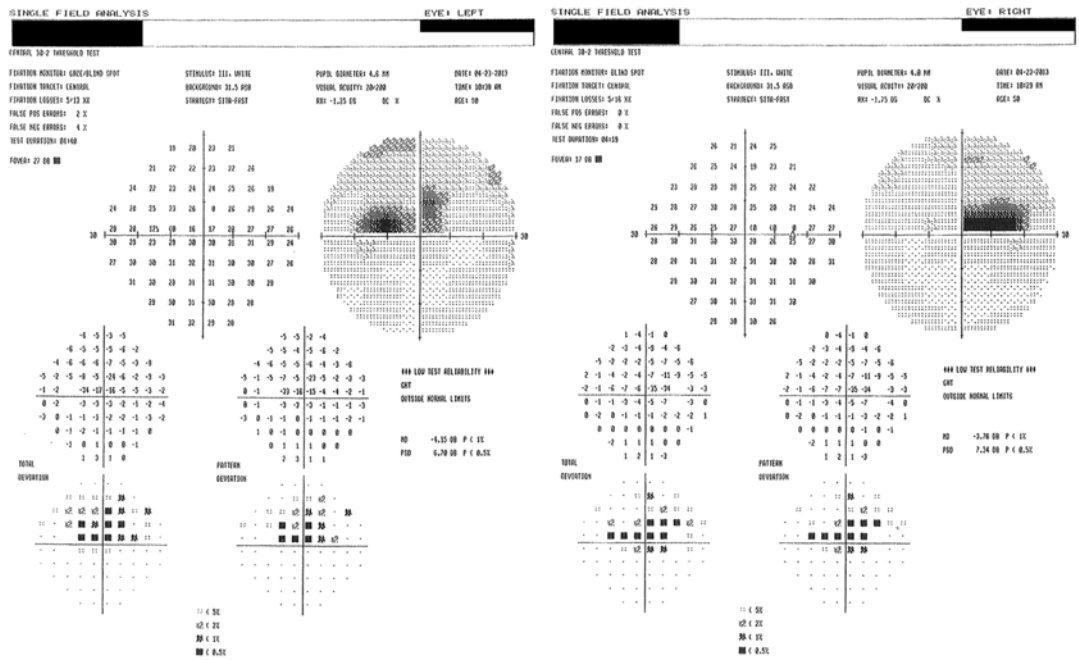

Fig. 7.6 The Humphrey visual field of a DOA patient demonstrating bilateral cecocentral scotoma in both eyes

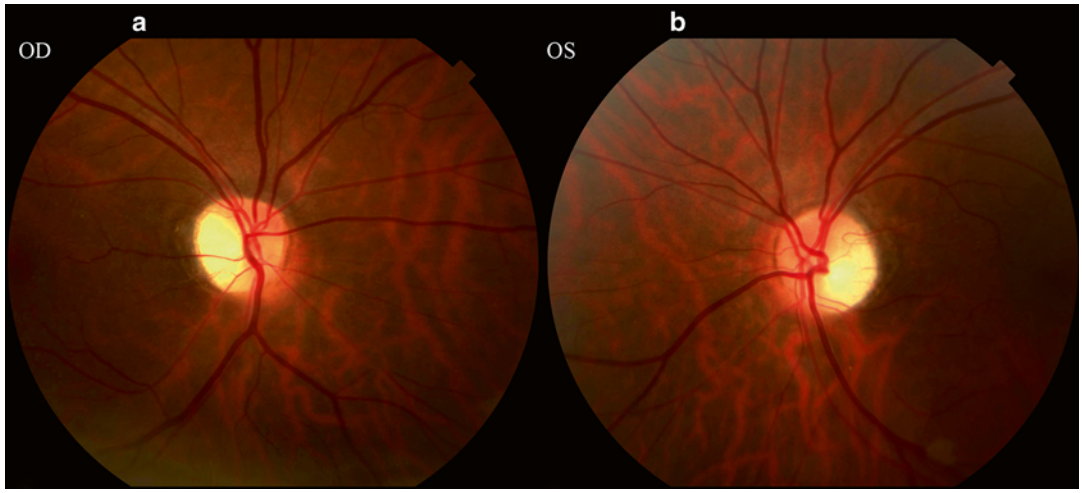

Fig. 7.7 Optic disc photos of a DOA patient demonstrating marked temporal pallor in both right eye (**a**) and left eye (**b**) with excavation (common in DOA) especially in the right eye (**a**)

extent of optic atrophy. Spontaneous recovery does not usually occur and there is currently no treatment for DOA. Unlike LHON, DOA rarely presents rapidly. However, the clinical endpoint of DOA is often indistinguishable from LHON; the bilateral and symmetrical loss of central vision with relative sparing of the peripheral visual field, dyschromatopsia, and a relatively preserved pupillary response are shared by both diseases.

Funduscopic Features

Ophthalmoscopically, the optic disc in DOA is characterized by temporal pallor, frequently accompanied by peripapillary atrophy, excavation of the temporal disc, and pallor or shallow shelving of the temporal neuroretinal rim (Fig. 7.7) [148]. Attenuation of blood vessels, temporal gray crescent, and nonglaucomatous cupping may also be present. OCT has shown significant thinning of the peripapillary nerve fiber layer at the temporal, superior, and inferior quadrants, correlating with the visual acuity (Fig. 7.8) [149]. Despite a remarkably different genetic basis and clinical history, the two genetic optic neuropathies, LHON and DOA, have similar fundus findings in that the temporal pallor of the optic atrophy reflects the selective loss of the PMB.

Optic disc excavation is frequently seen in end-stage DOA, and in normal-tension glaucoma (NTG) [150], and is reported in LHON [83, 151–153]. In a study by Votruba et al., DOA patients with OPA1 mutations show optic disc excavation with enlarged cup-to-disc ratio, frequent peripapillary atrophy, and temporal gray crescent, most of which are features also seen in glaucomatous optic neuropathy [148]. The temporal aspect of the disc characteristically has a triangular wedge-like excavation and is pale without fine superficial capillaries [154]. The smallest fibers of the PMB are located in the temporal optic disc. In another study by Votruba et al. [155], optic atrophy may be subtle involving the temporal aspect of the disc in 55 % of patients, or may involve the entire disc in 44 % of patients. Fournier et al. [156] examined optic disc morphology in patients with DOA to elucidate features that would distinguish DOA from NTG. The DOA patients had a mild to moderate reduction in visual acuity and color vision. Seventy-eight percent had a temporal wedge-shaped area of optic disc excavation. All involved eyes had moderate to severe pallor of the temporal neuroretinal rim, with milder pallor of the remaining noncupped rim. All eyes had a slate-gray crescent within the neuroretinal rim tissue and some degree of peripapillary

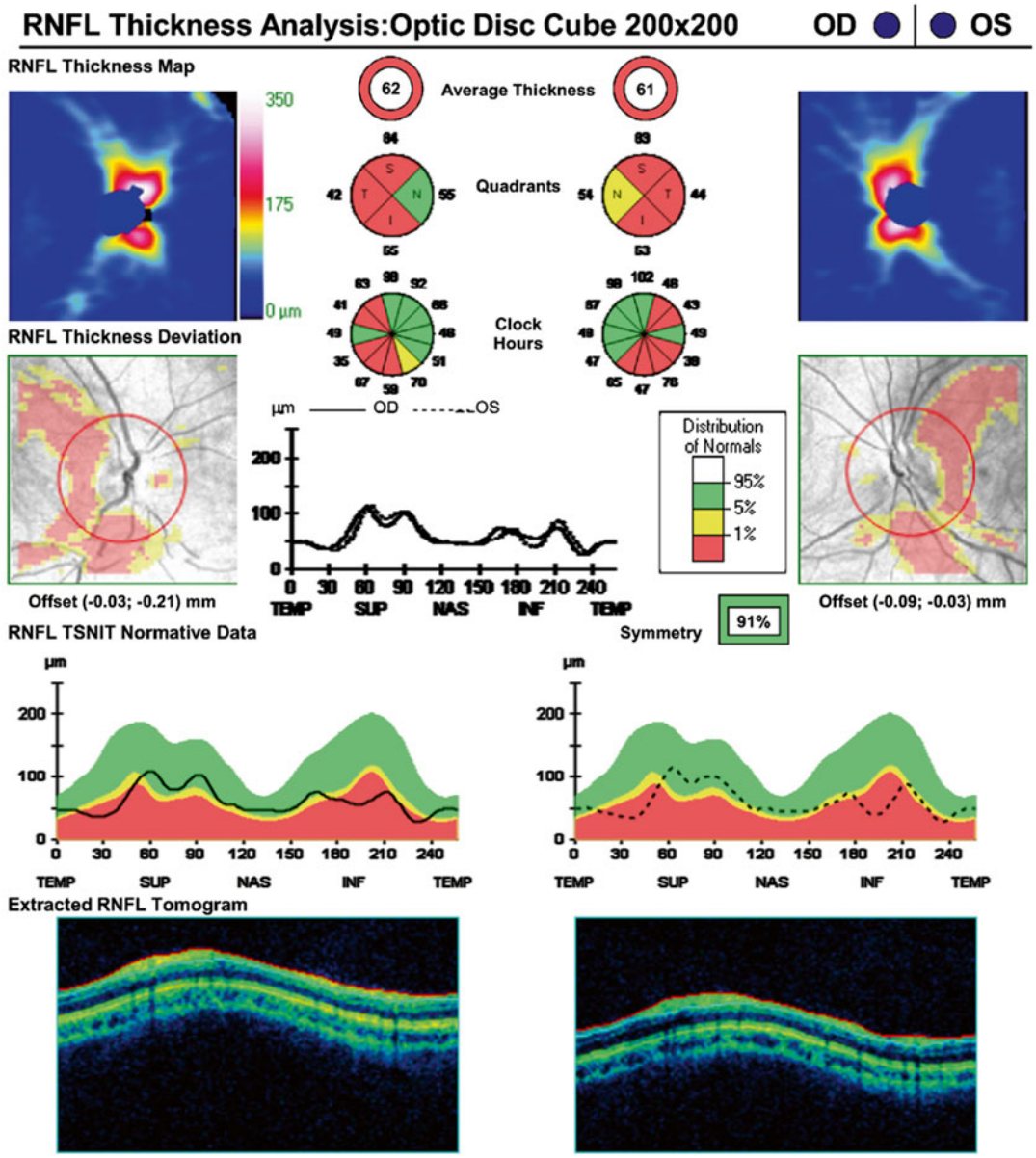

Fig. 7.8 The OCT RNFL analysis of a DOA patient demonstrates marked thinning in RNFL in temporal, superior, and inferior quadrants with the nasal quadrant being less affected

atrophy. Several clinical features, including early age of onset, preferential loss of central vision, sparing of the peripheral fields, pallor of the remaining neuroretinal rim, and a family history of unexplained visual loss or optic atrophy, help distinguish patients with DOA from those with NTG.

Diagnostic Testing

Genetic testing for the OPA1 gene can be performed on whole blood. Humphrey visual field and OCT are extremely helpful testings. Electrophysiological testing shows a normal flash electroretinogram, absent or delayed pattern visually evoked poten-

tials suggestive of a conduction deficit, and N95 waveform reduction on the pattern electroretinogram, consistent with a primary ganglion cell pathology [155].

Histopathology of DOA

The site of pathology in DOA is thought to be the RGCs. The outer retina appears to be structurally normal and RGC loss occurs primarily in the macula and in the PMB of the optic nerve. In one postmortem study by Johnston et al. [157], marked decrease in the number of RGCs in the macular region with a variable degree of degenerative changes was seen. Axons had variable degrees of noninflammatory demyelination. In another postmortem study by Kjer et al. [158], similar findings were reported and demyelination of the optic chiasm, optic tracts, and transsynaptic degeneration in the lateral geniculate body was also observed.

Pathophysiology of DOA

The pathogenic characteristics of OPA1 resemble those of LHON, which results from a defect of the mitochondria. Mutations in the mitochondrial gene presumably lead to insufficient energy supply in the highly energy-demanding neurons of the optic nerve, especially the PMB, and cause blindness by a compromise of axonal transport in RGCs. Alexander et al. [139] hypothesized that mutations in the OPA1 gene affect mitochondrial integrity, resulting in an impairment of energy supply. On phosphorus magnetic resonance spectroscopy [139], defective oxidative phosphorylation has been demonstrated in six OPA1 patients from two unrelated families with a 4-bp deletion in the OPA1 gene. The time constant of postexercise phosphocreatine resynthesis was significantly increased in patients compared to controls, indicating a reduced rate of mitochondrial ATP production in the patients. Similar findings have been observed in patients with LHON.

Payne et al. [159] hypothesized that although OPA1 is a nuclear gene, the fact that the gene product localizes to mitochondria suggests that mitochondrial dysfunction might be the final common pathway for many forms of syndromic and nonsyndromic optic atrophy, hearing loss, and external ophthalmoplegia. With quantitative real-time polymerase chain reaction (PCR) [160], significantly decreased levels of cellular mtDNA in blood from four of eight patients with OPA1 were found (range, 412–648 copies per cell) compared to controls (1,149 ± 407). Three patients had decreased levels (813–1,134), and one patient had normal levels (1,455). The findings were consistent with the hypothesis that OPA1 gene mutations may result in decreased numbers of mitochondrial organelles by apoptosis. However, neither mtDNA content nor genotype correlated with phenotype, indicating that additional epigenetic factors are involved. It was postulated that selective damage to RGCs in OPA1 may result from a combination of high energy requirements of retinal cells in the macular area and increased sensitivity of RGCs to free radicals and oxidative stress.

Molecular Genetics and the Genetic Heterogeneity of DOA

DOA is an inherited mitochondrial disease but the genetic mutation affects autosomal DNA, not mtDNA as does LHON. About 60 % of DOA cases are now linked to mutations in the OPA1 gene (chromosome 3q28-q29) [141, 161]. Four other loci have been reported, including OPA3 (chromosome 19q13.2-q13.3) [161], OPA4 (chromosome 18q12.2-q12.3) [162], OPA5 (chromosome 22q12.1-q13.1) [163], and OPA8 (chromosome 16q21-q22) [164].

OPA1 protein comprises a highly basic amino-terminal that has a MTS, a dynamin-GTPase domain, and C-terminus of unknown function. OPA1 is a dynamin-related protein that may be a major organizer of the mitochondrial inner membrane, contributing to cristae maintenance, mitochondrial structure, and cytochrome c sequestration [161].

There is a wide spectrum of mutations and more than 100 have been reported, including missense,

nonsense, deletion/insertion, and splicing mutations [165–167]. Mutations are located throughout the gene, but three clusters most commonly occur at the leader sequence for mitochondrial import, the GTPase domain, and the –COOH terminus [166]. Because most mutations result in a truncated protein, these mutations probably represent null alleles, and dominant inheritance of the disease may result from haploinsufficiency of OPA1. Further evidence for haploinsufficiency as the predominant mechanism of the disease has been provided by the identification of a 560- to 860-kb microdeletion on chromosome 3q28 that results in the complete loss of one copy of the OPA1 gene [168]. Missense mutations are less common, are clustered in the GTPase domain, and probably lead to a loss of function of the protein and to haplotype insufficiency. A cluster of truncation mutations affect the C-terminus, and a dominant-negative effect has been hypothesized in these cases [165]. Asymptomatic carriers of OPA1 mutations have been identified within families, leading to the recalculation of a consistently lower penetrance [167]. A frameshift mutation, the 2708del (TTAG), appears to be the most frequent in Caucasian patients [165, 166].

OPA1 mutations inducing haploinsufficiency also impair ATP synthesis to cause a coupling defect in mitochondrial respiration in both DOA and LHON [169]. A subset of OPA1 missense mutations, affecting mostly the GTPase domain of OPA1, have been shown to be linked to multisystemic mitochondrial encephalopathy, early onset optic atrophy and deafness, and later mitochondrial myopathy with progressive external ophthalmoplegia, cerebellar involvement, white matter abnormalities, peripheral neuropathy, and spastic paraplegia [170–172]. Other neurological abnormalities have occasionally been associated with DOA. An R445H mutation in the OPA1 gene results in optic atrophy, sensorineural hearing loss, ptosis, and ophthalmoplegia [159].

There is wide variability in both penetrance and clinical severity, from family to family with the same mutation and from mutation to mutation. Unknown genetic or epigenetic and environmental factors may play a role in the phenotypic expression of DOA [173].

Other Autosomal Dominant Optic Atrophy and Sensorineural Hearing Loss Syndromes

Other syndromes involving autosomal DOA and sensorineural hearing loss without any other systemic or neurologic abnormalities have been shown to have OPA1 mutations, similar to DOA. New loci in the WFS1 (Wolfram) gene have been identified to cause mitochondrial dysfunction [170]. A missense mutation was found in the WFS1 gene on chromosome 4 (4p16.1) to cause DOA and deafness without diabetes insipidus and diabetes mellitus [174]. Another DOA pedigree with hearing loss and impaired glucose regulation was found to have another missense mutation in the WFS1 (Wolfram) gene without any mutations in the OPA1, OPA3, OPA4, or OPA5 genes [175]. The OPA8 gene on chromosome 16 (16q21-q22) was found in a pedigree with optic neuropathy that was indistinguishable from that in OPA1-DOA and associated with late-onset sensorineural hearing loss, increased central conduction times in somatosensory evoked potentials, and cardiac abnormalities [164]. Other "DOA Plus" syndromes with OPA1 mutations have been characterized to have other neurological manifestations that can affect up to 20 % of all mutational carriers. These include ataxia, myopathy, peripheral neuropathy, progressive external ophthalmoplegia from the third decade onwards. Other features mimicked hereditary spastic paraplegia (HSP) and a MS-like illness [170].

Treatment of DOA

There is currently no effective treatment to reverse or prevent visual loss from DOA, but genetic testing for OPA1 gene and genetic counseling can help in family planning. A variety of low-vision devices are also available to patients [176].

Gene Therapy

Animal models carrying mutant OPA1 gene have been generated to study the RGC loss in DOA

[177]. These mouse models are characterized by about 50 % reduction of OPA1 expression with demyelination, axonal degeneration, and ultrastructural abnormalities of mitochondria [178, 179]. While it is embryonically lethal to be homozygous, heterozygous animals produce mild age-dependent ocular phenotype with evidence of RGC dysfunction. Interestingly, both models showed mild neuromuscular signs and symptoms such as decreased locomotor activity and abnormal clutching reflex and tremor as seen in human patients with DOA "plus" syndrome [170].

ROS production was increased in the Drosophila model of OPA1, and superoxide dismutase 1, vitamin E, and genetically overexpression of human superoxide dismutase 1 was able to reverse the phenotype of mutant model, suggesting that ROS plays an important role in the pathophysiology [180].

The dendritic distribution of mitochondria has been shown to be essential for enhancing the number and plasticity of synapses [181], supporting the crucial role of OPA1 and mitochondrial fusion in maintaining dendrites and their synapses. Recently, OPA1 animal models showed that the earliest pathological changes in RGCs does indeed occur in the dendritic pruning [182, 183]. These studies have shed light on the sequence of pathologic events taking place in DOA.

Gene therapy has been shown to be feasible for mitochondrial diseases due to nuclear gene defects. A reliable genetic model for isolated complex I defect, known as the Harlequin mouse, is characterized by progressive degeneration of cerebellar and retinal neurons [184]. This model is produced by the loss of function of apoptosis-inducing factor (AIF) which expresses a clinical phenotype resembling the human complex I deficiency, including RGC loss and optic atrophy. Bouaita et al. delivered the AIF1 gene contained in an AAV2 vector intravitreally and found protection of RCGs and optic nerve integrity, preservation of complex I function in optic nerves, and prevention of glial and microglial responses [185]. This study serves as the first proof of feasibility of gene therapy targeted at rescuing RGCs, providing a platform for future studies in optic nerve disorders due to nuclear genetic defects such as DOA.

Optic Neuropathy in Mitochondrial Diseases: Syndromic

LHON and DOA are the two most common hereditary MONs with monosymptomatic expression. However, there are many multisystemic mitochondrial disorders that also result in optic neuropathy. Some of these disorders are caused by mtDNA mutations whereas others are due to nuclear gene mutation encoding mitochondrial proteins.

Mitochondrial DNA-Based Disorders

LHON/Dystonia/Myoclonic Epilepsy, Ragged-Red-Fibers (MERRF)/ Mitochondrial Encephalomyopathy, Lactic Acidosis, and Stroke-Like Episodes (MELAS)/Leigh Overlapping Syndrome

Optic atrophy can be found in MERRF, MELAS, and Leigh syndrome. MERRF and MELAS are usually due to mtDNA point mutation affecting tRNAs whereas Leigh syndrome may be caused by both nuclear and mtDNA mutations, most often affecting the complex I subunit gene [186]. The 14459/ND6 mutation is the first mutation that showed an overlapping clinical expression ranging from LHON to dystonia and Leigh syndrome [187, 188]. The 13513/ND5 mutation was later found associated with MELAS and LHON-like severe optic neuropathy [189, 190]. The LHON-like optic neuropathy may be a spectrum of diseases with different degrees of CNS involvement. The common pathogenic mechanism may be related to mitochondrial angiopathy [51]. Vascular changes are well-known features in LHON. Similarly, mitochondrial angiopathy has been described in MELAS and Leigh syndrome patients [191, 192].

Wolfram Syndrome/Diabetes Insipidus, Diabetes Mellitus, Optic Atrophy, and Hearing Loss (DIDMOAD)

Wolfram's syndrome, an autosomal recessive disorder, is also known as DIDMOAD, or diabetes insipidus, diabetes mellitus, optic atrophy, and deafness from sensorineural hearing loss. The gene for this disorder is located on chromosome 4 (4p16.1). Because of wide phenotypic variations in DIDMOAD, some patients have ataxia, hypogonadism, and psychiatric illness. The exact prevalence of this syndrome is unknown [193, 194].

Symptoms and Signs

The order of development of the clinical signs of Wolfram syndrome is variable. In general, however, insulin-dependent diabetes develops first, followed by optic atrophy and diabetes insipidus; deafness occurs later. Progressive optic atrophy is usually diagnosed before 12 years of age. Other clinical signs may appear at various ages before 25 years. Some less common features may include ptosis, anosmia, ataxia, nystagmus, seizures, mental retardation, psychiatric disorders, and hypogonadotropic hypogonadism [195].

Visual acuity may be normal in the early stages, despite mild dyschromatopsia and optic atrophy. Visual loss then progresses to worse than 20/200. The visual field defect is most often concentric and is occasionally associated with a central scotoma. Abnormal pupillary reflexes and horizontal nystagmus have also been reported. The optic disc often has diffuse pallor with mild to moderate cupping. Pigmentary retinopathy and abnormal ERG findings have been reported in 30 % of patients and diabetic retinopathy in 20 %. The VEPs to flash and checkerboard stimuli reveal reduced amplitudes [195].

Diabetes insipidus and sensorineural hearing loss affecting high frequencies often begin in the first or second decade of life. Approximately 75 % of those affected develop diabetes insipidus and about 60 % develop sensorineural hearing loss. Neurogenic bladder dysfunction develops early in the third decade and multiple neurological abnormalities early in the fourth decade. About 60 % have neurological complications, such as gait ataxia, seizures, startle myoclonus, depression, mental retardation, central apnea, anosmia, megaloblastic and sideroblastic anemia, ptosis, Adie's pupil, ophthalmoplegia, convergence insufficiency, vertical gaze palsy, and nystagmus [196].

Diagnostic Testing

The diagnosis of Wolfram syndrome requires the presence of optic atrophy and juvenile-onset diabetes mellitus that cannot be explained by other causes [196]. The diagnosis of DIDMOAD syndrome should be investigated in children who present with unexplained visual loss or with persistent polyuria and polydipsia despite adequate blood sugar control. A baseline and annual MRI of the brain, hearing test, ultrasound study of the urinary tract, and ophthalmologic examination should be performed.

MRI of the brain reveals diffuse atrophy of the brainstem, middle cerebellar peduncle, and cerebellum. The hypointense signal in the posterior pituitary represents degeneration of the supraoptic and paraventricular nuclei of the hypothalamus [197].

The differential diagnosis of optic atrophy and diabetes mellitus includes Friedreich's ataxia, Alstrom syndrome, infantile Refsum disease, and Bardet–Biedl syndrome [196]. DIDMOAD should be distinguished from other syndromes involving optic atrophy and hearing loss, such as Sylvestor syndrome [198], Jensen syndrome [199], and another syndrome involving optic atrophy, hearing loss, and peripheral neuropathy [200].

Molecular Genetics and Genetic Heterogeneity of DIDMOAD

Wolfram syndrome is an autosomal recessive disorder linked to a gene located at 4p16.1 [201]. The gene responsible for Wolfram syndrome, at locus

WFS1, encodes for gene product, wolframin, an endoplasmic reticulum protein which plays a role in the regulation of intracellular calcium [202]. Mutations of WFS1 may include nonsense mutations, missense mutations, in-frame deletions, in-frame insertions, and frameshift mutations [201]. Hardy et al. [195] performed direct DNA sequencing to screen the entire coding region of the WFS1 gene in 30 patients from 19 British kindreds with Wolfram syndrome. DNA was also screened for structural rearrangements (deletions and duplications) and point mutations in mtDNA. No pathogenic mtDNA mutations were found in this cohort. The authors identified 24 mutations in the WFS1 gene: eight nonsense mutations, eight missense mutations, three in-frame deletions, one in-frame insertion, and four frameshift mutations. Of these, 23 were novel mutations, and most occurred in exon 8. Most patients were compound heterozygotes for two mutations, and there was no common founder mutation. No clear-cut correlations between any of the observed mutations and disease severity were found. There were no obvious mutation hotspots or clusters.

The clinical manifestations of Wolfram syndrome have some similarities with mitochondrial disease, such as those with chronic progressive ophthalmoplegia. Some patients with Wolfram syndrome also have the 11778 mtDNA mutation associated with LHON, a condition which is believed to represent the random overlap of the two disorders. Clinical manifestations from both autosomal mutations on chromosome 4p (Wolfram's syndrome) and multiple deletions in mtDNA have been observed in two studies [201, 203]. In the first study, by Rotig et al. [203], a female infant presented with insulin-dependent diabetes mellitus and then gradually had optic atrophy and sensorineural deafness, consistent with the diagnosis of Wolfram's syndrome. Her multi-organ involvement and development of mild elevated lactate represented a deficiency of the respiratory chain and a 7.6-kb heteroplasmic deletion of the mtDNA. In the second study, by Barrientos et al. [201], four sisters whose parents were first cousins presented with insulin-dependent diabetes mellitus and dyschromatopsia followed by severe optic atrophy in their thirties. These patients initially were thought to have had Wolfram's syndrome until they later developed psychiatric abnormalities, sphincter disturbances, anosmia, walking instability, tremor, dysphagia, and swallowing difficulties. Genetic testing in the sisters showed that both nuclear and mitochondrial genomic abnormalities were present in their recessive disorder.

As Wolfram syndrome has features of mitochondrial dysfunction, idebenone was used in a case report with promising result [110]. More studies are necessary to confirm the efficacy of this therapy.

Nuclear DNA-Based Disorders

Optic Neuropathy in Hereditary Ataxias Friedreich's Ataxia (FA)

FA is the most common of the autosomal recessive spinocerebellar ataxias and accounts for at least half of the hereditary ataxias in most large case series reported [204]. The prevalence of FA is estimated to be between 1 in 22,000 and 2 in 100,000 internationally and slightly higher in Quebec. It affects mostly Caucasians and almost always presents before 20 years of age. Males and females are equally affected [204].

Clinical Features of FA

In a clinical and genetic study of 90 families by Harding [205], the onset of symptoms was before the age of 25 years (mean, 10.52 years) in all the index cases. In early cases of FA, limb and truncal ataxia and absent tendon reflexes in the legs within 5 years of presentation appeared to be the only consistent diagnostic criteria. Dysarthria, signs of pyramidal tract dysfunction in the legs, and loss of joint position and vibration sense were not necessarily present during the first 5 years of symptoms, but appeared to develop eventually in all cases. Most patients are visually asymptomatic, but optic atrophy occurred in 25 % of patients with FA and resulted in occasional blindness [206]. VEPs were abnormal in two-thirds of patients, typically displaying reduced amplitude and delayed latency [205, 207]. Nystagmus was observed in approximately

20 % of patients with FA, but extraocular movements were nearly always abnormal, with abnormal smooth pursuit, dysmetric saccades, square wave jerks, failure of fixation, and suppression of the vestibulo-ocular reflex. Significant sensorineural deafness occurred in 10 % of persons with FA. About 10 % of patients with FA have diabetes mellitus, which appeared to be associated with a higher incidence of optic atrophy and deafness. Cardiac abnormalities were found in more than 75 % of patients. Clinical evidence of ventricular hypertrophy, systolic ejection murmurs, and third or fourth heart sounds were observed [205, 208]. This gradual progressive disorder leads to the inability to walk at about 25 years of age. Ninety-five percent became wheelchair bound by the age of 44 years.

Molecular Genetics of FA

Classic FA is an autosomal recessive disorder caused by a gene mutation at the centromeric region of chromosome 9 (9q13-21.1) at the site of the gene encoding for the 210-amino-acid protein frataxin [209, 210]. This mutation is characterized by an excessive number of repeats of the GAA (guanine adenine adenine) trinucleotide DNA sequence in the first intron of the gene coding for frataxin [209]. It is the only disease known to be the result of a GAA trinucleotide repeat. This expansion alters the expression of the gene, decreasing the synthesis of frataxin protein. The expanded GAA repeat is thought to result in frataxin deficiency by interfering with transcription of the gene by adopting an unstable helical structure [210]. The larger the number of repeats, the more profound is the reduction in frataxin expression. Variability in the clinical presentation of FA may be explained by the extent of this trinucleotide repeat expansion. The age of disease onset, its severity, rate of progression, and extent of neurological involvement vary with the number of repetitive GAA sequences. Larger GAA expansions correlate with earlier age of onset and shorter times to loss of ambulation [210].

Point mutations not only reduce levels of the frataxin protein but are also responsible for the creation of abnormal protein. They also represent another source of variability in the clinical presentation of FA [211]. Seventeen different point mutations have so far been described in FA [211]. Between 1 and 5 % of the point mutations are single base changes in the sequence of the FA gene causing missense, nonsense, or splicing mutations. Patients with missense mutations have either mild or severe symptoms, whereas those with splicing, nonsense, and initiation codon mutations, which are associated with nonfunctional frataxin, have a severe phenotype [211]. Point mutations of the frataxin gene involving the amino-terminal typically present with a more benign course than those of the carboxy-terminal. The three most common point mutations include the Il54F mutation among southern Italians, the ATG to ATT mutation of the start codon, and the G130V mutation. Patients with the G130V mutation tend to have slower disease progression [211].

Pathophysiology of FA

Cells and tissues of the body are differentially sensitive to frataxin deficiency. Cells normally requiring and producing greater amounts of frataxin tend to be most affected by FA [212]. For example, sensory neurons in the dorsal root ganglion express the frataxin gene and are affected greatly in FA. Frataxin has been shown to be essential for normal mitochondrial function, both for oxidative phosphorylation and for iron homeostasis [213]. Strong evidence suggests that frataxin deficiency results in iron accumulation within mitochondria of affected cells as shown in cell culture lines. The excessive mitochondrial accumulation of iron affects cytosolic iron levels. Excess intracellular iron stimulates the increased generation of free radicals and mitochondrial damage. Iron excess inactivates mitochondrial enzymes essential for the production of ATP. Cell death, particularly of neurons of the spinal cord and peripheral nervous system (PNS), ensues [212].

On histological cross section through the lower cervical cord, loss of myelinated fibers of the dorsal columns, corticospinal tracts, and some of the

spinocerebellar tract may be seen. The affected tracts have compact fibrillary gliosis but no breakdown products or macrophages because of the very slow rate of fiber degeneration. The dorsal spinal root ganglia show shrinkage and eventual disappearance of neurons associated with proliferation of capsular cells. The posterior roots are nearly devoid of large myelinated fibers. Neuronal degeneration is seen in Clarke's column within the thoracic spinal cord, brainstem (cranial nerve nuclei VIII, X, and XII), and cerebellum (dentate nucleus and the Purkinje cells of the superior vermis) [212].

Diagnosis of FA

The diagnosis of FA is a clinical one. A specific trinucleotide repeat expansion assay is available commercially in the United States and should be performed in all suspected cases of FA [204]. The CSF abnormality is usually normal in patients with FA. MRI of the brain and spinal cord in patients with FA often reveals atrophy of the cervical spinal cord with minimal evidence of cerebellar atrophy [204]. On echocardiogram hypertrophic cardiomyopathy is present in approximately 40 % of patients. The severity of left ventricular hypertrophy is related to the number of GAA repeats. The electrocardiogram is abnormal in approximately two-thirds of patients, with widespread T-wave inversion [205]. Unlike in Charcot–Marie–Tooth (CMT) syndrome, the motor nerve conduction velocities are normal, while the sensory ones are normal or mildly reduced, especially in the lower extremities. VEPs are abnormal in two-thirds of patients with FA. Absent or delayed latency and reduced amplitude of the P100 wave are seen [207]. Brainstem auditory evoked responses are typically abnormal in FA, displaying absent waves III and IV with preservation of wave I. Somatosensory evoked potentials reveal delayed, dispersed potentials at the sensory cortex, as well as abnormal central motor conduction [204].

Management of FA

No effective therapy to delay the progression of FA is yet available. Free radical scavengers and antioxidants (e.g., coenzyme Q, acetylcysteine, vitamin E) currently are being considered for treatment trials. Iron chelation therapy may also be a possibility [213].

Optic Neuropathy in Hereditary Ataxias

Spinocerebellar Ataxia Type 1 (SCA-1)

Spinocerebellar ataxia type 1 (SCA-1) is an autosomal dominant disorder caused by a gene mutation that is an expanded CAG repeat on chromosome 6p22-p23. The triplet nucleotides are expanded from 42 to 82 repeats compared to the normal 19 to 36 CAG repeats [232]. This mutation involves a gain of function resulting in a protein, ataxin-1. Age of onset and severity of the disease depend upon the length of the CAG expansion. A longer expansion of the trinucleotide repeat is correlated with an earlier onset and more severe presentation of the disease. Anticipation, or amplification of the CAG repeats with each successive generation, also occurs [232].

The onset of clinical symptoms and signs is usually at 40 years of age. Gait and extremity ataxia, dysarthria, and bulbar dysfunction are followed by loss of vibration sense and proprioception. Pyramidal tract signs, optic atrophy, and dysphagia are more frequent in SCA-1 than in SCA-2 and SCA-3 patients [233]. In contrast to SCA-2, in which optic atrophy is secondary to retinal degeneration, up to 30 % of patients with SCA-1 have primary optic atrophy. The severity of this optic atrophy varies among patients, and visual acuity is not severely impaired [233]. Oculomotor disorders are also seen in most patients, including impaired smooth pursuit and optokinetic nystagmus, gaze-evoked nystagmus, supranuclear ophthalmoplegia, and lid retraction [234]. Facial palsy, bulbar symptoms, and extrapyramidal features, such as dystonia and chorea, develop later in the disease [233].

The exact pathophysiological mechanisms underlying SCA-1 are not yet entirely understood. On histopathology, degeneration of

Purkinje cells; dentate nucleus; inferior olive; red nucleus; and cranial nerve nuclei III, X, and XII are often seen. Occasionally, the substantia nigra, putamen, pallidum, and subthalamic nucleus are also affected [235, 236].

MRI of the brain reveals mild olivopontocerebellar atrophy (OPCA), less severe than that in SCA-2 and OPCA patients [236]. Definitive diagnosis of SCA-1 is based upon demonstration of an expanded CAG repeat on chromosome 6p22-p23 [233].

Low vision, occupational, speech, and physical therapy can be offered to improve or maintain patients' functional capacities and help them adapt to their limitations [233].

Deafness, Dystonia, and Optic Neuropathy (DDON or Mohr–Tranebjaerg Syndrome)

DDON syndrome is an X-linked disorder that presents by 20 years of age with sensorineural hearing loss, dystonia, and ataxia in late childhood, followed by optic atrophy. Cognitive and psychiatric abnormalities are usually present by 50 years of age. Most patients are legally blind by 40 years old. Mutations in the TIMM8A gene on chromosome X (Xq22) produce a gene product that localizes to the mitochondrial intermembrane space [170].

Hereditary Spastic Paraplegia

The hallmark of HSP is a slowly progressive lower extremity weakness and spasticity. The age of onset is variable and is classified as pure, if spasticity is the only feature, or as complicated if other features, such as optic atrophy, ataxia, peripheral neuropathy, extrapyramidal defects, and dementia are present [214]. One of the key mitochondrial proteases is paraplegin, which is encoded by SPG7 (chromosome 16q24.3). Mutations in SPG7 have been identified in an autosomal recessive form of HSP, and in some patients with bilateral optic neuropathy this is a prominent feature [215].

Disorders Related to Fission/Fusion Genes

Neurodegenerative diseases associated with mitochondrial fission/fusion defect include syndromic forms of DOA in combination with chronic progressive external ophthalmoplegia (CPEO) with specific missense mutations in the GTPase domain of the OPA1 gene (DOA plus syndrome) [171, 172], Charcot–Marie–Tooth disease type 2A (CMT2A) with optic atrophy or HMSN VI associated with mutations in the MFN2 gene encoding mitofusin 2 (MFN 2) [216, 217], and infantile encephalopathy in association with mutant dynamin-like protein 1 (DLP1) gene [218].

CPEO is the most frequent manifestation of mitochondrial myopathy which can be associated with either mtDNA single deletions and point mutations or with nuclear gene mutations resulting in mtDNA multiple deletions [186]. The OPA1/R445H mutation was found associated with mitochondrial myopathy and mtDNA multiple deletions, suggesting molecular overlapping of CPEO and DOA [171, 172]. The CPEO/DOA plus phenotype is characterized by severe sensorineural deafness, cerebellar ataxia, axonal sensorymotor polyneuropathy, severe early-onset optic atrophy, and late CPEO/mitochondrial myopathy.

A number of cases of CMT2A with optic atrophy fulfilling the diagnostic criteria for HMSN VI were found to be due to mutations in the MFN2 gene. The optic neuropathy is similar to the LHON 14484/ND6 mutation which has higher likelihood than the other LHON mutations for spontaneous recovery [217]. The HMSN VI/CMT2A patients usually present with subacute visual loss, central scotomas, dyschromatopsia, and pale optic discs followed by variable degrees of recovery over time. Unlike LHON, late onset is a favorable predictive factor whereas early childhood onset tends to lead to slowly progressive course without visual recovery as in DOA. Hence, LHON, DOA, and HMSNVI/CMT2A with optic neuropathy likely represent a continuum along the spectrum of optic nerve disorders.

Hereditary motor and sensory neuropathy type VI (HMSN6) is an autosomal dominant

subtype of CMT that involves optic atrophy. It is caused by MFN2 mutations (chromosome 1p36.2) [216]. The MFN2 mutation is a mitochondrial outer membrane protein with dynamin GTPase domains that overlap structurally and functionally with OPA1 involved in DOA and with the mitochondrial encoded oxidative phosphorylation proteins seen in LHON [217].

Affected patients present with visual loss starting at 7–10 years of age. As patients with HMSN6 develop optic atrophy, decreased visual acuity occurs in the twentieth decade and worsens to light perception by age 30. An axonal sensorimotor polyneuropathy that may be associated with peroneal muscular atrophy also develops in early childhood, causing gait difficulties [219].

Phenotypic variability occurs in the neurological and ophthalmologic features of HMSN type VI. In a study by Voo et al. [220], 58 members of a family were affected by autosomal dominant HMSN VI. Twelve had both peripheral neuropathy and optic atrophy; three others had either peripheral neuropathy or optic atrophy. Although there was clinical variability, most had childhood onset of progressive visual loss associated with optic atrophy, abnormal gait, distal sensory impairment, and hyporeflexia. Other variable features included hearing loss, tinnitus, cogwheel ocular pursuit, and anosmia. Incomplete penetrance was observed. In another report by Zuchner et al. [217], ten affected patients from six unrelated families had inherited HMSN VI as an autosomal dominant disorder. All had an early onset of a severe axonal peripheral neuropathy starting at about 2 years of age. Optic atrophy began later at about 19 years of age. Most experienced subacute loss of visual acuity with dyschromatopsia, central scotoma, and pale optic discs. Sixty percent of the patients experienced significant recovery of their visual acuity after several years. The mechanism involved in this visual recovery is not yet fully understood.

DLP1-related encephalopathy is characterized by severe infantile encephalopathy with optic atrophy and hypoplasia, dysmyelination and abnormal gyral patterns of cerebral cortex, and severe respiratory dysfunction with lactic acidosis. Cell studies identified a heterozygous dominant-negative mutation in the DLP1, a protein involved in mitochondrial fission, as the genetic defect in the disease [218].

Behr and Costeff Syndromes

Behr's syndrome is a rare disorder with an autosomal recessive pattern of inheritance, presenting in children. Optic atrophy usually occurs in the first 8 years of life. Visual loss becomes moderate to severe, and sensory nystagmus develops. Other systemic abnormalities also develop, including ataxia, hypertonia, pyramidal and extrapyramidal dysfunction, spastic paresis, pes cavus, mental retardation, and urinary incontinence. In most cases, abnormalities do not progress after childhood. MRI of the brain may show cerebellar atrophy [221]. Histopathological examination may show central atrophy of the optic nerves and total disarray of the normal laminar pattern of the lateral geniculate nucleus, neuronal loss, and gliosis. Numerous axonal spheroids can also be seen [221, 222].

Behr syndrome may present similarly to other types of hereditary ataxias associated with optic atrophy. The differential diagnosis includes NARP (nyctalopia, ataxia, retinitis pigmentosa) syndrome [223], Marinesco–Sjogren syndrome (autosomal recessive disorder of cataracts, cerebellar ataxia, and mental retardation) [224], CAMOS (cerebellar ataxia, mental retardation, optic atrophy, and skin abnormalities) syndrome (15q24-q26) [225], CAPOS (cerebellar ataxia, arreflexia, pes cavus, optic atrophy, and sensorineural hearing loss) syndrome [226], and other spinocerebellar degenerations. Therefore, the diagnosis of Behr syndrome is one of exclusion [227].

Considerable overlap exists between Behr syndrome and Costeff syndrome. Some patients fulfilled the diagnostic criteria for Behr syndrome and had elevated urinary 3-methylglutaconic acid [228]. Costeff syndrome, or Type III 3-methylglutaconic aciduria (MGA), is a rare syndrome reported in persons of Iraqi-Jewish ancestry. The gene for type III MGA has been mapped to the long arm of chromosome 19 at 19q13.2-q13.3 or OPA3. OPA3 consists of two

exons and encodes a peptide of 179 amino acid residues, which localizes to the mitochondrial inner membrane [229]. Homozygous mutations lacking the OPA 3 gene product occur in Costeff syndrome, while missense mutations in one copy of the OPA3 gene cause autosomal DOA with cataract [230].

Costeff et al. [231] described 19 patients with a familial syndrome consisting of infantile optic atrophy and an early-onset extrapyramidal movement disorder dominated by chorea. About half the patients developed spastic paraparesis at 20 years of age. Mild cognitive impairment and ataxia were common. Urinary excretion of 3-methylglutaconic acid and 3-methylglutaric acid were elevated. Nine of the ten families, including all those with multiple affected siblings, belonged to the Iraqi-Jewish community in Israel, a group with an estimated minimal prevalence rate of 1 in 10,000. The disorder had some similarities to Behr's syndrome, but the neurological aspects were distinctive. In general, patients with Costeff syndrome have more extrapyramidal abnormalities without ataxia, whereas those with Behr syndrome have more ataxia without extrapyramidal problems [230].

Optic Neuropathy in Hereditary Polyneuropathies

X-linked Charcot–Marie–Tooth (CMTX5) Disease or Rosenberg–Chutorian Syndrome

The X-linked form of hereditary optic atrophy with progressive deafness and polyneuropathy is represented by X-linked Charcot–Marie–Tooth disease. The locus of this gene is CMTX5 on chromosome Xq21.32-q24 [237]. Few case reports describe the phenotype of this disorder. In a report by Rosenberg and Chutorian [238], two brothers developed early-onset hearing loss, lower extremity weakness and atrophy during childhood, and progressive optic atrophy at about 20 years of age. The older brother had pes cavus, and both brothers required a cane for walking by 15 years of age. As adults, both had severe distal weakness and atrophy in all extremities, with broad-based gait and atrophy of the intrinsic hand muscles. They had a sensorimotor peripheral neuropathy. A 3-year-old nephew showed a similar phenotype. Later evidence suggested that the mother, grandmother, and great-grandmother of the affected nephew also had slowly progressive hearing loss, suggesting X-linked semi-dominant inheritance. In a another report by Kim et al. [239], a Korean family had six males who had early-onset hearing loss, decreased visual acuity, and motor impairment in an X-linked recessive pattern of inheritance. Bilateral profound sensorineural hearing loss was present at an early age. They had progressive lower extremity weakness by 10–12 years of age. All developed bilateral progressive visual failure starting at 8–13 years of age. The proband had bilateral optic disc pallor and abnormal VEPs consistent with an optic neuropathy. Obligate female carriers were unaffected. The phenotype of the affected males in this family resembled that described in the previous study by Rosenberg and Chutorian [238].

Hereditary Optic Atrophy with Progressive Deafness and Polyneuropathy

Hereditary optic atrophy with progressive deafness and polyneuropathy may be inherited as an autosomal dominant, autosomal recessive, or X-linked form. Hagemoser et al. [200] reported two unrelated families with a disorder characterized by optic atrophy, hearing loss, and peripheral neuropathy. In the first family, 13 affected members spanning four generations had male-to-male transmission of the disorder. Most patients developed bilateral hearing loss and visual loss with optic atrophy by 5–6 years of age. Neurological features were only seen in a subset of patients as adults, and consisted mainly of decreased vibratory sensation and lower extremity hyporeflexia. Nerve conduction velocities suggested an axonal sensory and motor neuropathy. The second family had three affected members over three generations. Optic atrophy was seen by 10 years of age. The proband had

visual loss by 5 years of age and hearing loss by 13 years. Sensory ataxia developed during adulthood. Therefore, it was concluded that this disorder showed autosomal dominant inheritance with initial presentation of optic atrophy followed by deafness and ataxia.

Hereditary optic atrophy with progressive deafness and polyneuropathy may also be inherited in an autosomal recessive form. In a report by Iwashita et al. [237], a Korean brother and sister developed optic atrophy, hearing loss, and distal neurogenic atrophy. The older brother, who was more severely affected, showed bilateral ulnar deviation and flexed fingers at 8 years of age. At 13, he developed progressive optic atrophy and hearing loss. At 25, his lower extremities had severe atrophy and sensory loss in all modalities. He had an ataxic, broad-based gait. Nerve conduction velocities were normal, and sural nerve biopsy showed slight demyelination. The sister had distal weakness and atrophy of the upper limbs with the same hand deformity as her brother, but no weakness or atrophy of the lower limbs. She had mild optic atrophy and hearing loss. She had no sensory impairment.

Hereditary Sensory and Autonomic Neuropathy Type III (HSAN3) or Familial Dysautonomia (Riley–Day Syndrome)

Hereditary sensory and autonomic neuropathy type III, or familial dysautonomia (FD), can be caused by mutations in the IKBKAP gene on chromosome 9q31-q33 [240]. This is an autosomal recessive disorder occurring almost exclusively in persons of Ashkenazi Jewish descent [241]. Neuropathological findings reveal that the mean volumes of the superior cervical sympathetic ganglion and the preganglionic neurons in the first three thoracic cord segments are characteristically reduced by about 30–50 % [242].

The criteria for the diagnosis of HSAN3 require the following five signs: (1) lack of axon flare after intradermal injection of histamine, (2) absence of fungiform papillae on the tongue, (3) miosis of the pupil after conjunctival instillation of methacholine chloride (2.5 %), (4) absent deep tendon reflexes, and (5) diminished tear flow 186. However, consistent neuropathological findings in sural nerve biopsies may be the best diagnostic criterion to differentiate familial dysautonomia from other forms of congenital sensory neuropathy [243].

Only a few case reports illustrate the neuro-ophthalmic features associated with this disorder. In a report by Rizzo et al. [244], patients with HSAN3 presented with optic atrophy after 10 years of age. Although optic atrophy appears to be an uncommon finding, the increasing life span of patients with HSAN3 could increase the probability of identifying optic atrophy in the future. Groom et al. described a patient with familial dysautonomia who presented with an optic neuropathy and chiasmal visual field defects [245]. Schnitzler et al. described a 21-year-old woman who presented with a slowly progressive tetraparesis, bilateral optic atrophy, and dysautonomia since early childhood [246]. Although the autonomic, motor, and visual symptoms and signs resembled familial dysautonomia, some hallmarks of familial dysautonomia were absent, such as absence of fungiform papillae of the tongue, abnormal reaction on intradermal histamine injection, and absent tendon reflexes. It was suggested that the progressive bilateral optic atrophy, tetraparesis, and dysautonomia could all be a variant of familial dysautonomia.

Other ophthalmological findings include severe corneal hypesthesia and absent tears which lead to corneal ulcerations; retinal vascular tortuosity, ptosis, anisocoria, exotropia, and tendency for myopia.

Optic Neuropathies in Neurodegenerative Disorders of Childhood

Although neurodegenerative disorders are commonly classified as gray or white matter disorders, most will eventually involve both gray and white matter to some degree. Disorders affecting pre-

dominantly the white matter involve corticospinal tract dysfunction, peripheral neuropathies, and optic atrophy. Those affecting mostly the gray matter cause seizures, movements disorders, and dementia. Neurodegenerative disorders commonly associated with optic atrophy include the mucopolysaccharidoses (MPS), Pelizaeus–Merzbacher disease, Canavan disease, X-linked adrenoleukodystrophy, Alexander disease, Leigh disease, metachromatic leukodystrophy, Krabbe disease, neuronal ceroid lipofuscinosis, MELAS, and spinocerebellar degenerations [247].

Mucopolysaccharidoses with Optic Neuropathy

MPS is an abnormal storage disease caused by a deficiency of the lysosomal enzymes that catalyze the degradation of glycosaminoglycans. Mucopolysaccharides are stored in the cornea, connective tissue, bone, cartilage, and reticuloendothelial system.

(Hurler-Scheie), MPS IIA and IIB (Hunter), MPS IIIA and IIIB (Sanfilippo), MPS IV (Morquio), and MPS VI (Maroteaux-Lamy) are all autosomal recessive diseases, except for type II, which is X linked [248].

In the various phenotypes of the MPS, meningeal deposition may lead to decreased CSF absorption and increased intracranial pressure causing eventual secondary (papilledema-associated) optic atrophy. Local compression of the optic nerve can be caused by meningeal or scleral mucopolysaccharide deposition. Accumulation of mucopolysaccharides within glial cells of the optic nerve has also been observed [249]. Corneal clouding and retinal degeneration commonly occur in MPS I. Other systemic features involve the brain, visceral organs, connective tissue, and bone. For example, abdominal hernia, dysostosis multiplex, stiff joints, visceromegaly, and mental retardation can be observed in the Hurler (MPS IH) phenotype [248].

Definitive diagnosis is established by alpha-l-iduronidase enzyme assay using artificial substrates (fluorogenic or chromogenic) in cultured fibroblasts or isolated leukocytes [250].

Allogeneic bone marrow transplantation (BMT) before the age of 2 years prevents disease progression in Hurler syndrome and prolongs life. Because allogeneic BMT is not available to all patients, gene therapy may offer effective treatment for patients with Hurler syndrome without a matched sibling donor. In a study by Fairbairn et al. [251], a retro-viral vector carrying the full-length cDNA for alpha-L-iduronidase was used to transduce bone marrow from patients with this disorder. The gene was then transferred into primitive CD34+ cells and subsequently expressed the enzyme in their maturing progeny. The efficiency of gene transfer, as assessed by PCR analysis of hematopoietic colonies, was about 25–56 %. The enzyme was then secreted into the medium, and functional localization was demonstrated by reversal of the phenotypic effects of lysosomal storage in macrophages.

Progressive Encephalopathy with Edema, Hypsarrhythmia, and Optic Atrophy (PEHO Syndrome)

This autosomal dominant disorder is a progressive encephalopathy presenting in the first 6 months of infancy, followed by severe hypotonia, seizures with hypsarrhythmia, profound mental retardation, microcephaly, hyperreflexia, extremity edema, and facial anomalies. Optic atrophy and nystagmus often develops by 10–20 years of age. In a report by Salonen et al. [247], 14 patients, from 11 families, who had this syndrome had no identifiable metabolic defect that could explain the clinical features. Neuropathological findings for eight of these patients revealed diffuse cerebral and particularly cerebellar atrophy. Cerebellar hypoplasia was considered a cardinal diagnostic feature of PEHO syndrome [252]. Neuronal loss was severe in the inner granular layer of the cerebellum. The Purkinje cells were relatively preserved in number but were small and deformed.

Infantile Neuroaxonal Dystrophy

Infantile neuroaxonal dystrophy is an autosomal recessive disorder that results from a mutation in the PLA2G6 gene located on chromosome 22q12.3-q13.2 [253].

This disorder is caused by the formation of neuroaxonal spheroids in axon terminals of the CNS and PNS [254]. Swollen eosinophilic spheroids throughout the gray matter lead to cerebral degeneration. This progressive disorder usually begins within the first 2 years of life with psychomotor deterioration, bilateral pyramidal tract signs, marked hypotonia, and early visual disturbances. VEPs are abnormal. The EEG often reveals high voltage and fast rhythms, and the EMG results are consistent with chronic denervation. T2-weighted MRI can reveal cerebellar atrophy with signal hyperintensity in the cerebellar cortex. In a report by Farina et al. [254], a thin optic chiasm was observed on MRI in four patients with infantile neuroaxonal dystrophy.

Both clinical and pathological features are necessary for the definitive diagnosis. Pathological diagnosis requires demonstrating neuroaxonal spheroids in peripheral nerve endings of the skin or conjunctiva. Treatment is supportive [255].

X-Linked Adrenoleukodystrophy

Adrenoleukodystrophy is an X-linked disorder that is secondary to a mutation in the ABCD1 gene, an ATPase-binding cassette protein [256]. This mutation causes a deficiency of peroxisomal acyl coenzyme A synthetase that leads to the accumulation of the saturated very long chain fatty acids. This disorder manifests primarily in the adrenal cortex, the myelin of the CNS, and the Leydig cells of the testes [256].

Boys are usually affected starting about age 7 years. Seizures and behavioral problems, including inattention, hyperactivity, and emotional lability, develop early. Visual and auditory deterioration, and motor incoordination, then develop rapidly. Periventricular demyelination, especially in the posterior cerebral hemisphere, contributes to visual loss. As demyelination affects the anterior pathways, optic atrophy becomes more apparent. MRI reveals symmetric involvement of the posterior parietooccipital white matter in 85 % of patients, frontal involvement in 10 %, and an asymmetric pattern in the remainder [257].

The diagnosis is established by measuring elevated levels of very long chain fatty acids in serum [258].

Asymptomatic individuals with the adrenomyeloneuropathy gene, as well as patients with this disorder and heterozygotes, may benefit from a combined oleic acid, VLCFA-restricted diet [259]. In a report by Aubourg et al. [260], reversal of early neurological and neuroradiologic features was achieved in an 8-year-old boy who received BMT from his fraternal twin brother. Malm et al. [261] described experience with BMT in three children with ALD. They concluded that BMT must be considered very early, even in a child without symptoms but with signs of demyelination on MRI, if a suitable donor is available.

Metachromatic Leukodystrophy

Metachromatic leukodystrophy is an autosomal recessive disorder caused by a deficiency of arylsulfatase A [262]. The progressive subcortical demyelination, mostly in the posterior cerebral white matter, causes dementia and blindness. Up to 50 % of patients with juvenile and adult forms have optic atrophy [262]. Histopathological studies in the infantile form of metachromatic leukodystrophy have shown storage of metachromatic complex lipids in the optic nerve, RGCs, and the ciliary nerves. Abnormal myelin metabolism also leads to peripheral demyelination causing weakness, spasticity, and ataxia [263].

Diagnosis is established by showing the absence of arylsulfatase A in leukocytes [263].

BMT may be a treatment option. Improvement in neurodevelopmental milestones was observed [264] in a boy with late infantile metachromatic

leukodystrophy after receiving a bone marrow transplant from an HLA-identical sister [265]. Improvement in neurophysiological function and sulfatide metabolism was also reported in an affected 10-year-old girl who had received a bone marrow transplant 5 years previously.

Krabbe Disease (Globoid Cell Leukodystrophy)

Krabbe disease is an autosomal recessive disorder localized to chromosome 14 [266]. This progressive demyelinating disease is caused by a deficiency of galactosylceramide- ß (beta)-galactosidase. Abnormal storage of galactosylceramide is seen as periodic acid-Schiff-positive material extracellularly and cerithin in microglial cells, which later appear as globoid cells in the white matter of the CNS [267].

Diffuse demyelination of the brain, including the entire visual pathway, and of the peripheral nerves, leads to blindness and psychomotor retardation in infancy. The optic neuropathy is more severe in the early-onset phenotype [266]. In neurophysiological studies by Husain et al. [268] of 20 patients with early-onset Krabbe disease, 53 % had abnormal flash VEPs compared to six patients with late-onset Krabbe disease who had normal flash VEPs. The abnormalities correlated well with disease severity as measured by MRI.

Diagnosis is established by showing the deficiency of galactosylceramide- ß (beta)-galactosidase in leukocytes or cultured fibroblasts [267].

BMT may be a treatment option. CNS manifestations of Krabbe disease can be reversed or prevented by allogeneic hematopoietic stem cell transplantation [267]. In a study by Krivit et al. [269], five children with Krabbe disease, one with the infantile type and four with late-onset disease, were treated with allogeneic hematopoietic stem cell transplantation. Four of the patients had clinical CNS abnormalities before transplantation. In all four cases, CNS deterioration was reversed. In the patient with the infantile form of the disease, the expected decline in CNS function had not occurred by the age of 16 months or 14 months posttransplantation.

Pelizaeus–Merzbacher Disease

Pelizaeus–Merzbacher disease is an X-linked demyelinating disorder caused by a mutation in the gene encoding proteolipid protein-1, leading to the defective synthesis of a proteolipid protein required in the myelin sheath. In the classic type of Pelizaeus–Merzbacher disease, demyelination of the cerebral hemispheres leads to the initial signs of nystagmoid eye movement and jerking and rolling head movements or head tremor. As nystagmus disappears, dementia, choreoathetosis, ataxia, and spasticity develop. Optic atrophy occurs late in the disease [270].

Diagnosis is established by showing the deletion of the exon coding the proteolipid protein on chromosome Xq22. MRI may be a suitable means for carrier detection. In obligate carriers, bilateral multiple areas with signal hyperintensity in the periventricular and subcortical white matter have been demonstrated [271]. Treatment is supportive [270].

Canavan's Syndrome

Canavan's disease is an autosomal recessive disorder caused by a point mutation in the ASPA gene mutation on chromosome 17pter-p13 [272]. This mutation causes a deficiency of aspartoacylase, leading to spongy degeneration of the white matter, swollen astrocytes, and normal neurons [273]. It is thought that the dysmyelination may result from failure of A-acetylaspartate to serve as a carrier of acetyl groups from mitochondria to the cytosol for lipogenesis [273]. A diffuse symmetric leukoencephalopathy develops before the manifestation of psychomotor retardation. In early infancy, hypotonia, hyperextension of legs and flexion of arms, blindness, severe cognitive delay, and megalencephaly develop. Optic atrophy is prominent at 6–10 months of age. Death occurs at about 18 months of age [273, 274].

Diagnosis is established by showing abnormal excretion of A-acetyl aspartate in the urine and showing a decreased level of aspartoacylase activity in culture fibroblasts [273]. MRI often

reveals diffuse leukodystrophy and high signal lesions in the globi pallidi on T2-weighted images. MRS of the brain shows an elevated ratio of N-acetyl aspartate/phosphocreatin + creatin (Cr) whereas the ratio of Cholin/Cr is reduced [275]. Treatment is supportive [273].

Many of these syndromes are very rare. Many are understandable only by recent molecular genetic characterization. What remains intriguing is that so many include vision loss and optic atrophy.

References

1. Carelli V. Leber's hereditary optic neuropathy. In: Schapira AHV, DiMauro S, editors. Mitochondrial disorders in neurology. Boston, MA: Butterworth-Heinemann; 2002. p. 115–42.
2. Sadun AA. Mitochondrial optic neuropathies. J Neurol Neurosurg Psychiatry. 2002;72:423–5.
3. Sadun AA, Carelli V. The role of mitochondria in health, ageing, and diseases affecting vision. Br J Ophthalmol. 2006;90:809–10.
4. Fontaine E, Bernardi P. Progress on the mitochondrial permeability transition pore: regulation by complex I and ubiquinone analogs. J Bioenerg Biomembr. 1999;31:335–45.
5. Sadun AA. Optic neuropathies and retinal ganglion cell death. J Neuroophthalmol. 2000;24:387–94.
6. Sadun AA. Acquired mitochondrial impairment as a cause of optic nerve disease. Trans Am Ophthalmol Soc. 1998;96:881–923.
7. Carelli V, Ross-Cisneros FN, Sadun AA. Mitochondrial dysfunction as a cause of optic neuropathies. Prog Retin Eye Res. 2004;23:53–89.
8. Zoumalan CI, Agarwal M, Sadun AA. OCT can measure axonal loss in patients with ethambutol-induced optic neuropathy. Graefe's Arch Clin Exp Ophthalmol. 2005;243:410–6.
9. Sadun AA, Martone JF, Muci-Mendoza R, Reyes L, DuBois L, Silva JC, et al. Epidemic optic neuropathy in Cuba. Eye findings. Arch Ophthalmol. 1994;112:691–9.
10. Pan BX, Ross-Cisneros FN, Carelli V, Rue KS, Salomao SR, Moraes-Filho MN, et al. Mathematically modeling the involvement of axons in Leber's hereditary optic neuropathy. Investig Ophthalmol Vis Sci. 2012;53:7608–17.
11. Fraser JA, Biousse V, Newman NJ. The neuro-ophthalmology ofmitochondrial disease. Surv Ophthalmol. 2010;55:299–334.
12. Wallace DC, Singh G, Lott MT, Hodge JA, Schurr TG, Lezza AM, et al. Mitochondrial DNA mutations associated with Leber's hereditary optic neuropathy. Science. 1988;242:1427–30.
13. Howell N, Bindoff LA, McCullough DA, Kubacka I, Poulton J, Mackey D, et al. Leber hereditary optic neuropathy: identification of the same mitochondrial ND1 mutation in six pedigrees. Am J Hum Genet. 1991;49:939–50.
14. Johns DR, Neufeld MJ, Park RD. An ND-6 mitochondrial DNA mutation associated with Leber hereditary optic neuropathy. Biochem Biophys Res Commun. 1992;187:1551–7.
15. Carelli V, Ghelli A, Bucchi L, Montagna P, De Negri A, Leuzzi V, et al. Biochemical features of mtDNA 14484 (ND6/M64V) point mutation associated with Leber's hereditary optic neuropathy. Ann Neurol. 1999;45:320–8.
16. Chinnery PF, Johnson MA, Wardell TM, Singh-Kler R, Hayes C, Brown DT, et al. The epidemiology of pathogenic mitochondrial DNA mutations. Ann Neurol. 2000;48:188–93.
17. Man PY, Griffiths PG, Brown DT, Howell N, Turnbull DM, Chinnery PF. The epidemiology of Leber hereditary optic neuropathy in the northeast of England. Am J Hum Genet. 2003;72:333–9.
18. Spruijt L, Kolbach DN, de Coo RF, Plomp AS, Bauer NJ, Smeets HJ, et al. Influence of mutation type on clinical expression of Leber hereditary optic neuropathy. Am J Ophthalmol. 2006;141:676–82.
19. Puomila A, Hämäläinen P, Kivioja S, Savontaus ML, Koivumäki S, Huoponen K, et al. Epidemiology and penetrance of Leber hereditary optic neuropathy in Finland. Eur J Hum Genet. 2007;15:1079–89.
20. Sadun AA, Carelli V, Salomao SR, Berezovsky A, Quiros P, Sadun F, et al. A very large Brazilian pedigree with 11778 Leber's hereditary optic neuropathy. Trans Am Ophthalmol Soc. 2002;100:169–78. discussion 178–9.
21. Wallace DC, Lott MT. Maternally inherited diseases. In: DiMauro S, Wallace DC, editors. Mitochondrial DNA in human pathology. New York, NY: Raven; 1993. p. 63–83.
22. Brown MD, Allen JC, Van Stavern GP, et al. Clinical, genetic, and biochemical characterization of a Leber hereditary optic neuropathy family containing both the 11778 and 14484 primary mutations. Am J Med Genet. 2001;104:331–8.
23. Seedorff T. The inheritance of Leber's disease. A genealogical follow-up study. Acta Ophthalmol (Copenh). 1985;63:135–45.
24. Giles RE, Blanc H, Cann HM, et al. Maternal inheritance of human mitochondrial DNA. Proc Natl Acad Sci U S A. 1980;77:6715–9.
25. Mackey DA, Oostra RJ, Rosenberg T, et al. Primary pathogenic mtDNA mutations in multigeneration pedigrees with Leber hereditary optic. Am J Hum Genet. 1996;59:481–5.
26. Howell N, Halvorson S, Burns J, et al. When does bilateral optic atrophy become Leber hereditary optic neuropathy? Am J Hum Genet. 1993;53:959–63.

27. Wissinger B, Besch D, Baumann B, et al. Mutation analysis of the ND6 gene in patients with Lebers hereditary optic neuropathy. Biochem Biophys Res Commun. 1997;234:511–5.
28. Newman NJ, Lott MT, Wallace DC. The clinical characteristics of pedigrees of Leber's hereditary optic neuropathy with the 11778 mutation. Am J Ophthalmol. 1991;111:750–62.
29. Singh G, Lott MT, Wallace DC. A mitochondrial DNA mutation as a cause of Leber's hereditary optic neuropathy. N Engl J Med. 1989;320:1300–5.
30. Huoponen K, Lamminen T, Juvonen V, et al. The spectrum of mitochondrial DNA mutations in families with Leber hereditary optic neuroretinopathy. Hum Genet. 1993;92:379–84.
31. Lott MT, Voljavec AS, Wallace DC. Variable genotype of Leber's hereditary optic neuropathy patients. Am J Ophthalmol. 1990;109:625–31.
32. Huoponen K, Vilkki J, Aula P, et al. A new mtDNA mutation associated with Leber hereditary optic neuroretinopathy. Am J Hum Genet. 1991;48:1147–53.
33. Johns DR, Heher KL, Miller NR, et al. Leber's hereditary optic neuropathy. Clinical manifestations of the 14484 mutation. Arch Ophthalmol. 1993; 111:495–8.
34. Novotny Jr EJ, Singh G, Wallace DC, et al. Leber's disease and dystonia: a mitochondrial disease. Neurology. 1986;36:1053–60.
35. Wallace DC, Singh G, Hopkins LC, et al. Maternally inherited diseases of man. In: Quagliariello E, Slater EC, Palmieri F, Saccone C, Kroon AM, editors. Achievements and perspectives of mitochondrial research. Amsterdam: Elsevier; 1985. p. 427–36.
36. Brown MD, Voljavec AS, Lott MT, et al. Leber's hereditary optic neuropathy; a model for mitochondrial neurodegenerative diseases. FASEB J. 1992;6:2791–9.
37. Howell N, Kubacka I, Halvorson S, et al. Leber's hereditary optic neuropathy: the etio-logical role of a mutation in the mitochondrial cytochrome b gene [Letter]. Genetics. 1993;133:133–6.
38. Carelli V, Achilli A, Valentino ML, Rengo C, Semino O, Pala M, et al. Haplogroup effects and recombination of mitochondrial DNA: novel clues from the analysis of Leber hereditary optic neuropathy pedigrees. Am J Hum Genet. 2006;78:564–74.
39. Hudson G, Carelli V, Spruijt L, Gerards M, Mowbray C, Achilli A, et al. Clinical expression of Leber hereditary optic neuropathy is affected by the mitochondrial DNA-haplogroup background. Am J Hum Genet. 2007;81:228–33.
40. Shankar SP, Fingert JH, Carelli V, Valentino ML, King TM, Daiger SP, et al. Evidence for a novel x-linked modifier locus for Leber hereditary optic neuropathy. Ophthalmic Genet. 2008;29:17–24.
41. Hudson G, Carelli V, Horvath R, Zeviani M, Smeets HJ, Chinnery PF. X-Inactivation patterns in females harboring mtDNA mutations that cause Leber hereditary optic neuropathy. Mol Vis. 2007;13:2339–43.
42. Sadun AA, Carelli V, Salomao SR, Berezovsky A, Quiros PA, Sadun F, et al. Extensive investigation of a large Brazilian pedigree of 11778/haplogroup J Leber hereditary optic neuropathy. Am J Ophthalmol. 2003;136:231–8.
43. Kirkman MA, Yu-Wai-Man P, Korsten A, Leonhardt M, Dimitriadis K, De Coo IF, et al. Gene-environment interactions in Leber hereditary optic neuropathy. Brain. 2009;132:2317–26.
44. Sanchez RN, Smith AJ, Carelli V, Sadun AA, Keltner JL, et al. Leber hereditary optic neuropathy possibly triggered by exposure to tire fire. J Neuroophthalmol. 2006;26:268–72.
45. Wang MY, Sadun AA. Drug-related mitochondrial optic neuropathies. J Neuroophthalmol. 2013;33: 172–8.
46. Mackey DA, Fingert JH, Luzhansky JZ, McCluskey PJ, Howell N, Hall AJ, et al. Leber's hereditary optic neuropathy triggered by antiretroviral therapy for human immunodeficiency virus. Eye. 2003;17:312–7.
47. Ikeda A, Ikeda T, Ikeda N, Kawakami Y, Mimura O, et al. Leber's hereditary optic neuropathy precipitated by ethambutol. Jpn J Ophthalmol. 2006;50: 280–3.
48. Carelli V, Franceschini F, Venturi S, Barboni P, Savini G, Barbieri G, et al. Grand rounds: could occupational exposure to n-hexane and other solvents precipitate visual failure in leber hereditary optic neuropathy? Environ Health Perspect. 2007; 115:113–5.
49. De Marinis M. Optic neuropathy after treatment with anti-tuberculous drugs in a subject with Leber's hereditary optic neuropathy mutation. J Neurol. 2001;248:818–9.
50. Cullom ME, Heher KL, Miller NR, et al. Leber's hereditary optic neuropathy masquerading as tobacco-alcohol amblyopia. Arch Ophthalmol. 1993;111:1482–5.
51. Carelli V, La Morgia C, Valentino ML, Barboni P, Ross-Cisneros FN, Sadun AA, et al. Retinal ganglion cell neurodegeneration in mitochondrial inherited disorders. Biochim Biophys Acta. 2009;1787:518–28.
52. Barboni P, Savini G, Valentino ML, La Morgia C, Bellusci C, De Negri AM, et al. Leber's hereditary optic neuropathy with childhood onset. Investig Ophthalmol Vis Sci. 2006;47:5303–9.
53. Yu-Wai-Man P, Griffiths PG, Chinnery PF. Mitochondrial optic neuropathies – disease mechanisms and therapeutic strategies. Prog Retin Eye Res. 2011;30:81–114.
54. Oostra RJ, Bolhuis PA, Wijburg FA, Zorn-Ende G, Bleeker-Wagemakers EM, et al. Leber's hereditary optic neuropathy: correlations between mitochondrial genotype and visual outcome. J Med Genet. 1994;31:280–6.
55. Carelli V, Ross-Cisneros FN, Sadun AA. Optic nerve degeneration and mitochondrial dysfunction: genetic and acquired optic neuropathies. Neurochem Int. 2002;40:573–84.

56. Hannibal J, Hindersson P, Knudsen SM, Georg B, Fahrenkrug J, et al. The photopigment melanopsin is exclusively present in pituitary adenylate cyclase-activating polypeptide-containing retinal ganglion cells of the retinohypothalamic tract. J Neurosci. 2002;22:RC191.
57. Hattar S, Liao HW, Takao M, Berson DM, Yau KW, et al. Melanopsincontaining retinal ganglion cells: architecture, projections, and intrinsic photosensitivity. Science. 2002;295:1065–70.
58. Moura AL, Nagy BV, La Morgia C, Barboni P, Oliveira AG, Salomão SR, et al. The pupil light reflex in Leber's hereditary optic neuropathy: evidence for preservation of melanopsin-expressing retinal ganglion cells. Investig Ophthalmol Vis Sci. 2013;54:4471–7.
59. La Morgia C, Ross-Cisneros FN, Hannibal J, Montagna P, Sadun AA, Carelli V. Melanopsin-expressing retinal ganglion cells: implications for human diseases. Vision Res. 2011;51:296–302.
60. La Morgia C, Ross-Cisneros FN, Sadun AA, Hannibal J, Munarini A, Mantovani V, et al. Melanopsin retinal ganglion cells are resistant to neurodegeneration in mitochondrial optic neuropathies. Brain. 2010;133:2426–38.
61. Ventura DF, Gualtieri M, Oliveira AG, Costa MF, Quiros P, Sadun F, et al. Male prevalence of acquired color vision defects in asymptomatic carriers of Leber's hereditary optic neuropathy. Investig Ophthalmol Vis Sci. 2007;48:2362–70.
62. Gualtieri M, Bandeira M, Hamer RD, Costa MF, Oliveira AG, Moura AL, et al. Psychophysical analysis of contrast processing segregated into magnocellular and parvocellular systems in asymptomatic carriers of 11778 Leber's hereditary optic neuropathy. Vis Neurosci. 2008;25:469–74.
63. Ventura DF, Quiros P, Carelli V, Salomão SR, Gualtieri M, Oliveira AG, et al. Chromatic and luminance contrast sensitivities in asymptomatic carriers from a large Brazilian pedigree of 11778 Leber hereditary optic neuropathy. Investig Ophthalmol Vis Sci. 2005;46:4809–14.
64. Sadun AA. Optic disc pits and associated serous macular detachment. In: Ryan SJ, editor. Retina, vol. 2. St. Louis: CV Mosby; 2006. p. 1883–9.
65. Quiros PA, Torres RJ, Salomao S, Berezovsky A, Carelli V, Sherman J, et al. Colour vision defects in asymptomatic carriers of the Leber's hereditary optic neuropathy (LHON) mtDNA 11778 mutation from a large Brazilian LHON pedigree: a case–control study. Br J Ophthalmol. 2006;90:150–3.
66. Sadun F, De Negri AM, Carelli V, Salomao SR, Berezovsky A, Andrade R, et al. Ophthalmologic findings in a large pedigree of 11778/Haplogroup J Leber hereditary optic neuropathy. Am J Ophthalmol. 2004;137:271–7.
67. Mann ES, Handler SP, Chung SM. Leber's hereditary optic neuropathy masquerading as retinal vasculitis. Arch Ophthalmol. 2000;118:1587–9.
68. Riordan-Eva P, Sanders MD, Govan GG, et al. The clinical features of Leber's hereditary optic neuropathy defined by the presence of a pathogenic mitochondrial DNA mutation. Brain. 1995;118:319–37.
69. Sadun AA, Carelli V. Mitochondrial function and dysfunction within the optic nerve. Arch Ophthalmol. 2003;121:1342–3.
70. Burde RM. Optic disk risk factors for nonarteritic anterior ischemic optic neuropathy. Am J Ophthalmol. 1993;116:759–64.
71. Ramos Cdo V, Bellusci C, Savini G, Carbonelli M, Berezovsky A, Tamaki C, et al. Association of optic disc size with development and prognosis of Leber's hereditary optic neuropathy. Investig Ophthalmol Vis Sci. 2009;50:1666–74.
72. Harding AE, Sweeney MG, Govan GG, et al. Pedigree analysis in Leber hereditary optic neuropathy families with a pathogenic mtDNA mutation. Am J Hum Genet. 1995;57:77–86.
73. Nikoskelainen E, Hoyt WF, Nummelin K. Ophthalmoscopic findings in Leber's hereditary optic neuropathy. I. Fundus findings in asymptomatic family members. Arch Ophthalmol. 1982;100:1597–602.
74. Sadun AA, Win PH, Ross-Cisneros FN, Walker SO, Carelli V, et al. Leber's hereditary optic neuropathy differentially affects smaller axons in the optic nerve. Trans Am Ophthalmol Soc. 2000;98:223–32. Discussion 232–5.
75. Nikoskelainen E, Hassinen IE, Paljärvi L, et al. Leber's hereditary optic neuroretinopathy, a mitochondrial disease? Lancet. 1984;2:1474.
76. Kerrison JB, Howell N, Miller NR, et al. Leber hereditary optic neuropathy. Electron microscopy and molecular genetic analysis of a case. Ophthalmology. 1995;102:1509–16.
77. Barboni P, Carbonelli M, Savini G, Ramos Cdo V, Carta A, Berezovsky A, et al. Natural history of Leber's hereditary optic neuropathy: longitudinal analysis of the retinal nerve fiber layer by optical coherence tomography. Ophthalmology. 2010;117:623–7.
78. Barboni P, Savini G, Valentino ML, Montagna P, Cortelli P, De Negri AM, et al. Retinal nerve fiber layer evaluation by optical coherence tomography in Leber's hereditary optic neuropathy. Ophthalmology. 2005;112:120–6.
79. Savini G, Barboni P, Valentino ML, Montagna P, Cortelli P, De Negri AM, et al. Retinal nerve fiber layer evaluation by optical coherence tomography in unaffected carriers with Leber's hereditary optic neuropathy mutations. Ophthalmology. 2005;112:127–31.
80. Barboni P, Savini G, Feuer WJ, Budenz DL, Carbonelli M, Chicani F, et al. Retinal nerve fiber layer thickness variability in Leber hereditary optic neuropathy carriers. Eur J Ophthalmol. 2012;22:985–91.

81. Sadun AA, La Morgia C, Carelli V. Leber's Hereditary Optic Neuropathy. Curr Treat Options Neurol. 2011;13:109–17.
82. Harding AE, Sweeney MG, Miller DH, Mumford CJ, Kellar-Wood H, Menard D, et al. Occurrence of a multiple sclerosis-like illness in women who have a Leber's hereditary optic neuropathy mitochondrial DNA mutation. Brain. 1992;115:979–89.
83. Ortiz RG, Newman NJ, Manoukian SV, Diesenhouse MC, Lott MT, Wallace DC, et al. Optic disk cupping and electrocardiographic abnormalities in an American pedigree with Leber's hereditary optic neuropathy. Am J Ophthalmol. 1992;113:561–6.
84. Olsen NK, Hansen AW, Norby S, et al. Leber's hereditary optic neuropathy associated with a disorder indistinguishable from multiple sclerosis in a male harbouring the mitochondrial DNA 11778 mutation. Acta Neurol Scand. 1995;91:326–9.
85. Flanigan KM, Johns DR. Association of the 11778 mitochondrial DNA mutation and demyelinating disease. Neurology. 1993;43:2720–2.
86. Kellar-Wood H, Robertson N, Govan GG, et al. Leber's hereditary optic neuropathy mitochondrial DNA mutations in multiple sclerosis. Ann Neurol. 1994;36:109–12.
87. Nikoskelainen EK, Marttila RJ, Huoponen K, et al. Leber's "plus": neurological abnormalities in patients with Leber's hereditary optic neuropathy. J Neurol Neurosurg Psychiatry. 1995;59:160164.
88. Nikoskelainen E, Hoyt WF, Nummelin K. Fundus findings in Leber's hereditary optic neuroretinopathy. Ophthalmic Paediatr Genet. 1985;5:125–30.
89. McLeod JG, Low PA, Morgan JA. Charcot-Marie-Tooth disease with Leber optic atrophy. Neurology. 1978;28:179–84.
90. Wallace DC. A new manifestation of Leber's disease and a new explanation for the agency responsible for its unusual pattern of inheritance. Brain. 1970;93: 121–32.
91. Funalot B, Reynier P, Vighetto A, et al. Leigh-like encephalopathy complicating Leber's hereditary optic neuropathy. Ann Neurol. 2002;52:374–7.
92. Paulus W, Straube A, Bauer W, et al. Central nervous system involvement in Leber's optic neuropathy. J Neurol. 1993;240:251–3.
93. Klopstock T, Yu-Wai-Man P, Dimitriadis K, Rouleau J, Heck S, Bailie M, et al. A randomized placebo-controlled trial of idebenone in Leber's hereditary optic neuropathy. Brain. 2011;134:2677–86.
94. Carelli V, La Morgia C, Valentino ML, Rizzo G, Carbonelli M, De Negri AM, et al. Idebenone treatment in Leber's hereditary optic neuropathy. Brain. 2011;134:e188.
95. Sadun AA, Chicani CF, Ross-Cisneros FN, Barboni P, Thoolen M, Shrader WD, et al. Effect of EPI-743 on the clinical course of the mitochondrial disease Leber hereditary optic neuropathy. Arch Neurol. 2012;69:331–8.
96. Guy J, Qi X, Koilkonda RD, Arguello T, Chou TH, Ruggeri M, et al. Efficiency and safety of AAV-mediated gene delivery of the human ND4 complex I subunit in the mouse visual system. Investig Ophthalmol Vis Sci. 2009;50:4205–14.
97. Pott JW, Wong KH. Leber's hereditary optic neuropathy and vitamin B12 deficiency. Graefes Arch Clin Exp Ophthalmol. 2006;244:1357–9.
98. Wheeler L, WoldeMussie E, Lai R. Role of alpha-2 agonists in neuroprotection. Surv Ophthalmol. 2003; 48:S47–51.
99. Yoles E, Wheeler LA, Schwartz M. Alpha-2-adenoreceptor agonists are neuroprotective in a rat model of optic nerve degeneration. Investig Ophthalmol Vis Sci. 1999;40:65–73.
100. WoldeMussie E, Ruiz G, Wijono M, Wheeler LA. Neuro-protection of retinal ganglion cells by brimonidine in rats with laser-induced chronic ocular hypertension. Investig Ophthalmol Vis Sci. 2001;42: 2849–55.
101. Lai RK, Chun T, Hasson D, Lee S, Mehrbod F, Wheeler L. Alpha-2 adrenoceptor agonist protects retinal function after acute retinal ischemic injury in the rat. Vis Neurosci. 2002;19:175–85.
102. Newman NJ, Biousse V, David R, Bhatti MT, Hamilton SR, Farris BK, et al. Prophylaxis for second eye involvement in Leber hereditary optic neuropathy: an open-labeled, nonrandomized multicenter trial of topical brimonidine purite. Am J Ophthalmol. 2005;140:407–15.
103. Ghelli A, Porcelli AM, Zanna C, Martinuzzi A, Carelli V, Rugolo M, et al. Protection against oxidant-induced apoptosis by exogenous glutathione in Leber hereditary optic neuropathy cybrids. Investig Ophthalmol Vis Sci. 2008;49:671–6.
104. Sala G, Trombin F, Beretta S, et al. Antioxidants partially restore glutamate transport defect in Leber hereditary optic neuropathy cybrids. J Neurosci Res. 2008;86:3331–7.
105. Huang CC, Kuo HC, Chu CC, Kao LY. Rapid visual recovery after coenzyme q10 treatment of leber hereditary optic neuropathy. J Neuroophthalmol. 2002;22:66.
106. Geromel V, Darin N, Chrétien D, Bénit P, DeLonlay P, Rötig A, et al. Coenzyme Q (10) and idebenone in the therapy of respiratory chain diseases: rationale and comparative benefits. Mol Genet Metab. 2002; 77:21–30.
107. Di Prospero NA, Baker A, Jeffries N, Fischbeck KH. Neurological effects of high-dose idebenone in patients with Friedreich's ataxia: a randomised, placebo-controlled trial. Lancet Neurol. 2007;6: 878–86.
108. Meier T, Perlman SL, Rummey C, Coppard NJ, Lynch DR. Assessment of neurological efficacy of idebenone in pediatric patients with Friedreich's ataxia: data from a 6-month controlled study followed by a 12-month open-label extension study. J Neurol. 2012;259:284–91.
109. Lekoubou A, Kouamé-Assouan AE, Cho TH, Luauté J, Nighoghossian N, Derex L. Effect of long-term oral treatment with L-arginine and idebenone on the

prevention of stroke-like episodes in an adult MELAS patient. Rev Neurol (Paris). 2011;167:852–5.
110. Bababeygy SR, Wang MY, Khaderi KR, Sadun AA. Visual improvement with the use of idebenone in the treatment of Wolfram syndrome. J Neuroophthalmol. 2012;32:386–9.
111. Mashima Y, Hiida Y, Oguchi Y. Remission of Leber's hereditary optic neuropathy with idebenone. Lancet. 1992;340:368–9.
112. Mashima Y, Kigasawa K, Wakakura M, Oguchi Y, et al. Do idebenone and vitamin therapy shorten the time to achieve visual recovery in Leber hereditary optic neuropathy? J Neuroophthalmol. 2000;20: 166–70.
113. Cortelli P, Montagna P, Pierangeli G, Lodi R, Barboni P, Liguori R, et al. Clinical and brain bioenergetics improvement with idebenone in a patient with Leber's hereditary optic neuropathy: a clinical and 31P-MRS study. J Neurol Sci. 1997;148:25–31.
114. Carelli V, Barboni P, Zacchini A, Mancini R, Monari L, Cevoli S, et al. Leber's hereditary optic neuropathy (LHON) with 14484/ND6 mutation in a North African patient. J Neurol Sci. 1998;160:183–8.
115. Eng JG, Aggarwal D, Sadun AA. Idebenone treatment in patients with Leber's hereditary optic neuropathy. Vis Sci. 2009;50:1440.
116. Shrader WD, Amagata A, Barnes A, Enns GM, Hinman A, Jankowski O, et al. α-Tocotrienol quinone modulates oxidative stress response and the biochemistry of aging. Bioorg Med Chem Lett. 2011;21:3693–8.
117. Kerr DS. Review of clinical trials for mitochondrial disorders: 1997–2012. Neurotherapeutics. 2013;10: 307–19.
118. Floreani M, Napoli E, Martinuzzi A, Pantano G, De Riva V, Trevisan R, et al. Antioxidant defences in cybrids harboring mtDNA mutations associated with Leber's hereditary optic neuropathy. FEBS J. 2005;272:1124–35.
119. Enns GM, Kinsman SL, Perlman SL, Spicer KM, Abdenur JE, Cohen BH, et al. Initial experience in the treatment of inherited mitochondrial disease with EPI-743. Mol Genet Metab. 2012;105:91–102.
120. Blankenberg FG, Kinsman SL, Cohen BH, Goris ML, Spicer KM, Perlman SL, et al. Brain uptake of Tc99m-HMPAO correlates with clinical response to the novel redox modulating agent EPI-743 in patients with mitochondrial disease. Mol Genet Metab. 2012;107:690–9.
121. Porcelli AM, Angelin A, Ghelli A, Mariani E, Martinuzzi A, Carelli V, et al. Respiratory complex I dysfunction due to mitochondrial DNA mutations shifts the voltage threshold for opening of the permeability transition pore toward resting levels. J Biol Chem. 2009;284:2045–52.
122. Giordano C, Montopoli M, Perli E, Orlandi M, Fantin M, Ross-Cisneros FN, et al. Oestrogens ameliorate mitochondrial dysfunction in Leber's hereditary optic neuropathy. Brain. 2011;134:220–34.
123. Wenz T, Diaz F, Spiegelman BM, Moraes CT. Activation of the PPAR/PGC-1alpha pathway prevents a bioenergetic deficit and effectively improves a mitochondrial myopathy phenotype. Cell Metab. 2008;8:249–56.
124. Gray RE, Law RH, Devenish RJ, Nagley P. Allotopic expression of mitochondrial ATP synthase genes in nucleus of Saccharomyces cerevisiae. Methods Enzymol. 1996;264:369–89.
125. Guy J, Qi X, Pallotti F, Schon EA, Manfredi G, Carelli V, et al. Rescue of a mitochondrial deficiency causing Leber hereditary optic neuropathy. Ann Neurol. 2002;52:534–42.
126. Qi X, Sun L, Lewin AS, Hauswirth WW, Guy J. The mutant human ND4 subunit of complex I induces optic neuropathy in the mouse. Invest Ophthalmol Vis Sci. 2007;48:1–10.
127. Ellouze S, Augustin S, Bouaita A, Bonnet C, Simonutti M, Forster V, et al. Optimized allotopic expression of the human mitochondrial ND4 prevents blindness in a rat model of mitochondrial dysfunction. Am J Hum Genet. 2008;83:373–87.
128. Lam BL, Feuer WJ, Abukhalil F, Porciatti V, Hauswirth WW, Guy J. Leber hereditary optic neuropathy gene therapy clinical trial recruitment: year 1. Arch Ophthalmol. 2010;128:1129–35.
129. Perales-Clemente E, Fernández-Silva P, Acín-Pérez R, Pérez-Martos A, Enríquez JA. Allotopic expression of mitochondrial-encoded genes in mammals: achieved goal, undemonstrated mechanism or impossible task? Nucleic Acids Res. 2011;39: 225–34.
130. Oca-Cossio J, Kenyon L, Hao H, Moraes CT. Limitations of allotopic expression of mitochondrial genes in mammalian cells. Genetics. 2003;165: 707–20.
131. Iyer S, Bergquist K, Young K, Gnaiger E, Rao RR, Bennett Jr JP. Mitochondrial gene therapy improves respiration, biogenesis, and transcription in G11778A Leber's hereditary optic neuropathy and T8993G Leigh's syndrome cells. Hum Gene Ther. 2012;23:647–57.
132. Yu H, Koilkonda RD, Chou TH, Porciatti V, Ozdemir SS, Chiodo V, et al. Gene delivery to mitochondria by targeting modified adenoassociated virus suppresses Leber's hereditary optic neuropathy in a mouse model. Proc Natl Acad Sci U S A. 2012; 109:E1238–47.
133. Lin CS, Sharpley MS, Fan W, Waymire KG, Sadun AA, Carelli V, et al. Mouse mtDNA mutant model of Leber hereditary optic neuropathy. Proc Natl Acad Sci U S A. 2012;109:20065–70.
134. Marella M, Seo BB, Matsuno-Yagi A, Yagi T. Mechanism of cell death caused by complex I defects in a rat dopaminergic cell line. J Biol Chem. 2007;282:24146–56.
135. Park JS, Li YF, Bai Y. Yeast NDI1 improves oxidative phosphorylation capacity and increases protection against oxidative stress and cell death in cells carrying

a Leber's hereditary optic neuropathy mutation. Biochim Biophys Acta. 2007;1772:533–42.
136. Marella M, Seo BB, Thomas BB, Matsuno-Yagi A, Yagi T. Successful amelioration of mitochondrial optic neuropathy using the yeast NDI1 gene in a rat animal model. PLoS One. 2010;5:e11472.
137. Chadderton N, Palfi A, Millington-Ward S, Gobbo O, Overlack N, Carrigan M, et al. Intravitreal delivery of AAV-NDI1 provides functional benefit in a murine model of Leber hereditary optic neuropathy. Eur J Hum Genet. 2013;21:62–8.
138. Newman NJ. Dominant optic atrophy. In: Newman NJ, Miller NR, editors. Walsh and Hoyt's clinical neuro-ophthalmology. Baltimore, MD: Williams & Wilkins; 1998. p. 753–6.
139. Alexander C, Votruba M, Pesch UE, Thiselton DL, Mayer S, Moore A, et al. OPA1, encoding a dynamin-related GTPase, is mutated in autosomal dominant optic atrophy linked to chromosome 3q28. Nat Genet. 2000;26:211–5.
140. Delettre C, Lenaers G, Griffoin JM, Gigarel N, Lorenzo C, Belenguer P, et al. Nuclear gene OPA1, encoding a mitochondrial dynamin-related protein, is mutated in dominant optic atrophy. Nat Genet. 2000;26:207–10.
141. Eiberg H, Kjer B, Kjer P, Rosenberg T, et al. Dominant optic atrophy (OPA1) mapped to chromosome 3q region. I. Linkage analysis. Hum Mol Genet. 1994;3:977–80.
142. Olichon A, Guillou E, Delettre C, Landes T, Arnauné-Pelloquin L, Emorine LJ, et al. Mitochondrial dynamics and disease, OPA1. Biochim Biophys Acta. 2006;1763:500–9.
143. Mantyjarvi MI, Nerdrum K, Tuppurainen K. Color vision in dominant optic atrophy. J Clin Neuro Ophthalmol. 1992;12:98–103.
144. Simunovic MP, Votruba M, Regan BC, et al. Colour discrimination ellipses in patients with dominant optic atrophy. Vision Res. 1998;38:3413–9.
145. Hoyt CS. Autosomal dominant optic atrophy. A spectrum of disability. Ophthalmology. 1980;87:245–51.
146. Votruba M, Aijaz S, Moore AT. A review of primary hereditary optic neuropathies. J Inherit Metab Dis. 2003;26:209–27.
147. Kok-van Alphen CC. Four families with the dominant infantile form of optic nerve atrophy. Acta Ophthalmol (Copenh). 1970;48:905–16.
148. Votruba M, Thiselton D, Bhattacharya SS. Optic disc morphology of patients with OPA1 autosomal dominant optic atrophy. Br J Ophthalmol. 2003;87:48–53.
149. Ito Y, Nakamura M, Yamakoshi T, Lin J, Yatsuya H, Terasaki H, et al. Reduction of inner retinal thickness in patients with autosomal dominant optic atrophy associated with OPA1 mutations. Investig Ophthalmol Vis Sci. 2007;48:4079–86.
150. Manchester Jr PT, Calhoun Jr FP. Dominant hereditary optic atrophy with bitemporal field defects. AMA Arch Ophthalmol. 1958;60:479–84.
151. Buono LM, Foroozan R, Sergott RC, et al. Is normal tension glaucoma actually an unrecognized hereditary optic neuropathy? New evidence from genetic analysis. Curr Opin Ophthalmol. 2002;13:362–70.
152. Weiner NC, Newman NJ, Lessell S, et al. Atypical Leber's hereditary optic neuropathy with molecular confirmation. Arch Neurol. 1993;50:470–3.
153. Mashima Y, Kimura I, Yamamoto Y, et al. Optic disc excavation in the atrophic stage of Leber's hereditary optic neuropathy: comparison with normal tension glaucoma. Graefes Arch Clin Exp Ophthalmol. 2003;241:75–80.
154. Li Y, Deng T, Tong Y, et al. Identification of two novel OPA1 mutations in Chinese families with autosomal dominant optic atrophy. Mol Vis. 2008;14:2451–7.
155. Votruba M, Moore AT, Bhattacharya SS. Clinical features, molecular genetics, and pathophysiology of dominant optic atrophy. J Med Genet. 1998;35:793–800.
156. Fournier AV, Damji KF, Epstein DL, et al. Disc excavation in dominant optic atrophy. Ophthalmology. 2001;108:1595–602.
157. Johnston PB, Gaster RN, Smith VC, et al. A clinicopathologic study of autosomal dominant optic atrophy. Am J Ophthalmol. 1979;88:868–75.
158. Kjer P, Jensen OA, Klinken L. Histopathology of eye, optic nerve and brain in a case of dominant optic atrophy. Acta Ophthalmol (Copenh). 1983;61:300–12.
159. Payne M, Yang Z, Katz BJ, et al. Dominant optic atrophy, sensorineural hearing loss, ptosis, and ophthalmoplegia: a syndrome caused by a mis-sense mutation in OPA1. Am J Ophthalmol. 2004;138:749–55.
160. Lodi R, Tonon C, Valentino ML, et al. Deficit of in vivo mitochondrial ATP production in OPA1-related dominant optic atrophy. Ann Neurol. 2004;56:719–23.
161. Kim JY, Hwang J-M, Ko HS, et al. Mitochondrial DNA content is decreased in autosomal dominant optic atrophy. Neurology. 2005;64:966–72.
162. Kerrison JB, Arnould VJ, Ferraz Sallum JM, et al. Genetic heterogeneity of dominant optic atrophy, Kjer type: identification of a second locus on chromosome 18q12.2-12.3. Arch Ophthalmol. 1999;117:805–10.
163. Barbet F, Hakiki S, Orssaud C, Gerber S, Perrault I, Hanein S, et al. A third locus for dominant optic atrophy on chromosome 22q. J Med Genet. 2005;42:e1.
164. Carelli V, Schimpf S, Fuhrmann N, Valentino ML, Zanna C, Iommarini L, et al. A clinically complex form of dominant optic atrophy (OPA8) maps on chromosome 16. Hum Mol Genet. 2011;20:1893–905.
165. Ozden S, Duzcan F, Wollnik B, et al. Progressive autosomal dominant optic atrophy and sensorineural hearing loss in a Turkish family. Ophthalmic Genet. 2002;23:29–36.

166. Toomes C, Marchbank NJ, Mackey DA, et al. Spectrum, frequency and penetrance of OPA1 mutations in dominant optic atrophy. Hum Mol Genet. 2001;10:1369–78.
167. Delettre C, Griffoin JM, Kaplan J, et al. Mutation spectrum and splicing variants in the OPA1 gene. Hum Genet. 2001;109:584–91.
168. Thiselton DL, Alexander C, Morris A, et al. A frameshift mutation in exon 28 of the OPA1 gene explains the high prevalence of dominant optic atrophy in the Danish population: evidence for a founder effect. Hum Genet. 2001;109:498–502.
169. Zanna C, Ghelli A, Porcelli AM, Karbowski M, Youle RJ, Schimpf S, et al. OPA1 mutations associated with dominant optic atrophy impair oxidative phosphorylation and mitochondrial fusion. Brain. 2008;131:352–67.
170. Yu-Wai-Man P, Griffiths PG, Gorman GS, Lourenco CM, Wright AF, Auer-Grumbach M, et al. Multisystem neurological disease is common in patients with OPA1 mutations. Brain. 2010;133:771–86.
171. Amati-Bonneau P, Valentino ML, Reynier P, Gallardo ME, Bornstein B, Boissière A, et al. OPA1 mutations induce mitochondrial DNA instability and optic atrophy 'plus' phenotypes. Brain. 2008;131:338–51.
172. Hudson G, Amati-Bonneau P, Blakely EL, Stewart JD, He L, Schaefer AM, et al. Mutation of OPA1 causes dominant optic atrophy with external ophthalmoplegia, ataxia, deafness and multiple mitochondrial DNA deletions: a novel disorder of mtDNA maintenance. Brain. 2008;131:329–37.
173. Marchbank NJ, Craig JE, Leek JP, et al. Deletion of the OPA1 gene in a dominant optic atrophy family: evidence that haploinsufficiency is the cause of disease. J Med Genet. 2002;39:e47.
174. Hogewind BF, Pennings RJ, Hol FA, Kunst HP, Hoefsloot EH, Cruysberg JR, et al. Autosomal dominant optic neuropathy and sensorineual hearing loss associated with a novel mutation of WFS1. Mol Vis. 2010;16:26–35.
175. Eiberg H, Hansen L, Kjer B, Hansen T, Pedersen O, Bille M, et al. Autosomal dominant optic atrophy associated with hearing impairment and impaired glucose regulation caused by a missense mutation in the WFS1 gene. J Med Genet. 2006;43:435–40.
176. Delettre C, Lenaers G, Pelloquin L, et al. OPA1 (Kjer type) dominant optic atrophy: a novel mitochondrial disease. Mol Genet Metab. 2002;75:97–107.
177. Williams PA, Morgan JE, Votruba M. Mouse models of dominant optic atrophy: what do they tell us about the pathophysiology of visual loss? Vision Res. 2011;51:229–34.
178. Alavi MV, Bette S, Schimpf S, Schuettauf F, Schraermeyer U, Wehrl HF, et al. A splice site mutation in the murine Opa1 gene features pathology of autosomal dominant optic atrophy. Brain. 2007;130:1029–42.
179. Davies VJ, Hollins AJ, Piechota MJ, Yip W, Davies JR, White KE, et al. Opa1 deficiency in a mouse model of autosomal dominant optic atrophy impairs mitochondrial morphology, optic nerve structure and visual function. Hum Mol Genet. 2007;16:1307–18.
180. Yarosh W, Monserrate J, Tong JJ, Tse S, Le PK, Nguyen K, et al. The molecular mechanisms of OPA1-mediated optic atrophy in Drosophila model and prospects for antioxidant treatment. PLoS Genet. 2008;4:e6.
181. Li Z, Okamoto K, Hayashi Y, Sheng M. The importance of dendritic mitochondria in the morphogenesis and plasticity of spines and synapses. Cell. 2004;119:873–87.
182. Williams PA, Morgan JE, Votruba M. Opa1 deficiency in a mouse model of dominant optic atrophy leads to retinal ganglion cell dendropathy. Brain. 2010;133:2942–51.
183. Williams PA, Piechota M, von Ruhland C, Taylor E, Morgan JE, Votruba M. Opa1 is essential for retinal ganglion cell synaptic architecture and connectivity. Brain. 2012;135:493–505.
184. Klein JA, Longo-Guess CM, Rossmann MP, Seburn KL, Hurd RE, Frankel WN, et al. The harlequin mouse mutation downregulates apoptosis-inducing factor. Nature. 2002;419:367–74.
185. Bouaita A, Augustin S, Lechauve C, Cwerman-Thibault H, Bénit P, Simonutti M, et al. Downregulation of apoptosis-inducing factor in Harlequin mice induces progressive and severe optic atrophy which is durably prevented by AAV2-AIF1 gene therapy. Brain. 2012;135:35–52.
186. DiMauro S, Schon EA. Mitochondrial disorders in the nervous system. Annu Rev Neurosci. 2008;31:91–123.
187. Jun AS, Brown MD, Wallace DC. A mitochondrial DNA mutation at nucleotide pair 14459 of the NADH dehydrogenase subunit 6 gene associated with maternally inherited Leber hereditary optic neuropathy and dystonia. Proc Natl Acad Sci U S A. 1994;91:6206–10.
188. Kirby DM, Kahler SG, Freckmann ML, Reddihough D, Thorburn DR. Leigh disease caused by the mitochondrial DNA G14459A mutation in unrelated families. Ann Neurol. 2000;48:102–4.
189. Santorelli FM, Tanji K, Kulikova R, Shanske S, Vilarinho L, Hays AP, et al. Identification of a novel mutation in the mtDNA ND5 gene associated with MELAS. Biochem Biophys Res Commun. 1997;238:326–8.
190. Corona P, Antozzi C, Carrara F, D'Incerti L, Lamantea E, Tiranti V, et al. A novel mtDNA mutation in the ND5 subunit of complex I in two MELAS patients. Ann Neurol. 2001;49:106–10.
191. Sakuta R, Nonaka I. Vascular involvement in mitochondrial myopathy. Ann Neurol. 1989;25:594–601.
192. Cavanagh JB, Harding BN. Pathogenic factors underlying the lesions in Leigh's disease. Tissue

responses to cellular energy deprivation and their clinico-pathological consequences. Brain. 1994;117: 1357–76.
193. Barrett TG, Bundey SE, Macleod AF. Neurodegeneration and diabetes: UK nationwide study of Wolfram (DIDMOAD) syndrome. Lancet. 1995;346: 1458–63.
194. Scolding NJ, Kellar-Wood HF, Shaw C, et al. Wolfram syndrome: hereditary diabetes mellitus with brainstem and optic atrophy. Ann Neurol. 1996;39:352–60.
195. Hardy C, Khanim F, Torres R, et al. Clinical and molecular genetic analysis of 19 Wolfram syndrome kindreds demonstrating a wide spectrum of mutations in WFS1. Am J Hum Genet. 1999;65: 1279–90.
196. Kinsley BT, Swift M, Dumont RH, et al. Morbidity and mortality in the Wolfram syndrome. Diabetes Care. 1995;18:1566–70.
197. Ito S, Sakakibara R, Hattori T. Wolfram syndrome presenting marked brain MR imaging abnormalities with few neurologic abnormalities. AJNR Am J Neuroradiol. 2007;28:305–6.
198. Sylvestor PE. Some unusual findings in a family with Friedreich ataxia. Arch Dis Child. 1958;33: 217–21.
199. Jensen PK, Reske-Nielsen E, Hein-Sørensen O, Warburg M. The syndrome of opticoacoustic nerve atrophy with dementia. Am J Med Genet. 1987;28:517–8.
200. Hagemoser K, Weinstein J, Bresnick G, Nellis R, Kirkpatrick S, Pauli RM. Optic atrophy, hearing loss, and peripheral neuropathy. Am J Med Genet. 1989;33:61–5.
201. Barrientos A, Volpini V, Casademont J, et al. A nuclear defect in the 4p16 region predisposes to multiple mitochondrial DNA deletions in families with Wolfram syndrome. J Clin Invest. 1996;97:1570–6.
202. Takei D, Ishihara H, Yamaguchi S, Yamada T, Tamura A, Katagiri H, et al. WFS1 protein modulates the free Ca(2+) concentration in the endoplasmic reticulum. FEBS Lett. 2006;16(580):5635–40.
203. Rotig A, Cormier V, Chatelain P, et al. Deletion of mitochondrial DNA in a case of early-onset diabetes mellitus, optic atrophy, and deafness (Wolfram syndrome, MIM 222300). J Clin Invest. 1993;91: 1095–8.
204. Durr A, Cossee M, Agid Y, et al. Clinical and genetic abnormalities in patients with Friedreich's ataxia. N Engl J Med. 1996;335:1169–75.
205. Harding AE. Friedreich's ataxia: a clinical and genetic study of 90 families with an analysis of early diagnostic criteria and intrafamilial clustering of clinical features. Brain. 1981;104:589–620.
206. Fortuna F, Barboni P, Liguori R, Valentino ML, Savini G, Gellera C, et al. Visual system involvement in patients with Friedreich's ataxia. Brain. 2009;132:116–23.
207. Camacho LM, Wenzel W, Aschoff JC. The pattern-reversal visual evoked potential in the clinical study of lesions of the optic chiasm and visual pathway. Adv Neurol. 1982;32:49–59.
208. Boyer IV SH, Chisolm AW, McKusick VA. Cardiac aspects of Friedreich's ataxia. Circulation. 1962;25: 493–505.
209. Chamberlain S, Shaw J, Rowland A, et al. Mapping of mutation causing Friedreich's ataxia to human chromosome 9. Nature. 1988;334:248–50.
210. Fujita R, Agid Y, Trouillas P, et al. Confirmation of linkage of Friedreich ataxia to chromosome 9 and identification of a new closely linked marker. Genomics. 1989;4:110–1.
211. Forrest SM, Knight M, Delatycki MB, et al. The correlation of clinical phenotype in Friedreich ataxia with the site of point mutations in the FRDA gene. Neurogenetics. 1998;1:253–7.
212. Koeppen AH. The hereditary ataxias. J Neuropathol Exp Neurol. 1998;57:531–43.
213. Voncken M, Ioannou P, Delatycki MB. Friedreich ataxia: update on pathogenesis and possible therapies. Neurogenetics. 2004;5:1–8.
214. Harding AE. Classification of the hereditary ataxias and paraplegias. Lancet. 1983;1:1151–5.
215. Casari G, De Fusco M, Ciarmatori S, Zeviani M, Mora M, Fernandez P, et al. Spastic paraplegia and OXPHOS impairment caused by mutations in paraplegin, a nuclear-encoded mitochondrial metalloprotease. Cell. 1998;93:973–83.
216. Züchner S, Mersiyanova IV, Muglia M, Bissar-Tadmouri N, Rochelle J, Dadali EL, et al. Mutations in the mitochondrial GTPase mitofusin 2 cause Charcot-Marie-Tooth neuropathy type 2A. Nat Genet. 2004;36:449–51.
217. Züchner S, De Jonghe P, Jordanova A, Claeys KG, Guergueltcheva V, Cherninkova S, et al. Axonal neuropathy with optic atrophy is caused by mutations in mitofusin 2. Ann Neurol. 2006;59:276–81.
218. Waterham HR, Koster J, van Roermund CW, Mooyer PA, Wanders RJ, Leonard JV. A lethal defect of mitochondrial and peroxisomal fission. N Engl J Med. 2007;356:1736–41.
219. Dyck PJ, Chance P, Lebo R, et al. Hereditary motor and sensory neuropathies. In: Dyck PJ, Thomas PK, Griffin JW, Low PA, Poduslo JF, editors. Peripheral neuropathy, vol. 2. Philadelphia, PA: Saunders; 1993. p. 1094–123.
220. Voo I, Allf BE, Udar N, et al. Hereditary motor and sensory neuropathy type VI with optic atrophy. Am J Ophthalmol. 2003;136:670–7.
221. Pizzatto MR, Pascual-Castroviejo I. Sindrome de Behr. Presentacion de siete casos. Rev Neurol. 2001;32:721–4.
222. Horoupian DS, Zucker DK, Moshe S, et al. Behr syndrome: a clinicopathologic report. Neurology. 1979;29:323–7.
223. Gillis L, Kaye E. Diagnosis and management of mitochondrial diseases. Pediatr Clin. 2002;49: 203–19.
224. Georgy BA, Snow RD, Brogdon BG, Wertelecki W. Neuroradiologic findings in Marinesco-Sjögren syndrome. AJNR Am J Neuroradiol. 1998;19:281–3.

225. Delague V, Bareil C, Bouvagnet P, Salem N, Chouery E, Loiselet J, et al. A new autosomal recessive non-progressive congenital cerebellar ataxia associated with mental retardation, optic atrophy, and skin abnormalities (CAMOS) maps to chromosome 15q24-q26 in a large consanguineous Lebanese Druze family. Neurogenetics. 2002;4:23–7.
226. Nicolaides P, Appleton RE, Fryer A. Cerebellar ataxia, areflexia, pes cavus, optic atrophy, and sensorineural hearing loss (CAPOS): a new syndrome. J Med Genet. 1996;33:419–21.
227. Felicio AC, Godeiro-Junior C, Alberto LG, Pinto AP, Sallum JM, Teive HG, et al. Familial Behr syndrome-like phenotype with autosomal dominantinheritance. Parkinsonism Relat Disord. 2008; 14:370–2.
228. Sheffer RN, Zlotogora J, Elpeleg ON, Raz J, Ben-Ezra D. Behr's syndrome and 3-methylglutaconic aciduria. Am J Ophthalmol. 1992;114:494–7.
229. Anikster Y, Kleta R, Shaag A, Gahl WA, Elpeleg O. Type III 3-methylglutaconic aciduria (optic atrophy plus syndrome, or Costeff optic atrophy syndrome): identification of the OPA3 gene and its founder mutation in Iraqi Jews. Am J Hum Genet. 2001;69: 1218–24.
230. Ho G, Walter JH, Christodoulou J. Costeff optic atrophy syndrome: new clinical case and novel molecular findings. J Inherit Metab Dis. 2008;31: S419–23.
231. Costeff H, Gadoth N, Apter N, et al. A familial syndrome of infantile optic atrophy, movement disorder, and spastic paraplegia. Neurology. 1989;39:595–7.
232. Orr HT, Chung MY, Banfi S, et al. Expansion of an unstable trinucleotide CAG repeat in spinocerebellar ataxia type 1. Nat Genet. 1993;4:221–6.
233. Burk K, Abele M, Fetter M, et al. Autosomal dominant cerebellar ataxia type I clinical features and MRI in families with SCA1, SCA2 and SCA3. Brain. 1996;119:1497–505.
234. Buttner N, Geschwind D, Jen JC, et al. Oculomotor phenotypes in autosomal dominant ataxias. Arch Neurol. 1998;55:1353–7.
235. Robitaille Y, Schut L, Kish SJ. Structural and immunocytochemical features of olivoponto-cerebellar atrophy caused by the spinocerebellar ataxia type 1 (SCA-1) mutation define a unique phenotype. Acta Neuropathol. 1995;90:572–81.
236. Vig PJ, Subramony SH, Burright EN, et al. Reduced immunoreactivity to calcium-binding proteins in Purkinje cells precedes onset of ataxia in spinocerebellar ataxia-1 transgenic mice. Neurology. 1998;50: 106–13.
237. Iwashita H, Inoue N, Araki S, et al. Optic atrophy, neural deafness, and distal neurogenic amyotrophy: report of a family with two affected siblings. Arch Neurol. 1970;22:357–64.
238. Rosenberg RN, Chutorian A. Familial opticoacoustic nerve degeneration and polyneuropathy. Neurology. 1967;17:827–32.
239. Kim H-J, Hong SH, Ki C-S, et al. A novel locus for X-linked recessive CMT with deafness and optic neuropathy maps to Xq21.32-q24. Neurology. 2005;64: 1964–7.
240. Slaugenhaupt SA, Blumenfeld A, Gill SP, et al. Tissue-specific expression of a splicing mutation in the IKBKAP gene causes familial dysautonomia. Am J Hum Genet. 2001;68:598–605.
241. Riley CM, Day RL, Greeley DM, et al. Central autonomic dysfunction with defective lacrimation: report of five cases. Pediatrics. 1949;3:468–78.
242. Pearson J, Pytel BA, Grover-Johnson N, et al. Quantitative studies of dorsal root ganglia and neuropathologic observations on spinal cords in familial dysautonomia. J Neurol Sci. 1978;35:77–92.
243. Axelrod FB, Pearson J, Tepperberg J, et al. Congenital sensory neuropathy with skeletal dysplasia. J Pediatr. 1983;102:727–30.
244. Rizzo 3rd JF, Lessell S, Liebman SD. Optic atrophy in familial dysautonomia. Am J Ophthlamol. 1986; 102:463–7.
245. Groom M, Kay MD, Corrent GF. Optic neuropathy in familial dysautonomia. J Neuroophthalmol. 1997; 17:101–2.
246. Schnitzler A, Witte OW, Kunesch E, et al. Early-onset multisystem degeneration with central motor, autonomic and optic nerve disturbances: unusual Riley-Day syndrome or new clinical entity? J Neurol Sci. 1998;154:205–8.
247. Salonen R, Somer M, Haltia M, et al. Progressive encephalopathy with edema, hypsarrhythmia, and optic atrophy (PEHO syndrome). Clin Genet. 1991; 39:287–93.
248. Scott HS, Bunge S, Gal A, et al. Molecular genetics of mucopolysaccharidosis type I: diagnostic, clinical, and biological implications. Hum Mutat. 1995;6:288–302.
249. Collins ML, Traboulsi EI, Maumenee IH. Optic nerve head swelling and optic atrophy in the systemic mucopolysaccharidoses. Ophthalmology. 1990;97: 1445–9.
250. Hall CW, Liebaers I, Di Natale P, et al. Enzymic diagnosis of the genetic mucopolysac-charide storage disorders. Methods Enzymol. 1978;50: 439–56.
251. Fairbairn LJ, Lashford LS, Spooncer E, et al. Long-term in vitro correction of alpha-L-iduronidase deficiency (Hurler syndrome) in human bone marrow. Proc Natl Acad Sci. 1996;93:2025–30.
252. Somer M. Diagnostic criteria and genetics of the PEHO syndrome. J Med Genet. 1993;30:932–6.
253. Morgan NV, Westaway SK, Morton JE, et al. PLA2G6, encoding a phospholipase A(2), is mutated in neurodegenerative disorders with high brain iron. Nat Genet. 2006;38:752–4.
254. Farina L, Nardocci N, Bruzzone MG, et al. Infantile neuroaxonal dystrophy: neuroradio-logical studies in 11 patients. Neuroradiology. 1999;41:376–80.
255. Aicardi J, Castelein P. Infantile neuroaxonal dystrophy. Brain. 1979;102:727–48.

256. Schaumburg HH, Powers JM, Raine CS, et al. Adrenoleukodystrophy: a clinical and pathological study of 17 cases. Arch Neurol. 1975;32:577–91.
257. Aubourg P, Chaussain JL, Dulac O, et al. Adrenoleukodystrophy in children: apropos of 20 cases. Arch Fr Pediatr. 1982;39:663–9.
258. Moser HW, Moser AB, Frayer KK, et al. Adrenoleukodystrophy: increased plasma content of saturated very long chain fatty acids. Neurology. 1981;31:1241–9.
259. Kolodny EH. The adrenoleukodystrophy-adrenomyeloneuropathy complex: is it treatable? [Editorial]. Ann Neurol. 1987;21:230–1.
260. Aubourg P, Blanche S, Jambaque I, et al. Reversal of early neurologic and neuroradiologic manifestations of X-linked adrenoleukodystrophy by bone marrow transplantation. N Engl J Med. 1990;322:1860–6.
261. Malm G, Ringden O, Anvret M, et al. Treatment of adrenoleukodystrophy with bone marrow transplantation. Acta Paediatr. 1997;86:484–92.
262. Percy AK, Brady RO. Metachromatic leukodystrophy: diagnosis with samples of venous blood. Science. 1968;161:594–5.
263. Austin J, McAfee D, Armstrong D, et al. Abnormal sulphatase activities in two human diseases (metachromatic leukodystrophy and gargoylism). Biochem J. 1964;93:15C–7.
264. Bayever E, Ladisch S, Philippart M, et al. Bone marrow transplantation for meta-chromatic leukodystrophy. Lancet. 1985;II:471–3.
265. Krivit W, Shapiro E, Kennedy W, et al. Treatment of late infantile metachromatic leukodys-trophy by bone marrow transplantation. N Engl J Med. 1990; 322:28–32.
266. Zlotogora J, Chakraborty S, Knowlton RG, et al. Krabbe disease locus mapped to chromosome 14 by genetic linkage. Am J Hum Genet. 1990;47:37–44.
267. D'Agostino AN, Sayre GP, Hayles AB. Krabbe's disease: globoid cell type of leukodystrophy. Arch Neurol. 1963;8:82–96.
268. Husain AM, Altuwaijri M, Aldosari M. Krabbe disease: neurophysiologic studies and MRI correlations. Neurology. 2004;63:617–20.
269. Krivit W, Shapiro EG, Peters C, et al. Hematopoietic stem-cell transplantation in globoid cell leukodystrophy. N Engl J Med. 1998;338:1119–26.
270. Renier WO, Gabreels FJM, Hustinx TWJ, et al. Connatal Pelizaeus-Merzbacher disease with congenital stridor in two maternal cousins. Acta Neuropathol. 1981;54:11–7.
271. Schinzel A, Boltshauser E, Wichmann W, Haller D, et al. Pelizaeus-Merzbacher disease: magnetic resonance imaging as a potential tool for carrier detection [Abstract]. J Med Genet. 1988;25:276–7.
272. Kaul R, Gao GP, Balamurugan K, Matalon R. Cloning of the human aspartoacylase cDNA and a common missense mutation in Canavan disease. Nat Genet. 1993;5:118–23.
273. Matalon R, Michals K, Sebesta D, et al. Aspartoacylase deficiency and N-acetylaspartic aciduria in patients with Canavan disease. Am J Med Genet. 1988;29:463–71.
274. Matalon R, Kaul R, Casanova J, et al. Aspartoacylase deficiency: the enzyme defect in Canavan disease. J Inherit Metab Dis. 1989;12:329–31.
275. Wittsack HJ, Kugel H, Roth B, et al. Quantitative measurements with localized 1H MR spectroscopy in children with Canavan's disease. J Magn Reson Imaging. 1996;6:889–93.

Congenital Disc Anomalies

8

Jane W. Chan

Congenitally Anomalous Disc Size

Optic Nerve Hypoplasia

Optic nerve hypoplasia is the most common congenital optic disc anomaly and is a common cause of congenital blindness. The increased prevalence of this disorder reflects its greater recognition by ophthalmologists and possibly the increased incidence of alcohol and drug abuse. It may be unilateral or bilateral, and may occur with or without any associated neurological or ocular abnormalities [1].

Optic nerve hypoplasia is an abnormally small optic nerve head that may appear gray or pale because of a decreased number of optic nerve axons with normal glial tissue [2]. The optic disc is surrounded by a yellowish peripapillary ring of sclera and an outer concentric ring of hyper- or hypopigmentation, known as the "double-ring" sign. The outer ring is located at the normal junction between the sclera and lamina cribosa. The inner ring represents the abnormal extension of retina and pigment epithelium into the outer aspects of the lamina cribosa. The surrounding large retinal veins are usually tortuous (Fig. 8.1) [3].

J.W. Chan, M.D. (✉)
Department of Neurology, Neuro-Ophthalmology,
University of Nevada School of Medicine,
975 Kirman Avenue (111), Reno, Nevada 89502, USA
e-mail: worjun@aol.com

The diagnosis of optic nerve hypoplasia is based upon small optic discs, decreased or normal vision, and visual field defects with corresponding nerve fiber bundle defects. Visual acuity ranges from 20/20 to no light perception. Localized defects with peripheral constriction are common. Visual acuity is determined mainly by the integrity of the papillomacular bundle and does not correlate with the size of the optic disc [4, 5].

Astigmatism is associated with optic nerve hypoplasia [6]. Visual evoked potentials (VEP) may be normal or abnormal. Unilateral or bilateral optic nerve hypoplasia may be associated with central nervous system (CNS) malformations [7], especially forebrain malformations and endocrinological abnormalities [8], as in septo-optic dysplasia (de Morsier syndrome) [3]. Focal thinning or absence of the side of the chiasm corresponding to the hypoplastic optic disc can be seen on magnetic resonance imaging (MRI). In bilateral optic nerve hypoplasia, the optic chiasm is atrophied and the prechiasmatic intracranial optic nerve corresponding to the hypoplastic disc is thinned. The diagnosis of optic nerve hypoplasia may be presumed based upon diminished intracranial optic nerves with other neuroradiologic features of septo-optic dysplasia [9].

Other CNS malformations associated with optic nerve hypoplasia include abnormalities in the cerebral hemispheres and the pituitary infundibulum [1, 8]. Hemispheric migration abnormalities, such as schizencephaly and cortical heterotopia, and hemispheric injury, such as periventricular

J.W. Chan (ed.), *Optic Nerve Disorders: Diagnosis and Management*,
DOI 10.1007/978-1-4614-0691-4_8,

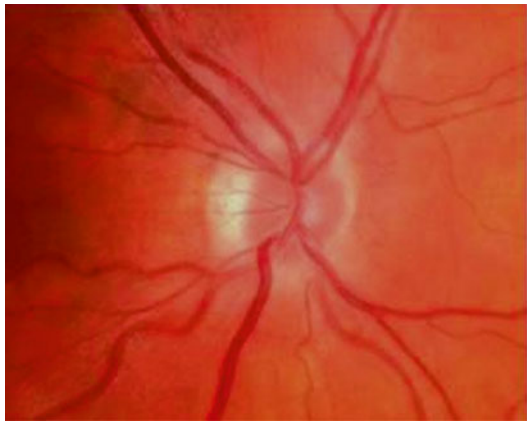

Fig. 8.1 Optic disc hypoplasia. Choroidal atrophy surrounds pink area of hypoplastic disc. Reprinted from Atlas of Ophthalmology. http://www.atlasophthalmology.com. Accessed June 11, 2012. With permission from Online Journal of Ophthalmology

leukomalacia and encephalomalacia, may occur in 45 % of patients with optic nerve hypoplasia [8]. Fifteen percent of patients with optic nerve hypoplasia may have perinatal injury of the pituitary infundibulum leading to necrosis. This brain abnormality is seen as posterior pituitary ectopia on MRI, in which the normal posterior pituitary hyperintensity is absent and an ectopic posterior pituitary hyperintensity is seen in place of the necrosed pituitary infundibulum [1, 8]. Posterior pituitary ectopia is pathognomonic of anterior pituitary hormonal deficiency with normal posterior pituitary function. The absence of a normal or ectopic posterior pituitary is associated with antidiuretic hormone deficiency. The type of hormonal deficiency may evolve over time in some patients. Growth hormone deficiency is most often associated with optic nerve hypoplasia. Hypothyroidism, hypocortisolism, panhypopituitarism, diabetes insipidus, and hyperprolactinemia may also occur [10–12]. Cerebral hemispheric abnormalities that are often associated with thinning or agenesis of the corpus callosum are predictive of neurodevelopmental defects [7]. Optic nerve hypoplasia with an intact septum pellucidum may be associated with pituitary hormonal deficiencies [7].

Based on studies with high resolution neuroimaging, it has been shown that early gestational CNS injury can disrupt optic nerve development [1, 7, 13, 14]. Mass lesions, such as a prenatal suprasellar tumor, may interfere with the normal migration of optic axons to their target sites [15]. Intrauterine injuries to midline CNS structures, such as the septum pellucidum and pituitary infundibulum, can injure or disrupt the migrating axons of the optic nerve [16]. This injury results in direct or trans-synaptic retrograde degeneration to cause segmental hypoplasia of both optic nerves [7, 15–17].

Megalopapilla

Megalopapilla refers to an enlarged optic disc with no other morphological abnormalities. In the more common phenotypic variant, megalopapilla more commonly is bilateral. The disc is greater than 2.1 mm in diameter, with an increased cup-to-disc ratio that may mimic normal tension glaucoma [18]. The cupping is usually round or horizontally oval without focal notching of the rim [19]. The axons are spread over a larger surface area causing the neuroretinal rim to appear pale [20]. The less common variant of megalopapilla is unilateral. An anomalous superior excavation obliterates the adjacent neuroretinal rim. This variant is distinguished from a colobomatous disc in which the excavation is located inferiorly on the disc and may be associated with other congenital abnormalities (Fig. 8.2).

In contrast to normal tension glaucoma or compressive optic atrophy, the visual acuity is usually normal or mildly decreased and is often associated with an enlarged blind spot. The differential diagnosis of megalopapilla includes glaucoma, optic disc coloboma, and orbital optic glioma [21].

Megalopapilla may rarely be seen with other congenital abnormalities, such as basal encephalocele and midline facial anomalies [22].

Segmental Optic Nerve Hypoplasia

Superior segmental optic nerve hypoplasia may occur in children of insulin-dependent diabetic mothers. These children have no other systemic

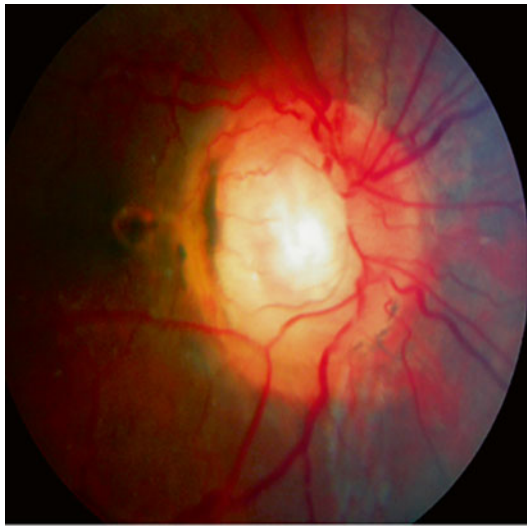

Fig. 8.2 Megalopapilla. Courtesy of Frank Lee

anomalies and present with incidental inferior visual field defects of segmental optic nerve hypoplasia. Characteristic features include superior entrance of the central retinal artery, superior disc pallor, superior peripapillary halo, and superior peripapillary nerve fiber layer thinning. These funduscopic signs are all suggestive of maternal diabetes [5, 23–25].

Homonymous Hemioptic Hypoplasia

Congenital lesions affecting the retina, optic nerve, chiasm, tract, or retrogeniculate pathways are associated with segmental hypoplasia of the corresponding sections of each optic nerve. Unilateral congenital hemispheric lesions affecting the postchiasmal afferent visual pathways may cause homonymous hemioptic hypoplasia. Trans-synaptic degeneration of the optic tract from a retrogeniculate lesion results in homonymous hemioptic hypoplasia, which leads to segmental hypoplasia of the nasal and temporal aspects of the optic disc contralateral to the hemispheric lesion. This optic disc may have horizontal, or "bowtie," pallor. The disc ipsilateral to the hemispheric lesion may be normal to mildly hypoplastic [13, 16, 26].

Congenital Tilted Disc Syndrome

The congenital tilted disc syndrome equally affects men and women in 1–2 % of the population and shows no particular hereditary pattern [27]. It has not been significantly associated with any systemic or neurological disorders. The tilted disc syndrome presents with the following characteristic features: (1) inferonasal "tilting" of the disc with an associated inferonasal crescent (conus); (2) hypoplasia of the retinal pigment epithelium (RPE), and choroid in the inferonasal fundus; (3) posterior staphyloma in the inferonasal region; and (4) situs inversus [28, 29].

The congenital tilted disc syndrome is considered a coloboma that varies in appearance depending upon the degree of malclosure of the embryonic ocular fissure. In the fourth week of gestation, the optic sulci begin to form and grow toward the ectoderm to form the optic vesicles. As the optic vesicle reaches the ectoderm, the distal face invaginates to form a goblet-shaped optic cup that is attached to the forebrain by the optic stalk [30]. This invagination with incomplete closure often results in a coloboma of the optic disc, retina, RPE, and choroids. Because the embryonic ocular fissure closes last in the inferior to inferior nasal aspect, most colobomas arise in this region. The congenital tilted disc syndrome is thought to result from incomplete closure of the ocular fissure at 6 weeks gestation with the formation of a typical coloboma of the disc, peripapillary retina, RPE, and choroids [28, 29, 31, 32].

The optic disc only appears to be tilted without actual rotation (Fig. 8.3) [3]. The superotemporal aspect is elevated and the inferonasal region is posteriorly positioned to form an oval-shaped disc with its long axis obliquely oriented. No actual rotation of the disc occurs in this syndrome. The congenital absence of inferonasal tissue that forms the coloboma gives the appearance that the inferior pole of the disc has been rotated. The superior aspect of the disc appears to be dislocated to the superonasal quadrant. Neural tissue is concentrated at the superior and superior temporal aspect of the disc, whereas the inferior and

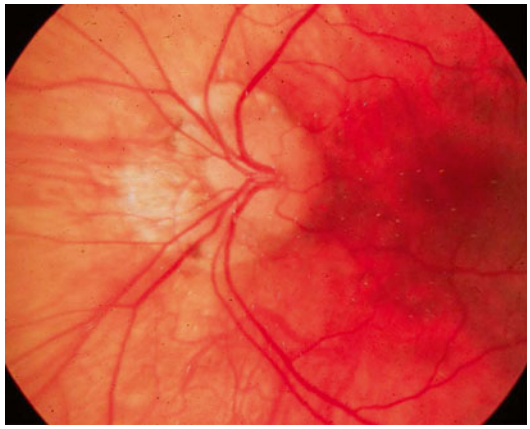

Fig. 8.3 Congenital tilted disc syndrome. Disc is tilted nasally with the disc vessels exiting nasally. Inverse conus is also located nasally. Reprinted from Atlas of Ophthalmology. http://www.atlasophthalmology.com. Accessed June 11, 2012. With permission from Online Journal of Ophthalmology

Table 8.1 Clinical features of the congenital tilted disc syndrome

Congenital tilted disc syndrome is bilateral and nonhereditary.
Myopia is mild to moderate associated with astigmatism, often with an oblique axis.
Myopia is nonprogressive, as in acquired high myopia.
Disc appears tilted inferiorly and nasally.
Inferior or inferonasal crescent or conus is usually present (Fuch's coloboma).
Blood vessels emerge from the temporal rather than the nasal aspect of the disc and course nasally before extending outward in the usual temporal distribution (situs inversus).
Inferonasal fundus appears pale from RPE hypoplasia.
Posterior, inferonasal staphyloma can be confirmed by computed tomography (CT) scan or B-scan ultrasound.
Superior temporal or bitemporal visual field defect that does not respect the vertical meridian and corresponds to the area of the inferonasal defect of the optic nerve and retina.
ERG response is sometimes decreased.

Reprinted from Apple DJ, Rabb MF, Walsh PM. Congenital anomalies of the optic disc. Surv Ophthalmol 1982;27(1):3–41. With permission from Elsevier

inferior nasal aspect is deficient in axons. The inferior nasal aspect of the disc is hollowed out and forms an inferonasal conus. The oblique deviation of major retinal vessels toward the inferior crescent contributes to the tilted appearance of the disc. The conus is associated with posterior staphyloma formation and is continuous with an area of hypoplasia of the retina, choroid, and RPE (Table 8.1) [29, 31, 32].

The region of hypoplasia of the retina, choroid, and RPE is associated with acquired, rare complications, especially choroidal and subretinal neovascularization and hemorrhage [33–36]. The staphylomatous formation is thought to cause stretching of the tissues to form lacquer cracks in Bruch's membrane and a localized nidus for the formation of choroidal neovascularization, which can be treated with parafoveal photocoagulation. Visual prognosis is relatively good [36]. Associated neovascular membranes that develop in the peripapillary and parafoveal areas do not usually progress [34]. Other less frequently observed findings include associated medullated nerve fibers, central retinal vein thrombosis, and peripapillary and macular subretinal hemorrhages [33–38].

The appearance of the congenital tilted disc may mimic other acquired ophthalmic syndromes. The lack of nerve fibers in both the disc and inferior peripapillary conus may cause the neuroretinal rim to be nonexistent and may mimic the appearance of notching seen in glaucoma. Furthermore, the inferior conus must be distinguished from the acquired temporal crescent seen in degenerative myopia that enlarges over time [28, 31].

The most common visual field defect seen in the congenital tilted disc syndrome is a superior bitemporal defect not respecting the vertical meridian. It actually represents a refractive scotoma related to the myopia from the inferonasal retina [29]. Larger refractive errors are generally associated with more characteristic presentations of the congenital tilted disc syndrome [37]. The visual field defect may often extend beyond the vertical meridian to form a complete altitudinal defect. Other less common bilateral field defects include arcuate scotomas, blind spot enlargements, and nasal constrictions of the visual field [37–39].

The most common electrophysiological abnormality observed in the congenital tilted disc

syndrome is a delayed latency or no response in the pattern reversal VEP [40, 41]. Reduced amplitude of photopic and scotopic b-waves in the electroretinogram (ERG) and reduced amplitude in the electro-oculogram (EOG) reflect defects of the inner retinal layer in the inferonasal area of hypoplasia [40]. The degree of abnormality of the ERG and EOG is proportional to the degree of hypoplasia. The reduced EOG is particularly associated with fundus hypopigmentation [40].

Ocular and systemic syndromes are associated with the congenital tilted syndrome. The chorioretinal ectasia adjacent with the conus causes the myopic astigmatism with the plus axis oriented parallel to the ectasia [27]. The astigmatic myopia is usually not clinically significant because it is easily correctable and central vision is not usually affected. In contrast to acquired high myopia, the myopia in congenital tilted disc syndrome is not progressive. The congenital tilted disc syndrome has also been reported to be associated with X-linked congenital stationary night blindness [27].

Suprasellar disorders have also been associated with the congenital tilted disc syndrome [42]. Suprasellar tumors have been found in patients with the congenital tilted disc syndrome who present with true bitemporal hemianopsia. These tumors may disrupt axons of the optic nerve during migration in embryogenesis [43]. Therefore, an MRI of the brain with contrast is necessary in any patient with the tilted disc syndrome who has a bitemporal hemianopia that respects the vertical meridian [44].

Excavated Optic Disc Anomalies

Morning Glory Disc Anomaly

The morning glory disc anomaly consists of an optic nerve coloboma associated with retinal vascular anomalies, glial proliferation and metaplasia, and peripapillary pigmentary changes. The embryological origin of this syndrome remains unclear at this time. No hereditary factors have been shown in this condition. The morning glory disc anomaly usually occurs unilaterally in females and rarely in African Americans [45].

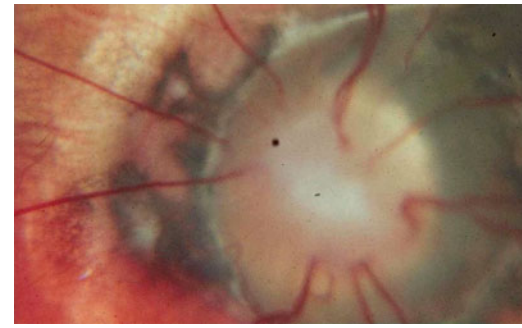

Fig. 8.4 Optic disc with features of both morning glory disc anomaly and peripapillary staphyloma. The central glial tuft, the radially oriented disc vessels, and the peripapillary pigmentary changes are all consistent with the morning glory disc anomaly. The disc is also relatively well defined and appears to be at the bottom of a deep, cup-shaped ectasia. These latter features are suggestive of a peripapillary staphyloma. Reprinted from Atlas of Ophthalmology. http://www.atlasophthalmology.com. Accessed June 11, 2012. With permission from Online Journal of Ophthalmology

The enlarged optic disc is orange-pink and is located centrally within a funnel-shaped peripapillary excavation. White glial proliferative tissue lies over the center. Chorioretinal pigmentation outlines the disc, and anomalous blood vessels emanate radially from the disc (Fig. 8.4) [3]. These vessels may be either large and tortuous with S-loops or abnormally straight, narrow, and branching at sharp angles in the periphery. The macula may occasionally be incorporated into the excavation [45, 46].

Visual acuity is often poor, ranging from 20/200 to finger counting. It is often associated with a myopic astigmatic refractive error [27]. Within the excavated zone, retinal folds and subretinal neovascularization within the surrounding peripapillary pigmentation may be seen. The most common complication of the morning glory disc anomaly is serous retinal detachment, which extends from the peripapillary region to the posterior pole in 26–38 % of patients [47, 48]. This complication can lead to transient to permanent visual loss [47–49]. Spontaneous contractile movements attributed to fluctuations in fluid volume between the subretinal and subarachnoid

spaces [45] and transient dilation of retinal veins [49] have been reported.

The morning glory disc anomaly can be associated with a transsphenoidal encephalocele [22, 50–52], which consists of midfacial deformities, including hypertelorism, depressed nasal bridge, upper lid notch, cleft palate, and herniation of pituitary-hypothalamic structures into an osseous defect in the anterior skull base. The optic chiasm may be absent in one-third of patients, but most have panhypopituitarism [53]. About three-fourths of patients with transsphenoidal encephalocele have absence of an optic chiasm, callosal agenesis associated with posterior dilatation of the lateral ventricles [54]. This midline congenital pouch, usually containing the chiasm and adjacent hypothalamus, protrudes through the sphenoid bone and into the nasopharynx to cause rhinorrhea, mouth-breathing, and snoring [54].

Because hypoplasia of the ipsilateral intracranial vasculature [55] may be associated with the morning glory disc anomaly, MR angiography should be performed. This hypoplasia may occur with or without Moyamoya syndrome [56].

The morning glory disc anomaly may be associated with ipsilateral orofacial hemangioma as part of the PHACE (posterior fossa malformations, large facial hemangioma, arterial anomalies, cardiac anomalies and aortic coarctation; and eye anomalies) syndrome affecting only females [57].

Optic Disc Coloboma

The optic disc coloboma may occur unilaterally or bilaterally with equal frequency [58]. Unlike the morning glory disc anomaly, there is no predilection for race or sex. The inheritance pattern may be sporadic or autosomal dominant [58]. It has been linked to a mutation of the PAX6 gene. Incomplete or abnormal apposition of the proximal end of the embryonic fissure leads to the development of an optic disc coloboma. The excavation represents the position of the embryonic fissure relative to the primitive epithelial papilla [58].

An optic disc coloboma appears as a well-demarcated white excavation lying within an enlarged optic disc. This excavation is off-centered and lies inferiorly within the disc, distinguishing it from the morning glory disc that lies centrally within the excavation (Fig. 8.5) [3]. The inferior neuroretinal rim is thin or absent, and the superior neuroretinal rim is relatively spared. In contrast to the morning glory disc anomaly, there is no central glial tuft, no anomalous retinal vasculature, and only minimal peripapillary pigmentary changes. If the defect extends inferiorly to involve the adjacent retina and choroid, then microphthalmia, and iris and ciliary colobomas, may form [58].

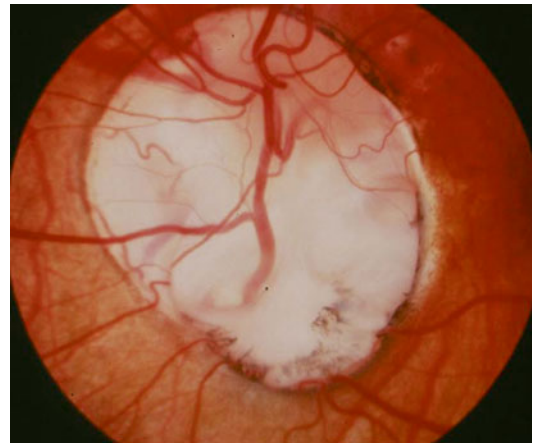

Fig. 8.5 Optic disc coloboma. A *white* excavated area located below a crescent of neuroretinal rim tissue which corresponds to the superior quadrant of the anomalous optic disc. Reprinted from Atlas of Ophthalmology. http://www.atlasophthalmology.com. Accessed June 11, 2012. With permission from Online Journal of Ophthalmology

Visual loss is variable and difficult to predict based upon disc appearance. Contractile movements from intrascleral smooth muscle arranged concentrically around the distal optic nerve have also been rarely reported in patients with optic disc colobomas [59–62]. Serous macular detachment can develop in patients with optic disc colobomas; these are nonrhegmatogenous, and spontaneous reattachment has been known to occur [62, 63].

Differing from the morning glory disc anomaly, optic disc colobomas may be associated with other multisystemic congenital syndromes, such as CHARGE [64, 65], Walker–Warburg syndrome [66], Goltz focal dermal hypoplasia [66],

Table 8.2 Systemic abnormalities that may be associated with optic disc colobomas

Optic disc colobomas and CNS malformations
Dandy Walker cyst
Arhinencephaly
Anencephaly
Agenesis of the corpus callosum
Sphenoidal encephalocoeles
Optic disc colobomas and chromosomal abnormalities
Trisomy 13–15 (Patau's syndrome)
Trisomy 18 (Edward's syndrome)
Optic disc colobomas and congenital syndromes
Meckel–Gruber syndrome (autosomal recessive): *coloboma*, *microphthalmos*, *cleft palate*, *micrognathia*, *polydactyly*, *renal abnormalities*, *encephalocoele*, *and cryptorchidism*
Goltz syndrome (X-linked dominant): *colobomas*, *focal dermal hypoplasia*, *and variable mental retardation*
Lenz microphthalmia syndrome (X-linked recessive): *colobomas*, *prominent ears*, *skeletal defects*, *and crowded teeth*
CHARGE association: with at least three of the following features:
Coloboma
Heart defects
Atresia of the choanae
Retarded growth and development
Genital hypoplasia
Ear abnormalities and/or hearing loss

Reprinted from Apple DJ, Rabb MF, Walsh PM. Congenital anomalies of the optic disc. Surv Ophthalmol 1982;27(1):3–41. With permission from Elsevier

Aicardi syndrome [67, 68], Goldenhar syndrome [69], and linear sebaceous nevus syndrome [66]. Orbital cysts may also be rarely seen with optic disc colobomas [70].

In the CHARGE syndrome, at least three of the following features must be present for the condition: *c*olobomatous microphthalmia, *h*eart defects, *c*hoanal *a*tresia, *r*etarded growth, *g*enital anomalies, and *e*ar anomalies or deafness (Table 8.2) [71].

Peripapillary Staphyloma

A peripapillary staphyloma appears as a deep, cup-shaped excavation with a relatively normal, well-formed optic disc with some temporal pallor but otherwise normal disc conformation and normal blood vessels. As opposed to the anomalous, poorly defined morning glory disc, the optic disc is located at the bottom of the excavated defect. Unlike the morning glory disc anomaly, central glial tissue and anomalous retinal vasculature are absent. Retinal pigment epithelial and choroidal atrophic changes appear in the walls of the staphyloma. The excavation in the peripapillary staphyloma appears deeper than that of the morning glory disc (Fig. 8.6). Rarely are contractile movements of the walls of the staphyloma observed [72]. Because the optic disc and blood vessels are normally developed, the peripapillary staphyloma formation must occur after the development of these structures. The staphyloma probably occurs during the fifth month of gestation when posterior scleral and neural crest cells are incompletely differentiated. It is believed that normal intraocular pressure may contribute to the herniation of tissue into the weakened scleral wall [72].

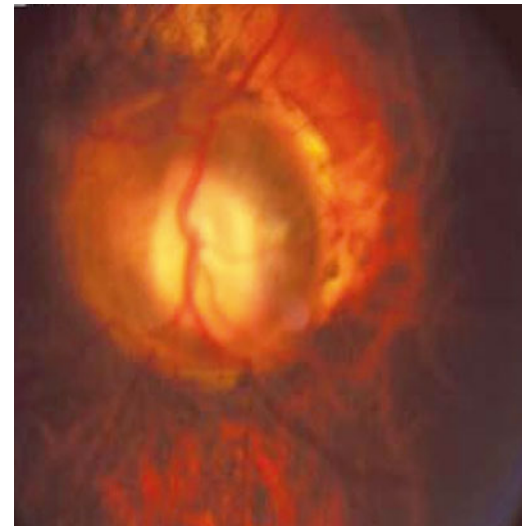

Fig. 8.6 Peripapillary staphyloma. Courtesy of William Eng, M.D.

Visual acuity is usually markedly decreased and is associated with a cecocentral scotoma. Peripapillary staphyloma is not usually associated with other congenital anomalies [72].

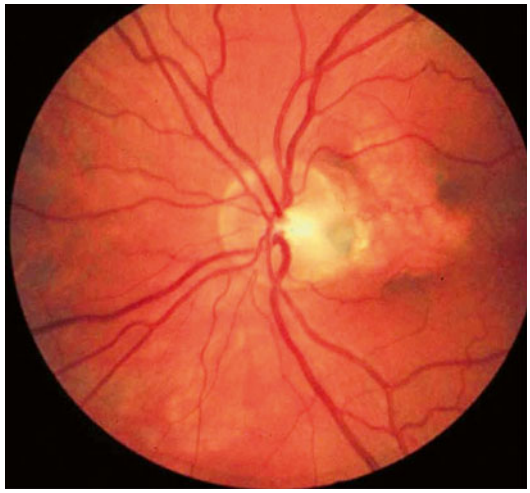

Fig. 8.7 Optic disc pit. The optic disc pit is located in the temporal aspect of the disc and appears to penetrate deeply. Reprinted from Atlas of Ophthalmology. http://www.atlasophthalmology.com. Accessed June 11, 2012. With permission from Online Journal of Ophthalmology

Optic Disc Pit

An optic disc pit is a congenital oval or round depression in the optic nerve head. The incidence of optic disc pits is 1 in 11,000 [73], and it usually occurs sporadically. Most optic disc pits occur unilaterally. Optic pits are formed from the herniation of dysplastic retina into a collagen-lined pocket extending posteriorly, often into the subarachnoid space, through a defect in the lamina cribosa [72]. In contrast to optic disc colobomas, optic pits often occur in locations unrelated to the embryonic fissure and are rarely associated with iris or retinochoroidal colobomas or other systemic anomalies [74].

In unilateral optic pits, the affected disc is slightly larger than the normal one. Optic pits may appear gray, white, or yellowish (Fig. 8.7) [3]. They average about 0.3 disc diameters in width and are often located temporally; 20 % occur centrally and 10 % are located in other regions of the disc [74]. When the pit is located temporally, abnormal peripapillary pigment epithelial changes are often observed. Centrally located pits are associated with temporal disc pallor [74].

Some common mimics of optic disc pits include glaucoma, central serous choroidopathy, presumed ocular histoplasmosis syndrome, astrocytic hamartoma, melanocytoma, and other types of disc colobomas [74].

Visual acuity is usually normal. Approximately 50 % of patients with optic disc pits have visual field defects, which may include a paracentral arcuate scotoma, an enlarged blind spot, a nasal step, a centrocecal scotoma, and generalized constriction [74].

Temporally located pits are usually associated with serous macular detachment and, occasionally, secondary macular edema and macular hole [75, 76]. Larger pits are associated with a higher frequency of serous maculopathy. Macular edema or detachment occurs in about 40–60 % of patients with optic disc pits. Central visual loss from these macular complications develops at 30–40 years of age [75, 76]. Spontaneous reattachment is seen in about 25 % of cases [75], but visual recovery has been observed to be variable [76]. The etiology of the intraretinal fluid associated with optic pits remains controversial.

Cilioretinal arteries emerge from or near the optic disc pit in 59 % of patients. Approximately 18 % of patients have arterial trifurcations [77].

Papillorenal Syndrome

The papillorenal syndrome consists of bilateral anomalous optic discs associated with hypoplastic kidneys [78]. This disorder has been attributed to mutations in the PAX2 gene, in which several families have been reported with similar eye findings and various renal abnormalities [79]. As the eyes and kidneys are the most highly perfused tissues in the body, lack of angiogenesis in the ocular and renal tissues during development may contribute to this malformation. Failure of the hyaloid system to convert to normal central retinal vessels may lead to optic disc and retinal anomalies.

The excavated disc is not a true coloboma. It has a normal diameter with a central excavation and peripheral pigmentation. Cilioretinal vessels emanate from the disc periphery and the central retinal vessels have variable attenuation [80]. The central retinal circulation is absent (Fig. 8.8).

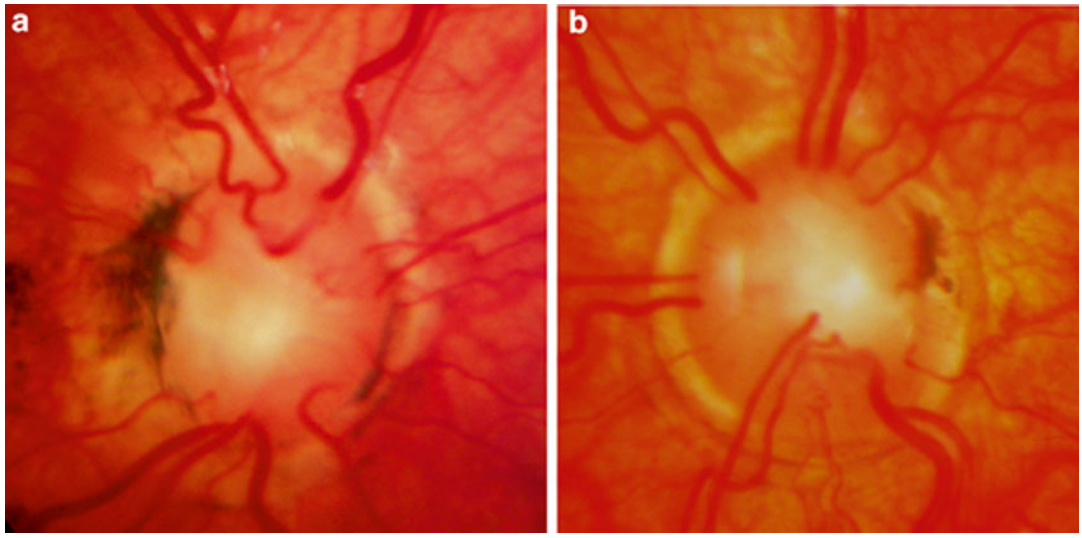

Fig. 8.8 Papillorenal syndrome. Reprinted from Taylor D. Developmental abnormalities of the optic nerve and chiasm. Eye. 2007;21:1271–1284. With permission from Nature Publishing Group

Visual acuity is usually normal and may be decreased by choroidal or retinal hypoplasia or by later complications of retinal detachments. Visual field defects correspond to the regions of retinal hypoplasia [80].

Optic Disc Dysplasia

Optic disc dysplasia refers to a deformed optic disc that cannot be classified in any specific diagnostic category. It is likely that these optic disc variants will be identified as distinct anomalies in the future [27].

Elevated Optic Disc Anomalies

Optic Disc Drusen

Optic disc drusen occurs in 3.4–24 per 1,000 population and occurs bilaterally in about 75 %, and even as high as 91.2 % [81]. Although no sex predilection was found in earlier studies, recent investigations note a higher incidence in females of 61 % [82] and 71 % [81], respectively. It is inherited as an irregularly autosomal dominant disorder [83].

The appearance of optic discs having drusen changes with age. In younger children, the drusen is buried within the optic disc, causing disc elevation [84]. In adults, drusen can be seen superficially and the remainder, about 60 %, is located deep within the papilla [85]. In a study of six patients [86], visual field defects can change as fast as within 2.5 years and as slowly as within 9 years.

It is believed that impaired axonal transport through a small scleral canal can lead to axonal degeneration [87]. Based on electron microscopic findings [88], impaired axonal transport leads to intracellular mitochondrial calcification. Some axons may rupture to release mitochondria in the extracellular space. Calcium continues to deposit in these mitochondria, which gradually degenerate into calcified microbodies to form drusen. Drusen contains calcium [89], mucopolysaccarides [90], amino acid [90], ribonucleic acids [91, 92], deoxyribonucleic acid [92], and iron [90].

Most patients with optic disc drusen are asymptomatic. Rarely is visual acuity severely affected by optic disc drusen. Visual loss may follow severe visual field defects [93]. Transient visual obscurations occur in up to 8.6 % of cases [94], and permanent monocular blindness [95] related to optic disc drusen without vascular

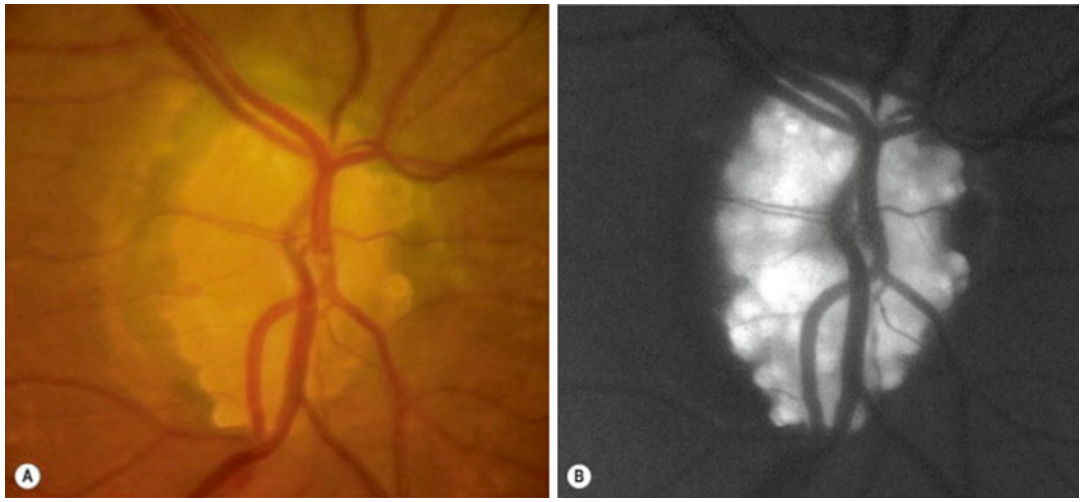

Fig. 8.9 Optic disc drusen. (**a**) Exposed drusen; (**b**) autofluorescence of drusen. Reprinted from Neuro-Ophthalmology. In: Kanski JJ, Bowling B, eds. Clinical Ophthalmology: A Systematic Approach. 7th ed. New York, NY: Elsevier; 2007;796–806. With permission from Elsevier

complications has been documented. When optic disc drusen causes unilateral or asymmetric visual field loss without affecting visual acuity, an afferent pupillary defect can be detected on examination [96]. Visual field defects are usually slowly progressive such that patients are not aware of the deterioration of their visual field [97]; sudden defects may rarely occur. Visual field defects increase in extent and frequency beginning in childhood [98]. In a study by Hoover et al. [98], 18 of 35 eyes in 31 children had an enlarged blind spot; 9 eyes had an inferior arcuate, sector, or altitudinal defect; and 3 eyes had both types of visual field defects. The frequency of visual field defects ranged from 24 to 87 % [97, 99–101] in adults with superficial drusen and prominent visual field defects. The nerve fiber bundle defects detected by Goldmann perimetry in adults include those in the inferior nasal quadrant, enlargement of the blind spot, and peripheral constriction [97, 99]. Most visual loss is in the periphery as a result of arcuate field defects. Blind spot enlargement may be related to concomitant papilledema and vessel leakage [99].

On fundoscopy, drusen may appear buried in the optic disc in children. With increasing age and as calcification progresses with nerve fiber atrophy, the buried drusen become more visible (Figs. 8.9 and 8.10) [100, 101]. In adults, drusen appear as irregular, whitish-yellow crystals within the optic nerve and on the surface of the disc. They are most often in the nasal aspect of the peripapillary area [102, 103]. The disc appears elevated with blurred disc margins, but without obscuration of disc vessels or elevation of the peripapillary nerve fiber layer. Drusen occasionally cannot be visually differentiated from intrapapillary refractile bodies in chronic papilledema [104, 105]. Disc blood vessels may appear in an anomalous pattern [103].

Various diagnostic tests are available to help detect and confirm the presence of drusen. Serial automated visual field testing can help determine progression of field defects that correspond to nerve fiber layer damage from the drusen. B-scan ultrasound can detect deeply buried calcified drusen in the optic nerve head, which is seen as bright areas. Deeper lesions can be visualized because of the highly reflective nature of drusen. B-scan ultrasound has been shown to be the most reliable method of detection of drusen [106]. CT scan is not as sensitive, as the slice thickness is usually 1.5 mm, which may not detect smaller drusen [106].

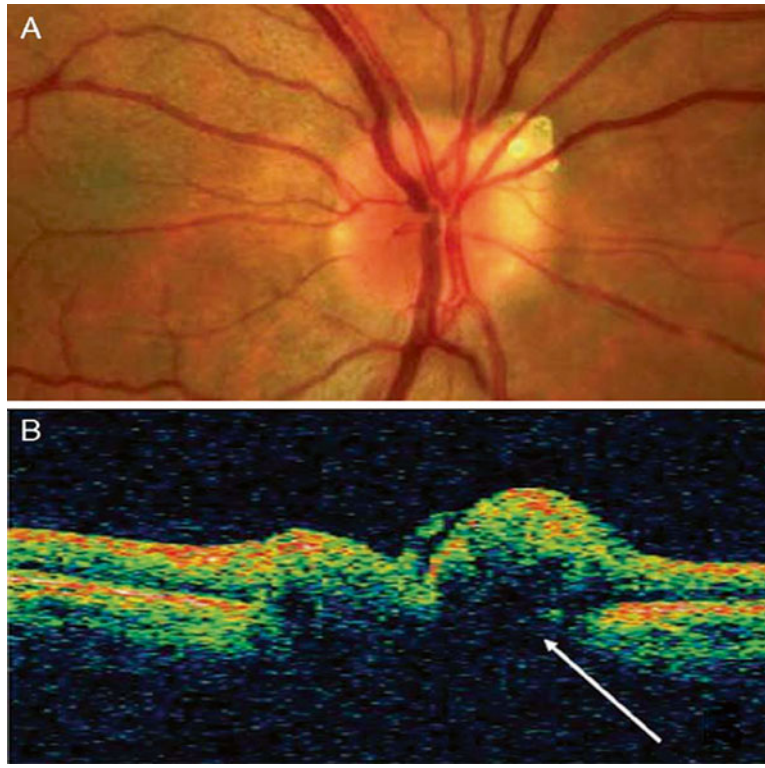

Fig. 8.10 (**a**) Fundus photograph of right optic disc with drusen located in the superior nasal border. (**b**) The Stratus OCT3 (Stratus Optical Coherence Tomography 3; Carl Zeiss Meditec, Dublin, CA) scan of the right optic disc showing an elevated optic nerve head with a low signal region below the surface. Courtesy of Robert Sykes, M.D.

On fluorescein angiography (FA), buried drusen is seen by autofluorescence. The sensitivity of FA is less than that of B-scan ultrasonography [106]. In the late phase of FA, sharply demarcated areas of uneven hyperfluorescence, not usually seen in papilledema, can also be seen.

Optic coherence tomography (OCT) and the GDx scanning laser polarimetry have been used to quantitatively monitor retinal nerve fiber layer (RNFL) loss that could be caused by glaucomatous atrophy obscured by drusen or by optic disc drusen itself. The nerve fiber layer analysis can reveal early subclinical RNFL not visible by fundoscopy. The GDx scanning laser polarimetry has been shown to reliably detect peripapillary thinning associated with optic disc drusen [107].

VEP is abnormal in 41–97 % of patients with optic disc drusen [108, 109] and represents the severity of peripapillary nerve fiber layer damage [108]. Prolongation of the P100 latency seems to depend on degree of visual impairment and check size used for testing [108]. Earlier VEP components can also be fragmented and of lower amplitude. Because of the wide range of VEP abnormalities seen in patients with optic disc drusen, VEP is not a reliable diagnostic modality for drusen [109, 110].

Sudden, substantial visual field defects can occur as a consequence of vascular complications from anomalies of the ophthalmic arteries and veins that are associated with disc drusen [111, 112]. The retinal vessels can be very tortuous and dilated and have abnormal branching with vascular loops [113]. Cilioretinal arteries occur in 20–40 % of patients with disc drusen [113] compared to 15 % in the normal population [112]. Optociliary shunts or venous retinochoroidal collaterals occur in 4–6 % of patients with disc drusen [111]. Disc drusen account for only 10 % of all causes of venous retinochoroidal collaterals [114].

The venous channel between the central retinal and the choroidal circulation may increase with advancing age because of the enlarging drusen that compresses the central retinal vein [115].

Optic disc drusen is associated with a variety of vascular complications. Non-arteritic ischemic optic neuropathy (NAION), occurring in patients with optic disc drusen, is usually related to vaso-occlusion [116]. It affects patients at 20 years of age or less. Optic discs with drusen have smaller diameters than those affected with NAION [117]. The smaller optic nerve canal could lead to more mechanical distortion of blood vessels and would predispose the optic disc to infarction. Enlarging drusen would also cause a compressive ischemia of these vessels [118].

Central retinal artery occlusion and central retinal vein occlusion also occur in a similar manner as in NAION in patients with disc drusen. Compression of the artery or vein by drusen predispose them to visual loss in the setting of risk factors, such as systemic hypertension, contraceptive use, migraine, high altitude, and atrioseptal defect [116, 118–120].

Subretinal neovascularization in young patients with optic disc drusen is usually located adjacent to the disc and may occasionally extend toward the macula. Visual acuity is usually 6/12 or better after hemorrhage from choroidal neovascular membranes that does not require treatment [121].

Retinal hemorrhages without subretinal neovascularization usually occur in association with disc drusen. The frequency of retinal hemorrhage is from 2 to 10 % [122]. These may be splinter hemorrhages within the nerve fibers, hemorrhages of the optic nerve head spreading to the vitreous, deep papillary hemorrhages, or deep peripapillary hemorrhages with or without extension into the macula. Visual outcome is often good. Visual impairment from macular involvement is rare [122]. The etiology of these hemorrhages is not yet clear. Some possible mechanisms include (1) erosion of the disc blood vessels by enlarging drusen, (2) congestion and venous stasis or retinociliary venous communication, and (3) ischemia [123].

Optic disc drusen is associated with retinitis pigmentosa and pseudoxanthoma elasticum and angioid streaks. Retinitis pigmentosa occurs up to 39 %, based on several series [124, 125]. Differing from the idiopathic type, optic disc drusen in retinitis pigmentosa appears adjacent to a normal-diameter disc with a normal scleral canal and a disc that is not elevated [126].

In pseudoxanthoma elasticum, the incidence of disc drusen ranges from 1.4 to 3.6 % [127]. Angioid streaks occur in 85 % of patients with pseudoxanthoma elasticum [126]. Disc drusen ranges from 4.5 to 21.6 % in some series [128]. These two disorders may have a common genetic biochemical defect of abnormal mineralization that predisposes to the development of disc drusen and angioid streaks. In patients with pseudoxanthoma elasticum, the abnormal accumulation of polyanions with high calcium affinity in the elastic fibers may lead to mineralization of the fibers in the lamina cribosa. Elastin mineralization, as in the angioid streaks, and the deposition of abnormal glycosaminoglycans to elastic fibers of the lamina cribosa both lead to thickening of the lamina cribosa. The thickened laminar portion of the optic nerve may impair axonal transport. This altered axonal metabolism can predispose to the formation of optic disc drusen despite a normal-sized optic canal [128].

Treatment for optic disc drusen is often not needed, but monitoring for elevated intraocular pressure and vascular complications as described earlier is recommended. When visual field defects occur, tonometry and visual field examinations should be done regularly. If visual field defects occur with enlargement of optic disc drusen, intraocular pressure-lowering agents should be considered. Optic disc drusen and glaucoma can cause similar types of visual field defects that may be indistinguishable if a patient has both disorders. If the intraocular pressure is elevated in an eye with disc drusen, but without cupping, OCT is recommended to evaluate for RNFL damage [129]. Rarely is surgery ever recommended, but optic nerve sheath decompression was done for visual field loss in 19 eyes, which resulted in significant visual improvement [130].

Vascular occlusions are treated in a similar manner as in situations without disc drusen. Subretinal neovascular membranes are treated only if central vision is affected. Peripapillary choroidal neovascular membranes related to disc drusen regress spontaneously and do not need photocoagulation. The visual prognosis is relatively good [122].

Hyaloid System Remnants

The persistence of epipapillary fibrous glial tissue can mimic an elevated optic disc. It can occur unilaterally or bilaterally and may be associated with amblyopia. The vessels in the vitreous during fetal development persist as fibrous glial tissue lying over the disc. The cup may be obliterated, and the disc margins may appear blurred [27].

The hyaloid vascular system and the glial sheath of Bergmeister, which envelops the posterior portion of the hyaloid artery, have failed to totally atrophy by the end of gestation. The persistence and proliferation of these normally transient vessels of the primary vitreous, especially the posterior tunica vasculosa lentis, leads to the formation of persistent hyperplastic primary vitreous [3]. Persistent hyperplastic primary vitreous causes a white pupillary reflex, which must be distinguished from retinoblastoma. Disc anomalies are determined by the extent of persistence of glial and/or vascular components.

A persistent Bergmeister's papilla represents a vascular remnant surrounded by fibroglial tissue or just the fibroglial tissue itself [131–133]. Glial sheath remnants of Bergmeister are epipapillary or peripapillary, off-white membranes, or glial cysts (Fig. 8.11) [131–133]. These remnants do not impair visual function, but must be distinguished from retinoblastomas, hamartomas of the optic disc, medullated retinal nerve fibers, and papilledema [27].

Anomalous, tortuous vessels and early branching of retinal vessels are commonly seen in patients with persistence of hyaloid remnants. Retinal and ciliary communications, such as cilioretinal, ciliochoroidal, and optociliary vessels, are also seen. Situs inversus, where retinal vessels emerge in a temporal-to-nasal direction, is another associated benign anomaly [27].

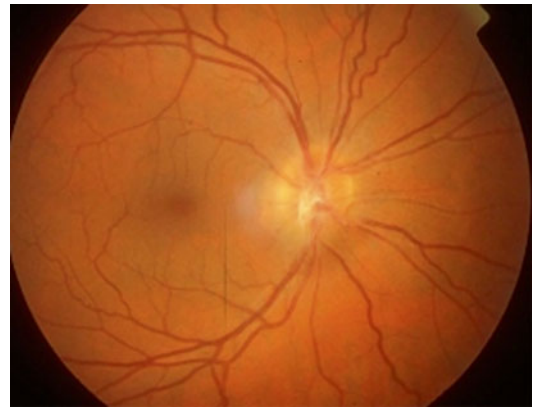

Fig. 8.11 Hyaloid remnants. Courtesy of Robert Sykes, M.D.

Myelinated Nerve Fibers

Myelination of the optic nerve fibers in the peripapillary retina occurs at a frequency of about 0.3–1 % [134]. This anomaly is inherited as an autosomal dominant disorder. It affects males and females equally and occurs unilaterally in 80 % of patients [134].

During fetal development at 5 months gestation, myelination progresses from the lateral geniculate body to the optic tracts, then the optic chiasm, and last to the optic nerve by 8 months gestation [135]. Anomalous myelinated nerve fibers develop when myelination extends beyond the posterior portion of the lamina cribosa and into disc and peripapillary areas. The exact pathogenesis of this abnormal extension of myelin is still not well understood [136].

The myelinated areas have a whitish, feathery appearance and are usually continuous with the disc at the upper or lower poles (Fig. 8.12) [3]. The myelination may progress after birth but does not usually extend into the macula. Visual acuity is usually normal. More distal myelination into the retina appears fan shaped. If the myelination is more severe, amblyopia, strabismus, nystagmus, enlarged blind spots, and relative

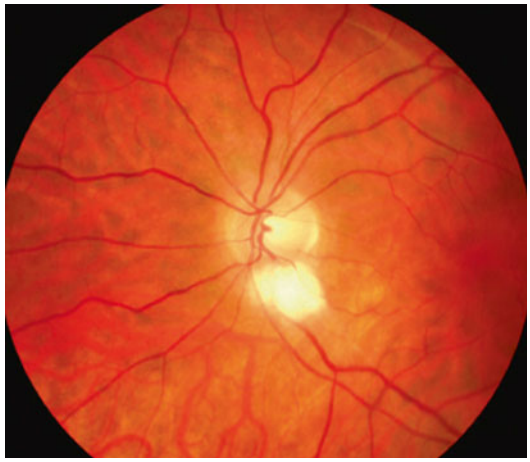

Fig. 8.12 Myelinated nerve fibers. Courtesy of Robert Sykes, M.D.

scotomas may develop. Myopia occurs in about half of all cases [134].

Myelinated nerve fibers may be associated with systemic disorders. The Gorlin syndrome (multiple basal cell nevi) is an autosomal dominant disorder that may present in children with myelinated nerve fibers and cutaneous lesions [135]. Typical lesions appear as small pits in the hands and feet that can increase in size and numbers, especially during puberty. Jaw cysts and other bony abnormalities may also develop. Early treatment with dermatological surgery and topical chemotherapy can help prevent progression of this disorder [137]. Myelinated nerve fibers are also associated with an autosomal dominant vitreoretinopathy with limb deformities. The RNFL is myelinated, and the vitreous degenerates to cause congenitally poor vision and night blindness [138].

Congenital Disc Pigmentation

Congenital optic disc pigmentation is defined as the deposition of melanin anterior to or within the lamina cribosa, giving the disc a slate-gray coloration. This deposition appears irregular and granular [139]. Visual acuity is usually good. Congenital optic disc pigmentation is a rare disorder, but it may be seen associated with Aicardi syndrome [140] and interstitial deletion of chromosome 17 [139].

Most infants with gray optic discs do not have true congenital disc pigmentation, but rather diffusely gray optic discs related to albinism and delayed visual maturation. This gray tint often disappears within the first year of life without visible pigment migration, and good vision develops. The etiology of this gray tint is unclear. It is thought that the gray color represents delayed myelination of the optic nerve in neonates, but it can also be seen in normal neonates [141].

References

1. Lambert SR, Hoyt CS, Narahara MH. Optic nerve hypoplasia. Surv Ophthalmol. 1987;32(1):1–9.
2. Hotchkiss ML, Green WR. Optic nerve aplasia and hypoplasia. J Pediatr Ophthalmol Strabismus. 1979;16(4):225–40.
3. Mosier MA, Lieberman MF, Green WR, Knox DL. Hypoplasia of the optic nerve. Arch Ophthalmol. 1978;96(8):1437–42.
4. Gardner HB, Irvine AR. Optic nerve hypoplasia with good visual acuity. Arch Ophthalmol. 1972;88(3):255–8.
5. Petersen RA, Walton DS. Optic nerve hypoplasia with good visual acuity and visual field defects: a study of children of diabetic mothers. Arch Ophthalmol. 1977;95(2):254–8.
6. Zeki SM. Optic nerve hypoplasia and astigmatism: a new association. Br J Ophthalmol. 1990;74(5):297–9.
7. Brodsky MC, Glasier CM. Optic nerve hypoplasia. Clinical significance of associated central nervous system abnormalities on magnetic resonance imaging. Arch Ophthalmol. 1993;111(1):66–74.
8. Hoyt WF, Kaplan SL, Grumbach MM, et al. Septo-optic dysplasia and pituitary dwarfism. Lancet. 1970;1(7652):893–4.
9. Brodsky MC, Glasier CM, Pollock SC, et al. Optic nerve hypoplasia. Identification by magnetic resonance imaging. Arch Ophthalmol. 1990;108(11):1562–7.
10. Arslanian SA, Rothfus WE, Foley Jr TP, et al. Hormonal, metabolic, and neuroradiologic abnormalities associated with septo-optic dysplasia. Acta Endocrinol (Copenh). 1984;107(2):282–8.
11. Izenberg N, Rosenblum M, Parks JS. The endocrine spectrum of septo-optic dysplasia. Clin Pediatr (Phila). 1984;23(11):632–6.
12. Margalith D, Tze WJ, Jan JE. Congenital optic nerve hypoplasia with hypothalamic-pituitary dysplasia. A review of 16 cases. Am J Dis Child. 1985;139(4):361–6.

13. Novakovic P, Taylor DS, Hoyt WF. Localising patterns of optic nerve hypoplasia: retina to occipital lobe. Br J Ophthalmol. 1988;72(3):176–82.
14. Skarf B, Hoyt CS. Optic nerve hypoplasia in children. Association with anomalies of the endocrine and CNS. Arch Ophthalmol. 1984;102(1):62–7.
15. Hoyt WF. Congenital occipital hemianopia. Neuro Ophthalmol Jpn. 1985;2:252–9.
16. Ragge NK, Barkovich AJ, Hoyt WF, et al. Isolated congenital hemianopia caused by prenatal injury to the optic radiation. Arch Neurol. 1991;48(10): 1088–91.
17. Taylor D. Congenital tumours of the anterior visual system with dysplasia of the optic discs. Br J Ophthalmol. 1982;66(7):455–63.
18. Francheschetti A, Bock RH. Megalopapilla; a new congenital anomaly. Am J Ophthalmol. 1950;33(2): 227–35.
19. Jonas JB, Gusek GC, Guggenmoos-Holzmann I, Naumann GO. Size of the optic nerve scleral canal and comparison with intravital determination of optic disc dimensions. Graefes Arch Clin Exp Ophthalmol. 1988;226(3):213–5.
20. Bynke H, Homdahl G. Megalopapilla: a differential diagnosis in suspected optic atrophy. Neuro Ophthalmol. 1971;71:423–5.
21. Grimson BS, Perry DD. Enlargement of the optic disk in childhood optic nerve tumors. Am J Ophthalmol. 1984;97(5):627–31.
22. Goldhammer Y, Smith JL. Optic nerve anomalies in basal encephalocele. Arch Ophthalmol. 1975;93(2): 115–8.
23. Kim RY, Hoyt WF, Lessell S, et al. Superior segmental optic hypoplasia. A sign of maternal diabetes. Arch Ophthalmol. 1989;107(9):1312–5.
24. Nelson M, Lessell S, Sadun AA. Optic nerve hypoplasia and maternal diabetes mellitus. Arch Neurol. 1986;43(1):20–5.
25. Petersen RA, Holmes LB. Optic nerve hypoplasia in infants of diabetic mothers. Arch Ophthalmol. 1986;104(11):1587.
26. Hoyt WF, Rios-Montenegro EN, Behrens MM, et al. Homonymous hemioptic hypoplasia. Fundoscopic features in standard and red-free illumination in three patients with congenital hemiplegia. Br J Ophthalmol. 1972;56(7):537–45.
27. Apple DJ, Rabb MF, Walsh PM. Congenital anomalies of the optic disc. Surv Ophthalmol. 1982;27(1): 3–41.
28. Dorrell D. The tilted disc. Br J Ophthalmol. 1978;62(1):16–20.
29. Young SE, Walsh FB, Knox DL. The tilted disk syndrome. Am J Ophthalmol. 1976;82(1):16–23.
30. Larsen WJ. Development of the eyes. In: Larsen WJ, editor. Human embryology. 2nd ed. New York, NY: Churchill Livingstone; 1993. p. 120–39.
31. Giuffre G. Chorioretinal degenerative changes in the tilted disc syndrome. Int Ophthalmol. 1991;15(1): 1–7.
32. Giuffré G. Hypothesis on the pathogenesis of the papillary dysversion syndrome. J Fr Ophthalmol. 1985;8(8–9):565–72.
33. Bottoni FG, Eggink CA, Cruysberg JR, et al. Dominant inherited tilted disc syndrome and lacquer cracks. Eye. 1990;4(pt 3):504–9.
34. Khairallah M, Chatti T, Messaoud R, et al. Peripapillary subretinal neovascularization associated with tilted disk syndrome. Retina. 1996;16(5): 449–51.
35. Prost M, De Laey JJ. Choroidal neovascularization in tilted disc syndrome. Int Ophthalmol. 1988;12(2): 131–5.
36. Stur M. Congenital tilted disk syndrome associated with parafoveal subretinal neovascularization. Am J Ophthalmol. 1988;105(1):98–9.
37. Manor RS. Temporal field defects due to nasal tilting of discs. Ophthalmologica. 1974;168(4):269–81.
38. Brazitikos PD, Safran AB, Simona F, et al. Threshold perimetry in tilted disc syndrome. Arch Ophthalmol. 1990;108(12):1698–700.
39. Giuffre G. The spectrum of the visual field defects in the tilted disc syndrome: clinical study and review. Neuro Ophthalmol. 1986;6:239–46.
40. Giuffre G, Anastasi M. Electrofunctional features of the tilted disc syndrome. Doc Ophthalmol. 1986;62(3): 223–30.
41. De Rouck A, Kayembe D, De Laey JJ, et al. Clinical and electrophysiological manifestations of the tilted disk syndrome. Bull Soc Belge Ophthalmol. 1981; 193:147–59.
42. Toussaint P, Turut P, Milazzo S, et al. Aspects of the tilted disk syndrome. Bull Soc Ophthalmol Fr. 1989;89(2):267–8. 271–272.
43. Hatten ME, Mason CA. Mechanisms of glial-guided neuronal migration in vitro and in vivo. Experientia (Basel). 1990;46(9):907–16.
44. Keane JR. Suprasellar tumors and incidental optic disc anomalies. Diagnostic problems in two patients with hemianopic temporal scotomas. Arch Ophthalmol. 1977;95(12):2180–3.
45. Pollock S. The morning glory disc anomaly: contractile movement, classification, and embryogenesis. Doc Ophthalmol. 1987;65(4):439–60.
46. Beyer WB, Quencer RM, Osher RH. Morning glory syndrome. A functional analysis including fluorescein angiography, ultrasonography, and computerized tomography. Ophthalmology. 1982;89(12):1362–7.
47. Haik BG, Greenstein SH, Smith ME, Abramson DH, Ellsworth RM. Retinal detachment in the morning glory anomaly. Ophthalmology. 1984; 91(12):1638–47.
48. Steinkuller PG. The morning glory disk anomaly: case report and literature review. J Pediatr Ophthalmol Strabismus. 1980;17(2):81–7.
49. Graether JM. Transient amaurosis in one eye with simultaneous dilatation of retinal veins in association with a congenital anomaly. Arch Ophthalmol. 1963;70:342–5.

50. Caprioli J, Lesser RL. Basal encephalocele and morning glory syndrome. Br J Ophthalmol. 1983; 67(6):349–51.
51. Hope-Ross M, Johnston SS. The Morning Glory syndrome associated with sphenoethmoidal encephalocele. Ophthalmic Paediatr Genet. 1990;11(2): 147–53.
52. Koenig SB, Naidich TP, Lissner G. The morning glory syndrome associated with sphenoidal encephalocele. Ophthalmology. 1982;89(12):1368–73.
53. Eustis HS, Sanders MR, Zimmerman T. Morning glory syndrome in children. Association with endocrine and central nervous system anomalies. Arch Ophthalmol. 1994;112(2):204–7.
54. Yokota A, Matsukado Y, Fuwa I, et al. Anterior basal encephalocele of the neonatal and infantile period. Neurosurgery. 1986;19(3):468–78.
55. Hansen MR, Price RL, Rothner AD, et al. Developmental anomalies of the optic disc and carotid circulation: a new association. J Clin Neuro Ophthalmol. 1985;5:3–8.
56. Massaro M, Thorarensen O, Liu GT, et al. Morning glory disc anomaly and moyamoya vessels. Arch Ophthalmol. 1998;116(2):253–4.
57. Metry DW, Dowd CF, Barkovich AJ, et al. The many faces of PHACE syndrome. J Pediatr. 2001;139(1): 117–23.
58. Francois J. Colobomatous malformations of the ocular globe. Int Ophthalmol Clin. 1968;8(4): 797–816.
59. Font RL, Zimmerman LE. Intrascleral smooth muscle in coloboma of the optic disk. Electron microscopic verification. Am J Ophthalmol. 1971;72(2): 452–7.
60. Foster JA, Lam S. Contractile optic disc coloboma. Arch Ophthalmol. 1991;109(4):472–3.
61. Willis R, Zimmerman LE, O'Grady R, et al. Heterotopic adipose tissue and smooth muscle in the optic disc, association with isolated colobomas. Arch Ophthalmol. 1972;88:139–46.
62. Lin CC, Tso MO, Vygantas CM. Coloboma of optic nerve associated with serous maculopathy. A clinicopathologic correlative study. Arch Ophthalmol. 1984;102(11):1651–4.
63. Schatz H. Central serous chorioretinopathy: the etiology of sequelae. Ophthalmology. 1988;95(7): 1007–8.
64. Chestler RJ, France TD. Ocular findings in CHARGE syndrome. Six case reports and a review. Ophthalmology. 1988;95(12):1613–9.
65. Russell-Eggitt IM, Blake KD, Taylor DS, et al. The eye in the CHARGE association. Br J Ophthalmol. 1990;74(7):421–6.
66. Pagon RA. Ocular coloboma. Surv Ophthalmol. 1981;25(4):223–36.
67. Carney SH, Brodsky MC, Good WV, et al. Aicardi syndrome: more than meets the eye. Surv Ophthalmol. 1993;37(6):419–24.
68. Hoyt CS, Billson F, Ouvrier R, et al. Ocular features of Aicardi's syndrome. Arch Ophthalmol. 1978; 96(2):291–5.
69. Limaye SR. Coloboma of the iris and choroid and retinal detachment in oculo-auricular dysplasia (Goldenhar syndrome). Eye Ear Nose Throat Mon. 1972;51(10):384–6.
70. Villalonga Gornes PA, Galan Terraza A, Gil-Gibernau JJ. Ophthalmoscopic evolution of papillary colobomatous malformations. J Pediatr Ophthalmol Strabismus. 1995;32(1):20–5.
71. Jacobs M, Taylor D. The systemic and genetic significance of congenital optic disc anomalies. Eye. 1991;5(pt 4):470–5.
72. Brown G, Tasman W. Congenital anomalies of the optic disc. New York, NY: Grune & Stratton; 1983.
73. Kranenburg EW. Crater-like holes in the optic disc and central serous retinopathy. Arch Ophthalmol. 1960;64:912–24.
74. Brown GC, Shields JA, Goldberg RE. Congenital pits of the optic nerve head. II. Clinical studies in humans. Ophthalmology. 1980;87(1):51–65.
75. Sobol WM, Blodi CF, Folk JC, et al. Long-term visual outcome in patients with optic nerve pit and serous retinal detachment of the macula. Ophthalmology. 1990;97(11):1539–42.
76. Gass JD. Serous detachment of the macula. Secondary to congenital pit of the optic nerve head. Am J Ophthalmol. 1969;67(6):821–41.
77. Theodossiadis GP, Kollia AK, Theodossiadis PG. Cilioretinal arteries in conjunction with a pit of the optic disc. Ophthalmologica. 1992;204(3):115–21.
78. Parsa CF, Silva ED, Sundin OH, et al. Redefining papillorenal syndrome: an underdiagnosed cause of ocular and renal morbidity. Ophthalmology. 2001;108(4):738–49.
79. Schimmenti LA, Cunliffe HE, McNoe LA, et al. Further delineation of renal coloboma syndrome in patients with extreme variability of phenotype and identical PAX2 mutations. Am J Hum Genet. 1997;60(4):869–78.
80. Parsa CF, Goldberg MF, Hunter DG. Papillorenal ("renal coloboma") syndrome. Am J Ophthalmol. 2002;134(2):300–1.
81. Kiegler HR. Comparison of functional findings with results of standardized echography of the optic nerve in optic disk drusen. Wien Klin Wochenschr. 1995;107(21):651–3.
82. Giarelli L, Ravalico G, Saviano S, et al. Optic nerve head drusen: histopathological considerations-clinical features. Metab Pediatr Syst Ophthalmol. 1990;13(2–4):88–91.
83. Lorentzen SE. Drusen of the optic disk, an irregularly dominant hereditary affection. Acta Ophthalmol (Copenh). 1961;39:626–43.
84. Boldt HC, Byrne SF, DiBernardo C. Echographic evaluation of optic disc drusen. J Clin Neuro Ophthalmol. 1991;11(2):85–91.

85. Friedman AH, Gartner S, Modi SS. Drusen of the optic disc. A retrospective study in cadaver eyes. Br J Ophthalmol. 1975;59(8):413–21.
86. Lansche RK, Rucker CW. Progression of defects in visual fields produced by hyaline bodies in optic disks. AMA Arch Ophthalmol. 1957;58(1):115–21.
87. Spencer WH. XXXIV Edward Jackson memorial lecture: drusen of the optic disc and aberrant axoplasmic transport. Ophthalmology. 1978;85(1):21–38.
88. Tso MO. Pathology and pathogenesis of drusen of the optic nerve head. Ophthalmology. 1981;88(10):1066–80.
89. Friedman AH, Henkind P, Gartner S. Drusen of the optic disc. A histopathological study. Trans Ophthalmol Soc U K. 1975;95(1):4–9.
90. Friedman AH, Beckerman B, Gold DH, et al. Drusen of the optic disc. Surv Ophthalmol. 1977;21(5):373–90.
91. Boyce SW, Platia EV, Green WR. Drusen of the optic nerve head. Ann Ophthalmol. 1978;10(6):695–704.
92. Seitz R. The intraocular drusen. Klin Monatsbl Augenheilkd. 1968;152(2):203–11.
93. Beck RW, Corbett JJ, Thompson HS, et al. Decreased visual acuity from optic disc drusen. Arch Ophthalmol. 1985;103(8):1155–9.
94. Sarkies NJ, Sanders MD. Optic disc drusen and episodic visual loss. Br J Ophthalmol. 1987;71(7):537–9.
95. Knight CL, Hoyt WF. Monocular blindness from drusen of the optic disk. Am J Ophthalmol. 1972;73(6):890–2.
96. Vicary DL, Swann PG. Relative afferent pupil defect associated with optic disc drusen. Aust NZ J Ophthalmol. 1991;19(3):245–8.
97. Pietruschka G, Priess G. Clinical importance and prognosis of drusen of the disc. Klin Monatsbl Augenheilkd. 1973;162(3):331–41.
98. Hoover DL, Robb RM, Petersen RA. Optic disc drusen and primary megalencephaly in children. J Pediatr Ophthalmol Strabismus. 1989;26(2):81–5.
99. Savino PJ, Glaser JS, Rosenberg MA. A clinical analysis of pseudopapilledema. II. Visual field defects. Arch Ophthalmol. 1979;97(1):71–5.
100. Kanski JJ, Bowling B. Clinical ophthalmology: a systematic approach. 7th ed. Philadelphia, PA: Saunders; 2007.
101. Mustonen E. Pseudopapilloedema with and without verified optic disc drusen. A clinical analysis II: visual fields. Acta Ophthalmol (Copenh). 1983;61(6):1057–66.
102. Lorentzen SE. Drusen of the optic disk. A clinical and genetic study. Acta Ophthalmol (Copenh). 1966;90(Suppl):1–180.
103. Erkkila H. Optic disc drusen in children. Acta Ophthalmol Suppl. 1977;129:3–44.
104. Okun E. Chronic papilledema simulating hyaline bodies of the optic disc. A case report. Am J Ophthalmol. 1962;53:922–7.
105. Sibony PA, Kennerdell JS, Slamovits TL, et al. Intrapapillary refractile bodies in optic nerve sheath meningioma. Arch Ophthalmol. 1985;103(3):383–5.
106. Kurz-Levin MM, Landau K. A comparison of imaging techniques for diagnosing drusen of the optic nerve head. Arch Ophthalmol. 1999;117(8):1045–9.
107. Roh S, Noecker RJ, Schuman JS, et al. Effect of optic nerve head drusen on nerve fiber layer thickness. Ophthalmology. 1998;105(5):878–85.
108. Scholl GB, Song HS, Winkler DE, et al. The pattern visual evoked potential and pattern electroretinogram in drusen-associated optic neuropathy. Arch Ophthalmol. 1992;110(1):75–81.
109. Stevens RA, Newman NM. Abnormal visual evoked potentials from eyes with optic nerve head drusen. Am J Ophthalmol. 1981;92(6):857–62.
110. Vieregge P, Rosengart A, Mehdorn E, et al. Drusen papilla with vision disorder and pathologic visual evoked potentials. Nervenarzt. 1990;61(6):364–8.
111. Erkkila H. Clinical appearance of optic disc drusen in childhood. Albrecht Von Graefes Arch Klin Exp Ophthalmol. 1975;193(1):1–18.
112. Lorentzen SE. Incidence of cilioretinal arteries. Acta Ophthalmol (Copenh). 1970;48(3):518–24.
113. Erkkila H. The central vascular pattern of the eye ground in children with drusen of the optic disk. Albrecht Von Graefes Arch Klin Exp Ophthalmol. 1976;199(1):1–10.
114. Masyama Y, Kodama Y, Matsumara Y, et al. Clinical studies on the occurrence and the pathogenesis of optociliary veins. J Clin Neuro Ophthalmol. 1990;10:1–8.
115. Karel I, Otradovec J, Peleska M. Fluorescence angiography in circulatory disturbances in drusen of the optic disk. Ophthalmologica. 1972;164(6):449–62.
116. Frohlich SJ, Ulbig MW, Klauss V. Sudden loss of vision without previous symptoms. 58-year-old patient with sudden and painless loss of vision of the right eye. Ophthalmologe. 1999;96(2):120–1.
117. Jonas JB, Gusek GC, Guggenmoos-Holzmann I, et al. Optic nerve head drusen associated with abnormally small optic discs. Int Ophthalmol. 1987;11(2):79–82.
118. Brown GC, Magargal LE, Shields JA, et al. Retinal arterial obstruction in children and young adults. Ophthalmology. 1981;88(1):18–25.
119. Newman NJ, Lessell S, Brandt EM. Bilateral central retinal artery occlusions, disk drusen, and migraine. Am J Ophthalmol. 1989;107(3):236–40.
120. Newsom RS, Trew DR, Leonard TJ. Bilateral buried optic nerve drusen presenting with central retinal artery occlusion at high altitude. Eye. 1995;9(Pt 6):806–8.
121. Saudax E, Martin-Beuzart S, Lesure P, et al. Submacular neovascular membrane and drusen of the optic disk. J Fr Ophthalmol. 1990;13(4):219–22.
122. Harris MJ, Fine SL, Owens SL. Hemorrhagic complications of optic nerve drusen. Am J Ophthalmol. 1981;92(1):70–6.

123. Brodrick JD. Drusen of the disc and retinal haemorrhages. Br J Ophthalmol. 1973;57(5):299–306.
124. van den Born LI, van Soest S, van Schooneveld MJ, et al. Autosomal recessive retinitis pigmentosa with preserved para-arteriolar retinal pigment epithelium. Am J Ophthalmol. 1994;118(4):430–9.
125. Grover S, Fishman GA, Brown Jr J. Frequency of optic disc or parapapillary nerve fiber layer drusen in retinitis pigmentosa. Ophthalmology. 1997;104(2):295–8.
126. Bouchet GC, Chabot J. Fluorographic diagnosis of papillary pseudo-edema related to the presence of hyalin verrucosity of the papilla. Bull Soc Ophthalmol Fr. 1970;70(11):1121–31.
127. Goodman RM, Smith EW, Paton D, et al. Pseudoxanthoma elasticum: a clinical and histopathological study. Medicine (Baltim). 1963;42:297–334.
128. Pierro L, Brancato R, Minicucci M, et al. Echographic diagnosis of drusen of the optic nerve head in patients with angioid streaks. Ophthalmologica. 1994;208(5):239–42.
129. Samples JR, van Buskirk M, Shults WT, et al. Optic nerve head drusen and glaucoma. Arch Ophthalmol. 1985;103(11):1678–80.
130. Jiraskova N, Rozsival P. Results of 62 optic nerve sheath decompressions. Cesk Slov Oftalmol. 1999;55(3):136–44.
131. Francois J. Pre-papillary cyst developed from remnants of the hyaloid artery. Br J Ophthalmol. 1950;34(6):365–8.
132. Gieser DK, Goldberg MF, Apple DJ, et al. Persistent hyperplastic primary vitreous in an adult: case report with fluorescein angiographic findings. J Pediatr Ophthalmol Strabismus. 1978;15(4):213–8.
133. Hamming NA, Apple DJ, Gieser DK, et al. Ultrastructure of the hyaloid vasculature in primates. Invest Ophthalmol Vis Sci. 1977;16(5):408–15.
134. Straatsma BR, Heckenlively JR, Foos RY, et al. Myelinated retinal nerve fibers associated with ipsilateral myopia, amblyopia, and strabismus. Am J Ophthalmol. 1979;88(3 pt 1):506–10.
135. De Jong PTVM, Bistervels B, Cosgrove J, et al. Medullated nerve fibers: a sign of multiple basal cell nevi (Gorlin's) syndrome. Arch Ophthalmol. 1985;103:1833–6.
136. Magoon EH, Robb RM. Development of myelin in human optic nerve and tract. A light and electron microscopic study. Arch Ophthalmol. 1981;99(4):655–9.
137. Kronish JW, Tse DT. Basal cell nevus syndrome. In: Gold DH, Weingeist TA, editors. The eye in systemic disease. Philadelphia, PA: Lippincott; 1990. p. 201–9.
138. Traboulsi EI, Lim JI, Pyeritz R, et al. A new syndrome of myelinated nerve fibers, vitreoretinopathy, and skeletal malformations. Arch Ophthalmol. 1993;111(11):1543–5.
139. Brodsky MC, Buckley EG, McConkie-Rosell A. The case of the gray optic disc! Surv Ophthalmol. 1989;33(5):367–72.
140. Taylor D. Optic nerve. In: Pediatric ophthalmology. Cambridge: Blackwell; 1990.
141. Halbertsma KTA. Pseudoatrophy of the optic nerve in infant 2 months old. Ned Tijdschr Geneeskd. 1937;81:1230–6.

Optic Disc Tumors

9

Jane W. Chan

Tumors of the Sensory Retina and Medullary Epithelium Affecting the Optic Disc

Retinoblastoma

Retinoblastoma affects the sensory retina and is the most common intraocular malignant tumor of childhood that occasionally may extend into the optic nerve. Up to 30 % of cases are bilateral. The incidence of retinoblastoma is about 1 in 20,000 live births in the United States [1]. Seventy percent of all retinoblastomas are unilateral and 30 % are bilateral. Bilateral cases are transmitted in an autosomal dominant manner with incomplete penetrance [2]. Only 10–15 % of unilateral cases are hereditary [3]. The average age at presentation in bilateral cases is about 10 months and in unilateral cases 21 months [2].

The most common presentation of a retinoblastoma is leukocoria, followed by strabismus, and then as an ocular disorder that simulates inflammation [4]. Rarely is retinoblastoma manifested as secondary angle-closure glaucoma, proptosis, or pinealoblastoma [5, 6]. Some conditions that may mimic a retinoblastoma include (1) persistent hyperplastic primary vitreous, (2) cataract, (3) retinopathy of prematurity, (4) toxocariasis, (5) colobomata of the choroids and disc, (6) uveitis, and (7) Coats' disease [7].

Retinoblastoma of the optic nerve appears as an elevated, circumscribed gray-white lesion that involves the peripapillary retina. Calcium deposits may be seen within the tumor as it spreads into the overlying vitreous cavity. Feeder vessels from the retina may also enter into the tumor [1].

About 75 % of retinoblastomas demonstrate findings indicative of calcium deposits, which can be detected on computed tomography (CT) scan of the orbits or ultrasound. Magnetic resonance imaging (MRI) of the brain may detect a pinealoblastoma. Ultrasonography may be more helpful in distinguishing retinoblastomas from nonneoplastic conditions [8, 9]. DNA analysis on blood specimens from the patient, parents, and any siblings will help confirm the diagnosis. Additionally, a pediatric oncologist should be consulted for a bone marrow aspiration and biopsy, and a lumbar puncture to assess for hematogenous spread of the tumor.

On histopathology the tumor may range from poorly differentiated with mitotic figures to well differentiated with Flexner–Wintersteiner rosettes. These rosettes are composed of columnar cells arranged in a circular manner around a clear central lumen.

Retinoblastoma of the optic nerve head may gradually extend into the lamina cribosa and then into the

J.W. Chan, M.D. (✉)
Department of Neurology, Neuro-Ophthalmology,
University of Nevada School of Medicine,
975 Kirman Avenue (111), Reno, Nevada 89502, USA
e-mail: worjun@aol.com

J.W. Chan (ed.), *Optic Nerve Disorders: Diagnosis and Management*,
DOI 10.1007/978-1-4614-0691-4_9,

retrolaminar nerve [2]. As it spreads posteriorly along the optic nerve, it may enter the subarachnoid space into the brain. By this time, metastases also occur in the bone and liver [10]. The incidence of optic nerve involvement is about 29.5 % (240/814) [11]. If the retinoblastoma remains in the optic nerve anterior to the lamina scleralis, the prognosis is good. If it spreads posterior to the lamina scleralis and into the line of surgical transection of the optic nerve, then the prognosis is worse.

The current main treatment strategies for retinoblastoma involve enucleation, intravenous chemoreduction, and intra-arterial chemotherapy. Enucleation is reserved for eyes with extensive retinoblastoma with poor visual prognosis. Intravenous chemoreduction provides favorable tumor control for most eyes classified as groups A, B, or C and some D eyes, using the International Classification of Retinoblastoma. Chemotherapy has also decreased the incidence of pinealoblastoma in children with germline mutation retinoblastoma. Intra-arterial chemotherapy into the ophthalmic artery under careful neurointerventional guidance has been the treatment of choice for those patients who fail standard treatments or as a primary treatment in selected cases. Visual outcomes from long-term follow-up data are still needed for intra-arterial chemotherapy [12].

Medulloepithelioma

Medulloepithelioma usually affects the ciliary body and is an exceedingly rare tumor to infiltrate the optic nerve. It is an embryonal tumor arising from the medullary epithelium that eventually develops into the nonpigmented ciliary body epithelium in adulthood [13]. It may develop more posteriorly in the optic nerve [14].

It appears as a white-yellow globular mass that may mimic an astrocytic hamartoma or retinoblastoma (Fig. 9.1) [14]. If it extends into the retrobulbar optic nerve, proptosis can occur. Visual prognosis is poor. If the tumor has malignant components, enucleation and removal of the affected optic nerve is the preferred treatment [14].

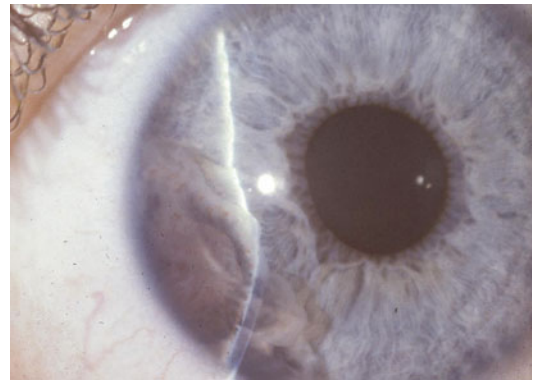

Fig. 9.1 Malignant teratoid medulloepithelioma of the ciliary body and iris. This nonpigmented tumor has an irregular surface filling of the anterior chamber angle. It may develop posteriorly in the optic nerve, mimicking an astrocytic hamartoma or retinoblastoma (Reprinted from Atlas of Ophthalmology. http://www.atlasophthalmology.com. Accessed June 11, 2012.With permission from Online Journal of Ophthalmology)

Glial Tumors of the Retina Affecting the Optic Disc

Astrocytic Hamartoma of the Optic Disc

Astrocytic hamartomas infiltrate the optic disc to appear to be above the optic disc or in the retina. They occur bilaterally in 50 % of patients with the tuberous sclerosis complex (TSC). The most common type appears as a smooth, flat, salmon-colored lesion that is either round or oval shaped. It is semitransparent and located in the superficial posterior pole of the retina. The second type appears as an opaque, elevated, white-yellow calcified tumor with well-defined borders and multiple nodules, resembling a mulberry (Fig. 9.2). The third type has a combination of features of the previous two variants. The center is calcified and nodular, while the periphery is smooth, semitranslucent, and salmon colored. The three variants of hamartomas may possibly represent various developmental stages of the tumor [15, 16].

On histopathology, astrocytic hamartomas develop from astrocytes located on the optic nerve head and in the nerve fiber layer of the posterior retina. Astrocytic hamartomas consist

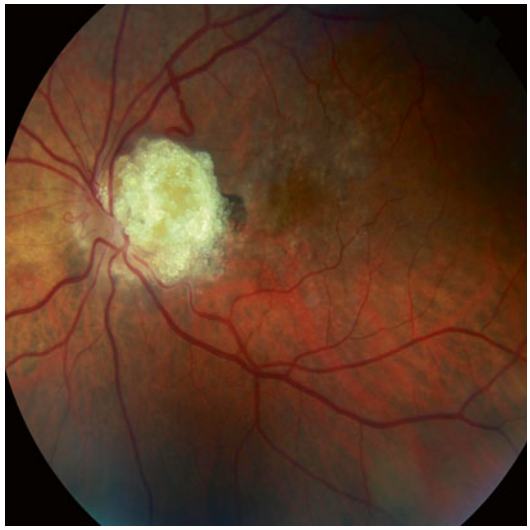

Fig. 9.2 Astrocytic hamartoma. This *white* nodular tumor arises from the superficial retina adjacent to the disc (This image was originally published in the Retina Image Bank. Freund, KB, Shah, VP. Astrocytic hamartoma. Retina Image Bank. 2012; Image Number 1258 © the American Society of Retina Specialists)

of benign astrocytes, calcium, and amorphous material [17]. The lesion is often limited to the prelaminar portion of the disc but may extend through the lamina cribrosa into the retrolaminar portion of the nerve [18].

On fluorescein angiography, calcified retinal and optic disc astrocytomas may demonstrate autofluorescence. The tumor appears avascular in the early and midphases of the study, and the prominent blood vessels become apparent in the late phases. Diffuse hyperfluorescence occurs because of leakage of dye from these vessels [19].

Visual function is usually normal unless the optic disc or macula is affected. Diagnosis is based mainly on funduscopic morphological findings, as already discussed. Retinoblastomas of the optic nerve and retina must be differentiated from astrocytic hamartomas. Vitreous hemorrhage may occur rarely, and hard exudates rarely appear surrounding the tumor. Because astrocytic hamartomas usually do not grow and vision is preserved, treatment is not needed [16].

Astrocytic hamartomas may appear as an isolated phenomenon in 30 % of cases [18, 19]. The exact prevalence of this tumor is unclear, but astrocytic hamartomas are believed to occur in approximately 53 % of patients with TSC [20], and, less commonly, in neurofibromatosis type I (NF-1) [18, 21–23].

TSC is thought to be transmitted by an autosomal dominant gene with low penetrance and variability of expression [22]. It exhibits locus heterogeneity with two causative loci on chromosome 9p34 (TSC1) and 16p13 (TSC2). The TSC1 gene codes for the protein hamartin, thought to be involved in actin cytoskeleton organization, and the TSC2 gene codes for the protein tuberlin. Both these proteins play a role in GTPase signaling. TSC2 mutations account for about 85 % of all cases and appear to cause a more severe disease than TSC1 [24].

Most patients with tuberous sclerosis present with mental retardation, seizures, and adenoma sebaceum, a papular rash in a butterfly distribution over the nose and cheeks [20]. These facial lesions are actually angiofibromas, which are seen in about 75 % of patients [25]. In about 25 % of patients, shagreen patches, irregularly shaped, raised white "ash leaf" lesions about several centimeters in diameter, can be seen in the lumbar or flank region. Ungual fibromas, nodular lesions adjacent to or underneath nails, are present in 20 % of patients [22].

Besides the retina and the optic disc, astrocytic hamartomas can affect other organs of the body. Calcified hamartomas may be seen in the basal ganglia and ventricles on MRI. Larger tubers may be seen in the cortical gray matter [22]. Hamartomatous lesions can also be found in the heart and are histopathologically classified as rhabdomyomas. In the kidney, they appear as angiomyolipomas and are present in about 80 % of patients with tuberous sclerosis [22].

Diagnosis is based on clinical criteria (Table 9.1) and can be confirmed with molecular gene testing for chromosome 9q34 and chromosome 16p13 [26].

Treatment for astrocytic hamartomas is not usually necessary as they are benign, stable lesions that often do not affect visual acuity. About 80 % of patients with TSC have epilepsy, mental retardation, developmental delay, and autism [26]. This neurological involvement is

Table 9.1 Diagnostic criteria for tuberous sclerosis complex: (1) definite tuberous sclerosis complex requires two major features or one major and two minor features; (2) probably tuberous sclerosis complex requires one major feature and one minor feature; (3) possible tuberous sclerosis complex requires either one major feature or two or more minor features

Major features	Minor features
Facial angiofibromas or forehead plaque	Dental pits
Nontraumatic ungula or periungual fibroma	Hamartomatous rectal polyps
More than three hypomelanotic macules	Bone cysts
Shagreen patch	Cerebral white matter migration lines
Multiple retinal nodular hamartomas	Gingival fibromas
Cortical tubers	Nonrenal hamartoma
Subependymal giant cell astrocytoma	Multiple renal cysts
Cardiac rhabdomyoma	
"Confetti" skin lesions	
Lymphangiomyomatosis	
Renal angiomyolipoma	

(Reprinted from Roach ES, Gomez MR, Northrup H. Tuberous sclerosis complex consensus conference: revised clinical diagnostic criteria. J Child Neurol 1998;13(12): 624–28. With permission from Sage Publications)

often the most common cause of morbidity in TSC patients. Therefore, a patient who presents with an isolated astrocytic hamartoma in the fundus needs a neurological examination and an MRI of the brain as part of the evaluation for TSC. Because astrocytic astrocytomas can also be rarely seen in NF-1, the neurological evaluation should also be focused on detecting this disorder [26].

Vascular Tumors of the Retina Affecting the Optic Disc

Capillary Hemangioma

Capillary hemangiomas are bilateral in one-third to one-half of affected persons between the ages of 15 and 40. Capillary hemangiomas may present as an endophytic lesion that looks circular, reddish-orange, elevated, and well circumscribed

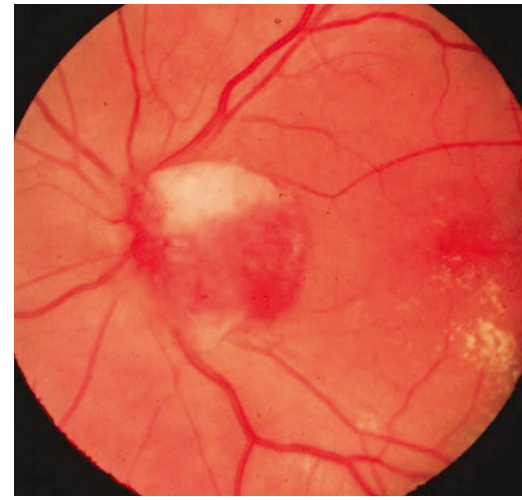

Fig. 9.3 Capillary hemangioma of the disc in von Hippel–Lindau syndrome. This *pink*, well-defined tumor over the disc is surrounded by mild hemorrhage and chronic macular exudates (Reprinted from Atlas of Ophthalmology. http://www.atlasophthalmology.com. Accessed June 11, 2012. With permission from Online Journal of Ophthalmology)

involving a portion of the disc or the entire disc and juxtapapillary retina (Fig. 9.3). It lies underneath the internal limiting membrane and grows inward toward the vitreous cavity. It may also mimic a peripapillary subretinal neovascular membrane. The exophytic type of capillary hemangioma appears as an indistinct lesion, causing a blurred and elevated disc margin, often with serous detachment, or the peripapillary sensory retina and a ring of lipid deposition. Although capillary hemangiomas of the optic disc may mimic optic disc granulomas, optic neuritis, peripapillary subretinal neovascularization, or even papilledema if presenting bilaterally, fluorescein angiography or ultrasound can demonstrate the vascular anomaly. The capillaries of the tumor fill in the retinal arterial phase of the angiogram, and the tumor becomes hyperfluorescent from leakage of fluorescein dye. These tumors in the optic disc do not demonstrate large feeding and draining vessels as do those in the peripheral retina [27, 28].

On histopathology, capillary hemangiomas of the optic disc consist of a proliferation of capillaries in the disc and vacuolated interstitial cells [27]. These capillaries may extend into the juxtapapillary

retina, which may have cystic changes in the outer plexiform layer [29].

On B-scan ultrasonography, the capillary hemangioma appears as a mass lesion with a smooth anterior border, acoustic solidity, and no choroidal excavation. A-scan ultrasonography reveals an initial high spike with low or medium internal reflectivity [30].

The most common presenting symptom, painless visual loss, occurs in 53 % of cases [31]. This visual loss is often a result of associated subretinal and intraretinal fluid and hard exudates. Blindness can occur if the tumor grows and a large nonrhegmatogenous retinal detachment evolves. Vitreous hemorrhage and neovascular glaucoma are rare [31, 32]. About one-third of affected patients have more than one lesion, which is often present at different stages of maturation. About 50 % of patients with a capillary hemangioma of the optic disc also have an associated retinal capillary hemangioma in the involved eye [33]. These vascular tumors do not extend into the optic nerve or chiasm.

About 25 % of patients with a capillary hemangioma of the optic disc and/or retina have an associated central nervous system (CNS) hemangioma. Capillary hemangiomas may be a feature of a rare disorder, von Hippel–Lindau disease (see following section: Optic Disc Hemangioblastoma). Other systemic abnormalities that can be associated with capillary hemangiomas include pheochromocytoma and renal cell carcinoma [34]. Angiomas and cysts of the pancreas, liver, spleen, kidney, lung, ovaries, epididymis, and bladder have been reported to be associated with this ocular vascular anomaly [31, 35].

Definitive criteria for treatment of capillary hemangiomas of the optic disc have not been established at this time. Small retinal capillary hemangiomas, less than about 2.5 mm disc diameters, that are not associated with the optic nerve can be treated with direct argon laser photocoagulation [36]. Cryotherapy [37] or perforating diathermy with or without scleral buckling [38] is reserved for larger lesions. These types of therapy are not applied to tumors of the optic disc because of the risk of permanent visual loss. Photocoagulation over the surface of the tumor has been done in patients with visual loss from macular edema or macular subretinal fluid. Only about a third of these patients maintained pretreatment vision after photocoagulation [39].

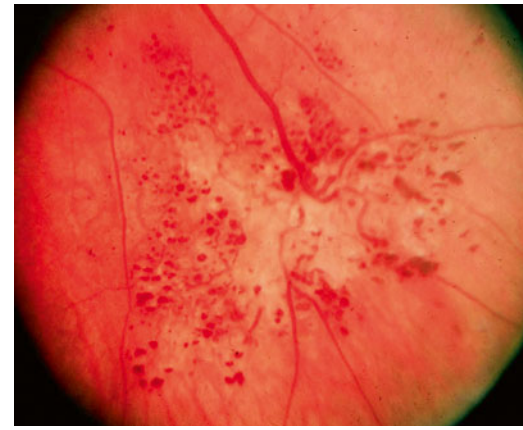

Fig. 9.4 Cavernous hemangioma of the retina. This cluster of small aneurysms, which are filled with stagnant blood, is located over the disc (Reprinted from Atlas of Ophthalmology. http://www.atlasophthalmology.com. Accessed June 11, 2012. With permission from Online Journal of Ophthalmology)

Cavernous Hemangioma

Cavernous hemangioma of the optic disc consists of grapelike clusters of aneurysmal dilatations of large-caliber vessels located within and above the optic disc (Fig. 9.4). The tumor may cover a portion or all of the optic nerve head and may even extend into the peripapillary retina. It usually occurs unilaterally and may be inherited in an irregular autosomal dominant pattern. According to a study by Lewis et al. [40], the average age of presentation was 23 years and 60 % of these tumors occurred in women. Less than 10 % were bilateral. Visual acuity is usually spared, unless the fovea is involved. Visual fields often reveal an enlarged blind spot. Progression of these lesions is rare, and vitreal hemorrhage is unusual. In contrast to capillary hemangiomas of the optic disc and retina, yellow intraretinal and subretinal exudation is not associated with cavernous hemangioma [40].

On histopathology, cavernous hemangiomas consist of large vascular spaces lined with epithelial cells. These spaces replace the normal nerve tissue but do not extend posterior to the lamina cribosa. These tumors extend through the full thickness of the peripapillary retina, but not to the choroid [41].

On fluorescein angiography, the flow through a cavernous hemangioma is slower and is often hypofluorescent in the early stages. The tumor may not entirely fill until the venous phase or later. Some saccules fill completely, whereas others demonstrate an upper portion of dye and a lower portion of erythrocyte plasma. Some tumors may remain hypofluorescent even in the late stages. Slight staining may be seen, but extravascular leakage from the tumor is not commonly seen [40].

On B-scan ultrasonography, the cavernous hemangioma appears as an elevated dome-shaped mass with an anechoic area inside, and no choroidal excavation. A-scan ultrasonography reveals a high initial spike and irregular reflectivity [30].

In contrast to capillary hemangiomas, cavernous hemangiomas may grow within the retrolaminar, intracanalicular, and intracranial optic nerve, optic chiasm [42, 43], or optic tracts to cause a gradual compressive optic neuropathy with subsequent visual loss. More commonly, sudden hemorrhage of the cavernous hemangioma may cause sudden headache, acute decrease in visual acuity, and visual field defects. Up to one-third of patients may present with transient visual loss. Cavernous hemangiomas localized only to the optic disc may grow in size and even cause vitreous hemorrhage severe enough to require vitrectomy [44]. Alcohol abuse, pregnancy-related hormonal changes, and Valsalva maneuver have been associated with a higher risk of aneurysmal rupture, especially in patients between 30 and 40 years of age [43, 44].

In contrast to capillary hemangiomas, cavernous hemangiomas are not associated with von Hippel–Lindau disease, but they are associated with systemic abnormalities, including various cavernous hemangiomas of the skin and brain. The intracranial hemangiomas may cause seizures and intracranial hemorrhage [43, 44].

Treatment is not necessary in most cases because cavernous hemangiomas grow slowly and rarely cause spontaneous vitreous hemorrhage. Cryopexy and photocoagulation might be useful in preventing further vitreous hemorrhage from retinal cavernous hemangiomas [45], but this therapy for optic disc variants is not established at this time.

Optic Nerve Hemangioblastoma

In contrast to capillary and cavernous hemangiomas, optic nerve hemangioblastomas are malignant [46]. Optic nerve hemangioblastomas grow within the nerve parenchyma to cause an anterior or retrobulbar optic neuropathy, which may be either unilateral or bilateral [46–48]. Optic nerve hemangioblastomas contain a vascular matrix with intervascular stromal cells with abundant cytoplasm. These vascular spaces are lined with endothelium and pericytes; lipid-filled stromal cells fill the intervascular areas [47].

Patients present with progressive visual acuity loss, a relative afferent pupillary defect, and variable visual field defects. On MRI, the affected optic nerve appears enlarged and fusiform, mimicking an optic nerve glioma [48].

Thirty percent of optic disc hemangioblastomas are associated with von Hippel–Lindau disease [45]. von Hippel–Lindau disease is an autosomal dominant disorder characterized by retinal and/or optic disc hemangioma and CNS hemangioblastoma, most commonly occurring in the cerebellum and less often in the medulla and spinal cord [49, 50]. The prevalence of von Hippel–Lindau disease has been found to be 1 in 10,000 to 1 in 22,000 [51]. The average age of onset of this disorder is 32 years, but retinal vascular lesions may occur at a younger age (10 years and older) to cause visual impairment from hemorrhage [52]. Up to half of cases of von Hippel–Lindau disease are autosomal dominant with variable penetrance [51]. The remainder of the cases are probably sporadic [32]. The tumor suppressor gene, VHL1, is located on chromosome 3p26 [49, 50], encoding for a protein that regulates hypoxia-inducible genes. Overexpression of

Table 9.2 Clinical diagnostic criteria for von Hippel–Lindau (vHL) disease

Without family history of vHL With family history of vHL
Two or more hemangioblastomas Single hemangioblastoma
OR single hemangioblastoma OR two of the following: Renal cell carcinoma Pheochromocytoma
AND one of the following: Multifocal renal cyst Renal cell carcinoma Pheochromocytoma

(Reprinted from Lonser RR, Glenn GM, Walther M, Chew EY, Libutti SK, Linehan WM, et al. Von Hippel-Lindau disease. The Lancet 2003;361:2059–67. With permission from Elsevier)

hypoxia-inducible mRNAs, such as vascular endothelial growth factor (VEGF), leads to the high vascularization of VHL-related tumors [50]. Systemic features essential for the diagnosis of VHL disease are summarized in Table 9.2 [53]. Ophthalmoscopy, renal ultrasound, and MRI of the brain with contrast should be done every 3 years [54].

Visual loss secondary to optic nerve hemangioblastomas may be preventable with surgical treatment [46, 55]. Resection of the hemangioblastoma with preservation of the optic nerve is possible because the pattern of growth produces a plane of section between the tumor and the optic nerve [45]. If the lesion grows circumferentially around the nerve, then resection may involve permanent damage to the optic nerve. Recent case reports show that anti-angiogenic agents, such as intravitreal bevacizumab, pegaptanib, and ranibizumab, along with photodynamic therapy resulted in a decrease in exudation, tumor regression, and improved visual acuity. Whether VEGF is the ideal target in the inhibition of VHL-related tumor growth is still unproven [56].

Racemose Hemangioma

Racemose hemangiomas are rare arteriovenous anastomoses, consisting of an engorged retinal vessel that enters the optic disc, then into the peripheral retina, and finally out of the optic disc. These hemangiomas usually occur unilaterally and are thought to be congenital abnormalities, but remodeling may occur over years [57]. On histopathology, racemose hemangiomas have a variable fibromuscular medial layer that makes it difficult to distinguish the vessels as either arterial or venous. These vessels may compress the optic nerve and replace normal tissue in the nerve and even the full thickness of the retina [58].

About one-third of racemose hemangiomas are associated with the Wyburn–Mason syndrome, involving arteriovenous malformations in the midbrain that are ipsilateral to a separate retinal lesion. Rarely, an intracranial arteriovenous malformation may extend anteriorly through the optic foramen, along the optic nerve to the retina, all as one lesion [59]. Growth into the orbit and orbital portion of the optic nerve can cause diplopia, proptosis that is usually nonpulsatile, an orbital bruit, and conjunctival vascular dilatation [60, 61]. Intracranial and retinal arteriovenous malformations are also associated with vascular malformations in the ipsilateral maxilla, pterygoid fossa, and mandible to cause epistaxis [62]. They can be located in the ipsilateral frontal areas to cause seizures, intracranial hemorrhage, hemiplegia, and homonymous visual field defects. They can also affect the posterior fossa to cause cranial nerve palsies and other brainstem signs [63–65].

Visual acuity is preserved when a racemose hemangioma has small arteriole–venule anastomoses that involve one sector of the retina and are difficult to detect on funduscopy. However, vision is often impaired when retinal veins grow tortuous and irregularly dilated, mimicking aneurysms. Occasionally several large vessels may grow to obscure the disc to impair vision. The most severe type involves markedly convoluted, dilated, and tortuous arteriovenous communications that drain the macula both superiorly and inferiorly to the horizontal raphe. Central retinal vein occlusion may be a complication, leading to neovascular glaucoma [21, 57, 66]. The enlarged veins, giving the appearance of a bulky lesion, can develop thrombosis or may directly compress the central retinal vein [67]. If an associated

intracranial hemangioma affects the optic tract, then a homonymous hemianopsia is seen [66].

On fluorescein angiography no leakage occurs in the racemose hemangioma, so flow is rapid. The vascular malformation may appear as small, abnormal vessel communications or as an extensive, tortuous "bag of worms" [65].

The workup of an isolated racemose hemangioma in the retina includes a neurological evaluation and neuroimaging, such as an MRI of the brain, to identify an intracranial arteriovenous malformation. If the neurological exam is abnormal, then cerebral angiography may also be considered. Visual prognosis of racemose hemangiomas depends on the location and size of the lesions. They are usually stable and often do not require treatment. Periodic ophthalmologic and neurological examinations should be performed to monitor this disorder [2].

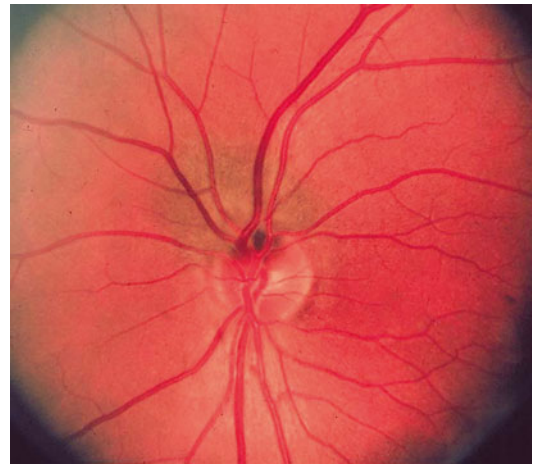

Fig. 9.5 Melanocytoma of the optic disc. Small pigmented tumor extending from the superior aspect of the disc into the choroid (Reprinted from Atlas of Ophthalmology. http://www.atlasophthalmology.com. Accessed June 11, 2012. With permission from Online Journal of Ophthalmology)

Melanocytic Tumors Affecting the Optic Disc

Melanocytoma

Melanocytoma of the optic nerve usually presents unilaterally as a congenital pigmented nevus that appears dark brown or black (Fig. 9.5) [68]. It is a relatively benign tumor of the optic disc that is often diagnosed at about 50 years of age and does not appear to have a racial predilection [69]. This tumor is not associated with systemic disorders, but it is associated with an 8 % incidence of ocular melanocytosis [69].

On histopathology, melanocytomas are composed mainly of two types of cells. The type 1 cell is oval or round, containing giant, round cytoplasmic melanosomes. Nuclei and nucleoli are small. The type 2 nevus cell is spindle shaped, with larger nucleoli, rod-shaped melanosomes, and more cytoplasmic organelles [70, 71].

Some conditions to consider in the differential diagnosis of an optic disc melanocytoma include juxtapapillary choroidal melanoma, choroidal nevus, hyperplasia of the retinal pigment epithelium (RPE), combined hamartoma of the retina and RPE, adenoma of the RPE, metastatic melanoma to the optic disc, and epipapillary vitreous hemorrhage [69].

Seventy-five percent of patients with melanocytoma have visual acuity ranging from 20/15 to 20/30 [68]. Mild visual loss is attributed to the tumor from retinal exudation involving the fovea or neuroretinitis from tumor necrosis [68]. Severe visual loss occurs rarely and is often a result of central retinal vein occlusion and/or spontaneous tumor necrosis [72–77].

An afferent pupillary defect occurs in about 30 % of patients with optic disc melanocytomas in the affected eye [78]. Mild compression of the optic nerve fibers by melanocytoma cells may lead to this pupillary defect in the setting of good visual acuity.

Visual field defects occur in most patients with optic disc melanocytomas. An enlarged blind spot occurs in 75 % of affected patients, arcuate scotomas in 20 %, a nasal step in 10 %, relative nerve fiber bundle defect in 20 %, and an absolute arcuate defect in 20 % [78]. Tumor extension beyond the disc margin may cause an enlarged blind spot. Nerve fiber layer field defects may be related to tumor compression of the axons in the optic disc.

An optic disc melanocytoma appears as a dark brown to black, elevated mass that grows within the substance of the optic disc. Approximately 90 % of melanocytomas measure two disc diameters or less, and most are 1 mm in height [68]. Eleven percent of these melanocytomas increase in size by 5 years and 32 % of them by 10 years [74]. Fifteen percent are confined to the optic disc, and the remainder may be located eccentrically on the disc to affect the nerve fiber layer of the peripapillary retina, giving the appearance of a feathery margin. In 54 % of affected patients, this tumor extends beyond the disc margin to involve the adjacent choroid. In 30 % of affected patients, it grows into the adjacent sensory retina [79].

Fluorescein angiography often reveals persistent hypofluorescence throughout the study.

This finding is related to the densely packed, deeply pigmented cells and avascularity of the tumor. If optic disc edema is present, then hyperfluorescence of the disc can be seen adjacent to the tumor [80, 81]. B-scan ultrasound or CT scan detect this tumor if it is elevated beyond the disc more than 0.5 mm. Optical coherence tomography can detect subretinal fluid and cystoid macular edema [82].

Optic disc melanocytomas display a variety of local complications that account for visual loss in about 26 % of affected patients. In a study of 115 patients with melanocytoma of the optic disc [74], optic disc edema was seen in 25 %, retinal edema in 16 %, localized subretinal fluid in 14 %, retinal exudation in 12 %, retinal hemorrhage in 5 %, vitreous seeds in 4 %, and retinal vein obstruction in 3 %. Optic disc edema adjacent to the tumor is seen more often in larger tumors. This edema is thought to represent axoplasmic stasis from chronic disc compression.

About 54 % of optic disc melanocytomas had a choroidal component and 30 % had a retinal component. Mild peripapillary subretinal fluid is seen in 10 %, and vascular sheathing may be seen in one-third of cases. The spread of the tumor to the retina and the development of subretinal fluid appear to be risk factors for visual loss that is usually not severe [74].

Severe visual loss, however, may be caused by tumor necrosis and retinal vascular occlusion. Rarely, patients may develop spontaneous necrosis of the tumor and surrounding neural tissue from chronic compression of disc vessels. This necrosis can induce obstruction of the central retinal vein and retinal hemorrhages [82]. The visual outcome is poor.

Although melanocytomas are considered to be benign lesions that do not usually require any treatment, they have the potential to produce the aforementioned ocular complications [82]. Tumor growth may lead to ischemic tumor necrosis and visual loss, and not be associated with malignant transformation. Therefore, affected patients should have fundus photos with their eye examination every year [82]. Clinical features suggestive of malignancy at presentation include moderate visual loss, marked elevation, and atypical B-scan echography are indications of possible malignant change de novo or from the juxtapapillary choroids [83]. If progressive growth of the tumor occurs with worsening visual loss, then enucleation should be considered [82].

Choroidal Melanoma

The most common symptoms in patients with a choroidal melanoma are visual loss, photopsias, and visual field defects. Some are asymptomatic. Visual loss is usually a result of the tumor extending to the disc or fovea, exudative retinal detachment involving the macula, or tumor encroaching on the lens. Choroidal melanomas have a racial predilection for Caucasians that is eight times that of blacks [84, 85] and three times that of Asians [86, 87].

Because a choroidal melanoma may have various atypical features, it can mimic other lesions, such as a choroidal nevus, a localized retinal hemorrhage, an RPE tumor, or a choroidal hemangioma. A melanocytoma of the optic disc may mimic a combined hamartoma of the retina and RPE, which has tortuous blood vessels and macular pucker, or an optic disc pit, which appears as an excavated lesion. In contrast to an optic disc melanocytoma, a peripapillary melanoma is not deep black and often grows over a period of months. Melanomas also do not have a feathery margin [88].

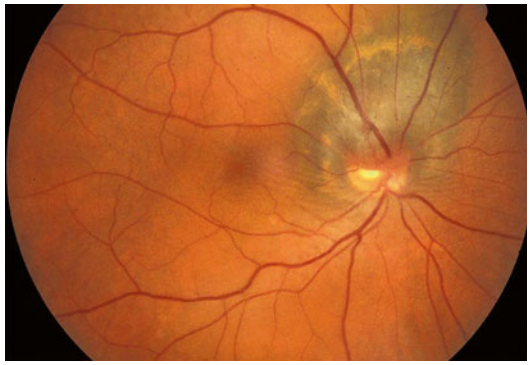

Fig. 9.6 tapapillary choroidal melanoma. Most optic disc melanomas arise from direct extension of juxtapapillary choroidal melanomas. This dark elevated tumor involves the upper aspect of the optic disc. Infiltration of the optic disc is more likely to occur from diffuse, rather than nodular, choroidal melanomas (Reprinted from Atlas of Ophthalmology. http://www.atlasophthalmology.com. Accessed June 11, 2012. With permission from Online Journal of Ophthalmology)

Although the classic choroidal melanoma presents as a pigmented, dome-shaped tumor with an associated exudative retinal detachment, it is the less common presentations of a choroidal melanoma that encroach onto the optic disc. Most optic disc melanomas arise from direct extension of juxtapapillary choroidal melanomas (Fig. 9.6). Infiltration of the optic disc and subarachnoid space is more likely to occur from diffuse choroidal melanomas than from nodular ones. They appear as juxtapapillary, subretinal, brown, or yellow lesions with variable surface pigmentation. Diffuse melanomas are flat, usually less than 5 mm thick, and cover more than 25 % of the uveal tract [89]. Gradual infiltration of the disc may cause worsening optic disc edema and central retinal vein obstruction [90].

On fluorescein angiography, diffuse choroidal melanomas affecting the optic disc appear as diffuse hyperfluorescence or as hyperfluorescence mottled with areas of hypofluorescence. Lesions that appear hyperemic on fundoscopy have uniform hyperfluorescence of the disc on angiography. These clinical findings correlate with tumor impinging upon the disc at the level of the lamina choroidalis without invasion of the optic nerve head. This compressive effect from the tumor may contribute to the disc edema. White tissue on the surface of the disc appears hypofluorescent in the earlier phases of the angiogram and correlates histopathologically with tumor tissue that may have infiltrated the optic nerve itself [90].

Tumor that has infiltrated the disc of a patient with poor vision is best managed by enucleation with a long resection of the optic nerve. Optic nerve invasion is correlated with development of metastases [91]. Radiotherapy, thermotherapy, and other techniques are more effective for local tumor control [92].

Combined Hamartoma of the Retina and RPE

The combined hamartoma of the retina and RPE is a benign, congenital hamartoma involving the pigment epithelium, sensory retina, retinal vasculature, and adjacent vitreous. It affects males and females equally and is usually diagnosed about 15 years of age [93].

On histopathology, the combined hamartoma of the retina and RPE on the disc is composed of glial, vascular, and pigmented cells that replace the normal tissues of the retina and optic nerve. Infiltration of the hyperplastic RPE into the retinal layers and along the inner retinal surface is seen. Glial and fibrous tissue gives a gray-white appearance to the center of the lesion. This gliosis accounts for the vascular tortuosity, tractional folding of the retina, and vitreoretinal interface changes [93, 94].

Visual loss is unilateral and painless. Visual acuity ranges from 20/40 to 20/200 [94–96]. Visual loss occurs more commonly in patients who have lesions involving the optic disc caused by contraction of surface glial tissue that leads to striae distorting the fovea [96]. In a study by Schachat et al. [96], 18 % of the tumors were located on the optic disc, 28 % were in the juxtapapillary area, 38 % involved the macula, 10 % involved both optic disc and fovea, and only 5 % were in the midperiphery. Other features can include hyperpigmentation, tortuosity of vessels, mild elevation, and occasionally an epiretinal membrane. Contraction of the inner aspects of the tumor causes surrounding vessels and retina

to be drawn toward its center. These tumors usually do not grow, but growth has been reported in a few patients [94, 97]. The contraction of the glial tissue can decrease vision and give the appearance of tumor growth [97].

On fluorescein angiography, the early venous filling phase shows tortuous vessels and dilated retinal capillaries. These abnormal vessels show leakage in the later phases of the study. Ultrasound may be useful in ruling out other disc tumors, because combined hamartoma of the retina and RPE is only minimally elevated and is not well seen on ultrasonography.

Complications of combined hamartomas of the retina and RPE include choroidal neovascularization, progressive retinoschisis, retinal hemorrhages, vitreous hemorrhages, exudative retinal detachment, and subretinal and intraretinal exudation [98–100].

It is important to distinguish combined hamartoma of the retina and RPE from retinoblastoma. Choroidal nevi, melanomas, reactive hyperplasia of the RPE, and melanocytoma may all mimic combined hamartomas of the retina and RPE. Gliosis and traction are often absent in nevi, melanomas, and melanocytomas. Reactive hyperplasia of the pigment epithelium appears more irregular than in combined hamartoma [93, 100].

Although the combined hamartoma of the retina and RPE usually occurs in individuals with no underlying systemic abnormalities, several reports have shown that they may be one of the ophthalmic manifestations of the phakomatoses, especially neurofibromatosis types I and II [101–104]. Juvenile nasopharyngeal angiofibroma has also been associated with combined hamartoma of the retina and RPE [105].

Some reports have shown visual improvement in patients with combined hamartoma of the retina and RPE after pars plana vitrectomy and membrane peeling for vitreoretinal traction [106–110]. Subfoveal choroidal neovascularization associated with combined hamartoma of the retina and RPE can be treated successfully by submacular surgery [109]. Based on the results from a study of 41 patients over 4 years by Schachat et al. [100], 66 % of patients remained within two lines of their initial visual acuity, 24 % decreased greater than or equal to two lines, and 10 % improved by greater than or equal to two lines. Three patients underwent patching, and one had vitreous surgery with membrane peeling. However, vitrectomy done on two other patients in this study did not improve vision. It is suggested that when peeling the macular epiretinal membrane, it is difficult to separate it from the tumor, and some of the retinal tractional folds remain after surgery.

Metastatic Tumors

Systemic Cancers, Leukemia

See Chap. 4.

Intrinsic Optic Nerve Tumors

Benign and Malignant Gliomas, Optic Nerve Sheath Meningiomas

See Chap. 4.

Other Granulomatous Lesions

Sarcoidosis

See Chap. 4.

References

1. Shields JA, Augsburger JJ. Current approaches to the diagnosis and management of retinoblastoma. Surv Ophthalmol. 1981;25(6):347–72.
2. Shields JA. Diagnosis and management of intraocular tumors. St. Louis: Mosby; 1983.
3. Knudson Jr AG. Mutation and cancer: statistical study of retinoblastoma. Proc Natl Acad Sci U S A. 1971;68(4):820–3.
4. Ellsworth RM. The practical management of retinoblastoma. Trans Am Ophthalmol Soc. 1969;67:462–534.
5. Kingston JE, Plowman PN, Hungerford JL. Ectopic intracranial retinoblastoma in childhood. Br J Ophthalmol. 1985;69(10):742–8.

6. Bader JL, Meadows AT, Zimmerman LE, et al. Bilateral retinoblastoma with ectopic intracranial retinoblastoma: trilateral retinoblastoma. Cancer Genet Cytogenet. 1982;5(3):203–13.
7. Howard GM, Ellsworth RM. Differential diagnosis of retinoblastoma. A statistical survey of 500 children. II. Factors relating to the diagnosis of retinoblastoma. Am J Ophthalmol. 1965;60(4):618–21.
8. Shields JA, Leonard BC, Michelson JB, et al. B-scan ultrasonography in the diagnosis of atypical retinoblastomas. Can J Ophthalmol. 1976;11(1):42–51.
9. Hermsen VM. Echographic diagnosis. In: Lodi FC, editor. Retinoblastoma. New York: Churchill Livingstone; 1985. p. 62–71.
10. Merriam Jr GR. Retinoblastoma: analysis of 17 autopsies. Arch Ophthalmol. 1950;44(1):71–108.
11. Abramson DH, Ellsworth RM. Optic nerve involvement in retinoblastoma. Ophthalmology. 1989;96(2): 217–22.
12. Shields CL, Shields JA. Retinoblastoma management: advances in enucleation, intravenous chemoreduction, and intra-arterial chemotherapy. Curr Opin Ophthalmol. 2010;21(3):203–12.
13. Karch SB, Urich H. Medulloepithelioma: definition of an entity. J Neuropathol Exp Neurol. 1972;31(1): 27–53.
14. Green WR, Iliff WJ, Trotter RR. Malignant teratoid medulloepithelioma of the optic nerve. Arch Ophthalmol. 1974;91(6):451–4.
15. Grover WD, Harley RD. Early recognition of tuberous sclerosis by funduscopic examination. J Pediatr. 1969;75(6):991–5.
16. Robertson DM. Astrocytic hamartomas. Ann N Y Acad Sci. 1991;615(1):17–25.
17. Barksy D, Wolter JR. The retinal lesion of tuberous sclerosis: an angiogliomatous hamartoma? J Pediatr Ophthalmol. 1971;8:261.
18. Foos RY, Straatsma BR, Allen RA. Astrocytoma of the optic nerve head. Arch Ophthalmol. 1965;74: 319–26.
19. Reeser FJ, Aaberg TM, van Horn D. Astrocytic hamartoma of the retina not associated with tuberous sclerosis. Am J Ophthalmol. 1978;86(5):688–98.
20. Lagos JC, Gomez MR. Tuberous sclerosis: reappraisal of a clinical entity. Mayo Clin Proc. 1967;42(1): 26–49.
21. Cleasby GW, Fung WE, Shekter WB. Astrocytoma of the retina. Report of two cases. Am J Ophthalmol. 1967;64 suppl 3:633–7.
22. Font RL, Ferry AP. The phakomatoses. Int Ophthalmol Clin. 1972;12(1):1–50.
23. Turek M, Raistrick ER, Hart CD. Retinal tumours in neurofibromatosis. Can J Ophthalmol. 1977;12(1): 68–70.
24. Darling TN, Skarulis MC, Steinberg SM, et al. Multiple facial angiofibromas and collagenomas in patients with multiple endocrine neoplasia type 1. Arch Dermatol. 1997;133(7):853–7.
25. Nickel WR, Reed WB. Tuberous sclerosis. Special reference to the microscopic alterations in the cutaneous hamartomas. Arch Dermatol. 1962;85:209–26.
26. Roach ES, Gomez MR, Northrup H. Tuberous sclerosis complex consensus conference: revised clinical diagnostic criteria. J Child Neurol. 1998; 13(12):624–8.
27. McLean EB. Hamartoma of the retinal pigment epithelium. Am J Ophthalmol. 1976;82(2):227–31.
28. Macmichael IM. Von Hippel-Lindau's disease of the optic disc. Trans Ophthalmol Soc U K. 1970;90: 877–85.
29. Nicholson DH, Green WR, Kenyon KR. Light and electron microscopic study of early lesions in angiomatosis retinae. Am J Ophthalmol. 1976;82(2): 193–204.
30. Pierro L, Guarisco L, Zaganelli E, et al. Capillary and cavernous hemangioma of the optic disc. Echographic and histological findings. Acta Ophthalmol Suppl. 1992;204:102–6.
31. Schindler RF, Sarin LK, MacDonald PR. Hemangiomas of the optic disc. Can J Ophthalmol. 1975;10(3):305–18.
32. Brown GC, Magargal LE, Schachat A, et al. Neovascular glaucoma. Etiologic considerations. Ophthalmology. 1984;91(4):315–20.
33. Augsburger JJ, Shields JA, Goldberg RE. Classification and management of hereditary retinal angiomas. Int Ophthalmol. 1981;4(1–2):93–106.
34. Hardwig P, Robertson DM. von Hippel-Lindau disease: a familial, often lethal, multi-system phakomatosis. Ophthalmology. 1984;91(3):263–70.
35. Carr RE, Noble KG. Retinal angiomatosis. Ophthalmology. 1980;87(9):956–9, 961.
36. Goldberg ME, Koenig S. Argon laser treatment of von Hippel-Lindau retinal angiomas. Arch Ophthalmol. 1974;92:121.
37. Annesley Jr WH, Leonard BC, Shields JA, et al. Fifteen year review of treated cases of retinal angiomatosis. Trans Sect Ophthalmol Am Acad Ophthalmol Otolaryngol. 1977;83(83 Pt1): OP446–53.
38. Cardoso RD, Brockhurst RJ. Perforating diathermy coagulation for retinal angiomas. Arch Ophthalmol. 1976;94(10):1702–15.
39. Salazar EG, Lamiell JM. Early identification of retinal angiomas in a large kindred with von Hippel-Lindau disease. Am J Ophthalmol. 1980;89:540.
40. Lewis RA, Cohen MH, Wise GN. Cavernous haemangioma of the retina and optic disc. A report of three cases and a review of the literature. Br J Ophthalmol. 1975;59(8):422–34.
41. Davies WS, Thumim M. Cavernous hemangioma of the optic disc and retina. Trans Am Acad Ophthalmol Otolaryngol. 1956;60(2):217–8.
42. Maruoka N, Yamakawa Y, Shimauchi M. Cavernous hemangioma of the optic nerve. Case report. J Neurosurg. 1988;69(2):292–4.
43. Castel JP, Delorge-Kerdiles C, Rivel J. Cavernous angioma of the optic chiasm. Neurochirurgie. 1989;35(4):252–6.
44. Kushner MS, Jampol LM, Haller JA. Cavernous hemangioma of the optic nerve. Retina. 1994;14(4): 359–61.

45. Manschot WA. Juxtapapillary retinal angiomatosis. Arch Ophthalmol. 1968;80(6):775–6.
46. Kerr DJ, Scheithauer BW, Miller GM, et al. Hemangioblastoma of the optic nerve: case report. Neurosurgery. 1995;36(3):573–80.
47. In S, Miyagi J, Kojho N, et al. Intraorbital optic nerve hemangioblastoma with von Hippel-Lindau disease. J Neurosurg. 1982;56(3):426–9.
48. Ginzburg BM, Montanera WJ, Tyndel FJ, et al. Diagnosis of von Hippel-Lindau disease in a patient with blindness resulting from bilateral optic nerve hemangioblastomas. AJR Am J Roentgenol. 1992; 159(2):403–5.
49. Nerad JA, Kersten RC, Anderson RL. Hemangioblastoma of the optic nerve. Report of a case and review of literature. Ophthalmology. 1988; 95(3):398–402.
50. Hardwig P, Robertson DM. von Hippel-Lindau disease: a familial, often lethal, multisystem phakomatosis. Ophthalmology. 1984;91(3):263–70.
51. Seizinger BR, Rouleau GA, Ozelius LJ, et al. Von Hippel-Lindau disease maps to the region of chromosome 3 associated with renal cell carcinoma. Nature. 1988;332(6161):268–9.
52. Krill AE. Hereditary retinal and choroidal diseases, vol. 2. Hagerstown: Harper and Row; 1997.
53. Lonser RR, Glenn GM, Walther M, Chew EY, Libutti SK, Linehan WM, et al. Von Hippel-Lindau disease. Lancet. 2003;361:2059–67.
54. Rosenberg RN, Prusiner SB, DiMauro S, et al. The molecular and genetic basis of neurologic and psychiatric disease. 3rd ed. Philadelphia, PA: Butterworth Heinemann; 2003.
55. Raila FA, Zimmerman J, Azordegan P, et al. Successful surgical removal of an asymptomatic optic nerve hemangioblastoma in von Hippel-Lindau disease. J Neuroimaging. 1997;7(1):48–50.
56. Wong WT, Chew EY. Ocular von Hippel-Lindau disease: clinical update and emerging treatments. Curr Opin Ophthalmol. 2008;19(3):213–7.
57. Archer DB, Deutman A, Ernest JT, et al. Arteriovenous communications of the retina. Am J Ophthalmol. 1973;75(2):224–41.
58. Cameron ME, Greer CH. Congenital arteriovenous aneurysm of the retina. A post mortem report. Br J Ophthalmol. 1968;52(10):768–72.
59. Theron J, Newton TH, Hoyt WF. Unilateral retinocephalic vascular malformations. Neuro-radiology. 1974;7(4):185–96.
60. Wyburn-Mason R. Arteriovenous aneurysm of the midbrain and retina, facial nevi and mental changes. Brain. 1943;66:163.
61. Kikuchi K, Kowada M, Sakamoto T, et al. Wyburn-Mason syndrome: report of a rare case with computed tomography and angiographic evaluations. J Comput Tomogr. 1988;12(2):111–5.
62. Ladow CS, McFall TA. Central hemangioma of the maxilla, with von Hippel's disease: report of a case. J Oral Surg Anesth Hosp Dent Serv. 1964;22:252–9.
63. Sperner J, Schmauser I, Bittner R, et al. MR imaging findings in children with Sturge-Weber syndrome. Neuropediatrics. 1990;21(3):146–52.
64. Rundles Jr WZ, Falls HF. Congenital arteriovenous (racemose) aneurysm of the retina; report of 3 cases. AMA Arch Ophthalmol. 1951;46(4):408–18.
65. Cameron ME. Congenital arteriovenous aneurysm of the retina. Br J Ophthalmol. 1958;42(11):655–66.
66. Destro M, D'Amico DJ, Gragoudas ES, et al. Retinal manifestations of neurofibromatosis. Diagnosis and management. Arch Ophthalmol. 1991;109(5):662–6.
67. Traboulsi EI. Neovascular glaucoma and ischemia. J Clin Neuro-Ophthalmol. 1986;6(2):126–7.
68. Joffe L, Shields JA, Osher RH, et al. Clinical and follow-up studies of melanocytomas of the optic disc. Ophthalmology. 1979;86(6):1067–83.
69. Shields JA, Demirci H, Mashayekhi A, et al. Melanocytoma of optic disc in 115 cases: the 2004 Samuel Johnson Memorial Lecture, part 1. Ophthalmology. 2004;111(9):1739–46.
70. Juarez CP, Tso MO. An ultrastructural study of melanocytomas (magnocellular nevi) of the optic disk and uvea. Am J Ophthalmol. 1980;90(1):48–62.
71. Mansour AM, Zimmerman L, La Piana FG, et al. Clinicopathological findings in a growing optic nerve melanocytoma. Br J Ophthalmol. 1989;73(6):410–5.
72. Apple DJ, Craythorn JM, Reidy JJ, et al. Malignant transformation of an optic nerve melanocytoma. Can J Ophthalmol. 1984;19(7):320–5.
73. Croxatto JO, Ebner R, Crovetto L, et al. Angle closure glaucoma as initial manifestation of melanocytoma of the optic disc. Ophthalmology. 1983;90(7):830–4.
74. Shields CL, Demirci H, Karatza E, et al. Clinical survey of 1643 melanocytic and nonmelanocytic conjunctival tumors. Ophthalmology. 2004;111(9): 1747–54.
75. Shields JA, Shields CL, Eagle Jr RC, et al. Malignant melanoma associated with melanocytoma of the optic disc. Ophthalmology. 1990;97(2):225–30.
76. Shields JA, Shields CL, Eagle Jr RC, et al. Central retinal vascular obstruction secondary to melanocytoma of the optic disc. Arch Ophthalmol. 2001;119(1): 129–33.
77. Wiznia RA, Price J. Recovery of vision in association with a melanocytoma of the optic disk. Am J Ophthalmol. 1974;78(2):236–8.
78. Osher RH, Shields JA, Layman PR. Pupillary and visual field evaluation in patients with melanocytoma of the optic disc. Arch Ophthalmol. 1979;97(6): 1096–9.
79. De Potter P, Shields CL, Shields JA, et al. Plaque radiotherapy for juxtapapillary choroidal melanoma. Visual acuity and survival outcome. Arch Ophthalmol. 1996;114(11):1357–65.
80. Gahankari MD, Jehangir R, Bhatti SS. Melanocytoma of the optic disc. J Postgrad Med. 1992;38(3): 135–6.
81. Shields JA. Melanocytoma of the optic nerve head: a review. Int Ophthalmol. 1978;1(1):31–7.

82. Shields JA, Demirci H, Mashayekhi A, et al. Melanocytoma of the optic disk: a review. Surv Ophthalmol. 2006;51(2):93–104.
83. Sharma PM, Sangal K, Malik P, et al. Malignant transformation of optic disc melano-cytoma? A clinical dilemma at presentation with a review of the literature. Ophthalmologica. 2002;216(4):292–5.
84. Graham BJ, Duane TD. Ocular melanoma task force report. Am J Ophthalmol. 1980;90(5):728–33.
85. Margo CE, McLean IW. Malignant melanoma of the choroid and ciliary body in black patients. Arch Ophthalmol. 1984;102(1):77–9.
86. Haukin T, Teppo L, Saxen F. Cancer of the eye: a review of trends and differentials. World Health Stat Q. 1978;31:143–58.
87. Scotto J, Fraumeni Jr JF, Lee JA. Melanomas of the eye and other noncutaneous sites: epidemiologic aspects. J Natl Cancer Inst. 1976;56(3):489–91.
88. Ferry AP. Lesions mistaken for malignant melanoma of the posterior uvea: a clinicopathologic analysis of 100 cases with ophthalmoscopically visible lesions. Arch Ophthalmol. 1964;72:463–9.
89. Font RL, Spaulding AG, Zimmerman LE. Diffuse malignant melanoma: a clinicopathologic report of 54 cases. Trans Am Acad Ophthalmol Otolaryngol. 1968;72(6):877–95.
90. Shields JA. Lesions simulating malignant melanoma of the posterior uvea. Arch Ophthalmol. 1973;89(6): 466–71.
91. Affeldt JC, Minckler DS, Azen SP, et al. Prognosis in uveal melanoma with extrascleral extension. Arch Ophthalmol. 1980;98(11):1975–9.
92. Shields CL, Shields JA. Recent developments in the management of choroidal melanoma. Curr Opin Ophthalmol. 2004;15(3):244–51.
93. Vogel MH, Zimmerman LE, Gass JD. Proliferation of the juxtapapillary retinal pigment epithelium simulating malignant melanoma. Doc Ophthalmol. 1969;26:461–81.
94. Cardell BS, Starbuck MS. Juxtapapillary hamartoma of retina. Br J Ophthalmol. 1961;45:672–7.
95. Gass JD. An unusual hamartoma of the pigment epithelium and retina simulating choroidal melanoma and retinoblastoma. Trans Am Ophthalmol Soc. 1973;71:171–83. discussions 184–185.
96. Schachat AP, Shields JA, Fine SL, et al. Combined hamartomas of the retina and retinal pigment epithelium. Ophthalmology. 1984;91(12):1609–15.
97. Rosenberg PR, Walsh JB. Retinal pigment epithelial hamartoma: unusual manifestations. Br J Ophthalmol. 1984;68(6):439–42.
98. Kahn D, Goldberg MF, Jednock N. Combined retinal pigment epithelial hamartoma presenting as a vitreous hemorrhage. Retina. 1984;4(1):40–3.
99. Flood TP, Orth DH, Aaberg TM, et al. Macular hamartomas of the retinal pigment epithelium and retina. Retina. 1983;3(3):164–70.
100. Schachat AP, Glaser BM. Retinal hamartoma, acquired retinoschisis, and retinal hole. Am J Ophthalmol. 1985;99(5):604–5.
101. Kaye LD, Rothner AD, Beauchamp GR, et al. Ocular findings associated with neurofibromatosis type II. Ophthalmology. 1992;99(9):1424–9.
102. Palmer ML, Carney MD, Combs JL. Combined hamartomas of the retinal pigment epithelium and retina. Retina. 1990;10(1):33–6.
103. Sivalingam A, Augsburger J, Perilongo G, et al. Combined hamartoma of the retina and retinal pigment epithelium in a patient with neurofibromatosis type 2. J Pediatr Ophthalmol Strabismus. 1991;28(6):320–2.
104. Vianna RN, Pacheco DF, Vasconcelos MM, et al. Combined hamartoma of the retina and retinal pigment epithelium associated with neurofibromatosis type 1. Int Ophthalmol. 2001;24(2):63–6.
105. Fonseca RA, Dantas MA, Kaga T, et al. Combined hamartoma of the retina and retinal pigment epithelium associated with juvenile nasopharyngeal angiofibroma. Am J Ophthalmol. 2001;132(1):131–2.
106. Mason III JO. Visual improvement after pars plana vitrectomy and membrane peeling for vitreoretinal traction associated with combined hamartoma of the retina and retinal pigment epithelium. Retina. 2002;22(6):824–5.
107. Sappenfield DL, Gitter KA. Surgical intervention for combined hamartoma of the retina and retinal pigment epithelial hamartoma. Retina. 1990;10(2): 119–24.
108. Stallman JB. Visual improvement after pars plana vitrectomy and membrane peeling for vitreoretinal traction associated with combined hamartoma of the retina and retinal pigment epithelium. Retina. 2002; 22(1):101–4.
109. Inoue M, Noda K, Ishida S, et al. Successful treatment of subfoveal choroidal neovascularization associated with combined hamartoma of the retina and retinal pigment epithelium. Am J Ophthalmol. 2004;138(1):155–6.
110. McDonald HR, Abrams GW, Burke JM, et al. Clinicopathologic results of vitreous surgery for epiretinal membranes in patients with combined retinal and retinal pigment epithelial hamartomas. Am J Ophthalmol. 1985;100(6):806–13.

10 Approach to the Diagnosis and Differentiation of Glaucomatous and Nonglaucomatous Optic Neuropathies

Christopher Kai Shun Leung and Carmen K.M. Chan

Introduction

This chapter highlights the important clinical features that distinguish glaucomatous from nonglaucomatous optic neuropathies. Neuroretinal rim narrowing and optic disc excavation characterize glaucomatous optic disc damage, whereas neuroretinal rim pallor is indicative of nonglaucomatous optic neuropathy. While retinal nerve fiber layer (RNFL) imaging with optical coherence tomography (OCT) plays an important role in confirming the presence of optic neuropathy, documenting the severity of optic nerve damage, and monitoring the progression of disease, the etiology of an optic neuropathy requires detailed history taking, clinical examination, and other appropriate investigations, including neuroimaging and laboratory tests, for confirmation. Perimetry, as well as central and color vision testing, is also essential in estimating functional damage and should be an integral part in the assessment of both glaucomatous and nonglaucomatous optic neuropathies.

C.K.S. Leung, M.D., M.B.Ch.B., B.MedSc., M.Sc., F.H.K.A.M., F.H.K.C.Ophth. (✉)
Department of Ophthalmology & Visual Sciences, University Eye Center, Hong Kong Eye Hospital, The Chinese University of Hong Kong,
147K Argyle Street, Kowloon, Hong Kong
e-mail: tlims00@hotmail.com

C.K.M. Chan, M.B.BChir., M.R.C.P., F.R.C.S.Ed(Ophth). (✉)
Department of Ophthalmology, Hong Kong Eye Hospital, The Chinese University of Hong Kong, 147 K, Argyle Street, Kowloon, Hong Kong
e-mail: kmcc2001@hotmail.com

History Taking

History taking provides important clues to the diagnosis of optic neuropathy. Glaucoma is the most common type of optic neuropathy. Except in patients with chronic angle-closure glaucoma who develop an acute angle-closure attack, it is often asymptomatic despite extensive visual field loss. Most glaucoma patients are not aware of progressive visual field loss because the rate of disease progression is often slow.

In the assessment of an optic neuropathy, sudden visual loss suggests an acute optic neuropathy, such as optic neuritis, traumatic optic neuropathy, and non-arteritic or arteritic ischemic optic neuropathy. Optic neuritis is often characterized by pain with eye movement. In the Optic Neuritis Treatment Trial (ONTT), 92 % of the patients had eye pain [1]. Sudden painful visual loss also needs to be differentiated from an acute angle-closure attack due to an elevated intraocular pressure (IOP).

Medical history, medication history, family history, and associated systemic symptoms are useful to formulate the differential diagnosis of an optic neuropathy. Some salient features of history taking in the work-up of an optic neuropathy are summarized in Table 10.1.

J.W. Chan (ed.), *Optic Nerve Disorders: Diagnosis and Management*,
DOI 10.1007/978-1-4614-0691-4_10,

Table 10.1 Salient features in history taking in the differentiation of various nonglaucomatous optic neuropathies

Type of optic neuropathy	Salient features in history taking
Compressive optic neuropathy	• History of neurosurgical procedures • Diplopia, ptosis, and proptosis may suggest other cranial nerve involvement or a retro-orbital lesion
Non-arteritic ischemic optic neuropathy	• History of acute visual loss • Vasculopathic risk factors, such as diabetes, hypertension, and tobacco use
Arteritic ischemic optic neuropathy	• History of acute visual loss • Headache, jaw claudication, general malaise, and weight loss
Demyelinating optic neuritis	• History of acute visual loss • Pain, especially on eye movement • History of multiple sclerosis or vaccinations
Hereditary optic neuropathy	• History of acute visual loss, as in Leber's hereditary optic neuropathy • Family history of optic neuropathy
Toxic/metabolic optic neuropathy	• History of tobacco and alcohol use • History of antituberculosis medication use
Traumatic optic neuropathy	• History of significant head or ocular trauma

Clinical Examination

Visual Acuity and Color Vision

Central vision is commonly well preserved in glaucoma until the end stages. Depending on the etiology and severity of the optic nerve damage, the presenting visual acuity in patients with nonglaucomatous optic neuropathies varies widely. Visual acuity is usually worse in eyes with a nonglaucomatous optic neuropathy compared with those with a glaucomatous optic neuropathy. In a case-controlled study comparing glaucomatous optic neuropathies with compressive optic neuropathies related to chronic intracranial mass lesions, 76.9 and 47.7 % of eyes had visual acuity better than 20/40, respectively [2]. In another study examining 386 eyes from 340 consecutive untreated patients with nonarteritic ischemic optic neuropathy, 49 % of eyes had presenting visual acuity ≥20/30 [3]. For eyes with presenting visual acuity ≤20/70 (31 %), 41 % improved at 6 months. Of the 457 eyes in the ONTT, 35.4 % had visual acuity ≥20/40 and 36.3 % had visual acuity ≤20/200 in the initial visit [1]. Most patients with typical demyelinating optic neuritis have good visual recovery. Seventy-two percent of the affected eyes in the ONTT had a visual acuity of ≥20/20 by 15 years [4].

Regarding color vision, blue-yellow color deficiency is more common in glaucomatous optic neuropathy, whereas red-green color deficiency is more common in nonglaucomatous optic neuropathy. Autosomal dominant optic neuropathy and ethambutol-related toxic optic neuropathy may exhibit tritanopia [5, 6].

Relative Afferent Pupillary Defect

The presence of a relative afferent pupillary defect (RAPD) is a hallmark feature of a unilateral or bilateral optic neuropathy with asymmetric involvement. Nonglaucomatous optic neuropathies can be predominantly unilateral, such as in optic neuritis, ischemic optic neuropathy, and traumatic optic neuropathy, or bilateral, such as in hereditary and toxic/metabolic optic neuropathies. A glaucomatous optic neuropathy is often bilateral with asymmetric involvement. In a systematic review examining a total of 30 clinical studies, an RAPD was evident in 9–82 % of patients with glaucoma [7]. Therefore, the presence of an RAPD does not always help distinguish between glaucomatous and nonglaucomatous optic neuropathies.

IOP and Central Corneal Thickness Measurement

Although the IOP adds no diagnostic value in differentiating glaucomatous from nonglaucomatous optic neuropathies, measurement of the IOP is pertinent to estimating the risk of glaucoma progression and monitoring the treatment response. Goldmann applanation tonometry (GAT) is considered the standard for IOP measurement. It is important to also measure the central corneal thickness for the interpretation of the

GAT measurement, since GAT overestimates IOP in thick corneas and underestimates it in thin corneas. Thin corneas are also at a higher risk for the development of glaucoma in patients with ocular hypertension, independent of the level of the IOP. Although various formulas have been suggested to correct the GAT IOP readings for the adjustment of central corneal thickness, such correction is not recommended in clinical practice and may result in readings further away from the true values [8, 9]. In eyes with abnormal corneal thickness and biomechanical properties, such as in those after corneal refractive surgery, dynamic contour tonometry would be more useful in providing reliable IOP measurements that are less dependent on corneal thickness and biomechanical properties [10, 11].

Examination of the Anterior and Posterior Segments

Careful examination of the anterior segment is important for the assessment of an optic neuropathy. The presence of anterior chamber cells, keratic precipitates, iris atrophy, posterior synechiae, and peripheral anterior synechiae are suggestive of an active or chronic anterior uveitis that may result in an elevation of IOP and uveitic glaucoma. The possibility of steroid-induced glaucoma should always be considered in these eyes. Gonioscopy is indispensable to detect peripheral anterior synechiae and to determine the angle width. Primary angle closure is diagnosed when $\leq 90°$ of the posterior trabecular meshwork is visible with evidence of peripheral anterior synechiae and/or increased IOP [>97.5th percentile for the population ($\geq$22 mmHg)] [12]. Primary angle-closure glaucoma is defined as having primary angle closure with a glaucomatous optic neuropathy. The finding of angle recessions and pupillary sphincter tears suggests either a traumatic optic neuropathy if a pale neuroretinal rim is seen, or angle-recession glaucoma if a pink and narrowed neuroretinal rim is present. Pigment in the endothelium (Krukenberg spindle), iris trans-illumination in the mid-peripheral iris, and heavy pigmentation of the trabecular meshwork are all indicative of pigment dispersion syndrome. The presence of white pseudoexfoliative material on the pupillary margin and the anterior lens surface is suggestive of pseudoexfoliation syndrome. Vitritis, snowballs, snowbanking, and peripheral retinal vasculitis are all signs of intermediate uveitis, which can be associated with optic neuritis. The presence of a macular hard exudate or macular star with an optic neuropathy is suggestive of a neuroretinitis, whereas parapapillary hard exudates are more consistent with recently resolved disc swelling.

Examination of the Optic Disc

A binocular examination is required to evaluate the extent of neuroretinal rim loss and the degree of optic disc cupping. Documentation of the morphology and color of the neuroretinal rim is best attained with color stereoscopic optic disc photographs.

The discrimination between glaucomatous from nonglaucomatous optic neuropathies is largely based on the assessment of the color and morphology of the neuroretinal rim. A pale neuroretinal rim suggests a nonglaucomatous optic neuropathy, whereas a narrowed neuroretinal rim signifies a glaucomatous one (Fig. 10.1). Glaucomatous optic discs may appear pale in the late stages because of extensive loss of the neuroretinal rim. The lamina cribrosa is exposed in advanced glaucoma. Light reflected from the lamina cribrosa is white, which gives the pale appearance of the optic discs. It is important to note that the residual neuroretinal rim tissue in glaucomatous optic discs often remains pink. It has been reported that neuroretinal rim pallor is 94 % specific for nonglaucomatous optic neuropathy, whereas focal or diffuse obliteration of the neuroretinal rim is 87 % specific for glaucomatous optic neuropathy [13].

Neuroretinal Rim Pallor

Accurate and reliable assessment of the color of the neuroretinal rim is not easy. Because of interobserver variations in the intensity and the angle

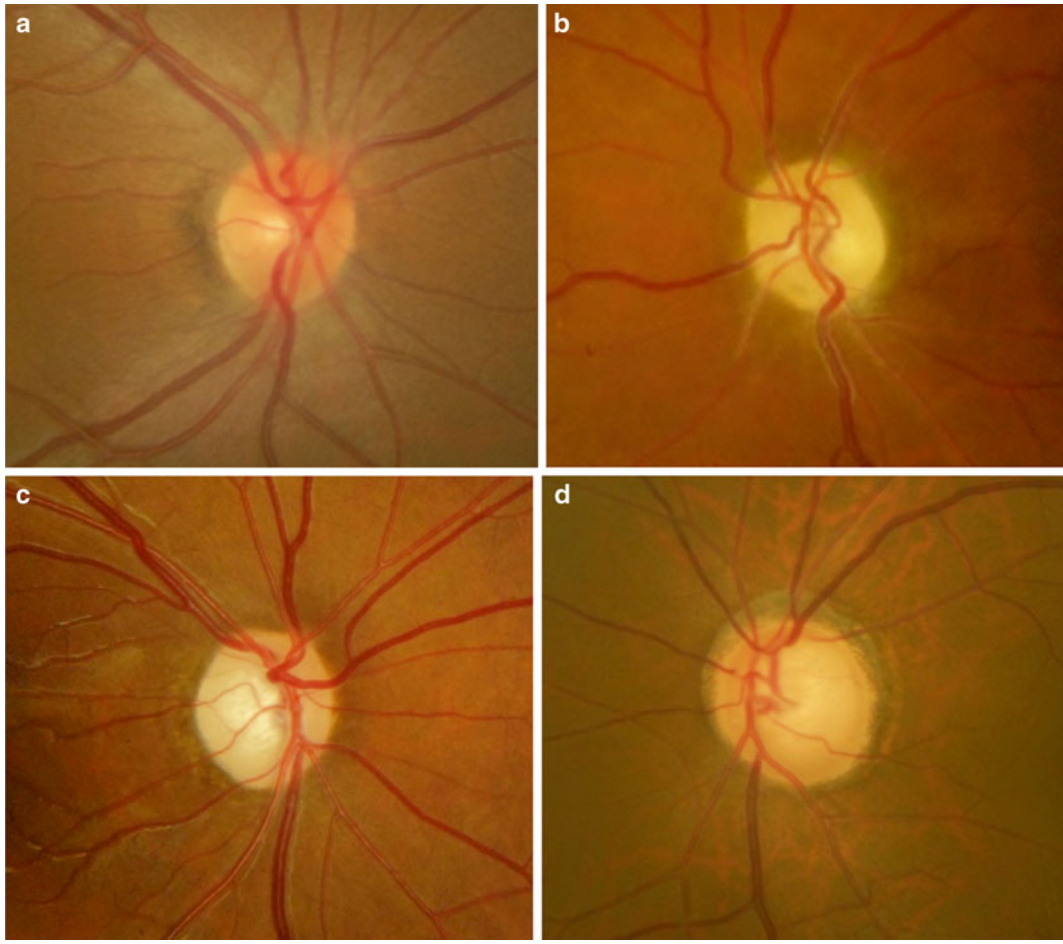

Fig. 10.1 (**a**) A normal healthy eye with a pink and intact neuroretinal rim. (**b**) A pale-looking optic disc with resolved non-arteritic anterior ischemic optic neuropathy. Although the neuroretinal rim is pale, there is no definite neuroretinal rim loss. (**c**) An optic disc with Leber's hereditary optic neuropathy that has an intact but pale neuroretinal rim, more noticeable on the temporal than the nasal aspect. (**d**) An advanced glaucomatous optic disc with diffuse narrowing of the neuroretinal rim and cupping

of incidence of illumination and interindividual differences in the density of the crystalline lens, interpretation of the neuroretinal rim color is highly subjective. The normal neuroretinal rim appears pink because of the presence of capillaries. The neuroretinal rim becomes pale when gliosis and retinal ganglion cell axonal loss occurs, with or without the loss of capillaries. Gliosis covers the capillaries to obscure their reflection. A pale neuroretinal rim is indicative of nonglaucomatous optic neuropathies. Superior or inferior segmental disc and rim pallor can be found in anterior ischemic optic neuropathy after the segmental swelling resolves. Bilateral segmental disc and rim pallor, or band atrophy, occurs in chiasmal lesions when there is a loss of nasal fibers crossing the optic chiasm. Therefore, the detection of neuroretinal rim pallor requires further investigation in order to identify the etiology of the optic nerve damage.

Loss of Neuroretinal Rim and Cupping

Both glaucomatous and nonglaucomatous optic neuropathies are characterized by loss of retinal ganglion cells, but glaucomatous differs from

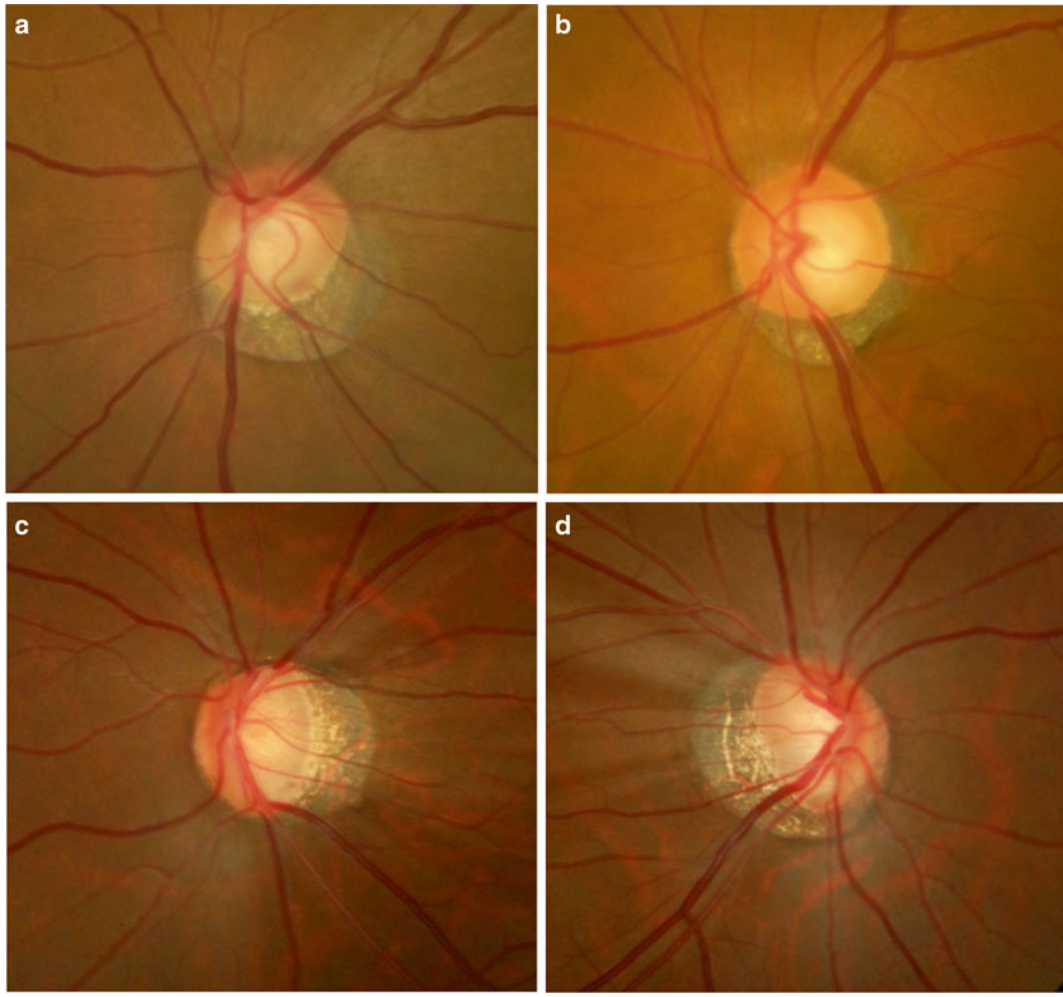

Fig. 10.2 (**a**) A glaucomatous optic disc with loss of the inferotemporal neuroretinal rim but relatively normal superotemporal neuroretinal rim. (**b**) Another glaucomatous optic disc with loss of the inferotemporal rim and early narrowing of the superotemporal neuroretinal rim. An inferotemporal retinal nerve fiber layer (RNFL) defect is also present. (**c**, **d**) show neuroretinal rim loss and RNFL thinning in both the inferotemporal and superotemporal sectors

nonglaucomatous optic neuropathies in having optic nerve head remodeling with progressive narrowing of the neuroretinal rim and excavation of the optic disc. Glaucomatous optic disc damage exhibits characteristic patterns, with the loss of neuroretinal rim commonly initiated in the inferotemporal followed by the superotemporal sector (Fig. 10.2). The inferotemporal and superotemporal sectors are the most frequent locations of neuroretinal rim loss and retinal nerve fiber layer (RNFL) thinning. The increase in cup-to-disc ratio is a result of the loss of neuroretinal rim.

Optic disc cupping is also a characteristic feature in glaucoma. Progressive optic nerve head remodeling and displacement of lamina cribrosa occurs during the course of glaucomatous progression. However, optic disc cupping can also be seen in other types of nonglaucomatous optic neuropathies. Cupping has been reported in 50 % of eyes after arteritic ischemic optic neuropathy and 10 % after non-arteritic ischemic optic neuropathy [14]. Disc cupping can be seen in hereditary optic neuropathy, compressive optic neuropathy involving the anterior visual

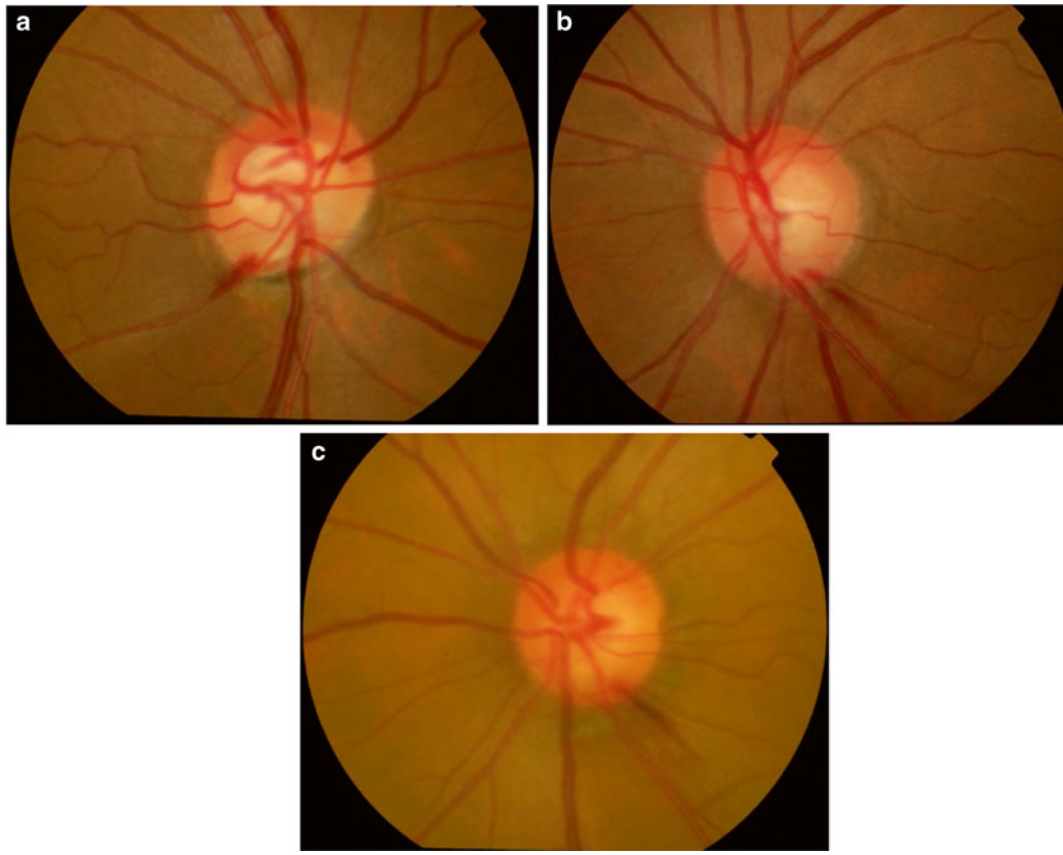

Fig. 10.3 Optic disc hemorrhages (**a**–**c**). All optic discs show loss of the inferotemporal neuroretinal rim and thinning of the inferotemporal retinal nerve fiber layer (RNFL). The disc hemorrhages are located along the temporal border of the RNFL defects

pathway, traumatic optic neuropathy, fusiform aneurysm of the intracranial carotid artery, and optic nerve infarction [15]. A large cup can even be present in a large healthy, normal optic disc. Careful history taking and examination of the neuroretinal rim are often informative to distinguish glaucomatous from nonglaucomatous optic disc cupping.

Other Optic Disc Features of Glaucoma

Other optic disc features, such as saucerization, notching, nasalization, and bayoneting of disc vessels, that have been used to describe glaucomatous optic discs, are consequences of diffuse or localized loss of the neuroretinal rim. Although beta zone peripapillary atrophy (atrophy of the retinal pigment epithelium and choriocapillaries) is more common in glaucoma, it can also be found in normal eyes, particularly in eyes with myopia. Optic disc hemorrhage is a relatively specific, albeit insensitive indicator of glaucoma (Fig. 10.3). Disc hemorrhage is also a risk factor for glaucoma progression. Disc hemorrhage can be found in nonglaucomatous optic neuropathies when there is concomitant optic disc swelling. Furthermore, diabetic retinopathy, posterior vitreous detachment, and anticoagulant therapy are other causes of disc hemorrhage. Table 10.2 compares some of the main differences in clinical findings between glaucomatous and nonglaucomatous optic neuropathy.

Table 10.2 Clinical features differentiating between glaucomatous and nonglaucomatous optic neuropathies

	Glaucomatous optic neuropathy	Nonglaucomatous optic neuropathy
Visual acuity	• Usually well preserved until the end stages	• Variable
Color vision	• Blue-yellow deficiency more common than red-green deficiency	• Red-green deficiency more common than blue-yellow deficiency, except for autosomal dominant optic neuropathy and ethambutol-related toxic optic neuropathy
Presence of RAPD	• Variable	• Variable
Optic disc color and morphology	• Pink neuroretinal rim • Narrowing of neuroretinal rim • Optic disc cupping	• Pale neuroretinal rim • Neuroretinal rim is usually intact, but optic disc cupping has been reported in anterior ischemic optic neuropathy, hereditary optic neuropathy, compressive optic neuropathy involving the anterior visual pathway, traumatic optic neuropathy, fusiform aneurysm of the intracranial carotid artery, and optic nerve infarction [15]

Further Testing

Perimetry

The static automated white-on-white perimetry is a common standard for the evaluation of visual field changes in patients with glaucoma, but different approaches for visual field evaluation have been adopted by neuro-ophthalmologists for the detection of a wide spectrum of nonglaucomatous optic neuropathies. Confrontational visual field examination is considered an integral part of a standard neuro-ophthalmic examination. For the detection of visual sensitivity loss in the peripheral visual field, manual kinetic perimetry, such as Goldmann perimetry, or full-field automated static perimetry, such as the Humphrey full-field 81 protocol, is useful. Patients with nonglaucomatous optic neuropathy generally have worse central vision compared with that in glaucoma patients. Manual kinetic perimetry may yield a more reliable result than automated static perimetry in patients who cannot fixate on the fixation target.

The differentiation between glaucomatous and nonglaucomatous optic neuropathies should not be based merely on the pattern of visual field defects (Fig. 10.4). Since perimetry is a subjective test, repeat testing is important to confirm the presence of visual field defects. Visual field defects may not be detectable in the early stages of glaucoma (Fig. 10.5). Superonasal, superior arcuate, inferonasal and inferior arcuate defects are visual field abnormalities commonly observed in glaucoma because of the propensity of neuroretinal rim loss and RNFL thinning in the inferotemporal and superotemporal sectors of the optic disc. The visual field defects in the early and moderate stages of glaucoma often respect the horizontal midline because the superior and inferior nerve fiber bundles do not cross the horizontal raphe. The superior and inferior neuroretinal rim loss and corresponding RNFL loss also develop asymmetrically. Although temporal field defects are considered atypical in glaucoma, patients with extensive beta zone peripapillary atrophy may have enlarged blind spots and temporal field defects. Bitemporal field defects respecting the vertical midline should be investigated further with neuroimaging in order to exclude a chiasmal lesion. The patterns of visual field defects in nonglaucomatous optic neuropathies are even more diverse. The typical visual field defects observed in various optic neuropathies are summarized in Table 10.3.

Neuroimaging

Although the patient history and clinical findings can usually lead to the correct diagnosis, a compressive optic neuropathy can only be excluded

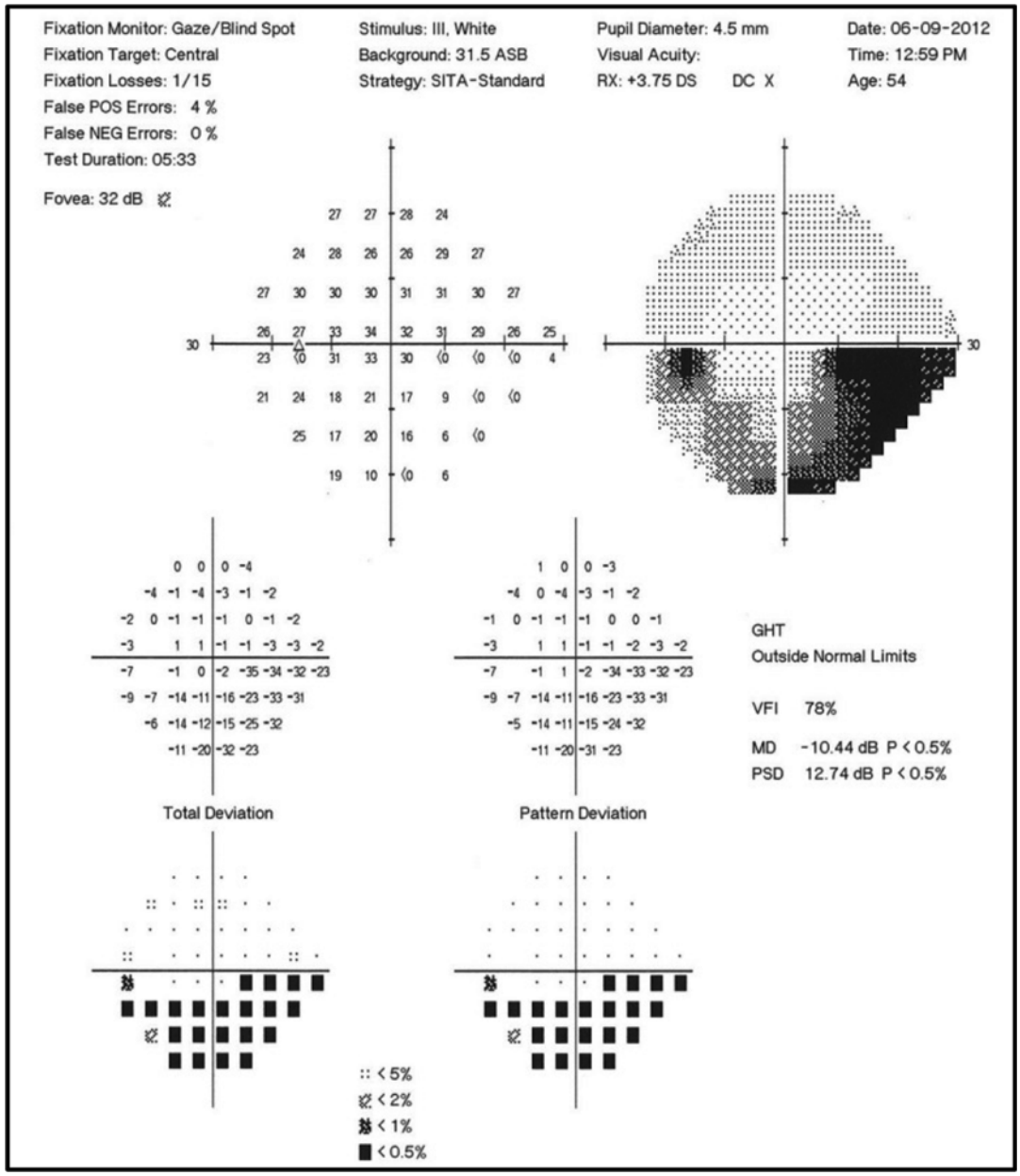

Fig. 10.4 The diagnosis of optic neuropathy should not be based merely on the pattern of visual field defects. Standard automated white-on-white perimetry of an eye with (**a**) non-arteritic anterior ischemic optic neuropathy and another with (**b**) glaucoma. Both eyes show inferior nasal visual field defects respecting the *horizontal midline*

with neuroimaging, preferably with magnetic resonance imaging (MRI) of the brain and orbit with and without gadolinium. Glaucoma is diagnosed based on the characteristic narrowing of neuroretinal rim, excavation of the disc, and thinning of the RNFL that can be confirmed with digital ocular imaging technologies. Neuroimaging is generally not required in the workup of glaucoma, with or without elevation of IOP. In an observational study evaluating the

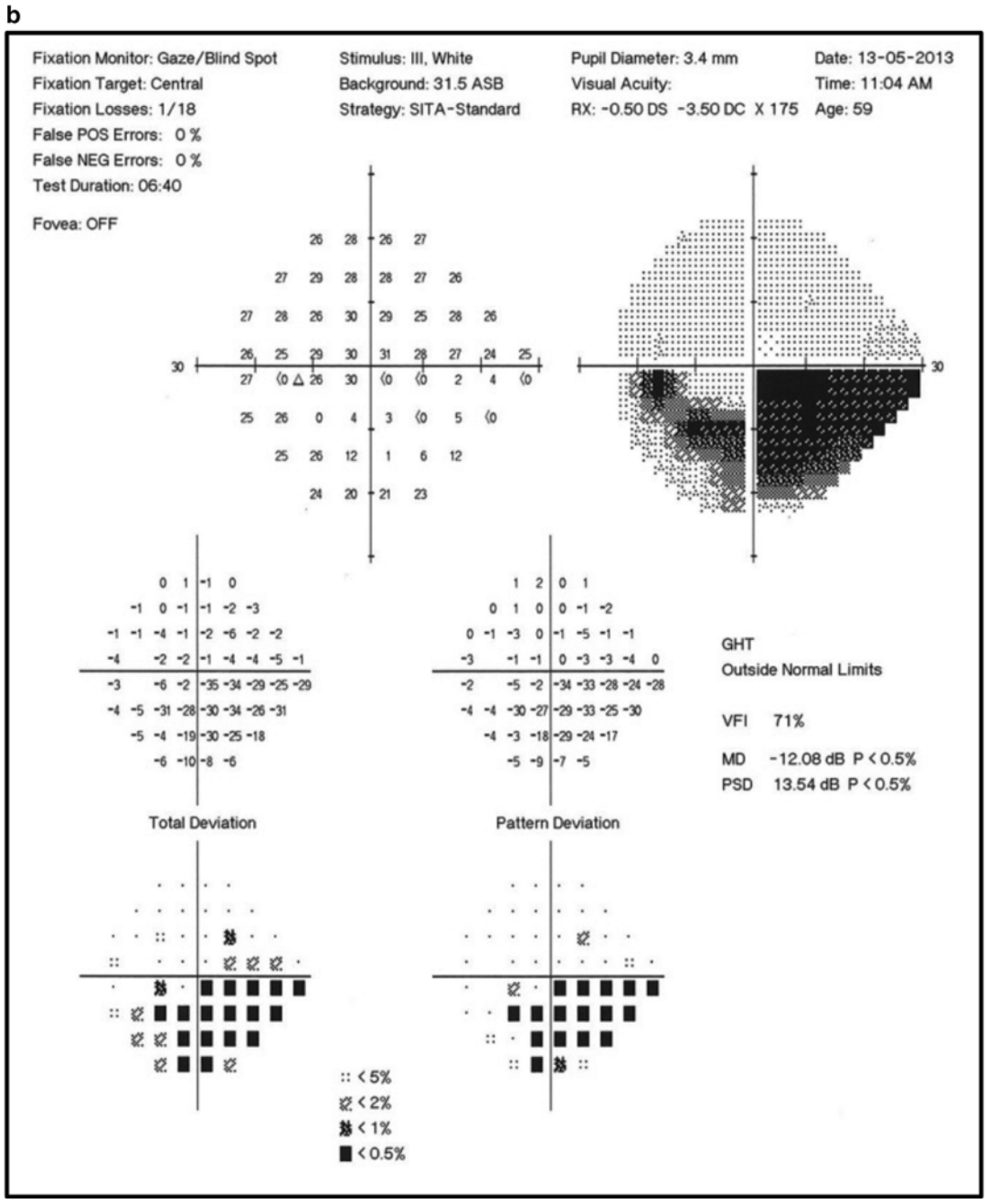

Fig. 10.4 (continued)

role of neuroimaging in patients with glaucoma without elevation of IOP, none of these patients had radiologic evidence of a mass lesion involving the anterior visual pathway [2]. In another case series, 4 of the 62 patients (6.5 %) diagnosed with "normal tension" glaucoma (IOP ≤ 21 mmHg) and none of the 70 patients with "high tension" glaucoma (>21 mmHg) had intracranial compressive lesions [16]. Two of the "normal tension" glaucoma patients had visual

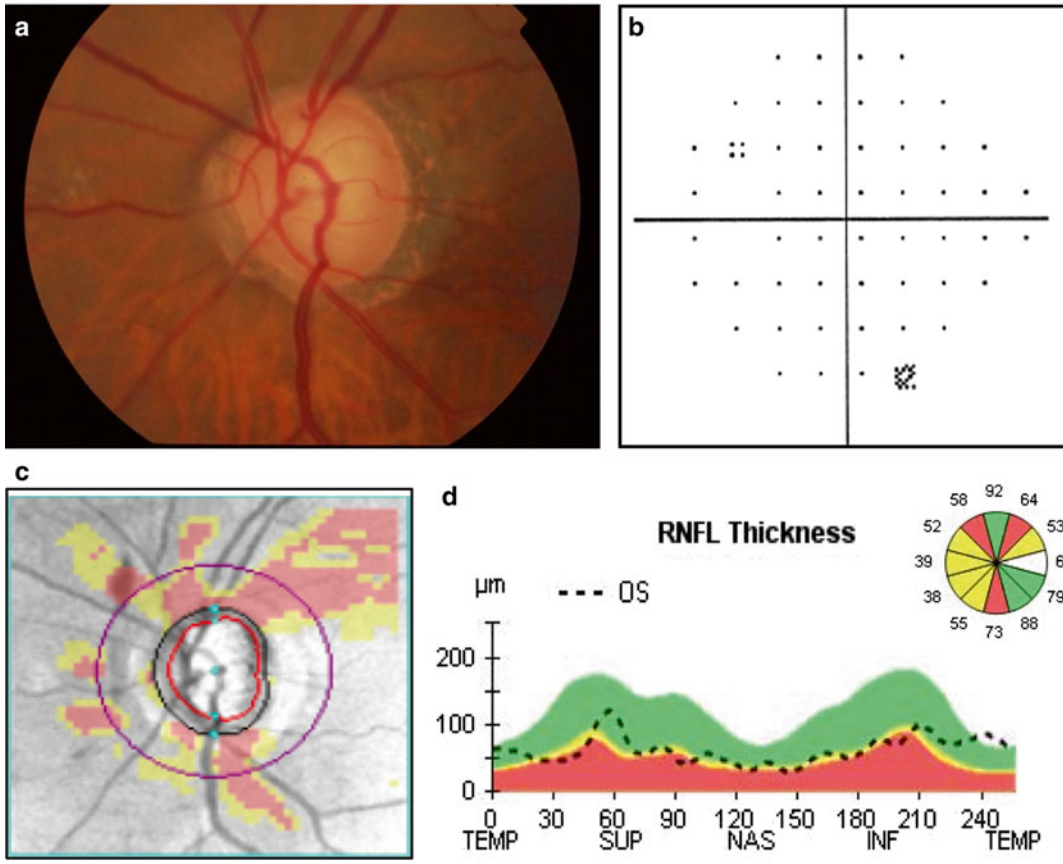

Fig. 10.5 Structural changes in the optic nerve head often precedes detectable functional loss in glaucoma. (**a**) Optic disc photograph shows diffuse narrowing of neuroretinal rim and optic disc excavation. (**b**) Automated white-on-white static perimetry shows no visual field defects in the pattern deviation plot. (**c**) Superotemporal and inferotemporal retinal nerve fiber layer (RNFL) thinning is evident in the RNFL thickness deviation map and (**d**) in the circumpapillary RNFL thickness profile obtained with a spectral-domain optical coherence tomography

Table 10.3 Typical patterns of visual field defects in glaucomatous and nonglaucomatous optic neuropathies

Optic neuropathy	Typical patterns of visual field defects
Glaucoma	• Superonasal, inferonasal, superior arcuate, and inferior arcuate defects
	• Early and moderate visual field defects respect the horizontal midline
Typical optic neuritis	• Acute stage: diffuse and central loss
	• Chronic stage: partial arcuate, paracentral, and arcuate defects
Ischemic optic neuropathy	• Non-arteritic anterior ischemic optic neuropathy (NAAION): central scotoma, followed by inferior altitudinal, superior arcuate, superior altitudinal, or inferior arcuate defects [37]
	• Arteritic anterior ischemic optic neuropathy (AAION): extensive diffuse visual field defects
Toxic/metabolic optic neuropathy	• Central or cecocentral scotoma [38]
Compressive optic neuropathy	• Variable—depending on the location of compression
Traumatic optic neuropathy	• Variable—depending on severity and mechanism of injury
Leber's hereditary optic neuropathy	• Dense central or cecocentral scotoma [39]
Dominant optic atrophy	• Central, cecocentral, and paracentral scotomas with sparing of the peripheral field [39]

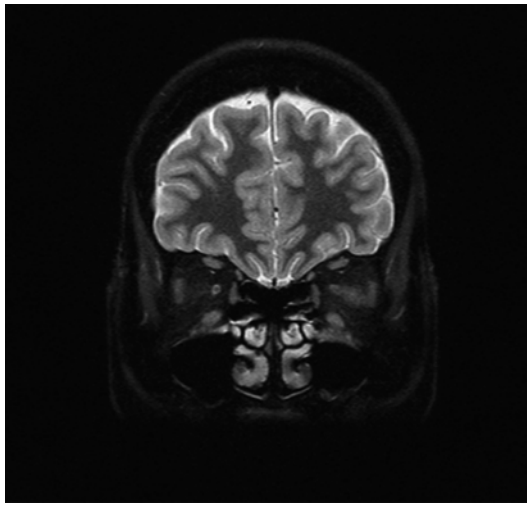

Fig. 10.6 T2 coronal brain MRI image with fat suppression showing increased T2 signal around the right optic nerve, reflecting extensive loss of nerve fiber bundles in a 56-year-old patient with right glaucoma, not acute optic neuritis

field loss more on the temporal side than the nasal side. Neuroimaging is required to exclude intracranial compressive lesions in patients who present with decreased visual acuity, a pale neuroretinal rim, and temporal field defects with or without excessive field loss.

In advanced glaucoma or optic atrophy with extensive loss of the optic nerve fiber bundles, a relative increase in the amount of cerebrospinal fluid around the nerve can cause an enhanced signal on T2 MRI images (Fig. 10.6). This finding may be misinterpreted as acute optic neuritis by inexperienced radiologists. It is the lack of contrast enhancement that distinguishes optic atrophy from acute optic neuritis.

Electrodiagnostics

Visual evoked potentials (VEPs) can help confirm the presence of an organic abnormality of the visual pathway, whereas electroretinograms (pattern/full-field/multifocal ERGs) can help differentiate between a retinopathy and an optic neuropathy. Electrodiagnostics have a limited role in the diagnostic work-up of an optic neuropathy. In optic neuropathies, such as early glaucoma, with peripheral visual field defects, VEP may not detect an abnormality if the stimulus field size is only 15°. Although multifocal VEP can be used to test the focal responses from a wider field of stimulus, considerable overlap in the multifocal VEP latencies exists among patients with optic neuritis, glaucoma, and retinal disease [17]. Both the N95 of the pattern ERG and the photopic negative response (PhNR) of the ERG, reflecting ganglion cell function, have been used for the detection of glaucoma [18]. But the ERG responses are not specific for glaucoma. For example, the amplitude of the PhNR can also be reduced in nonglaucomatous optic neuropathies, such as in optic neuritis [19].

Laboratory Tests

Further laboratory testing is sometimes necessary to diagnose chronic nonglaucomatous optic neuropathies. For example, serum B12 and thiamine (B1) are required for the diagnosis of nutritional optic neuropathy. Dominant optic atrophy and Leber's hereditary optic neuropathy require genetic testing to confirm. Secondary syphilis can present as an acute optic neuropathy (retrobulbar, papillitis, perineuritis, neuroretinitis), whereas tertiary syphilis can manifest as a chronic progressive optic neuropathy [20] (For further details regarding laboratory testing in other optic neuropathies, see the chapters on optic neuritis, papilledema, ischemic optic neuropathies, hereditary optic neuropathies, and toxic and nutritional optic neuropathies.).

Evaluation of Optic Neuropathies with OCT

While clinical examination of the optic disc is pertinent to the diagnosis and monitoring of glaucomatous and nonglaucomatous optic neuropathies, the advent of digital imaging technologies has provided objective and quantitative documentation of optic nerve damage. Among the various measurement techniques, including confocal scanning laser ophthalmoscopy, scanning laser polarimetry, and OCT, only OCT measures both the optic disc parameters (rim/cup area and volume) and the RNFL thickness. The scanning

speed has substantially improved from 100 to 400 A-scans/s in time-domain OCT to 26,000–53,000 A-scans/s in spectral-domain OCT. The axial resolution has also improved from 10 μm in time-domain OCT to ~4 μm in spectral-domain OCT. These improvements have provided the opportunity to examine the optic nerve head structures in three dimensions. Spectral-domain OCT has been widely adopted in detecting and following glaucomatous optic nerve degeneration, and its application in nonglaucomatous optic neuropathies is expanding. This section reviews the application of OCT for measurement of the RNFL, the interpretation of the analysis printout, the roles of OCT in detecting and monitoring optic nerve damage, and the limitations of this technology.

OCT Measurement of the Retinal Nerve Fiber Layer

Degeneration of the retinal ganglion cells is the hallmark of many optic neuropathies. Although it is not yet feasible to visualize the retinal ganglion cells clinically, RNFL imaging is a sensitive and reliable method to quantify the extent of retinal ganglion cell damage in the detection and monitoring of glaucomatous and nonglaucomatous optic neuropathies. The RNFL is the innermost layer of the retina which is largely composed of the axonal fiber bundles of retinal ganglion cells. In OCT images, it is a highly reflective layer bounded anteriorly by the vitreoretinal interface and posteriorly by the anterior border of the ganglion cell layer (Fig. 10.7). Almost all commercially available time- and spectral-domain OCT instruments use the circle scan protocol to report the average and clock hour RNFL thicknesses. The conventional approach in measuring the RNFL thickness is based on a circle scan with a diameter of approximately 3.46 mm. The selection of this circle size was based on a study showing that the average RNFL thickness obtained with the 3.46 mm diameter circle scan was more reproducible compared with other circle sizes [21].

The test–retest variability of the 3.46 mm circumpapillary RNFL measurement is low. In a study comparing the inter-visit reproducibility of time- and spectral-domain OCT, the reproducibility coefficients of RNFL thicknesses obtained with a spectral-domain OCT were less than those of the time-domain OCT [22]. The inter-visit reproducibility coefficient of the average RNFL thickness measured with the spectral-domain OCT (Cirrus HD-OCT, Carl Zeiss Meditec) is ~5 μm, meaning that the difference in average RNFL thickness obtained on two separate occasions would be less than ~5 μm with a probability of 95 %. By contrast, it is ~11 μm for the time-domain OCT (Stratus OCT, Carl Zeiss Meditec). The smaller test–retest variability suggests that the spectral-domain OCT is more sensitive for the detection of RNFL changes.

Table 10.4 compares some of the commercially available spectral-domain OCT instruments for RNFL imaging. At the moment, only a few spectral-domain OCT instruments can image the RNFL in a volumetric scan and display the RNFL measurements in a RNFL thickness map. The Cirrus HD-OCT (Carl Zeiss Meditec) measures the RNFL thickness in 200×200 pixels over 6×6 mm^2 of the optic disc region (Fig. 10.8b). RNFL abnormalities are displayed in the RNFL thickness deviation map (Fig. 10.8c), which comprises of 50×50 pixels. If the RNFL thickness value is smaller than the lower 95^{th} percentile value of normal individuals, the pixel is color-coded in yellow and in red if the RNFL thickness is below the lower 99^{th} percentile. The RNFL thickness map is more sensitive in detecting RNFL damage compared with the circumpapillary RNFL measurement at a comparable level of specificity [23]. In Fig. 10.9, the RNFL thickness map shows the RNFL defects missed on circumpapillary RNFL measurement.

A Step-by-Step Approach in the Interpretation of the Retinal Nerve Fiber Layer Analysis Printout

1. *Check the signal-to-noise ratio* (*signal strength*) *of the OCT image*
   The signal-to-noise ratio, or signal strength, is a key determinant of RNFL measurement.

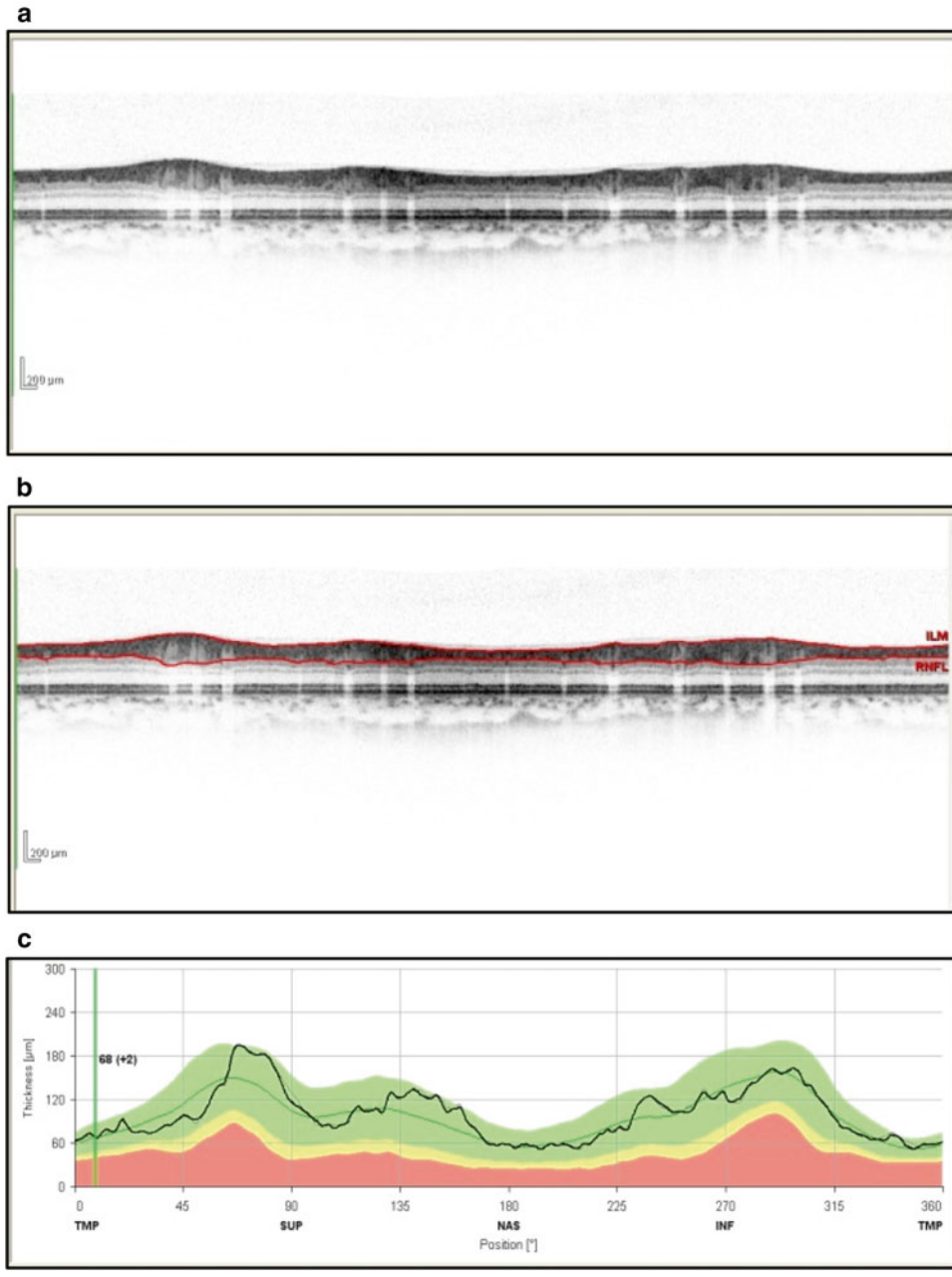

Fig. 10.7 Cross-sectional imaging of the retina around the optic nerve head obtained by a spectral-domain optical coherence tomography (Spectralis OCT, Heidelberg Engineering). (**a**) The retinal nerve fiber layer (RNFL) is visualized as the innermost reflective layer bounded anteriorly by the vitreoretinal interface and posteriorly by the anterior border of the ganglion cell layer. (**b**) The instrument software automatically segments the RNFL (*red lines*) and (**c**) reports the circumpapillary RNFL thickness profile. The normal RNFL thickness reference ranges are indicated in *green* (within normal range), *yellow* (borderline), and *red* (outside the normal range)

Table 10.4 Commercially available spectral-domain optical coherence tomography systems for retinal nerve fiber layer (RNFL) imaging

	RTVue SD-OCT	Cirrus HD-OCT	Spectralis OCT	Topcon 3D OCT	RS-3000 OCT	Envisu C-Class SDOIS
Manufacturer	Optovue	Carl Zeiss Meditec	Heidelberg Engineering	Topcon	NIDEK	Bioptigen
Superluminescent diode wavelength (nm)	840±10	840	870	840	880	840/870
Scan speed (A-scans/s)	26,000	27,000	40,000	27,000	53,000	32,000
Axial resolution (μm)	5	5	3.9	5–6	7	4–6
Transverse resolution (μm)	15	15	14	20	20	20
Circumpapillary scan for RNFL imaging	3.45 mm in diameter 1,024 A-scans 16 Sectors analysis	3.46 mm in diameter 256 A-scans 12 Clock hours analysis	3.45 mm in diameter 1,536 or 1,024 A-scans Six sectors analysis	3.40 mm in diameter 1,024 A-scans 12 Clock hours analysis	3.45 mm in diameter 1,024 A-scans 12 Clock hours analysis	Not available
Volumetric scan for RNFL imaging and analysis	12 Radial line (3.4 mm) and 13 concentric ring (1.3–4.9 mm in diameter) scans centered at the optic disc 14,105 A-scans in total	200×200 A-scans over 6×6 mm^2 centered at the optic disc	Not available	512×128 A-scans over 6×6 mm^2 centered at the optic disc	512×128 A-scans over 6×6 mm^2 centered at the optic disc	Not available
Normative database for RNFL analysis	Circumpapillary scan Volumetric scan	Circumpapillary scan Volumetric scan	Circumpapillary scan	Circumpapillary scan	Circumpapillary scan Volumetric scan	Not available

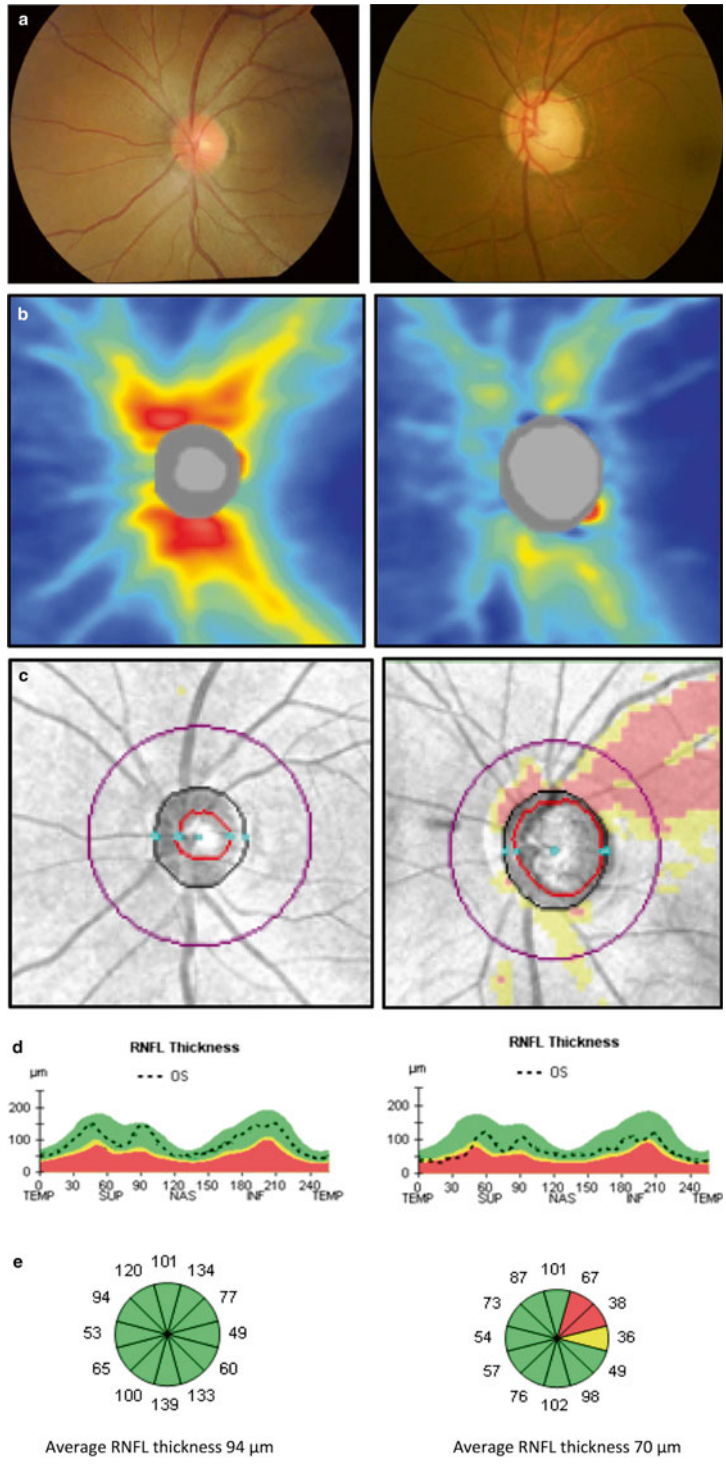

Fig. 10.8 Analysis of retinal nerve fiber layer (RNFL) thickness with spectral-domain optical coherence tomography (OCT) (Cirrus HD-OCT, Carl Zeiss Meditec). (**a**) Optic disc photograph, (**b**) RNFL thickness map, (**c**) RNFL thickness deviation map, (**d**) circumpapillary RNFL thickness profile, and (**e**) clock hour and average RNFL thicknesses of a normal (*left panel*) and a glaucomatous (*right panel*) eye. The RNFL thickness map (200 × 200 pixels) is color coded with hot colors representing high and cold colors representing low RNFL measurements. Abnormal RNFL thicknesses are encoded in yellow and red in the RNFL thickness deviation map (50 × 50 pixels) when the measurements fall below the lower 95 and 99 % centile ranges, respectively. For the glaucomatous eye, the RNFL measurements in the superotemporal region are outside the normal ranges and highlighted in red in the RNFL thickness deviation map

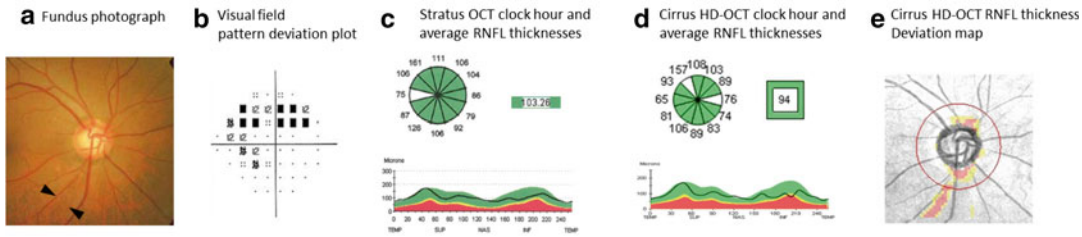

Fig. 10.9 A glaucomatous eye with an inferotemporal retinal nerve fiber layer (RNFL) defect barely visible in the fundus photograph (**a**) had superonasal defects in the visual field pattern deviation plot (**b**). While Stratus OCT (**c**) and Cirrus HD-OCT (**d**) clock hour and average RNFL thicknesses failed to show any abnormality (all were within normal limits), the inferotemporal RNFL defect was evident in the RNFL thickness deviation map (**e**). Abnormal pixels of RNFL measurement are indicated in *yellow* or *red* [Adapted from Leung CK, Lam S, Weinreb RN, Liu S, Ye C, Liu N, He J, Lai G, Li T, Lam DS. Retinal Nerve Fiber Layer Imaging with Spectral-Domain Optical Coherence Tomography – Analysis of the RNFL Map for Glaucoma Detection. Ophthalmology.2010; 117:1684–91. With permission from Elsevier]

Images with poor signal have smaller RNFL thickness values that may lead to erroneous interpretations of the RNFL defects (Fig. 10.10). A positive association between signal strength and RNFL thickness has been shown in both time- and spectral-domain OCT [24, 25]. The optimal signal-to-noise ratio/signal strength for reliable RNFL measurement varies among different OCT instruments. Therefore, obtaining OCT images with the best possible quality is recommended for reliable interpretation of RNFL measurement.

2. *Examine the RNFL boundaries in the OCT image*
   All commercially available OCT instruments provide automated segmentation of the RNFL. RNFL segmentation errors commonly occur in images with a poor signal-to-noise ratio (Fig. 10.11). It is not uncommon to have an abnormal increase in RNFL thickness from an edematous nerve fiber layer (Fig. 10.12). RNFL splitting can also cause an abnormal measurement of the RNFL. Therefore, checking the RNFL reflectivities and boundaries in the OCT image is essential before analyzing the RNFL measurement.
3. *Interpret the circumpapillary RNFL thickness profile or the RNFL thickness map with reference to the normative data.*
   While the average quadrant, or clock hour, RNFL measurements are often reported in clinical studies to quantify the degree of RNFL damage, the color-coded circumpapillary RNFL profile and the RNFL thickness map generated with reference to the normative database are most useful in detecting RNFL defects in clinical practice (Figs. 10.8 and 10.9). Most OCT instruments have built-in data collected from normal individuals. RNFL measurements falling below the lower 95th and 99th percentile ranges are encoded in yellow and red, respectively. Since the normative database in most OCT instruments only include eyes with a mild degree of refractive errors, caution is needed in interpreting the RNFL profile in myopic eyes. The detection of RNFL abnormalities in the OCT printout does not necessarily imply the presence of RNFL defects. Healthy myopic eyes often have a different RNFL distribution pattern, rendering the analysis of RNFL measurements unreliable (Fig. 10.13).

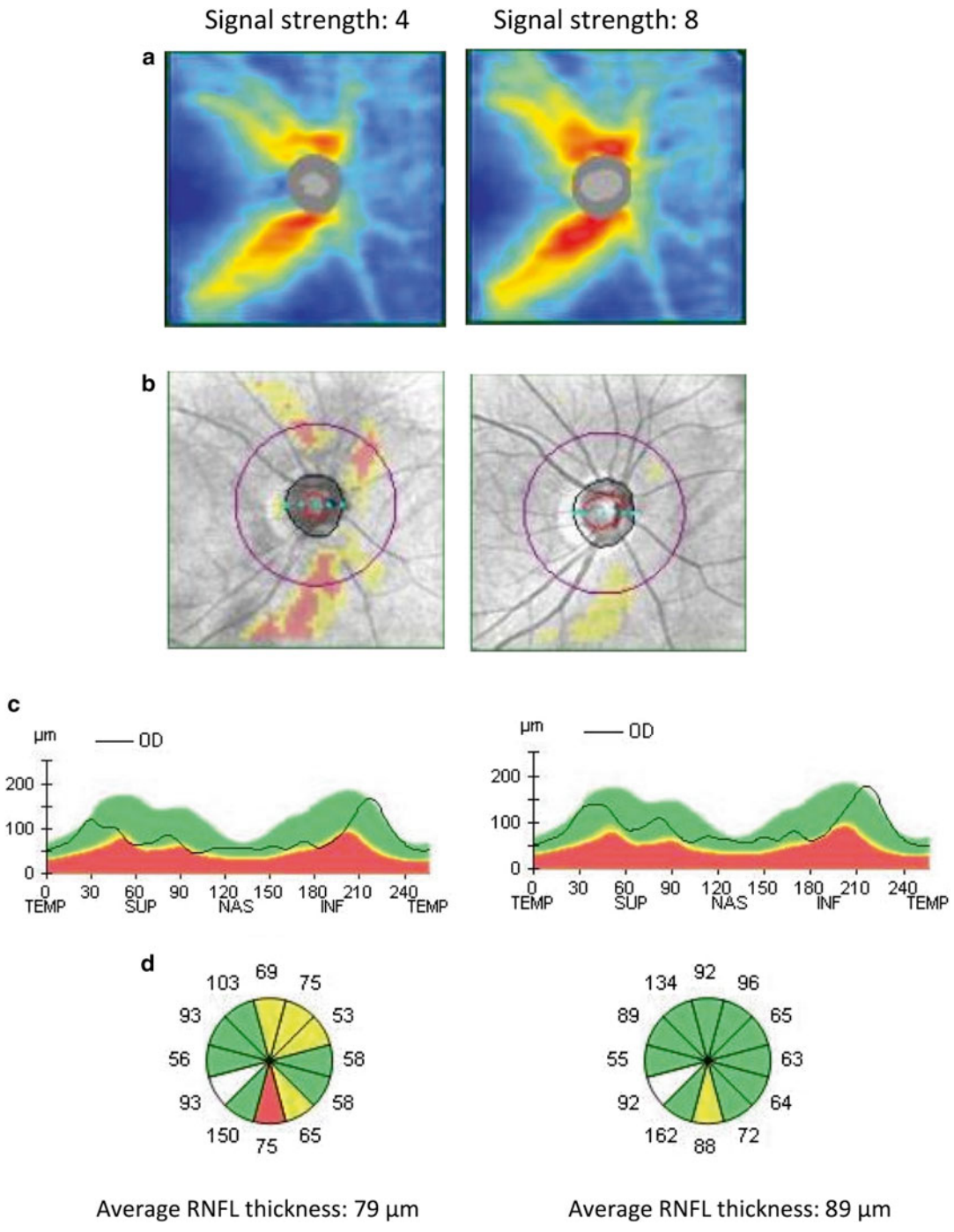

Fig. 10.10 A normal healthy pseudophakic eye with retinal nerve fiber layer (RNFL) imaging obtained by a spectral-domain optical coherence tomography (Cirrus HD-OCT, Carl Zeiss Meditec) (**a**) The RNFL thickness map, (**b**) RNFL thickness deviation map, (**c**) circumpapillary RNFL thickness profile, and (**d**) clock hour and average RNFL thicknesses are shown before (*left panel*) and after (*right panel*) laser capsulotomy. The signal strength of the OCT image increases from 4 to 8 after laser capsulotomy. The clock hour and average RNFL thickness are less in the OCT scan with a lower signal strength

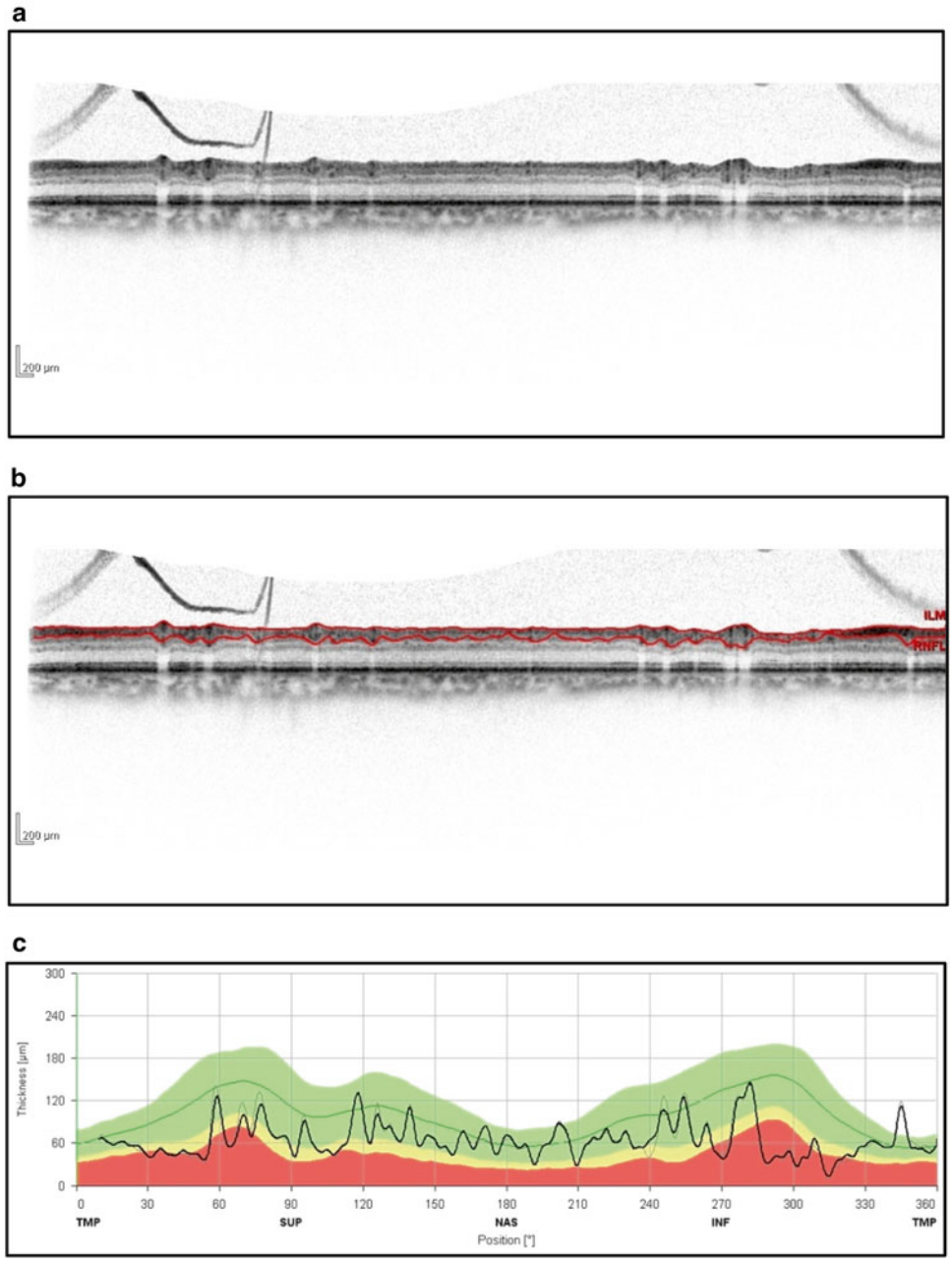

Fig. 10.11 (**a**) The cross-sectional parapapillary retinal image was obtained with a spectral-domain optical coherence tomography (Spectralis OCT, Heidelberg Engineering) and (**b**) the instrument software automatically segments the RNFL (*red lines*) and (**c**) displays the circumpapillary RNFL thickness profile with reference to the normal reference ranges. It is noteworthy that while the anterior boundary of the RNFL is correctly detected along the vitreoretinal interface, the posterior boundary of the RNFL in the superonasal, nasal, and inferonasal sectors is detected along the posterior boundary (instead of anterior boundary) of the ganglion cell layer, rendering the RNFL measurements in these sectors greater than the actual values. Segmentation error occurs even when the signal-to-noise ratio is considered acceptable in this image (quality score: 27)

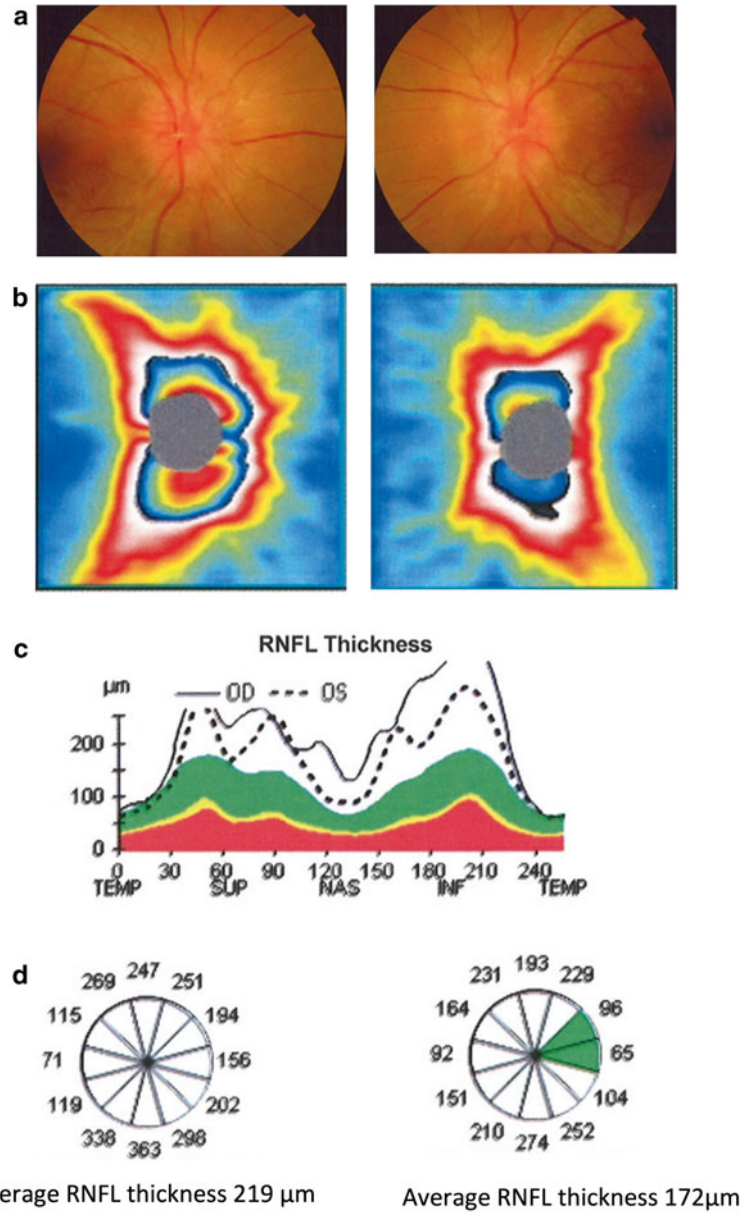

Fig. 10.12 Retinal nerve fiber layer (RNFL) analysis in eyes with optic disc swelling. **(a)** Optic disc photograph, (**b**) RNFL thickness map (Cirrus HD-OCT, Carl Zeiss Meditec), (**c**) circumpapillary RNFL thickness profile, and (**d**) clock hour and average RNFL thicknesses are illustrated for the right (*left panel*) and left (*right panel*) eyes. The nerve fiber bundles are edematous and the RNFL measurements are above the normal reference ranges. The RNFL thickness map indicates that the RNFL is substantially thickened, and the clock hour and average RNFL thicknesses are above the normal ranges

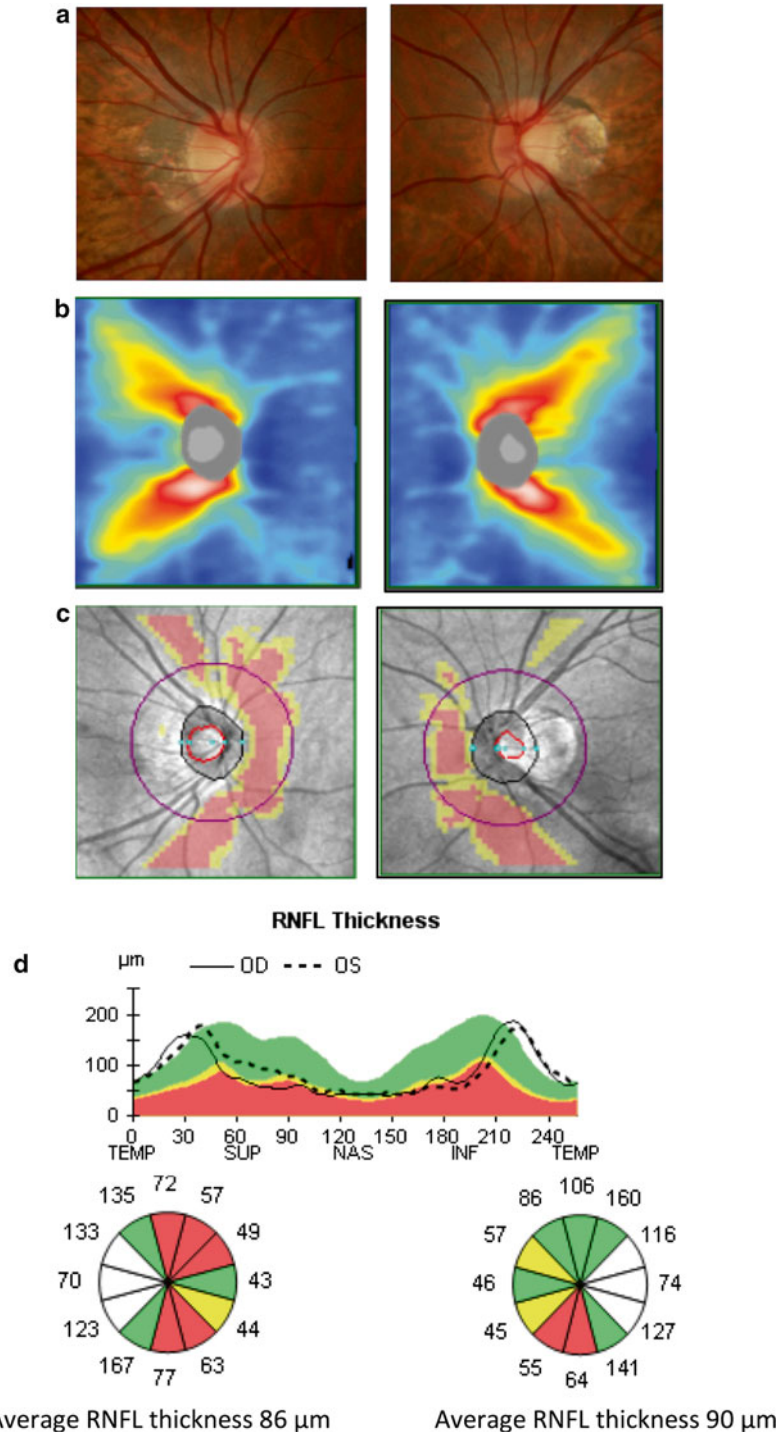

Fig. 10.13 (**a**) Optic disc photograph, (**b**) retinal nerve fiber layer (RNFL) thickness map (Carl Zeiss Meditec), (**c**) RNFL thickness deviation map, (**d**) circumpapillary RNFL thickness profile, and (**e**) clock hour and average RNFL thicknesses of the right (*left panel*) and left (*right panel*) eyes of a normal healthy lady with high myopia (OD: −8.25D OS: −7.50D). Both eyes show relatively normal RNFL thickness distribution in the RNFL thickness maps although the RNFL thickness deviation maps, circumpapillary RNFL thickness profiles, and clock hour RNFL thicknesses suggest abnormal RNFL measurements (area highlighted in *red*). This should not be interpreted as RNFL defects, as the superotemporal and inferotemporal RNFL bundles tend to converge temporally in myopic eyes. Therefore, the interpretation of RNFL measurements in myopic eyes requires careful consideration of the distribution pattern in the RNFL bundles

Application of OCT in Detecting Optic Nerve Damage

Since dysfunction or loss of retinal ganglion cells is universal in all types of optic neuropathies, it is important to note that RNFL thinning detected by OCT only represents the presence of an optic neuropathy and is not diagnostic of a specific disease. The differentiation between glaucomatous and nonglaucomatous optic neuropathies requires careful examination of the color and configuration of the neuroretinal rim. Narrowing of the neuroretinal rim and excavation of the optic disc are the most important diagnostic features of glaucoma. The neuroretinal rim is often pink in glaucoma, even in the end stages, whereas segmental or diffuse neuroretinal rim pallor is indicative of nonglaucomatous optic neuropathy. In the assessment of an optic neuropathy, the roles of OCT include the following: (1) to confirm the presence of RNFL defects, (2) to stage the severity of disease, and (3) to monitor the progress of disease. OCT can help visualize both localized and diffuse thinning of the RNFL (Fig. 10.14) [26]. Early localized RNFL defects can be better visualized in the RNFL thickness map than in the circumpapillary RNFL profile (Fig. 10.9). In glaucoma, RNFL defects are most often detected in the inferotemporal, followed by the superotemporal sectors of the optic disc. This is concordant with the observation that the inferotemporal followed by the superotemporal neuroretinal rim has predilection for glaucomatous damage. Isolated RNFL loss in the nasal quadrant is not typical in glaucoma. Although less is known about the patterns of RNFL defects in nonglaucomatous optic neuropathies, it is often possible to determine the etiology of an optic neuropathy with detailed history taking and examination of the optic disc.

Figure 10.15 compares the OCT RNFL thickness maps and RNFL thickness deviation maps of an eye with glaucoma (left panel), and an eye with non-arteritic ischemic optic neuropathy (right panel). Both eyes show a similar pattern of RNFL defects, with inferotemporal thinning greater than superotemporal thinning. The neuroretinal rim narrowing and excavation of the optic disc distinguishes glaucoma from an ischemic optic neuropathy. The vertical cup-disc ratio is also larger in the glaucomatous eye. In this case, the color and cup/disc ratio of the eye with ischemic optic neuropathy appears normal. Figure 10.15 illustrates how OCT is essential in confirming the presence and severity of optic nerve damage.

Application of OCT in Monitoring Glaucomatous Optic Nerve Damage

Glaucoma is a chronic progressive optic neuropathy. Monitoring disease progression helps to guide appropriate treatment. With objective and reproducible measurement of the RNFL, OCT facilitates the detection of progressive RNFL thinning and estimation of the rate of disease progression. Similar to the evaluation of visual field progression, RNFL thickness progression analysis can be performed with event- and trend-based approaches. The Guided Progression Analysis (GPA, Carl Zeiss Meditec) is a commercially available statistical package that provides an event analysis of the RNFL thickness map and trend analysis of the average superior and inferior RNFL thickness based on the circumpapillary RNFL measurement. In the progression analysis of the RNFL thickness map (50×50 pixels), the differences in RNFL thickness of individual pixels between two baseline visits and a follow-up visit are computed. If the differences are greater than the pixel test–retest variabilities, the pixels are encoded in yellow. The pixels are encoded in red if the significant differences are confirmed in a consecutive follow-up visit. Pixels of progressive RNFL thinning are displayed in the RNFL thickness change map (Fig. 10.16). The RNFL thickness change map is useful not only to detect the presence of disease progression, but also to discern different patterns of progressive RNFL thinning. Three different RNFL progression patterns have been observed in glaucoma: (1) enlargement of RNFL defects, (2) deepening of

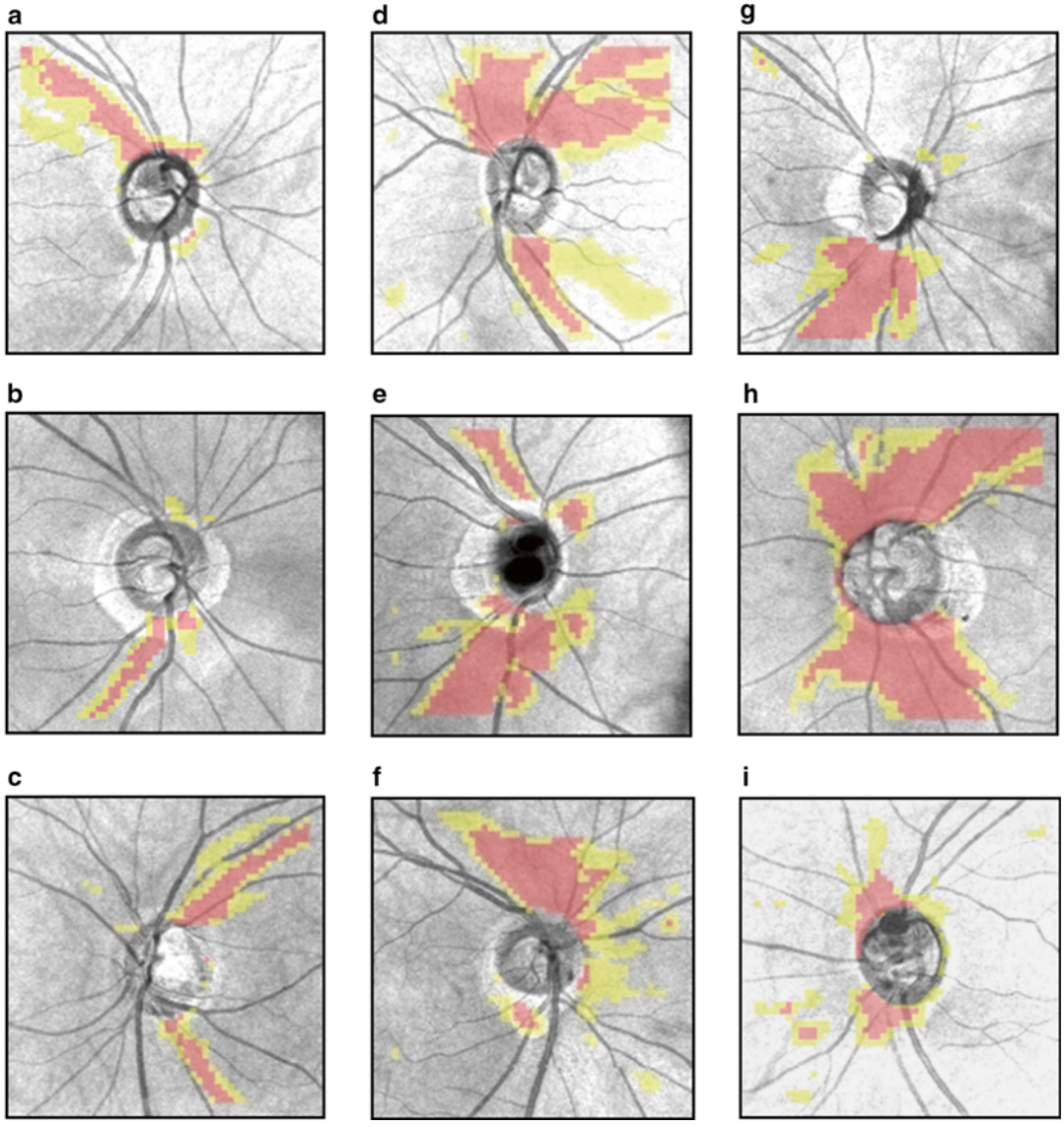

Fig. 10.14 Distribution patterns (**a**–**i**) of retinal nerve fiber layer (RNFL) defects visualized in the RNFL thickness deviation maps (Cirrus HD-OCT, Carl Zeiss Meditec) in glaucomatous eyes. Patterns (**a**–**c**) represent localized RNFL defects with angular width ≤30° involving the superior, inferior, and both the superior and inferior quadrants, respectively. Patterns (**d**, **e**) indicate localized RNFL defects in one quadrant and diffuse RNFL (angular width>30°) defect in the fellow quadrant. Patterns (**f**–**h**) represent diffuse RNFL defects with angular width >30° involving the superior, inferior, and both the superior and inferior quadrants, respectively. In pattern (i), RNFL defects are close to the optic disc margin not involving the conventional RNFL measurement circle of a diameter 3.46 mm [Adapted from Leung CK, Choi N, Weinreb RN, Liu S, Ye C, Lai G, Lau J, Lam DS. Retinal Nerve Fiber Layer Imaging with Spectral-Domain Optical Coherence Tomography – Pattern of RNFL defects in Glaucoma. Ophthalmology. 2010;117:2337–44. With permission from Elsevier]

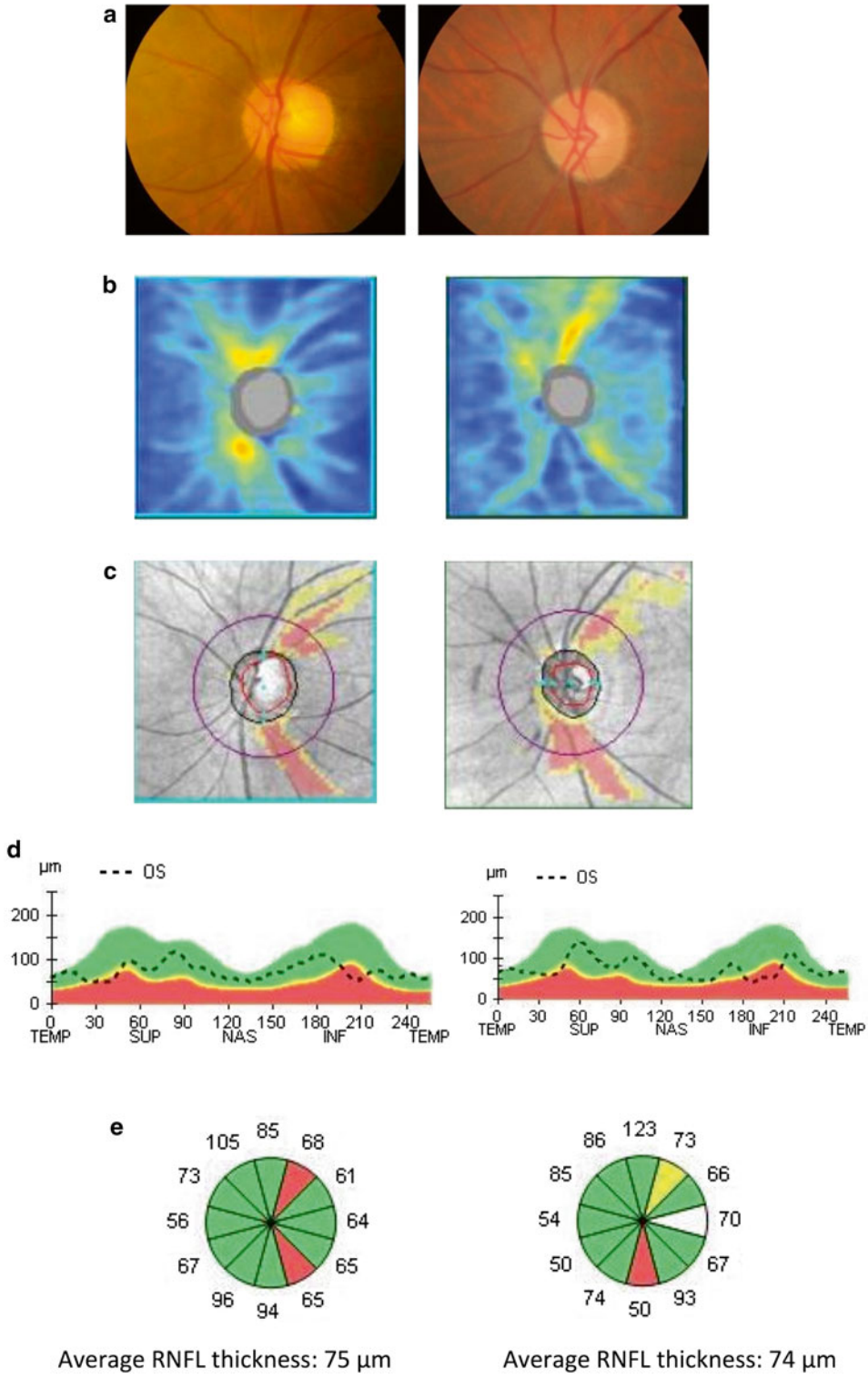

Fig. 10.15 (**a**) Optic disc photograph, (**b**) retinal nerve fiber layer (RNFL) thickness map (Carl Zeiss Meditec), (**c**) RNFL thickness deviation map, (**d**) circumpapillary RNFL thickness profile, and (**e**) clock hour and average RNFL thicknesses of a glaucomatous eye (*left panel*) and an eye with non-arteritic anterior ischemic optic neuropathy (*right panel*). The pattern of RNFL thinning is similar between the eyes, both with inferotemporal and superotemporal RNFL defects. The optic disc features that distinguish between the two are neuroretinal rim loss with an increase in optic/disc ratio and optic disc excavation in glaucoma

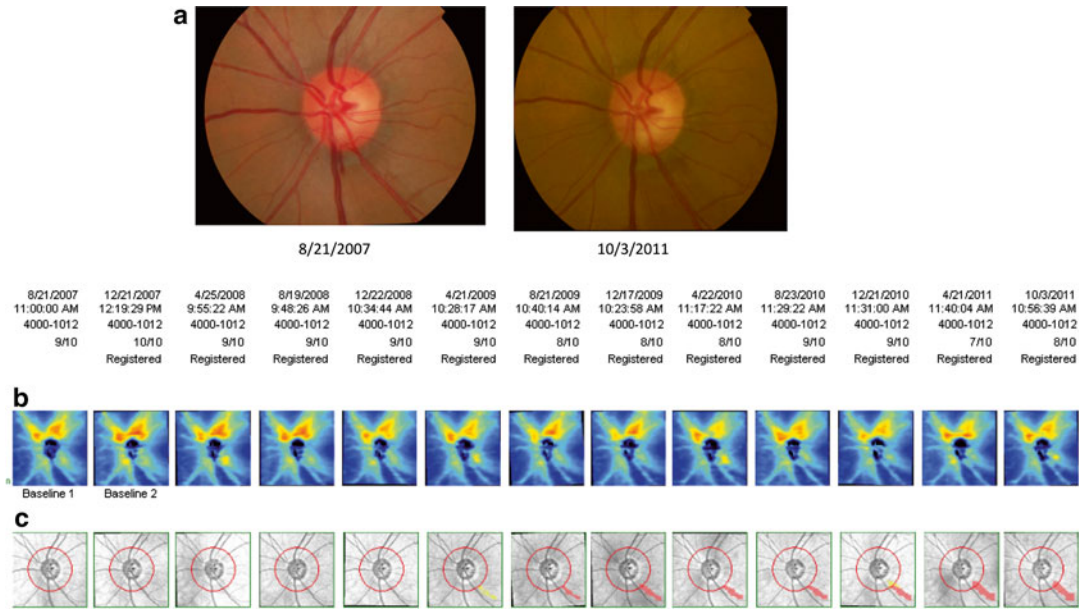

Fig. 10.16 (**a**) Optic disc photograph, and serial (**b**) retinal nerve fiber layer (RNFL) thickness maps (Carl Zeiss Meditec) and (**c**) RNFL thickness change maps analyzed by the Guided Progression Analysis printout (GPA) of a glaucomatous eye with an inferotemporal RNFL defect. Pixels with a RNFL thickness difference exceeding the test–retest variability between follow-up and the first and the second baseline images are encoded in *yellow* in the RNFL thickness change map. If the same changes are evident in an additional follow-up image, the pixels are encoded in *red*. Significant progressive loss of the RNFL was first detected in the RNFL thickness change map in the inferotemporal sector on 4/21/2009. An expansion of the inferotemporal RNFL defects from 8/21/2007 to 10/3/2011 is also evident in the optic disc photographs [Modified from Leung CK, Yu M, Weinreb RN, Lai G, Xu G, Lam DS. Retinal Nerve Fiber Layer Imaging with Spectral-Domain Optical Coherence Tomography: Patterns of RNFL Progression. Ophthalmology.2012; 119:1858–66. With permission from Elsevier]

preexisting RNFL defects, and (3) development of new RNFL defects [27]. Progressive RNFL thinning is apparent most frequently at the inferotemporal meridians, approximately 2 mm away from the optic disc center. In other words, analysis of the RNFL measurement based on the 1.73 mm radius circle scan alone would be inadequate to detect disease progression; RNFL loss may take place in regions outside the 3.46 mm diameter circle scan. The RNFL thickness map is helpful in detecting the presence of progressive RNFL thinning, whereas the circumpapillary average RNFL thickness is more useful in analyzing the rate of disease progression. Previous studies have estimated that the rate of change of average RNFL thickness ranges between approximately −0.3 and −15 μm/year in glaucoma patients [28–33]. Patients with a rapid rate of progression may require closer follow-up and a more aggressive treatment plan. Some nonglaucomatous optic neuropathies, including optic neuritis, compressive optic neuropathies, and hereditary optic neuropathies, also demonstrate progressive RNFL thinning. Therefore, RNFL monitoring at regular intervals of time would be useful to track disease progression and evaluate treatment response.

Limitations of OCT in Retinal Nerve Fiber Layer Measurement

The Floor Effect in RNFL Measurement

Although OCT is useful in monitoring the progression of optic neuropathies, detecting progressive RNFL thinning becomes difficult in the advanced stages when the loss of the RNFL is very extensive. In a cross-sectional study investigating eight eyes with no light perception as a

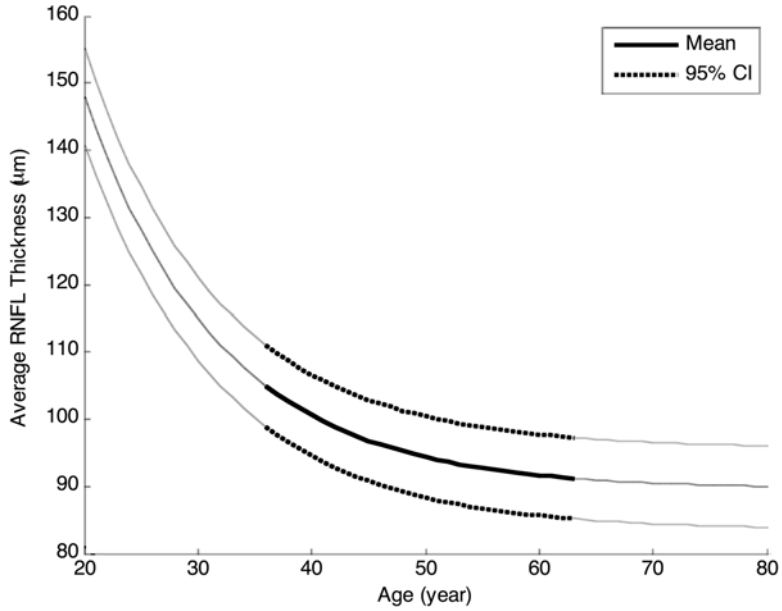

Fig. 10.17 Age-related decline of average retinal nerve fiber layer (RNFL) thickness. *Solid line*: linear mixed modeling estimation analyzed using a dataset of 70 eyes of 35 normal individuals who had been followed in 4-month intervals for RNFL imaging with a spectral-domain optical coherence tomography for a mean of 30 months. *Dash line*: estimation extrapolated from the linear mixed model. Dotted lines: 95 % confidence interval (CI) [Adapted from Leung CK, Yu M, Weinreb RN, Ye C, Liu S, Lai G, Lam DS. Retinal nerve fiber layer imaging with spectral-domain optical coherence tomography: a prospective analysis of age-related loss. Ophthalmology. 2012;119:731–7. With permission from Elsevier]

result of end-stage optic neuropathies, the average RNFL thickness measured by time-domain OCT ranged between 38 and 51 μm [34]. This finding suggests that there are components in the RNFL other than neuronal tissue, such as retinal blood vessels and glial tissue, measured by OCT. Since retinal blood vessels are embedded in the RNFL and commercially available OCT instruments do not separate these blood vessels from the measurement of RNFL, OCT becomes less sensitive in detecting further change in the advanced stages of optic nerve damage. The contribution of retinal blood vessels to RNFL thickness measurements is considerable when the RNFL is thin.

Age-Related Loss of the RNFL

Not all of the progressive RNFL thinning is related to the optic neuropathy itself. It has been shown that progressive reduction of the RNFL thickness can be detected with OCT in normal healthy eyes [35]. The rate of change of RNFL thickness is associated with the baseline RNFL measurement, with a more rapid loss at a younger age when the RNFL is relatively thick (Fig. 10.17). Estimation of the rate of change of RNFL thickness would be useful to differentiate disease-related from age-related change in the assessment of progressive RNFL thinning in monitoring patients with optic neuropathies.

Interpretation of RNFL Measurement in Myopic Eyes

The evaluation of optic disc morphology can be challenging in myopic eyes. The pattern of distribution of the RNFL in myopic eyes is different from that of non-myopic eyes. The RNFL is thickest over the superotemporal and inferotemporal

sectors of the optic disc. In moderate and high myopic eyes, the superotemporal and inferotemporal nerve fiber bundles tend to converge temporally (Fig. 10.13) [36]. Since most of the normative databases for RNFL measurement have been collected from eyes with small refractive errors, these databases would not be considered appropriate references in defining the "normal" percentile ranges in high myopic eyes. Therefore, the RNFL thickness of myopic eyes may fall below the "normal" range. The superior and inferior RNFL measurements may be signaled as "outside the normal range" in eyes with a long axial length. Consideration of the distribution pattern in the circumpapillary RNFL profile and the RNFL thickness map is required in the interpretation of RNFL abnormalities in eyes with myopia.

Disclosures C.L.: Speaker honorarium—Carl Zeiss Meditec, Heidelberg Engineering, Topcon; Research support—Carl Zeiss Meditec, Optovue, Tomey.

References

1. Beck RW, Cleary PA, Anderson Jr MM, et al. A randomized, controlled trial of corticosteroids in the treatment of acute optic neuritis. The Optic Neuritis Study Group. N Engl J Med. 1992;326:581–8.
2. Greenfield DS, Siatkowski RM, Glaser JS, et al. The cupped disc. Who needs neuroimaging? Ophthalmology. 1998;105:1866–74.
3. Hayreh SS, Zimmerman MB. Nonarteritic anterior ischemic optic neuropathy: natural history of visual outcome. Ophthalmology. 2008;115:298–305.
4. Optic Neuritis Study Group. Visual function 15 years after optic neuritis: a final follow-up report from the optic neuritis treatment trial. Ophthalmology. 2008;115:1079–82.
5. Berninger TA, Jaeger W, Krastel H. Electrophysiology and colourperimetry in dominant infantile optic atrophy. Br J Ophthalmol. 1991;75:49–52.
6. Lee EJ, Kim SJ, Choung HK, et al. Incidence and clinical features of ethambutol-induced optic neuropathy in Korea. J Neuroophthalmol. 2008;28:269–77.
7. Chang DS, Xu L, Boland MV, Friedman DS. Accuracy of pupil assessment for the detection of glaucoma: a systematic review and meta-analysis. Ophthalmology. 2013;120:2217–25.
8. Weinreb RN, Brandt JD, Garway-heath D, editors. Intraocular pressure. Consensus series 4. The Hague, The Netherlands: Kugler Publications; 2007. p. 17–58.
9. Park SJ, Ang GS, Nicholas S, et al. The effect of thin, thick, and normal corneas on Goldmann intraocular pressure measurements and correction formulae in individual eyes. Ophthalmology. 2012;119:443–9.
10. Kaufmann C, Bachmann LM, Thiel MA. Intraocular pressure measurements using dynamic contour tonometry after laser in situ keratomileusis. Investig Ophthalmol Vis Sci. 2003;44:3790–4.
11. Kniestedt C, Nee M, Stamper RL. Dynamic contour tonometry: a comparative study on human cadaver eyes. Arch Ophthalmol. 2004;122:1287–93.
12. Foster PJ, Buhrmann R, Quigley HA, Johnson GJ. The definition and classification of glaucoma in prevalence surveys. Br J Ophthalmol. 2002;86:238–42.
13. Trobe JD, Glaser JS, Cassady J, et al. Nonglaucomatous excavation of the optic disc. Arch Ophthalmol. 1980;98:1046–50.
14. Quigley H, Anderson DR. Cupping of the optic disc in ischemic optic neuropathy. Trans Sect Ophthalmol Am Acad Ophthalmol Otolaryngol. 1977;83:755–62.
15. Piette SD, Sergott RC. Pathological optic-disc cupping. Curr Opin Ophthalmol. 2006;17:1–6.
16. Ahmed II, Feldman F, Kucharczyk W, Trope GE. Neuroradiologic screening in normal-pressure glaucoma: study results and literature review. J Glaucoma. 2002;11:279–86.
17. Hood DC, Chen JY, Yang EB, et al. The role of the multifocal visual evoked potential (mfVEP) latency in understanding optic nerve and retinal diseases. Trans Am Ophthalmol Soc. 2006;104:71–7.
18. Bach M, Poloschek CM. Electrophysiology and glaucoma: current status and future challenges. Cell Tissue Res. 2013;353:287–96.
19. Wang J, Cheng H, Hu YS, et al. The photopic negative response of the flash electroretinogram in multiple sclerosis. Investig Ophthalmol Vis Sci. 2012;53:1315–23.
20. Kiss S, Damico FM, Young LH. Ocular manifestations and treatment of syphilis. Semin Ophthalmol. 2005;20:161–7.
21. Schuman JS, Pedut-Kloizman T, Hertzmark E, et al. Reproducibility of nerve fiber layer thickness measurements using optical coherence tomography. Ophthalmology. 1996;103:1889–98.
22. Leung CK, Cheung CY, Weinreb RN, Qiu Q, Liu S, Li H, et al. Retinal nerve fiber layer imaging with spectral-domain optical coherence tomography: a variability and diagnostic performance study. Ophthalmology. 2009;116:1257–63.
23. Leung CK, Lam S, Weinreb RN, Liu S, Ye C, Liu N, et al. Retinal nerve fiber layer imaging with spectral-domain optical coherence tomography – analysis of the RNFL Map for glaucoma detection. Ophthalmology. 2010;117:1684–91.
24. Cheung CY, Leung CK, Lin D, Pang CP, Lam DS. Relationship between retinal nerve fiber layer measurement and signal strength in optical coherence tomography. Ophthalmology. 2008;115:1347–51.

25. Cheung CY, Chan N, Leung CK. Retinal nerve fiber layer imaging with spectral-domain optical coherence tomography – Effect of signal strength on analysis of the RNFL map. Asia-Pac J Ophthalmol. 2012;1: 19–23.
26. Leung CK, Choi N, Weinreb RN, Liu S, Ye C, Lai G, et al. Retinal nerve fiber layer imaging with spectral-domain optical coherence tomography – pattern of RNFL defects in Glaucoma. Ophthalmology. 2010;117: 2337–44.
27. Leung CK, Yu M, Weinreb RN, Lai G, Xu G, Lam DS. Retinal nerve fiber layer imaging with spectral-domain optical coherence tomography: patterns of RNFL progression. Ophthalmology. 2012;119:1858–66.
28. Medeiros FA, Zangwill LM, Alencar LM, et al. Detection of glaucoma progression with stratus OCT retinal nerve fiber layer, optic nerve head, and macular thickness measurements. Investig Ophthalmol Vis Sci. 2009;50:5741–8.
29. Leung CK, Cheung CY, Weinreb RN, et al. Evaluation of retinal nerve fiber layer progression in glaucoma: a study on optical coherence tomography guided progression analysis. Investig Ophthalmol Vis Sci. 2010;51:217–22.
30. Leung CK, Liu S, Weinreb RN, et al. Evaluation of retinal nerve fiber layer progression in glaucoma: a prospective analysis with neuroretinal rim and visual field progression. Ophthalmology. 2011;118:1551–7.
31. Lee EJ, Kim TW, Weinreb RN, et al. Trend-based analysis of retinal nerve fiber layer thickness measured by optical coherence tomography in eyes with localized nerve fiber layer defects. Investig Ophthalmol Vis Sci. 2011;52:1138–44.
32. Leung CK, Chiu V, Weinreb RN, et al. Evaluation of retinal nerve fiber layer progression in glaucoma: a comparison between spectral-domain and time-domain optical coherence tomography. Ophthalmology. 2011;118:1558–62.
33. Grewal DS, Sehi M, Paauw JD, Greenfield DS. Advanced Imaging in Glaucoma Study Group. detection of progressive retinal nerve fiber layer thickness loss with optical coherence tomography using 4 criteria for functional progression. J Glaucoma. 2012;21: 214–20.
34. Chan CK, Miller NR. Peripapillary nerve fiber layer thickness measured by optical coherence tomography in patients with no light perception from long-standing nonglaucomatous optic neuropathies. J Neuroophthalmol. 2007;27:176–9.
35. Leung CK, Yu M, Weinreb RN, Ye C, Liu S, Lai G, et al. Retinal nerve fiber layer imaging with spectral-domain optical coherence tomography: a prospective analysis of age-related loss. Ophthalmology. 2012;119: 731–7.
36. Leung CK, Yu M, Weinreb RN, Mak HK, Lai G, Ye C, et al. Retinal nerve fiber layer imaging with spectral-domain optical coherence tomography: interpreting the RNFL maps in healthy myopic eyes. Investig Ophthalmol Vis Sci. 2012;53:7194–200.
37. Scherer RW, Feldon SE, Levin L, et al. Visual fields at follow-up in the Ischemic optic neuropathy decompression trial: evaluation of change in pattern defect and severity over time. Ophthalmology. 2008;115: 1809–17.
38. Sadun AA. Metabolic optic neuropathies. Semin Ophthalmol. 2002;17:29–32.
39. Yu-Wai-Man P, Griffiths PG, Chinnery PF. Mitochondrial optic neuropathies – disease mechanisms and therapeutic strategies. Prog Retin Eye Res. 2011;30:81–114.

Application of Optical Coherence Tomography in Neuro-Ophthalmic Disorders

11

Joseph Ho, Geetha Athappilly, Timothy B. Tivnan, and Thomas R. Hedges III

Basic Principles of Optical Coherence Tomography (OCT)

OCT technology is based on the principle of "indirect inferometry" which superimposes light waves for imaging [1]. The summation of waves results in either constructive or destructive interference of light, and this information is then translated into an A-scan. The horizontal summation of a series of A-scans is a B-scan, which is represented as the OCT cross-sectional image. A summation of B-scans results in C-scans or three-dimensional cross-sections.

Early OCT employed time domain technology. In time domain OCT, the reference arm contains a light source and mobile mirror, which changes the path length of the light with time [2]. When the time delay from both arms is congruent, constructive interference occurs, and when they are not the same, varying levels of constructive and destructive interference patterns are formed. An example of an OCT using time domain technology is Zeiss Stratus OCT.

More recently, spectral, or Fourier domain OCT, has been developed. In this technology, the reference arm is fixed, resulting in a spectrum of interference pattern detected by the camera at any time point [3]. A mathematical algorithm known as the Fourier transformation is then carried out to generate the OCT image [3]. With this technology, the imaging speed is dramatically improved, allowing for acquisition of a dense level of data and in effect decreasing motion artifacts and generation of three-dimensional data. In addition, the use of a broad wavelength light source results in high-resolution imaging. Examples of OCT devices using spectral domain are Spectralis (Heidelberg Engineering, Carlsbad, CA), Cirrus HD-OCT (Carl Zeiss Meditec, Dublin, CA), 3D-OCT (Topcon Medical Systems, Oakland, NJ), and RTVue (Optovue, Fremont, CA) [4, 5].

Although both technologies follow the same basic principle, studies comparing the two types of machines have found differences in the results generated. In addition to variability between time domain and spectral domain OCT, there is also variability in the results between the different spectral domain OCTs. This variability limits the longitudinal assessment of data when a patient's results are obtained on different machines over time. The differences between the reproducibility of data among the different machines will also be highlighted.

J. Ho, M.D.
Department of Ophthalmology, New England Eye Center-Tufts Medical Center, Boston, MA, USA

G. Athappilly, M.D. (✉)
Tufts Medical Center, Boston, MA, USA

Lahey Clinic Ophthalmology Department, Burlington, MA, USA
e-mail: gathappilly@tuftsmedicalcenter.org; Geetha.k.athappilly@lahey.org

T.B. Tivnan, B.S., C.R.A.
Department of Ophthalmology, Lahey Clinic Medical Center, Mashpee, MA, USA

T.R. Hedges III, M.D.
Department of Ophthalmology, Tufts Medical Center, Boston, MA, USA

J.W. Chan (ed.), *Optic Nerve Disorders: Diagnosis and Management*,
DOI 10.1007/978-1-4614-0691-4_11,

OCT in the Analysis of Neuro-Ophthalmic Disorders

OCT does not replace the role of a careful neuro-ophthalmic evaluation. It supplements the clinical examination and can provide quantitative and longitudinal information. In this section, examples of neuro-ophthalmic disorders are shown in which OCT demonstrates areas of pathology not always clearly visualized on fundus examination.

Non-arteritic Ischemic Optic Neuropathy with Subretinal Fluid

Patients with a non-arteritic ischemic optic neuropathy (NAION) typically present with altitudinal field loss. Central vision may be mildly to moderately affected. Hedges et al. first reported several patients with central vision loss due to subretinal fluid (SRF) associated with NAION [6]. These patients, unlike those with classic NAION, have more central visual loss due to SRF extending to the fovea. SRF can be difficult to identify on fundus exam (Fig. 11.1) but can be clearly seen on macular OCT (Fig. 11.2). As treatment of NAION is developed, exactly how therapy affects the nerve and/or the retina must be considered.

Papilledema with Secondary Choroidal Neovascularization and Subretinal Fluid

Patients with papilledema typically do not present with acute central visual loss. An exception is when there are associated macular changes from SRF or a choroidal neovascular membrane (CNV) (see Fig. 11.3). Line scans through the macula help in locating the heme as subretinal and identifying the CNV (see Fig. 11.4).

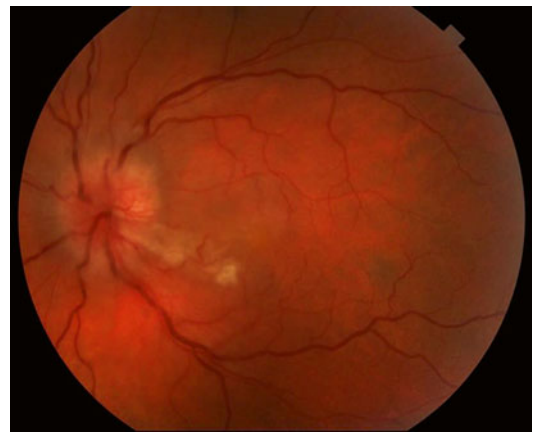

Fig. 11.1 Fundus photograph of non-arteritic ischemic optic neuropathy (NAION) in the left eye revealing a hyperemic, swollen nerve, nerve fiber layer infarct, and dull foveal reflex due to sub-retinal fluid

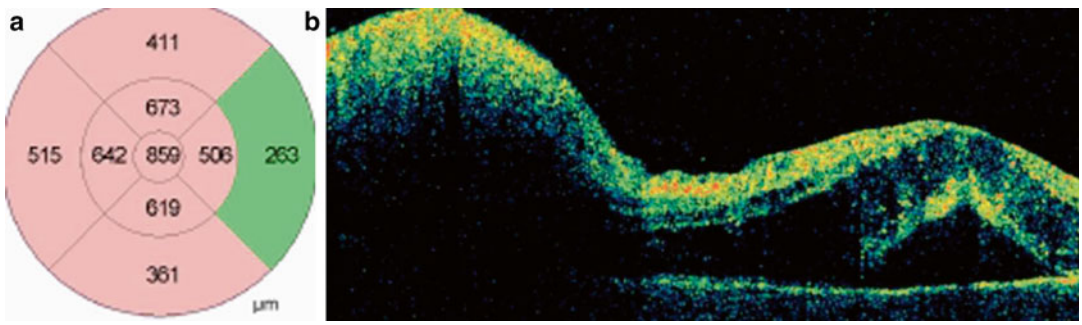

Fig. 11.2 Fast macular scan in above patient with non-arteritic ischemic optic neuropathy (NAION) in the left eye revealing increased macular thickness in the affected eye (**a**). Line scan through the optic nerve and macula clearly revealing severe disc edema with intraretinal and subretinal fluid in the macula (**b**)

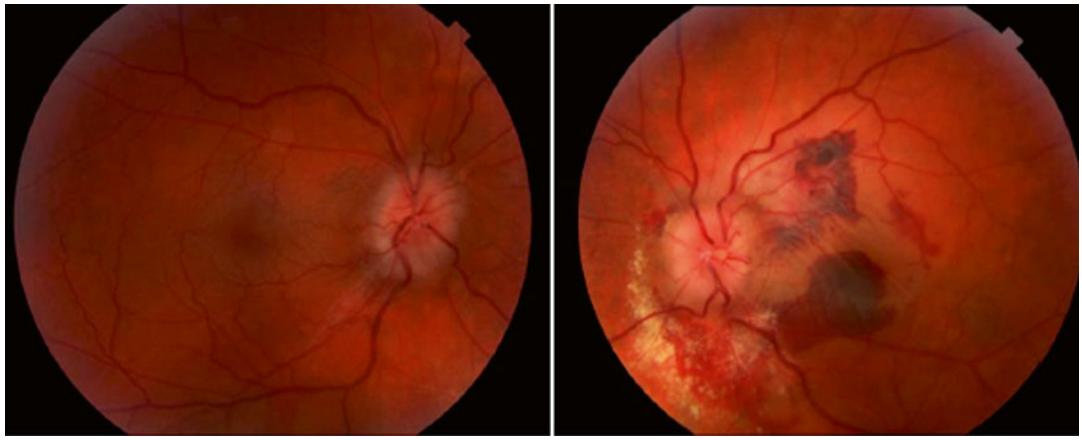

Fig. 11.3 Fundus photographs of a patient with long-standing poorly controlled papilledema presenting with acute, central, vision loss in her left eye due to a choroidal neovascular membrane affecting the macula

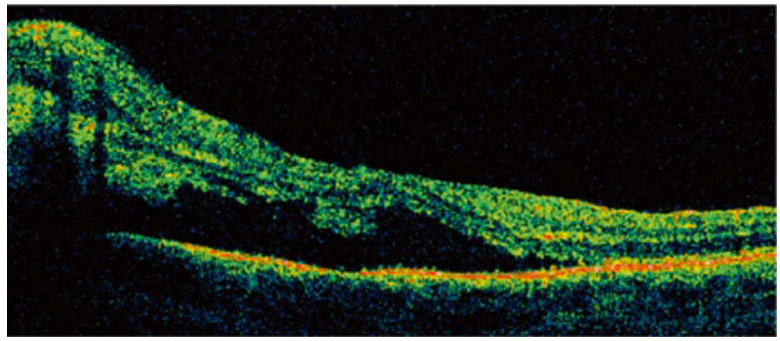

Fig. 11.4 Line scan from the left optic nerve to the macula revealing subretinal hemorrhage from choroidal neovascular membrane as the etiology of her central vision loss

Avastin injections have been beneficial in treating CNV associated with papilledema. SRF involving the macula, as described by Hoye et al. in 1998, usually resolves, and visual acuity improves spontaneously as the cause of the papilledema is treated [7, 8].

Toxic Optic Neuropathy

Patients with visual loss from toxic, hereditary, or nutritional optic neuropathies maybe mistaken for functional visual loss due to minimal abnormalities on fundus examination. The temporal pallor and dull foveal reflex on fundus exam is subtle (see Fig. 11.5). Retinal nerve fiber layer (RNFL) and macular OCT studies clearly demonstrate abnormalities in RNFL thickness temporally and in the distribution of the papillomacular bundle fibers (see Fig. 11.6) [9].

Optic Nerve Drusen

Optic nerve drusen can give the appearance of blurred disc margins, similar to the appearance of true disc edema, or papilledema (see Fig. 11.7). RNFL scans show atrophy in optic nerve head drusen, whereas it shows increased RNFL thickness in optic nerve edema (see Fig. 11.8).

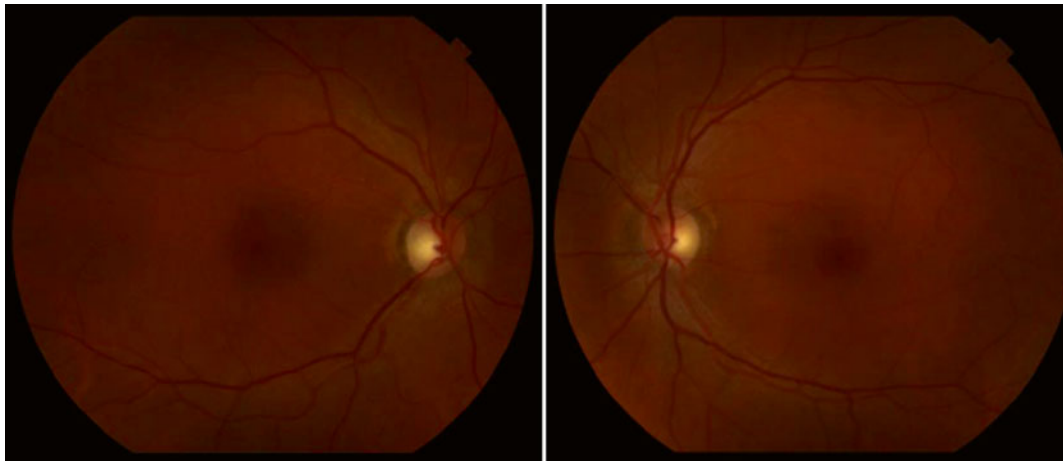

Fig. 11.5 Fundus photographs of a patient with bilateral toxic optic neuropathy demonstrating subtle optic nerve pallor and dull foveal reflexes

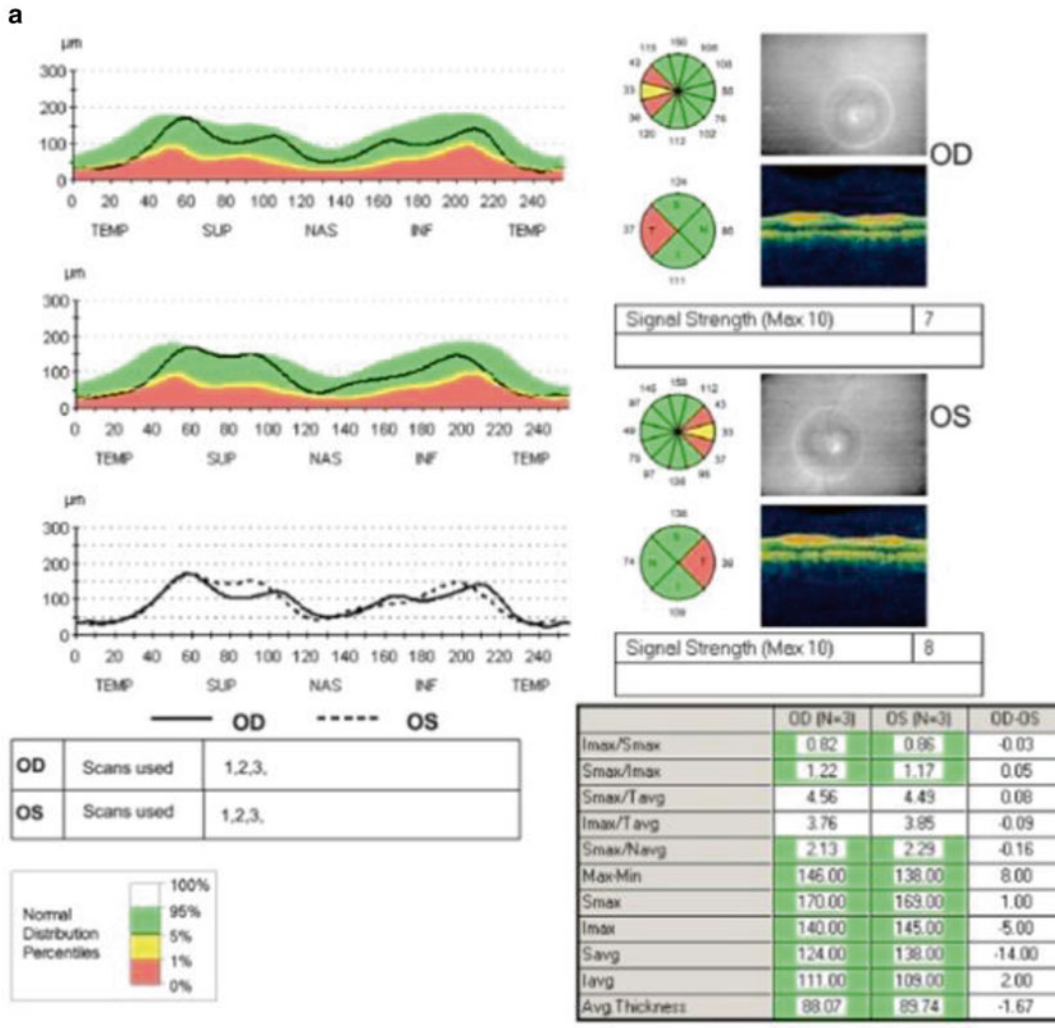

	OD (N=3)	OS (N=3)	OD-OS
Imax/Smax	0.82	0.86	-0.03
Smax/Imax	1.22	1.17	0.05
Smax/Tavg	4.56	4.49	0.08
Imax/Tavg	3.76	3.85	-0.09
Smax/Navg	2.13	2.29	-0.16
Max-Min	146.00	138.00	8.00
Smax	170.00	169.00	1.00
Imax	140.00	145.00	-5.00
Savg	124.00	138.00	-14.00
Iavg	111.00	109.00	2.00
Avg Thickness	88.07	89.74	-1.67

Fig. 11.6 Retinal nerve fiber layer (RNFL) studies showing bilateral temporal thinning (**a**). Macular optical coherence tomography (OCT) demonstrating macular thinning in same patient with toxic optic neuropathy (**b**)

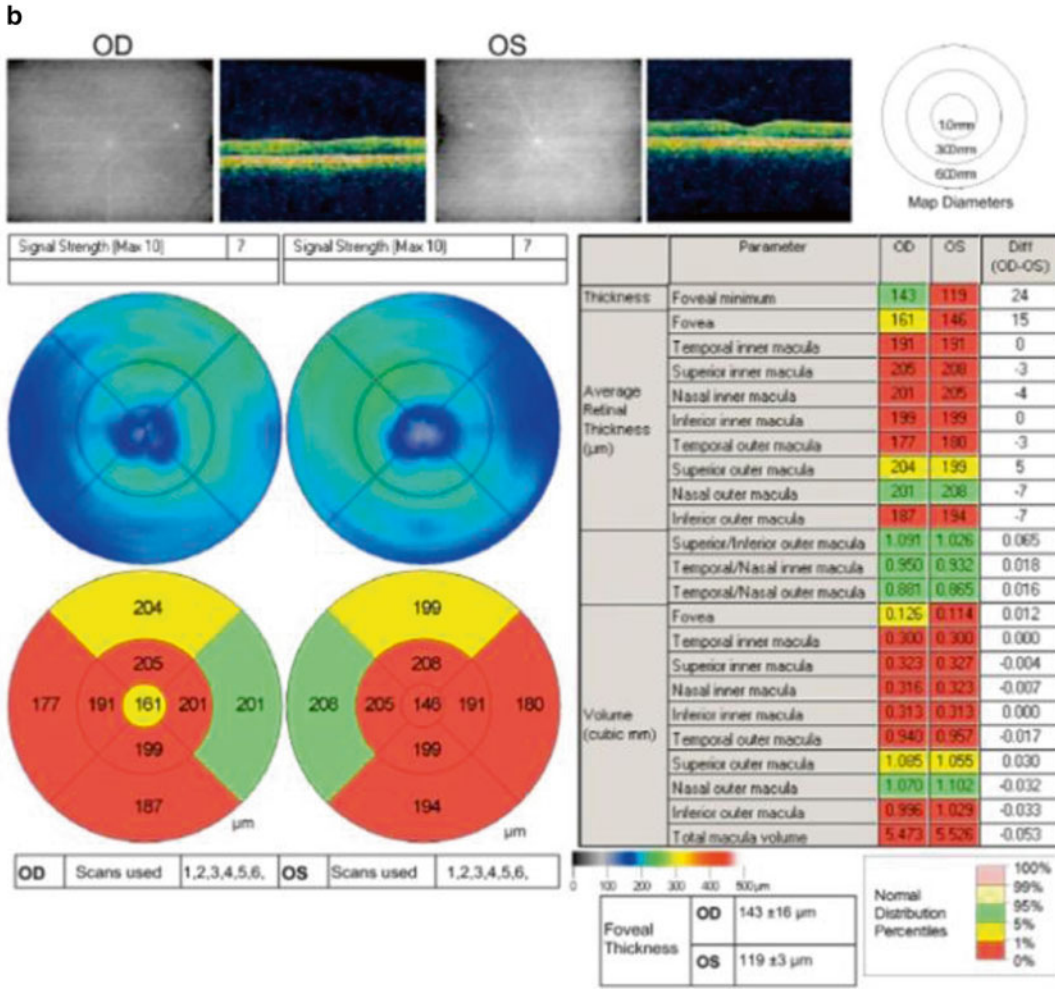

Fig. 11.6 (continued)

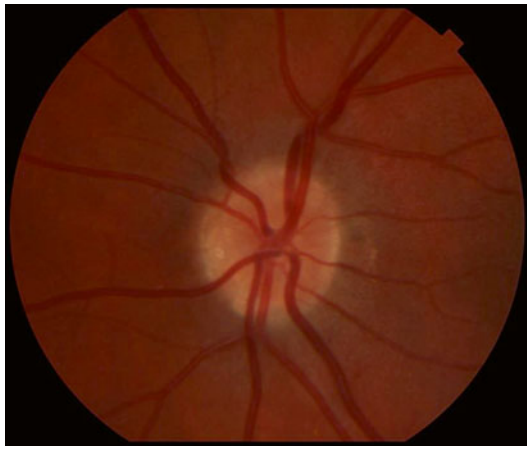

Fig. 11.7 Fundus photograph of blurred disc margins in the left eye of a patient with a presumed diagnosis of papilledema

In addition, line scans through the optic nerve reveal differences in the contour of the optic nerve. Various studies have shown a characteristic "bumpy" appearance of the internal contour of the optic nerve in optic nerve drusen, compared to the more smooth borders of elevation seen with true disc edema (see Fig. 11.9) [10, 11].

Optic Nerve Pit

Patients with optic nerve pits have an optic nerve appearance that may be mistaken for an optic neuropathy or glaucoma. In characteristic cases, there may be a grayish appearance to the inferior

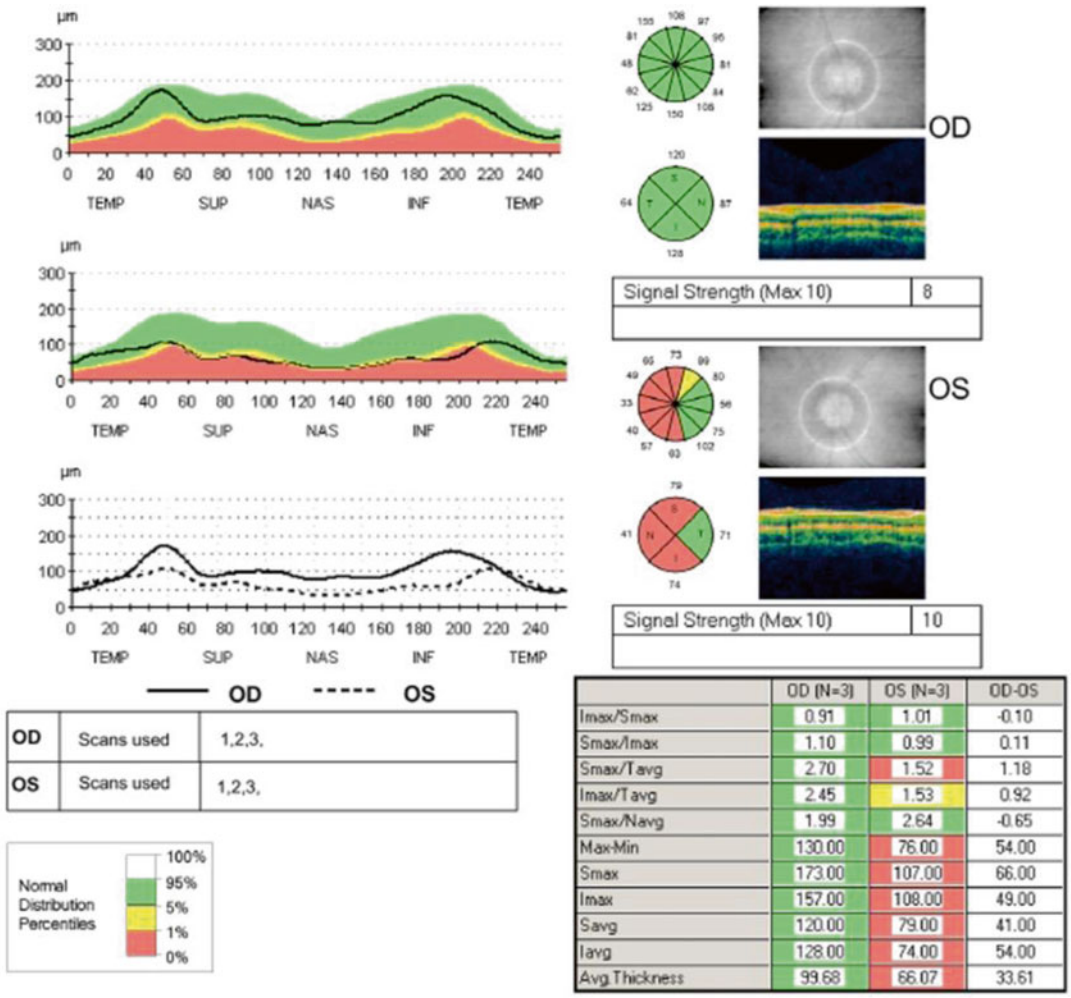

Fig. 11.8 Fast retinal nerve fiber layer (RNFL) scan of the left eye showing optic atrophy, as commonly seen in patients with optic nerve drusen

temporal rim (see Fig. 11.10). In more subtle cases, this may not be present. OCT can help clarify the diagnosis. Optic nerve pits often have inferior-temporal RNFL thinning on fast RNFL scan (see Fig. 11.11). When patients with an optic nerve pit present with central visual loss from neurosensory retinal fluid, this may be further mistaken for an acquired optic neuropathy (see Fig. 11.12). The correct diagnosis can be made by doing a line scan from the optic nerve to the macula, which reveals the "pit" as a schisis contiguous with fluid in the neurosensory retina (see Fig. 11.13).

Macular Edema from Fingolimod

A rare complication in the use of fingolimod in multiple sclerosis (MS) patients is visual loss from macular edema [12]. Macular edema may sometimes be difficult to diagnose on fundus examination (see Fig. 11.14). When MS patients present with central visual loss, it may be inaccurately diagnosed as retrobulbar optic neuritis. Macular OCT (see Fig. 11.15) helps distinguish visual loss from macular edema versus that from retrobulbar optic neuritis by clearly demonstrating the intraretinal fluid in the macula.

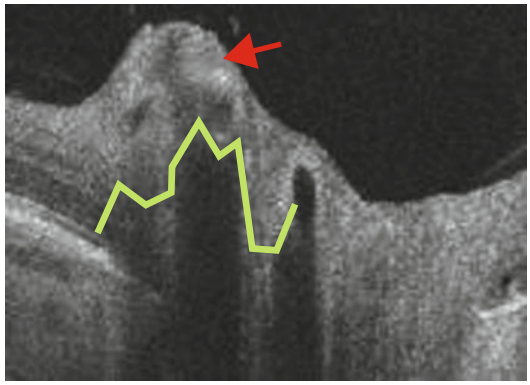

Fig. 11.9 Line scan through the optic nerve showing characteristic "bumpy" internal contour of the optic nerve (*green wavy line*), seen with optic nerve drusen. Drusen is seen as a hyper-reflective mass (*arrow*) with a hypo-reflective shadow

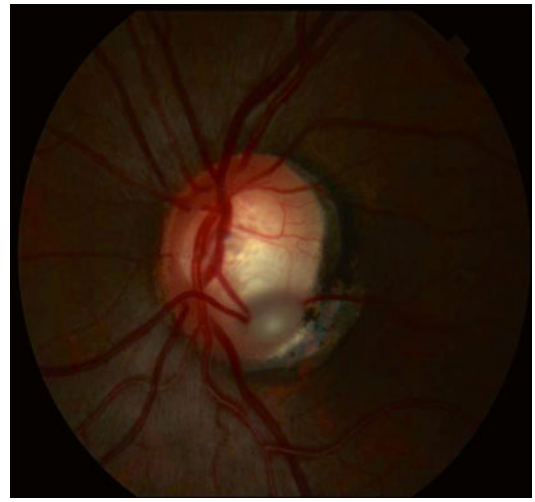

Fig. 11.10 Fundus photograph of the left eye showing an optic nerve pit with an abnormal inferior disc rim which, in subtle cases, may be mistaken for disc pallor or thinning

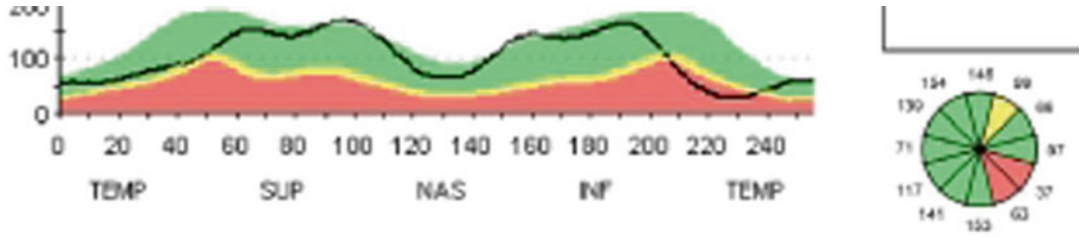

Fig. 11.11 Fast retinal nerve fiber layer (RNFL) scan showing an inferior-temporal segmental thinning of the left optic nerve that corresponds to the location of the optic nerve pit

Central Serous Retinopathy

Central serous retinopathy and optic neuritis can present with similar symptoms which can be especially confusing in MS patients. The findings of central visual loss, color defect, and a relative afferent pupillary defect can be present in both central serous retinopathy and optic neuritis. Similar to macular edema, central serous retinopathy can be difficult to identify on fundus exam. Macular OCT (see Fig. 11.16) is especially helpful in these cases by demonstrating the SRF (Fig. 11.17).

Central Retinal Artery Occlusion

Patients with central retinal artery occlusion (CRAO) may also have clinical features suggestive of an optic neuropathy because of the presence of central visual loss, color defect, and relative afferent pupillary defect, with occasional optic nerve edema (see Fig. 11.18). In the early stages of CRAO, the fundus examination often shows mild changes. Macular OCT more clearly demonstrates acute retinal thickening (see Fig. 11.19) [13] followed by more chronic inner retinal thinning in the chronic stages of CRAO.

Demyelinative and Neurodegenerative Disorders

The use of OCT extends beyond the evaluation of the eye and retrobulbar optic nerve to provide insight into intracranial pathology. MS, Parkinson's disease (PD), and Alzheimer's disease (AD) all show changes on OCT specific to central nervous

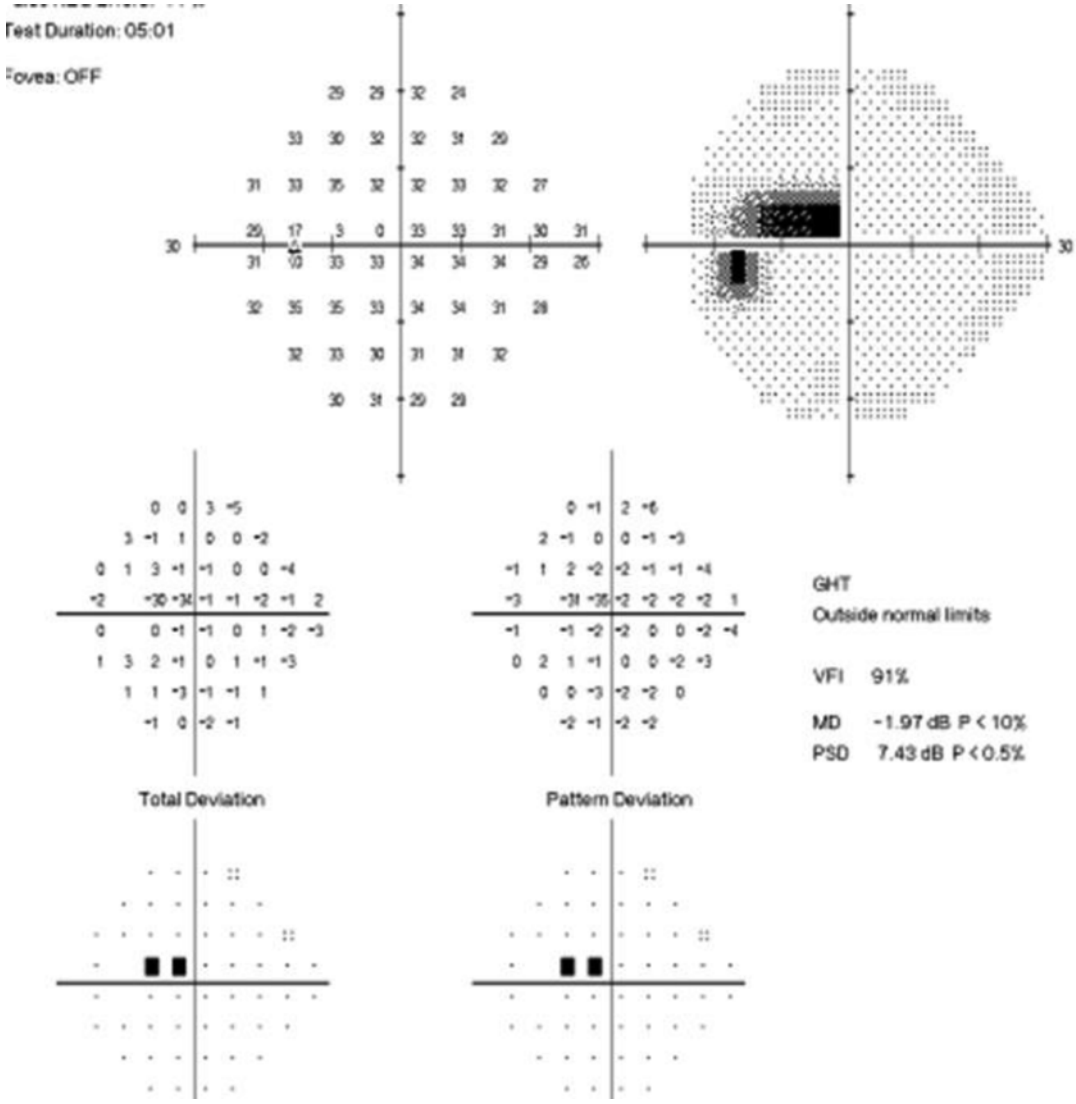

Fig. 11.12 Central scotoma on Humphrey central threshold 30–2 visual field test of a patient with a left optic nerve pit and subretinal fluid

system disease, which may help in the diagnosis and management of these conditions.

A current area of intensive investigation is the use of OCT in demyelinating disease. When a patient presents with new onset optic neuritis, it is important to distinguish if he or she has MS, neuromyelitis optica (NMO), or a clinically isolated syndrome (CIS). Unlike CIS patients, those with MS may show subclinical RNFL loss in the unaffected eye. Over time, MS patients also develop further RNFL loss in the affected eye, presumably from additional optic neuritis events compared to those patients with only CIS [14–16].

OCT can help distinguish patients with NMO from MS. Studies have shown that more severe RNFL loss occurs after a single episode of optic neuritis in NMO compared to that in MS [17]. It is important to distinguish among patients with CIS, MS, and NMO, as the overall prognosis and management of these diseases are different.

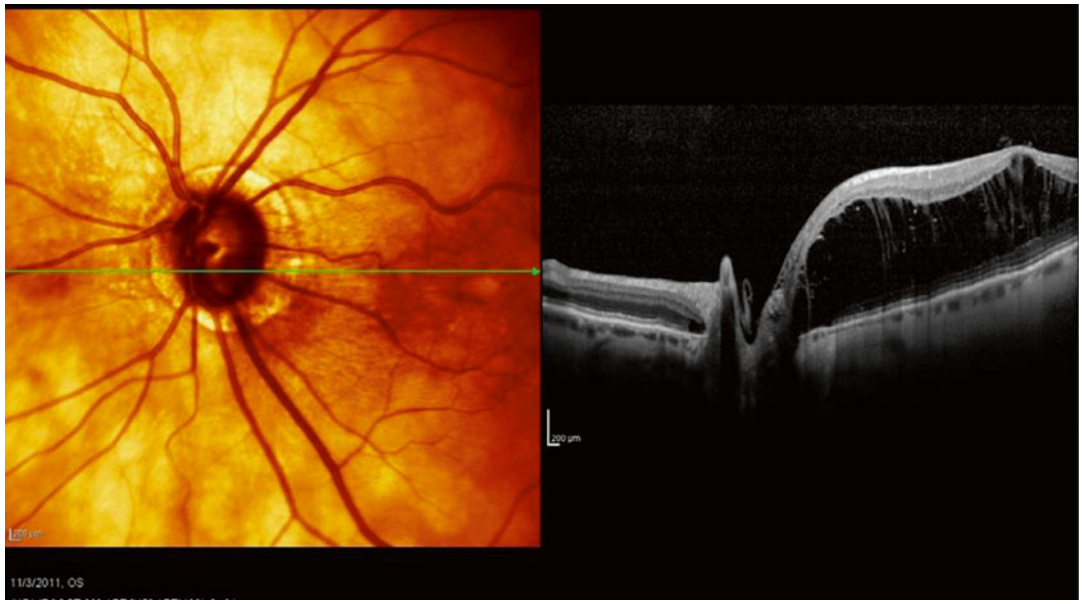

Fig. 11.13 Line scan through the left optic nerve showing the characteristic opening or "pit" (*arrow*) with fluid extending into the neurosensory retina

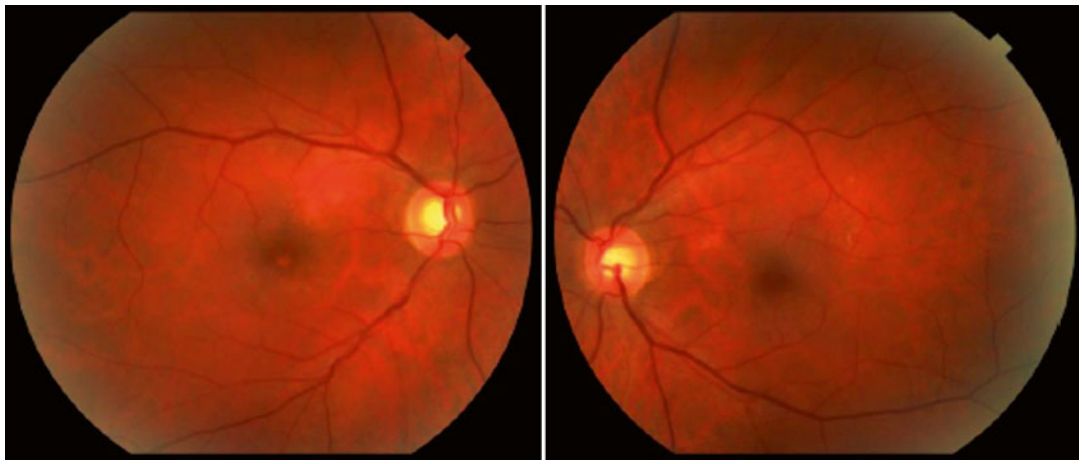

Fig. 11.14 Fundus photographs of a patient with multiple sclerosis with macular edema related to fingolimod use

OCT can also provide information regarding the type of MS. In a study by Costello, lower RNFL values were found with more severe forms of MS such as primary and secondary progressive MS compared to patients with relapsing, remitting MS [18].

In addition to the RNFL, recent OCT studies evaluating macular thickness have provided further insight into the pathologic course of MS. Macular thinning was found to be at the level of the inner and outer nuclear layer, and the ganglion cell layer (GCL) [19]. These patients with macular thinning did not have RNFL thinning, as one would expect, but did have more severe forms of MS. Multiple sclerosis not only causes demyelination, but also neuronal loss. Microcystic changes

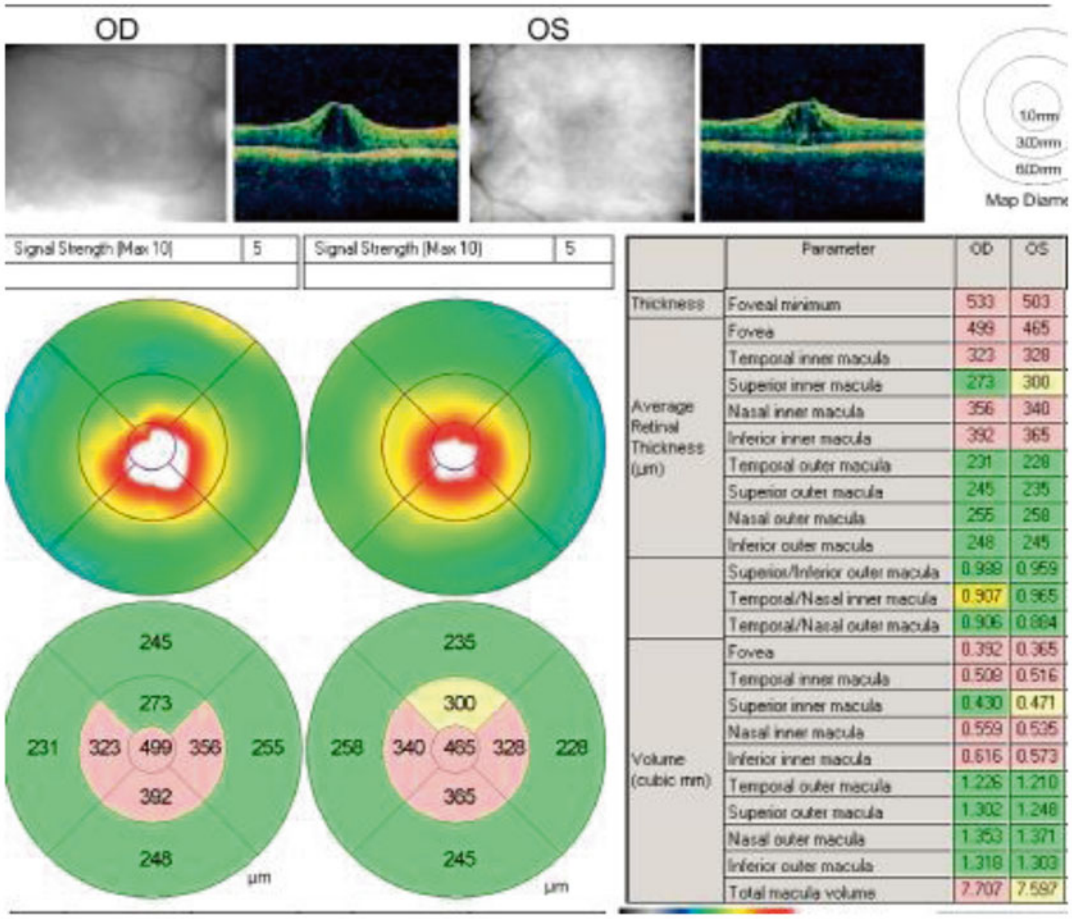

Fig. 11.15 Fast MAC scan revealing bilateral macular edema as the cause of visual loss

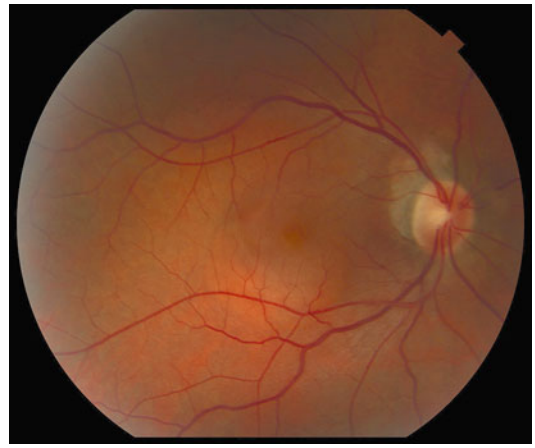

Fig. 11.16 Fundus photograph of right central serous retinopathy in a patient with multiple sclerosis

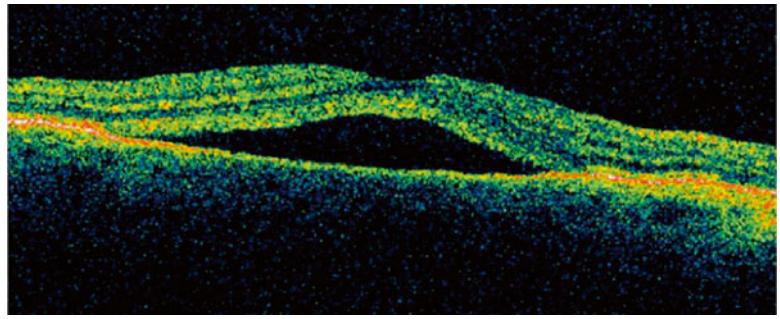

Fig. 11.17 Line scan through the macula revealing subretinal fluid as the etiology of visual loss

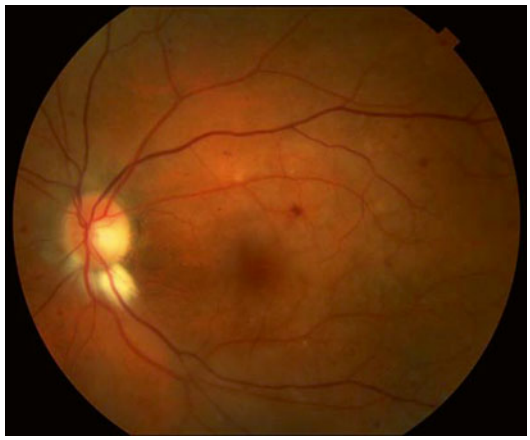

Fig. 11.18 Fundus photograph of mild macular changes from a left central retinal artery occlusion in a patient with diabetic retinopathy complaining of acute, severe visual loss

in the retina have also been seen in optic neuritis, but this pathology is now being interpreted as a nonspecific secondary change that can be seen in a variety of other optic nerve disorders [20–23].

In other neurodegenerative diseases, such as PD and AD, the distinctive patterns of RNFL thinning on OCT may play a role in the diagnosis and monitoring of these disorders and may give further insight into the understanding of associated visual symptoms. Degenerative changes occurring in the optic nerve in AD patients are seen as RNFL thinning. Marziani et al. [24] demonstrated that the RNFL and RNFL and GCL thickness measurements on spectral domain OCT were reduced in all RNFL quadrants in AD patients compared with healthy subjects. In another study by Moreno-Ramos et al. [25], RNFL thinning was statistically correlated with both the Mini Mental State Examination and the Mattis Dementia Rating Scale scores in not only AD, but also in PD and dementia of Lewy bodies. Greater cognitive deterioration correlated with more severe RNFL thinning. These studies support RNFL measurement as a possible biomarker for the diagnosis and monitoring of various dementias.

Patients with PD have decreased dopamine levels that play an important role for various visual functions, including color vision and spatial sensitivity. Dopamine is an important neurotransmitter in the visual pathways, and pathology specimens have revealed its widespread location in the retina [26, 27]. Previous studies have shown ERG and VEP changes in patients with PD [28–30]. Time domain OCT can show macular and RNFL layer changes in patients with early stages of PD [31]. Moschos et al. [32] found that patients with PD with no clinical optic nerve pathology had statistically significant RNFL thinning in the inferior and temporal quadrants. Hajee et al. [33] also found paramacular thinning in PD patients without associated macular pathology. In both of these studies, the OCT findings support that subclinical visual dysfunction can be detected in the early stages of PD.

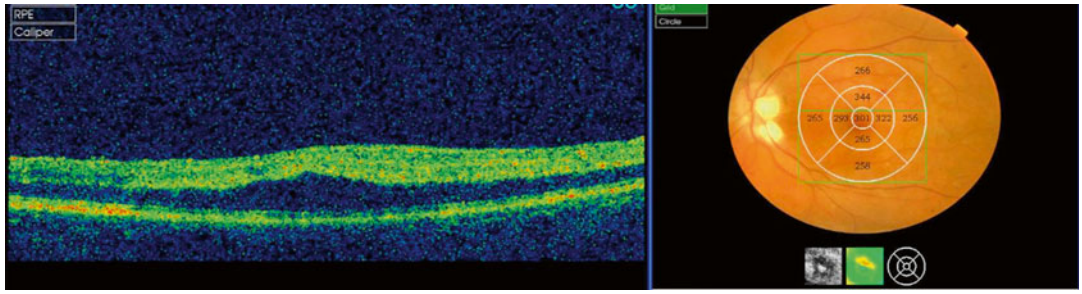

Fig. 11.19 Line scan through the macula showing edema of the retinal layers, as often seen in patients with a central retinal artery occlusion

Limitations of OCT in Neurologic Disorders

Limitations in OCT Software

Accurate quantitative analysis of the macular and RNFL thickness in neuro-ophthalmic disorders requires proper segmentation of the RNFL anatomy. In cases where the anatomy is altered from pathology or media opacities, "software breakdown" may occur and limit the accuracy of the data. For example, with optic nerve pathologies such as severe disc edema or papilledema, placement of the 3.4 mm circular scan in the center of the optic nerve can be challenging because of the uneven elevation of the optic nerve along its circumference. This contour distortion can result in inaccurate measurements and difficulty in assessing progression or improvement of optic nerve edema. In media opacities like cataract or corneal scarring, degradation of the signal strength can limit the quality of the scan and give inaccurate results, especially with signal strengths under 7 [34]. Therefore, clinical decisions cannot be based solely on numeric RNFL thickness measurements, and the quality and reliability of each OCT scan must be individually evaluated for various possible artifacts. Research in improving the retinal segmentation software to reduce the incidence of "software breakdown" is currently underway.

With spectral domain OCT, limitations from motion and spatial resolution have been reduced. Scanning speed has tremendously increased with spectral domain OCT so that blink artifact, an inherent limitation in time domain technology, is decreased. Newer generation spectral domain technology also uses a broader imaging wavelength, which improves axial resolution from approximately 10 μm to about 4 μm for most commercial devices. This improved resolution has allowed greater accuracy in detecting subtle pathology with spectral domain OCT.

Limitations of OCT Based on Patient Cooperation, Operator Skills, and Ocular Anatomy

Patient cooperation is an important factor that may influence the quality of a scan. Patients with neurologic disorders often have cognitive difficulties that impair attention and concentration during the OCT procedure. For example, if a patient cannot maintain fixation on the scan target or if he/ she blinks during the scan, this may result in motion or blink artifacts. These errors are seen as distorted, or "cut- off" OCT images. Spectral domain OCT technology decreases the incidence of these errors by operating at a faster scan speed. Some spectral domain OCTs, such as the Heidelberg Spectralis, also have a retinal tracker feature which decreases the incidence of motion artifact.

In addition to patient cooperation, signal strength is also affected by the operator and it can vary depending on the operator's skill. Scans with a signal strength of less than 7 are associated with lower reproducibility [34]. Different results in the

peripapillary RNFL measurements in time domain and spectral domain OCT can also be seen because of the variability in the manual placement of the 3.4 mm circle around the optic nerve among operators. Even in situations where the patient is cooperative and the operator is skilled, OCT values can have reduced reliability based on the patient's ocular anatomy. For example, a longer axial length in high myopia, or a markedly temporally tilted optic disc [35] can give higher variability in RNFL thickness measurements. (For further details regarding how ocular anatomy and age-related changes can affect RNFL measurement, see "Limitations of OCT in Retinal Nerve Fiber Layer Measurement" in the chapter entitled, "Approach to the Diagnosis and Differentiation of Glaucomatous and Nonglaucomatous Optic Neuropathies.")

Measurement Variability in OCT Technology in Multiple Sclerosis

Although the mean RNFL thickness in patients with MS can be reproducibly measured by skilled technicians with excellent interrater (ICC, 0.89), intrarater (ICC, 0.98), and intervisit (ICC, 0.91) results [36], the differences in technology and software can result in different RNFL measurements between the time and spectral domain OCT devices. Although the RNFL thickness measurements in optic neuritis scanned from Stratus OCT have been shown to correlate well with those taken from Cirrus OCT, these measurements are not the same [37]. In a study of 18 patients with monocular acute optic neuritis within 6 months of presentation, Rebolleda et al. [37] showed that the RNFL in the nasal and temporal quadrants was thicker with Stratus OCT than with Cirrus OCT, except when the RNFL was very thin. When the average RNFL thickness was ≤56 μm, Cirrus OCT gave a higher value than Stratus. These measurement differences may be due to differences in registration, processing, and analysis. Differences in software segmentation algorithms may also account for this variation. The Cirrus spectral domain OCT aims to measure the bottom of the RNFL layer, whereas the Stratus time domain OCT focuses more at the top of the GCL [38].

Furthermore, the Cirrus spectral domain OCT, compared with the Stratus time domain OCT, identified a higher proportion of eyes with optic neuritis based on the internal normative database (44.4 % vs. 38 %). This greater sensitivity in measurement could be attributed to higher scan resolution and more accurate data registration of the instrument. In another study by Lange et al. [39] comparing MS eyes without optic neuritis to those with optic neuritis and to normal controls using Spectralis spectral domain OCT and Stratus time domain OCT, measurements between time domain and spectral domain OCT were highly correlated, but the absolute measurements were not interchangeable. These results were also similar to those in a study done by Bock et al. [40] in which they compared differences in RNFL thicknesses in RRMS patients compared to normal controls, using time domain and Cirrus spectral domain OCT.

Studies have also shown differences in measurements generated among the different spectral domain OCT equipment themselves. In a study by Watson et al. [4] five different OCT devices (the Stratus time domain OCT, along with four spectral domain OCTs, including Topcon 3D OCT 1000, Optovue RTVue-100, Cirrus HD OCT, and Heidelberg Spectralis SD OCT) yielded statistically significant differences in RNFL and central macular thickness (CMT) measurements in 92 eyes of patients with a history of optic neuritis and/or MS. The Cirrus and Spectralis OCT yielded lower RNFL measurements, while the RTVue-100 and 3D OCT 1000 yielded higher measurements compared to those of the Stratus OCT. The differences in CMT could arise from the nonstandard placement of the outer macular segmentation boundary line. The boundary line of the Stratus OCT aligns at the inner segment/outer segment junction, while it aligns at the outer RPE of the Cirrus/RTVue-100, at the inner RPE in the 3D OCT-1000, and at the Bruchs membrane in the Spectralis. Differences in sampling density, in the placement of the outer circle (Stratus/Cirrus at 3.46 mm, RTVue-100/Spectralis at 3.45 mm, and

3D OCT-1000 at 3.40 mm), and in the signal strength scale are all likely to contribute to RNFL and CMT measurement differences.

Because of this variability between spectral domain and time domain OCT and among various spectral domain OCTs, it is important to use the same instrument when following patients longitudinally.

References

1. Huang D, Swanson EA, Lin CP, Schuman JS, Stinson WG, Chang W, et al. Optical coherence tomography. Science. 1991;254(5035):1178–81.
2. Fujimoto JG, Brezinski ME, Tearney GJ, et al. Optical biopsy and imaging using optical coherence tomography. Nat Med. 1995;9:970–2.
3. Yaqoob Z, Wu J, Yang C. Spectral domain optical coherence tomography: a better OCT imaging strategy. Biotechniques. 2005;9(6 Suppl):S6–13.
4. Watson GM, Keltner JL, Chin EK, Harvey D, Nguyen A, Park SS. Comparison of retinal nerve fiber layer and central macular thickness measurements among five different optical coherence tomography instruments in patients with multiple sclerosis and optic neuritis. J Neuroophthalmol. 2011;31:110–6.
5. Buchser NM, Wollstein G, Ishikawa H, Bilonick RA, Ling Y, Folio LS, et al. Comparison of retinal nerve fiber layerthickness measurement bias and imprecision across three spectral-domain opticalcoherence tomography devices. Investig Ophthalmol Vis Sci. 2012;53(7):3742–7.
6. Hedges 3rd TR, Vuong LN, Gonzalez-Garcia AO, Mendoza-Santiesteban CE, Amaro-Quierza ML. Subretinal fluid from anterior ischemic optic neuropathy demonstrated by optical coherence tomography. Arch Ophthalmol. 2008;126(6):812–5.
7. Hoye 3rd VJ, Berrocal AM, Hedges 3rd TR, Amaro-Quireza ML. Optical coherence tomography demonstrates subretinal macular edema from papilledema. Arch Ophthalmol. 2001;119(9):1287–90.
8. Savini G, Barboni P, Carbonelli M, Carelli V, Sadun AA. Optical coherencetomography for optic disc edema. Arch Ophthalmol. 2011;129(9):1245–6.
9. Moura FC, Monteiro ML. Evaluation of retinal nerve fiber layer thickness measurements using optical coherence tomography in patients with tobacco-alcohol-induced toxic optic neuropathy. Indian J Ophthalmol. 2010;58(2):143–6.
10. Johnson LN, Diehl ML, Hamm CW, Sommerville DN, Petroski GF. Differentiating optic disc edema from optic nerve head drusen on optical coherence tomography. Arch Ophthalmol. 2009;127:45–9.
11. Kupersmith MJ, Sibony P, Mandel G, Durbin M, Kardon RH. Optical coherence tomography of the swollen optic nerve head: deformation of the peripapillaryretinal pigment epithelium layer in papilledema. Investig Ophthalmol Vis Sci. 2011;52(9):6558–64.
12. Afshar AR, Fernandes JK, Patel RD, Ksiazek SM, Sheth VS, Reder AT, et al. Cystoid macular edema associated with fingolimod use for multiple sclerosis. JAMA Ophthalmol. 2013;131(1):103–7.
13. Rodrigues IA. Acute and chronic spectral domain optical coherence tomography features of branch retinal artery occlusion. BMJ Case Rep. 2013;pii: bcr2013009007.
14. Costello F, Hodge W, Pan YI, Eggenberger E, Coupland S, Kardon RH. Tracking retinal nerve fiber layer loss after optic neuritis: a prospective study using optical coherence tomography. Mult Scler. 2008;14(7):893–905.
15. Costello FE, Klistorner A, Kardon R. Optical coherence tomography in the diagnosis and management of optic neuritis and multiple sclerosis. Ophthalmic Surg Lasers Imaging. 2011;42(Suppl):S28–40.
16. Talman LS, Bisker ER, Sackel DJ, Long Jr DA, Galetta KM, Ratchford JN, et al. Longitudinal study of vision and retinal nerve fiberlayer thickness in multiple sclerosis. Ann Neurol. 2010;67(6):749–60.
17. Fernandes DB, Raza AS, Nogueira RG, Wang D, Callegaro D, Hood DC, et al. Evaluation of inner retinal layers in patients with multiple sclerosis orneuromyelitisoptica using optical coherence tomography. Ophthalmology. 2013;120(2):387–94.
18. Costello F, Hodge W, Pan YI, Eggenberger E, Freedman MS. Using retinal architecture to help characterize multiple sclerosis patients. Can J Ophthalmol. 2010;45(5):520–6.
19. Saidha S, Syc SB, Ibrahim MA, Eckstein C, Warner CV, Farrell SK, et al. Primary retinal pathology in multiple sclerosis asdetected by optical coherence tomography. Brain. 2011;134(Pt 2):518–33.
20. Gelfand JM, Nolan R, Schwartz DM, Graves J, Green AJ. Microcystic macular oedema in multiple sclerosis is associated with disease severity. Brain. 2012;135(Pt 6):1786–93.
21. Gelfand JM, Cree BA, Nolan R, Arnow S, Green AJ. Microcystic inner nuclear layer abnormalities and neuromyelitisoptica. JAMA Neurol. 2013;70(5):629–33.
22. Abegg M, Zinkernagel M, Wolf S. Microcystic macular degeneration from optic neuropathy. Brain. 2012; 135(Pt 12):e225.
23. Wolff B, Basdekidou C, Vasseur V, Mauget-Faÿsse M, Sahel JA, Vignal C. Retinal inner nuclear layer microcystic changes in optic nerve atrophy: a novel spectral-domain OCT finding. Retina. 2013;33:2133–8.
24. Marziani E, Pomati S, Ramolfo P, Cigada M, Giani A, Mariani C, et al. Evaluation of retinal nerve fiber layer and ganglion cell layer thickness in Alzheimer's disease using spectral-domain optical coherence tomography. Investig Ophthalmol Vis Sci. 2013;54(9):5953–8.
25. Moreno-Ramos T, Benito-León J, Villarejo A, Bermejo-Pareja F. Retinal nerve fiber layer thinning in dementia associated with Parkinson's disease, dementia with lewy bodies, and Alzheimer's disease. J Alzheimers Dis. 2013;34(3):659–64.

26. Spund B, Ding Y, Liu T, Selesnick I, Glazman S, Shrier EM, et al. Remodeling of the fovea in Parkinson disease. J Neural Transm. 2013;120(5):745–53.
27. Bodis-Wollner I. Foveal vision is impaired in Parkinson's disease. Parkinsonism Relat Disord. 2013; 19(1):1–14.
28. Jaffe MJ, Bruno G, Campbell G, Lavine RA, Karson CN, Weinberger DR. Ganzfeldelectroretinographic findings in parkinsonism: untreated patients and the effect of levodopa intravenous infusion. J Neurol Neurosurg Psychiatry. 1987;50(7):847–52.
29. Bodis-Wollner I, Yahr MD. Measurements of visual evoked potentials in Parkinson's disease. Brain. 1978;101(4):661–71.
30. Gawel MJ, Vincent S, Clifford RF. Visual evoked potentials in patients with Parkinson disease. J Neurol Neurosurg Psychiatry. 1981;44:227–32.
31. Kirbas S, Turkyilmaz K, Tufekci A, Durmus M. Retinal nerve fiber layer thickness in Parkinson disease. J Neuroophthalmol. 2013;33(1):62–5.
32. Moschos MM, Tagaris G, Markopoulos I, Margetis I, Tsapakis S, Kanakis M, et al. Morphologic changes and functional retinal impairment in patients with Parkinson disease without visual loss. Eur J Ophthalmol. 2011;21(1):24–9.
33. Hajee ME et al. Inner retinal layer thinning in Parkinson disease. Arch Ophthalmol. 2009;127: 737–41.
34. Wu Z, Huang J, Dustin L, Sadda SR. Signal strength is an important determinant of accuracy of nerve fiber layer thickness measurement by optical coherencetomography. J Glaucoma. 2009;18(3):213–6.
35. Hwang YH, Yoo C, Kim YY. Myopic optic disc tilt and the characteristics ofperipapillary retinal nerve fiber layer thickness measured by spectral-domainoptical coherence tomography. J Glaucoma. 2012;21(4): 260–5.
36. Cettomai D, Pulicken M, Gordon-Lipkin E, Salter A, Frohman TC, Conger A, et al. Reproducibility of optical coherence tomography in multiple sclerosis. Arch Neurol. 2008;65(9):1218–22.
37. Rebolleda G, García-García A, Won Kim HR, Muñoz-Negrete FJ. Comparison ofretinal nerve fiber layer measured by time domain and spectral domain opticalcoherence tomography in optic neuritis. Eye. 2011; 25(2):233–8.
38. Knight OJ, Chang RT, Feuer WJ, Budenz DL. Comparison of retinal nerve fiber layer measurements using time domain and spectral domain optical coherenttomography. Ophthalmology. 2009;116(7):1271–7.
39. Lange AP, Sadjadi R, Saeedi J, Lindley J, Costello F, Traboulsee AL. Time-domain and spectral-domain optical coherence tomography of retinal nervefiber layer in MS patients and healthy controls. J Ophthalmol. 2012;2012:564627.
40. Bock M, Brandt AU, Dörr J, Pfueller CF, Ohlraun S, Zipp F, et al. Time domain and spectral domain optical coherence tomography in multiple sclerosis: acomparative cross-sectional study. Mult Scler. 2010; 16(7):893–6.

12 The Use of Multifocal Electroretinograms and Multifocal Visual Evoked Potentials in Optic Nerve Disorders

Donald C. Hood and Karen Holopigian

Introduction

Electrophysiological tests of vision measure the electrical activity generated by the eye, the optic pathways, and the visual cortex, and thus provide important diagnostic information to the clinical ophthalmologist. Traditionally, these electrophysiological tests involved stimulation of relatively large areas of the retina [1]. For example, for the standard electroretinogram (ERG) and the flash visual evoked potential (VEP) tests, the entire retina is illuminated. Other tests, such as the pattern ERG (PERG) and VEP tests, use a stimulus which typically exceeds 15° in diameter. The size of the stimuli used for these tests presents a problem if the clinician is interested in the local topography of the damage to the retina or optic nerve. Although ERG and VEP responses can be elicited to relatively small stimuli using traditional measures, each retinal area would have to be tested separately. Since the time and effort required to obtain these multiple responses would be burdensome, the multifocal technique was developed [2]. With both the multifocal electroretinogram (mfERG) and multifocal visual evoked potential (mfVEP) techniques, local responses can be recorded simultaneously from many regions of the visual field. These local electrophysiological measures can be interpreted with visual fields obtained with static automated perimetry (SAP) and with imaging scans obtained with optical coherence tomography (OCT). Both the mfERG and mfVEP allow the clinician to rule out nonorganic causes of vision loss, to rule out retinal, or preganglionic causes, and to occasionally distinguish among diseases of the ganglion cells/optic nerve. This chapter provides an introduction to these techniques and focuses on the use of these techniques to rule out retinal causes and to diagnose optic nerve disorders.

The mfERG

The standard ERG is a massed potential, the result of the summed electrical activity of the cells of the retina. With the multifocal technique, many local ERG responses can be recorded from the cone-driven retina in minutes. The mfERG is widely used to diagnose and study retinal diseases [3, 4]. Before describing how the mfERG can be of use in ruling out retinal causes and diagnosing optic nerve disease, it is necessary to understand some of the basics of how it is recorded and which retinal components contribute to the responses.

D.C. Hood, B.A., M.Sc., Ph.D. (✉)
Departments of Psychology and Ophthalmology, Columbia University, 406 Schermerhorn Hall, 1190 Amsterdam Ave., MC5501, New York, NY 10027, USA
e-mail: dch3@columbia.edu

K. Holopigian, Ph.D.
Clinical Sciences and Innovation, Novartis Pharmaceuticals, East Hanover, NJ, USA

J.W. Chan (ed.), *Optic Nerve Disorders: Diagnosis and Management*,
DOI 10.1007/978-1-4614-0691-4_12,

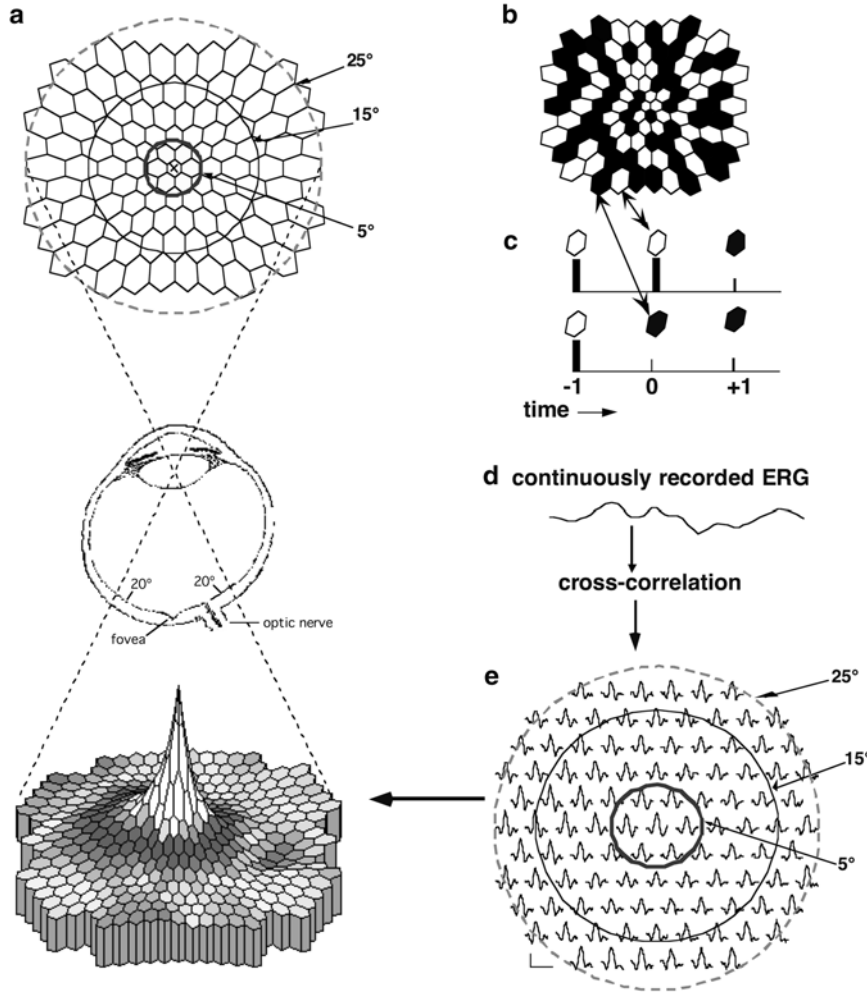

Fig. 12.1 The multifocal electroretinogram (mfERG). (**a**) *Top*: AmfERG display with 103 scaled hexagons. *Circles* have been drawn to indicate radii of 5° (*thick dark gray*), 15° (*thin black*), and 25° (*dashed light gray*). *Middle*: A schematic of the eye illustrating where the image of the display falls. *Bottom*: The 3D density plot of the responses (**e**) from a control subject's right eye. (**b**) The mfERG display at one moment in time. (**c**) The stimulation sequence of two sectors in (**b**). (**d**) The single continuous ERG record generated by the display. (**e**) The 103 mfERG trace array. The responses (first-order kernels) are extracted by correlating the stimulus sequence (**c**) with the continuous ERG record (**d**) [Reprinted from Hood DC, Odel JG, Chen CS, Winn BJ. The multifocal electroretinogram. J Neuroophthalmol. 2003 23(3): 225–35. With permission from Wolters Kluwer Health]

Recording of the mfERG

The display contains an array of hexagons; the most commonly used displays contain either 61 or 103 hexagons (Fig. 12.1a, b). The hexagons are usually scaled with eccentricity so as to produce local ERG responses of approximately equal amplitude in individuals with normal vision [2]. The retinal size of the display varies across laboratories and clinics, but is generally 40°–50° in diameter. Guidelines regarding recommended stimulus and recording parameters have been established [4, 5].

When the recording starts, the display (Fig. 12.1b) appears to flicker because each hexagon goes through a pseudorandom sequence of black and white presentations (Fig. 12.1c). With the same electrodes and amplifiers used for

standard, full-field ERG recordings, a single continuous ERG record is obtained (Fig. 12.1d). The continuous record is typically 4–8 min in length and is obtained in 15–30 s segments for the subject's comfort (Fig. 12.1d). Technically, the mfERG responses are derived as the first-order kernels of the cross correlation between the stimulation sequence and the continuously recorded ERG [2–4, 6, 7]. The recording is done with a contact lens or thread-type electrode, usually with a dilated pupil. The 103 mfERG responses from the right eye of a control subject are shown in Fig. 12.1e, in which the responses are similar in waveform and amplitude as a function of eccentricity.

Presentation of the mfERG Responses

The responses in Fig. 12.1e are positioned so that they do not overlap. The scaling is nonlinear compared to that in the iso-degree circles in Fig. 12.1a, e. The trace array in Fig. 12.1e is the most common and useful method to display the results. In some cases, the summed responses within various regions of the display are more informative. For example, the responses within rings around fixation may be examined. In Fig. 12.2b, the responses from Fig. 12.1e are grouped by rings and the amplitudes are summed, as shown in Fig. 12.2a. The responses become larger with eccentricity because progressively larger areas of the retina are stimulated. Another approach takes retinal area into consideration. The amplitude of the summed response is divided by the total area of the hexagons in the associated ring. The resulting responses in Fig. 12.2c are expressed as a measure of response amplitude per unit area or as a response density in nanoVolt/degrees [2]. The response per unit area is highest in the fovea. In addition, the average response per hexagon in a ring can be shown [4]. Although these analyses by rings are useful for many purposes, they are not an appropriate display for summarizing the effects of retinal diseases that have naso-temporal asymmetries. Most commercially available software allow for arbitrary groupings of responses so that regional response densities can be compared.

The mfERG results can also be displayed in a 3D plot, an example of which is shown at the bottom of Fig. 12.1a. For the 3D plot, the response amplitude at each point is divided by the area of the hexagon to obtain a response density. The depression is associated with the optic disc and the peak is associated with the fovea. Because the 3D plots can be misleading, it is important to compare them with the associated trace arrays [3, 4, 8, 9]. For example, it is possible to see a peak in a 3D plot when there is no recordable signal present. But when the foveal peak and the optic disc depression are both present in the 3D plot, they can be useful for assessing the location of fixation [3, 4, 8].

Measurement of the Latency and Amplitude

When analyzing mfERG responses for abnormalities, it is important to examine both the amplitude and the latency of the responses. In some diseases, damage to the outer retina can result in mfERG responses of reasonably normal amplitudes, but with markedly delayed latencies [3], such as in retinitis pigmentosa (RP) [10–13], cone rod dystrophy (CRD) [3], cone dystrophy [14], diabetic retinopathy (DR) [15–17], and occult macular dystrophy [18] (Fig. 12.3).

The upper left panel of Fig. 12.3 shows the waveforms delayed compared to those of normal controls. Although both commercial and specialized software [19] provide measures of latency, restricting the time scale so that only the first portion of the response is displayed allows for an easy analysis of latency changes.

In Fig. 12.4, the responses from a patient with RP appear to be truncated because they have not yet reached their peak amplitude at 35 msec. The responses from the control subject, however, have reached the maximum response and are decreasing in amplitude until 35 msec. These results demonstrate the differences in implicit time between the control subject and the patient with RP.

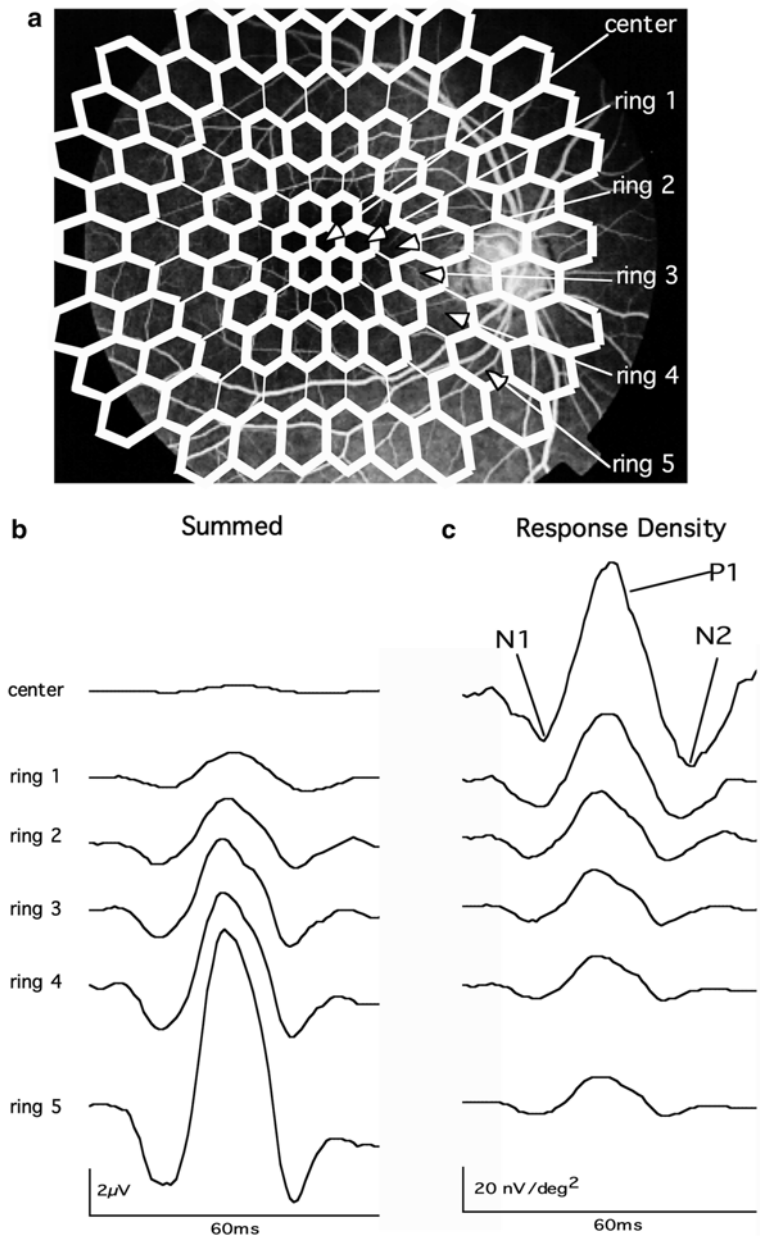

Fig. 12.2 The mfERG in relation to retinal anatomy. (**a**) The mfERG stimulus overlaid on top of a fundus photograph. The sectors are grouped by rings around the center and marked by *arrows*. (**b**) The summed mfERG responses for each of the rings marked in (**a**). (**c**) The same responses as in (**b**) but expressed in units of response density (nV/deg2). That is, the summed responses in (**b**) are divided by the total area of stimulation in the associated rings. The principal mfERG components N1, P1, and N2 are labeled for one of the responses [Reprinted from Hood DC, Odel JG, Chen CS, Winn BJ. The multifocal electroretinogram. J Neuroophthalmol. 2003 23(3): 225–35. With permission from Wolters Kluwer Health]

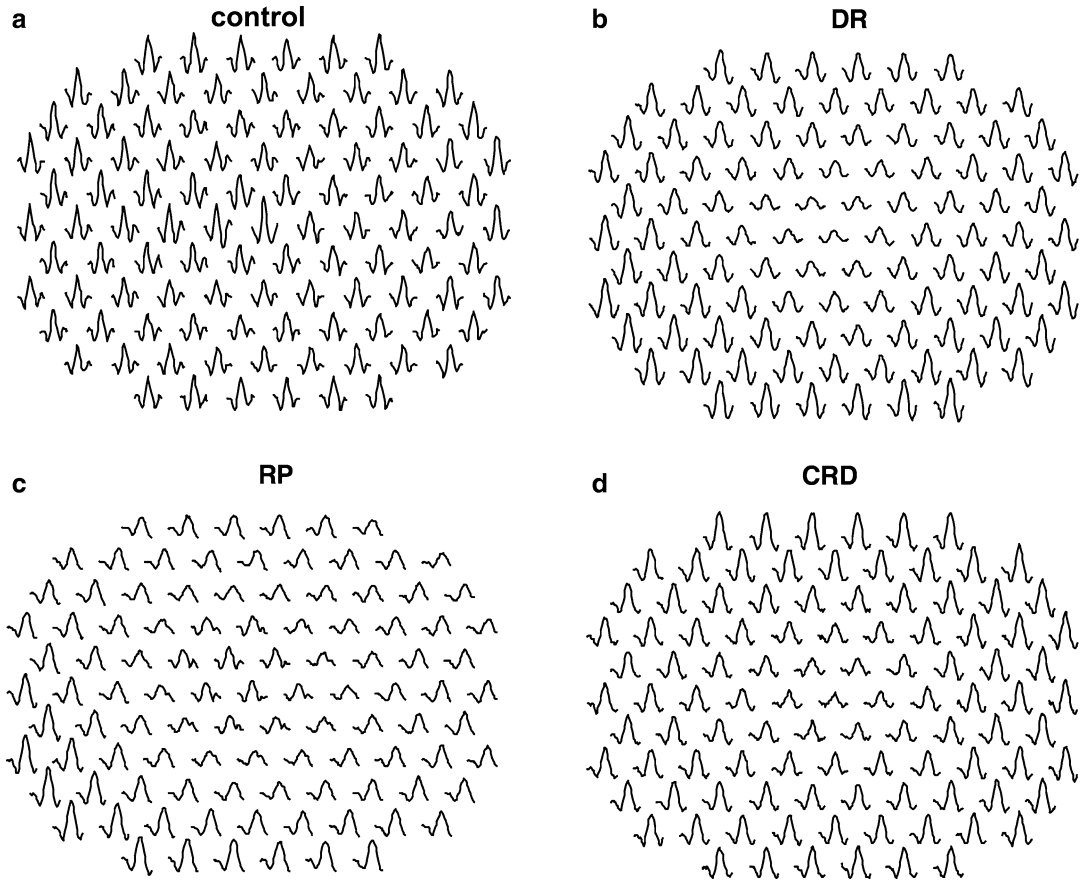

Fig. 12.3 Examples of mfERG trace arrays for 103 hexagons. (**a**) Results from a control subject. (**b**) Results from a patient with diabetic retinopathy (DR) and CME. (**c**) Results from a patient with retinitis pigmentosa (RP). (**d**) Results from a patient with cone-rod dystrophy (CRD). The responses from the patients are delayed relative to the results from the control subject

The Origin of the mfERG

The mfERG, like the standard full-field ERG, has only a relatively small contribution from retinal ganglion cells under standard recording conditions [3, 20]. The term "standard recording conditions" refers to a fast flicker sequence, as shown in Fig. 12.1c where the individual hexagons have a probability of 50 % of being white or black on every frame change. In primates the standard mfERG is largely determined by bipolar cell activity with smaller contributions from the photoreceptor cells and the inner retinal amacrine and ganglion cells [21]. Therefore, the standard mfERG provides a functional measure of the outer retinal cone photoreceptors and bipolar cells and can be used to help distinguish between diseases of the outer retinal preganglionic cells from diseases of the ganglion cells and/or optic nerve.

The mfERG and the Diagnosis of Retinal and Optic Nerve Disorders

For a number of years, our laboratory has been recording standard mfERGs from patients referred by neuro-ophthalmologists, especially Dr. J. Odel. Here we summarize the most common uses of the mfERG in diagnosing optic nerve disorders in a neuro-ophthalmological practice. (For more examples, see ref. [8].)

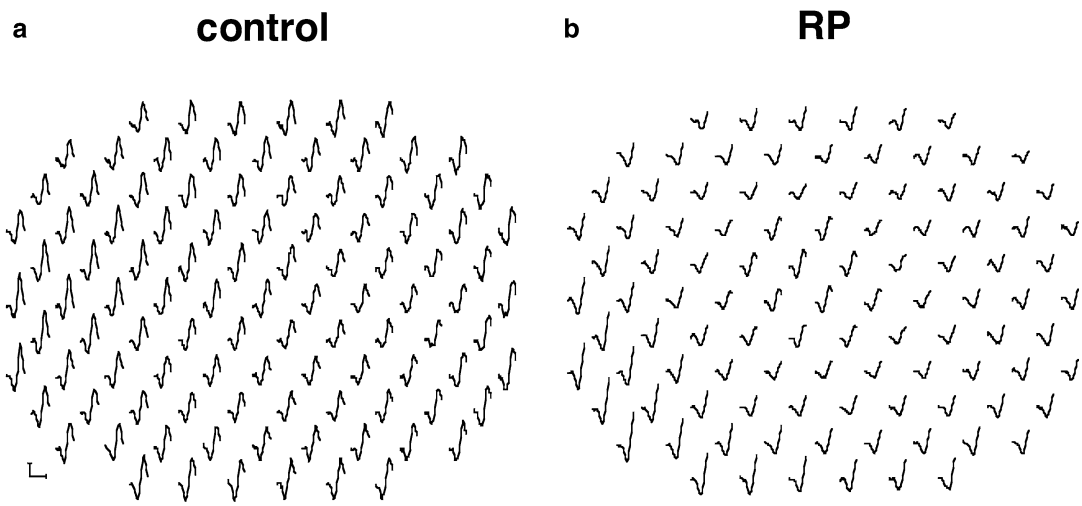

Fig. 12.4 The mfERG responses are shown on a time axis from 0 to 35 ms, showing the delayed responses from the patient. (**a**) Results from a control subject (**b**) Results from a patient with retinitis pigmentosa (RP). The horizontal calibration bar indicates 35 ms and the vertical bar 100 nV [Reprinted from Hood DC. Assessing retinal function with the multifocal technique. Prog Retin Eye Res. 2000 19(5): 607–46. With permission from Elsevier]

Ruling Out Diseases of the Outer Retina

Determining whether a visual defect is related to an optic nerve or to an outer retinal lesion is a common neuro-ophthalmologic problem. A normal mfERG can be used to rule out outer retinal disease. An abnormal mfERG, especially if it corresponds to abnormal visual field defects and/or to an abnormal OCT scan, can confirm an outer retinal etiology. For example, Fig. 12.5a shows the visual fields of a 16-year-old girl who had optic neuritis. Her full-field ERG was normal and she had a normal fundus examination. The retinal specialist suspected optic neuritis, but her mfERGs showed depressed responses in the central regions (Fig. 12.5b), suggestive of a retinal disorder. Since normal variations, as well as fixation errors, may produce mfERG responses that are reduced in amplitude, it is important to compare the mfERG findings with the visual field and OCT results. In Fig. 12.5, to help compare the visual field and the mfERG topographies, iso-degree contours were added to the figures. While more sophisticated procedures for comparing visual fields to the mfERG are available [22], these contours are sufficient for most clinical purposes. The recordings in Fig. 12.5c show the mfERG responses averaged as a response density (Fig. 12.2c) within the central 5°, between 5° and 15°, and between 15° and 25°. The depressed amplitudes of the mfERG (Fig. 12.5b, c) were clinically consistent with the visual field defects (Fig. 12.5a), confirming a retinal etiology. A reduced mfERG amplitude with a relatively normal latency can be seen in Stargardt's disease e.g., [23]. In another example, a 41-year-old male engineer noticed a paracentral visual field defect in his left eye and reported that his right eye was normal (Fig. 12.6). His visual acuity was 20/20 in both eyes and he had a normal funduscopic examination. But his visual fields (Fig. 12.6a) showed paracentral ring scotomas in both eyes. The differential diagnosis included glaucoma and a retinal disorder. Both the trace arrays (Fig. 12.6b) and the responses averaged by rings (Fig. 12.6c) showed reduced mfERG amplitudes in regions corresponding to his visual field defects, which were suggestive of a retinal abnormality. Subsequent studies revealed elevated antibodies for melanoma associated retinopathy (MAR).

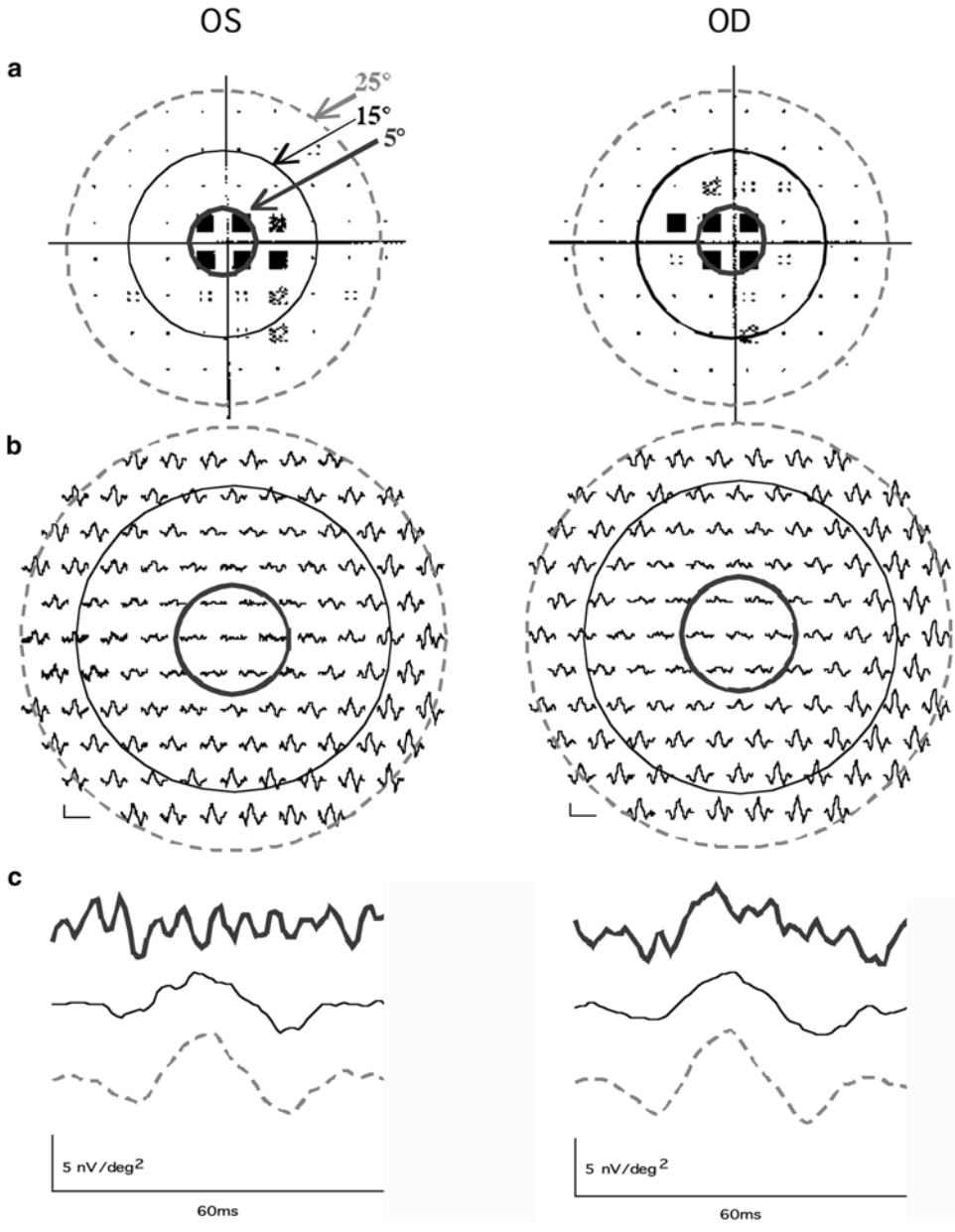

Fig. 12.5 Humphrey visual fields and mfERGs for the right (*right side*) and left (*left side*) eyes of a patient with Stargardt's disease. (**a**) 24–2 Humphrey visual fields (total deviation probability plots) show abnormal thresholds for the central areas. (**b**). The mfERG responses show reduced central amplitudes, but relatively unchanged implicit times, typical of early Stargardt's disease. The vertical and horizontal calibration bars indicate 100 nV and 60 ms and the *thick dark gray*, *thin black*, and *dashed light gray circles* indicate radii of 5°, 15°, and 25°, respectively. (**c**) The amplitudes for the three rings shown in (**b**) are plotted as response densities. [Modified from Hood DC. Electrophysiologic imaging of retinal and optic nerve damage: the multifocal technique. Ophthalmol Clin North Am. 2004 17(1): 69–88. With permission from Elsevier]

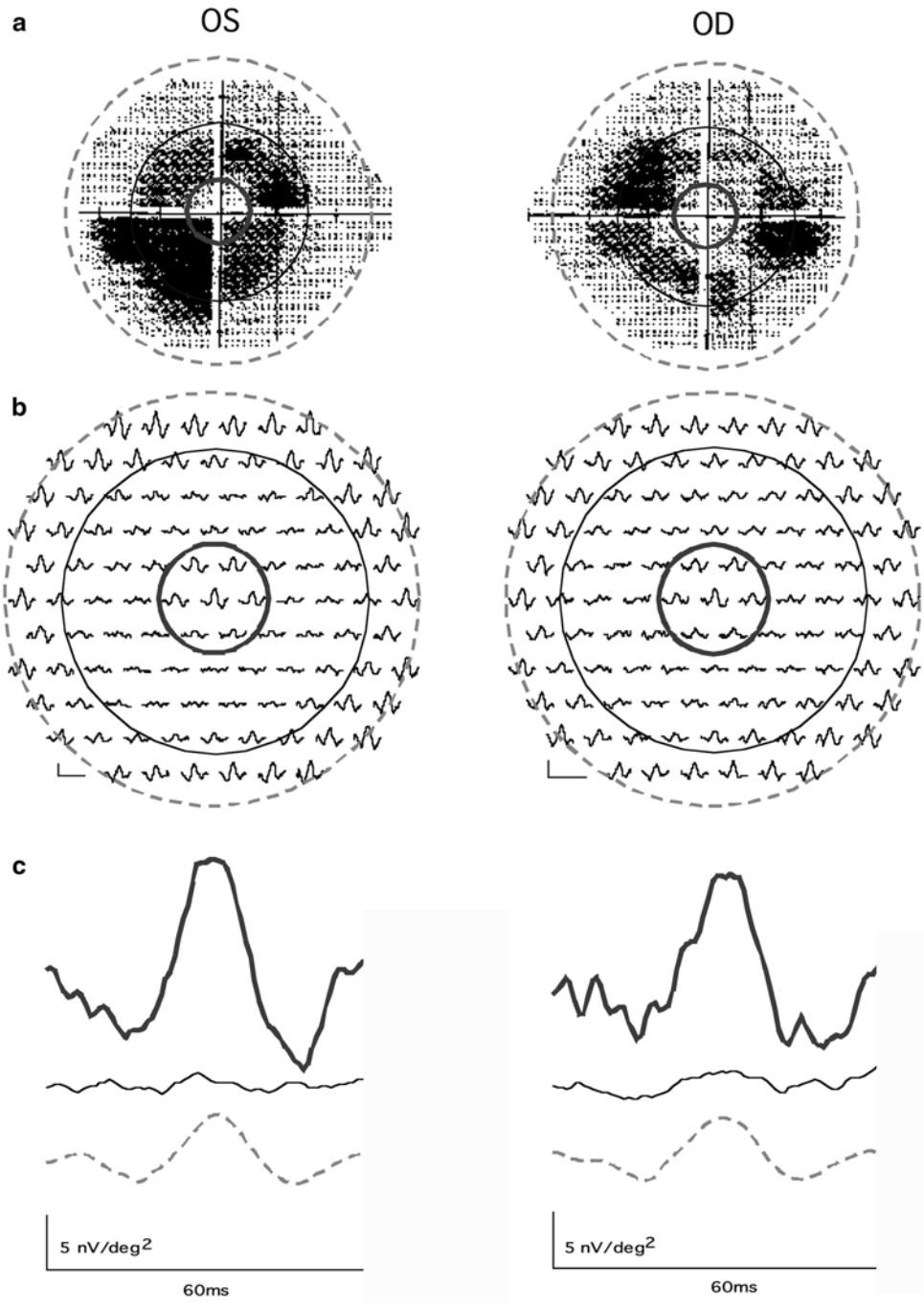

Fig. 12.6 Humphrey visual fields and mfERGs for the left (*left side*) and right (*right side*) eyes of a patient with suspected melanoma associated retinopathy (MAR). (**a**) 24–2 Humphrey visual fields show abnormal thresholds for parafoveal regions. (**b**) The mfERG responses show the same pattern of parafoveal loss as in the visual field. The *vertical* and *horizontal calibration bars* indicate 100 nV and 60 ms and the *thick dark gray*, *thin black*, and *dashed light gray circles* indicate radii of 5°, 15°, and 25°, respectively. (**c**) The amplitudes for the three rings shown in (**b**) are plotted as response densities [Modified from Hood DC, Holopigian K, Greenstein V, Seiple W, Li J, Sutter EE, Carr RE. Assessment of local retinal function in patients with retinitis pigmentosa using the multi-focal ERG technique. Vision Res. 1998 38(1): 163–79. With permission from Elsevier]

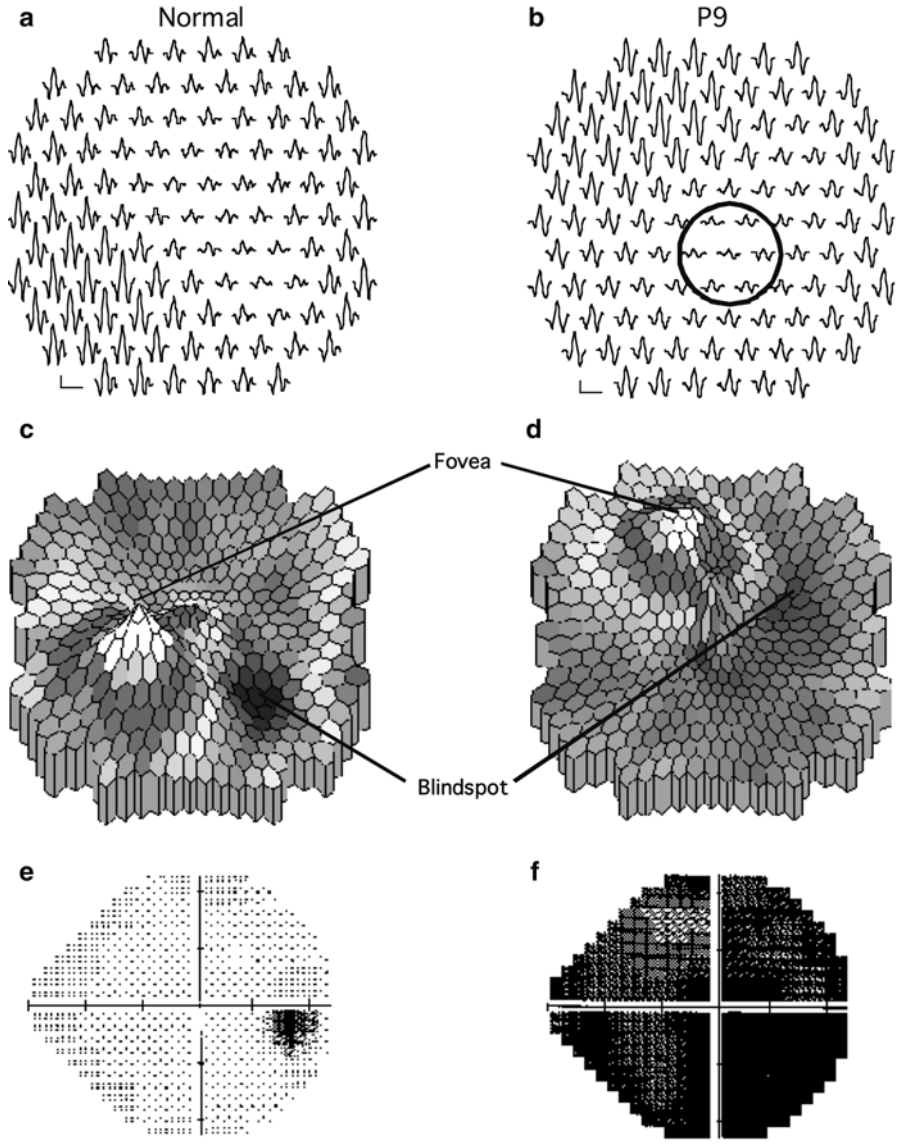

Fig. 12.7 The problem of eccentric fixation. (**a**) The mfERG from a control subject instructed to fixate at a target 8.5° down and to the left of center. (**b**) The mfERG from a patient. The *black circle* indicates an area of apparently decreased mfERG responses due to fixation error. (**c**) The 3D plot for the mfERG in (**a**). (**d**) The 3D plot for the mfERG in (**b**) of the patient. The reduced amplitudes in the patient's mfERG are likely due to eccentric fixation and not to retinal damage. (**e**) The visual field from the control subject. (**f**) The visual field from the patient [Modified from Hood DC, Holopigian K, Greenstein V, Seiple W, Li J, Sutter EE, Carr RE. Assessment of local retinal function in patients with retinitis pigmentosa using the multi-focal ERG technique. Vision Res. 1998 38(1): 163–79. With permission from Elsevier]

The Problem of Fixation Errors

One of the most common errors in the interpretation of multifocal ERG is attributing an abnormal result to a retinal problem when it is actually due to a fixation problem. For example, a 64-year-old woman with right visual loss had an mfERG showing a decreased amplitude in the central 5° (Fig. 12.7b). Because her right visual acuity was 20/400, she could not see the fixation target, but her fixation which was monitored by an infrared

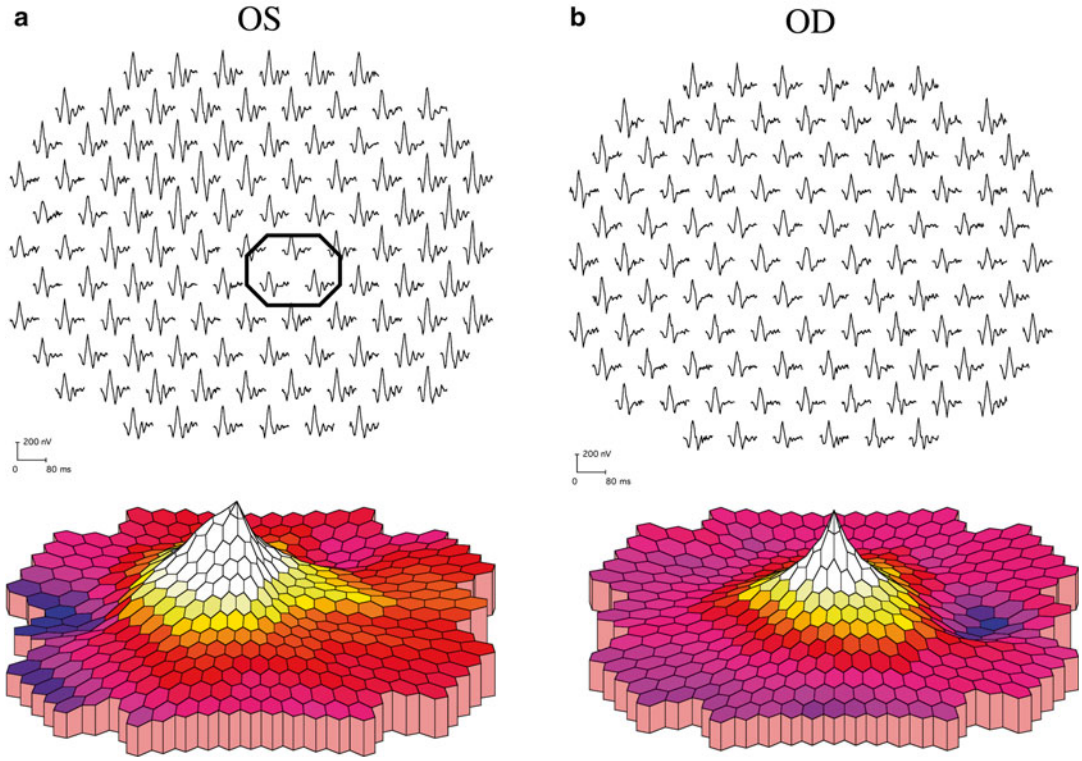

Fig. 12.8 The problem of eccentric fixation. (**a**) The mfERG from the two eyes of a patient. The left eye has a small central defect on the visual field and the right eye has a normal visual field result. The *black circle* indicates an area of apparently decreased mfERG responses. (**b**) The 3D plots for the mfERGs in (**a**). The 3D plot for the *left eye* indicates that the patient is fixating slightly off center and this could account for the reduced mfERG amplitudes in this area

camera appeared steady. Whenever the macular area is potentially involved and/or there is any question about the patient's ability to fixate steadily, the accuracy of fixation must be further investigated. There are two relatively easy ways to check fixation accuracy using the mfERG. First, the mfERG responses can be compared to the visual field results. In this case, her field depression extended to at least 25° (Fig. 12.7f), which was not consistent with the location of the depression on the mfERG (circle in Fig. 12.7b). Based on this evidence alone, this patient may not have a retinal lesion. Second, the foveal peak can be compared with the optic disc depression on the 3D plot. Figure 12.7d shows that both the foveal peak and the optic disc depression were displaced compared to those of the control subject with normal fixation (Fig. 12.1a, bottom). The patient was fixating eccentrically and all the abnormalities seen in the trace array in Fig. 12.7b were based on poor fixation.

The left column of Fig. 12.7 also illustrates features of poor fixation of another patient who had normal vision and was asked to fixate down and to the left 8.5° from the center. The mfERG resembled that of the control patient in Fig. 12.7a, c, but the patient was fixating up and to the left of the target.

Figure 12.8 illustrates the characteristics of a more subtle fixation error seen on the mfERGs from a woman with a small central visual field defect in her left eye. Her acuity was good and her fixation appeared steady. It was initially thought that her problem was retinal because some of her paracentral responses (inside rectangle of Fig. 12.8) appeared reduced in amplitude. The comparison of her 3D plots between the left affected eye and the right

unaffected eye indicated that she was actually fixating slightly off center.

Therefore, depressed mfERG responses due to fixation errors can be misinterpreted as a retinal problem.

Ruling Out Functional, or Nonorganic, Causes

When diagnosing optic nerve disorders, it is often important to rule out functional, or nonorganic, causes. The advantage of the mfERG technique over the conventional ERG is that it provides a topographical representation that can be compared to the patient's visual fields. If the mfERG is abnormal in the *same* location as the field defect, then a nonorganic cause can be ruled out. If the mfERG is normal, then further tests, such as the mfVEP, are needed to rule out a nonorganic cause.

Will the OCT Replace the mfERG?

Because the frequency domain (fd) OCT is now widely available for clinical use, it would be reasonable to ask if OCT imaging will replace mfERG testing. In our opinion, the simple answer is, in some cases, yes, but in general, no. The OCT is a structural measurement, while the mfERG, like the visual field, is a functional one. In a study [24] comparing the ability of the mfERG and fdOCT to detect retinal abnormalities, the retina of 52 eyes (36 patients) was categorized as abnormal based upon mfERG and/or fdOCT. Of this group, 25 eyes (20 patients) were abnormal on both tests. However, 20 eyes (13 patients) were abnormal on mfERG, while the fdOCT was normal/inconclusive; and 7 eyes (7 patients) had normal or inconclusive mfERG, but abnormal fdOCT. Considerable disagreement exists between these two methods for detection of retinal abnormalities. The mfERG tends to miss small local abnormalities that are detectable on the fdOCT. On the other hand, the fdOCT can appear normal in the face of clearly abnormal mfERG and SAP results. While improved imaging and analysis may show fdOCT abnormalities in some cases, in others early damage may not appear on structural tests.

The OCT can miss the outer retinal damage detected by both visual fields and mfERGs [25]. In Fig. 12.9, a patient presented with sudden left visual loss after cataract surgery. The visual field showed a dense central scotoma. The mfERG responses were markedly reduced in the same region (red rectangle in Fig. 12.9), but the fdOCT in this region appeared normal compared to healthy controls. In Fig. 12.10, a patient presented with right blurred vision with a visual acuity of 20/25 + 2. The Humphrey 24–2 visual field showed reduced sensitivity centrally, consistent with the foveal lesion detected on OCT. The spatial resolution of the mfERG is limited due to the size of the test hexagons and aberrant light. It will miss relatively small (less than about 3°) outer retinal defects [3]. For example, the OCT scan and the visual field can be both abnormal, but the mfERG is normal (Fig. 12.11).

Despite the above illustrations of possible testing discrepancies, the visual field, mfERG, and OCT are often consistent and can help confirm the clinical diagnosis (Fig. 12.12). Given that the OCT is easier and faster to perform on a patient compared to the mfERG, an OCT would be the preferred test in investigating a patient with central retinal symptoms with an outer retinal lesion. If the OCT is definitively abnormal and spatially consistent with the visual field, then there is no need for further testing; if not, a mfERG test should then be performed.

Special Techniques for Detecting Ganglion Cell Damage with the mfERG

The effectiveness of the human mfERG for detecting local ganglion cell damage is still debated [26]. Although some contradictory findings can be found in the literature, the evidence is relatively clear on the following points. First, there is a component generated at the optic nerve head that appears to reflect local ganglion cell activity. Sutter and Bearse [27] first identified

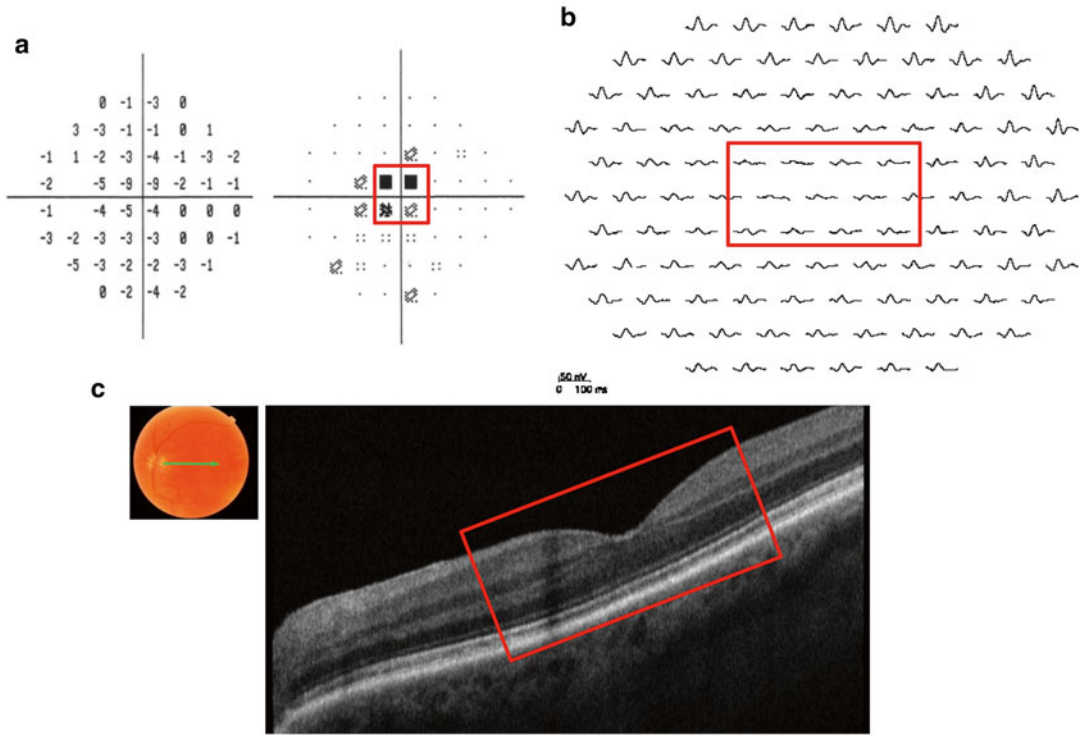

Fig. 12.9 An eye with an abnormal visual field and mfERG but normal-appearing OCT. (**a**) The 24–2 Humphrey visual field shows a central defect. (**b**) The mfERG responses are diminished in amplitude in the same region. (**c**) The frequency domain OCT appears reasonably normal. The *red rectangle* indicates corresponding regions of the three tests [Reprinted from Talamini CL, Raza AS, Dale EA, Greenstein VC, Odel JG, Hood DC. Abnormal multifocal ERG findings in patients with normal-appearing retinal anatomy. Doc Ophthalmol. 2011 123(3):187–92. With permission from Springer Science + Business Media]

this component in the human mfERG and called it the optic nerve head component (ONHC). Second, a component similar to the ONHC has been identified in the monkey mfERG and it appears to depend upon ganglion cell activity [28]. Thus far, attempts to detect glaucomatous damage with standard mfERG recordings show relatively poor sensitivity and/or specificity [20, 29–31]. But the relatively small ONHC in humans can be enhanced with specialized paradigms of mfERG stimulation [32–35] and/or methods of analysis [27]. Thus, although some remain optimistic [36], we question the clinical utility of the mfERG for detecting early glaucomatous damage. The mfERG technique still needs to be compared with other objective tests of ganglion cell function, such as the PERG, the photopic negative response, the mfVEP, and OCT imaging.

The mfVEP

The visual evoked potential (VEP) has long been used to diagnosis disorders of the optic nerve. Delayed VEP responses in patients with optic neuritis/multiple sclerosis (ON/MS) were reported almost 25 years ago [37, 38]. While the conventional VEP, elicited by either a pattern-reversal stimulus or bright flash, is still used to help in the diagnosis of ON/MS or to rule out nonorganic causes, the conventional VEP has its limitations. First, conventional VEPs are dominated by responses from the lower field in most individuals, e.g., [39–41]. In some cases, large upper visual field defects can be missed with the conventional VEP. Second, the conventional pattern reversal VEP represents an area of at least

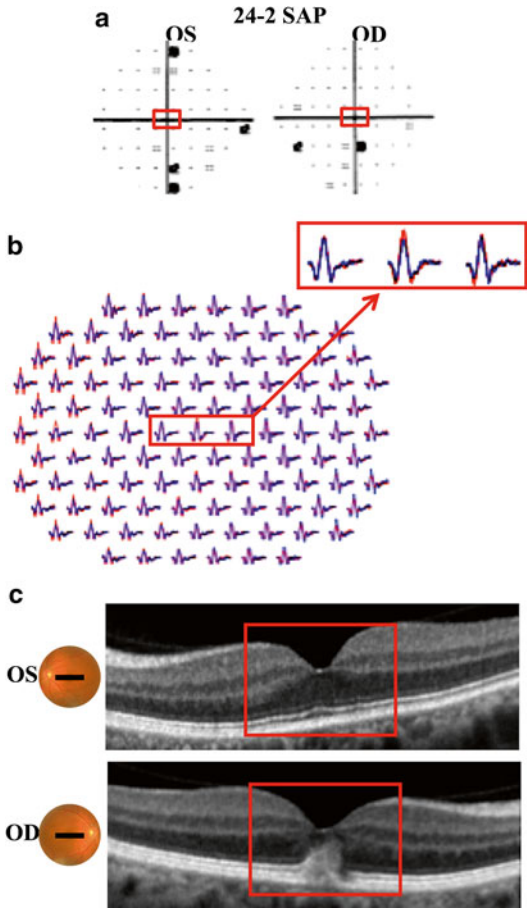

Fig. 12.10 An eye with an abnormal visual field and OCT, but a normal mfERG. (**a**) The Humphrey 24–2 visual field shows reduced sensitivity in the central visual field. (**b**) The mfERG in the same region is within normal limits. The *blue records* are from the right affected eye and the *red* from the left eye. The *blue records* are flipped so that the equivalent portions of the retina are being compared. (**c**). The OCT in this region is abnormal. The *red rectangle* indicates corresponding regions of the three tests [Reprinted from Dale EA, Hood DC, Greenstein VC, Odel JG. A comparison of multifocal ERG and frequency domain OCT changes in patients with abnormalities of the retina. Doc Ophthalmol. 2010 120(2):175–86. With permission from Springer Science + Business Media]

15° in diameter [42] such that smaller localized defects can be missed.

The mfVEP, developed by Baseler, Sutter and colleagues [43, 44], allows the recording of local VEP responses from the visual field by combining conventional VEP recording techniques with multifocal technology. Similar to the mfERG, each region of the display is an independent stimulus. From a single, continuous EEG signal, the software extracts the VEP responses generated from each of the independent regions. Local VEP responses are typically generated simultaneously from 60 regions of the central 20–25° of the visual field to create a topographic profile of the VEP.

Recording of the mfVEP

Similar electrodes and amplifiers used for conventional VEP recordings are also used for the mfVEP, but the parameters of the stimulus and display, and the analysis of the raw data are different. Although different paradigms have been developed [45], most of the published mfVEP data have been recorded with pattern reversal stimulation and a display similar to the one shown in Fig. 12.13. This display, first introduced by Baseler, Sutter and colleagues [43, 44], contains 60 sectors approximately scaled to account for cortical magnification. Each sector contains 16 checks, 8 black and 8 white.

The mfVEP is recorded monocularly with electrodes placed over the occipital region. There is currently no agreement regarding the standard placement for the electrodes, but all mfVEP recordings include at least one midline electrode placement. For example, for our midline channel we use two electrodes. One is placed at the inion plus 4 cm and serves as the "active," while the other, on the inion, serves as the "reference"; a third electrode, the ground, is placed on the forehead. It is not uncommon to record from more than one channel at a time [46–48]. For example, we use three "active" electrodes, one placed 4 cm above the inion and two placed 1 cm above and 4 cm lateral to the inion on each side of the midline [46, 48]. Every active electrode is referenced to the inion.

Presentation and Analysis of the mfVEP Responses

Similar to the mfERG, each of the individual mfVEP waveforms in the array does not represent

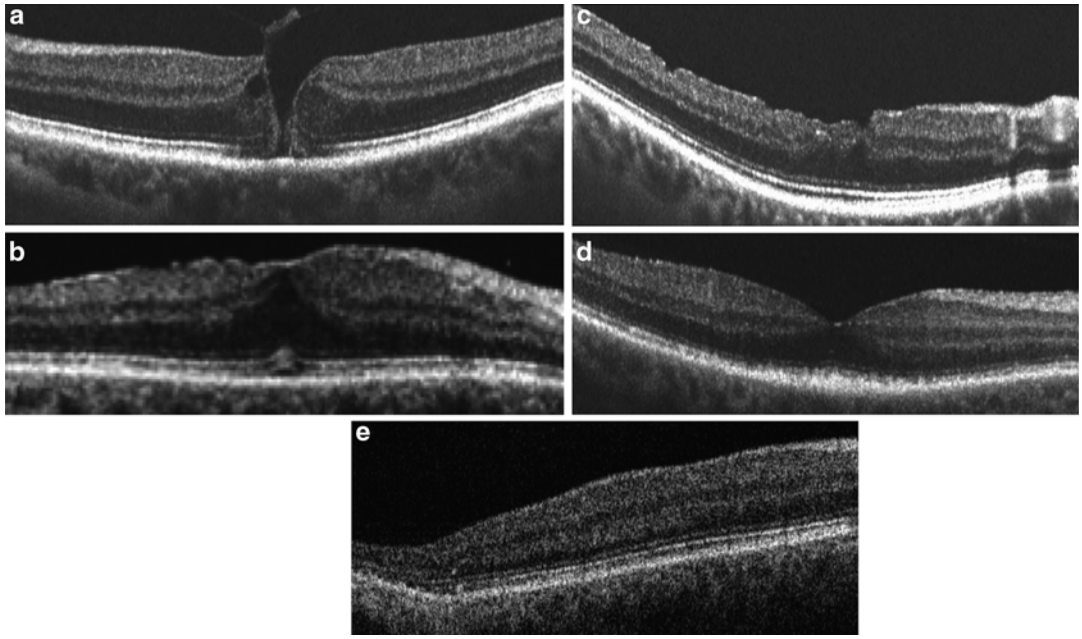

Fig. 12.11 OCT scans from five eyes with an abnormal visual field but a reasonably normal mfERG. (**a**) macular hole; (**b**) premacular fibrous; (**c**) macular hole postsurgery; (**d**) disorganized inner segment/outer segment region; (**e**) abnormal receptor region [Reprinted from Dale EA, Hood DC, Greenstein VC, Odel JG. A comparison of multifocal ERG and frequency domain OCT changes in patients with abnormalities of the retina. Doc Ophthalmol. 2010 120(2):175–86. With permission from Springer Science + Business Media]

a single response, but is a derivation from the stimulation and the continuously recorded signal. Figure 12.14 shows software-derived mean mfVEP responses from 30 control subjects. The black traces are the responses for monocular stimulation of the right eye and the gray traces are the responses from the left eye. It is important to note that when the mfVEPs are displayed in an array, the responses are positioned arbitrarily so that they do not overlap. The spatial scale for this array is nonlinear and can be seen in the comparison between the iso-degree circles in Fig. 12.14 to the display in Fig. 12.13. (For further details about the mfVEP technique) [36, 48, 49].

Nearly Identical mfVEP Responses Between the Two Eyes

There is considerable inter-subject variability in the amplitudes and the waveforms of the mfVEP responses. This variability is due to individual differences in the location and folding of the visual cortex, [22, 48] but the responses of the two eyes from any individual with normal vision are nearly identical. This can be seen in the mean mfVEP responses shown in Fig. 12.14. These mean responses from the two eyes are nearly identical because they are generated in the same general cortical regions. The responses from the two eyes differ in relatively minor ways. First, there is a small amplitude asymmetry along the horizontal meridian. Second, there is a small interocular latency difference of 4 or 5 ms across the midline. These small differences can be seen in the insets in Fig. 12.14. The amplitudes of the responses from the left eye are reduced, but the latencies are slightly less than the responses from the right eye in the left visual field. The reverse situation is present in the right visual field. (For further discussion of the reasons for these differences, see ref. [48]).

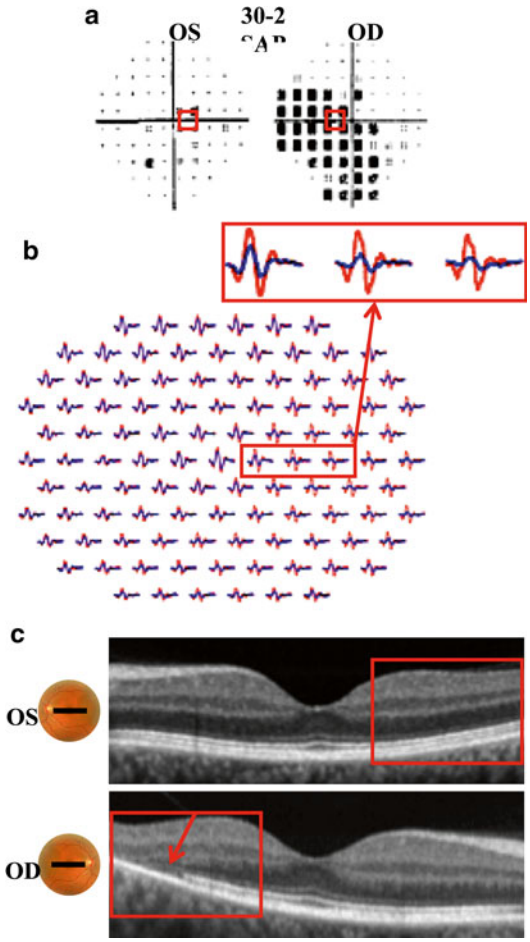

Fig. 12.12 An eye with an abnormal visual field, mfERG, and OCT. (**a**) The Humphrey 24–2 visual field shows a dense scotoma in the right eye. (**b**) The mfERG in the same region is markedly reduced (*blue*) compared to the left eye (*red*). (**c**) The OCT in this region is abnormal. The *red rectangle* indicates corresponding regions of the three tests [Reprinted from Dale EA, Hood DC, Greenstein VC, Odel JG. A comparison of multifocal ERG and frequency domain OCT changes in patients with abnormalities of the retina. Doc Ophthalmol. 2010 120(2):175–86. With permission from Springer Science + Business Media]

Topographical Representation of the mfVEP

Unlike the mfERG, there are no accepted standards for analyzing and presenting mfVEP results. The mfVEP analyses discussed in the following paragraphs are based upon our own software. In Fig. 12.15a, a patient has unilateral glaucomatous damage in the left eye. The corresponding visual field defects in the left eye are circled in gray and black. The mfVEP responses obtained from the patient's left eye (red) and right eye (blue) are shown in Fig. 12.15b. Iso-degree contours representing the same areas of visual space are shown for both the visual field and the mfVEP responses. In order to determine which of the responses from the left eye (red recordings in Fig. 12.15b) are abnormal, mfVEP probability plots analogous to the visual field probability plot in Fig. 12.15a are developed. Monocular mfVEP probability plots (left two panels in Fig. 12.15c) are obtained by comparing the patient's monocular mfVEPs to the averaged mfVEPs from the left and right eyes of a group of control subjects (Fig. 12.14). For each sector, the amplitude of the patient's mfVEP is compared to that from a control group [46, 48, 50, 51]. Each square is then plotted at the center of one of the sectors of the mfVEP display (Fig. 12.13). A colored square indicates that the mfVEP was significantly different from the control data at either the 5 % (desaturated color) or 1 % (saturated color) level, while the color indicates whether it is the left (red) or right (blue) eye that is significantly smaller than normal.

Since the visual field (Fig. 12.15a) and mfVEP (Fig. 12.15c) probability plots are shown on the same linear scale, a direct comparison can be made. To illustrate this comparison, the black and gray ellipses from Fig. 12.15a are overlaid onto Fig. 12.15c. Notice that the mfVEP results confirm the visual field defect within the black ellipse, but not the defect within the gray ellipse.

In some patients, especially those with unilateral damage, an interocular comparison of the mfVEP results is a more sensitive indicator of damage than is the monocular comparison to the control group [48, 52]. To obtain the interocular mfVEP plot in Fig. 12.15c (right-hand panel), the ratio of the mfVEP amplitudes of the two eyes is measured for each sector of the display and compared to the ratios from the group of controls [22, 46, 48, 53, 54]. The information is coded for the monocular fields. The defect within the gray ellipse is not apparent, but an arcuate defect is detected in the lower field that was not present in

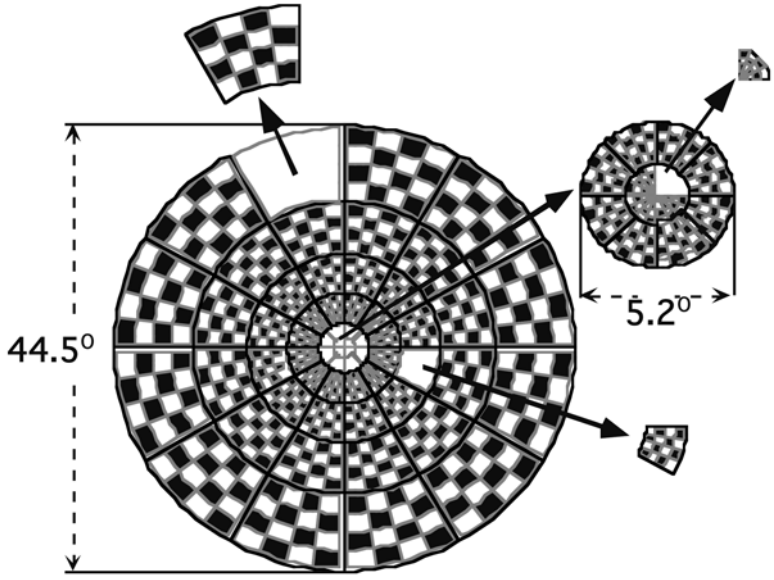

Fig. 12.13 The multifocal VEP stimulus. This display contains 60 sectors that are approximately scaled to account for cortical magnification. Each sector contains 16 checks, 8 black and 8 white

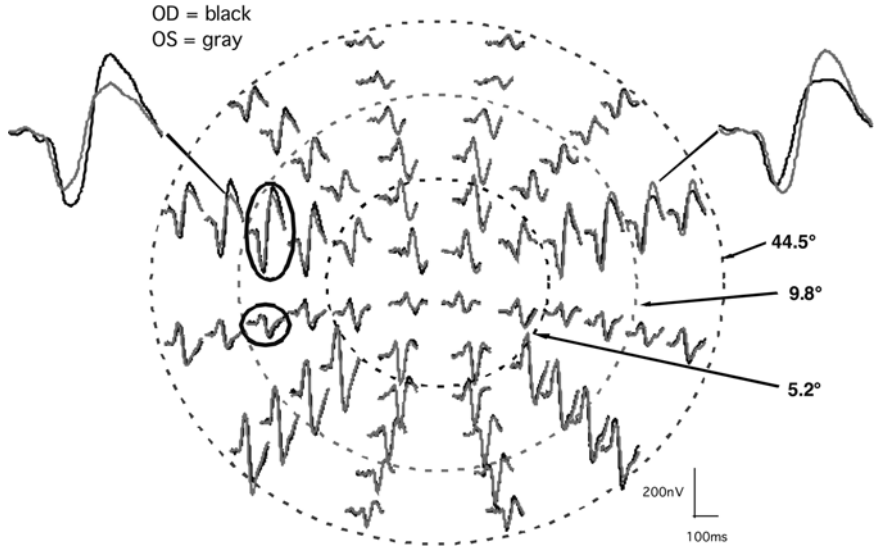

Fig. 12.14 The software-derived mean mfVEP responses from 30 control subjects. The black traces are the responses for monocular stimulation from the right eye and the gray traces are the responses from the left eye [Reprinted from Hood DC. Electrophysiologic imaging of retinal and optic nerve damage: the multifocal technique. Ophthalmol Clin North Am. 2004 17(1): 69–88. With permission from Elsevier]

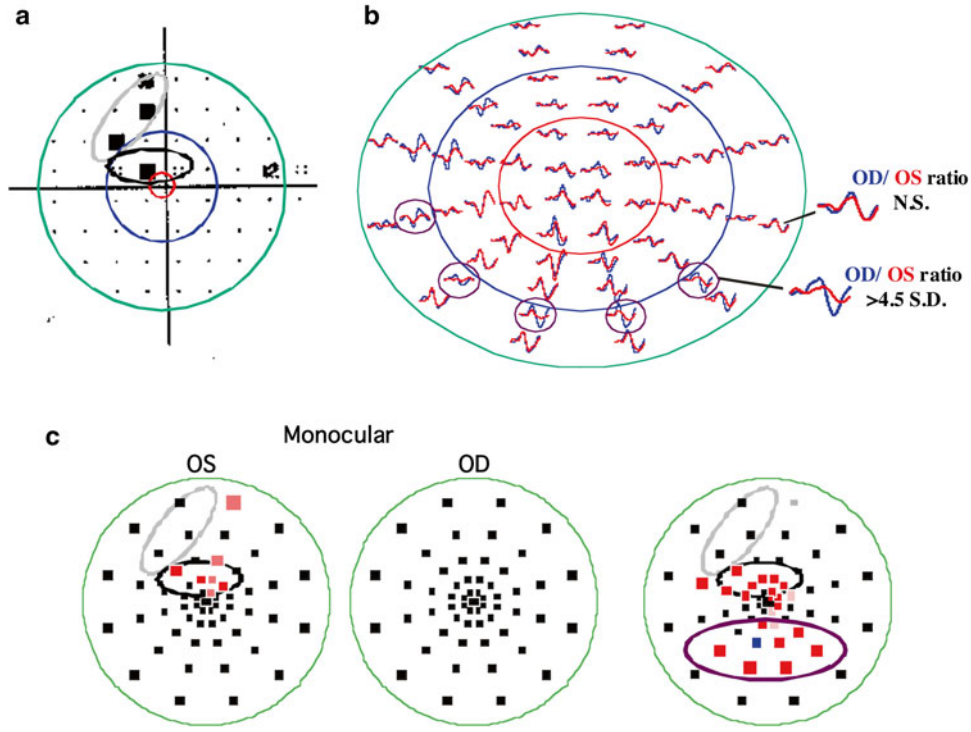

Fig. 12.15 Results from a patient with glaucoma. (**a**) The 24–2 Humphrey visual field probability plot for the patient's left eye with the defects circled in *gray* and *black*. (**b**) The mfVEP responses from the patient's left eye (*red*) and right eye (*blue*). The *inset* shows the results of comparing the root mean square ratios of two pairs of responses to those from a group of control subjects. N.S. means that the ratio of amplitudes is not significantly different from normal. Iso-degree contours representing the same areas of visual space are shown for both the visual field and the mfVEP responses. (**c**) Monocular and interocular mfVEP probability plots. Each symbol is in the center of a sector of the mfVEP display. A *black square* indicates that there is no significant difference between the two eyes. The *colored squares* indicate that there is a significant difference at greater than the 5 % (desaturated) or 1 % (saturated) level. The color denotes whether the right (*blue*) or left (*red*) eye has the smaller response. A *gray square* indicates that the responses from both eyes are too small to allow for comparison [Modified from Hood DC, Holopigian K, Greenstein V, Seiple W, Li J, Sutter EE, Carr RE. Assessment of local retinal function in patients with retinitis pigmentosa using the multifocal ERG technique. Vision Res. 1998 38(1): 163–79. With permission from Elsevier]

the visual field. Subsequent tests confirm that this defect was real. (For a review of the derivation and use of both monocular and interocular probability plots, see ref. [48]).

Measurement of the Latency and the Amplitude

The latency of individual mfVEP waves can also be measured [55–57]. In Fig. 12.16a, a woman has a left visual field defect with corresponding mfVEPs from the right and left eyes (Fig. 12.16b). Figure 12.17a shows the amplitude probability plots of her mfVEPs which are normal on the monocular plots, but the interocular plot shows a relative loss in amplitude for the left eye. Figure 12.17b shows the results of the latency analysis plotted in an analogous fashion to the amplitude plots. The colored circle indicates that the mfVEP latency is significantly delayed at either the 5 % (desaturated color) or 1 % (saturated color) level, while the color indicates whether it was the left (red) or right (blue) eye that was significantly more delayed than normal. In this example, the latency of the left eye was

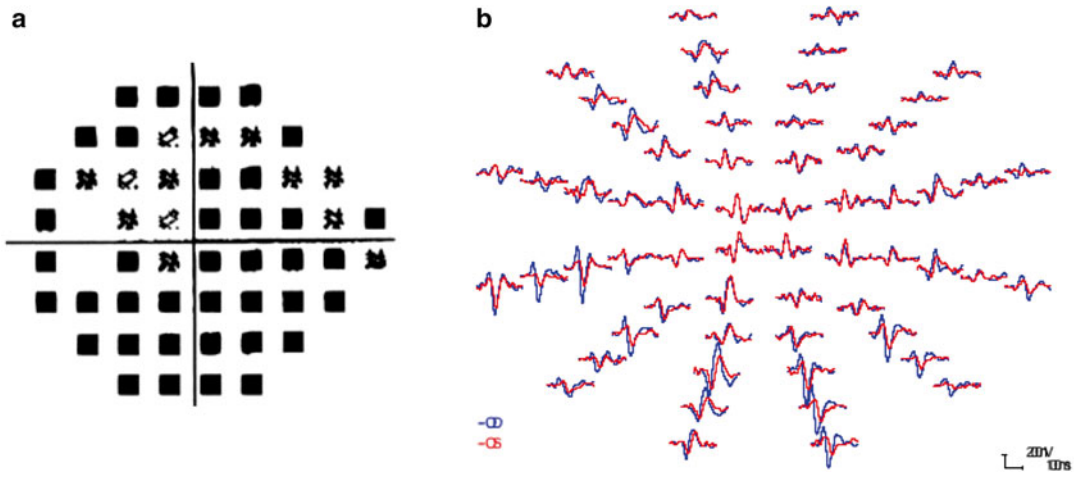

Fig. 12.16 Results from a patient with left visual loss. (**a**) The 24–2 Humphrey visual field probability plot is abnormal in the left eye; the right eye is normal. (**b**) The mfVEPs from the right (*blue*) and left (*red*) eyes of the patient

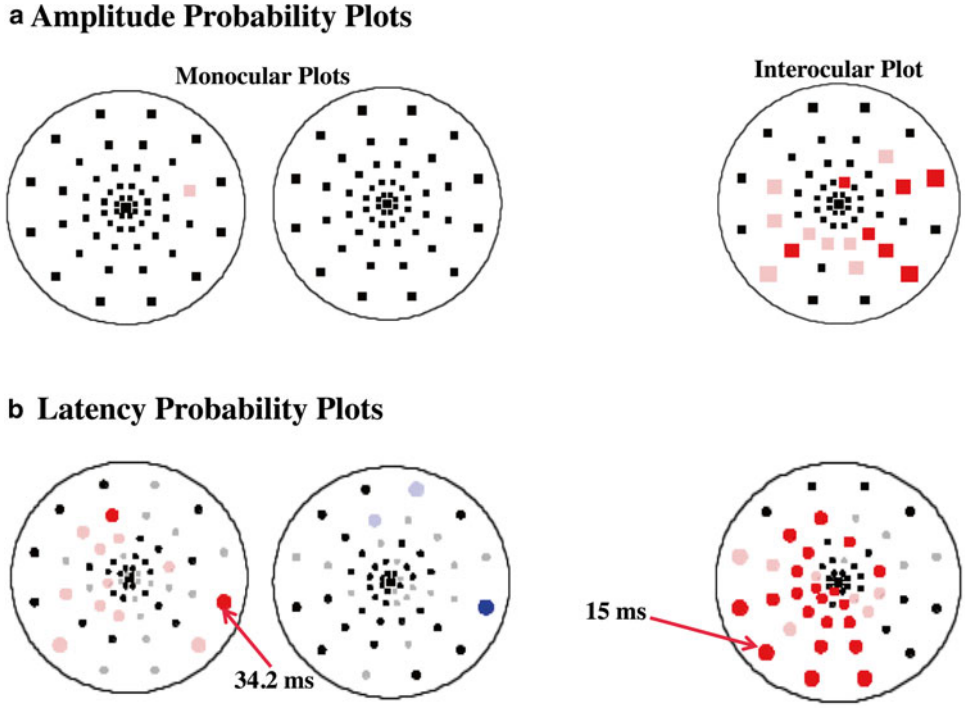

Fig. 12.17 Monocular and interocular probability plots derived from the VEP results shown in Fig. 12.16. (**a**) Amplitude results. A *colored square* indicates that the mfVEP amplitude is significantly smaller at either the 5 % (desaturated color) or 1 % (saturated color) level, while the color indicates whether it is the left (*red*) or right (*blue*) eye that is significantly smaller than normal. (**b**) Latency results. A *colored circle* indicates that the mfVEP latency is significantly delayed at either the 5 % (desaturated color) or 1 % (saturated color) level, while the color indicates whether it is the left (*red*) or right (*blue*) eye that is significantly delayed than normal

on average 7.8 ms more delayed than the right, as compared to the normal control subjects. An individual point is shown that is 15 ms slower on the interocular comparison (i.e., her left eye was delayed relative to her right eye) and another one that is 34.2 ms slower on the monocular comparison relative to the control group.

The Origins of the mfVEP

There are two lines of evidence that the mfVEP is generated largely in V1. First, as originally pointed out by Baseler et al. [43], the mfVEP waveforms reverse polarity as one crosses the horizontal meridian (reversal of the waveforms in Fig. 12.14 and see ref. [58]). The mfVEP from the upper visual field is reversed in polarity compared to the lower, while the conventional VEP from the upper and lower field has the same polarity [41]. Only potentials generated within the calcarine fissure have these characteristics. Second, a mathematical analysis of the multifocal VEP sources suggests that most of the signal is generated in V1 [59]. Third, using an application of principal component analysis, Zhang and Hood [60] provided evidence that the first principal component of the mfVEP is generated within the calcarine fissure or V1. The clinical implication is that damage beyond V1 will not necessarily produce abnormal mfVEPs.

The mfVEP and the Diagnosis of Optic Nerve Disorders

The mfVEP is a very sensitive measure of local optic nerve/ganglion cell damage. Hood et al. [52] showed that the signal in the mfVEP response is linearly related to the loss in visual field sensitivity, such that a loss of 10 dB in visual field sensitivity would reduce the amplitude of the signal in the mfVEP response by a factor of 10. This reduction in the mfVEP response would be indistinguishable from noise. Therefore, relatively small visual field sensitivity losses of approximately 6 dB due to optic nerve damage can produce profound reductions in the mfVEP amplitude.

Diagnosing and Monitoring Optic Neuritis/Multiple Sclerosis

During the acute phase of optic neuritis/multiple sclerosis (ON/MS), mfVEP amplitudes are depressed in the regions where the visual field sensitivity is decreased [61]. Partial or complete recovery of optic neuritis occurs within about 3 months, and this recovery is reflected in the mfVEP. Patients with normal visual fields after recovery will have normal or near normal mfVEP amplitudes, although the latency in some regions will be markedly delayed [61, 62]. These regions with the delayed mfVEP presumably correspond to the portions of the optic nerve that were demyelinated. The mfVEP in Fig. 12.18b shows the range of findings that can be observed in a patient who had optic neuritis in the left eye [61, 62]. In this patient, the visual field probability plot (Fig. 12.18a) shows a paracentral defect and the amplitude of the mfVEP is depressed in this region (ellipse in Fig. 12.18b). Outside of this region (Fig. 12.18b), there are areas with delayed mfVEP responses (asterisks) and regions with reasonably normal mfVEP responses (plus signs). The regions with mfVEP delays can border regions that have normal amplitude and latency. Therefore, the mfVEP can detect focal demyelination [61, 63–66].

In the diagnosis of patients with ON/MS, the mfVEP can detect delays even when the visual field results and conventional VEPs appear normal [49, 64, 65]. In some patients with ON/MS, the mfVEP is abnormal, while the conventional VEP is normal. Whether the conventional VEP is normal will depend upon the relative contributions of the normal and abnormal regions of the visual field. The conventional VEP is most likely to miss local delays if the delays involve very small areas or occur in the upper field, which typically contributes less to the conventional VEP signal than does the lower field [41]. Figure 12.19 shows the SAP probability plot (panel A) and mfVEP responses (panel B) of a 45-year-old man who had blurred vision in the superior visual field of his left eye. His MRI of the orbits revealed a left optic nerve lesion. His conventional pattern VEP and his visual fields (panel A) were normal. The insets in panel B

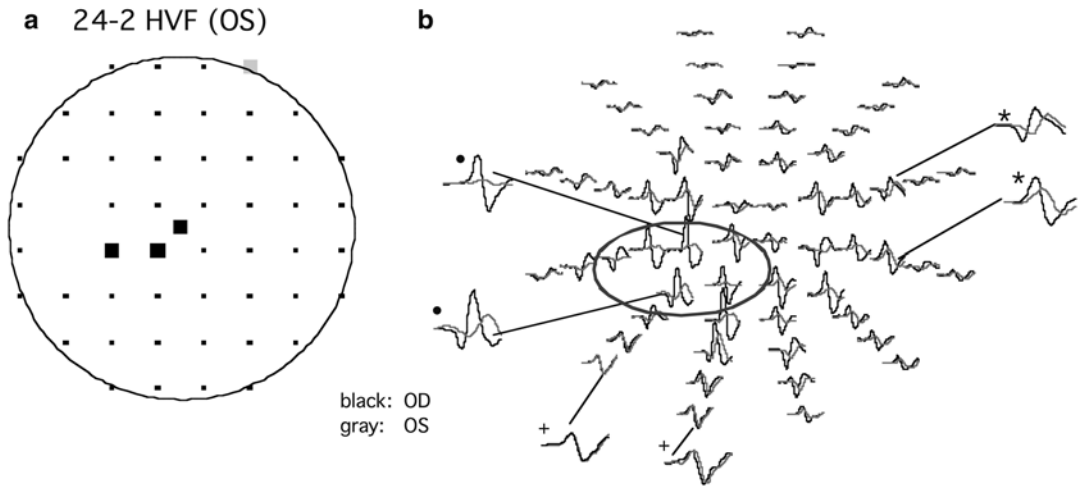

Fig. 12.18 The mfVEP and visual fields in a patient with left optic neuritis. (**a**) The visual field probability plot from the left eye shows a paracentral defect. The right visual field is normal. (**b**) The mfVEPs from the left eye show depressed amplitudes in the area that is affected on the visual field (ellipse). Outside of this region are areas with delayed mfVEP responses (*asterisks*) and regions with reasonably normal mfVEP responses (plus signs) [Reprinted from Hood DC. Electrophysiologic imaging of retinal and optic nerve damage: the multifocal technique. Ophthalmol Clin North Am. 2004 17(1): 69–88. With permission from Elsevier]

show the mfVEPs summed within each quadrant. The mfVEPs are delayed in the upper field for the left eye. This was missed on the conventional VEP, presumably because the upper field contributed relatively little to the conventional VEP.

Although the diagnosis of ON can usually be made based upon the patient's history and visual fields, a small percentage of patients with ON can present with swollen discs but without pain. The mfVEP is very useful in distinguishing ON, ischemic optic neuropathy (ION), or a compressive lesion [49].

Finally, the mfVEP is particularly useful for following patients with ON/MS, especially when the visual field is normal. Recovery of local mfVEP latencies occurs in some patients whose visual field thresholds are normal and Stable [67].

Although the conventional VEP is faster and technically less demanding than the mfVEP, the mfVEP has a higher sensitivity and specificity compared to the conventional VEP, but the differences were not large [64, 65]. Therefore, we suggest that the conventional VEP should be used for screening patients for MS/ON and that the mfVEP test should be added if the conventional VEP is normal in patients clinically suspected of having optic neuritis.

Ruling Out Functional, or Nonorganic, Causes

The conventional VEP has been used to rule out functional, or nonorganic, causes of visual field defects. Because multiple, local responses are obtained, the mfVEP is more effective than the conventional VEP for this purpose. For example, a local defect can be identified on the mfVEP and can be missed on the conventional VEP if the defect involves a small part of the total stimulated field. In these cases, the incorrect diagnosis of a functional cause can be avoided. In Fig. 12.20 a patient with a scotoma was suspected to be functional. He had emotional stress at home and work. His visual fields were unreliable and his mfVEP confirmed a localized defect corresponding to his visual symptom. The mfVEP abnormalities corresponded to his visual field defect. Genetic testing confirmed his diagnosis of Leber's hereditary optic atrophy. In patients such as this one with localized deficits, the conventional VEP is often normal.

Compared to the conventional VEP, the mfVEP provides more topographical information and is more reliable in determining nonorganic etiologies. The diagnosis of a functional etiology

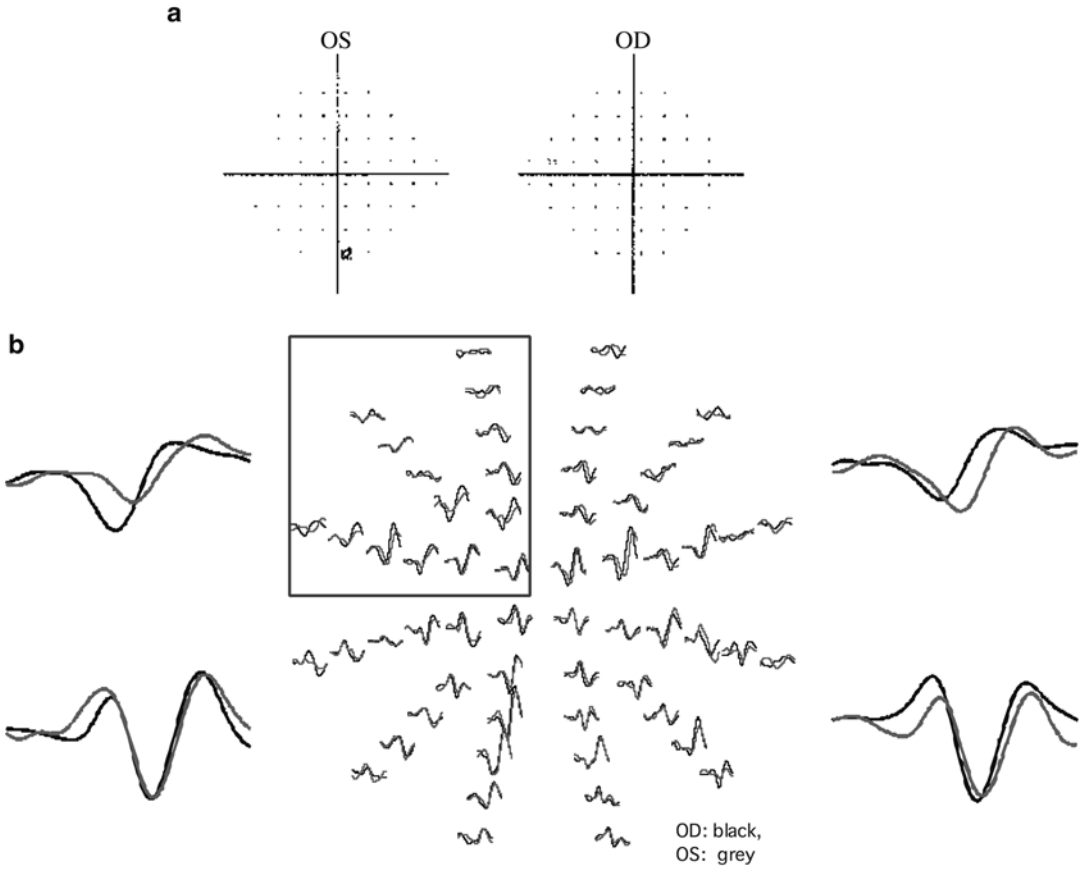

Fig. 12.19 The mfVEP and visual fields in a patient with a left superior visual field defect. (**a**) The visual fields for the left and right eyes are normal. (**b**) The mfVEP response arrays for the left (*gray*) and right (*black*) eyes. The *insets* show the mfVEPs summed within each quadrant, indicating delayed mfVEPs in the upper field of the left eye [Modified from Hood DC, Holopigian K, Greenstein V, Seiple W, Li J, Sutter EE, Carr RE. Assessment of local retinal function in patients with retinitis pigmentosa using the multi-focal ERG technique. Vision Res. 1998 38(1): 163–79. With permission from Elsevier]

would be supported by normal mfVEP responses in the areas corresponding to the visual field defect [68].

Finally, the mfVEP can assess the patient with "functional overlay." It is not uncommon to have a patient with clear indications of organic disease, but whose visual fields are so unreliable that they cannot be explained by an organic etiology. A careful quantitative comparison of the mfVEP amplitudes can help distinguish the nonorganic from the organic ones.

Questionable Visual Fields that Need Confirmation

A related category of patients are those whose visual fields are questionable to the ophthalmologist even though the reliability indices are within the normal ranges. For example, some patients produce visual fields that are reproducible and of good quality (e.g., low false positives, low false negatives, and minimal fixation errors), but they are not a good indicator of what the patient actually sees. The mfVEP can help resolve such dilemmas when insufficient or contradictory evidence can make it difficult to diagnose the cause of a visual field defect. In Fig. 12.21, a 74-year-old woman produced abnormal visual fields that were unreliable. Her 24–2 Humphrey total deviation plots in Fig. 12.21b show that both eyes had regions of sensitivity loss that exceeded 15 dB. Although her cup-to-disc ratios [0.6 (OD) and 0.5 (OS)] were relatively normal, her visual fields were abnormal.

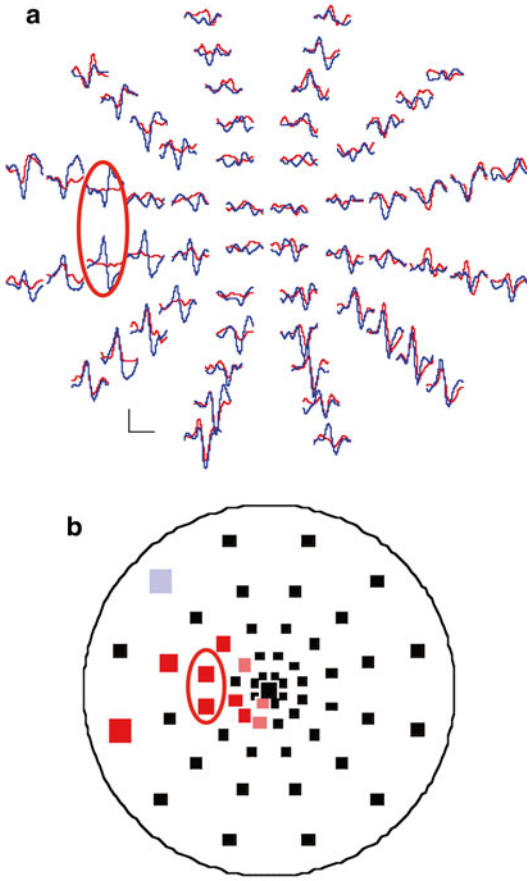

Fig. 12.20 The mfVEP and mfVEP interocular probability plot in a patient with localized visual loss. (**a**) The mfVEPs for the left (*red*) and right (*blue*) eyes. (**b**) The mfVEP interocular probability plot reveals focal losses (*red circle*)

Since she did not have any optic nerve damage, the mfVEP responses from both eyes (Fig. 12.21a) were normal and were not consistent with the large visual field sensitivity losses. (For further examples on the uses of mfVEP to verify questionable visual fields, see ref. [48].

Unreliable Visual Field Takers

Some patients cannot or will not reliably perform visual field tests because of various reasons, such as poor attention and concentration related to dementia. For most of these patients, the mfVEP provides an alternative method of testing.

Detecting Glaucomatous Damage

Most of the research on mfVEP has been focused on its applications in glaucoma. A detailed description of this work is beyond the scope of this chapter. (For details regarding the use of mfVEPs in detecting and following glaucoma, see refs. [48, 49, 69]). In a prospective study by de Moraes et al. [70], glaucoma suspects, ocular hypertensives, and glaucoma patients were referred for mfVEP testing by a single glaucoma specialist over a 2-year period. All patients underwent standard automated perimetry (SAP) and mfVEP testing within 3 months. Two hundred and ten patients (420 eyes) were referred for mfVEP testing for the following reasons: (1) normal SAP tests suspected of early functional loss (ocular hypertensives and glaucoma suspects on the basis of suspicious optic discs); (2) suspected central SAP defects in normal tension glaucoma (NTG); and (3) SAP abnormalities needing confirmation. All glaucoma suspects with normal SAP and mfVEP results remained untreated. Of those with abnormal mfVEP results, 68 % (15/22) were treated because the abnormal regions on the mfVEP were consistent with the abnormal funduscopic disc findings. The mfVEP was abnormal in 86 % (69/80) of eyes with glaucomatous optic neuropathy and SAP damage. In NTG patients, the mfVEP showed central defects in 44 % (12 of 27) of the eyes with apparently normal central fields and confirmed central scotomas in 92 % (36 of 39), leading to more rigorous monitoring of these patients. Therefore, the mfVEP can be used to test unreliable visual field takers, patients with questionable fields, or fields that need confirmation. However, it will not replace SAP. While there are clinical situations in which the mfVEP can detect damage missed on SAP [48, 54, 71–73], there are conditions in which the reverse is true [48, 72, 73]. Furthermore, the widespread availability of OCT has decreased the need for the mfVEP. Many cases that once required the mfVEP to confirm VF defects can now be resolved with the OCT [73], if the OCT is properly analyzed and interpreted.

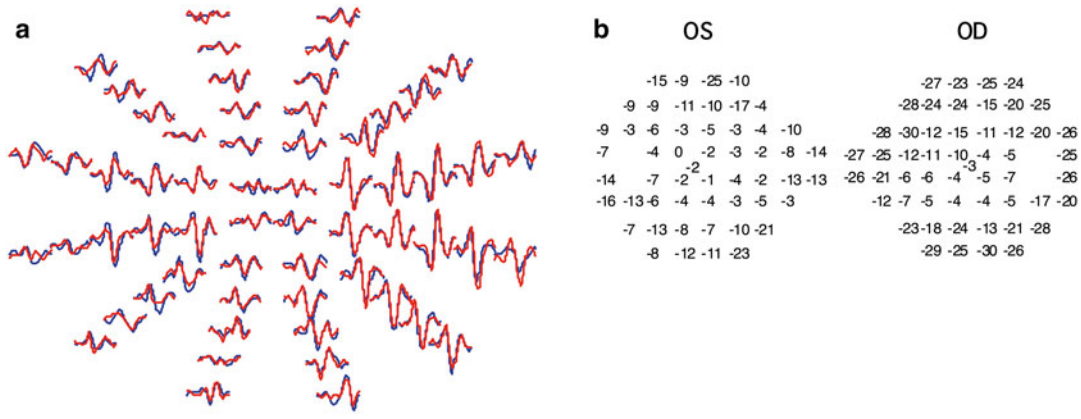

Fig. 12.21 Results from a patient with abnormal visual fields. (**a**) The mfVEPs for the left (*red*) and right (*blue*) eyes. (**b**) The Humphrey 24–2 total deviation plots for this patient reveal profound sensitivity losses that are not consistent with the mfVEP findings in (**a**)

The Problem of Fixation Error

Inaccurate or unsteady fixation can cause erroneous results on the mfVEP [48, 72]. While monitoring the eye would ensure steady fixation, it would not guarantee that the fixation is accurate. Patients with central visual problems often have eccentric fixation. Fig. 12.22 shows the effects of a 3° fixation error. A control subject was instructed to maintain steady fixation that was down and to the left by 3° for the right eye, while the left eye was tested for central fixation. Compared to control (Fig. 12.22a, b), the eccentric fixation result (Fig. 12.22c, d) showed apparent defects in both eyes on the interocular probability plot. The probability plot revealed smaller responses in diagonally opposite parts of the field. Some of the responses near the midline (inset in Fig. 12.22d) showed a polarity reversal between the two eyes, which helped confirm that these symmetrical defects were related to eccentric fixation. Therefore, it is important to monitor eye position to avoid false positives due to *unsteady* fixation. The mfVEP plot and responses (Fig. 12.22) should also be examined to avoid false positives due to *eccentric* fixation.

Unreliable mfVEP Testing

Similar to unreliable SAP takers, there are also patients who are unreliable mfVEP takers. In a few cases, these can be the same individuals. They may refuse to cooperate or may have poor attention and concentration. Most patients who are poor SAP takers are able to perform the mfVEP test. On the other hand, there are a small percentage of patients who are good SAP takers, but who do not produce reliable mfVEP recordings. In these cases, the responses are difficult to discern because of a high noise level secondary to either a large alpha wave contribution or to a poor signal-to-noise ratio.

Clinical Indications for the Multifocal ERG and/or the Multifocal VEP

The mfERG and mfVEP are not necessarily the best electrophysiological tests for every patient. In deciding whether an mfERG or mfVEP is the appropriate test, the following points should be considered:

1. If there is no advantage to performing a multifocal test over a full-field test, then the standard full-field ERG, or conventional wide-field VEP, should be performed first. In general, the multifocal tests require more time to administer, require more technical expertise to perform and analyze, and are less readily available than the conventional ERG or VEPs. For example, if the problem involves a large abnormal visual field defect and retinal involvement is suspected, then a standard

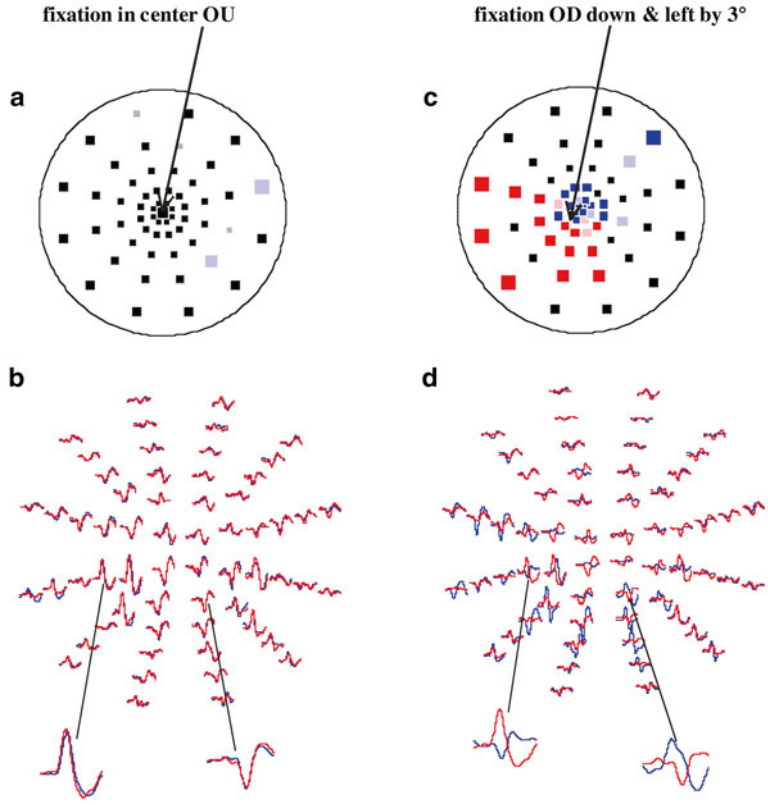

Fig. 12.22 The consequences of eccentric fixation. Eccentric fixation can give the appearance of an abnormality in an otherwise normal eye. (**a**) The interocular mfVEP probability plot for a control subject fixating at the center of the stimulus with both eyes. (**b**) The 60 mfVEP responses corresponding to the probability plot in (**a**). Responses in the inset are of the same polarity and appear normal. (**c**) The interocular mfVEP probability plot for the same subject instructed to fixate down and to the left by 3° when testing the right eye and fixating in the center when testing the left eye. (**d**) The 60 mfVEP responses corresponding to the probability plot in (**c**). Responses in the inset show polarity reversals and amplitude differences between the two eyes [Reprinted from Hood DC, Odel JG, Winn BJ. The multifocal visual evoked potential. J Neuroophthalmol. 2003 23(4): 279–89. With permission from WolterKluwers Health]

full-field ERG [74] is the test of choice. In the case of ON/MS, we suggest a conventional VEP first. If the latencies are normal, then the mfVEP may be considered.

2. The mfVEP and mfERG are not useful for problems in the far periphery. In general, these tests assess visual function in the central 20–30° from fixation (Figs. 12.1a and 12.13).
3. If a panretinal disorder is suspected, then the standard full-field ERG, which evaluates the function of the rod and cone systems, should be performed. The cone receptors and cone bipolars are assessed when recording the mfERG, while the mfVEP assesses the cone pathways up to V1. The rod system is not assessed.
4. These mfVEP and mfERG are not appropriate for patients who have unsteady fixation or eye movement disorders, such as nystagmus. The standard ERG and VEP would be preferable in these patients.
5. The mfVEP and the mfERG provide topographical information that requires a reliable SAP visual field for comparing corresponding defects.
6. OCT testing should be considered prior to mfERG or mfVEP testing, as it is faster and easier on the patient. OCT can miss retinal and

optic nerve damage. If the OCT results are within the normal range and/or ambiguous, then mfERG or mfVEP should be performed.

In patients who have localized visual field defects with steady fixation, the mfERG and mfVEP are useful for diagnosing and monitoring optic nerve disorders. They should be interpreted in conjunction with visual fields and/or OCT imaging.

References

1. Holopigian K, Hood DC. Electrophysiology. Ophthalmol Clin North Am. 2003;16(2):237–51.
2. Sutter EE, Tran D. The field topography of ERG components in man – I. The photopic luminance response. Vision Res. 1992;32(3):433–46.
3. Hood DC. Assessing retinal function with the multifocal technique. Prog Retin Eye Res. 2000;19(5): 607–46.
4. Hood DC, Bach M, Brigell M, Keating D, Kondo M, Lyons JS, et al. ISCEV standard for clinical multifocal electroretinography (mfERG) (2011 edition). Doc Ophthalmol. 2012;2012(124):1–13.
5. Keating D, Parks S, Malloch C, Evans A. A comparison of CRT and digital stimulus delivery methods in the multifocal ERG. Doc Ophthalmol. 2001;102(2): 95–114.
6. Sutter E. The interpretation of multifocal binary kernels. Doc Ophthalmol. 2000;100(2–3):49–75.
7. Keating D, Parks S, Evans A. Technical aspects of multifocal ERG recording. Doc Ophthalmol. 2000; 100(2–3):77–98.
8. Hood DC, Odel JG, Chen CS, Winn BJ. The multifocal electroretinogram. J Neuroophthalmol. 2003;23(3): 225–35.
9. Hood DC. Electrophysiologic imaging of retinal and optic nerve damage: the multifocal technique. Ophthalmol Clin North Am. 2004;17(1):69–88.
10. Hood DC, Holopigian K, Greenstein V, Seiple W, Li J, Sutter EE, et al. Assessment of local retinal function in patients with retinitis pigmentosa using the multi-focal ERG technique. Vision Res. 1998;38(1): 163–79.
11. Seeliger MW, Kretschmann UH, Apfelstedt-Sylla E, Zrenner E. Implicit time topography of multifocal electroretinograms. Investig Ophthalmol Vis Sci. 1998;39(5):718–23.
12. Holopigian K, Seiple W, Greenstein VC, Hood DC, Carr RE. Local cone and rod system function in patients with retinitis pigmentosa. Investig Ophthalmol Vis Sci. 2001;42(3):779–88.
13. Wolsley CJ, Silvestri G, O'Neill J, Saunders KJ, Anderson RS. The association between multifocal electroretinogram and OCT retinal thickness in retinitis pigmentosa patients with good visual acuity. Eye. 2009;23(7):1524–31.
14. Holopigian K, Seiple W, Greenstein VC, Hood DC, Carr RE. Local cone and rod system function in progressive cone dystrophy. Investig Ophthalmol Vis Sci. 2002;43(7):2364–73.
15. Greenstein VC, Holopigian K, Hood DC, Seiple W, Carr RE. The nature and extent of retinal dysfunction associated with diabetic macular edema. Investig Ophthalmol Vis Sci. 2000;41(11):3643–54.
16. Fortune B, Schneck ME, Adams AJ. Multifocal electroretinogram delays reveal local retinal dysfunction in early diabetic retinopathy. Investig Ophthalmol Vis Sci. 1999;40(11):2638–51.
17. Han Y, Bearse Jr MA, Schneck ME, Barez S, Jacobsen CH, Adams AJ. Multifocal electroretinogram delays predict sites of subsequent diabetic retinopathy. Investig Ophthalmol Vis Sci. 2004;45(3):948–54.
18. Piao CH, Kondo M, Tanikawa A, Terasaki H, Miyake Y. Multifocal electroretinogram in occult macular dystrophy. Investig Ophthalmol Vis Sci. 2000;41(2): 513–7.
19. Hood DC, Li J. A technique for measuring individual multifocal ERG records. In: Yager D, editor. Noninvasive assessment of the visual system, vol. 11. Washington, DC: Optical Society of America; 1997. p. 33–41.
20. Hood DC, Greenstein VC, Holopigian K, Bauer R, Firoz B, Liebmann JM, et al. An attempt to detect glaucomatous damage to the inner retina with the multifocal ERG. Investig Ophthalmol Vis Sci. 2000; 41(6):1570–9.
21. Hood DC, Frishman LJ, Saszik S, Viswanathan S. Retinal origins of the primate multifocal ERG: implications for the human response. Investig Ophthalmol Vis Sci. 2002;43(5):1673–85.
22. Hood DC, Zhang X. Multifocal ERG and VEP responses and visual fields: comparing disease-related changes. Doc Ophthalmol. 2000;100(2–3):115–37.
23. Kretschmann U, Seeliger MW, Ruether K, Usui T, Apfelstedt-Sylla E, Zrenner E. Multifocal electroretinography in patients with Stargardt's macular dystrophy. Br J Ophthalmol. 1998;82(3):267–75.
24. Dale EA, Hood DC, Greenstein VC, Odel JG. A comparison of multifocal ERG and frequency domain OCT changes in patients with abnormalities of the retina. Doc Ophthalmol. 2010;120(2):175–86.
25. Talamini CL, Raza AS, Dale EA, Greenstein VC, Odel JG, Hood DC. Abnormal multifocal ERG findings in patients with normal-appearing retinal anatomy. Doc Ophthalmol. 2011;123(3):187–92.
26. Chan HH, Ng YF, Chu PH. Applications of the multifocal electroretinogram in the detection of glaucoma. Clin Exp Optom. 2011;94(3):247–58.
27. Sutter EE, Bearse Jr MA. The optic nerve head component of the human ERG. Vision Res. 1999;39(3): 419–36.
28. Hood DC, Bearse Jr MA, Sutter EE, Viswanathan S, Frishman LJ. The optic nerve head component of the monkey's (Macacamulatta) multifocal electroretinogram (mERG). Vision Res. 2001;41(16):2029–41.
29. Hasegawa S, Takagi M, Usui T, Takada R, Abe H. Waveform changes of the first-order multifocal

electroretinogram in patients with glaucoma. Investig Ophthalmol Vis Sci. 2000;41(6):1597–603.
30. Fortune B, Johnson CA, Cioffi GA. The topographic relationship between multifocal electroretinographic and behavioral perimetric measures of function in glaucoma. Optom Vis Sci. 2001;78(4):206–14.
31. Palmowski AM, Allgayer R, Heinemann-Vemaleken B. The multifocal ERG in open angle glaucoma – a comparison of high and low contrast recordings in high- and low-tension open angle glaucoma. Doc Ophthalmol. 2000;101(1):35–49.
32. Shimada Y, Li Y, Bearse Jr MA, Sutter EE, Fung W. Assessment of early retinal changes in diabetes using a new multifocal ERG protocol. Br J Ophthalmol. 2001;85(4):414–9.
33. Fortune B, Bearse Jr MA, Cioffi GA, Johnson CA. Selective loss of an oscillatory component from temporal retinal multifocal ERG responses in glaucoma. Investig Ophthalmol Vis Sci. 2002;43(8):2638–47.
34. Rodrigues AR, Filho MS, Silveira LC, Kremers J. Spatial distribution of on- and off-responses determined with the multifocal ERG. Doc Ophthalmol. 2010;120(2):145–58.
35. Palmowski AM, Allgayer R, Heinemann-Vernaleken B, Ruprecht KW. Multifocal electroretinogram with a multiflash stimulation technique in open-angle glaucoma. Ophthalmic Res. 2002;34(2):83–9.
36. Palmowski-Wolfe AM, Allgayer RJ, Vernaleken B, Schötzau A, Ruprecht KW. Slow-stimulated multifocal ERG in high- and normal-tension glaucoma. Doc Ophthalmol. 2006 May;112(3):157–68.
37. Halliday AM, McDonald WI, Mushin J. Delayed visual evoked response in optic neuritis. Lancet. 1972; 1(7758):982–5.
38. Halliday AM, McDonald WI, Mushin J. Visual evoked response in diagnosis of multiple sclerosis. Br Med J. 1973;4(5893):661–4.
39. Halliday AM, Michael WF. Changes in pattern-evoked responses in man associated with the vertical and horizontal meridians of the visual field. J Physiol. 1970;208(2):499–513.
40. Michael WF, Halliday AM. Differences between the occipital distribution of upper and lower field pattern-evoked responses in man. Brain Res. 1971;32(2):311–24.
41. Fortune B, Hood DC. Conventional pattern-reversal VEPs are not equivalent to summed multifocal VEPs. Investig Ophthalmol Vis Sci. 2003;44(3):1364–75.
42. Odom JV, Bach M, Barber C, Brigell M, Marmor MF, Tormene AP, et al. Visual evoked potentials standard (2004). Doc Ophthalmol. 2004;108(2):115–23.
43. Baseler HA, Sutter EE, Klein SA, Carney T. The topography of visual evoked response properties across the visual field. Electroencephalogr Clin Neurophysiol. 1994;90(1):65–81.
44. Baseler HA, Sutter EE. M and P components of the VEP and their visual field distribution. Vision Res. 1997;37(6):675–90.
45. James AC, Ruseckaite R, Maddess T. Effect of temporal sparseness and dichoptic presentation on multifocal visual evoked potentials. Vis Neurosci. 2005;22(1): 45–54.
46. Hood DC, Zhang X, Greenstein VC, Kangovi S, Odel JG, Liebmann JM, et al. An interocular comparison of the multifocal VEP: a possible technique for detecting local damage to the optic nerve. Investig Ophthalmol Vis Sci. 2000;41(6):1580–7.
47. Klistorner A, Graham SL. Objective perimetry in glaucoma. Ophthalmology. 2000;107(12):2283–99.
48. Hood DC, Greenstein VC. Multifocal VEP and ganglion cell damage: applications and limitations for the study of glaucoma. Prog Retin Eye Res. 2003;22(2): 201–51.
49. Hood DC, Odel JG, Winn BJ. The multifocal visual evoked potential. J Neuroophthalmol. 2003;23(4): 279–89.
50. Hood DC, Zhang X, Hong JE, Chen CS. Quantifying the benefits of additional channels of multifocal VEP recording. Doc Ophthalmol. 2002;104(3):303–20.
51. Zhang X, Hood DC, Chen CS, Hong JE. A signal-to-noise analysis of multifocal VEP responses: an objective definition for poor records. Doc Ophthalmol. 2002;104(3):287–302.
52. Hood DC, Greenstein VC, Odel JG, Zhang X, Ritch R, Liebmann JM, et al. Visual field defects and multifocal visual evoked potentials: evidence of a linear relationship. Arch Ophthalmol. 2002;120(12): 1672–81.
53. Graham SL, Klistorner AI, Grigg JR, Billson FA. Objective VEP perimetry in glaucoma: asymmetry analysis to identify early deficits. J Glaucoma. 2000;9(1): 10–9.
54. Goldberg I, Graham SL, Klistorner AI. Multifocal objective perimetry in the detection of glaucomatous field loss. Am J Ophthalmol. 2002;133(1):29–39.
55. Hood DC, Ohri N, Yang EB, Rodarte C, Zhang X, Fortune B, et al. Determining abnormal latencies of multifocal visual evoked potentials: a monocular analysis. Doc Ophthalmol. 2004;109(2):189–99.
56. Hood DC, Zhang X, Rodarte C, Yang EB, Ohri N, Fortune B, et al. Determining abnormal interocular latencies of multifocal visual evoked potentials. Doc Ophthalmol. 2004;109(2):177–87.
57. Sriram P, Klistorner A, Arvind H, Graham SL. Reproducibility of multifocal VEP latency using different stimulus presentations. Doc Ophthalmol. 2012; 125(1):43–9.
58. Klistorner AI, Graham SL, Grigg JR, Billson FA. Multifocal topographic visual evoked potential: improving objective detection of local visual field defects. Investig Ophthalmol Vis Sci. 1998;39(6): 937–50.
59. Slotnick SD, Klein SA, Carney T, Sutter E, Dastmalchi S. Using multi-stimulus VEP source localization to obtain a retinotopic map of human primary visual cortex. Clin Neurophysiol. 1999;110(10):1793–800.
60. Zhang X, Hood DC. A principal component analysis of multifocal pattern reversal VEP. J Vis. 2004;4(1): 32–43.
61. Hood DC, Odel JG, Zhang X. Tracking the recovery of local optic nerve function after optic neuritis: a multifocal VEP study. Investig Ophthalmol Vis Sci. 2000;41(12):4032–8.

62. Kardon RH, Givre SJ, Wall M, Hood DC. Comparison of threshold and multifocal-VEP perimetry in recovered optic neuritis. In: Perimetry update 2000: proceedings of the XVII International Perimetric Society Meeting. New York, NY: Kugler; 2001.
63. Fraser C, Klistorner A, Graham S, Garrick R, Billson F, Grigg J. Multifocal visual evoked potential latency analysis: predicting progression to multiple sclerosis. Arch Neurol. 2006;63:847–50.
64. Grover LK, Hood DC, Ghadiali Q, Grippo TM, Wenick AS, Greenstein VC, et al. A comparison of multifocal and conventional visual evoked potential techniques in patients with optic neuritis/multiple sclerosis. Doc Ophthalmol. 2008;117:121–8.
65. Klistorner A, Fraser C, Garrick R, Graham S, Arvind H. Correlation between full-field and multifocal VEPs in optic neuritis. Doc Ophthalmol. 2008;116: 19–27.
66. Laron M, Cheng H, Zhang B, et al. Comparison of multifocal visual evoked potential, standard automated perimetry and optical coherence tomography in assessing visual pathway in multiple sclerosis patients. Mult Scler. 2010;16:412–26.
67. Yang EB, Hood DC, Rodarte C, Zhang X, Odel JG, Behrens MM. Improvement in conduction velocity after optic neuritis measured with the multifocal VEP. Investig Ophthalmol Vis Sci. 2007;48(2): 692–8.
68. Miele DL, Odel JG, Behrens MM, Zhang X, Hood DC. Functional bitemporalquadrantopia and the multifocal visual evoked potential. J Neuroophthalmol. 2000;20(3):159–62.
69. Graham SL, Klistorner AI, Goldberg I. Clinical application of objective perimetry using multifocal visual evoked potentials in glaucoma practice. Arch Ophthalmol. 2005;123(6):729–39.
70. De Moraes CG, Liebmann JM, Ritch R, Hood DC. Clinical use of multifocal visual-evoked potentials in a glaucoma practice: a prospective study. Doc Ophthalmol. 2012;125(1):1–9.
71. Thienprasiddhi P, Greenstein VC, Chu DH, Xu L, Liebmann JM, Ritch R, et al. Detecting early functional damage in glaucoma suspect and ocular hypertensive patients with the multifocal VEP technique. J Glaucoma. 2006;15(4):321–7.
72. Hood DC, Thienprasiddhi P, Greenstein VC, Winn BJ, Ohri N, Liebmann JM, et al. Detecting early to mild glaucomatous damage: a comparison of the multifocal VEP and automated perimetry. Investig Ophthalmol Vis Sci. 2004;45(2):492–8.
73. De Moraes CG, Liebmann JM, Ritch R, Hood DC. Understanding disparities among diagnostic technologies in glaucoma. Arch Ophthalmol. 2012;130(7): 833–40.
74. Marmor MF, Holder GE, Seeliger MW, Yamamoto S. Standard for clinical electroretinography (2004 update). Doc Ophthalmol. 2004;108(2):107–14.

Index

A
A-acetylaspartate, 238
Acetazolamide, 95, 101
Acetylsalicylic acid, 61
Activated protein C resistance, 52
Acute ischemic optic neuropathy
  age of onset, 3
  definition of, 3
  optic neuritis versus, 3
Acute optic neuritis. *See* Optic neuritis
Acute sphenoid sinusitis, 4
Adeno-associated virus vector, 221
Adenosine triphosphate
  deficiency of, 180
  mitochondrial production of, 209
Adrenoleukodystrophy, X-linked, 237
Afferent pupillary defect, in melanocytoma, 274
AION. *See* Anterior ischemic optic neuropathy
Aldehyde dehydrogenases, 185–186
Amantadine, 168
Amiodarone-associated optic neuropathy, 189–191
Amplitude
  multifocal electroretinogram measurement, 327
  multifocal visual evoked potential measurement, 341–343
Anemia
  megaloblastic, 179
  nonarteritic anterior ischemic optic neuropathy and, 49, 51
  pernicious, 179
  pseudotumor cerebri syndrome and, 92
Aneurysm
  anterior communicating artery, 64, 125
  carotid-ophthalmic artery, 125–126
  internal carotid artery, 125
Angiography
  cerebral
    endovascular stenting, 99
    giant cell arteritis, 60
  fluorescein. *See* Fluorescein angiography
  magnetic resonance
    giant cell arteritis evaluations, 60
    suprasellar meningiomas, 121
Angioid streaks, 260
Angiotensin-converting enzyme, 141
Annulus of Zinn, 156–157
Anterior communicating artery aneurysm, 64, 125
Anterior ischemic optic neuropathy
  amiodarone-induced optic neuropathy versus, 190
  arteritic
    choroid ischemia in, 55
    clinical findings in, 54
    etiology of, 63
    giant cell arteritis as cause. of *See* Giant cell arteritis
    inflammation in, 54
    visual loss in, 54
    visual prognosis of, 62–63
  bilateral, 50
  nonarteritic. *See* Nonarteritic anterior ischemic optic neuropathy
  retinal nerve fiber layer in, 43–44
  shock-induced, 49–50
Anterior segment, 283
Anterior visual pathway
  compression of, 109–112
  dysfunction of
    imaging of, 15–16
    in optic neuritis, 11–16
Anterior visual pathway gliomas
  chemotherapy for, 134
  course of, 132
  description of, 128–129
  histopathology of, 131–132
  magnetic resonance imaging of, 130–131
  malignant
    epidemiology of, 134
    neuroimaging of, 135
    optic disc in, 135
    pathology of, 135
    prognosis for, 135–136
    signs and symptoms of, 134–135
    treatment of, 135–136
    visual loss caused by, 134

J.W. Chan (ed.), *Optic Nerve Disorders: Diagnosis and Management*,
DOI 10.1007/978-1-4614-0691-4, © Springer Science+Business Media New York 2014

Anterior visual pathway gliomas (*cont.*)
management of, 132–134
monitoring of, 132–133
neuroimaging of, 130–131
prognosis for, 132
radiation therapy for, 133–134
signs and symptoms of, 129–130
surgery for, 133
visual field defects in, 129
Anticoagulants, for cerebral sinus thrombosis, 85
Anticytokine therapies, for Graves' ophthalmopathy, 116
Antimyelin phospholipid protein antibodies, 7
Antioxidants
Graves' ophthalmopathy treated with, 115–116
Leber's hereditary optic neuropathy treated with, 219
Antiphospholipid antibody syndrome, 5
Anti-vascular endothelial growth factor agents, for cystoid macular edema in POEMS syndrome, 29
Apoptosis, 162
Apoptosis-inducing factor, 227
Aquaporin-4, 22, 24–25
Aqueductal stenosis, in papilledema, 82
Arachidonic acid, 163
Arachnoiditis, 64
Arachnoid trabeculae, 156
Arcuate scotoma
optic neuritis as cause of, 2
in pseudotumor cerebri syndrome, 94
ARRON syndrome. *See* Autoimmune-related retinopathy and optic neuropathy syndrome
Arteriovenous malformation, 273
Arylsulfatase A deficiency, 237
Ascites, 133
Aspergillus fumigatus, 64
Aspirin, nonarteritic anterior ischemic optic neuropathy recurrence lessened using, 46–47
Astigmatism, 249
Astrocytic hamartoma, 268–270
Asymmetric papilledema, 80
ATP. *See* Adenosine triphosphate
Atrophic papilledema, 79
Autoantibodies
in neuromyelitis optica, 24
thyrotropin receptor, 114
Autoimmune-related retinopathy and optic neuropathy syndrome, 29
Autosomal dominant optic atrophy, 226
Autosomal dominant optic neuropathy, 282
Azathioprine
giant cell arteritis treated with, 62
neuromyelitis optica treated with, 25–26
Azidothymidine, 185

B

Bariatric surgery, 98
B-cell depletion therapies, 116
bcl-2, 166
Behcet's disease, 5
Behr syndrome, 233–234
BENEFIT study, 19
Biliopancreatic bypass surgery, 181
Birdshot retinochoroiditis, 5
Bitemporal hemianopsia, 118, 253
Blepharoplasty, optic nerve injury after, 170
Blood–brain barrier, 6
Bone marrow transplantation
Krabbe disease treated with, 238
metachromatic leukodystrophy treated with, 237–238
Bradykinin, 163
Brimonidine
Leber's hereditary optic neuropathy treated with, 219
nonarteritic anterior ischemic optic neuropathy treated with, 47
Bromocriptine, for pituitary adenoma, 119
Bruch's membrane, 252
B-scan ultrasonography, 272

C

Cabergoline, for pituitary adenoma, 119
CADASIL. *See* Cerebral autosomal dominant arteriopathy with subcortical infarcts and leukoencephalopathy
Calcific uremic arteriolopathy, 50
Calcified hamartomas, 269
Calpain, 7
Canavan's syndrome, 238–239
Capillary hemangioma, 270–271
Carbonic anhydrase inhibitors, 94–95
Carotid artery disease, 64
Carotid artery stenosis, 45
Carotid-ophthalmic artery, 125–126
Cataract surgery
nonarteritic anterior ischemic optic neuropathy after, 168–169
optic nerve injury after, 168–169
Cavernous hemangioma, 271–272
Cavernous sinus syndrome, 121
Cecocentral scotoma
in dominant optic atrophy, 222
in Leber's hereditary optic neuropathy, 214
in peripapillary staphyloma, 255
Cell-mediated damage, 6–7
Central macular thickness, 321–322
Central retinal artery
description of, 156
occlusion of
optical coherence tomography of, 315, 319–320
in optic disc drusen, 260
Central retinal vein
description of, 156
occlusion of, 260, 273
Central serous retinopathy, 315, 318–319
Central vision
optic neuritis-related loss of, 1
papilledema effects on, 80
Cerebral angiography
endovascular stenting, 99

giant cell arteritis, 60
Cerebral autosomal dominant arteriopathy with subcortical infarcts and leukoencephalopathy, 53
Cerebral venous sinuses, 84
Cerebral venous sinus thrombosis, 83–86, 92
Cerebrospinal fluid. *See also specific disorders*
carbonic anhydrase inhibitors to decrease production of, 94–95
diversion procedures for, 96–98, 100
lumboperitoneal shunting for, 96–98
ventriculoperitoneal shunting for, 96–97
CHAMPS/CHAMPIONS study, 18
Charcot–Marie–Tooth syndrome
description of, 231–232
X-linked, 234
CHARGE syndrome, 255
Chemotherapy
optic gliomas treated with, 134
optic nerve sheath meningiomas treated with, 112
Chiasmal gliomas
computed tomography of, 130
hydrocephalus secondary to, 133
ophthalmoplegias in, 130
prognosis for, 132
radiation therapy for, 133–134
surgery for, 133
Children
craniopharyngiomas in, 122–124
infantile neuroaxonal dystrophy in, 237
neurofibromatosis type 1 in, 129
optic nerve sheath meningiomas in, 112
optic neuritis in, 1, 9
optic neuropathies in neurodegenerative disorders of, 235–236
pseudotumor cerebri syndrome in, 101
traumatic optic neuropathy in, 165
Chlamydia, in nonarteritic anterior ischemic optic neuropathy, 49
Chlamydia pneumoniae, 57
Chloramphenicol-associated optic neuropathy, 184
Choroidal folds, 78–79
Choroidal melanoma, 275–276
Choroidal metastases, 137
Choroidal neovascularization, papilledema with, 310–311
Chronic papilledema, 79–80
Chronic progressive external ophthalmoplegia, 232
Cilioretinal arteries, 256
Circle of Zinn-Haller, 156
Circumpapillary telangiectatic microangiopathy, 4
Cirrus spectral domain optical coherence tomography, 321
Clinically definite multiple sclerosis
definition of, 1
intravenous methylprednisolone and, 18
magnetic resonance imaging of, 9–10
risk factors for, 9–10
risk of developing, 9, 19–20
Clinically isolated syndrome, 316
Clomiphene citrate-associated optic neuropathy, 192
Coagulopathies, 51–52
Coenzyme Q10, 168, 219
Collapsing response-mediating-protein-5, 27
Collapsing response-mediating-protein-5–immunoglobulin G, 27–28
Coloboma, optic disc, 250, 254–255
Color duplex ultrasonography, of giant cell arteritis, 59
Color vision
in glaucomatous optic neuropathies, 282
optic neuritis effects on, 2–3
Combined hamartoma of retina and retinal pigment epithelium, 274, 276–277
Compressive optic neuropathy, 113, 290
Computed tomography
craniopharyngiomas, 123
Graves' ophthalmopathy, 113–114
idiopathic orbital inflammatory pseudotumor, 117
sphenoid sinus mucocele, 126–127
traumatic optic neuropathy, 160–161
Cone rod dystrophy, 327
Congenital optic disc anomalies. *See* Optic disc anomalies
Congenital tilted disc syndrome, 251–253
Connective tissue diseases, 24
Continuous positive airway pressure, 53, 92–93
Contrast sensitivity, optic neuritis effects on, 2–3
Cortical plasticity, multifocal visual evoked potentials for detection of, 15
Corticosteroids. *See also specific drug*
giant cell arteritis treated with, 60–62
Graves' ophthalmopathy treated with, 114–115
idiopathic orbital inflammatory pseudotumor treated with, 117
lymphomatous infiltration of optic nerve treated with, 139
nonarteritic anterior ischemic optic neuropathy treated with, 47
papilledema treated with, 95
pituitary apoplexy treated with, 120
in pregnancy, 101
radiation-induced optic neuropathy treated with, 196
sarcoidosis treated with, 142
traumatic optic neuropathy treated with, 164
Costeff syndrome, 233–234
Cotton wool spots, 54
Craniopharyngioma, 122–124, 133
Craniosynostosis, 82
C-reactive protein, in giant cell arteritis, 57–58
Cryotherapy, for capillary hemangioma, 271
Cryptococcosis, 143–144
Cryptococcus neoformans, 143
CT. *See* Computed tomography
CTLA-4, 116
Cuban epidemic of optic neuropathy, 187, 189
Cup/disc ratio. *See also* Optic disc
in diabetic papillopathy, 48
in nonarteritic anterior ischemic optic neuropathy, 43–45
in shock-induced anterior ischemic optic neuropathy, 49
Cupping, of optic disc, 285
Cyanocobalamin, 180

Cyclosporin A, for giant cell arteritis, 62
Cystoid macular edema, in POEMS syndrome, 29
Cytomegalovirus, 145

D
DDON syndrome, 232
Deafness, dystonia, and optic neuropathy. *See* DDON syndrome
Deceleration injury, 155
de Morsier syndrome, 249
Demyelinating optic neuritis, 4
Demyelination, in optic neuritis, 6
Demyelinative disorders, 315–317, 319
Diabetes insipidus, diabetes mellitus, optic atrophy, and hearing loss syndrome, 228–229
Diabetes mellitus, 45
Diabetic papillopathy, 48
DIDMOAD. *See* Diabetes insipidus, diabetes mellitus, optic atrophy, and hearing loss syndrome
Diet-related optic neuropathy, 181
Diffusion tensor imaging tractography, 16
Diffusion-weight imaging, 16
Digital biochemical information transfer and sensing compounds, 220
Digoxin-associated optic neuropathy, 189–191
Diplopia, from optic nerve sheath decompression, 96
Disease-modifying antirheumatic drugs, 192
Disulfiram-associated optic neuropathy, 191
Dominant optic atrophy
  autosomal, 226
  cecocentral scotoma in, 222
  clinical presentation of, 222–223
  description of, 209
  epidemiology of, 222
  funduscopic features of, 223–224
  gene therapy for, 226–227
  genetic heterogeneity of, 225–226
  histopathology of, 225
  molecular genetics of, 225–226
  OPA1 gene in, 222, 225–226
  optical coherence tomography of, 224–225
  optic disc excavation in, 223
  pathophysiology of, 225
  treatment of, 226–227
  visual field defects in, 290
Dominant optic atrophy plus syndrome, 226–227
Dopamine, 319
Dopamine receptor agonists, for pituitary adenoma, 119
"Double-ring" sign, 249
Drug-related optic neuropathy
  chloramphenicol, 184
  ethambutol, 182–184
  linezolid, 184–185
  overview of, 181–182
Drusen. *See* Optic disc drusen
Dural sinus stenosis, 90
Dural venous sinus stenting, for pseudotumor cerebri syndrome, 100
Dynamin-like protein 1-related encephalopathy, 232–233
Dysplasia, optic disc, 257

E
Eating disorders, 181
Eccentric fixation, with multifocal visual evoked potentials, 347–348
Electro-oculogram, 253
Electroretinogram
  congenital tilted disc syndrome findings, 253
  description of, 325
  multifocal
    amplitude measurement using, 327
    applications of, 325
    fixation errors associated with, 333–335
    indications for, 347–349
    latency measurement using, 327
    optical coherence tomography versus, 335
    optic nerve disorders diagnosed using, 329–335
    origin of, 329
    outer retina diseases ruled out using, 330–333
    recording of, 326–327
    responses, 327
    retinal ganglion cell damage detected using, 335–336
    trace arrays, 329
  pattern, 325
Empty delta sign, 85
Encephalomalacia, 250
Endoscopic sinus surgery, 170
Endovascular stenting, 99
Enucleation, 268
EPI-743, 220
Epidermal growth factor receptor inhibitors, 165
ERG. *See* Electroretinogram
Erythrocyte folate, 180
Erythrocyte sedimentation rate, in giant cell arteritis, 57
Erythromycin, 185
Ethambutol-associated optic neuropathy, 182–184
Ethylene glycol-associated optic neuropathy, 186
ETOMS study, 19
Exophytic gliomas, 130

F
FA. *See* Friedreich's ataxia
Familial dysautonomia, 235
Farnsworth–Munsell 100-hue test, 3
Fibrous dysplasia, 127–128
Fingolimod, 314
Fistula, posterior ischemic optic neuropathy caused by, 64
Flavonoids, 168
Flexner–Wintersteiner rosettes, 267
Fluorescein angiography
  astrocytic hamartoma findings, 269
  cavernous hemangioma findings, 272
  choroidal melanoma findings, 276
  combined hamartoma of retina and retinal pigment epithelium findings, 277
  giant cell arteritis findings, 59
  melanocytoma findings, 275
  optic disc drusen, 259
  optic disc metastasis findings, 137
  papilledema evaluations, 81

paraneoplastic optic neuropathy findings, 28
POEMS syndrome findings, 29
racemose hemangioma findings, 274
Folate deficiency anemia, 51
Folic acid deficiency optic neuropathy, 180
Formate, 187
Foster-Kennedy syndrome, 80, 121
Fourier domain optical coherence tomography, 309
Frataxin, 230
Free radicals, 162
Friedreich's ataxia
clinical features of, 229–230
diagnosis of, 231
epidemiology of, 229
magnetic resonance imaging of, 231
management of, 231
molecular genetics of, 230
pathophysiology of, 230–231
Functional magnetic resonance imaging, 17
Fundus, optic neuritis involvement of, 3
Furosemide, 95

G
Galactosylceramide, 238
Gastric achlorhydria, 188
GCA. *See* Giant cell arteritis
Gene therapy
dominant optic atrophy treated with, 226–227
Leber's hereditary optic neuropathy treated with, 220–221
Germinoma, 133
Ghrelin, 90
Giant cell arteritis
acetylsalicylic acid for, 61
age at diagnosis, 53
azathioprine for, 62
cerebral angiography of, 60
color duplex ultrasonography of, 59
corticosteroids for, 60–62
C-reactive protein in, 57–58
cyclosporin A for, 62
diagnosis of, 57–60
erythrocyte sedimentation rate in, 57
fluorescein angiography of, 59
genetic background of, 53
granuloma formation in, 55
histologic findings, 58
immune mechanisms of, 55
immunosuppressive agents for, 61
incidence of, 53
infliximab for, 62
lymphocytes in, 59
magnetic resonance angiography of, 60
magnetic resonance imaging of, 60
methylprednisolone for, 60
microorganisms involved in, 57
pathology of, 58–59
pathophysiology of, 54–57
prednisone for, 60–61
signs and symptoms of, 54
temporal artery biopsy for, 58
treatment of, 60–62
tumor necrosis factor blockers for, 62
ultrasound biomicroscopy of, 59–60
visual loss in, 54
visual prognosis in, 62–63
Ginkgo biloba, 168
Glatiramer acetate, for neuromyelitis optica, 27
Glaucomatous optic neuropathies
anterior segment in, 283
clinical examination for, 282–286
clinical features of, 287
color vision in, 282
cup-disc ratio in, 301
description of, 281
electrodiagnostics of, 291
history-taking, 281–282
intraocular pressure measurement in, 282–283
laboratory tests for, 291
multifocal visual evoked potentials for detection of, 346
neuroimaging of, 287–291
neuroretinal rim in, 283–286
nonglaucomatous optic neuropathies versus, 287–306
optical coherence tomography of
description of, 291–292
retinal nerve fiber layer, 292–306
optic disc in
examination of, 283
features of, 286
optic nerve head remodeling in, 284
perimetry of, 287–290
posterior segment in, 283
primary angle-closure glaucoma, 283
relative afferent pupillary defect in, 282
visual acuity in, 282
visual evoked potentials of, 291
visual field defects in, 290
Glial sheath of Bergmeister, 261
Gliomas. *See* Anterior visual pathway gliomas; Optic gliomas
Globoid cell leukodystrophy. *See* Krabbe disease
Glycolate, 186
GM6001, 166
Goldmann applanation tonometry, 282–283
Goltz syndrome, 255
Gorlin syndrome, 262
Graves' hyperthyroidism, 113
Graves' ophthalmopathy
anticytokine therapies for, 116
antioxidants for, 115–116
B-cell depletion therapies for, 116
compressive optic neuropathy caused by, 113
computed tomography of, 113–114
corticosteroids for, 114–115
diagnostic testing of, 113–114
epidemiology of, 113
management of, 114–115
pathology of, 114
pathophysiology of, 114
radiotherapy for, 115
rituximab for, 116

Graves' ophthalmopathy (*cont.*)
signs and symptoms of, 113
smoking and, 113
surgery for, 115
T-cell depletion therapies for, 116
thyrotropin receptor autoantibodies in, 114
transantral orbital decompression for, 115
Growth hormone deficiency, 250
Guided progression analysis, 301
Guillain-Barre syndrome, 83

H
Halo sign, 59
Headaches
lumboperitoneal shunting for, 97–98
management of, 94
in pseudotumor cerebri syndrome, 94
ventriculoperitoneal shunting as cause of, 97
Head trauma-related optic neuropathy
chiasmal injuries, 159
computed tomography of, 160–161
corticosteroids for, 164
deceleration injury, 155, 161
diagnosis of, 159–161
epidemiology of, 155
indirect injuries, 159, 161
localization, 158–159
magnetic resonance imaging of, 160–161
management of, 163–165
methylprednisolone for, 163–164
motorcycle accidents, 155
neuroimaging of, 160–161
optic canal decompression for, 162, 164
optic nerve anatomy, 155–158
pathogenesis of, 162–163
pathology associated with, 161–162
posterior indirect injury, 159
shearing forces associated with, 162
sphenoid bone fractures, 161
visual prognosis for, 161
Hemangioblastoma, 272–273
Hemangioma
capillary, 270–271
cavernous, 271–272
racemose, 273–274
Heparin
cerebral sinus thrombosis treated with, 86
extracorporeal LDL/fibrinogen precipitation induced by, 47–48
Hereditary ataxias
Friedreich's ataxia. *See* Friedreich's ataxia
spinocerebellar ataxia type 1, 231–232
Hereditary motor and sensory neuropathy type VI, 232–233
Hereditary optic atrophy with progressive deafness and polyneuropathy, 234–235
Hereditary optic neuropathies
Behr syndrome, 233–234
Costeff syndrome, 233–234
dominant optic atrophy. *See* Dominant optic atrophy
hereditary optic atrophy with progressive deafness and polyneuropathy, 234–235
hereditary sensory and autonomic neuropathy type III, 235
Leber's. *See* Leber's hereditary optic neuropathy
overview of, 209
Hereditary sensory and autonomic neuropathy type III, 235
Hereditary spastic paraplegia, 232
Highly active anti-retroviral therapy, 185
HIV, 4
HLA-DRB1*04, 53
Homocysteine metabolism, 52
Homonymous hemioptic hypoplasia, 251
Human leukocyte antigen-DR2, 8
Hurler syndrome, 236
Hyaloid system remnants, 261
Hydrocephalus, 133
Hydroxyurea, for optic nerve sheath meningiomas, 112
Hyperbaric oxygen therapy
nonarteritic anterior ischemic optic neuropathy treated with, 47
radiation-induced optic neuropathy treated with, 196–197
Hypertension, 45
Hypopituitarism, 130
Hypotension
nonarteritic anterior ischemic optic neuropathy and, 46, 49
posterior ischemic optic neuropathy caused by, 64
Hypothalamic gliomas, 128

I
Idebenone, 168, 219–220
Idiopathic orbital inflammatory pseudotumor
computed tomography of, 117
corticosteroids for, 117
diagnostic testing for, 117
epidemiology of, 116–117
histopathology of, 117
management of, 117
signs and symptoms of, 117
Idiopathic perioptic neuritis, 142
IgG test, for neuromyelitis optica, 24
Immune-mediated thrombocytopenia, 86
Immunosuppressive agents, for giant cell arteritis, 61
Indirect inferometry, 309
Infants. *See also* Children
gray optic discs in, 262
neuroaxonal dystrophy in, 237
Infiltrative optic neuropathies
description of, 128
infectious
cryptococcosis, 143–144
toxoplasmosis, 144–145
tuberculosis, 142–143
inflammatory
idiopathic perioptic neuritis, 142
sarcoidosis. *See* Sarcoidosis

Infliximab
giant cell arteritis treated with, 62
optic neuropathy caused by, 192
thyroid eye disease treated with, 116
Insulin-like growth factor-1, 114
Intensity-modulated radiotherapy, 194
Interferon ß, for neuromyelitis optica, 27
Interferon-alpha-associated optic neuropathy, 191–192
Interferon-gamma-producing T cells, 7
Interleukin-1 inhibitors, 116
Interleukin-6 receptor blockers, 116
Internal carotid artery aneurysm, 125
Intracanalicular optic nerve, 157–158
Intracranial masses, 82
Intracranial optic nerve, 158–159
Intracranial pressure, increased
choroidal folds associated with, 78–79
headaches associated with, 77
iatrogenic causes of, 83
intracranial masses as cause of, 82
medications that cause, 93
meningitis as cause of, 83
papilledema caused by. *See* Papilledema
pseudotumor cerebri as cause of, 89
secondary causes of, 82–83
spinal cord tumors as cause of, 83
subarachnoid hemorrhage as cause of, 82–83
subhyaloid hemorrhages caused by, 79
systemic disorders associated with, 91
Intraocular pressure
elevated, nonarteritic anterior ischemic optic neuropathy and, 50–51
measurement of, in glaucomatous and nonglaucomatous optic neuropathies, 282–283
Intravenous immunoglobulin
neuromyelitis optica treated with, 26
optic neuritis treated with, 18
Intravenous methylprednisolone
neuromyelitis optica treated with, 25
optic neuritis treated with, 18
Intravitreal triamcinolone acetonide, for nonarteritic anterior ischemic optic neuropathy, 47
Intrinsically photosensitive retinal ganglion cells, 214
IONDT. *See* Ischemic Optic Neuropathy Decompression Trial
Ischemic optic neuropathy
nonarteritic anterior. *See* Nonarteritic anterior ischemic optic neuropathy
visual field defects in, 290
after vitrectomy, 169
Ischemic Optic Neuropathy Decompression Trial, 41, 45

J
Junctional or anterior chiasmal syndrome, 123

K
Kallidin, 163
Krabbe disease, 238
Krukenberg spindle, 283
Kjer's optic neuropathy. *See* Dominant optic atrophy

L
Lamina cribrosa, 137, 283
Latency
multifocal electroretinogram measurement, 327
multifocal visual evoked potential measurement, 341–343
Lateral geniculate nucleus, 17
Leber's hereditary optic neuropathy
alcohol consumption and, 213
asymptomatic carriers of, 215
cecocentral scotoma in, 214
circumpapillary telangiectatic microangiopathy associated with, 4
clinical presentation of, 213–215
Cuban epidemic of optic neuropathy and, 187
definition of, 212
description of, 177, 209
diagnosis of, 216–218
differential diagnosis of, 216
discovery of, 212
epidemiology of, 212
ethambutol and, 185
funduscopic features of, 215–216
genetic heterogeneity of, 212–213
genetic testing for, 218
histopathology of, 216
management of
anti-apoptotic drugs, 220
antioxidants, 219
brimonidine, 219
coenzyme Q10, 219
EPI-743, 220
gene therapy, 220–221
idebenone, 219–220
mitochondrial biogenesis-activating drugs, 220
overview of, 218–219
vitamins, 219
mitochondrial DNA mutations associated with, 212–213, 218, 221
molecular genetics of, 212–213
mouse model of, 221
multiple sclerosis and, 218
optical coherence tomography of, 216–217
optic disc findings in, 215
optic nerve head in, 215–216
optic neuritis versus, 3–4
retinal nerve fiber layer in, 216–217
risk factors for, 213
smoking and, 213
systemic diseases associated with, 218
visual field defects in, 214, 290
visual loss in, 185, 213–215
"Leber's plus" syndrome, 218
Lenz microphthalmia syndrome, 255
Leptin, 90
Leptomeningeal metastases, to optic nerve, 136–137

Leukemic infiltration, of optic nerve, 139–140
Leukocoria, 267
Leukomalacia, 250
Levodopa/carbidopa, for nonarteritic anterior ischemic optic neuropathy, 47
Lewy body dementia, 319
Lhermitte's sign, 21
LHON. *See* Leber's hereditary optic neuropathy
Linezolid-associated optic neuropathy, 184–185
Low-contrast letter acuity and contrast sensitivity testing, 14
Lown–Ganong–Levine syndrome, 218
Lumboperitoneal shunting, for cerebrospinal fluid diversion, 96–98, 100
Lymphocytes, in giant cell arteritis, 59
Lymphomatous infiltration, of optic nerve, 138–139
Lymphomatous infiltrative optic neuropathy, 138

M
Macroadenomas, 118–119
Macular edema
  cystoid, in POEMS syndrome, 29
  fingolimod as cause of, 314
  in optic disc pit, 256
  in papilledema, 79
Macular thinning, 317
Macular volume, 11–14
Magnetic resonance angiography
  giant cell arteritis evaluations, 60
  suprasellar meningiomas, 121
Magnetic resonance imaging
  clinically definite multiple sclerosis, 9–10
  craniopharyngiomas, 123
  Friedreich's ataxia findings, 231
  giant cell arteritis, 60
  idiopathic orbital inflammatory pseudotumor, 117
  infantile neuroaxonal dystrophy findings, 237
  neuromyelitis optica, 23
  optic gliomas, 130–131
  optic nerve sheath meningiomas, 110
  optic neuritis, 10
  pituitary adenoma, 118–119
  pituitary apoplexy, 120–121
  pseudotumor cerebri syndrome, 87
  suprasellar meningiomas, 121
  traumatic optic neuropathy, 160–161
Magnetization transfer ratio, 16–17
Malabsorption syndrome, 181
Malignant anterior visual pathway gliomas
  epidemiology of, 134
  neuroimaging of, 135
  optic disc in, 135
  pathology of, 135
  prognosis for, 135–136
  signs and symptoms of, 134–135
  treatment of, 135–136
  visual loss caused by, 134
Malignant teratoid medulloepithelioma, 268
Mammalian target of rapamycin, 128
Matrix metalloproteinases, 166
Meckel–Gruber syndrome, 255
Medulloepithelioma, 268
Megaloblastic anemia, 179
Megalopapilla, 250–251
Melanocytic tumors, 274–277
Melanocytoma, 274–275
Memantine, 168
Meningeal metastases, to optic nerve, 136–137
Meningiomas
  optic nerve sheath. *See* Optic nerve sheath meningiomas
  sphenoid wing, 124–125
  suprasellar, 121–122
Meningitis, 83, 144
MERRF, MELAS, and Leigh syndrome, 227
Metachromatic leukodystrophy, 237–238
Metastases
  choroidal, 137
  leptomeningeal, to optic nerve, 136–137
  optic disc, 137–140
Methanol-associated optic neuropathy, 185–186
Methazolamide, 95
Methylmalonyl CoA, 179
Methylprednisolone
  giant cell arteritis treated with, 60
  papilledema treated with, 95
  traumatic optic neuropathy treated with, 163–164
Methyltetrahydrofolate reductase, 51–52, 179–180
mfERG. *See* Multifocal electroretinogram
mfVEP. *See* Multifocal visual evoked potentials
Migraines, 52–53 *See also* Headaches
Mitochondria
  biogenesis in, drugs for activation of, 220
  dendritic distribution of, 227
  description of, 209–210
  fission/fusion defects of, 232–233
Mitochondrial DNA
  description of, 209
  disorders associated with, 227–229
  mutations of, in Leber's hereditary optic neuropathy, 212–213, 218, 221
Mitochondrial optic neuropathies
  classification of, 177, 210
  clinical features of, 211
  clinical presentation of, 211
  definition of, 177
  Leber's hereditary optic neuropathy. *See* Leber's hereditary optic neuropathy
  papillomacular bundle in, 210–211
  screening for, 211
  signs and symptoms of, 211
Mitochondrial permeability transition pores, 209
Mohr–Tranebjaerg syndrome. *See* DDON syndrome
Morning glory disc anomaly, 253–254
MRA. *See* Magnetic resonance angiography
MRI. *See* Magnetic resonance imaging
MS. *See* Multiple sclerosis
Mucopolysaccharidoses, 82, 236
Müller cells, 165

Multifocal electroretinogram
amplitude measurement using, 327
applications of, 325
fixation errors associated with, 333–335
indications for, 347–349
latency measurement using, 327
optical coherence tomography versus, 335
optic nerve disorders diagnosed using, 329–335
origin of, 329
outer retina diseases ruled out using, 330–333
recording of, 326–327
responses, 327
retinal ganglion cell damage detected using, 335–336
trace arrays, 329
Multifocal visual evoked potentials
amplitude measurements, 341–343
conventional visual evoked potentials versus, 344–345
description of, 15, 325, 336–337
eccentric fixation with, 347–348
fixation errors with, 347
glaucomatous damage detection using, 346
indications for, 347–349
inter-subject variability in, 338
latency measurements, 341–343
mechanism of action, 337
optic nerve disorders diagnosed using, 343–347
optic neuritis/multiple sclerosis diagnosis and monitoring using, 343–344
origins of, 343
recording of, 337
responses of, 337–338
stimulus, 340
topographical representation of, 339–341
unreliable testing with, 347
visual fields evaluated using, 345–346
Multiple sclerosis
central serous retinopathy in, 318
clinically definite
definition of, 1
intravenous methylprednisolone and, 18
magnetic resonance imaging of, 9–10
risk factors for, 9–10
risk of developing, 9, 19–20
environmental factors, 8
epidemiologic factors, 8
fingolimod for, 314
Leber's hereditary optic neuropathy and, 218
macular volume measurements in, optical coherence tomography of, 11–14
multifocal visual evoked potentials for diagnosis and monitoring of, 343–344
neuromyelitis optica versus, 21
optical coherence tomography of, 317
optic neuritis in. *See* Optic neuritis
optic-spinal, 5
in pediatric optic neuritis, 9
peripheral retinal venous sheathing in, 3
retinal nerve fiber layer in, optical coherence tomography measurements of, 11–14
retinal nerve fiber layer thickness in, 321
risk factors for, 8
Mycobacterium tuberculosis, 142–143, 182
Mycophenolate mofetil, for neuromyelitis optica, 26
Myelinated nerve fibers, 261–262
Myelin basic protein, 6
Myopia, retinal nerve fiber layer in, 305–306

N
N-acetyl aspartate, 196
NADH dehydrogenase, 221
NAION. *See* Nonarteritic anterior ischemic optic neuropathy
Nanotechnology, 166
Neurodegenerative disorders, 315–317, 319
Neurofibromatosis-1
in children, 129
incidence of, 128
optic gliomas associated with, 128–136
orbital gliomas in, 131
Neurofibromatosis-2, 112
Neuroimaging. *See also* Computed tomography; Fluorescein angiography; Magnetic resonance imaging
of glaucomatous optic neuropathies, 287–291
of head trauma-related traumatic optic neuropathy, 160–161
of malignant anterior visual pathway gliomas, 135
of nonglaucomatous optic neuropathies, 287–291
of optic gliomas, 130–131
of optic nerve sheath meningiomas, 110
of pseudotumor cerebri syndrome, 93
of traumatic optic neuropathy, 160–161
Neuromyelitis optica
autoantibodies in, 24
azathioprine for, 25–26
clinical course of, 24–25
connective tissue diseases and, 24
diagnosis of, 20–23
epidemiology of, 20
glatiramer acetate for, 27
humoral immune mechanism in, 25
IgG test for, 24
interferon ß for, 27
intravenous immunoglobulin for, 26
intravenous methylprednisolone for, 25
laboratory studies, 23–24
magnetic resonance imaging of, 23
multiple sclerosis versus, 21
mycophenolate mofetil for, 26
neuro-ophthalmic findings in, 21–22
optical coherence tomography of, 316
optic neuritis in, 21–23
pathogenesis of, 25
pathology of, 25
prednisone for, 25–26
prevalence of, 20
relapsing
description of, 24–25

Neuromyelitis optica (*cont.*)
prevention of, 25–26
rituximab for, 26
treatment of, 25–27
in women, 20
Neuroretinal rim
loss of, 284–286
pallor of, 283–284
Neuroretinitis
infectious causes of, 5
optic disc edema in, 4
Nitric oxide, 194
Nitric oxide synthase, 162–163
NMDA receptors, 162–163
Nocturnal hypotension, 46
Nonarteritic anterior ischemic optic neuropathy
altitudinal defect in, 41
amiodarone-associated optic neuropathy and, 189–190
anemia and, 51
aspirin therapy for, 46–47
atypical features of, 43
bilateral simultaneous, 43
brimonidine tartrate for, 47
carotid artery stenosis and, 45
after cataract surgery, 168–169
Chlamydia in, 49
coagulopathies and, 51–52
corticosteroids for, 47
course of, 42–43
cup/disc ratio in, 43–45
diabetes mellitus and, 45
diabetic papillopathy as form of, 48
diagnostic tests for, 43–44
differential diagnosis of, 43
elevated intraocular pressure and, 50–51
heparin-induced extracorporeal LDL/fibrinogen precipitation for, 47–48
homocysteine metabolism impairments in, 52
hyperbaric oxygen therapy for, 47
hypertension and, 45
incidence of, 41
interferon-α treatment as cause of, 191–192
intravitreal triamcinolone acetonide for, 47
levodopa/carbidopa for, 47
methyltetrahydrofolate reductase mutation and, 52
migraines and, 52–53
nocturnal hypotension and, 46
nutritional anemia and, 51
optical coherence tomography of, 310
optic atrophy versus, 43
optic disc in
description of, 42–43
drusen, 48–49, 260
edema of, 47
filling delays, 45
optic nerve decompression surgery for, 46
optic neuritis versus, 43
pathogenesis of, 45–46
in perioperative period, 50
peripapillary splinter hemorrhages in, 42
predisposing factors for, 52
prednisone for, 47
primary open angle glaucoma versus, 44
prognosis for, 42–43
prothrombotic abnormality evaluations in, 52
recurrence rate, 42
retinal nerve fiber layer in, 43–44
risk factors for, 42, 44–45
signs and symptoms of, 41–42
sleep apnea syndrome and, 53
subretinal fluid with, 310
transvitreal optic neurotomy for, 48
treatment of, 46–48
Nonglaucomatous optic neuropathies
clinical features of, 287
glaucomatous optic neuropathies versus, 287–306
intraocular pressure measurement in, 282–283
laboratory tests for, 291
neuroimaging of, 287–291
optic disc examination in, 283
perimetry of, 287–290
visual acuity in, 282
visual field defects in, 290
Non-mitochondrial optic neuropathies
amiodarone, 189–191
clomiphene citrate, 192
digoxin, 189–191
disulfiram, 191
infliximab, 192
interferon-alpha, 191–192
radiation, 194–197
sildenafil, 193–194
tadalafil, 193–194
tamoxifen, 193
Nonsecreting adenomas, 119
Null cell adenomas, 119
Nutritional anemia, 51
Nutritional optic neuropathies
diet-related, 181
differential diagnosis of, 179
eating disorders and, 181
evaluation of, 178–179
folic acid deficiency, 180
malabsorption syndrome, 181
signs and symptoms of, 177–178
thiamine deficiency, 180–181
tobacco–alcohol amblyopia, 188, 213
toxic optic neuropathies and, combined types of, 187–189
vitamin B12, 178–180
vitamin B1 deficiency, 180–181
vitamin E deficiency, 181
zinc deficiency, 181
Nystagmus, 130

O

OCT. *See* Optical coherence tomography
Ocular motility defects, 123
Olfactory tract, 158

OPA1 gene, 222, 225–226
Ophthalmic artery, 156–157
Ophthalmoplegia
in chiasmal gliomas, 130
chronic progressive external, 232
in optic gliomas, 130
Optical coherence tomography
central macular thickness evaluations, 321–322
central retinal artery occlusion, 315, 319–320
central serous retinopathy, 315, 318–319
Cirrus spectral domain, 321
demyelinative disorders, 315–317, 319
devices/instruments for, 292, 294, 309
dominant optic atrophy, 224–225
Fourier domain, 309
indirect inferometry principle of, 309
Leber's hereditary optic neuropathy, 216–217
limitations of, 320–322
macular volume measurements using, 11–14
measurement variability in, based on technology, 321–322
multifocal electroretinogram versus, 335
multiple sclerosis, 317
neurodegenerative disorders, 315–317, 319
neuromyelitis optica, 316
nonarteritic anterior ischemic optic neuropathy, 310
operator skills-related limitations of, 320–321
optic disc drusen, 259
optic nerve applications of
description of, 301
drusen, 311, 313, 315
pit, 313–317
optic neuritis in multiple sclerosis diagnosis and monitoring using, 11–15
papilledema
description of, 80
with secondary choroidal neovascularization and subretinal fluid, 310–311
patient cooperation during, 320–321
principles of, 309
retinal ganglion cell loss, 13
retinal nerve fiber layer measurements using, 11–14, 259
software for, 320
spectral domain, 309, 320
Stratus, 321
toxic optic neuropathy, 311–313
traumatic optic neuropathy, 160
Optic atrophy
in anterior visual pathway gliomas, 129
in Leber's hereditary optic neuropathy, 215
neurodegenerative disorders associated with, 236
nonarteritic anterior ischemic optic neuropathy versus, 43
in progressive encephalopathy with edema, hypsarrhythmia, and optic atrophy, 236
in suprasellar meningiomas, 121
Optic canal fracture, 159
Optic chiasm compression, 118
Optic disc. *See also* Cup/disc ratio
astrocytic hamartoma of, 268–270
congenital pigmentation of, 262
cupping of, 285
edema of
in anterior visual pathway gliomas, 129
in leukemia, 139
in melanocytoma, 275
in neuroretinitis, 4
in nonarteritic anterior ischemic optic neuropathy, 42
in posterior scleritis, 5
in posterior uveitis, 5
sarcoid-related, 141
examination of, for glaucomatous versus nonglaucomatous optic neuropathies, 283
excavation of
anomalies associated with, 253–257
in dominant optic atrophy, 223
in glaucomatous optic neuropathies, 286
gray, 262
hemorrhages of, 286
ischemia of, in papilledema, 82
in Leber's hereditary optic neuropathy, 215
in malignant anterior visual pathway gliomas, 135
metastases to, 137–140
in nonarteritic anterior ischemic optic neuropathy, 42
in optic nerve sheath meningiomas, 109–110
in papilledema, 77–78
Optic disc anomalies
coloboma, 250, 254–255
congenitally anomalous size, 249–253
congenital pigmentation, 262
congenital tilted disc syndrome, 251–253
drusen. *See* Optic disc drusen
dysplasia, 257
elevated, 257–262
extracavated, 253–257
homonymous hemioptic hypoplasia, 251
hyaloid system remnants, 261
megalopapilla, 250–251
morning glory disc anomaly, 253–254
myelinated nerve fibers, 261–262
optic nerve hypoplasia, 249–250
papillorenal syndrome, 256–257
peripapillary staphyloma, 255
segmental optic nerve hypoplasia, 250–251
Optic disc drusen
asymptomatic presentation of, 257–258
central retinal artery occlusion in, 260
central retinal vein occlusion in, 260
diagnosis of, 258
epidemiology of, 257
fluorescein angiography of, 259
funduscopic findings, 258–259
nonarteritic anterior ischemic optic neuropathy associated with, 48–49, 260
optical coherence tomography of, 259
optic nerve sheath decompression for, 260
retinal hemorrhages associated with, 260
retinitis pigmentosa and, 260

Optic disc drusen (*cont.*)
treatment of, 260–261
visual evoked potentials in, 259
visual field defects in, 257–259
Optic disc pit, 256
Optic disc tumors
astrocytic hamartoma, 268–270
capillary hemangioma, 270–271
cavernous hemangioma, 271–272
choroidal melanoma, 275–276
combined hamartoma of retina and retinal pigment epithelium, 274, 276–277
hemangioblastoma, 272–273
medulloepithelioma, 268
melanocytic, 274–277
melanocytoma, 274–275
racemose hemangioma, 273–274
retinoblastoma, 267–268, 277
Optic gliomas
chemotherapy for, 134
computed tomography of, 130
course of, 132
growth of, 132
histopathology of, 131–132
incidence of, 128
intraneural growth pattern of, 132
magnetic resonance imaging of, 130–131
malignant, 134–136
management of, 132–134
monitoring of, 132–133
in neurofibromatosis type 1, 128–136
neuroimaging of, 130–131
ophthalmoplegia in, 130
perineural growth of, 131
prognosis for, 132
recurrence of, 132
signs and symptoms of, 129–130
spontaneous regression of, 133
surgery for, 133
visual loss caused by, 129
Optic nerve
anatomy of, 155–158
avulsion of, 158–160
blood supply to, 156–157
compression of, 113–116
crush injury of, 162–164
demyelination of, 6
drusen of, 311, 313, 315
ganglioglioma of, 136
hypoplasia of, 249–251
injury to
blepharoplasty and, 170
cataract surgery and, 168–169
endoscopic sinus surgery and, 170
head trauma as cause of. *See* Traumatic optic neuropathy, head trauma-related
periorbital injections as cause of, 168
trabeculectomy and, 170
vitrectomy and, 169–170
intracanalicular, 157–158
intracranial, 158–159
leptomeningeal metastases to, 136–137
leukemic infiltration of, 139–140
lymphomatous infiltration of, 138–139
lymphoreticular tumor infiltration of, 140
myelomatous infiltration of, 140
neuroprotective strategies for, 167–168
optical coherence tomography of, 301
orbital segment of, 156–157
primary tumors infiltrating, 128–136
regeneration of, 165
sarcoidosis involvement of, 140–142
sellar compressive lesions on, 118–128
stem cell transplantation for regeneration of, 165–166
suprasellar compressive lesions on, 118–128
swelling of, 159
Optic nerve decompression surgery
fibrous dysplasia treated with, 127
lumboperitoneal shunting versus, 97
nonarteritic anterior ischemic optic neuropathy treated with, 46
optic disc drusen-related visual loss treated with, 260
pseudotumor cerebri syndrome treated with, 95–98
traumatic optic neuropathy treated with, 164–165
Optic nerve head
anatomy of, 155–156
blood supply to, 156–157
in Leber's hereditary optic neuropathy, 215–216
remodeling of, in glaucomatous optic neuropathy, 284
retinal ganglion cells of, 155–156
retinoblastoma of, 267–269
Optic nerve pit, 313–317
Optic nerve sheath meningiomas
age of presentation, 109
chemotherapy for, 112
in children, 112
epidemiology of, 109
histopathology of, 110–111
hydroxyurea for, 112
magnetic resonance imaging of, 110
neurofibromatosis-2 associated with, 112
neuroimaging of, 110
observation of, 111
optic disc in, 109–110
pneumosinus dilatans associated with, 157
prognosis for, 111
radiotherapy for, 111
signs and symptoms of, 109–110
surgical treatment of, 112
treatment of, 111–112
visual acuity monitoring in, 111
visual field defects in, 109
Optic neuritis
acute ischemic optic neuropathy versus, 3
anterior visual pathway dysfunction in, 11–14
atypical, 11
in autoimmune diseases, 5
biomarkers, 20
cell-mediated damage as cause of, 6–7
central vision loss caused by, 1

in children, 1, 9
clinically definite multiple sclerosis and risks, 9, 19–20
treatment to delay progression to, 19–20
clinical presentation of, 1–3
color vision affected by, 2–3
contrast sensitivity affected by, 2–3
cortical plasticity after, 17
demyelinating, 4
demyelination associated with, 6
diagnostic testing for, 9–13
differential diagnosis of, 3–6, 43
early diagnosis and monitoring techniques
high-contrast visual acuity testing, 14
low-contrast letter acuity and contrast sensitivity testing, 14
multifocal visual evoked potentials, 343–344
optical coherence tomography, 11–15
visual evoked potentials, 15
epidemiologic factors, 8
fundal findings in, 3
gender predilection of, 1
genetic factors, 7–8
in HIV-infected patients, 4
incidence of, 1
laboratory tests for, 10–11
Leber's hereditary optic neuropathy versus, 3–4
macular volume measurements in, optical coherence tomography of, 11–14
magnetic resonance imaging of, 10
in neuromyelitis optica, 21–23
nonarteritic anterior ischemic optic neuropathy versus, 43
orbital pain associated with, 1
parainfectious, 4
in paraneoplastic syndrome, 6
pathogenesis and pathophysiology of, 6–8
posterior visual pathway involvement in, 16–17
pupillary abnormality associated with, 3
retinal nerve fiber layer in, optical coherence tomography measurements of, 11–14
in sarcoidosis, 4
signs and symptoms of, 1–3
treatment of
BENEFIT study findings, 19
CHAMPS/CHAMPIONS study, 18
to delay progression to multiple sclerosis, 19–20
ETOMS study findings, 19
intravenous immunoglobulin, 18
intravenous methylprednisolone, 18
plasmapheresis, 18
PreCISe study findings, 19
visual acuity in
decreases in, 1–2
high-contrast testing of, 14
visual evoked potentials for detection of, 11, 15, 336
visual field defects caused by, 2, 290
visual prognosis in, 8
Optic Neuritis Treatment Trial, 2, 8, 281
Optic-spinal multiple sclerosis, 5
Orbital emphysema, 158
Orbital hemorrhage, 158
Orbital inflammatory pseudotumor, idiopathic
computed tomography of, 117
corticosteroids for, 117
diagnostic testing for, 117
epidemiology of, 116–117
histopathology of, 117
management of, 117
signs and symptoms of, 117
Orbital optic nerve, 156–157
Orbital pain, 1
Orbital rim fractures, 159

P

Papilledema
acetazolamide for, 95, 101
aqueductal stenosis associated with, 82
asymmetric, 80
atrophic, 79
central vision affected by, 80
choroidal neovascularization with, 310–311
chronic, 79–80
computed tomography of, 81
corticosteroids for, 95
in craniofacial dysostosis, 82
definition of, 77
diagnostic testing for, 80–81
fluorescein angiography of, 81
furosemide for, 95
grade 1, 78
grade 2, 78
grade 3, 78, 94
grade 4, 79, 95
grade 5, 79, 95
macular edema in, 79
medical treatment of, 94–95
meningitis and, 83
methazolamide for, 95
mucopolysaccharidosis as cause of, 82
optical coherence tomography of, 80, 310–311
optic disc ischemia in, 82
optic nerve pathology in, 81–82
in otitis media, 83
pathology of, 81–82
progression of, 80
in pseudotumor cerebri syndrome, 86. *See also* Pseudotumor cerebri syndrome
retinal nerve epithelium/basement membrane in, 80–81
retinal nerve fiber layer in, 81
signs of, 77–80
splinter hemorrhages in, 78
symptoms of, 77
traumatic optic neuropathy and, 160
unilateral, 80
venous drainage decreases as cause of, 83
visual acuity affected by, 80
visual loss in, 79, 82, 95, 311

Papillitis, 3
Papillomacular bundle, 177, 210–211, 223
Papillorenal syndrome, 256–257
Paragangliomas, 83
Parainfectious optic neuritis, 4
Paraneoplastic optic neuropathies, 27–29
Paraneoplastic syndromes, 6
Parkinson's disease, 319
Pars plana vitrectomy, 277
Paton's lines, 78
PAX2 gene, 255
PCS. *See* Pseudotumor cerebri syndrome
PEHO syndrome. *See* Progressive encephalopathy with edema, hypsarrhythmia, and optic atrophy
Pelizaeus–Merzbacher disease, 238
Perimetry, 287–290
Perioperative posterior ischemic optic neuropathy, 64–66
Perioptic neuritis, idiopathic, 142
Periorbital injections, 168
Peripapillary staphyloma, 255
Peripheral nerve grafts, 165
Peripheral retinal venous sheathing, 3
Periventricular demyelination, 237
Pernicious anemia, 179
PHACE syndrome, 254
Phosphenes, 1
Phosphodiesterase-5 inhibitors, 193
Pilocystic astrocytoma, 131
Pinealoblastoma, 268
PION. *See* Posterior ischemic optic neuropathy
Pituitary adenoma, 118–120
Pituitary apoplexy, 120–121
Pituitary macroadenomas, 119
Plasmapheresis, for optic neuritis, 18
Platelet-derived growth factor, 55
Pneumosinus dilatans, 157
POEMS syndrome (polyneuropathy, organomegaly, endocrinopathy, monoclonal gammopathy, and skin changes), 28–29
Posterior ischemic optic neuropathy
  arachnoiditis and, 64
  carotid artery disease as cause of, 64
  fistula as cause of, 64
  incidence of, 63
  inflammatory diseases that cause, 64
  pathophysiology of, 63–64
  perioperative, 64–66
  in sickle cell disease, 64
  signs and symptoms of, 63
  in systemic disorders, 64
  treatment of, 66
Posterior pituitary ectopia, 250
Posterior scleritis, 5
Posterior segment, 283
Posterior uveitis
  autoimmune-related, 5
  optic disc edema in, 5
  in primary ocular disorders, 5
  viral causes of, 5
Posterior visual pathways
  cortical plasticity of, multifocal visual evoked potentials for detection of, 15
  imaging of, 16–17
  optic neuritis involvement of, 16–17
PreCISe study, 19
Prednisone. *See also* Corticosteroids
  giant cell arteritis treated with, 60–61
  idiopathic orbital inflammatory pseudotumor treated with, 117
  neuromyelitis optica treated with, 25–26
  nonarteritic anterior ischemic optic neuropathy treated with, 47
  sarcoidosis treated with, 142
Pregnancy
  corticosteroids in, 101
  pseudotumor cerebri syndrome in, 100–101
Primary angle-closure glaucoma, 283
Primary CNS lymphoma, 138
Primary open angle glaucoma, 44
Primary progressive multiple sclerosis, 12, 15
Progressive encephalopathy with edema, hypsarrhythmia, and optic atrophy, 236
Prolactinoma, 119
Proptosis, 129–130
Protein C deficiency, 51
Protein S deficiency, 51
Proteolipid protein-1, 238
Psammoma bodies, 110
Pseudotumor cerebri syndrome
  anemia and, 92
  carbonic anhydrase inhibitors for, 94–95
  central vision loss in, 94
  cerebrospinal fluid features of, 93
  in children, 101
  diagnostic criteria for, 86–87
  dural venous sinus stenting for, 100
  epidemiology of, 88
  gender and, 92
  genetics of, 88
  headaches in, 94
  hereditary conditions associated with, 92
  hypercoagulable states that cause, 92
  incidence of, 90
  increased intracranial pressure in, 89
  magnetic resonance imaging of, 87
  management of, 93–101
  medical treatment of, 94–95
  neuroimaging features of, 93
  optic nerve sheath decompression for, 95–98
  papilledema in, 86
  pathogenesis of, 89–91
  pediatric, 101
  in pregnancy, 100–101
  prognosis for, 88–89
  recombinant human growth hormone and, 93
  recurrence of, 101
  signs and symptoms of, 86
  sleep apnea associated with, 92–93
  systemic disorders associated with, 91–93
  venous sinus stenting for, 100

ventriculoperitoneal shunting for, 96–98
visual acuity affected by, 88
visual course of, 88–89
weight loss for, 94, 98
without papilledema, 87–88
Pseudoxanthoma elasticum, 260
PTCS. *See* Pseudotumor cerebri syndrome
Pulsatile tinnitus, 77
Pyridoxine, 143

Q
Quinagolide, for pituitary adenoma, 119

R
Racemose hemangioma, 273–274
Radiotherapy
chiasmal gliomas treated with, 133–134
complications of, 111, 134
Graves' ophthalmopathy treated with, 115
intensity-modulated, 194
optic disc metastases treated with, 138
optic gliomas treated with, 133–134
optic nerve sheath meningiomas treated with, 111
optic neuropathy caused by, 111–112, 194–197
pituitary adenoma treated with, 120
sphenoid wing meningiomas treated with, 124
Reactive oxygen species, 55, 209, 220
Recombinant human growth hormone, 93
Recombinant human mitochondrial transcription factor A, 221
Relative afferent pupillary defect, 159–160, 282
Retina
combined hamartoma of, and retinal pigment epithelium, 274, 276–277
glial tumors of, 268–270
sensory, tumors of, 267–268
vascular tumors of, 270–274
Retinal ganglion cells
apoptosis of, 220
axons of, 155–156, 211
degeneration of, 292
intracellular calcium effects on, 162
intrinsically photosensitive, 214
multifocal electroretinogram for detection of damage to, 335–336
optical coherence tomography for evaluation of, 13
optic nerve crush injury effects on, 164
stem cell transplantation for, 165–166
survival of, strategies for promoting, 167
Retinal hemorrhages, 260
Retinal nerve epithelium/basement membrane, 80–81
Retinal nerve fiber layer
age-related loss of, 305
in anterior ischemic optic neuropathy, 43–44
definition of, 292
floor effect in measurement of, 304–305
in Leber's hereditary optic neuropathy, 216–217
in multiple sclerosis, 321
in myopic eyes, 305–306
optical coherence tomography measurements of
in glaucomatous optic neuropathies, 292–306
in nonarteritic anterior ischemic optic neuropathy, 43
in optic nerve drusen, 311
in optic neuritis, 11–15
in toxic optic neuropathy, 311–312
in papilledema, 77, 81
thickness of, 301–302, 306
thinning of
in glaucomatous optic neuropathy, 285
in nonarteritic anterior ischemic optic neuropathy, 44
Retinal pigment epithelium
combined hamartoma of retina and, 276
reactive hyperplasia of, 277
Retinitis, 27
Retinitis pigmentosa, 260, 327
Retinoblastoma, 267–269, 277
Retinopathy
central serous, 315, 318–319
radiation therapy-related, 111
Retrobulbar optic nerve ischemia, 64
Retrobulbaroptic neuritis, 192
RGCs. *See* Retinal ganglion cells
Riley–Day syndrome. *See* Familial dysautonomia
Rituximab
Graves' ophthalmopathy treated with, 116
neuromyelitis optica treated with, 26
RNFL. *See* Retinal nerve fiber layer
Rosenberg–Chutorian syndrome, 234
Roux-en-Y gastric bypass, 98

S
Sarcoidosis
diagnostic testing of, 141–142
epidemiology of, 140–141
optic neuritis in, 4
signs and symptoms of, 141
visual loss in, 141
Schilling test, 180
Scleral canal, 156
Secondary progressive multiple sclerosis, 12
Secretory adenomas, 119
Segmental optic nerve hypoplasia, 250–251
Selenium, 115–116
Sensorineural hearing loss syndromes, 226
Serous macular detachment, 254
Sheehan's syndrome, 120
Shock-induced anterior ischemic optic neuropathy, 49–50
Sickle cell disease, posterior ischemic optic neuropathy in, 64
Sildenafil-associated optic neuropathy, 193–194
Sleep apnea syndrome
nonarteritic anterior ischemic optic neuropathy and, 53
pseudotumor cerebri syndrome associated with, 92–93
Smoking
Graves' ophthalmopathy and, 113
Leber's hereditary optic neuropathy and, 213
tobacco–alcohol amblyopia and, 188
Spectral domain optical coherence tomography, 309, 320
Sphenoid bone fractures, 161

Sphenoid sinusitis, acute, 4
Sphenoid sinus mucocele, 126–127
Sphenoid wing meningioma, 124–125
Spinal cord tumors, 83
Spindle cells, 110
Spinocerebellar ataxia type 1, 231–232
Splinter hemorrhages, in papilledema, 78
Stem cell transplantation, 165–167
Stereotactic radiosurgery, 194
Strachan syndrome, 188
Stratus optical coherence tomography, 321
Streptokinase, for cerebral sinus thrombosis, 85
Subarachnoid hemorrhage, 82–83
Subfoveal choroidal neovascularization, 277
Subhyaloid hemorrhages, 79
Subretinal fluid, 310–311, 319
Superior sagittal sinus, 83
Suprasellar disorders, 253
Suprasellar meningiomas, 121–122
Supratentorial tumors, 82
Surgery
  anterior visual pathway gliomas treated with, 133
  chiasmal gliomas treated with, 133
  craniopharyngiomas treated with, 124
  Graves' ophthalmopathy treated with, 115
  optic gliomas treated with, 133
  optic nerve sheath meningiomas treated with, 112
  sphenoid wing meningiomas treated with, 124
  suprasellar meningiomas treated with, 122
  thyroid eye disease treated with, 115
Syphilis, 5

T
Tadalafil-associated optic neuropathy, 193–194
Tamoxifen-associated optic neuropathy, 193
T-cell depletion therapies, 116
Temporal artery biopsy, 58
Tetrahydrofolate, 180
Th1 cells, 55
Thiamine deficiency optic neuropathy, 180–181
Thrombolytic agents, for cerebral sinus thrombosis, 85
Thyroid eye disease
  description of, 114
  surgery for, 115
  visual loss caused by, 114–115
Thyroid ophthalmopathy, 113
Thyrotropin receptor autoantibodies, 114
Tobacco–alcohol amblyopia, 188, 213
Toluene-associated optic neuropathy, 186–187
Topiramate, 94
Toxic optic neuropathies
  differential diagnosis of, 179
  ethylene glycol, 186
  evaluation of, 178–179
  infliximab treatment affected by, 192
  methanol, 185–186
  nutritional optic neuropathies and, combined types of, 187–189
  optical coherence tomography of, 311–313
  optic nerve pallor in, 312
  signs and symptoms of, 177–178
  toluene, 186–187
  visual field defects in, 290
Toxoplasmosis, 144–145
Trabeculectomy, optic nerve injury after, 170
Transantral orbital decompression, for Graves' ophthalmopathy, 115
Transsphenoidal encephalocele, 254
Transsphenoidal microsurgical decompression, of sphenoid sinus mucocele, 126
Transverse myelitis, 23
Transvitreal optic neurotomy, for nonarteritic anterior ischemic optic neuropathy, 48
Traumatic optic neuropathy
  in adolescents, 165
  anatomy of, 155–158
  in children, 165
  corticosteroids for, 164
  diagnosis of, 159–161
  direct, 158–159
  after endoscopic sinus surgery, 170
  epidemiology of, 155
  head trauma-related
    chiasmal injuries, 159
    computed tomography of, 160–161
    corticosteroids for, 164
    deceleration injury, 155, 161
    diagnosis of, 159–161
    epidemiology of, 155
    indirect injuries, 159, 161
    localization, 158–159
    magnetic resonance imaging of, 160–161
    management of, 163–165
    methylprednisolone for, 163–164
    motorcycle accidents, 155
    neuroimaging of, 160–161
    optic canal decompression for, 162, 164
    optic nerve anatomy, 155–158
    pathogenesis of, 162–163
    pathology associated with, 161–162
    posterior indirect injury, 159
    shearing forces associated with, 162
    sphenoid bone fractures, 161
    visual prognosis for, 161
  incidence of, 155
  indirect, 159, 161
  loss of consciousness secondary to, 155
  management of, 163–165
  methylprednisolone for, 163–164
  neuroimaging of, 160–161
  optical coherence tomography of, 160
  optic nerve decompression surgery for, 164–165
  papilledema and, 160
  periorbital injections as cause of, 168
  relative afferent pupillary defect associated with, 159–160
  visual evoked potentials of, 160
  visual field defects in, 290
  visual loss caused by, 155
  visual prognosis for, 161
Tuberculomas, 143

Tuberculosis, 142–143, 182
Tuberous sclerosis complex, 268–270
Tumor necrosis factor blockers
  giant cell arteritis treated with, 62
  infliximab. *See* Infliximab
Type III 3-methylglutaconic aciduria, 233

U
Ultrasound biomicroscopy, of giant cell arteritis, 59–60

V
Venous sinus compression, 92
Venous sinus stenoses, 89
Venous sinus stenting, for pseudotumor cerebri syndrome, 100
Ventriculoperitoneal shunting
  ascites secondary to, 133
  cerebrospinal fluid diversion using, 96–98
VEPs. *See* Visual evoked potentials
Visual acuity
  in glaucomatous optic neuropathies, 282
  in morning glory disc anomaly, 253
  in nonglaucomatous optic neuropathies, 282
  in optic nerve sheath meningiomas, 111
  optic neuritis effects on, 1–2
  papilledema effects on, 80
  in peripapillary staphyloma, 255
  pseudotumor cerebri syndrome effects on, 88
  in racemose hemangioma, 273
Visual evoked potentials
  multifocal
    amplitude measurements, 341–343
    conventional visual evoked potentials versus, 344–345
    description of, 15, 325, 336–337
    eccentric fixation with, 347–348
    fixation errors with, 347
    glaucomatous damage detection using, 346
    indications for, 347–349
    inter-subject variability in, 338
    latency measurements, 341–343
    mechanism of action, 337
    optic nerve disorders diagnosed using, 343–347
    optic neuritis/multiple sclerosis diagnosis and monitoring using, 343–344
    origins of, 343
    recording of, 337
    responses of, 337–338
    stimulus, 340
    topographical representation of, 339–341
    unreliable testing with, 347
    visual fields evaluated using, 345–346
  in optic disc drusen, 259
  optic nerve hypoplasia, 249
  optic neuritis detection using, 11, 15, 336
  traumatic optic neuropathy detection using, 160
Visual field defects
  in anterior visual pathway gliomas, 129
  in arteritic anterior ischemic optic neuropathy, 54
  in congenital tilted disc syndrome, 252
  in craniopharyngiomas, 122–123
  in dominant optic atrophy, 290
  in glaucomatous optic neuropathies, 290
  in ischemic optic neuropathy, 290
  in Leber's hereditary optic neuropathy, 214, 290
  in melanocytoma, 274
  in nonglaucomatous optic neuropathies, 290
  in optic disc drusen, 257–259
  in optic nerve sheath meningiomas, 109
  in optic neuritis, 2, 290
  in pituitary adenoma, 118
  in suprasellar meningiomas, 121
  in traumatic optic neuropathy, 290
Visual loss
  after blepharoplasty, 170
  in combined hamartoma of retina and retinal pigment epithelium, 276
  in cryptococcosis, 143
  ethambutol-associated, 182
  in giant cell arteritis, 54
  in Leber's hereditary optic neuropathy, 185, 213–215
  in malignant anterior visual pathway gliomas, 134
  in optic disc coloboma, 254
  in optic gliomas, 129
  in optic nerve hemangioblastoma, 273
  in papilledema, 79, 82, 95, 311
  in sarcoidosis, 141
  after trabeculectomy, 170
Vitamin B1 deficiency optic neuropathy, 180–181
Vitamin B12 optic neuropathy, 178–180
Vitamin E deficiency optic neuropathy, 181
Vitrectomy
  optic nerve injury after, 169–170
  pars plana, 277
Vitritis, 3
von Hippel–Lindau syndrome, 270–272

W
Wallerian degeneration, 162
Wegener's granulomatosis, 5
Weight loss
  bariatric surgery for, 98
  pseudotumor cerebri syndrome managed with, 94, 98
WFS1 gene, 226
Wolff–Parkinson–White syndrome, 218
Wolfram's syndrome, 228–229
Wyburn–Mason syndrome, 273

X
X-linked adrenoleukodystrophy, 237
X-linked Charcot–Marie–Tooth syndrome, 234

Z
Zinc deficiency optic neuropathy, 181
Zonal oblique multislice echo planar imaging, 16